ANNUAL REVIEW OF NUCLEAR SCIENCE

JAMES G. BECKERLEY, *Editor*
Schlumberger Well Surveying Corporation

MARTIN D. KAMEN, *Associate Editor*
Washington University Medical School

LEONARD I. SCHIFF, *Associate Editor*
Stanford University

VOLUME 5

1955

PUBLISHED BY
ANNUAL REVIEWS, INC.
IN CO-OPERATION WITH THE
NATIONAL RESEARCH COUNCIL
OF THE NATIONAL ACADEMY OF SCIENCES

ON SALE BY
ANNUAL REVIEWS, INC.
STANFORD, CALIFORNIA, U.S.A.

Engin. Library
QC
770
.A65
v. 5

ANNUAL REVIEWS, INC.
STANFORD, CALIFORNIA, U.S.A.

FOREIGN AGENCIES

H. K. Lewis & Company, Ltd.
136 Gower Street
London, W.C. 1

Maruzen Company, Ltd.
6 Tori-Nichome Nihonbashi
Tokyo

PRINTED AND BOUND IN THE UNITED STATES OF AMERICA BY
THE GEORGE BANTA PUBLISHING COMPANY

Engin
Nucl

PREFACE

The present volume marks the first half-decade of publication of the *Annual Review of Nuclear Science.* Therefore it seems appropriate to note here some of the basic problems which the Editorial Committee has faced in determining the content of these volumes and to record the method by which these problems have been resolved.

One important question has been, "To whom are the individual reviews directed?" We have concluded that a variety of readers must be considered, ranging from the specialists in the field under review, who probably will not learn very much new, to the scientists in neighboring fields, who will probably profit substantially. Other readers will profit mainly from those chapters dealing with common phenomena of broad scientific interest and those written by authors particularly adept in expressing novel and complex ideas in simple terms. Because of these realities the individual chapters will have a varying usefulness to those working in fields remote from the ones under review.

Another difficult question is, "What is the proper scope of the volumes?" We have been unable to find a rigid definition of "Nuclear Science"; in fact, we are not certain any can exist. An expanding field has by its nature undefined boundaries. We feel certain that nuclear physics, pure and applied, experimental and theoretical, belongs here. But, for example, radiation chemistry—does this belong to these volumes, or is it properly a matter for the *Annual Review of Physical Chemistry*? We have gradually come to the conclusion that it is physical chemistry and will place it in that category. Nevertheless, we may, with appropriate consents, reprint a chapter on this subject from the *Annual Review of Physical Chemistry* whenever we believe it will make the nuclear science series self-contained.

It has also been difficult in defining the scope of these volumes to decide the extent of coverage appropriate to radiobiology. All agree that nuclear science includes the interactions of nuclear radiations and matter. But does "matter" include living organisms and biological materials? We have taken the position that the answer is in the affirmative and have included chapters on this subject. We have been influenced by the increasingly frequent encounters between radiobiologists on the one hand and nuclear physicists, solid state physicists, *et al.* on the other. These professional interactions may be during competition for reactor irradiation facilities, or in mutual efforts to bring order into radiation dosage definitions and measurements, or in the rather personal concerns over the health and safety aspects of research with nuclear radiations. Obviously no rigid rules can be set for the amount of discussion on biological topics in any volume.

Of the many other problems faced by the Editorial Committee in planning each volume, one stands out in difficulty. This is the question of timing. Complete coverage in any one volume is clearly impossible. Consequently we have to be concerned with when to include a review on any particular

subject. Is the topic "ripe" for reviewing? Has anything of consequence happened since the last review? Have journals or books appeared (or are they about to appear) which would make a review at this time inappropriate? There seems to be no simple formula for obtaining the answers to such questions. It is a matter of predicting each year the activity and accomplishments expected during the next year and a half or more (the interval between the invitation to the author and the appearance of the corresponding volume). Some topics seem always timely (e.g., mesons, big and little). Others are referred to in books as "closed" (e.g., positronium). Most are intermediate, and the Editorial Committee is forced to prognosticate.

Of comparable difficulty to the timing question is the space allocation. This is, of course, related to the scope of the review and to the intended audience. Even with these latter items fixed, the optimum number of pages to be available for each chapter is still debatable. Too few pages tends to stimulate a review which is essentially an annotated reference list; too many pages encourages inclusion of material of secondary interest. Although there is a happy medium, unfortunately this is also a function of subject and author. Experience of the Editorial Committee indicates fewer and longer chapters per volume to encourage more valuable articles. As a consequence the present pattern is about fifteen chapters per 450 page volume. Of these chapters, perhaps one-third are twenty pages or less, the balance being substantially longer. Further reduction in the number of articles per volume could be accomplished only by reducing the scope of the volume or by requesting each individual author to cover much more ground than his specialization might support. (One other concern associated with the practice of having relatively few, lengthy chapters is the possibility of fluctuation, i.e., the unexpected loss of any one article reduces the volume size by an appreciable fraction.)

In spite of these and other problems, the Editorial Committee believes the results to date have been well worth the effort. The steadily increasing proliferation of research papers in the literature of nuclear science steadily increases the value of such integrating activities as these volumes represent.

It should not be construed from the above comments that the Editorial Committee considers its actions as creative. The real creators of each *Annual Review* are the contributing authors. To them belongs the credit, and to them we express our appreciation.

As an aid in using the first five volumes, a chapter title and author index for volumes 1 through 5 has been included following the present volume index.

J.G.B. M.D.K.
C.D.C. L.I.S.
L.F.C. E.S.
R.E.Z.

ERRATA

Volume 4

page 274: In the second paragraph following the subtitle *Range:* The authors regret their oversight in the references cited (on the range-energy relation) of the following: Menon, M. G. K., and O'Ceallaigh, C., *Phil. Mag.*, **44**, 1291 (1953); Baroni, G., Castagnoli, C., Cortini, G., Franzinetti, C., and Manfredini, A., *C.E.R.N., Rept. BS-9* (July, 1954).

page 276, line 26: for "other events, etc.," read "other events and measurement of mass."

page 286: Delete second sentence of the last paragraph and replace with: "They are derived from the potential path length of the particle in the chamber and the observed path length to the point of decay."

pages 291–92: The authors wish to point out that Figure 3 refers to evidence up to May, 1954, and is not consistent with text on page 293. A copy of a revised Figure 3, based on July, 1954, evidence, may be secured on request from the authors.

page 293, lines 12 ff.: Add the following sentence to conclusion (*a*): "After a special search for negative tracks among the apparent protons, one was found of mass $(1250 \pm 90)m_e$." Replace conclusion (*e*) with "Two *S*-particles which are observed in both chambers have secondaries with ranges consistent with the unique value of 90 gm./cm.^{2} Pb." Delete second sentence of conclusion (*f*) and replace with: "The Indiana group (47) finds that two of their *V*-particles' secondaries whose momenta in the center of mass system are measurable both have p consistent with 220 Mev/c."

page 295, ninth line from the bottom of the page: In the description of event Br2, the distance cited should read 1.1 mm. instead of 5.67 mm.

page 301, line 15: For "In view of" read "Even admitting."

page 303: Delete sentence immediately preceding Figure 7 ("It is not . . . fill the gap."), and replace with the following: "As happened with the τ, it is possible that other new groups of particles may be found with the increased range afforded by the emulsion stacks."

page 305: Footnote 4 should refer to "E.P. group" instead of "P.E.P. group."

page 315: The following acknowledgment was omitted from "Penetration of Heavy Charged Particles in Matter," by E. A. Uehling:

This report has been prepared at the suggestion of the Subcommittee on Penetration of Charged Particles in Matter of the National Research Council Committee on Nuclear Science. Its preparation has been assisted by the joint programs of the Office of Naval Research and the Atomic Energy Commission.

CONTENTS

PAGE

ELECTROMAGNETIC TRANSITIONS IN NUCLEI, *M. Goldhaber and J. Weneser* 1

THE DISTRIBUTION OF CHARGE IN THE NUCLEUS, *K. W. Ford and D. L. Hill* 25

NUCLEAR RADIATION SHIELDING, *E. P. Blizard* 73

NUCLEAR REACTIONS OF INTERMEDIATE ENERGY HEAVY PARTICLES, *D. C. Peaslee* 99

NUCLEAR PARTICLE DETECTION (CLOUD CHAMBERS AND BUBBLE CHAMBERS), *W. B. Fretter* 145

DESIGN COMPARISON OF REACTORS FOR RESEARCH, *L. B. Borst* . . 179

INDUSTRIAL APPLICATIONS (MASS SPECTROMETRY), *C. E. Berry and J. K. Walker* 197

RADIATION CHEMISTRY, *F. S. Dainton* 213

MASS SPECTRA AND THE CHEMICAL SPECIES PRODUCED BY THE IMPACT OF LOW ENERGY ELECTRONS, *M. Krauss, A. L. Wahrhaftig, and H. Eyring* 241

RADIOCHEMICAL SEPARATION TECHNIQUES, *H. L. Finston and J. Miskel* 269

THE FUNDAMENTALS OF RADIOAUTOGRAPHY, *W. P. Norris and L. A. Woodruff* 297

CELLULAR RADIOBIOLOGY, *R. K. Mortimer and C. A. Beam* . . . 327

REMOVAL OF RADIOELEMENTS FROM THE MAMMALIAN BODY, *J. Schubert* 369

VERTEBRATE RADIOBIOLOGY: PHYSIOLOGY, *A. Edelmann* 413

INDEX, AUTHOR 425

INDEX, SUBJECT 438

INDEX, CHAPTER TITLE, VOLUMES 1–5 445

INDEX, AUTHORS OF CHAPTERS IN VOLUMES 1–5 448

Annual Reviews, Inc., the National Research Council, and the Editors of this publication assume no responsibility for the statements expressed by the contributors to this *Review*.

ELECTROMAGNETIC TRANSITIONS IN NUCLEI[1]

By M. Goldhaber and J. Weneser
Brookhaven National Laboratory,[2] Upton, New York

Introduction

Since the properties of the electromagnetic radiation field are well understood, it appears to be an excellent probe to test the details of nuclear structure. For a long time it has been known from studies of the photodisintegration of the deuteron that the simple nonrelativistic convection and spin-currents explain the main features of nuclear electromagnetic interactions. However, finer questions still remain to be answered. These questions arise in connection with the type and magnitude of exchange currents which one is forced to postulate, e.g. because of the magnetic moment anomalies found for H^3 and He^3, and in consonance with ideas on the role of mesons in nuclear interactions. The evidence indicates that these currents are probably small. If we assume, therefore, that the exchange currents can be neglected in first approximation, we can make use of electromagnetic interactions to test certain aspects of nuclear models, and correlate them with the many other types of information.

It should be noted that there is a close relationship between the static moments of nuclei (e.g. magnetic dipole moment, electric quadrupole moment) and the multipole moments obtained from the probabilities of radiative transitions between nuclear states. In the region of practical interest, the region of relatively low photon energies, the transition multipoles are the off-diagonal elements of the same operator of which the static multipoles are the diagonal elements.

We have here adopted the simplest assumptions on charge and current densities and have used these in discussions of the one-particle shell model, the many-particle shell model, and the collective model. There is a region of low A ($A \lesssim 20$), where the intermediate coupling shell model appears successful. In the rare earth region ($A \sim 170$) the collective model appears successful. In the great intermediate region there seems as yet to be no definitive model for the low-lying levels. Finally, we discuss the evidence on the forms and magnitudes of exchange currents.

Since the experimental material on γ-ray transition probabilities was recently reviewed (1) and has not changed essentially in the intervening period, we emphasize the theoretical basis in this review, going back over the developments of the last few years.[3] We shall, however, confine ourselves

[1] The survey of literature pertaining to this review was concluded in April, 1955.

[2] Under the auspices of the United States Atomic Energy Commission.

[3] For a review of earlier work see E. Segrè and A. C. Helmholz, *Rev. Modern Phys.*, 21, 27 (1949).

only to those topics that shed light on the basic nuclear electromagnetic interactions, in order to delimit our subject from nuclear structure as a whole.

The Multipole Expansion

The interaction of the nucleus with the electromagnetic field is described in terms of a charge and current density. The part of the Hamiltonian, H_{rad}, that contains the interaction corresponding to the absorption or emission of one photon is

$$H_{\text{rad}} = -\frac{1}{c}\int \boldsymbol{J}\cdot\boldsymbol{A}d\tau. \qquad 1.$$

Here $\boldsymbol{J}$ is the current density and $\boldsymbol{A}$ is the vector potential of the radiation field. In this section we shall develop expressions for the matrix elements of H_{rad}, which are convenient for nuclear physics. These expressions are based on the properties of the radiation field and are independent of the nuclear model assumed. One property of the current that will be used is the continuity equation for the current density:

$$\nabla\cdot\boldsymbol{J} + \partial\rho/\partial t = \nabla\cdot\boldsymbol{J} + \frac{i}{\hbar}[H,\rho] = 0. \qquad 2.$$

A familiar form for quantization of the electromagnetic field is that in terms of plane waves (2). The matrix element for the emission of a photon of energy $E=\hbar c\, k$, direction $\boldsymbol{k}$ and definite circular polarization is

$$\left(f\left|\,(2\pi c\hbar/k)^{1/2}(-1/c)\int \boldsymbol{J}\cdot\boldsymbol{e}_\lambda e^{i\mathbf{k}\cdot\mathbf{r}}d\tau\,\right|i\right); \qquad 3.$$

here $\lambda=\pm 1$, $\boldsymbol{e}_1$ and $\boldsymbol{e}_{-1}$ are the circular polarization vectors, and i,f refer to the initial and final states. This plane wave expansion, while very convenient for problems involving essentially plane-wave particle states, is not so suitable for the calculation of transition probabilities between nuclear states of well-defined angular momentum and parity. It is far more convenient to expand the electromagnetic radiation field in eigenfunctions of the angular momentum and party operators (3):

$$\boldsymbol{e}_\lambda e^{i\mathbf{k}\cdot\mathbf{r}} = \pi\sum_{L=1}^{\infty}\sum_{M=-L}^{L} i^L(2L+1)^{1/2}D_{M,\lambda}{}^{L}(R)\left\{\boldsymbol{A}_e(L,M) + (-\lambda)\boldsymbol{A}_m(L,M)\right\}. \qquad 4.$$

The $D_{M,\lambda}{}^{L}(R)$ are the elements of the transformation corresponding to the rotation, R, that carries $\boldsymbol{k}$, $\boldsymbol{e}_\lambda$ into the co-ordinate axes; $D_{M,\lambda}{}^{L}$ completely de-describes the transformation properties of a tensor of rank L and of an eigenfunction of total angular momentum $L\hbar$. The $\boldsymbol{A}_e(L,M)$, $\boldsymbol{A}_m(L,M)$ can be written in the operator form

$$\boldsymbol{A}_e(L,M) = \left(\frac{2}{\pi}\right)^{1/2}\frac{1}{[L(L+1)]^{1/2}}\frac{1}{k}(\nabla\times\boldsymbol{L})j_L(kr)Y_L{}^{M}(\theta,\phi), \qquad 5.$$

$$\boldsymbol{A}_m(L,M) = \left(\frac{2}{\pi}\right)^{1/2}\frac{1}{[L(L+1)]^{1/2}}\boldsymbol{L}j_L(kr)Y_L{}^{M}(\theta,\phi), \qquad 6.$$

where $\boldsymbol{L} = -i\boldsymbol{r}\times\boldsymbol{\nabla}$. This is just an expansion in terms of the usual multipole fields (3, 4); $\boldsymbol{A}_e(L, M)$ is the vector potential of the electric L-multipole field, $\boldsymbol{A}_m(L, M)$ of the magnetic L-multipole field. $\boldsymbol{A}(L, M)$ corresponds to a total angular momentum of $L\hbar$ and a z-component of $M\hbar$. Under the parity transformation (reflection), the $\boldsymbol{A}_e(L, M)$, $\boldsymbol{A}_m(L, M)$ transform differently:

$$\begin{aligned}\boldsymbol{A}_e(L, M) &\to (-1)^{L+1}\boldsymbol{A}_e(L, M)\\ \boldsymbol{A}_m(L, M) &\to (-1)^{L}\boldsymbol{A}_m(L, M).\end{aligned} \qquad 7.$$

The total transition probability, T, is formed by summing over all possible photon directions and polarizations:

$$T = 4\pi^2\frac{e^2}{\hbar c}ck\sum_{\sigma=e,m}\sum_{L=1}^{\infty}\sum_{M=-L}^{L}\left|\left(f\left|\frac{1}{ec}\int \boldsymbol{J}\cdot\boldsymbol{A}_\sigma(L, M)\mathrm{d}\tau\right|i\right)\right|^2. \qquad 8.$$

Suppose we are concerned with a transition between the states i and f of characters (spin, parity) (J_i, π_i) and (J_f, π_f) respectively; defining a quantity p, which is 0 for even parity and $+1$ for odd parity, we see that the multipoles that can contribute are delimited by

$$J_i + J_f \geqq L \geqq |J_i - J_f|,$$

and by the further conditions:

$$\begin{aligned}p_i + p_f + L &= \text{odd for magnetic multipoles}\\ p_i + p_f + L &= \text{even for electric multipoles.}\end{aligned}$$

The parity rules are easily derived from the form of the operator entering in the matrix element (equation 3) if we use the parity transformation properties of the $\mathbf{A}(L, M)$ (equation 7) and remember that the current $\mathbf{J}$ changes sign under a parity transformation.

Designate the electric multipoles by $E1$, $E2$, etc., and the magnetic multipoles by $M1$, $M2$, etc.; Table I shows all the hitherto observed multipole

TABLE I

OBSERVED MULTIPOLE TRANSITIONS

Multipole L		1	2	3	4	5
Parity change	Yes	$E1$ ——	$M2$	$E3$	$M4$	$E5$
	No	$M1$ ——	$E2$	$M3$	$E4$	

transitions. In practice, however, only a few multipoles need to be considered in any particular case. To see this, we note the order of magnitude of the combination $(kr)^2$ that appears throughout:

$$(kr)^2 \sim (2\pi R/\lambda)^2 \sim \frac{A^{2/3}E^2(\text{Mev})}{2\times 10^4},$$

and this is $\ll 1$ for transitions between the low lying states, $E<1$ Mev. Since the quantity that enters in the vector potential of the L-multipole is:

$$j_L(kr) \cong \frac{(kr)^L}{(2L+1)!!}, \qquad 9.$$

we see that the lowest possible multipole transition is greatly favored for $kr \ll 1$. The range of energies for which $(kr) \ll 1$ is frequently called the "long wave-length" region. In fact, usually only the lowest possible multipole contributes, but sometimes also the next order will appear. It is this fact that makes the measurement of multipole order so useful a tool in the assignment of characters to levels. The most important examples of mixed multipoles are found for $M1+E2$ and $E1+M2$ transitions; these are indicated in the above table by connecting lines.

In the following sections we shall give the results of the application of various models in calculations of the basic quantity:

$$\left(f\left|\frac{1}{ec}\int J\cdot A_\sigma(L,M)\mathrm{d}\tau\right|i\right), \qquad \sigma = e, m. \qquad 10.$$

It is worth remarking here that the rather cumbersome forms for these quantities are simplified in the long wavelength approximation. Thus:

$$\frac{1}{ec}\int J\cdot A_e(L,M)\mathrm{d}\tau = -\left(\frac{2}{\pi}\right)^{1/2}\left(\frac{L+1}{L}\right)^{1/2}\frac{k^L}{(2L+1)!!}\frac{1}{e}\int \rho r^L Y_L^M(\theta,\phi)\mathrm{d}\tau + \text{higher order terms}, \qquad 11.$$

where we have used the current continuity equation. The fact that the electric multipole matrix elements depend only on ρ, the charge density, has been derived in other but equivalent ways (5). The magnetic part of the interaction Hamiltonian is:

$$\frac{1}{ec}\int J\cdot A_m(L,M)\mathrm{d}\tau = \left(\frac{2}{\pi}\right)^{1/2}\frac{i}{[L(L+1)]^{1/2}}\frac{1}{ec}\int [\nabla j_L(kr)Y_L^M(\theta,\phi)]\cdot(r\times J)\mathrm{d}\tau. \qquad 12.$$

The $M1$ transitions ($L=1$) are especially interesting; in the long wavelength approximation the matrix element corresponding to (equation 12) becomes proportional to

$$\left(f\left|e^{(M)}\cdot\int (r\times J)\mathrm{d}\tau\right|i\right).$$

The connection between this transition matrix element and the static magnetic dipole moment is readily seen from the expression for the latter:

$$\mu = \left(J, M=J\left|\frac{1}{2c}e^{(0)}\cdot\int (r\times J)\mathrm{d}\tau\right|J, M=J\right).$$

Thus, the magnetic dipole moment is proportional to the diagonal element of the same operator that gives in its off-diagonal terms magnetic dipole transi-

tions. The electric quadrupole moment and the electric quadrupole transition matrix element are similarly related.

We summarize the results for the transition probabilities for electric and magnetic L-multipoles, in the long wavelength limit:

$$T_e(L) = 8\pi c \frac{e^2}{\hbar c} \frac{L+1}{L[(2L+1)!!]^2} k^{2L+1} B_e(L) \qquad 13.$$

$$T_m(L) = 8\pi c \frac{e^2}{\hbar c} \frac{L+1}{L[(2L+1)!!]^2} k^{2L+1} B_m(L), \qquad 14.$$

where

$$B_e(L) = \sum_M \sum_{Mf} \left| \left(J_f, M_f \left| \frac{1}{e} \int \rho r^L Y_L^M(\theta, \phi) d\tau \right| J_i, M_i \right| \right)^2$$

$$B_m(L) = \sum_M \sum_{Mf} \left| \left(J_f, M_f \left| \frac{1}{L+1} \frac{1}{ec} \int [\nabla r^L Y_L^M(\theta, \phi)] \cdot r \times J d\tau \right| J_i, M_i \right) \right|^2.$$

In later sections we shall evaluate these expressions for various models.

Zero Angular Momentum Transitions

It is well known that since the radiation field is purely transverse there can be no one photon transitions in which zero angular momentum is carried off. Transitions between two $J=0$ states of the same parity occur by internal conversion or internal pair formation (6, 7, 8);[4] formally, these can be thought of as one-photon longitudinal transitions, which are given the name "$E0$ transitions."

By a suitable choice of gauge for the $L=0$ multipole, the $E0$ transition can be written in terms of the matrix element of the instantaneous Coulomb interaction between the nuclear protons and the electrons. The nuclear part of this matrix element—in lowest approximation—is proportional to:

$$\int \psi_f^* \sum_p r_p^2 Y_0^0(\theta_p, \phi_p) \psi_i d\tau,$$

$\sum_p$ signifying a sum over all the protons. The electron part has been calculated to date only in the point-nucleus approximation for the wave function.

It has been pointed out by Church (9) that there is an $E0$ contribution in the heavy elements of possibly considerable magnitude for all ($\Delta J=0$, *No*) transitions. However, since a nuclear matrix element different from that in either the $M1$ or $E2$ parts of the transition probability appears in the $E0$ part, no a priori predictions of the relative importance can be made. For orientation purposes one can compute the $E0$ transition probability by using Thomas' formula (6), which involves the point nucleus approximation for the electron wave functions, and estimating the nuclear matrix element by:

$$\int \psi_f^* \sum_p r_p^2 Y_0^0(\theta_p, \phi_p) \psi_i d\tau \sim R_0^2/(4\pi)^{1/2}, \qquad 15.$$

[4] Nonrelativistic calculations are given by Blatt & Weisskopf, and by Sachs (8).

where R_0 is the nuclear radius. From a study of 0-0 transitions (7) it appears that, empirically, $E0$ transitions may be about a factor of 10 slower than this estimate; even with such a slow-down factor the $E0$ may be important in some ($\Delta J=0$, *No*) transitions in the high Z region.

Calculations on Various Models

A reasonable first choice for a charge and current density is that based on ascribing to each nucleon the convection and spin current density it would have if it were a point particle independent of the other nucleons,

$$J=\sum_\alpha e_\alpha \mathfrak{p}_\alpha/m_\alpha \delta(r-r_\alpha)-\sum \nabla\times \mu_\alpha \mathfrak{s}_\alpha \delta(r-r_\alpha), \tag{16.}$$

and a charge density localized on the point, nucleon,

$$\rho=\sum_\alpha e_\alpha \delta(r-r_\alpha),$$

where e_α is the charge, μ_α the magnetic moment, m_α the mass of the αth nucleon. On introducing the isotopic spin notation these can be written in the useful form:

$$\begin{aligned} J=&\frac{e}{2}\sum \mathfrak{p}_\alpha/m_\alpha\delta(r-r_\alpha)-\tfrac{1}{2}(\mu_N+\mu_p)\sum \nabla\times \mathfrak{s}_\alpha\delta(r-r_\alpha)\\ &-e_\alpha\sum_\alpha \tau_\alpha{}^0\mathfrak{p}_\alpha/m_\alpha\delta(r-r_\alpha)-(\mu_N-\mu_p)\sum_\alpha \nabla\times \sigma_\alpha\tau_\alpha{}^0\delta(r-r_\alpha), \end{aligned} \tag{18.}$$

where $\tau_\alpha{}^0=+\frac{1}{2}$ for a neutron, $-\frac{1}{2}$ for a proton. Similarly

$$\rho=\frac{e}{2}\sum_\alpha \delta(r-r_\alpha)-e\sum_\alpha \tau_\alpha{}^0\delta(r-r_\alpha). \tag{19.}$$

Isotopic spin selection rules.—For the low Z nuclei it has long been thought that isotopic spin, T, is a good quantum number, and that charge independence of nuclear forces applies. From the fact that J and ρ are the sum of isotopic spin scalar and vector parts it follows directly that only $\Delta T=0,\ \pm1$ is allowed for any multipole transition (10). However, for electric dipole transitions still more restrictive rules apply. In the long wavelength region the relevant quantity is:

$$B_e(1)=\frac{3}{4\pi}\sum_M\sum_{M_f}\left|\int \psi_f{}^*(J_f,M_f)\sum_\alpha(\tfrac{1}{2}r_\alpha-\tau_\alpha{}^0r_\alpha)\cdot e^{(M)}\psi_i(J_i,M_i)d\tau\right|^2, \tag{20.}$$

where $e^{(M)}$ are the usual co-ordinate vectors. The first term, the scalar part, is, for a system of particles of equal mass, just proportional to the coordinate of the center-of-mass; so $\sum_\alpha r_\alpha=0$ and

$$B_e(1)=\frac{3}{4\pi}\sum_M\sum_{M_f}\left|\int \psi_f{}^*(J_f,M_f)\sum_\alpha \tau_\alpha{}^0r_\alpha\cdot e^{(M)}\psi_i(J_i,M_i)d\tau\right|^2. \tag{21.}$$

There remain, then, for electric dipole transitions the additional stronger, vector selection rules (10, 11, 12) ($T=0\rightarrow T=0$) forbidden, and $\Delta T=0$ forbidden for $T_z=0$ (self-conjugate nuclei).

There is a very similar consequence from the less-restrictive charge symmetry hypothesis (11, 13). This is based on an equality between neutron-neutron and proton-proton forces, without specifying the relation between these and neutron-proton forces. Then, since in a self-conjugate nucleus, the Hamiltonian is invariant to interchange of neutrons and protons, charge-parity is a good quantum number. That is, the wave-functions are odd or even with respect to an interchange of neutrons and protons. Since the operator in $B_e(1)$ as written in equation 21 is odd in the interchange there is the selection rule: (even→even), (odd→odd) forbidden. This is included in the results of the charge-independence hypothesis under the selection rule: $\Delta T=0$ is forbidden for $T_z=0$.

Wilkinson and collaborators (14) have shown experimentally that in several light nuclei for which $T_z=0$ the $\Delta T=0$ transitions are, in fact, markedly impeded, while in nuclei for which $T_z\neq 0$ the $\Delta T=0$ transitions go at normal speed.[5] These, then, only test the weaker charge symmetry hypothesis. It would be most interesting to test experimentally whether the stronger hypothesis (charge independence) can also be verified for electromagnetic transitions, although it seems difficult to devise reliable tests of the selection rule that $\Delta T=2$ is forbidden.

While the above-mentioned $E1$ transitions are impeded, they are not completely stopped. Theoretically, there are small contributions to the matrix elements from a number of sources: the slight difference between the neutron and proton mass, the terms neglected in the long wavelength approximation, and, most important, the Coulomb forces that mix different isotopic spin states. The observed intensities of the "T forbidden" electric dipole transitions appear to be compatible with what is expected from these contributions (15, 16). It should also be remarked here that the charge density, ρ, can be altered by the addition of exchange contributions without altering the "T selection rules," provided these additions have the same transformation properties as the Z-component of an isotopic spin vector (17).

The one-particle shell model.—The Mayer-Jensen (18) shell model has achieved great successes in affording an understanding of the spins and parities of the low-lying levels. Its quantitative results for magnetic moments, quadrupole moments, and β and γ transition probabilities have been less uniformly successful. However, its order of magnitude predictions have been useful; the failures of these have pointed to the drastic revision made by the collective model which we discuss later.

The shell model of the nucleus is based on the postulate that as a first approximation the last few nucleons see the remaining nucleons only as an average, central potential of a shape intermediate between a square-well and a harmonic oscillator. A large spin-orbit interaction is postulated to split up the one-particle levels according to their spin-directions, lowering the $j=l+\frac{1}{2}$ states and raising the $j=l-\frac{1}{2}$ states. The states are, then, roughly as shown in Table 2.

[5] See also reference (12) for a comparison with experiments.

TABLE II

NUCLEAR SHELL CONFIGURATIONS ON THE MAYER-JENSEN SCHEME

Shell	I	II	III	III′	IV
Configurations	$1s_{1/2}$	$1p_{3/2}1p_{1/2}$	$1d_{5/2}1d_{3/2}2s_{1/2}$	$1f_{7/2}$	$1f_{5/2}2p_{3/2}2p_{1/2}1g_{9/2}$
Total Occupation Number	2	4	20	28	50

Shell	V	VI
Configurations	$1g_{7/2}2d_{5/2}2d_{3/2}3s_{1/2}1h_{11/2}$	$1h_{9/2}2f_{7/2}2f_{5/2}3p_{3/2}3p_{1/2}i_{13/2}$
Total Occupation Number	82	126

In this section we shall discuss the case of a nucleus with one particle outside a closed shell. The wave-function of this state is

$$\psi(n, l; J, M) = R_{n,l}(r)\Phi(J, M) \qquad 22.$$

$\Phi(J, M)$ is the spin and angular part. $R_{n,l}(r)$ is the radial part corresponding to the orbital angular momentum, l, and is further specified by the additional quantum number, n; $(n-1)$ is defined as the number of eigenstates corresponding to the same l that have appeared at lower energies; alternatively, $(n-1)$ is the number of nodes other than at the origin or at infinity. $R_{n,l}(r)$ alone depends on the shape of the central potential.

Consideration of electric multipole transitions (19 to 22) require the evaluation of

$$B_e(L) = \sum_M \sum_{M_f} \left| \int \psi_f^*(J_f, M_f) \sum_\alpha \epsilon_\alpha r_\alpha^L Y_L^M(\theta_\alpha, \phi_\alpha)\psi_i(J_i, M_i)d\tau \right|^2, \qquad 23.$$

where $\epsilon = 1$ for a proton, 0 for a neutron. There still remains, however, the constraint of the constancy of the center-of-mass. Actually this constraint condition makes the calculations intractable and for this reason has not been properly resolved. However, an approximation frequently used is based on considering a simple two-body problem, the outer nucleon and the core. Then,

$$B_e(L) = \sum_M \sum_{M_f} \epsilon_L^2 \left| \int R_{n_f,l_f}^*(r)\Phi^*(J_f, M_f) r^L Y_L^M(\theta, \phi) R_{n_i,l_i}(r)\Phi(J_i, M_i)d\tau \right|^2, \qquad 24.$$

where ϵ_L is an effective charge given by

$$\epsilon_L^2 = \left| \epsilon \left(\frac{A-1}{A}\right)^L + (-1)^L \frac{Z-\epsilon}{A^L} \right|^2. \qquad 25.$$

In view of the uncertainties of the calculation, ϵ_L is usually approximated as

$$L = 1 \qquad \epsilon_L = \pm \tfrac{1}{2}$$
$$L \geqq 2 \qquad \epsilon_L = 1 \text{ if } \epsilon = 1 \text{ (proton)},$$
$$\epsilon_L \sim 0 \text{ if } \epsilon = 0 \text{ (neutron)}.$$

While this recoil mechanism allows a small effective charge for neutrons in electric multipole transitions, this provides only a very weak radiation mechanism for $L \geqq 2$.

The simplest and most elegant way of evaluating equation 24 makes use of the Racah methods (21, 22), since we have here to do with the evaluation of the matrix elements of irreducible tensor operators in a representation in which the angular momentum is diagonalized. As these have been extensively applied, we repeat only the results:

$$B_e(L) = \epsilon_L^2 \frac{R_0^{2L}}{4\pi} \left| \int R_{n_f, l_f}^* \frac{r^L}{R_0^L} R_{n_i, l_i} r^2 dr \right|^2 S_e(J_i, J_f, L), \tag{26.}$$

where S_e, called the statistical factor, is given by

$$S_e(J_i, J_f, L) = [Z^0(l_i, J_i, l_f, J_f; \tfrac{1}{2}L)]^2/(2J_i + 1), \tag{27.}$$

and where R_0 is some conventional radius. Since the Z^0 functions have been rather completely tabulated (23), the angular integrals are easily available. The several selection rules are those given by angular momentum and parity conservation. The radial part,

$$R(n_i, l_i; n_f, l_f) = \left| \int R_{n,l_f}^* \frac{r^L}{R_0^L} R_{n_i, l_i} r^2 dr \right|^2, \tag{28.}$$

depends on the details of the potential. It will be written in abbreviated form as $R(L)$, the specific dependence on the initial and final state being understood.

In summary

$$T_e(L) = 2c \frac{e^2}{\hbar c} \frac{L+1}{L[(2L+1)!!]^2} k^{2L+1} \epsilon_L^2 R_0^{2L} S_e(J_i, J_f, L) R(L). \tag{29.}$$

The calculation of the magnetic multipole matrix elements (19 to 22) is more complicated and requires amplification of the Racah techniques. The results [as taken directly from Kennedy & Sharp (22)] are

$$B_m(L) = \frac{M_\mu^2}{4\pi} \left(\frac{\hbar}{mc}\right)^2 R_0^{2L-2} \left| \int R_{n_f, l_f}^* \frac{r^{L-1}}{R_0^{L-1}} R_{n_i, l_i} r^2 dr \right|^2 S_m \tag{30.}$$
$$S_m = [Z^0(l_i \pm 1, J_i, l_f, J_f; \tfrac{1}{2}, L)]^2/(2J_i + 1),$$

where the signs in the Z^0 coefficients are determined by

$$(l_i + 1) \leftrightarrow J_i = l_i + \tfrac{1}{2}, \qquad (l_i - 1) \leftrightarrow J_i = l_i - \tfrac{1}{2}.$$

The M_μ is fairly complicated and is given in Table 3. However, the situation is especially simple for the case of a basic transition (defined by $|J_i - J_f| = L$):

$$M_\mu = \left(\mu_p L - \frac{L}{L+1}\right) \quad \text{proton}$$
$$= \mu_N L \quad \text{neutron;} \qquad 31.$$

there should, then, be an especially simple relation between proton and neutron transitions if the configurations involved are otherwise the same.

TABLE III

COEFFICIENT M_μ FOR MAGNETIC MUTIPOLE MATRIX ELEMENT*

	$j=l+\frac{1}{2}$		$j=l-\frac{1}{2}$	
	$j'=l'+\frac{1}{2}$	$j'=l'-\frac{1}{2}$	$j'=l'+\frac{1}{2}$	$j'=l'-\frac{1}{2}$
G	$j+j'-L$	$-(L+j'-j+1)$	$-(L+j-j'+1)$	$-(j+j'+L+2)$
F	$\frac{1}{2}(j+j'+L+1)$	$\frac{1}{2}(L+j-j')$	$\frac{1}{2}(L-j+j')$	$\frac{1}{2}(j+j'-L+1)$

* $M_\mu = F_\mu + FG(\epsilon/L+1)$
$\epsilon=1$ proton
$\epsilon=0$ neutron

Besides the selection rules that follow from angular momentum and parity conservation, there is the additional model dependent rule:

$$l_i = l_f + (L-1). \qquad 32.$$

So, magnetic transitions in which $\Delta l > (L-1)$ are forbidden. In the special case of an $M1$ transition the rules require $l_f = l_i$; the radial integral is, however,

$$\int R_{n_f,l} R_{n_i,l} r^2 dr,$$

which because of the orthogonality is zero unless $n_f = n_i$. Thus, in the one-particle shell model only spin-flip $M1$ transitions are allowed, e.g., $1p_{3/2} \rightarrow 1p_{1/2}$ but not $1d_{3/2} \rightarrow 1s_{1/2}$ or $2p_{3/2} \rightarrow 1p_{1/2}$, $1p_{3/2}$. Whether a selection rule is obeyed or not throws light on the nature of the wave functions and currents. It is interesting that there are many "$d_{3/2} \rightarrow s_{1/2}$" transitions which appear to be considerably slower than the theoretical value, but which are still quite sizeable (24). An explanation in terms of exchange current effects has been put forward (25, 26). Configuration mixing (27, 28) would also cause violation of the simple selection rules; the deviation of the magnetic moments from the Schmidt limits is just one piece of evidence in favor of such configuration mixing effects. The allowed spin-flip transitions are generally of a fairly high energy and so have lifetimes too short, as a rule, to be measured with present techniques. It should be remarked here, however, that these are not the only allowed $M1$ transitions; for an example of these consider the odd-odd nuclei. The coupling between the neutron and proton

configurations gives rise to splitting between the states of different J. Since there is no change in configuration, the $M1$ transitions between these states should be allowed, and since the energies of splitting may be low there is hope of measuring these lifetimes.

Center-of-mass effects in magnetic transitions are fairly small and of interest only for low A nuclei. We have therefore omitted them here [Kennedy & Sharp (22)]. In summary we write

$$T_m(L) = M_\mu^2 c \frac{e^2}{\hbar c} \frac{2(L+1)}{L[(2L+1)!!]^2} k^{2L+1} R_0^{2L-2} \left(\frac{\hbar}{mc}\right)^2 R(L-1) S_m. \qquad 33.$$

In Figures 1, 2, and 3 are plotted all the known data on multipole transitions. The ordinate corresponds to a reduced transition probability, the point being to remove the energy and radius dependence predicted by the relations for the transition probabilities, T_e and T_m. Also indicated are the theoretical values for these reduced probabilities as given by the relations equation 29 and equation 33, with the respective statistical factors, S_e and S_m, placed equal to 1, $M_\mu^2 = [\mu_p L - L/(L+1)]^2$, as for a basic proton transition, $R(L)$ approximated by $[3/(L+3)]^2$, and $R_0 = 1.2A^{1/3} \times 10^{-13}$. These are applicable because the more accurate values of the statistical factors and the fuller considerations of the many-particle shell model do not change the orders of magnitude. It is seen that there is a definite separation between the different multipole orders, as predicted by the theory. However, the wide fluctuations in values indicate that the nuclear wave-functions may be very different from the one-particle cases, so that each should be considered more closely.

It would be well to point out here some of the limitations imposed on obtaining information on electromagnetic transition probabilities. First of all, the transition probability must be measurable by the available techniques: (*a*) Direct lifetime measurements are possible only if $\tau \gtrsim 10^{-9}$ sec. Thus for the lowest multipoles, $E1$ and $M1$, the measurable cases are as a rule restricted to transitions where the matrix element is very small. Among the $E2$, $M2$ multipoles most of the lower energy transitions can be reached by this technique; (*b*) Coulomb excitation measurements are possible on $E1$ and fast $E2$ transitions that connect with the ground state; (*c*) Resonance fluorescence of γ-rays are being used, especially by Metzger, to study fast ground state transitions, $\tau < 10^{-9}$ sec.

Secondly, the miltipole transitions available for measurement depend on the accidents of nuclear level order. In fact, the nature of the low-energy nuclear levels is such that only a few kinds of multipole transitions between pure states can appear. The existing data are most exhaustive for $E2$ transitions in even-even nuclei and $M4$ transitions in odd-even nuclei. It is important to note that just these data show a most regular behavior. While more exact models will have to fit quantitatively all the transitions in any given nucleus, we shall here confine our further considerations principally to the $M4$, $E2$ and "l-forbidden" $M1$ transitions which shed light on the general

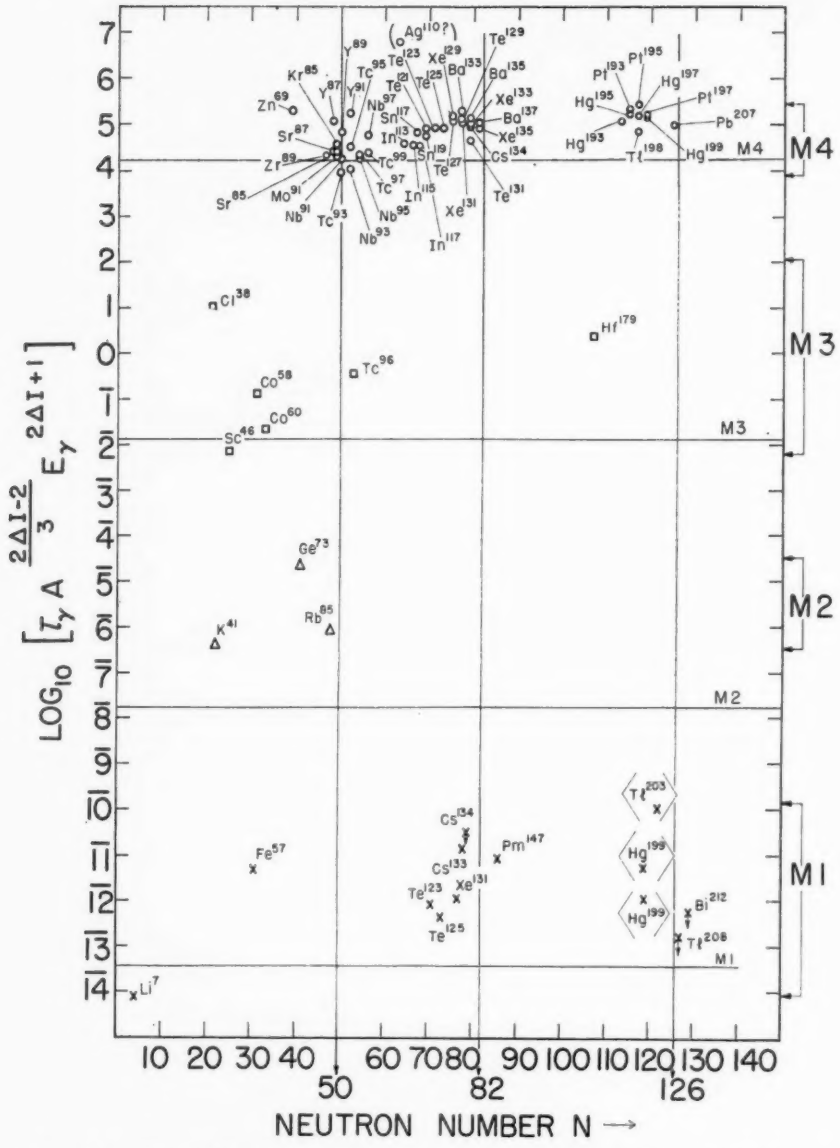

FIG. 1. Reduced lifetimes for $M1$, $M2$, $M3$, $M4$ transitions plotted against neutron number, N. The lines correspond to the theoretical values for single proton transitions, with the statistical factor, S_m, taken equal to unity, and the radius given by $R_0=1.2\times10^{-13}A^{1/3}$. [A modified version of a plot given by Goldhaber & Sunyar (1).]

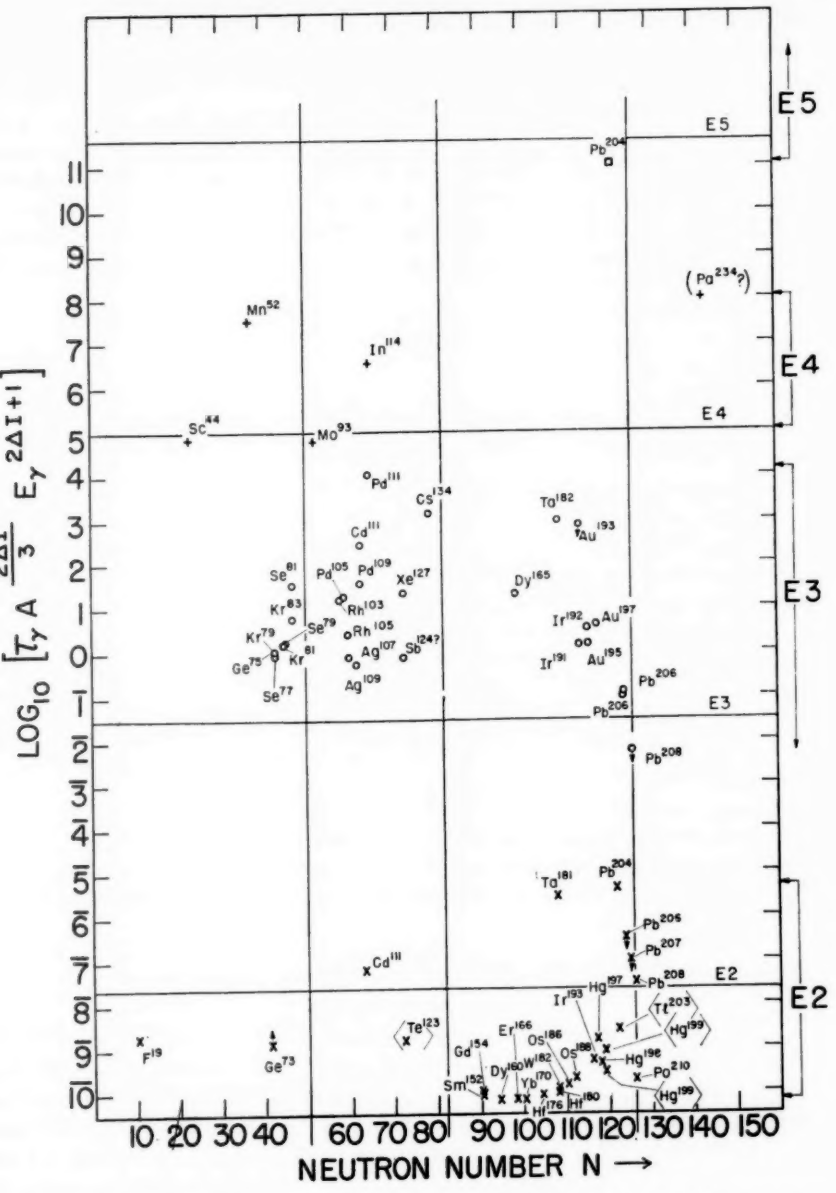

FIG. 2. Reduced lifetimes for $E2$, $E3$, $E4$, $E5$ transitions plotted against neutron number, N. The lines correspond to the theoretical values for single proton transitions, with the statistical factor, S_n, taken equal to unity and the radius given by $R_0=1.2\times10^{-13}A^{1/3}$. [A modified version of a plot given by Goldhaber & Sunyar (1).]

features of nuclear structure and currents. Before doing this, some many-particle shell model formulae are obtained.

Many-particle shell model.—Suppose now we have several particles in a sub-shell. Just what form of interaction exists between these particles is not known, since it is not clear what part has been already included in the shell model approximation. The configurations involved can be more definitely specified; since excitation to higher shells involves high energies, it is reasonable to assume that the low-lying states correspond to those configurations formed by occupation of the sub-shells of the last unfilled shell only. By

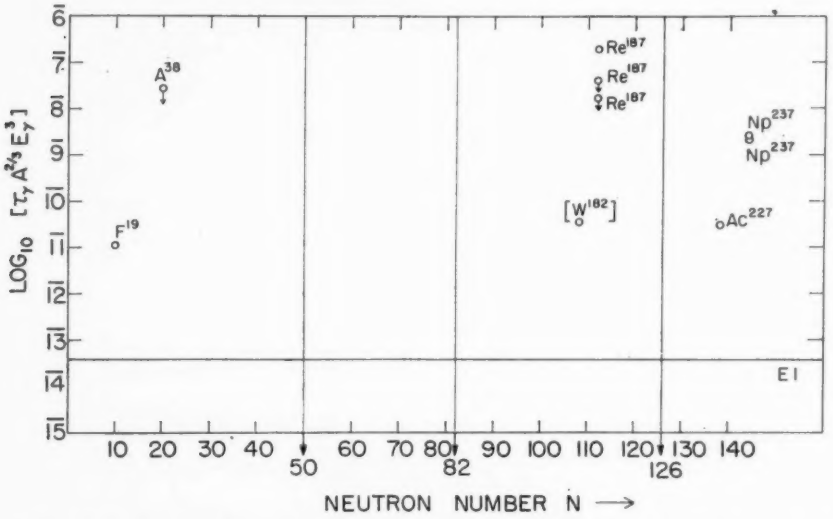

FIG. 3. Reduced lifetimes for $E1$ transitions. The line corresponds to the theoretical value for single proton transitions, with the statistical factor, S_ν, taken equal to unity, the radius given by $R_0=1.2\times10^{-13}A^{1/3}$. [A modified version of a plot given by Goldhaber & Sunyar (1).]

making simple assumptions about these points we present below some general results that can be expected from a shell model.

The shell model has been most adequately applied and tested in the region $A\lesssim20$, where a consistent scheme has been attained for the energy levels, magnetic moments, nuclear level widths, and electromagnetic and β-ray transition probabilities (29). This has been based on a central force acting between the outer nucleons, leading to an intermediate coupling situation. It should be especially noted that only the conventional currents, defined above, were introduced.

For the intermediate to heavy nuclei there has been as yet no such complete program[6] except for some recent work in the region around $A=40$ (31).

[6] See, however, the work of B. H. Flowers, A. R. Edmonds, and others, some of which are referred to in the reviews given in reference (18).

Furthermore, there are reasons to believe that such a shell model is not completely applicable in this region. First, at $A \sim 170$ there is now very good evidence to support the belief that any spherical shell model, such as we have been discussing, is not applicable to the low-lying states. The Bohr-Mottelson-Rainwater theory, to which we shall return below, introduces an additional parameter; it is based on a core highly deformed to the energetically more favored ellipsoidal shape. This non-spherical potential together with the dynamical properties of the core so completely determines the nature of the low lying levels that a simple shell model is no longer applicable in this region. Second, there is fairly convincing evidence (32) that the dynamical properties of the core deformability either determine or greatly affect the properties of the low-lying nuclear states in the whole region of $60 < A < 150$. We shall present the shell model results only for the sake of the qualitative ideas rather than in the hope of a precise comparison with experiment.

Since the charge and current densities are one-particle operators, there exists the general selection rule that many-particle transitions are forbidden. However, such a rule depends greatly on the purity of the wave-functions, and the rule is relieved by admixing the proper impurities. This is particularly relevant to the case of $E0$ transitions, since low-lying states of the same character usually differ in the coupling or configuration of at least two particles. It is, then, expected that $E0$ transition probabilities should depend on the relatively small wave-function impurities and thus should be appreciably smaller than those based on the estimate of equation 15; the few known 0-0 transitions are not completely consonant with such an interpretation (7) and indicate that further work is required here.

For the purposes of a comparison of the data with shell model calculations, we shall assume that only like particles in the same j sub-shell interact strongly. We shall further classify these according to seniority number, s (33, 34). While the seniority number is not expected to be a perfect quantum number, for short range forces it may be quite good (34); for $j \leqq 7/2$ it is, in fact, a perfect quantum number.

Consider the transition $i \to f$ in an odd-even nucleus;

$$J_i = j_1 \quad (j_1^{n_1+1}, J_1 = j_1, s_1 = 1)(j_2^{n_2}, J_2 = 0, s_2 = 0)(\cdots)(j_N^{n_N} J_N = 0\ s_N = 0)$$
$$J_f = j_2 \quad (j_1^{n_1}, J_1 = 0, s_1 = 0)(j_2^{n_2+1} J_2 = j_2, s_2 = 1)(\cdots)(j_N^{n_N} J_N = 0\ s_N = 0),$$

where the occupation numbers $n_1, n_2, \cdots, n_N$ are even. As an example of such a transition consider the possible $M4$ transition $(h_{11/2})^2(d_{3/2})^2 \to (h_{11/2})^2 (d_{3/2})^2$. The result (20) is given by multiplying the one-particle transition probability for $j_1 \to j_2$ by the factor S, where

$$S = \frac{2j_1 + 1 - n_1}{2j_1 + 1} \frac{2j_2 + 1 - n_2}{2j_2 + 1}. \qquad 34.$$

Alternatively, we can consider the somewhat different transition

$$J_i = j_1 \quad (j_1^{n_1-1} J_1 = j_1, s_1 = 1)(j_2^{n_2}, J_2 = 0, s_2 = 0)(\cdots)(j_N^{n_N} J_N = 0\ s_N = 0)$$
$$J_f = j_2 \quad (j_1^{n_1} J_1 = 0, s_1 = 0)(j_2^{n_2-1}, J_2 = j_2, s_2 = 1)(\cdots)(j_N^{n_N} J_N = 0\ s_N = 0).$$

This result (20) is given by multiplying the one particle transition probability for $j_1 \to j_2$ by S', where

$$S' = \frac{n_1}{2j_1+1}\,\frac{n_2}{2j_2+1}\,. \qquad 35.$$

This can be exemplified by the $M4$ transition $(h_{11/2})^1(d_{3/2})^4 \to (h_{11/2})^2(d_{3/2})^3$. Both these results show that the many-particle transition probability is slower than the one-particle transition probability. Moreover, they indicate a regular dependence on shell position. However, while the first possibility indicates a decrease, the second indicates an increase as the shell edge is approached.

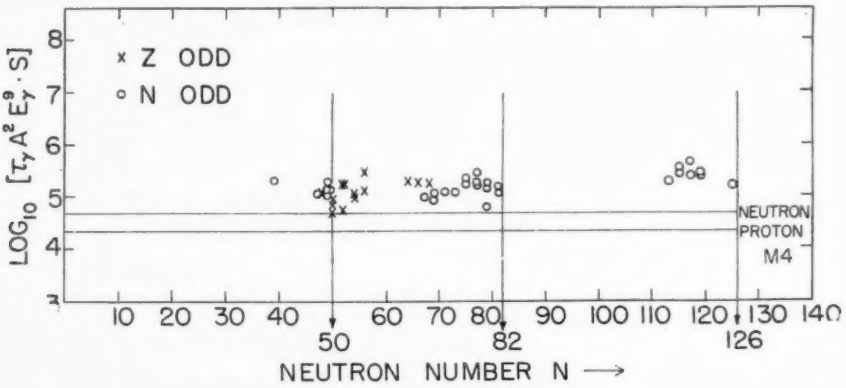

FIG. 4. Reduced lifetimes for $M4$ transitions plotted against neutron number, N. The relevant statistical factor, S_m, has been applied. The lines correspond to the theoretical values for single neutron and proton transitions; the radius is given by $R_0 = 1.2 \times 10^{-13} A^{1/3}$. [A modified version of a plot given by Goldhaber & Sunyar (1).]

Relations such as these can only be tested if data for sufficiently long sequences of nuclei are known. The only information of this type known to us occurs for the $M4$ transitions ($g_{9/2} \leftrightarrow p_{1/2}$; $h_{11/2} \leftrightarrow d_{3/2}$; $i_{13/2} \leftrightarrow f_{5/2}$). The data are characterized by a remarkably great uniformity of the reduced transition probability, there being at most deviations from the mean by a factor of 2 either way. This is a rather noteworthy result if it is recalled that the lifetimes vary over tremendously greater factors. The reduced transition probabilities have been replotted in Figure 4, using the one-particle statistical factors. The theoretical reduced transition probabilities would be just those given by the indicated lines for protons and neutrons. Actually, the data lie at lifetimes about a factor of 3 to 5 greater. The proton points seem to lie among the neutron points, instead of showing the theoretical difference of almost a factor 2. Further, there is no evidence that either of the simple dependences on shell position, (equation 34) or (equation 35), is obeyed. So,

while the order of magnitude of the transition probabilities is demonstrated to agree with the simple theory, more refined theories seem necessary to obtain detailed agreement.

The even-even nuclei are known to show great regularities (32, 35). The ground state invariably has the character $0+$, the first excited state almost without exception $2+$. The $E2$ transitions between these levels have been some of the most systematically studied. If we consider the first excited state to be the seniority 2, $J=2$ state of the configuration j^n, and the ground state the $s=0$, $J=0$ state of j^n, the transition probability is given by replacing the statistical factor, S_E, by S'', where

$$S'' = \frac{1}{4} \frac{(2j+3)(2n)(2j+1-n)}{(2j)(2j+2)} \qquad 36.$$

for $j=9/2$ the maximum $S''\sim 1.5$. A glance at the $E2$ data in the region $N \sim 100$ shows that $S\sim 100$ is required (36).[7] Therefore in this region the shell model does not suffice even for order of magnitude estimates for electric quadrupole transitions. It is noteworthy that these fast $E2$ transitions occur in a region of large static quadrupole moments (37). The failure of natural modifications of the shell model to describe such large coherent effects remains in contrast to the successes of the collective model of the nucleus.

However, before discussing this model, it should be remarked that the unmodified shell model does not even suffice for $E2$ transitions in the region $N \leqq 82$. There is recent evidence (36) that, in this region too, the $E2$ transitions between the first excited states and the ground states are faster than the shell model estimate by a factor of 10 to 20. This appears to imply that collective modes of motion play an important part.

The collective model.—To describe the cooperation of the large numbers of charges required to explain the large static and transition quadrupole moments in terms of a spherical shell model would require a great many partly filled shells, a most complicated form of description. The Bohr-Mottelson-Rainwater model gives up the sphericity of the potential and uses the shape of the core as a parameter.

Rainwater (38) found that it is energetically favorable for a nonclosed shell nucleus to take on a spheroidal shape. The static and dynamic effects of a deformed core have been the basis for the collective model of the nucleus of Bohr and Mottelson. Such a core shares angular momentum with the outer nucleons and contributes to the kinetic energy of the nucleus. In fact, for large core deformations it is expected that the low-lying levels correspond to just such motion. The identification of the bands of rotational levels has been a striking confirmation of the model. Further, the large core deformations contain intrinsically the collective effects needed to explain the electric quadrupole moments. Also, the sharing of the angular momentum be-

[7] We have not included on this plot the $E2$ transition probabilities measured by Coulomb excitation. See (36).

tween the particles and the core is in the right direction to explain the well-known deviations of the magnetic moments from the Schmidt limits. We cannot here go into the details of the development of the model. The principal work was carried out by A. Bohr and B. Mottelson and we must refer the reader to their extensive and thorough monograph (39) for a complete development of the theory. We have below used their results, limiting ourselves, however, to a very few topics.

The core properties appear in the moments of inertia and in the electrical moments. The total angular momentum, $\boldsymbol{I}$, is made up of core and particle angular momenta; calling the core angular momentum $\boldsymbol{R}$, the particle angular momentum $\mathbf{j}$, we have

$$\boldsymbol{I} = \boldsymbol{R} + \boldsymbol{j}. \tag{37.}$$

In the approximation of strong coupling between the core deformation and the particles, the components of $\boldsymbol{j}$ and $\boldsymbol{I}$ along the 3-axis, the symmetry axis of the core, are good quantum numbers; these are called Ω and K respectively. A state is, then, specified by the quantum numbers I, K, Ω and, of course, the usual Z-component of the total angular momentum, M. In terms of these quantum numbers the contribution to the energy from the rotational motion of the core is

$$E_{rot} = \frac{\hbar^2}{2\mathfrak{I}}[I(I+1) - K^2 + j(j+1) - \Omega^2] + \frac{\hbar^2}{4\mathfrak{I}_3^2}(K-\Omega)^2, \tag{38.}$$

where $\mathfrak{I}_1 = \mathfrak{I}_2 = \mathfrak{I}$, $\mathfrak{I}_3$ are the moments of inertia about the respective body axes. Since the details of the theory fix $\mathfrak{I}_3 \cong 0$, it is expected that the low-lying levels form a rotational band with $K = \Omega$, whose energies are given by

$$E_K(I) - E_K(K) = \frac{\hbar^2}{2\mathfrak{I}} I(I+1). \tag{39.}$$

In even-even nuclei the lowest rotational band is given by $K = 0$, $I = 0, 2, 4, \cdots$, the odd I not appearing because of symmetry considerations. In other nuclei the band is defined by $I = K, K+1, \cdots$. The identification of such a band structure allows the determination of the moment of inertia, $\mathfrak{I}$. The moment of inertia can be related to the deformation parameter only through a detailed theory; the Bohr hydrodynamical model leads to

$$\mathfrak{I} = \frac{9}{8\pi} AMR_0^2\beta^2, \tag{40.}$$

where A is the mass number, M the nucleon mass, R_0 the radius, and β the deformation parameter. The deformed surface is defined by R_0 and β through the equation for the distance from the center to the surface:

$$R = R_0[1 + \beta Y_2^0(\theta, \phi)]. \tag{41.}$$

The core possesses an intrinsic quadrupole moment, Q_0, that arises from the deformation. On the assumption of a uniform charge distribution

$$Q_0 = \frac{3}{\sqrt{5\pi}} ZR_0^2\beta. \qquad 42.$$

Since both the moment of intertia and the intrinsic quadrupole moment are simply related to the deformation, through β, it is interesting to test the relationship empirically; we shall come to this later. The intrinsic magnetic dipole of the core also follows from general considerations. It is reasonable to assume that the spins of the core particles are paired off to a zero resultant; the only currents present are, then, convection currents. If it is further assumed that the current is everywhere proportional to the matter velocity, the intrinsic magnetic dipole moment is directly proportional to the angular momentum, and is given in terms of a core g-factor,

$$\mu = g_R L. \qquad 43.$$

The uniform charge distribution leads to

$$g_R \cong Z/A \sim 0.4 \qquad 44.$$

These values of Q_0, μ, used by Bohr & Mottelson, are based on the uniformity of the charge distribution. The transition probabilities for $M1$ and $E2$ radiation can now be evaluated directly from equation 13 and equation 14 in terms of the intrinsic multipole moments.

Two types of electromagnetic transitions are possible: (*a*) core transitions in which the particles do not change their state, and (*b*) particle transitions. We shall discuss (*a*) first. The transition between the first excited state, $I=2+$, $K=\Omega=0$ and the ground state $I=0$, $K=\Omega=0$ of an even-even nucleus is given by

$$B_e(2) = \frac{1}{16\pi} Q_0^2 = \frac{9}{80\pi^2} Z^2 R_0^4 \beta^2, \qquad 45.$$

if we omit the small particle contributions. It is worth noting that the cooperative effect inherent in the model is reflected here by the presence of the factor Z^2. Similar results apply to transitions between other levels. For odd-even nuclei, transitions between levels of a rotational band $K=\Omega$, $I=K$, $K+1$, $\cdots$, are characterized by

$$I+1 \to I \qquad B_e(2) = \frac{15}{16\pi} Q_0^2 \frac{K^2(I+1-K)(I+1+K)}{I(I+1)(I+2)(2I+3)}, \qquad 46.$$

$$B_m(1) = \frac{3}{16\pi} \left(\frac{\hbar}{mc}\right)^2 (g_\Omega - g_R)^2 \frac{\Omega^2(I+1-K)(I+1+K)}{(I+1)(2I+3)}, \qquad 47.$$

$$I+2 \to I \qquad B_e(2) = \frac{15}{32\pi} Q_0^2 \frac{(I+1-K)(I+1+K)(I+2-K)(I+2+K)}{(I+1)(I+2)(2I+3)(2I+5)}, \qquad 51.$$

where g_Ω is the particle g-factor, g_R the core g-factor. The static magnetic dipole moment is given by : $\mu=(I/I+1)[Ig_\Omega+g_R]$.

The above relations have been applied to the data from the nuclei in the rare-earth region. The comparison is presented in Figure 5 in the form of a plot (40) of the deformation parameter as obtained from the moment of

inertia, $\mathfrak{I}$, through the energies and from Q_0 through the transition probabilities. It is seen that there is a discrepancy of a factor of about 5 in determinations of β^2 (40, 41). This is a definite failure of the details of the theory, but it still leaves the more general ideas applicable. A number of suggestions (40, 41) have been made to account for the discrepancy, but have not yet been worked out quantitatively.

Measurements of g_R, the core g-factor, are very relevant to a discussion of the discrepancy; if the discrepancy were attributable to a nonuniform charge distribution, it would affect g_R as it does Q_0. Since g_Ω, g_R appear in different combinations in the $M1$ transition probability and in the ground state magnetic moment, both g_Ω and g_R can be obtained if the two quantities

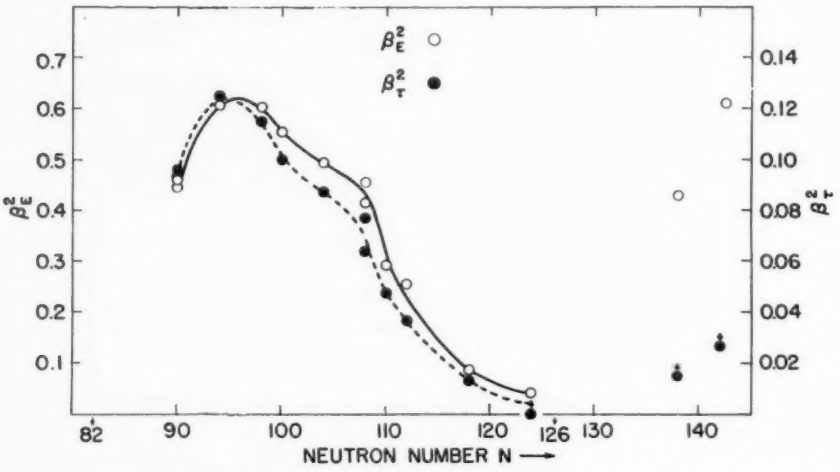

FIG. 5. A plot against neutron number, N, of the deformation parameters as obtained from the energies, β_E^2, and from the lifetimes, β_τ^2. Note that the scale for β_E^2 is five times that for β_τ^2. The β^2 are obtained from the empirical data, using the Bohr-Mottelson theory; the radius is given by $R_0=1.2\times10^{-13}A^{1/3}$. [Taken from Sunyar (40).]

are measured. This has been carried out for two nuclei; for $_{73}Ta^{181}$ $g_R\sim.25$ and for $_{63}Eu^{153}$ $g_R\sim.5$ (42).

Finally, a word about particle transitions. Because of the strong coupling to the core, only some substates of the particle states available in the shell model can contribute. Further, if the core differs in shape in the two different particle-configurations, the incomplete overlap will cut down the transition probabilities. Bohr & Mottelson suggest this as an explanation of the slow but regular $M4$ transitions; it must be remarked, however, that in the region in which the $M4$ data are best known, the nuclei do not show the simple rotational band structure displayed in the rare-earth region.

The collective model has, then, explained the important anomalously large static and transition electric quadrupole moments. The deformed

core and the strong coupling with the particles has further important implications for nuclear spectroscopy, that are being developed. While the details may not yet be completely correct, it is felt that the general ideas are valid.

The Nature of Modifications of the Charge and Current Densities

We have up to now accepted the simple choice of charge and current densities. In this section we discuss the evidence for modifications. That additional currents may exist is implied by the fact that the exchange of charged mesons is important for nuclear forces (43). The meson theory of nuclear forces implies a distribution of currents dependent on the coordinates of more than just one nucleon. However, since the meson theory has not yet reached the stage of development required for quantitative predictions and since heavy nuclei represent a highly complex problem, a more empirical approach has been taken.

The approach consists basically of writing down the most general form for the charge and current operators subject to the restrictions that the Hamiltonian obey the usual invariance conditions. These have been used to construct the most general magnetic dipole operator. While the procedure can be extended to the higher magnetic multipoles, there is not much point in doing so. For the dipole operator, the static magnetic moments in conjunction with some well understood $M1$ transition probabilities provide good tests which, however, allow but very tentative conclusions. A similar approach has been adopted in regard to modifications of the charge density and of the electric dipole operators (17). We shall here limit ourselves to a discussion of the magnetic dipole operator.

A complete knowledge of the interactions of nucleons only specifies in part the nature of the currents (44). The presence of an exchange potential requires a modification of the currents, leading to a contribution known variously as exchange moment, or longitudinal moment (45 to 49). Velocity-dependent forces also require additions to the currents (50, 51). A particular example (52) of a velocity-dependent one-nucleon force is the spin-orbit interaction so vital to the shell-model. But in addition to these currents directly correlated with the interactions, there are possible additional terms unrestricted except by invariance and the continuity equation. The possible forms of these magnetic dipole terms, further restricted to two-nucleon effects only and to velocity independence, have been written out by various authors (46, 47, 51, 53). We shall call these last interaction moments.

The dipole moment operators have then to be compared with the data: (*a*) the anomaly in the H^3, He^3 magnetic moments of about $\frac{1}{4}$ nuclear magneton; (*b*) the difference of a few per cent between the observed and calculated photomagnetic thermal neutron capture cross section in hydrogen; (*c*) the absence of any important anomaly in the magnetic moment of the deuteron. The evidence points to the existence and forms of small interaction moments (47, 51, 54).

At this point it is interesting to recall the $M1$ transitions, $d_{3/2} \leftrightarrow s_{1/2}$, we

discussed above, which are forbidden for the ordinary magnetic dipole operator in the absence of configuration mixing. It is especially interesting that Ross (25, 26) and Sachs (25) have found that these transitions can be understood in terms of the interaction magnetic dipole operators as fixed by the above data. It would be interesting to find cases where configuration mixing is less possible as in nuclei involving one nucleon or one hole outside a closed shell. It should also be noted that $\Delta l = 2$ transitions are allowed by the moment operator that arises from the velocity-dependent spin-orbit force, if the particle making the transition is a proton. For odd proton nuclei there may be interference effects between the interaction and spin-orbit moment operators, which have not yet been considered in detail.

We turn next to a less clear line of evidence, that is concerned with the static magnetic dipole moments of the heavier nuclei. The fairly regular deviations from the Schmidt limits have led to the suggestion (55) that the deviations be interpreted as a quenching of the intrinsic nucleon spin moment in nuclear matter. The quenching needed would be large, of the order of 1 nuclear magneton. Now, of the several possible forms for the interaction moments, not all have been fixed by the data given above. If the quenching effect is ascribed to these interaction moments (47, 56), large modifications of the simple currents would be present. However, the evidence for such large modifications rests on the rather shaky framework of the applicability of the Schmidt limits, since it is not yet clear how much of the deviation should be ascribed to the wave function. For example, application of the Bohr-Mottelson strong-coupling model produces sizeable deviations in the correct directions. Further, the work on the light elements discussed above described the static and transition magnetic dipole moments without the need of large interaction effects.

Deduction of additional terms from relativistic forms for the electromagnetic interactions have been considered (57), and small effects found.

We conclude, therefore, that there is evidence for small modifications of the currents, but not yet convincing evidence for large effects. It seems wise, therefore, to assume that the main features of nuclear electromagnetic phenomena involve only the ordinary currents.

LITERATURE CITED

1. Goldhaber, M., and Sunyar, A. W., *Beta and Gamma Ray Spectroscopy*, Chap. 16 (Siegbahn, K., Ed., Interscience Publishers, New York, N. Y., 959 pp., 1955)
2. Heitler, W., *The Quantum Theory of Radiation*, 3rd ed. (Oxford University Press, London, England, 430 pp., 1954)
3. Biedenharn, L. C., and Rose, M. E., *Revs. Mod. Phys.*, **25**, 729 (1954); (especially equations 54, 55, 105)
   Rose, M. E., *Multipole Fields* (John Wiley and Sons, Inc., New York, N. Y., 99 pp., 1955)
4. Hansen, W. W., *Phys. Rev.*, **47**, 139 (1955)
   Heitler, W., *Proc. Cambridge Phil. Soc.*, **37**, 112 (1936)
   Franz, W., *Z. Physik*, **127**, 363 (1950)
   Tralli, N., and Goertzel, G., *Phys. Rev.*, **83**, 399 (1951)

Blatt, J. M., and Weisskopf, V., *Theoretical Nuclear Physics* (John Wiley and Sons, Inc., New York, N. Y., 1952); (especially Appendix B).
Wallace, P. R., *Can. J. Phys.*, **29**, 393 (1951)
French, J. B., and Shimamoto, Y., *Phys. Rev.*, **91**, 898 (1953)
Bouwkamp, C. J., and Casimir, H. B. G., *Physica*, **20**, 539 (1954)
5. Sachs, R. G., and Austern, N., *Phys. Rev.*, **81**, 705 (1951)
6. Yukawa, H., and Sakata, S., *Proc. Phys. Math. Soc. Japan*, **17**, 397 (1935)
Thomas, R., *Phys. Rev.*, **58**, 714 (1940)
7. Drell, S. D., *Oak Ridge Natl. Lab. Rept., ORNL-792*, 1954
8. Blatt, J. M., and Weisskopf, V., *Theoretical Nuclear Physics* (John Wiley and Sons, Inc., New York, N. Y., 864 pp., 1952)
Sachs, R. G., *Nuclear Theory* (Addison-Wesley, Cambridge, Mass., 383 pp., 1953)
9. Church, E., (Personal communication); Church, E., and Weneser, J., *Phys. Rev.* (In press)
10. Radicati, L. A., *Phys. Rev.*, **87**, 521 (1952)
11. Trainor, L. E. H., *Phys. Rev.*, **85**, 962 (1952)
12. Gell-Mann, M., and Telegdi, V. L., *Phys. Rev.*, **91**, 169 (1953)
13. Kroll, N. M., and Foldy, L. L., *Phys. Rev.*, **88**, 1177 (1952)
14. Wilkinson, D. H., *Phil. Mag.*, **44**, 450 (1953)
Wilkinson, D. H., and Jones, G. A., *Phil. Mag.*, **44**, 542 (1953)
Wilkinson, D. H., *Phil. Mag.*, **44**, 1019 (1953)
Wilkinson, D. H., and Clegg, A. B., *Phil. Mag.*, **44**, 1269, 1322 (1953)
15. MacDonald, W. M., *University of California Radiation Lab. Rept., UCRL-2746* (1954)
16. MacDonald, W. M., *Phys. Rev.*, **98**, 60 (1955)
17. Foldy, L. L., *Phys. Rev.*, **92**, 178 (1953)
18. Mayer, M. G., and Jensen, J. H. D., *Elementary Theory of Nuclear Shell Structures* (John Wiley and Sons., Inc., New York, N. Y., 269 pp., 1955)
Feenberg, E., *Shell Theory of Nuclei* (Princeton University Press, Princeton, N. J., 211 pp., 1955)
Flowers, B. H., *Prog. Nuclear Phys.*, **5**, 2 (1952)
These review articles describe the earlier work· they are intended also as general references for the sections for the shell model.
19. Moszkowski, S. A., *Phys. Rev.*, **83**, 1071 (1951)
Weisskopf, V. F., *Phys. Rev.*, **83**, 1073 (1951)
Stech, B., *Z. Naturforsch.*, **7a**, 401 (1952)
20. Moszkowski, S. A., *Phys. Rev.*, **89**, 474 (1953)
21. Lane, A. M., and Radicati, L. A., *Proc. Phys. Soc.* (*London*), [A]**67**, 167 (1954)
Satchler, G. R., *Proc. Phys. Soc.* (*London*), [A]**67**, 1024 (1954)
22. Kennedy, J. M., and Sharp, W. T., *Statistical Factors for Electromagnetic Transitions, Chalk River Project, CRT-580* (1954). (This is a detailed and complete review of the calculations of the matrix elements.)
23. Sharp, W. T., Kennedy, J. M., Sears, B. J., and Hoyle, M. G., *Chalk River Project CRT-556* (1953)
Biedenharn, L. C., *Oak Ridge Natl. Lab. Report, ORNL 1501* (1953)
Simon, A., Vander Sluis, J. H., and Biedenharn, L. C. *Oak Ridge Natl. Lab. Report, ORNL-1679* (1953)
Biedenharn, L. C., Blatt, J., and Rose, M. E., *Rev. Mod. Phys.*, **24**, 249 (1952)
24. Goldhaber, M., and Sunyar, A. W., *Phys., Rev.* **83**, 906 (1951)
Graham, R. L., and Bell, R. E., *Can. J. Phys.*, **31**, 377 (1953)
25. Sachs, R. G., and Ross, M., *Phys. Rev.*, **84**, 379 (1951)

26. Ross, M., *Phys. Rev.*, **88,** 935 (1952)
27. de Shalit, A., and Goldhaber, M., *Phys. Rev.*, **92,** 1211 (1953)
28. Volkov, A. B., *Phys. Rev.*, **94,** 1664 (1954)
Feenberg, E., *Shell Theory of Nuclei*, 176 (Princeton University Press, Princeton, N. J., 211 pp., 1955)
29. Inglis, D. R., *Rev. Mod. Phys.*, **25,** 390 (1953)
Lane, A. M., *Proc. Phys. Soc.* (*London*), [A]**66,** 977 (1953)
Lane, A. M., and Radicati, L. A., *Proc. Phys. Soc.* (*London*), [A]**67,** 167 (1954)
Lane, A. M., *Proc. Phys. Soc.* (*London*), [A]**68,** 189, 197 (1955)
30. Flowers, B. H., *Progr. Nuclear Phys.*, **5,** 2 (1952); (See footnote 6)
31. Ford, K., and Levinson, C., *Phys. Rev.* (To be published)
32. Scharff-Goldhaber, G., and Weneser, J., *Phys. Rev.*, **98,** 212 (1955)
33. Racah, G., *Phys. Rev.*, **63,** 367 (1943)
Racah, G., *Phys. Rev.*, **76,** 1352 (1949)
Schwartz, C., and de Shalit, A., *Phys. Rev.*, **94,** 1257 (1954)
34. Flowers, B. H., *Proc. Roy. Soc.* (*London*), [A]**212,** 248 (1952)
Edmonds, A. R., and Flowers, B. H., *Proc. Roy. Soc.* (*London*), [A]**214,** 515 (1952)
Edmonds, A. R., and Flowers, B. H., *Proc. Roy. Soc.* (*London*), [A]**215,** 120 (1953)
Flowers, B. H., *Proc. Roy. Soc.* (*London*), [A]**215,** 398 (1953)
35. Scharff-Goldhaber, G., *Phys. Rev.*, **90,** 587 (1953)
36. McClelland, C., Mark, H., and Goodman, C., *Phys. Rev.*, **97,** 1191 (1955)
Temmer, G. M., and Heydenburg, N. P., *Phys. Rev.* (To be published June 1, 1955)
Alder, F., Bohr, A., Huns, T., Mottelson, B., Winther, A., and Zupancic, O., (Personal communication)
37. Townes, C. H., Foley, H. M., and Low, W., *Phys. Rev.*, **76,** 1415 (1949)
38. Rainwater, J., *Phys. Rev.*, **79,** 432 (1950)
Feenberg, E., and Hammack, K. C., *Phys. Rev.*, **81,** 285 (1951)
39. Bohr, A., and Mottelson, B., *Kgl. Danske Videnskab. Selskab, Mat.-fys. Medd.*, **27,** 16 (1953)
40. Sunyar, A. W., *Phys. Rev.*, **98,** 653 (1955)
41. Ford, K. W., *phys. Rev.*, **95,** 1250 (1954)
42. Bohr, A., Princeton University Lecture Notes, Physics Dept. (1954)
43. Villars, F., *Helv. Phys. Acta*, **20,** 476 (1947)
44. Siegert, A. J. F., *Phys. Rev.*, **52,** 787 (1937)
45. Sachs, R. G., *Phys. Rev.*, **74,** 433 (1948)
46. Osborn, R. K., and Foldy, L., *Phys. Rev.*, **79,** 795 (1950)
47. Berger, J. M., and Foldy, L., *Case Inst. of Tech. Rept. 18, AECU-2303* (n.d.)
48. Spruch, L., *Phys. Rev.*, **80,** 372 (1950)
49. Dalitz, R. H., *Phys. Rev.*, **95,** 799 (1954)
50. Blanchard, C. H., Avery, R., and Sachs, R. G., *Phys. Rev.*, **78,** 292 (1950)
51. Austern, N., and Sachs, R. G., *Phys. Rev.*, **81,** 710 (1950)
52. Jensen, J. H. D., and Mayer, M. G., *Phys. Rev.*, **85,** 1040 (1952)
53. Kynch, G. J., *Phys. Rev.*, **81,** 1060 (1951)
54. Austern, N., *Phys. Rev.*, **92,** 670 (1953)
55. Miyazawa, H., *Progr. Theoret. Phys.* (*Japan*), **6,** 801 (1951)
Bloch, F., *Phys. Rev.*, **83,** 839 (1951)
de Shalit, A., *Helv. Phys. Acta*, **24,** 296 (1951)
56. Russek, A., and Spruch, L., *Phys. Rev.*, **87,** 1111 (1952)
57. Stech, B., *Z. Naturforsch.*, **9a,** 1 (1954)

THE DISTRIBUTION OF CHARGE IN THE NUCLEUS[1]

By Kenneth W. Ford

Department of Physics, Indiana University, Bloomington, Indiana

AND

David L. Hill

Theoretical Physics Division, Los Alamos Scientific Laboratory, University of California, Los Alamos, New Mexico

I. INTRODUCTION AND PRÉCIS

Lord Rutherford's famous experiments (1) over forty years ago on the scattering of α-particles by thin foils gave the first quantitative evidence on the distribution of positive charge in the atom, his results showing that the positive charge is condensed into a volume almost negligible in comparison with the atomic volume. This work, and extensions of it which soon followed (see 2), not only provided the necessary foundation for the understanding of atomic structure and for the science of nuclear physics, but it stands as the greatest single step forward in the search for detailed understanding of the distribution of charge in the atomic nucleus. Rutherford's value for the nuclear radius has changed little with time, and it has become possible only in the past few years to probe more deeply into the nucleus and to learn something about the detailed distribution of charge. It is interesting that among recent experiments related to the nuclear charge distribution are several studies of the elastic scattering of α-particles [Farwell & Wegner (3); Blair (4); Wall, Rees, & Ford (5); Eisberg, Igo & Wegner (6)].

Early methods of determining nuclear radii were the elastic scattering of α-particles, α-decay, and other scattering processes (7). As the science of nuclear physics developed, other methods could be used—barrier penetration factors for charged particle reactions, mirror nuclei energy separations, proton scattering, and especially elastic scattering of high energy neutrons. All of these methods gave just one parameter of the nucleus, its "radius," and all had the feature that they depended not just on the distribution of charge or of mass, but also on the spatial distribution of nuclear potential energy, or, in the case of mirror nuclei energies, on special features of nuclear structure. These methods led to the relation $R=r_0A^{1/3}$, with $r_0=(1.4 \text{ to } 1.5)\times10^{-13}$ cm., which became an accepted value of nuclear radius (8).

More recent work on the elastic scattering of electrons by nuclei (9 to 13) afforded for the first time a way to study the distribution of charge in the nucleus by means of the well-understood electric interaction between

[1] This article was submitted for publication April 1, 1955. The literature survey does not, therefore, go beyond March, 1955.

electrons and protons, independent of any uncertainties associated with nuclear forces, or with nuclear structure. Although the earliest work on electron scattering led to "small" values of the radius of the nuclear charge distributions, there was sufficient uncertainty in the experiments and in their interpretation that the significance of the results was not generally appreciated.

The x-rays emitted by negative μ-mesons captured into bound states about nuclei were first observed by Chang (14), and their possible significance for studying nuclei was pointed out by Wheeler (15). Fitch & Rainwater (16) first obtained quantitative results for the energies of these μ-mesonic x-rays, and the interpretation of their results (16, 17, 18) led unambiguously to "small" nuclear radii ($r_0 = 1.20 \times 10^{-13}$ cm.), provided the μ-meson, like the electron, was assumed to be a Fermi-Dirac particle with negligibly small nonelectric interaction with the nucleus. The experiments of Fitch & Rainwater, in particular, stimulated renewed interest in the size of the nucleus, since their results seemed to require a change by 20 per cent of a well-accepted number in nuclear physics.

Among experiments sensitive to the nuclear charge distribution, the recent studies by Hofstadter *et al.*, (13, 19, 20, 21) of the electric scattering of very high energy electrons by nuclei are undoubtedly of the greatest significance, since their results make it possible to delineate the shape as well as the size of the nuclear charge distribution.

One expects that the distribution of neutrons in the nucleus is not very different from the distribution of protons, so that the determination of the distribution of charge is of fundamental interest to studies of nuclear structure. (Such differences as there are between neutron and proton distribution are, of course, of great interest. See section IV.) From the point of view of theoretical interpretation, purely electric measures of nuclear size and shape are the most clear-cut and least uncertain. It is these measurements and their interpretation in terms of the nuclear charge distribution that we especially wish to review in the present paper. In section IV we also mention briefly results of measurements of nuclear size and shape which depend in an important way on nuclear forces, mostly in order to compare the results of these measurements with the purely electric measurements and to see to what extent all measurements fit into a single consistent picture of the distribution of charge in the nucleus.

We shall distinguish three properties of an assumed continuous nuclear charge distribution: (*a*) The size of the charge distribution, i.e., the nuclear "radius"; (*b*) The radial variation of the charge distribution, which to avoid ambiguity with geometrical shape, we shall call the "radial shape" of the charge distribution. Its description requires one or more parameters in addition to the nuclear "radius"; (*c*) The angular variation of the charge distribution, which we shall call the "angular shape" of the distribution. None of these quantities, of course, is measured alone. Most experiments can be interpreted in terms of certain weighted averages over the charge distribution—

e.g., a mean square radius instead of a radius alone, or a radial moment instead of a radial shape, or a quadrupole moment instead of an angular shape. But, ideally, the picture one seeks is a successively more detailed description in terms of the size, the deviations of the radial variation from zero (corresponding to a constant density distribution), and the deviation of the angular variation from spherical symmetry.

For purposes of discussion, we divide electrical measurements of nuclear size and shape into four kinds:

1. Scattering of relativistic electrons by nuclei. Because of the great disparity in the masses of electron and nucleus, even relativistic electrons may have wave lengths great compared to the nuclear size. Electron energies of the order of 1 Mev are required before the effect of the finite size of the nucleus becomes appreciable in their scattering angular distributions. In the method of treatment and in discussion of what one learns about nuclei, it is convenient to divide relativistic electrons into "low," "medium," and "high" energy groups.

(*a*) Low energy electrons ($E \lesssim 16$ Mev) experience only S-wave effects in scattering from nuclei. Phase shifts may be determined from pertubation theory. The scattering measures a single parameter of the nucleus: the mean square radius of charge.

(*b*) Medium energy electrons (16 Mev$\lesssim E \lesssim$80 Mev) have several partial waves affected in scattering from nuclei, but a description of the scattering in terms of radial moments of the charge distribution may still be feasible.

(*c*) High energy electrons ($E \gtrsim 80$ Mev) have a substantial number of partial waves affected by the nucleus, and show a cross section sensitive to finer features of the charge distribution. Adequate theoretical interpretation of high energy electron scattering so far has required rather complicated exact numerical calculations. But high energy electron scattering has been more fruitful than any other single source of information in learning about the nuclear charge distribution.

2. Effect of the nucleus on bound electrons. The effect of the finite size of the nucleus on electronic energy levels has been a subject of interest since the first theoretical discussions of the subject by Racah (22) and by Rosenthal & Breit (23). The very small magnitude of the effect is to some extent compensated by the very high accuracy of measurements of optical and x-ray spectra. Two features of atomic spectra in particular have yielded information about the nuclear charge distribution: (*a*) the fine structure splitting of the $2p$ state observed in x-ray spectra, and (*b*) the isotope shift, which in heavy nuclei comes predominantly from the finite nuclear size.

3. The interaction of μ-mesons and nuclei. If μ-mesons are well-behaved fermions obeying the Dirac equations, and interacting with nuclei only electromagnetically and through the very weak β-coupling, as appears to be the case (24, 25, 26), then they are ideal nuclear probe particles. Moderate energy mesons have wave lengths short enough that they can feel out the

nuclear charge distribution in some detail.

(*a*) The scattering of μ-mesons from nuclei has not yet been attacked quantitatively, but there seems to be no doubt that it soon will be [Rochester & Wolfendale (27)]. It will be a valuable tool to measure charge distributions.

(*b*) The transition energies of negative μ-mesons bound to nuclei have been measured for some nuclei (16). An extension of this work will also be of real interest in learning about the nuclear charge distribution as well as in obtaining more detailed information about the μ-meson itself.

4. Nuclear Coulomb energy. This quantity is not strictly independent of nuclear forces, since its magnitude will depend on correlations between proton positions and on the degree of overlap of proton probability distributions in the nucleus. Information on Coulomb energy comes from two sources: (*a*) the energy differences of mirror nuclei, and (*b*) the Coulomb energy term in the semi-empirical mass formula.

We divide the discussion of nuclear charge distribution into two parts: (*a*) the size and radial shape of the distribution, discussed in section II, and (*b*) the angular shape, discussed in section III. In the discussion of radial shape, spherical symmetry is assumed. The effects of angular shape are then considered separately. Although the emphasis in this paper is on the interpretation of experiments which shed light on the nuclear charge distribution, we also mention in section IV some theories of nuclear size and shape. These theories are for the most part nonquantitative, but it is nonetheless of considerable interest to compare theoretical predictions with the improved experimental information now available.

The consistent and rather detailed picture which we now have of the nuclear charge distribution comes in large measure from the excellent electron scattering experiments of Hofstadter *et al.* (13, 19, 20, 21) coupled with the rather accurate measurement of a single parameter of the charge distribution by the μ-mesonic experiment of Fitch & Rainwater (16). This picture for heavy nuclei is a nearly uniform density of charge in the interior of the nucleus, with a rather rapid fall-off of density at the nuclear surface such that the density drops from 90 per cent to 10 per cent of its maximum value over a distance $\Delta r \cong 2.2 \times 10^{-13}$ cm., with a mean square radius (r^2).

$$R = [(5/3)\langle r^2 \rangle]^{1/2} = r_0 A^{1/3}, \qquad r_0 = 1.2 \times 10^{-13} \text{ cm.}$$

For the Pb nucleus in particular, more detailed analysis (16, 17, 18, 28) of the experimental data has led to $r_0 = (1.19 \pm 0.01) \times 10^{-13}$ cm., where the indicated error is probably an overestimate. Radii determined from electron scattering and from μ-mesonic x-rays are in agreement to within 1 per cent.

Notations and Definitions

For convenience, we summarize here some of the notations which will be used in the succeeding sections. Let the radial distribution of charge be represented by

$$\rho(r) = \rho_0 f(r/r_1) \qquad 1.$$

where ρ_0 is the central density of charge, $f(0)=1$, and r_1 is the "range" parameter related to the size of the nucleus. In practice $f(x)$ is taken to be some one- or two-parameter family of possibly reasonable radial shapes, which is amenable to calculation. In case the nucleus is not spherically symmetric, equation 1 should be regarded as the density distribution along a radius vector at some orientation relative to nuclear body-fixed axes. There is no basis at present for considering the general situation that the form of the radial shape function $f(x)$ itself depends on angle. Rather we suppose that the functional form of f does not vary with angle but that the range parameter r_1 is a function of θ and ϕ. Although there may be important effects where deformations of higher than second order play a role (e.g., fission and α-decay) we shall consider in this paper only effects which can be interpreted in terms of ellipsoidal deformation, described, for small α_μ, by

$$r_1 = \overline{r_1}[1 + \textstyle\sum_\mu \alpha_\mu Y_{2\mu}(\theta, \phi)]. \qquad 2.$$

If the axes to which the angles θ, ϕ refer are major axes of the nuclear ellipsoid, then $\alpha_2=\alpha_{-2}$, and $\alpha_1=\alpha_{-1}=0$. The two independent parameters in equation 2 may conveniently be taken to be a deformation parameter, β, and an asymmetry parameter, γ, defined by

$$\begin{aligned} \alpha_0 &= \beta \cos\gamma \\ \alpha_2 &= \alpha_{-2} = 2^{-1/2}\beta \sin\gamma. \end{aligned} \qquad 3.$$

$\gamma=0$ defines a prolate spheroid (if β is always taken positive), and $\gamma=\pi$ defines an oblate spheroid. Since the simplest radial shape function, f, is that of a uniform distribution—$f(x)=1$, $x<1$; $f(x)=0$, $x<1$—and since in this case $r_1=R=$an unambiguously defined nuclear radius, it is convenient to define for nonuniform shapes an "equivalent" radius, $R_{eq.}$, such that, for a given experiment, a uniform distribution with $R=R_{eq.}$ would yield the same result as the given distribution. This definition applies only to those experiments which measure a single parameter of the charge distribution. For example, low energy electron scattering measures the average value of r^2:

$$\overline{r^2} = r_1^2 \int_0^\infty f(x)x^4dx \Big/ \int_0^\infty f(x)x^2dx. \qquad 4.$$

The equivalent radius for the distribution $f(x)$ and for this particular experiment is found by equating the right side of equation 4 to the corresponding quantity evaluated for a uniform distribution: $(3/5)\ R_{eq.}^2$.

Both equations 1 and 2 define average distributions. For sufficiently short wave length effects, the difference between the continuous distribution (equation 1) and a distribution of point charges must be recognized. Similarly, some applications require that the dynamic properties of the deformation parameters α_μ be considered in addition to the average static deformation defined by equation 2.

II. ELECTRIC MEASURES OF NUCLEAR SIZE AND RADIAL SHAPE

A. Electron Scattering

The advantages of electrons as nuclear probe particles are the ease of obtaining energetic mono-ergic beams of high intensity and the well-understood nature of the electron-nucleon interaction. The disadvantages are the small mass and consequent long wave length of the electron which make it insensitive to nuclear effects except at very high energy. To very good approximation, the electron interacts with the nucleus only through the Coulomb forces between electrons and protons, and the motion of the electrons is described by the Dirac equation for a static central field. Refinements to this picture are the following: (*a*) The proton distribution may not be spherically symmetric. Corrections attributable to this effect are considered in section III. (*b*) The contribution of the nucleon magnetic moment to the scattering of electrons by protons has been calculated by Rosenbluth (29); and to the scattering of electrons by deuterons by Jankus (30), who finds a 5 per cent correction to the scattering of 350 Mev electrons at 90 degrees. For heavy nuclei, the coherent scattering resulting from magnetic effects should not be much greater than for a single nucleon, and, for even-even nuclei, possibly less. At great energies and large angle, however, the elastic cross section from a heavy nucleus is less than from a single proton. In this limit, the nonCoulomb interaction may become important, although there is as yet no experimental evidence for such an effect [see Fig. 1(d)]. The electron-nucleon β-decay interaction has an entirely negligible effect on the scattering. (*c*) The nuclear charge is discrete, not continuous. See end of this section. (*d*) The field is not static. The largest radiative correction is attributable to bremsstrahlung, but Suura (31) has recently extended Schwinger's work (32) and shown that, to all orders in the Born approximation, electrons which have emitted soft photons are scattered with very nearly the same angular distribution as electrons which have emitted no photons. The role of other processes and of higher order corrections (in number of photons) has not been assessed, but Suura's work suggests that corrections to angular distributions may be small even in the hundred Mev region, and for high Z.

The Born approximation affords the simplest way to gain qualitative insight into the effect of the size and radial shape of the charge distribution on electron scattering [see, e.g., Schiff (33)]. The Born approximate cross section is proportional to the square of a form factor,

$$F = (Ze)^{-1} \int_0^\infty \rho(r)(\sin qr/qr)4\pi r^2 dr, \qquad 5.$$

where q is the magnitude of the momentum change of the electron divided by $\hbar$ [$q=(2E/\hbar c)\sin\theta/2$]. At $\theta=0$, $F=1$. For a given shape of charge distribution, F falls away from 1 more rapidly for larger size. For a given

size of nucleus, the angular variation of F depends on the smoothness of the charge distribution. A uniform distribution gives rise to maxima and minima in the form factor, while a sufficiently gradual variation of charge density (e.g., exponential or gaussian) gives rise to a monotonically decreasing form factor.

For sufficiently low energy electrons ($qr \ll 1$ within the nucleus), or at small angles for any energy, $\sin qr/qr$ may be expanded to yield

$$F = 1 - (1/6)q^2\langle r^2\rangle_{\text{av}} + \cdots \qquad 6.$$

This result, that at low energy the scattering depends only on the mean square nuclear radius, is characteristic not only of the Born approximation, but has been derived by Feshbach (34) by means of a partial wave expansion, and holds when only s wave electrons are substantially affected by the finite size of the nucleus.

It is to be noted that, because one is in the relativistic domain, the usual rule that the Born approximation improves with increasing energy does not hold. The linear relation between energy and momentum means that phase shifts ($\sim R\Delta k$) do not diminish with increasing energy, since Δk is then independent of energy. The phase shift of a relativistic electron in passing through a heavy nucleus is not small compared to one radian. Consequently, the Born approximation is not accurate at any energy for heavy nuclei.

Low energy.—For electron energy less than about 16 Mev, only the s wave phase shift deviates appreciably from that for a point nucleus. For low Z, the cross section may be fit to the very simple Born approximation formula,

$$\sigma/\sigma_c = [1 - (1/6)(2E/hc)^2\langle r^2\rangle_{\text{av}} \sin^2 \tfrac{1}{2}\theta] \qquad 7.$$

The evaluation of the point nucleus cross section, σ_c, which appears in this equation is itself a sizable task of numerical computing, but has been carried out to an accuracy sufficient for low energy scattering by Bartlett & Watson (35) and by Feshbach (36). More accurate evaluations of point nucleus cross sections have been carried out at higher energy by Yennie, Wilson & Ravenhall (37), and by Hill, Freeman & Ford (28). For high Z, an accurate fit to low energy scattering data requires the numerical evaluation of the s-wave phase shift. Such work has been carried out by Acheson (38), Glassgold (39), Bitter & Feshbach (40), and by Bodmer (41). In either case, the results yield the mean square radius of the nuclear charge distribution. These results are summarized in Table I in terms of the radius of an equivalent uniform distribution:

$$R_{\text{eq}} = [(5/3)\langle r^2\rangle_{\text{av}}]^{1/2} \qquad 8.$$

Medium energy.—We designate energies from about 16 to 80 Mev as medium energy. This energy region is characterized by having more than a single electron partial wave influenced by the nucleus, but by being still in an energy region where approximate or perturbation means of analysis are possible. The most convenient description is then in terms of radial moments of the charge distribution.

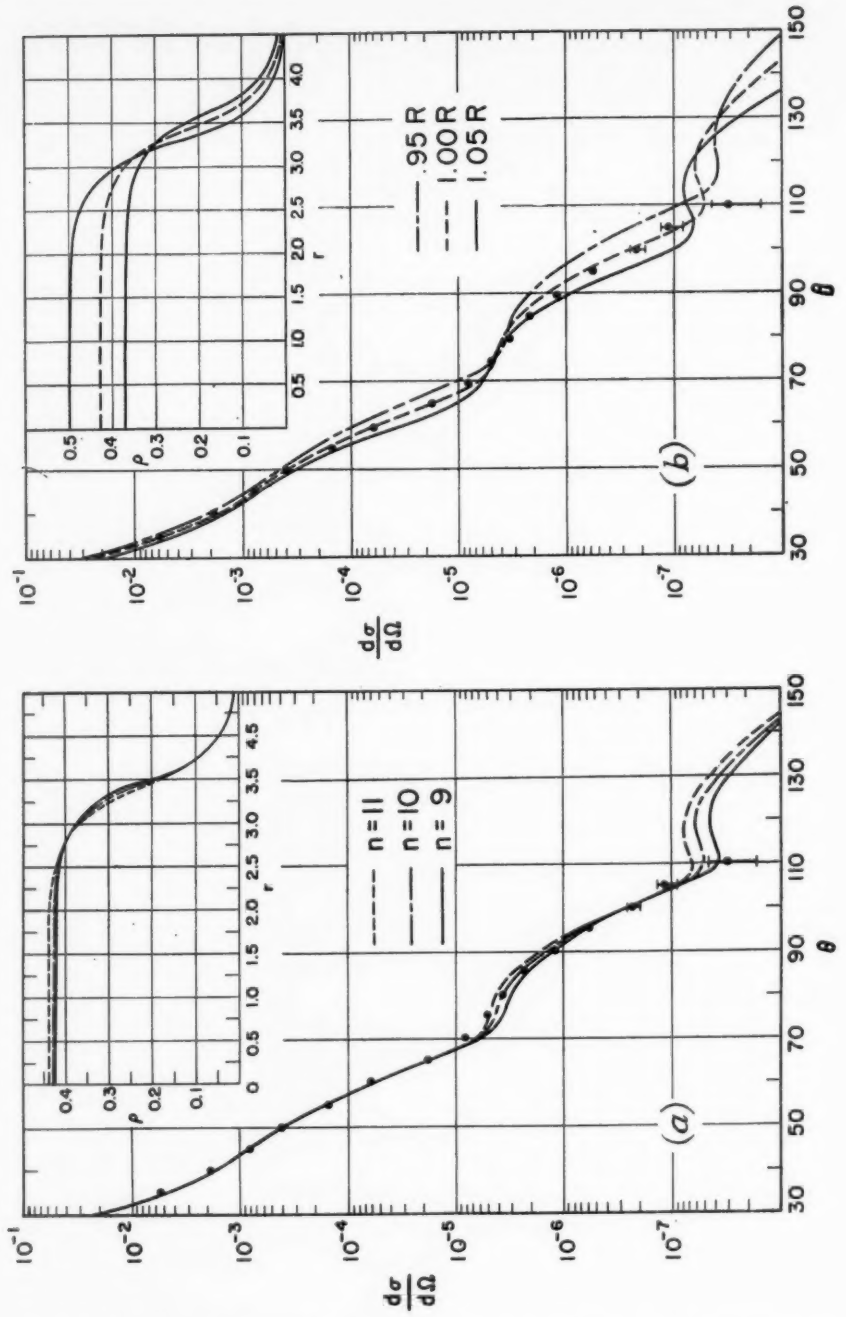

FIG. 1. Absolute differential cross sections for fast electron elastic scattering on heavy nuclei as functions of the angle θ). Illustrations are given (28) for gold, with charge distributions in the neighborhood of the best fit ($n=10$, $R=1.00$, $S=0$) as described in Table II. (a), (b), and (c) are for 183 Mev and illustrate the effect on $d\sigma/d\Omega$ of varying n (about $n=10$, $R=1.00$, $S=0$), R (about $n=10$, $R=1.00$, $S=0$),

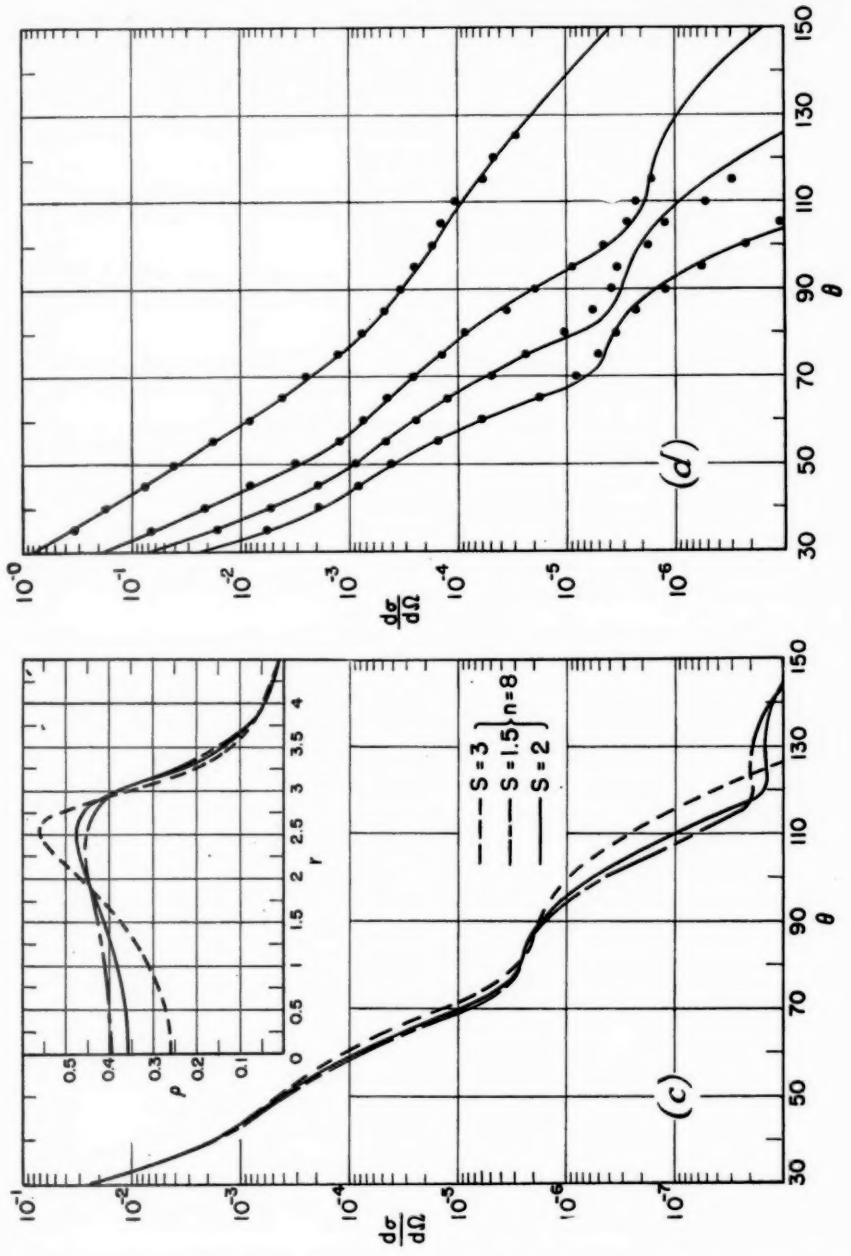

and S (about $n=8$, $R=1.00$, $S=2$) respectively. The inserts show the corresponding appearance of the charge density. Part (d) shows the scatter of the experimental data (20) about $d\sigma/d\Omega$ computed for $n=10$, $R=1.00$, $S=0$. The curves, proceeding from top to bottom, are for 84, 126, 154, and 183 Mev. The experimental data are normalized by γ, defined after equation 14.

TABLE I

NUCLEAR RADIUS MEASUREMENTS FROM MEDIUM ENERGY (15 TO 80 MEV) ELECTRON SCATTERING

Element	Z	Energy	Reference for Data	Reference for Analysis	Result for $10^{13}r_0$(cm)*
Silver	47	15.7 Mev	(9)	(9)	1.15 ± 0.1
Gold	79	15.7 Mev	(9)	(9)	1.15 ± 0.1
Tin	50	30–45 Mev	(10)	(10)	$1.1\ \pm0.1$
Tungsten	74	30–45 Mev	(10)	(10)	$1.0\ \pm0.1$
Copper	29	15.7 Mev	(9)	(40)	1.0
Silver	47	15.7 Mev	(9)	(40)	1.1
Gold	79	15.7 Mev	(9)	(40)	1.2
Tungsten	74	31–60 Mev	(12)	(12)	1.18 ± 0.10

* Results are given in terms of r_0 where $R_{eq}=r_0A^{1/3}$, and the equivalent radius R_{eq} is defined by equation 8. The first clear-cut evidence for the presently accepted electrical radius of the nucleus appears to have come in the work of Lyman, Hanson & Scott 9.

Consider the radial Dirac equations for an electron in a central field:

$$\begin{aligned}(dF/d\xi) - (k/\xi)F + [\epsilon - 1 - U(\xi)]G = 0\\ (dG/d\xi) + (k/\xi)G - [\epsilon + 1 - U(\xi)]F = 0\end{aligned} \qquad 9.$$

G and F are the large and small components of the wave function, in arbitrary units; E is the total energy and $U(\xi)$ the potential energy, both in units of mc^2; ξ is the radius in units of $\lambda\!\!\!^{-}_c=\hbar/(mc)$; and k, the angular quantum number, is $\mp(j+1/2)$ for $j=l\pm1/2$. (The integer l is of course not a good quantum number associated with orbital angular momentum. Rather it is a convenient way to describe the relativistic solution in nonrelativistic language. Thus we refer to the $k=-1$ solution as the "$s_{1/2}$" solution, the $k=+1$ solution as the "$p_{1/2}$" solution, etc.)

The phase shift η_k depends on the ratio $F/G=X$ evaluated at some radius $\xi=a$ outside the nucleus. It is, therefore, convenient to reduce equations 9 to a single equation for the ratio F/G. We consider alternative integral forms depending on the sign of k:

$$(F/G)_\xi=-\xi^{2k}\int_0^\xi(\epsilon-1-U)[1+(\epsilon+1-U)/(\epsilon-1-U)\cdot(F/G)^2]\xi^{-2k}d\xi, \quad k<0 \qquad 10.$$

$$(G/F)_\xi=+\xi^{-2k}\int_0^\xi(\epsilon+1-U)[1+(\epsilon-1-U)/(\epsilon+1-U)\cdot(G/F)^2]\xi^{2k}d\xi, \quad k>0 \qquad 11.$$

We suppose, for the energy region in question, that for $k=\pm1$ (and therefore for all k) there are no nodes of F or G for ξ smaller than the "fitting" radius, a. In fact, in the medium energy region, the second terms in the square brackets of equations 10 and 11 contribute a small part of the total values of the integrals. For 40 Mev electrons on Pb for example, these terms

contribute only a few per cent. (This assumes that the fitting radius a is just outside the conventional nuclear radius. For long tailed charge distributions, the second terms contribute more.) In lowest approximation, then, the terms in the integrands involving F and G may be ignored. In next approximation, the point nucleus solution for F and G may be substituted on the right of the equations. We consider here only the lowest approximation. Then for positive k,

$$(G/F)_a \cong a^{-2k} \int_0^a [\epsilon + 1 - U(\xi)]\xi^{2k} d\xi, \qquad 12.$$

with a similar relation for negative k. If the part of equation 12 involving $U(\xi)$ is integrated twice by parts, one finds:

$$(G/F)_a \cong \frac{a(\epsilon+1)}{2k+1} + \frac{1}{2k}\frac{Ze^2}{ch}\left[1 - \frac{1}{2k+1}\frac{\langle r^{2k}\rangle_{av}}{R_a{}^{2k}}\right], \qquad 13.$$

where $R_a = a\lambda\!\!\!^{-}_c$. The corresponding expression for negative k may be obtained by replacing $(\epsilon+1)$ by $(\epsilon-1)$ in this formula, and replacing k by $|k|$. Thus, for $k = \pm 1$, the charge distribution affects the scattering in this approximation only through the mean square radius. For higher $|k|$, higher moments of the charge distribution enter. More detailed considerations of this kind have been given by Glassgold (39), who showed that in general only even moments of the charge distribution enter.

Table I summarizes the experiments and analysis on low and medium energy electron scattering.

High energy.—The greatest amount of information regarding the radial shape of the nuclear charge distribution has come from experiments on the elastic scattering of high energy electrons ($E \gtrsim 80$ Mev). The analysis of these experiments, especially for high Z, has taken the form of numerical integration of the radial Dirac equations to obtain the required phase shifts for low angular momentum, and of numerical summing of the scattering amplitude series. A beautiful series of experiments in the energy range 80 to 200 Mev has been carried out by Hofstadter and collaborators (13, 19, 20, 21); analysis of these experiments has been carried out by Yennie, Ravenhall, and others (28, 37, 42, 43). Theoretical studies of high energy electron scattering have also been made by Schiff (44), Elton (45), and others (46 to 54).

A typical set of data and of theoretical cross section curves are shown in Figure 1. The cross section deviates from Coulomb at very small angles and diminishes with angle at a much greater rate than does the Coulomb cross section. This behavior accords with naive expectation, since that part of the point-charge potential responsible for scattering through considerable angles has been replaced by the finite Coulomb potential of the nucleus.

The detailed analysis of the high energy scattering has shown the following: (*a*) To extract useful information from the data requires careful and detailed numerical computations. Early efforts to understand the data by means of a Born approximate analysis were unsuccessful (33). (*b*) The

size and "surface thickness" of the charge distribution are well determined by the data: the central charge density is less well determined.

It has been found possible to fit the data of a given element at several energies with the same nuclear charge distribution. This affords indirect evidence that radiative corrections do not significantly alter the angular distributions.

Hill, Freeman & Ford (28) have applied a quantitative measure of the "best fit" of a theoretical to an experimental cross section. This procedure has made it possible to refine the fits to the data and, in particular, has led to two conclusions with regard to the Pb nucleus: (*a*) The radius of the distribution which best fits the electron scattering also fits to within 1 per cent the μ-mesonic $2P \rightarrow 1S$ transition energy (part B of this section). (*b*) The distribution which best fits the scattering does not have an appreciable central depression of charge density. The latter point is of special interest, since central depressions of charge density are to be expected for uniform neutron distribution. The absence of a central depression of proton density implies—because of Coulomb forces—that the central density of neutrons must be slightly peaked. However, it has been shown by Yennie *et al.* (42) and by Hill, Freeman & Ford (28) that the predicted angular distributions are not very sensitive to the central charge density.

Figure 2 illustrates the method (28) of measuring quantitatively the deviation of theoretical prediction from the experimental data. The measure of closeness of fit is taken to be D where

$$D^2 = \frac{\sum_{i=1}^{I} w_i(\gamma_i - \bar{\gamma})^2}{\bar{\gamma}^2 \, \Sigma \, w_i} \qquad 14.$$

and $\gamma_i = \sigma_{\text{exp}}/\sigma_{\text{th}}$ is the ratio of observed to calculated cross section at the angle θ_i. Here $\bar{\gamma} = \sum w_i\gamma_i / \sum w_i$, the weights w_i being chosen such that each value γ_i makes the same probable contribution to the error in $\bar{\gamma}$. Plotted in Figure 2 are the values of D for various values of the parameters n and R in the neighborhood of the best fit for a charge distribution described by

$$f\left(\frac{r}{r_1}\right) = f(x) = \frac{1}{1 - \frac{1}{2}e^{-n}} \begin{cases} 1 - \frac{1}{2}e^{-n(1-x)}, & x < 1 \\ \frac{1}{2}e^{-n(x-1)}, & x \geq 1. \end{cases} \qquad 15.$$

Both from the behavior of individual cases, such as the one illustrated in Figure 2, and from the consistency of results obtained as the electron energy and the target atomic number are varied, we conclude that the charge distribution in the neighborhood of Pb^{208} is determined to one unit in n and to 1 per cent in r_1. When the right member of equation 15 is generalized by introduction of the factor $[(\sinh sx)/sx]$ to describe some depression of the charge density in the center of the nucleus, the best fit to the experimental data is in all cases obtained for $s = 0$, corresponding to no central depression. See Table II.

The only detailed determinations of charge distribution from electron

TABLE II A

FITTING OF EXPERIMENTAL DATA

		Pb at 153 Mev			Au at 183 Mev		
$D_{statistical}$		0.0771			0.0637		
$D_{observed}$ ↘		0.95R	R	1.05R	0.95R	R	1.05R
Shape parameters							
n	s						
0	0 (exp.)					0.5063	
∞	0 (unif.)		0.3176			0.3206	
9	0	0.2165	0.1016	0.1450	0.2452	0.1231	0.1983
10	0	0.2018	0.1064	0.1713	0.2275	0.1214	0.2208
11	0	0.2017	0.1271	0.1957	0.2225	0.1354	0.2418
8	1.5		0.1921			0.2162	0.1198
8	2.0		0.2423			0.2637	0.1554
8	3.0		0.3583			0.3658	0.2947

TABLE II B

BEST VALUES OF PARAMETERS IN CHARGE DISTRIBUTION

	Au				Pb		
E(Mev)	84	126	154	183	84	153	186
$R(D_{min})$	0.998	1.010	1.020	1.002	1.018	1.014	0.987
$n(D_{min})$	11.37	9.56	10.05	9.58	10.20	8.44	10.88
$D(_{min})$	0.0656	0.0723	0.1868	0.1209	0.0575	0.0979	0.1343

	Au	Pb	Au & Pb
$\langle R(D_{min})\rangle_{av}$	1.008	1.006	1.007
$\langle n(D_{min})\rangle_{av}$	10.14	9.84	10.01

Table II (a) Comparison of experimental results (13, 19, 20, 21) on high energy electron scattering with predictions (28) for an illustrative set of assumed charge distributions, energies, and targets. The values of D, as defined in equation 14, are tabulated for shapes of charge distribution defined by equation 15 *et seq.* The restriction to spherical symmetry probably involves no significant error for nuclei in the neighborhood of Pb^{208}. Also tabulated is $D_{statistical}$, the most probable value of D for an optimal theoretical fit if the only source of experimental error were the fluctuations attributable to a finite number of counts. The parameter labeled R is the ratio of the radial constant used to the radial constant determined by the μ-mesonic x-ray analysis (18). The best fit for all energies for both lead and gold is in the neighborhood of $n=10$, $s=0$, and $R=1.00$. The possible charge distribution $n=8$, $s=1.5$, $R=1.05$ seems unlikely in view of the close agreement of all other good fits (small D) with the radius determined from the μ-mesonic $2P\rightarrow 1S$ transition, as indicated in part (b) of the table. Further increases in R for the cases with $s\neq 0$ do not give better fits than the best fits shown in the table.

(b) In the second part of the table are listed the values of n and R (for $s=0$) which locate the minimum of D in each case, as determined by the procedure described in the caption of Figure 2.

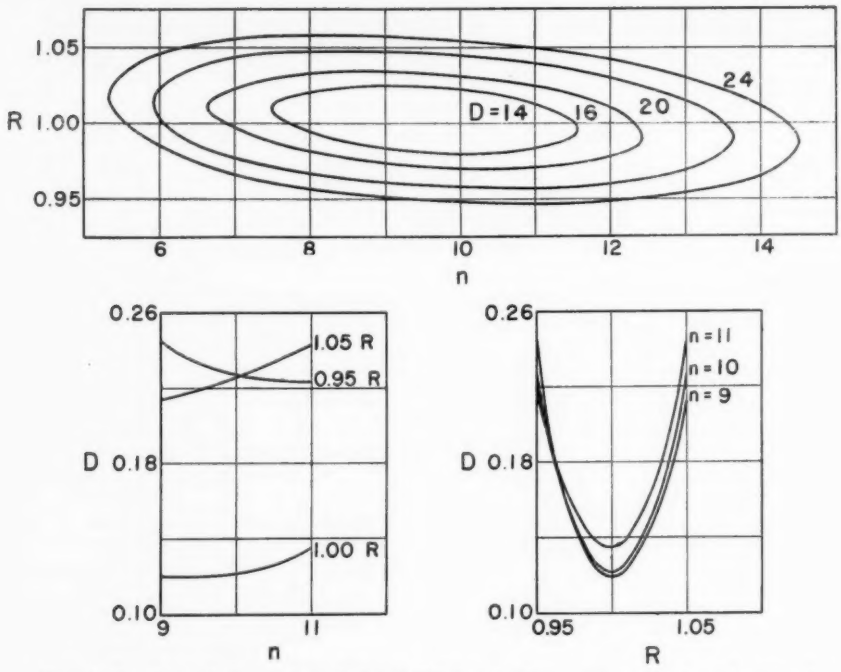

FIG. 2. Sections of the surface defined (28) by the fit measure, D, given in equation 14 and listed in Table II, for high energy elastic scattering of electrons on nuclei. The values of D in the top drawing should be divided by 100. The particular domain of D illustrated is for gold at 183 Mev, and is obtained by fitting the expansion,

$$D(n,R,S=0)=D_0+D_n n+D_R R+2D_{nR}nR+D_{nn}n^2+D_{RR}R^2$$

to the nine values of D corresponding to $n=9$, 10, and 11 for $R=0.95$, 1.00, and 1.05.

scattering reported so far are for gold and lead. It is of interest to compare the results of different workers. Hill, Freeman & Ford (28) used the functional form of charge density given by equation 15, while Ravenhall & Yennie (43) used

$$f(x) = [1 + e^{\kappa(x-1)}]^{-1}. \qquad 16.$$

The former authors fit the gold data shown in Figure 1(d) with parameters $n=10$, $r_1=6.55$; the latter authors fit the same data with $\kappa=14.6$, $r_1=6.63$ (distances in units 10^{-13} cm.). These distributions are very similar. Ravenhall & Yennie (43) define a measure of nuclear size,

$$c = r_1 \int_0^\infty f(x)dx, \qquad 17a.$$

a measure of nuclear surface thickness,

$$s^2 = -\int_0^\infty (r-c)^2(df/dx)dx, \qquad 17b.$$

and a "mean square radial constant,"

$$r_0 = [(5/3)\langle r^2\rangle A^{-2/3}]^{1/2}. \qquad 18.$$

For Au, they obtain $c=6.63$, $s=1.65$, $r_0=1.19$, while the distribution of Hill *et al.*, used for Figure 1(d), leads to $c=6.55$, $s=1.85$, $r_0=1.18$. The optimal distribution of Hill *et al.* (Table II) has radius larger by 0.8 per cent, i.e., $r_0=1.19$. The approximate formula for r_0 given in reference (43) over estimates r_0 by about one per cent for these distributions; we have therefore reduced the quoted value of $r_0=1.20$ in this reference to 1.19). Comparison of the fits in reference (43) and in Figure 1(d) indicates that such differences as exist between theory and experiment can be accounted for by the limitations of the particular two parameter family of charge distributions used to fit the data.

Corrections to the theoretical analysis.—Corrections necessitated by nonspherical symmetry of the charge distribution are discussed in Part III. We consider here some corrections to the analysis required as well for spherically symmetric distributions.

(*a*) Inelastic scattering. This affects the elastic scattering in two ways. First, because of finite resolution in the experiment, particles scattered inelastically with small energy loss may be counted as elastic particles. Such inelastic collisions may be attributable to bremsstrahlung (discussed below) or to excitation of low-lying nuclear states [Thie, Mullin & Guth (55), Schiff (56)]. The latter effect, although it provides an interesting new way to study nuclear levels, is not of great theoretical significance for the study of charge distributions, since there exists a considerable number of nuclei for which the scattered particles which leave the nucleus excited may be experimentally discriminated against. A special kind of inelastic scattering with small energy loss, leaving the nucleus in an excited rotational state is mentioned again in Part III.

The second effect of inelastic scattering may be more important. The existence of inelastic processes modifies the outgoing elastic wave. This effect has not yet received enough study to establish fully its significance. In Born approximation, elastic and inelastic processes are independent. Although the Born approximation is not accurate at high Z, it still has some qualitative value. In particular, in the true situation, as in the Born approximation, the outgoing elastic wave is only slightly distorted from a plane wave at high energy ($E \gtrsim 100$ Mev). For electrons of several hundred Mev scattered from a heavy element, the outgoing surface of constant phase differs from a plane by only a few degrees. Therefore, in spite of the fact that at appreciable angles elastic and inelastic cross sections are comparable in magnitude, the processes may still be approximately independent because of the approximate validity of the Born approximation.

The magnitude of the inelastic cross section may be crudely estimated with the help of the Born approximation. If closure over all nuclear states is used (based on the assumption that the more probable excitation energies

ΔE are small compared to the electron energy), then it is easy to derive the result (54),

$$\frac{d\sigma}{d\Omega} = \sigma_c[\,|F|^2 + Z^{-1}(1 - |F|^2)], \qquad 19.$$

where σ_c is the point-nucleus cross section and F is the form factor defined by equation 5. The inelastic term is of order Z^{-1}; it vanishes in the forward direction but may become dominant at large angles, where $|F| \ll 1$. Alternatively, if one supposes that the inelastic cross section arises from elastic collisions between the electrons and single protons in the nucleus, and if the exclusion principle is ignored, the second term in equation 19 becomes just Z^{-1}. This form agrees with equation 19 at large angles, where the proton recoil is large, but disagrees at small angles, where the exclusion principle would, in fact, cut off the inelastic scattering from single proton encounters. For this reason, 19 is the better approximation.

The qualitative conclusion is thus that if the energy resolution is poor, the observed scattering in the backward direction will be too great, and consequently the analysis will lead to the conclusion that the charge distribution falls too rapidly to zero. If the energy resolution is high, these qualitative arguments as to the effect of the inelastic cross section do not apply.

(*b*) NonCoulomb forces. These have been mentioned earlier and are probably negligible at energies and angles studied so far.

(*c*) Radiative corrections. These have been mentioned earlier. Suura's work shows that in an experiment with good energy resolution, bremsstrahlung does not alter the angular distribution, for arbitrary strength of scattering field. This may account for the fact that a consistent analysis of scattering at different energies has been carried out (28, 42, 43) using similar nuclear charge distributions.

(*d*) Granularity of nuclear charge. The difference between the idealized smooth charge distribution and the actual distribution of point charges makes itself felt primarily in inelastic processes. The effect on elastic scattering has not been analyzed, but the qualitative expectation is that for coherent scattering, the difference between a collection of point scatterers and a smoothed average potential is not significant; however, this point requires further study.

B. Mu Mesons

There is rather good evidence that the μ-meson is a Dirac particle which, like the electron, has no significant interaction with nucleons (for the present discussion) aside from the Coulomb interaction (24, 25, 26). As a nuclear probe particle it has the further advantage of large mass compared to the electron, and consequent short wave length and localizability. It suffers at present the practical disadvantage that intense monoenergetic beams cannot be produced, and in fact, μ-mesonic beams free of considerable background of other radiations are hard to obtain. Nonetheless, great prog-

ress has been made in obtaining spectra of bound μ-mesons, and experiments to measure the elastic scattering of μ-mesons from nuclei have been begun.

Bound mu-mesons.—The significant role of bound μ-meson spectra in determining the electric properties of nuclei was first pointed out by Wheeler (15). The bound meson in the lowest few states is well within the electronic K-orbit. Therefore, the problem is essentially hydrogenic for all Z, with the important difference, of course, that the finite size of the nucleus is of great importance. For the lowest bound state in Pb, for example, the meson is bound only half as tightly as for a point nucleus of the same charge. The $2P \rightarrow 1S$ transition of the meson was observed first by Chang (14) and studied quantitatively in the work of Fitch & Rainwater (16). Transitions among higher states were also observed, these being, for the lighter nuclei, primarily of interest in providing an accurate measure of the μ-meson mass.

The $2P \rightarrow 1S$ transition energy of the μ-meson fixes unambiguously a single parameter of the nuclear charge distribution. Although the angular distribution of high energy electron scattering contains in principle more parameters of the charge distribution, each of these parameters is less accurately determined. The μ-meson measurement, therefore, provides a useful constraint on the charge distribution, and, when used in conjunction with electron scattering measurements, helps to specify more precisely the shape of the charge distribution.

Higher transitions (than $2P \rightarrow 1S$) and the $2P$ doublet splitting do not measure the same parameter of the charge distribution as does the $2P \rightarrow 1S$ transition (18). Therefore, for the heaviest elements, accurate measurements of several μ-mesonic x-ray energies will in part specify the radial shape of the charge distribution. The required accuracy of measurement is, however, high—to within a few tens of kev for transition energies of several Mev, i.e., to within 1 per cent or less.

Analysis of the mesonic x-ray data and predictions of transition energies have been made on the basis of the Dirac equation for the μ-meson in the static, smooth, spherically symmetric, electric potential of the nucleus. Exact calculations of energy levels and eigenfunctions have been carried out by Fitch & Rainwater (16), Cooper & Henley (17) and Hill & Ford (18). For light nuclei, where perturbation treatment is possible, the $1S_{1/2}(k=-1)$ and $2P_{1/2}(k=1)$ levels are raised above their point nucleus values by an amount proportional to

$$\langle r^{2\sigma} \rangle_{\text{av}} = (4\pi/Ze) \int_0^\infty \rho(r) r^{2\sigma+2} dr, \qquad 20.$$

where $\sigma = [1-(\alpha Z)^2]^{1/2}$. The coefficient of the $2P_{1/2}$ shift, governed by the small component of the Dirac radial solution, is small compared to the coefficient of the $1S_{1/2}$ shift. The energy shifts of higher angular momentum states measure higher moments of the charge distribution, but are negligible in comparison to the shifts of the $|k|=1$ states. Since the perturbation ap-

proximation is valid only for low Z, where $\sigma \cong 1$, the $2P \rightarrow 1S$ transition energy for the light elements measures $\langle r^2 \rangle_{av}$, the mean square radius of the charge distribution. This is the same quantity that is measured by low energy electron scattering. The results of Fitch & Rainwater, summarized in Table III, give an equivalent radius for the light elements (defined by equation 8),

$$R_{eq} = (1.20 \pm 0.03)10^{-13}A^{1/3}\text{cm}. \qquad 21.$$

For the heavy elements, a perturbation treatment is no longer suitable, and exact numerical calculation is required. Extensive calculations have been carried out, especially for element ${}_{82}$Pb, for which the equivalent radius (no longer determined by $\langle r^2 \rangle$) is $R_{eq} = 1.17 \times 10^{-13}A^{1/3}$ cm.

TABLE III

Z	$E(2P_{3/2} \rightarrow 1S)$ (experimental, Mev)	r_0 (10^{-13} cm.)*
22	0.955	1.17
29	1.55	1.21
51	3.50	1.22
82	6.02	1.17

* Assuming the muon mass to be $\mu = 210m_e$ and using a uniform nuclear model with $R_0 = r_0A^{1/3}$, values of r_0 shown in column 3 gave the best fit to the measured $2P_{3/2} \rightarrow 1S$ transition energies given in column 2 as a function of Z. (This table taken from the work of Fitch & Rainwater (16)).

The most easily determined energies (experimentally) besides the $2P \rightarrow 1S$ transition energy are the $2P$ doublet splitting and the $3D \rightarrow 2P$ energy. As a gauge of sensitivity of the μ-meson spectra to the shape of the charge distribution, we note that for Pb, and for a fixed $2P \rightarrow 1S$ energy, the $3D \rightarrow 2P$ energy varies by 4.5 per cent between the uniform and the exponential charge distribution. Although small, this difference is about four times the theoretical uncertainty of the calculations, so that refined measurements of μ-mesonic spectra can roughly check the shapes as well as sizes of charge distributions determined by electron scattering.

The various significant perturbations to the calculated μ-mesonic energies, for spherically symmetric nuclei, have been considered by Cooper & Henley (17), Hill & Ford (18), Corben (57), and others (58, 59, 60), and are summarized in reference (18). (These exclude the interesting quadrupole effects studied by Wheeler (61), by Wilets (62), and by Jacobsohn (63), and discussed in Section III.) Two effects account for most of the perturbing energy shift, and one of these for most of the theoretical uncertainty. First is the polarization of the vacuum by electrons (18, 59). (Other radiative corrections involve intermediate states with a μ-meson created, and are less probably by order 10^{-2}.) The electron vacuum polarization is readily calcu-

lated to lowest order using results of Schwinger (64). The magnitude of the effect is, for heavy elements, of order 1 per cent of the $2P \rightarrow 1S$ transition energy. It has been crudely calculated so far to about 20 per cent, or 0.2 per cent, of the $2P \rightarrow 1S$ energy, but it could easily be refined to less than 0.1 per cent uncertainty in the transition energy. A point more important than accurate calculations of the first order effect is the magnitude of higher order effects. Wichman & Kroll (60) have shown that, in spite of the large value of αZ for the heavy elements, higher order corrections are in fact quite small. Radiative corrections account therefore for a noticeable shift in the energy but do not give rise to any important uncertainty.

The second important perturbing effect is nuclear polarization—the admixture of excited nuclear states to the ground state configuration attributable to the presence of the μ-meson (17, 58). This is estimated to be, for heavy nuclei, also of order 1 per cent of the $2P \rightarrow 1S$ energy, but its magnitude is uncertain by about a factor two. The uncertainty may be minimized in two limits: (*a*) If there are no nuclear excited states close to the ground state (e.g., Pb 208) the whole effect, and, therefore, its uncertainty, is diminished; (*b*) If the nature of the low excited states, and their mode of coupling to the μ-mesons are understood, the polarization effect, although not small, is calculable to reasonable accuracy. This is the case for nuclear rotational states (Part III).

Other perturbations have been estimated to be much smaller than these two. An interesting fact for heavy nuclei is that the $2P \rightarrow 1S$ energy is very insensitive (17, 18) to the μ-meson mass (65, 66). For Pb, this transition energy varies near the true mass approximately as $m^{0.2}$. This insensitivity, first pointed out by Wheeler (15) is attributable to the shape of the potential. For a parabolic potential, as that within the nucleus, energies vary as $m^{-1/2}$. For a $1/r$ potential, as that outside the nucleus, energies vary as m. The result, for a meson which finds itself half the time in each kind of potential, is a weak dependence of energies on meson mass.

For the Pb nucleus, it has been estimated that the error of theoretical transition energy for a given charge distribution is at most 1 per cent of the energy (18). Therefore, a measurement of the $2P \rightarrow 1S$ transition energy ($\sim$6 Mev) to less than 1 per cent determines a single parameter of the charge distribution to about 1 per cent, slightly more accurately than a single parameter can be determined by any other means at present.

Mu-meson scattering.—The scattering of μ-mesons from nuclei (27) affords in principle an interesting new way to study the distribution of nuclear charge. There are, of course, great practical difficulties, but preliminary experiments have been carried out. The advantage of μ-meson scattering over electron scattering is that a given wave length may be achieved at lower energy for the μ-meson, although this advantage largely disappears for energies in the hundred Mev region, where electrons and muons are kinematically almost equivalent.

C. Bound Electrons

The smallness of effects resulting from the finite size of the nucleus on the energies of bound electrons is to a considerable extent compensated by the very great accuracy with which electronic energy level differences may be measured. Thus observations on electronic energies can yield some information on the nuclear charge distribution. The evidence from this source is of several kinds.

x-Ray fine structure.—Christy & Keller (67) have calculated the fine structure splitting of the $2P$ states of heavy elements. The accuracy of their work is attested to by the accurate value of the fine structure constant which can be derived from it. Schawlow & Townes (68) have shown that the observed x-ray fine structure can be fit only if one adds to the theory of Christy & Keller a very small, but a very sharply Z-dependent term. The finite nucleus effect has such a strong Z-dependence because it depends, in addition to the usual Z^3 rate of increase of electron density at the nucleus, on the rapid rate of increase of the small component of the $P_{1/2}$ wave function with Z, as relativistic effects become more important. The value of nuclear radius obtained by Schawlow & Townes on the basis of an analysis in terms of a uniform charge distribution, was

$$R_{eq} = (1.77 \pm .27) \times 10^{-13} A^{1/3} \text{ cm.}, \qquad 22.$$

which is in disagreement with all other sources of evidence on the electromagnetic radius of the nucleus. As shown in another paper (69), the difference cannot be explained in terms of the shape of the charge distribution, since the quantity measured by the $P_{1/2}$ energy shift is $\langle r^{2\sigma} \rangle_{av}$, where $\sigma = [1 - (\alpha Z)^2]^{1/2}$, which is not very different from the quantity measured by low energy electron scattering, and is the same as the quantity measured by the isotope shift (see below). The discrepancy is probably associated with the radiative corrections to the $P_{1/2}$ level (69, 70, 71). These are in the right direction to explain the large size of nuclear radius in equation 22, and their Z dependence, although not as sharp as the Z-dependence of the nuclear volume effect, is sharper than the highest order Z-dependent term in the theory of Christy & Keller. The Lamb shift could, therefore, in part be included in the nuclear volume effect determined by Schawlow & Townes. Until the appropriate radiation corrections have been estimated, the radius given in equation (22) will have to be discounted.

x-Ray isotope shift.—An excellent way in principle to divorce the radiative effects and the volume effect would be to compare the x-ray fine structure for different isotopes of the same element. The radiative corrections depend almost exclusively on Z, so that the isotopic difference would be attributable to the difference of nuclear volumes. Such measurements are now just within experimental reach, but positive results have not as yet been reported (72). As a way to measure the nuclear radius, however, the x-ray isotope shift suffers from the same uncertainties as those in the isotope shifts of less tightly bound levels.

Optical isotope shift.—The comprehensive work of Brix & Kopfermann (73) in particular, has led to an understanding of the regularities in the atomic isotope shifts (74 to 78) and to a theoretical interpretation of these shifts (79 to 83). The observed isotope shift measures the difference,

$$\delta\langle r^{2\sigma}\rangle = \langle r^{2\sigma}\rangle_{Z,N+1} - \langle r^{2\sigma}\rangle_{ZN} \qquad 23.$$

If the nuclei are spherically symmetric, and if an $A^{1/3}$ law of radius holds, then the fractional increase of radius is just $\delta A/3A$, and

$$\delta\langle r^{2\sigma}\rangle = (2\sigma/3)(\delta A/A)\langle r^{2\sigma}\rangle. \qquad 24.$$

Indeed the fact that nuclei are not spherically symmetric (with rare exceptions) has a large effect on isotope shifts (Sec. III). From a knowledge of the regular variation of nuclear deformation, however, and the associated regular variation of isotope shifts, one can find the magnitude of the isotope shift corresponding to spherical symmetry. Still assuming an $A^{1/3}$ law, we find

$$R_{eq} = (0.90 \pm .1) \times 10^{-13} A^{1/3} \text{ cm.}) \qquad 25.$$

appreciably too small to agree with the μ-meson or electron-scattering determined values. The explanation offered has been that the nucleus possesses a finite compressibility [Wilets, Hill & Ford (83)]. This means that the nuclear density depends slightly on the neutron-proton ratio and is not a constant. When a neutron is added to a nucleus, the density increases slightly as a result of the diminished Coulomb energy, and the resultant fractional increase of radius is less than $(1/3A)$. The isotope shift is consequently smaller than for constant density nuclei, and one is led to the anomalously low radius given by equation 25. The magnitude of the nuclear compressibility is quite uncertain. Early estimates by Feenberg (84) and recent evidence from a theory of nuclear saturation (85) are in approximate agreement. They give for the "inverse nuclear compressibility" E_0'' (defined in reference 84),

$$E_0'' \sim 50 A mc^2, \qquad 26.$$

uncertain to perhaps 50 per cent. This value of compressibility, if used to correct the analysis of the isotope shifts, leads to radii larger than given by equation (25) by a factor which increases slowly with Z, and, at $Z=80$, is 1.27 (83). Thus, near $Z=80$, the revised estimate of R_{eq} from isotope shifts is

$$R_{eq} = (1.16 \pm .13) \times 10^{-13} A^{1/3}, \qquad 27.$$

for the compressibility given by equation 26.

It is clear from the discussion above that the x-ray fine structure and isotope shift do not at present provide an accurate means to determine nuclear radii. The theoretical analysis of the effect of the finite nucleus on these quantities, however, can be usefully applied for quite other purposes. Since one now knows the nuclear electric radius quite accurately from other experiments, this quantity may be regarded as known. More accurately stated, the μ-mesonic and electron scattering measurements together pro-

vide enough information on the charge distribution to calculate $\langle r^{2\sigma} \rangle$ accurately. If this quantity be inserted into the theory of the effect of the nuclear extension on bound electrons, the remaining discrepancy then provides a measure of other interesting quantities—the Lamb shift of the $2P_{1/2}$ electronic level from the fine structure data, and the nuclear compressibility from the isotope shift data. We have not attempted to carry out the former analysis. About the latter, we conclude that the experimentally determined nuclear compressibility is

$$E_0'' = (90 \pm 30) A mc^2. \qquad 28.$$

The limits of error in equation 28 are a crude guess, since a detailed analysis has been carried out only for the values 50 Amc^2 and 100 Amc^2 (83).

D. Coulomb Energy

The Coulomb energy difference between mirror nuclei is one of the oldest means to determine nuclear radii, but the difficulties of exact interpretation were recognized early (7, 86) and have been reemphasized recently (17, 87 to 91), although they have not been stressed in the interim, possibly because the simplest interpretation of the data without corrections led to radii in agreement with those obtained by α-decay and by fast neutron total cross sections for the heavier elements. The difficulty is associated, of course, with the fact that the Coulomb energy, in spite of its purely electrical nature, is dependent on certain details of the nuclear structure.

On a classical theory of uniformly distributed charge over a volume $4/3\ \pi R^3$, the nuclear Coulomb energy is

$$E_c = (3/5) Z(Z-1) e^2/R, \qquad 29.$$

and the Coulomb energy difference between mirror nuclei (Z and $Z+1$),

$$\Delta E_c = (6/5) Ze^2/R. \qquad 30.$$

When the mirror nuclei are interpreted in this way, one finds resulting radii which follow quite closely an $A^{1/3}$ law (8), given by

$$R = 1.46 \times 10^{-13} A^{1/3} \text{ cm.}, \qquad 31.$$

up to $A = 43$. There are two reasons why this simple interpretation is not correct. First, the antisymmetrization of the ground state proton wave function leads to exchange terms which diminish the Coulomb energy and, therefore, diminish the calculated radius. Cooper & Henley (17) give the approximate formula which includes the exchange energy,

$$E_c \cong (3/5) Z(Z-1) e^2/R - 0.46\, Z^{4/3} e^2/R. \qquad 32.$$

This leads for the light nuclei to an average reduction of radius of about 10 per cent, i.e., a change of the radial constant in equation 31 from 1.46 to 1.3. A more detailed study of the correction term in equation 32 has led to an explanation of an alternation in magnitude of the correction for very light nuclei on the basis of the symmetry properties of the ground state wave function (89).

A second and more difficult correction to equation 30 comes about from

the difference between the density distribution of the proton participating in the β-decay and the average density distribution of all protons. Although equation 32 might provide a good estimate of the total nuclear Coulomb energy, the difference $E_c(Z+1)-E_c(Z)$ evaluated from equation 32 could be in considerable error if the disappearing proton had a very nonuniform density distribution. The nuclear shell model suggests that this is the case, and calculations of Coulomb energy differences on the basis of the shell model have been carried out by Cooper & Henley (17), by Jancovici (90), and by Carlson & Talmi (91). The results generally tend to give nuclear electrical radii smaller than equation 31 by 10 to 15 per cent, but no longer so smoothly varying with A as the results of the simpler analysis. The final result of the mirror nucleus analysis is a radius given by

$$R = (1.3 \pm .1) \times 10^{-13} A^{1/3} \text{ cm.} \qquad 33.$$

It is still uncertain whether this slightly high value results from inadequacies of the analysis, or from the fact that the proton density in light nuclei is indeed somewhat lower than in heavy nuclei. The latter conclusion is suggested by Carlson & Talmi (91), who find an increasing trend of nuclear density between $A=13$ and $A=27$. Two omissions in the analysis so far which may be of significance are the following. (*a*) Nonuniform nuclear density. Since the Coulomb energy and electron scattering measure different properties of the charge distribution, the nuclear radii obtained should agree only for a uniform distribution. For a gaussian distribution, the radius, R_{eq}, deduced from Coulomb energy should be smaller by 5 per cent than that deduced from low energy scattering (69) (or any other effect measuring $\langle r^2 \rangle$). Since the radius in equation 33 is already larger than that found from electron scattering, this effect would increase the discrepancy somewhat. (*b*) The short range correlations in proton positions within the nucleus brought about by repulsive cores in the nuclear forces would reduce the Coulomb energy. This effect would further decrease the radius deduced from the mirror nuclei energy difference, and would be in the direction to diminish the discrepancy between the radius in equation 33 and the radius deduced from the more purely electromagnetic means.

The two corrections to equation 29 stressed for the mirror transitions are not important for the total Coulomb energy term appearing in the semi-empirical mass formula for medium and heavy nuclei. From this term one may therefore deduce an electrical radius by means of equation 29. It is unfortunately very difficult to estimate the probable error of the nuclear Coulomb energy obtained in this way. We therefore state, without indicated error, the nuclear electric radius deduced by this means (40) from a recently revised semi-empirical mass formula (92):

$$R_{eq} = 1.23 \times 10^{-13} A^{1/3} \text{ cm.} \qquad 34.$$

III. ELECTRIC MEASURES OF NUCLEAR ANGULAR SHAPE

Simple considerations of the energetics of nuclear deformation show that

the predominant mode of deformation should be ellipsoidal, as expressed by equation 2. As noted under that equation, such deformations are characterized by two parameters, a deformation parameter, β, related to the absolute magnitude of the deformation, and an asymmetry parameter, γ, measuring the deviation from cylindrical symmetry. These are classically defined quantities, however, assuming a static nucleus. For large nuclear deformations, β and γ may indeed have classical significance (amplitude of surface vibration$\ll$deformation), but even then approximate degeneracies between different combinations of β, γ may lead to mixing of different deformational configurations. For small deformations, β and γ have significance only as expectation values.

A. Quadrupole Moments

The shell model of the nucleus in its simplest form (nucleons moving independently in a common central potential) predicts quadrupole moments for any number of particles which are of the same order or less than the quadrupole moment of a single particle. This is because closed shells have zero quadrupole moments and groups of equivalent particles have quadrupole moments less than one particle of the group. Many observed moments are many times larger than can be explained by the central-well shell model. These large moments can be explained in the same shell model language in terms of very great configuration mixing in which many partly filled shells contribute additively to the quadrupole moment. An equivalent but far simpler explanation is in terms of a collective description of deformation of the whole nucleus. The shell model together with a finite nuclear deformability offers a ready explanation of the mechanism of the deformation and also accounts for the order of magnitude of the observed quadrupole moment.

Townes, Foley & Low (93) first pointed out the regularities in quadrupole moments as a function of mass number, and the correlation of these regularities with nuclear shell structure. Rainwater (94) showed that surface coupling of extra nucleons can account for the large magnitude of some observed moments, and the theory of this surface coupling was developed by Bohr (95), Hill & Wheeler (96), and Bohr & Mottelson (97). In a more recent survey of quadrupole moments, Goeppert-Mayer (98) has considered the combined contributions of extra-shell protons and of total nuclear deformation. She finds that in the vicinity of closed shells, the moments can be accounted for with zero deformation, while far from closed shells quite substantial deformations are required. The general picture obtained from observed moments is therefore a regularly varying nuclear deformation with minima for either proton or neutron closed shells, and maxima between closed shells.

Since we wish to avoid detailed discussion of the shell model and nuclear structure, we merely emphasize here that for nuclei with small quadrupole moments the nuclear deformation appears to be almost negligible. This

conclusion comes both from the quadrupole evidence given by Goeppert-Mayer, and from the success near closed shells of shell model calculations based on spherical symmetry (99, 100, 101). There are, then, at least a few nuclei for which a spherically symmetric charge distribution is a very good approximation.

For nuclei in the opposite limit, with very large quadrupole moments, it is reasonable to ignore the extra-particle contribution and to evaluate the angular shape of the nucleus on the assumption that all of the observed quadrupole moment is caused by the deformation of a homogeneous charge distribution. The "intrinsic" quadrupole moment, or moment relative to body fixed axes (or "classical" moment appropriate for angular momentum, $I \to \infty$), may then be defined for the charge distribution having the form given by equations 1 and 2:

$$Q_0 = e^{-1} \int_0^\infty \rho(r')(3Z'^2 - r'^2) r'^2 dr' d\Omega' \qquad 35a.$$

$$\cong (5/\pi)^{1/2} Z \langle r^2 \rangle_{av} \alpha_0 = (5/\pi)^{1/2} Z \langle r^2 \rangle_{av} \beta \cos \gamma. \qquad 35b.$$

In equation 35a the primes denote body-fixed axes such as are used in equation 2. Equation 35b is only accurate to order α; higher terms are omitted. The mean square radius which appears here is averaged over angle, i.e.,

$$\langle r^2 \rangle_{av} = (4\pi\rho_0/Ze) r_1^5 \int_0^\infty f(x) x^4 dx. \qquad 36.$$

Equations 35 and 36 have the same form as the usual definitions for a uniform charge distribution, but they hold (to order α) for an arbitrary radial shape, $f(x)$. If the angular momentum is directed along the Z' axis in the body, then the observed quadrupole moment is less than Q_0 by a projection factor (97),

$$P_I = \frac{I(2I-1)}{(I+1)(2I+3)} \qquad 37.$$

The simplest interpretation of observed quadrupole moments is then obtained by supposing that the deformation is cylindrically symmetric about the axis defined by the total angular momentum. On ethen sets $\cos \gamma = \pm 1$ according as $Q_0 \gtrless 0$, and uses 35b together with the projection factor, 37, to obtain $\beta \langle r^2 \rangle_{av}$ as the parameter of the nuclear charge distribution measured by experiment. Whether the number so determined is indeed $\beta \langle r^2 \rangle_{av}$ depends on the orientation of the angular momentum in the body fixed system and on the magnitude of the deformation, both of which change the projection factor of equation 37; on the direct contribution of extra-shell protons to the quadrupole moment; and on the degree of asymmetry of the charge distribution, which changes $\cos \gamma$. The last effect, in particular, could cause a small observed moment and a consequent underestimate of β. Near closed shells the direct particle contribution causes instead, with this interpretation, an overestimate of β. However, in the region of large deformations, the only region where the simple picture of a deformed homogene-

ous charge distribution is appropriate, the assumptions described above are expected to be nearly correct.

Although the quantity determined by the quadrupole moment is $\beta\langle r^2\rangle_{av}$, we can take $\langle r^2\rangle_{av}$ as a known quantity from the μ-mesonic energies or from electron scattering results, and therefore determine from the data the deformation, β, alone, by the formula

$$\beta = (\pi/5)^{-1/2}[Z\langle r^2\rangle]^{-1}\langle P_I\rangle^{-1}\,|\,Q\,|. \qquad 38.$$

Nuclear deformations determined from quadrupole moments (102) by this formula are shown in Figure 3, except that $\beta \cos \gamma$ is plotted in order to illustrate the sign of Q. The values are expected to be meaningful measures of the actual deformation of total nuclear charge only where they are large ($\beta \gtrsim 0.1$ for the heavy nuclei, $\beta \gtrsim 0.2$ for the intermediate nuclei). Measured quadrupole moments are not of high accuracy, but Figure 3 nonetheless gives valuable evidence as to the magnitude of nuclear charge deformation, as to the regularity of this deformation as a function of neutron number (for $N \gtrsim 70$), and as to the marked preference of large deformations for the prolate shape.

B. Electric Quadrupole Transition Rates

Electric Quadrupole ($E2$) transition rates measure the off-diagonal matrix elements of the same operator whose diagonal element is the ground state quadrupole moment. As a means to measure nuclear deformation, the transition rate has one disadvantage, but several advantages, as compared to the quadrupole moment measurement. The disadvantage is that two nuclear states are involved; if the excited state deformation differs from that of the ground state, one does not measure the desired quantity, the ground state deformation. There is a good theoretical reason to believe, however, that certain low excited states of nuclei with large deformation have nearly the same angular shape as the ground state (97). For such nuclei, whose angular shape is in fact of the greatest interest, this feature is therefore not a serious disadvantage. The advantages of the transition rate measurements, relative to quadrupole moments are: (*a*) the available data is more extensive; (*b*) the accuracy of measurement is frequently much greater; (*c*) the quadrupole matrix elements may be determined even for spin zero or one half, when quadrupole moments vanish, and therefore, in particular, the deformations of even-even nuclei may be determined.

As in the discussion of quadrupole moments, we shall avoid consideration of nuclei which are spherically symmetric or have only very small deformations, since the $E2$-transition rates in these nuclei will depend on shell structure effects as well as collective effects. For nuclei with large deformations, there are two simplifying features: (*a*) The contribution to $E2$ rates of extra-shell protons will be small compared to the contribution of the collective nuclear deformation. We therefore consider only the collective contribution; (*b*) Nuclear rotational states are expected to have deformations

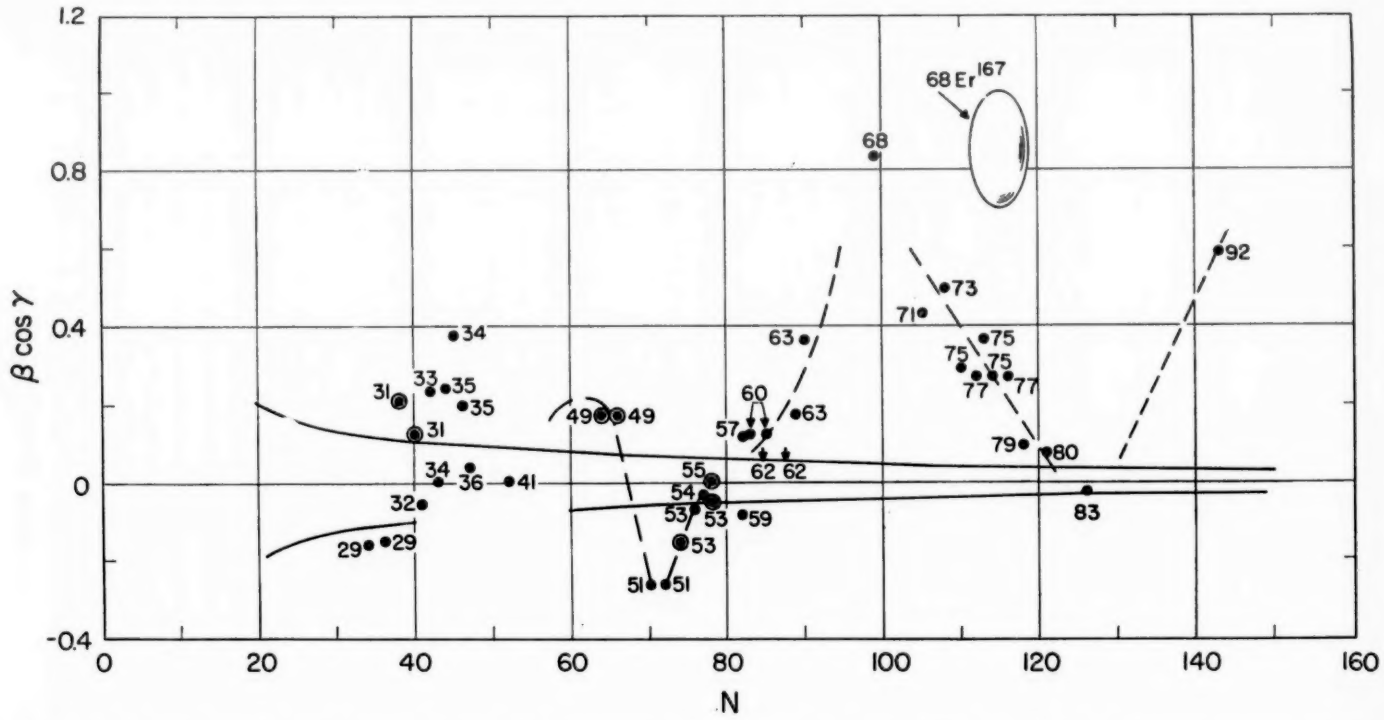

FIG. 3. Deformations deduced from static quadrupole moments. The deformation, $\beta \cos \gamma$ (equation 38) is plotted versus neutron number, and Z values are indicated by each point. A dashed line shows the approximately regular behavior of the deformation among the heavy nuclei. Most points are not accurate, errors being about 10 per cent to a factor two. Those points which are accurate to within a few per cent are doubly circled. The solid lines enclose the region the points would be expected to occupy if the moments were attributable to one or a few protons outside a spherically symmetric closed shell. The shape of the Er 167 nucleus, with a measured quadrupole moment of 10 barns, is illustrated. (However, transition rates suggest that this very large deformation may be spurious. See Fig. 4.)

nearly the same as the ground state, and to be connected by large quadrupole matrix elements to the ground state (for $\Delta I \leq 2$). Moreover, the theoretical treatment of $E2$ rates is very easy in the limit of large deformations.

The collective quadrupole operator for a homogeneous distribution of charge, defined by equations 1 and 2 is (analogous to equations 35),

$$Q_{2m}' = \varepsilon^{-1} \int_0^\infty \rho(r') Y_{2m}(\theta'\phi') r'^4 dr' d\Omega' \qquad 39a.$$

$$\simeq (5/4\pi) Z \langle r^2 \rangle \alpha_m', \qquad 39b.$$

where $\langle r^2 \rangle$ is defined by 36 for an arbitrary radial shape function, $f(x)$. Note that the normalizations of 39b and 35b are different: $Q_0 = 4(\pi/5)^{1/2} Q_{20}$. The factor of difference stems from the standard practice of defining the quadrupole moment in terms of $3Z^2 - r^2$, but the quadrupole transition operator in terms of $r^2 Y_{2m}(\theta, \phi)$.

Since the radial shape of the charge distribution enters only through the mean square radius, $\langle r^2 \rangle$, which is determined from other experiments, the problem is only to determine α_0' and $\alpha_2'(\alpha_{-2}' = \alpha_2', \alpha_{\pm 1}' = 0)$, the two independent deformation parameters in the body fixed system. One supposes, on the theoretical basis of the collective model, and the experimental basis of the symmetric top rotational energies proportional to $I(I+1)$, that in fact most nuclei with large deformations are cylindrically symmetric. Therefore $\alpha_2' = 0$, and $\alpha_0'(= \pm\beta)$ is the single deformation parameter determined by experiment. There is very little experimental information so far which bears on the interesting question whether there are nuclei with large but asymmetric deformations.

The theory of the fast $E2$ transitions of deformed nuclei is based on the collective theory of nuclear rotational states (97, 103, 104). The particle structure is assumed the same in initial and final state, and the relevant part of the nuclear wave function is written as the product [aside from symmetrization, For more detailed discussion, see reference (97)],

$$\psi \sim \phi^{\Omega, K}(\beta, \gamma) D_{MK}^I(\theta, \Phi, \psi). \qquad 40.$$

The function ϕ describes the vibration of the β, γ deformation parameters, D is the eigenfunction of a rigid rotator, with principle axes defined by Euler angles θ, Φ, ψ relative to space-fixed axes, and the quantum numbers are I, total angular momentum; M, Z-component of I; K, component of I along 3-axis of body-fixed system; and Ω, the component of extra-nucleon angular momentum along the 3-axis. In case the deformation is large, and the connected states belong to the same rotational band ($\Delta K = \Delta\Omega = 0$), the vibration function is unchanged, and only the angular function D_{MK}^I is important. This rotational factor in the wave function is not sensitive to the model. It would be the same for a rigid rotation as for an irrotational flow. The observed transition rates should therefore provide a measure of the deformation of charge, independently of the detailed nature of the rotational states.

The quadrupole operator in the spaced fixed system is

$$Q_{2m} = (5/4\pi) Z \langle r^2 \rangle \alpha_m, \qquad 41.$$

but the α_m are related to the body-fixed deformation parameters α_m', by

$$\alpha_m = \sum_k \overline{D}_{mk}^{(2)}(\theta, \Phi, \psi)\alpha_k', \qquad 42.$$

in which the $\overline{D}_{mk}^{(2)}$, the transformation functions of the spherical harmonics, are just the complex conjugates of the eigenfunctions of the rotator, except for a different normalization, and the α_k' are given by equation 3.

Following the notation of reference (97), we note that an electric quadrupole transition rate measures a reduced probability, $B_e(2)$, given by

$$B_e(2) = (2I_i + 1)^{-1} \sum_{M_i M_f m} |(f|\, eQ_{2m}\,|\, i)|^2 \qquad 43a.$$

$$= (2I_i + 1)^{-1} |(f\|eQ_2\|i)|^2. \qquad 43b.$$

The evaluation of the reduced probability involves, according to equations 40 and 42, integrals of the type

$$\int \overline{D}_{MK}^{I}\overline{D}_{mk}^{(2)}D_{M'K'}^{I'} \cos\theta d\theta d\Phi d\psi. \qquad 44.$$

Evaluations have been carried out, for example, by Bohr & Mottleson (97). For $\Delta K = 0$ (transition within a rotational band, the usual case), the results are

$$B(I \to I+1) = (5Ze/4\pi)^2[\langle r^2\rangle]^2\langle\beta\cos\gamma\rangle^2 \frac{3K^2(I+1+K)(I+1-K)}{I(I+1)(I+2)(2I+1)} \qquad 45.$$

and

$$B(I \to I+2) = (5Ze/4\pi)^2[\langle r^2\rangle]^2 < \beta\cos\gamma\rangle^2 \times \frac{3(I+2+K)(I+1+K)(I+2-K)(I+1-K)}{2(I+1)(I+2)(2I+1)(2I+3)}. \qquad 46.$$

The quantity $\langle\beta\cos\gamma\rangle$ means the matrix element of $\beta\cos\gamma$ between initial and final vibrational wave functions. It is this expectation value which, for large deformations, we refer to simply as the classically-defined nuclear deformation, $\beta\cos\gamma$. According to the theory of rotational states, the quantum number K is set equal to I_0, the lowest spin-value of the given rotational band (frequently the ground state spin). We further note the rule for the inverse transitions:

$$B(I \to I')/B(I' \to I) = (2I' + 1)/(2I + 1). \qquad 47.$$

The theory for transitions between different rotational bands is less clean cut, because the particle structure is in general expected to be changed. In case it is not, however, such transitions provide evidence on the asymmetry of the charge deformation. It is not certain whether such transitions have yet been observed. The general selection rule on the angular momentum projection quantum number is $\Delta K = 0, \pm 2$. For $\Delta K = 0$, the reduced probabilities are given by equations 45 and 46 and measure $\langle\beta\cos\gamma\rangle^2$. For $\Delta K = \pm 2$, the reduced probabilities measure $\langle\beta\sin\gamma\rangle^2$ and have the form:

$$B = \tfrac{1}{2}(5Ze/4\pi)^2[\langle r^2\rangle]^2\langle\beta\sin\gamma\rangle^2\Omega(I). \qquad 48.$$

The factors $\Omega(I)$ depending on the angular quantum numbers in the transition are given in Table IV for the cases that the transition begins or ends at the lowest member of one rotational band. These factors come from inte-

TABLE IV

ANGULAR FACTORS, $\Omega(I)$, REQUIRED IN EQUATION 48 FOR EVALUATION OF TRANSITION PROBABILITIES BETWEEN ROTATIONAL BANDS, IN CASE PARTICLE STRUCTURE IS UNCHANGED. INITIAL STATE IS $K=I$.

ΔK	I_f	$\Omega(I)$
+2	$I+2$	1
−2	$I-2$	$(2I-3)/(2I+1)$
	$I-1$	$4(2I-1)/(2I+1)(2I+2)$
	I	$12/(2I+2)(2I+3)$
	$I+1$	$96/(2I+1)(2I+2)(2I+4)$
	$I+2$	$576/(2I+1)(2I+2)(2I+3)(2I+4)$

grals of the type in equation 44, which may be evaluated, for example, by using the expression of the normalized D_{MK}^{I} functions in terms of Jacobi Polynomials:

$$D_{MK}^{I} = (2\pi)^{-1} \exp\left[iM\phi + iK\psi\right] \cdot \chi(\cos\theta), \tag{49a.}$$

$$\chi(x) = \eta(1-x)^{(1/2)\alpha}(1+x)^{(1/2)\beta} P_n^{(\alpha,\beta)}(x), \tag{49b.}$$

where $P_n^{(\alpha,\beta)}(x)$ is the Jacobi Polynomial as defined in reference (105), and the normalization constant is,

$$\eta = \left[\frac{2n+\alpha+\beta+1}{2^{\alpha+\beta+1}} \cdot \frac{n!(n+\alpha+\beta)!}{(n+\alpha)!(n+\beta)!}\right]^{1/2}, \tag{49c.}$$

and

$$\alpha = |M-K|, \quad \beta = |M+K|, \quad n = I - \tfrac{1}{2}(\alpha+\beta).$$

It should be stressed that the importance of the collective theory of rotational states in this discussion is just that it predicts that many nuclei have a classically definable angular shape (in general spheroidal) and provides a ready means to determine this shape from $E2$ transition rate measurements. Although the interpretation of the transition rates in terms of charge deformation rests on this theory of nuclear structure, it is, as pointed out earlier, insensitive to all details, depending only on the idea of rotational states.

Gamma decay.—Lifetimes of nuclear states undergoing $E2$ transitions have been measured for a number of nuclei among the heavy elements (97, 106, 107). The determination is limited to transition energies sufficiently small to make the lifetime measurably long, but this condition is satisfied for most of the low-lying rotational states of heavy nuclei. These lifetimes determine a charge deformation, β_E, within the limits set by the assumptions

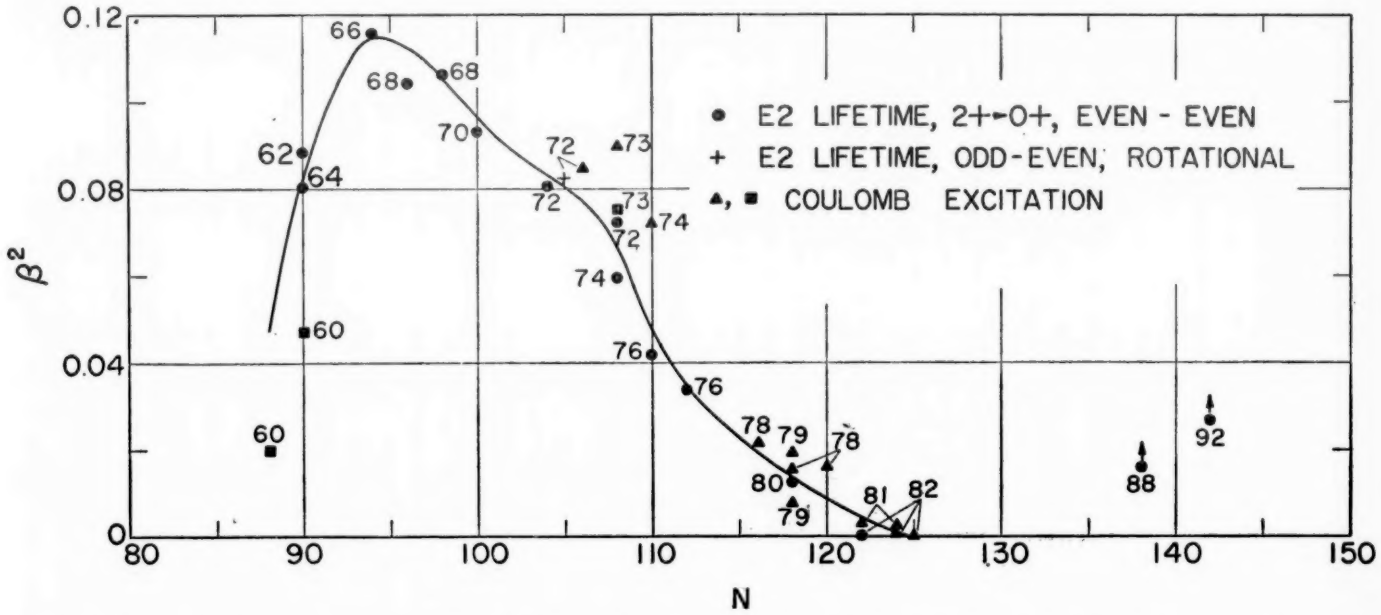

FIG. 4. Nuclear deformations determined from $E2$ transition rates, versus neutron number N. *Circles:* from directly measured lifetimes, as summarized in reference 107. *Squares:* from Coulomb excitation cross sections of Stelson & McGowan (110). *Triangles:* from Simmons *et al.*, [B. E. Simmons, D. M. Van Patter, K. F. Famularo & R. V. Stuart (*Phys. Rev.*, to be published)], and Huus & Zupancic (108). The nuclear electric radius is taken to be $1.20\times10^{-13}A^{1/3}$ cm. Errors are not indicated, but the direct lifetime measurements are, on the average, of higher accuracy.

above (rotational theory, direct particle contribution small), and with the further assumptions of cylindrical symmetry,

$$\beta_E^2 \equiv \langle \beta \cos \gamma \rangle^2, \qquad 50.$$

and of known mean square electric radius. From the available data, we plot in Figure 4, β_E^2 versus neutron number N, with mean square radius taken to be

$$\langle r^2 \rangle = (3/5)(1.20 \times 10^{-13} A^{1/3} \text{ cm})^2. \qquad 51.$$

The data is taken from a recent compilation by Sunyar (107), and his estimates of internal conversion coefficients are used. The deformation shows a very regular trend with neutron number in agreement with the trend from quadrupole moments (Fig. 3). The transition rates lead, however, to β^2 smaller by about a factor two than β^2 from quadrupole moments. (An exception is the quadrupole moment of 68 Er^{167}, for which the discrepancy is greater). According to Figure 4, $\beta^2_{MAX} \cong 0.12$ in the rare earth region, or $\beta_{MAX} \cong 0.35$. This corresponds to a nuclear shape $\sim[1+0.22\ P_2(\cos\theta)]$, which we shall call a 22 per cent deformation. The quadrupole moment of Er^{167}, if taken seriously, gives a 50 per cent deformation for that nucleus.

Coulomb excitation.—The process of electric excitation of nuclear levels has been exploited recently to measure the $E2$ transition rates of many transitions. The method is in a sense complementary to lifetime measurements, being most easily applied to fast $E2$ transitions (although the dependence of the excitation cross section on transition energy also favors low-lying levels). Also the Coulomb excitation process has the advantage of picking out almost exclusively the $E2$ rate between levels of the same parity, not being affected by the possible competition of $M1$ in the decay process (important in the odd-even nuclei).

Coulomb excitation cross sections have been measured by a number of workers (108 to 111). In particular, Temmer & Heydenburg (109), McGowan & Stelson (110), and McClelland, Mark & Goodman (111) have surveyed a large number of nuclear levels. Some results kindly furnished in advance of publication by McGowan & Stelson are included in Figure 4, reduced to the square of the nuclear deformation, β_E^2, according to the formulae 45 and 46 and the assumed relations 50 and 51, for the symmetry of the deformation, and for the electric radius. These results are seen to be in good agreement with deformations determined by lifetime measurements.

C. Isotope Shifts

The atomic isotope shift provides the most sensitive measure now available of the change of nuclear electric radius from one isotope to another. Specifically, the measured quantity is $\delta\langle r^{2\sigma} \rangle$ (equation 23), where $\langle r^2 \rangle$ is averaged over the radius and over angle. As discussed in section II, part C, the important role of nuclear compressibility in the phenomenon invalidates the isotope shift as an accurate way to measure nuclear electric radii. Since, however, the isotope shift depends on the angular shape as well as the radial

shape of the charge distribution, one may regard as known the radial shape, and seek to extract information from the isotope shift on the angular shape.

Brix & Kopfermann (73) first suggested that nuclear deformation might account for certain anomalously large isotope shifts (by more than a factor two) in the neighborhood of neutron number 90. Wilets further suggested that nuclear deformation might explain all of the anomalies, and the regular variation of the reduced isotope shift with neutron number. An analysis of isotope shifts from this point of view (83) confirmed the idea that all of the variation of anomaly with mass number could be accounted for in terms of the deformation of nuclear charge. Moreover, the isotope shift provides a measure of the change of nuclear deformation which is independent of uncertainty associated with the nuclear compressibility.

Consider the nuclear charge distribution defined by equations 1 and 2 and suppose that the deformation is spheroidal. Then $\alpha_{u'} = \beta \cos \gamma \delta_{\mu 0}$, and the mean value of $r^{2\sigma}[\sigma = \{1-(\alpha Z)^2\}^{1/2}]$ is given, to second order in β, by

$$\langle r^{2\sigma} \rangle = (4\pi\rho_0/Ze)\bar{r}_1^{3+2\sigma} \int f(x)x^{2\sigma+2}dx \times [1 + (8\pi)^{-1}(3 + 2\sigma)(2 + 2\sigma)\beta^2]. \quad 52.$$

Now the radial constant, $\bar{r}_1$, is independent of β only to first order [cf. equation 36, where second order terms were ignored]. To second order, the normalization of charge gives

$$1 = (4\pi\rho_0/Ze)\bar{r}_1^3 \int f(x)x^2dx[1 + (3/4\pi)\beta^2]. \quad 53.$$

A revised radial constant, $\bar{\bar{r}}_1$, is therefore defined such that $\rho_0\bar{\bar{r}}_1^3$ is a constant through second order in β:

$$\bar{\bar{r}}_1 = \bar{r}_1[1 + (1/4\pi)\beta^2]. \quad 54.$$

Substitution of equations 53 and 54 into 52 gives

$$\langle r^{2\sigma} \rangle = (\bar{\bar{r}}_1)^{2\sigma} \cdot \mathcal{R} \cdot [1 + (8\pi)^{-1}2\sigma(2\sigma + 3)\beta^2]. \quad 55.$$

where $\mathcal{R}$ is the ratio of two integrals over the radial shape function, $f(x)$:

$$\mathcal{R} = \int f(x)x^{2\sigma+2}dx \Big/ \int f(x)x^2dx. \quad 56.$$

Now we suppose that two isotopes of a given element differ in nuclear radius, or in central charge density ($\bar{\bar{r}}_1$ changes), and in deformation (β changes), but not in the radial shape of the charge distribution (R does not change). In that case, the change in $\langle r^{2\sigma} \rangle$, which is proportional to the isotope shift, is given by,

$$\delta\langle r^{2\sigma} \rangle = \mathcal{R}[\delta(\bar{\bar{r}}_1^{2\sigma}) + (\bar{\bar{r}}_1^{2\sigma})(8\pi)^{-1}2\sigma(2\sigma + 3)\delta\beta^2]. \quad 57.$$

In the second term within the brackets, the change of $\bar{\bar{r}}_2$ between the isotopes is ignored, since in general the fractional change of β^2 is much greater than the fractional change of $\bar{\bar{r}}_1$. The isotope shift has been calculated for spherical incompressible nuclei,—i.e., assuming $\beta^2 = 0$, and

$$\delta(\bar{r}_1^{2\sigma})/(\bar{r}_1^{2\sigma}) = (2\sigma/3)(\delta A/A).$$

If this model is called the "standard," then

$$[\delta\langle r^{2\sigma}\rangle]\text{st'd} = \mathcal{R}[\delta(\bar{r}_1^{2\sigma})]\text{st'd}, \qquad 58.$$

and the ratio of the observed isotope shift to the standard shift is just the ratio of the expressions in equations 57 and 58:

$$[(\text{Shift})_{\text{EXP.}}/(\text{Shift})_{\text{STD}}] = \{\delta(\bar{r}_1^{2\sigma})/[\delta(\bar{r}_1^{2\sigma})]_{\text{STD}}\} + \{(3/8\pi)A(2\sigma + 3)(\delta\beta^2/\delta A)\}. \qquad 59.$$

This discussion is a slight generalization of that given in reference (83) to include nonuniform charge distributions. The result, however, is not essentially altered. The ratio given by the left side of equation 59 has first been plotted by Brix & Kopfermann (73) who showed that the deviations of the ratio from unity are large but regular.

The right side of equation 59 breaks up very conveniently into two terms, one associated only with the change of mean charge density between the two isotopes, the other only with the change of deformation. All of the uncertainty coming from the nuclear compressibility comes in the first term. The ratio in the first braces in equation 59 should be less than 1. Experimentally, it appears to be about 0.64 for the heavy elements, which is in good agreement with what is expected for a reasonable nuclear compressibility, as pointed out in section II, part C. The final assumption required in order to interpret the isotope shifts in terms of nuclear deformation is that the value of the ratio in the first braces is nearly constant, or only slowly varying with A, among the heavy elements. This assumption would be wrong if, for example, shell structure effects caused a change in the average nuclear density among isotopes. However, it is the Coulomb energy which causes the ratio in question to be $\sim$0.64 instead of 1. Shell energies are smaller than Coulomb energies in the heavy elements and should therefore change this ratio by a lesser amount.

Within the framework of the assumptions outlined above, the change of nuclear deformation, $\delta\beta^2$, between isotopes can be found as follows. The ratio of observed isotope shift to the "standard" shift is plotted versus N or A. One reads off the ratio at several points where, on the basis of other evidence, $\delta\beta^2$ is expected to be nearly zero (e.g., near Pb 208 or at the maximum of β^2 versus N shown in Figures 3 and 4). These values should be (and are) nearly the same. They determine the value of the first braces on the right of 59. For the rest of the plotted points, the value of the first braces is taken to be the same, whence the values of the second braces, and therefore of $\delta\beta^2/\delta A$, are read off. Figure 5 shows a plot of $(\text{Shift})_{\text{EXP.}}/(\text{Shift})_{\text{STD.}}$, which differs from that given in reference (73) only in that the nuclear electric radius is here taken to be $1.20\times10^{-13}A^{1/3}$ cm. instead of $1.40\times10^{-13}A^{1/3}$ cm. Values of $\delta\beta^2/\delta A$ determined from this curve are plotted in Figure 6, together with the same quantity obtained by differencing values of β^2 plotted in Figure 4, where these are known for more than one isotope of a given element. The agreement is excellent in view of the magnification of error inherent in taking small differences of numbers from experimental sources. The marked asym-

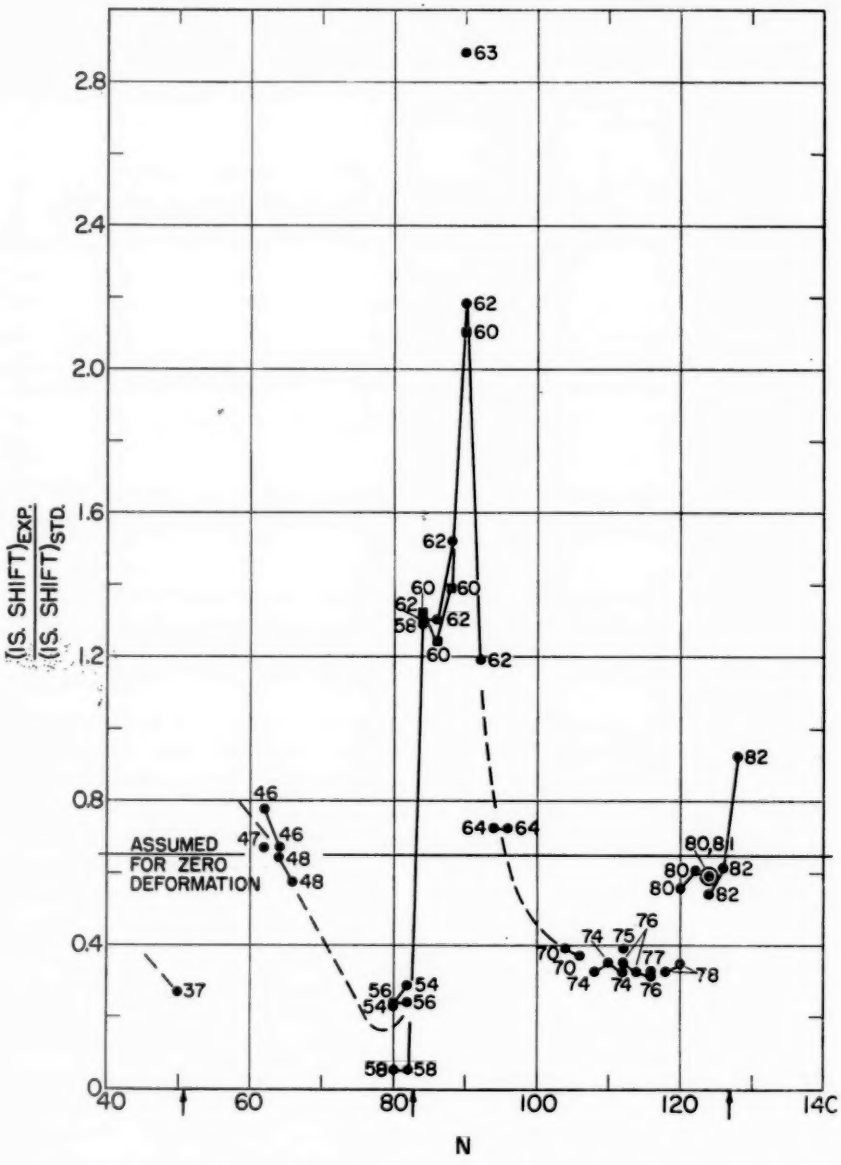

FIG 5. Ratio of observed isotope shift to "standard" shift for uniform density nuclei with $R=1.20\times10^{-13}A^{1/3}$, plotted versus neutron number N. Z values are indicated on graph. The assumed line of zero deformation is drawn in at ordinate 1.65. (The *Nd* points ($Z=60$) are only known relatively, but are included because they confirm the large anomaly at $N=88$ to 90.) Points are placed at the higher N value of each pair of isotopes.

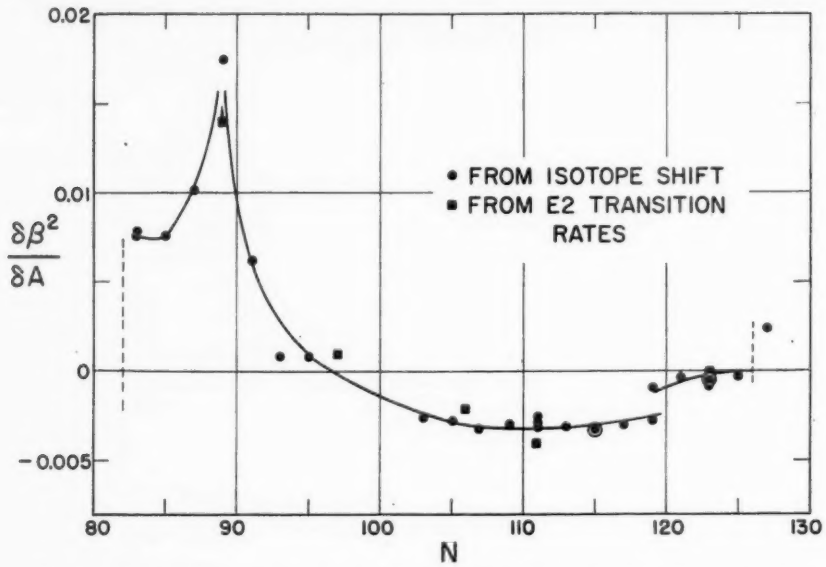

FIG. 6. Rate of change of nuclear deformation with mass number, versus neutron number, N. Circles are the derivatives $\delta\beta^2/\delta A$ evaluated from isotope shift data (Fig. 5). The squares are obtained by differencing the values of β^2 for fixed Z, which are calculated from $E2$ transition rates and illustrated in Fig. 4.

metry of this curve is attributable to the fact that large deformations develop very rapidly between neutron numbers 88 and 90, while the deformation falls off gradually and smoothly between $N=100$ and 120. The small discontinuity at $N=118$ is probably real, since it is seen also in the energies of the first excited state of even-even nuclei. The isotopes of Hg and Pb appear to be nearly spherically symmetric.

D. Mu-Mesonic x-Rays

Wheeler (15, 61) first pointed out that the effect of the quadrupole moment of the nucleus on the levels of the bound μ-meson might be quite appreciable, possibly of the same order as the fine-structure splitting in some cases, which amounts to several tenths of an Mev for heavy nuclei. He has calculated some quadrupole patterns, although the experiments have not as yet resolved the quadrupole effect. In interesting recent papers, Wilets (62) and Jacobsohn (63) have shown that the dynamic interaction of the μ-meson with a deformed nucleus is as important as the static interaction, and that, in addition, the dynamic interaction modifies the fine structure of the μ-meson even for even-even nuclei of spin-zero, for which, of course, the static interaction vanishes. This large effect comes about from the large electric quadrupole interaction of the μ-meson with the nuclear rotational states, which causes nuclear excitation with substantial probability by the cascad-

ing μ-meson. Wilets and Jacobsohn calculate typical fine structure patterns to be expected for $2P \rightarrow 1S$ μ-mesonic transitions. A particularly interesting feature is that this pattern depends on the sign of the intrinsic nuclear deformation (sign of cos γ), and affords the only method known at present which permits in principle the measurement of this quantity for even-even nuclei. From the calculations of Wilets and Jacobsohn it appears that, although individual lines of the fine structure pattern will not all be resolved with conventional techniques, the intensity patterns for positive and negative cos γ will be sufficiently different that a determination of the sign of the deformation will be possible without unreasonable demands on the experimental energy resolution of the γ-rays. Such measurements will be of great interest, since one anomaly of the large nuclear deformations in heavy nuclei not explained theoretically is the marked predominance of positive cos γ for the odd-even nuclei. As shown by Wilets and Jacobsohn, the order of magnitude of the deformation will also be determined by the $2P \rightarrow 1S$ fine structure pattern, but not with the accuracy expected of transition rate measurements.

E. Electron Scattering

A characteristic of the high energy electron scattering angular distributions from the highly deformed nuclei is a smoother variation with angle than is shown by the distribution from nearly spherical nuclei (112). It is reasonable to attribute this behavior largely to the averaging over angles of the highly deformed nuclear surface so that the radial distribution of charge which is effective in the scattering is more gradually tapered at the nuclear surface than in the case of spherically symmetric nuclei. One such calculation has recently been performed by Downs, Ravenhall & Yennie (113) for the element Ta^{181}, a nucleus whose charge deformation has been rather accurately determined by other means, and is large. The quadrupole effect on the scattering has been treated as a perturbation on the exactly calculated scattering for a spherically symmetric nucleus (113, 114). The large deformation of the nucleus perturbs the scattering in three ways: (*a*) The electrons which excite the nucleus to low-lying rotational states (137 Kev and 300 Kev in this case) and which are inelastically scattered are included experimentally as part of the elastic group [see Schiff (56)]; (*b*) The quadrupole field contributes to the elastic scattering. (This effect is averaged over orientations of the nucleus, i.e., over M values, and contributes only for $I \geqq 1$); (*c*) The deformation averaged classically over all angles extends and smooths the radial charge distribution. For even-even nuclei and for ideal energy resolution, this effect is the only one present and could not be distinguished from a change in the radial shape of the charge distribution. The effect of the subtraction of the inelastic electrons on the elastic amplitude is considered to be of negligible importance and is hence omitted in this discussion.

The measured angular distribution of 180 Mev electrons from Ta, together with fits made by Downs *et al.* (113) for various assumed nuclear deformations, are shown in Figure 7. The best fit to the data gives a value of

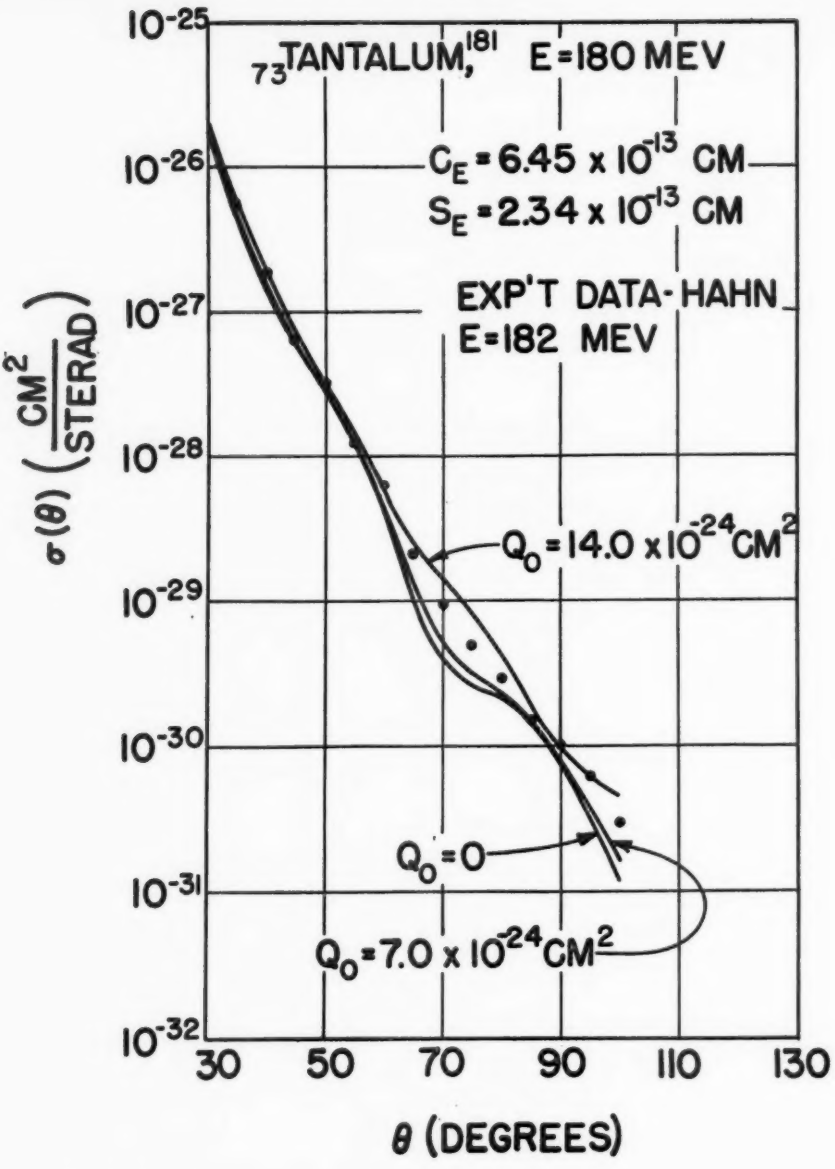

FIG. 7. Effect of nuclear deformation on scattering of high energy electrons. The charge distribution employed is that of equation 16, multiplied by $[1+\alpha P_2(\cos\theta)]$. The parameters c_E and s_E are the size and surface thickness parameters as given in equations 17, except that they are averaged over angle. (This figure kindly furnished by Downs, Ravenhall & Yennie (113) in advance of publication.)

intrinsic quadrupole moment of about 10 barns, in good agreement with other values for the same nucleus.

IV. OTHER EVIDENCE ABOUT NUCLEAR CHARGE DISTRIBUTION[2]

A. Nuclear Radius by Nonelectric Means

Most measures of nuclear size which utilize nuclear forces give radii $R \cong (1.4 \text{ to } 1.5) \times 10^{-13} A^{1/3}$ cm. These sources include total neutron cross sections at medium (115) and at high (116) energy, α-particle scattering (3 to 6), α-decay (117), and charged particle reaction rates (118). From angular distributions of low-energy neutron scattering, Emmerich (119) finds

$$R \cong 1.3 \times 10^{-13} A^{1/3} \text{ cm.}, \qquad 60.$$

while from analysis of high energy neutron cross sections, Brenner & Williams (120) obtain $R \cong 1.1 \times 10^{-13} A^{1/3}$ cm., smaller than any other nuclear force determination of radius. A recent careful analysis of proton scattering in the neighborhood of 20 Mev by Woods & Saxon (121, 122) has been carried out in terms of the complex well,

$$V = \frac{V_0 + iW_0}{1 + \exp k(r - R)}, \qquad 61.$$

and leads to perhaps the most reliable estimates of the radius of the nuclear potential. They obtain $R = 1.36 \times 10^{-13} A^{1/3}$ cm. and $k^{-1} = 0.5 \times 10^{-13}$ cm. (with $V_0 = 38$ Mev, $W_0 = 9$ Mev). Gatha & Riddell (123) find from an analysis of very high energy proton scattering, $R = 1.25 \times 10^{-13} A^{1/3}$ cm. Thus the nuclear force-determined radii, although quite scattered, seem to be predominantly from 5 to 20 per cent larger than the radius of the charge distribution. The evidence is that the nuclear potential strength becomes large at a radius where the charge density is only from 10 to 20 per cent of its value in the interior of the nucleus.

B. Nonelectric Measures of Nuclear Angular Shape

Rotational states.—The collective theory of nuclear rotational states (97, 103) has had remarkable qualitative success, and therefore its quantitative failure is surprising (103, 124). These facts seem well established for a number of heavy nuclei well removed from closed shells: (*a*) These nuclei have large deformations as deduced from the consistent evidence of several methods of measuring the deformation of charge; (*b*) These nuclei possess rotational states with energies given, very accurately in some cases, by

$$E_I = [I(I+1) - I_0(I_0+1)]\hbar^2/2\mathfrak{I}; \qquad 62.$$

(*c*) The moments of inertia, $\mathfrak{I}$, are approximately proportional to the square of the charge deformation,

[2] References included in this section are intended to be illustrative only, and by no means complete.

$$\mathfrak{I} = \text{const.} \times \beta^2. \qquad 63.$$

This detailed correlation of moments of interia and charge deformations is especially well-illustrated in a recent paper by Sunyar (107), who evaluates β^2 from lifetime measurements of $E2$ transitions. He finds that the qualitative form of the curves β^2 versus N evaluated from these two sources is very closely the same.

The quantitative failure arises in the magnitude of the proportionality constant in equation 63. It is easy to show that a classical spheroidal liquid droplet rotating about an axis perpendicular to its symmetry axis with irrotational flow possesses a moment of inertia,

$$\mathfrak{I} = 3B\beta \qquad 64.$$

where $B = \frac{1}{2}\rho_0 R^5$ for a uniform density droplet of mean radius R. The same result follows from the strong coupling limit of the collective model, the irrotational flow in this case stemming actually from the independent particle model. In the opposite limit of rigid body rotation we have

$$\mathfrak{I} = (16\pi/15)B, \qquad 65.$$

a constant. The approximate experimental proportionality of $\mathfrak{I}$ to β^2 therefore favors the irrotational picture. However, if equation 64 is used to fit the data, one obtains very large nuclear deformations,

$$\beta^2_{\text{rot}} = (6 \pm 2)\beta^2_{\text{charge}}. \qquad 66.$$

These deformations at the maximum are in fact unreasonably large. If taken seriously, they would require the inclusion of terms of higher than second order in β, and perhaps more complicated shapes than ellipsoidal. Indeed, such may be the case. Moszkowski & Townes (125), for example, have suggested that terms proportional to $P_4(\cos\theta)$ in the nuclear angular shape may be important and may account for the predominance of positive quadrupole moments.

A part of the discrepancy represented by the factor in equation 66 may be understood in terms of a neutron distribution larger than the proton distribution (126). The mass parameter B is proportional to $\langle r^2\rangle_{\text{mass}}$, and the factor of discrepancy in equation 66 should therefore be multiplied by $\langle r^2\rangle_{\text{charge}}/\langle r^2\rangle_{\text{mass}}$. Even if this correction factor is as small as $(1.20/1.40)^2 = 0.75$, a large discrepancy remains. Another explanation for the discrepancy has been offered, but not yet treated quantitatively. Teller & Wheeler (127) some time ago pointed out the role of symmetry conditions in nuclear rotation, made important by the finite number of particles. Brueckner (128) has recently suggested that analogous arguments may apply to deformed nuclei to prevent the occurrence of low-lying rigid body rotations, but to permit a semirigid body rotation in which only the displaced mass in the deformation participates. Although this is only a qualitative suggestion, it leads to the expectation that the moment of inertia might be proportional to β rather than to β^2, since the displaced mass is proportional to the first power of β. We put this idea to the test in Figure 8. According to the collective theory,

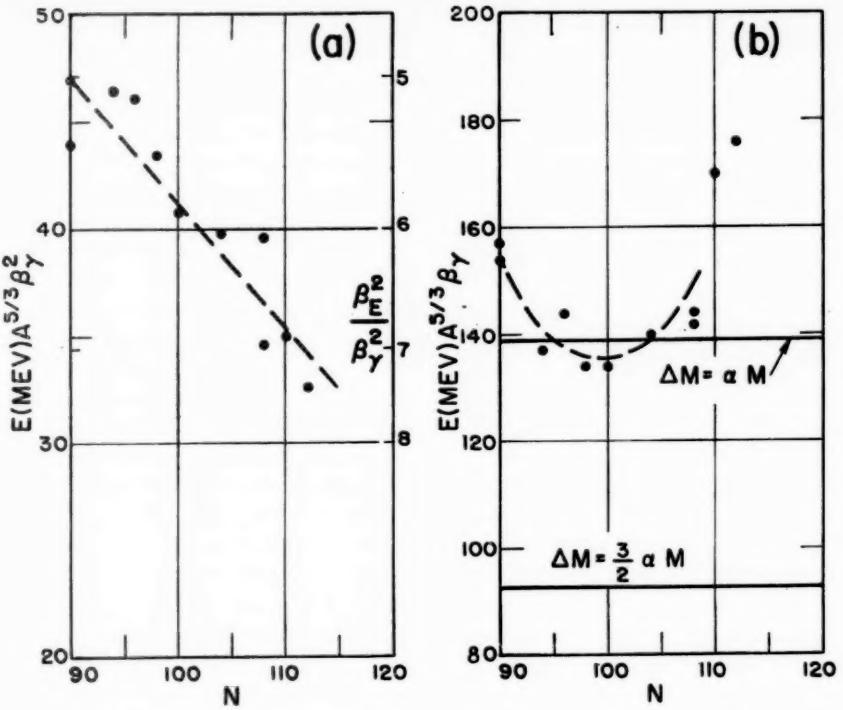

FIG. 8. Comparison of electric deformations and rotational moments of inertia. E is the energy of the first excited state of an even-even nucleus, only those states being selected which have the characteristics of rotational states. β_γ is the deformation of the nucleus determined by the lifetime for $E2$ γ-emission (107). (a) The quantity $EA^{5/3}\beta_\gamma^2$ is plotted versus N. This should be, according to the simple collective theory, a constant equal to 240 Mev. It shows instead a regular variation between a factor of discrepancy of about 5 and 7 given by comparing the deformations from the energies of rotational states with the deformations from γ-emission rates (shown on right hand scale). (b) The alternate hypothesis that the deformed "hump" on the nucleus rotates rigidly is tested. $EA^{5/3}\beta_\gamma$ is plotted versus N. Horizontal lines are shown for $\Delta M=\alpha M$ and $(3/2\alpha)M$, where ΔM is defined by the relation: moment of inertia, $I=\Delta MR^2$. R is taken to be $1.20\times10^{-13}A^{1/3}$ cm., and $\alpha=\beta(5/4\pi)^{1/2}$=fractional extension of radius along symmetry axis. Although the quantities vary somewhat, the order of magnitude of $EA^{5/3}\beta_\gamma$ is correct for a rigid rotation with $\Delta M=\alpha M$.

$EA^{5/3}\beta^2$ should be a constant for all deformed even-even nuclei (where E is the energy of the first excited state). Accordingly, we plot this quantity in Figure 8a for those nuclei whose deformation β has been independently evaluated by an $E2$ transition rate measurement [Sunyar (107], other measures (e.g., Coulomb excitation, quadrupole moments) being too inaccurate for this purpose. If instead the moment of inertia is linear in β, the quantity $EA^{5/3}\beta$ (Fig. 8b) should be constant, corresponding to a semirigid rotation

of the mass displaced by the deformation. (The $A^{5/3}$ factor is not expected to change, because it arises from the over-all proportionality of moment of inertia to MR^2.) From the figure it is evident that the latter assumption is at least closer to quantitative validity. This deviation of the rotational moment of inertia away from a proportionality to β^2, together with the large quantitative discrepancy, raises a major question of interpretation for nuclear theory. For the present discussion, however, we only need to note that it is probably necessary to discount the rotational energies as a measure of nuclear deformation and to accept the electrically-determined deformations, e.g., those shown in Figure 4.

Alpha decay.—The very strong dependence of α-decay rate on the Coulomb barrier thickness makes α-decay rates and angular distributions (from hypothetically aligned nuclei) sensitive to the nuclear deformation [Hill & Wheeler (96)]. Certain anomalously high decay rates among the rare earth α-emitters may be attributable to large deformations. Also, certain relative features of the α-decay fine-structure intensity in the heavy elements have been interpreted in terms of strongly deformed nuclei (129, 130, 131).These considerations, however, although interesting and important from the viewpoint of nuclear structure, do not lead at present to measures of the magnitude of the deformation.

Shell theory.—The deformation of nuclei is of great significance for nuclear structure and has received much theoretical attention. It is of interest to cite recent work which suggests that, in the near vicinity of closed shells, nuclei are unusually rigid, and the charge distribution is, therefore, very nearly spherically symmetric. The direct electric evidence from quadrupole moments favors this idea. The nucleus O^{17}, for example, has an extremely small quadrupole moment (102), and, at the other end of the periodic table, the nucleus Bi^{209} has a moment of the same order as a single proton (102). Goeppert-Mayer (98) has pointed out that, throughout the periodic table, quadrupole moments suggest a varying nuclear deformability which has minima near closed shells.

Indirect evidence for nearly spherical symmetry near closed shells comes from the quantitative success of several recent shell model calculations based on spherical symmetry: for example the work of Elliott & Flowers (99), and of Redlich (132), near ${}_8O^{16}$; the work of Levinson & Ford (101) near ${}_{20}Ca^{40}$; and the work of Pryce (see 100) and of True (133), near ${}_{82}Pb^{208}$. This work rounds out the picture of nuclear deformation, since the theories described in part III were applicable principally to nuclei with large deformations.

C. Theories of Nuclear Charge Distribution

Radial shape.—Early theories of the distribution of charge in spherically symmetric nuclei have been given by Feenberg (84) and by Wigner (134), and more recent discussions by Swiatecki (135) and by Born & Yang (136). These authors were concerned especially with the role of the Coulomb forces

in modifying the distribution away from uniform. Feenberg considered as well the difference between neutron and proton densities, amounting, for the heavy nuclei, to the order of 5 per cent fractionally. Swiatecki considered as well the finite thickness of the nuclear surface. Finite surface thickness attributable to particles in a well has also been considered by Gottfried & Weisskopf (137), and by Brueckner (138). It is interesting to note that the empirically-determined surface thickness is of the same order as these simple estimates. That is, one finds the charge to be as nearly uniform as is consistent with the finite wave length of the nucleons in the nucleus.

It is still undecided experimentally whether there exists an appreciable depression of charge density in the center of the nucleus. Evidence so far gives instead a uniform distribution in the nuclear interior. The fundamental energetic considerations of Feenberg, therefore, imply that the neutron distribution should be slightly peaked in the center of the nucleus. A similar conclusion has been reached by Born & Yang (136) on quite different grounds: that in the absence of Coulomb forces nuclear densities would be peaked at the center.

Not only should the central densities of neutrons and protons be slightly different, but their radial extents could also be different. Johnson & Teller (126) have suggested that the edge of the nucleus should be neutron-rich. Their argument is based on the idea that neutrons and protons see the same nuclear potential, but, of course, a different electric potential. Their argument would be weakened, but perhaps not invalidated, if a redistribution of neucleons is imagined, such that neutrons and protons do not experience the same nuclear potential.

A considerably more eleaborate theory of the radial shape of the nuclear charge distribution has been given by Gombas (139). He used a statistical treatment with only one adjustable parameter, the strength of the two-body interaction, but with several assumptions probably not in accord with experimental evidence: the assumption of a pure Majorana force, and of a Yukawa radial dependence. Nuclear binding energies and radii were well predicted over a wide range of A, but density distributions were peaked at the center of the nucleus with gradual tapering to the nuclear surface. In more recent work, Gombas has found that indeed the shape of the density distribution is somewhat sensitive to the radial dependence of the two-body force (140). He finds more nearly uniform distributions in approximate accord with experiment for two-body potentials which are finite at the origin (exponential and gaussian).

Angular shape.—The theories of nuclear angular shape have already been outlined in section III. The first quantitative treatment of nuclear deformation was given in the now classic Bohr-Wheeler (141) paper on nuclear fission. The role of deformations in quadrupole moments was pointed out by Rainwater (94), and theories of nuclear deformation emphasizing the dynamic aspects of nuclear vibration and rotation have been given by Hill & Wheeler (96), and by Bohr and Mottelson (97). The important theoretical

conclusions regarding the ground state deformation can be summarized as follows. The dominant mode of deformation should be ellipsoidal, and the lowest energy configuration should in general have cylindrical symmetry. Positive and negative deformations (prolate or oblate) should occur with about equal frequency (not borne out by experiment). For some nuclei, an approximate energy degeneracy of the oblate and prolate forms can result in a shape oscillation and an anomalously small observed quadrupole moment in spite of a large intrinsic deformation. There is no doubt experimentally that large deformations do occur. The theory of the mechanism for these deformations—the "pressure" of extra nucleons in unfilled shells—has not, however, received a direct check, and indeed the quantitative discrepancy in the energies of rotational states points to some failure of the theory. The mechanism of deformation postulated by the collective model is based on the independent particle model. It is to be noted that, even in the absence of an independent particle model, tensor forces could produce nuclear deformations. With independent particle motion, the tensor forces could, of course also produce deformation, with the regular shell structure behavior which is observed. These are qualitative remarks only, and magnitudes could be quite wrong. Yet the tensor force has a certain "threshold" property which fits with the rapid change of nuclear deformation sometimes observed. For a nucleus held in a spherical configuration by central forces, the tensor force averages to zero, but for a strongly deformed nucleus, the contribution of the tensor forces to the total binding might be quite appreciable. Thus the theory of nuclear deformation is still in an uncertain state, and experimental studies of the angular shape of the charge distribution remain, therefore, of fundamental interest.

REFERENCES CITED

1. Rutherford, E., *Phil. Mag.*, **21,** 669 (1911)
2. Rutherford, E., Chadwick, J., and Ellis, C. D., *Radiations from Radioactive Substances* (The University Press, Cambridge, England, 588 pp., 1930)
3. Farwell, G., and Wegner, H., *Phys. Rev.*, **93,** 356 (1954); **95,** 1212 (1954)
4. Blair, J. S., *Phys. Rev.*, **95,** 1218 (1954)
5. Wall, N. S., Rees, J. R., and Ford, K. W., *Phys. Rev.*, **97,** 726 (1955)
6. Eisberg, R., Igo, G., and Wegner, H., *Phys. Rev.* (To be published)
7. Bethe, H. A., and Bacher, R. F., *Rev. Modern Phys.*, **8,** 82 (1936)
8. Blatt, J. M., and Weisskopf, V. F., *Theoretical Nuclear Physics* (John Wiley & Sons, New York, N. Y., 864 pp., 1952)
9. Lyman, E., Hanson, A., and Scott, M., *Phys. Rev.*, **84,** 626 (1951)
10. Hammer, C. L., Raka, E. C., and Pidd, R. W., *Phys. Rev.*, **90,** 341 (1953); Pidd, R. W., Hammer, C. L., and Raka, E. C., *Phys. Rev.*, **92,** 436 (1953)
11. Paul, W., and Reich, H., *Z. Physik*, **131,** 326 (1952)
12. Pidd, R. W., and Hammer, C. L., *Phys. Rev.* (To be published)
13. Hofstadter, R., Fechter, H., and McIntyre, J., *Phys. Rev.*, **92,** 978 (1953)
14. Chang, W. Y., *Rev. Modern Phys.*, **21,** 166 (1949)
15. Wheeler, J. A., *Rev. Modern Phys.*, **21,** 133 (1949)
16. Fitch, V., and Rainwater, J., *Phys. Rev.*, **92,** 789 (1953) (References to earlier work here)
17. Cooper, L. N., and Henley, E. M., *Phys. Rev.*, **92,** 801 (1953)
18. Hill, D. L., and Ford, K. W., *Phys. Rev.*, **94,** 1617 (1954)
19. Hofstadter, R., *Phys. Rev.*, **94,** 773 (1954)
20. Hofstadter, R., Hahn, B., Knudsen, A., and McIntyre, J., *Phys. Rev.*, **95,** 512 (1954)
21. Hahn, B., and Hofstadter, R., *Phys. Rev.*, **98,** 178 (1955)
22. Racah, G., *Nuovo Cimento*, **8,** 178 (1931)
23. Rosenthal, J., and Breit, G., *Phys. Rev.*, **41,** 459 (1932)
24. Amaldi, E., and Fidecaro, G., *Phys. Rev.*, **81,** 339 (1951)
25. Kennedy, J. M., *Phys. Rev.*, **87,** 953 (1952)
26. Ferrari, F., and Villi, C., *Phys. Rev.*, **96,** 1159 (1954)
27. Rochester, G. D., and Wolfendale, A. W., *Phil. Mag.*, **45,** 980 (1954)
28. Hill, D. L., Freeman, B. E., and Ford, K. W., *Phys. Rev.* (To be published)
29. Rosenbluth, M., *Phys. Rev.*, **79,** 615 (1950)
30. Jankus, V. Z. (Personal communication)
31. Suura, H., *Phys. Rev.* (Accepted for publication)
32. Schwinger, J., *Phys. Rev.*, **75,** 898 (1949)
33. Schiff, L. I., *Phys. Rev.*, **92,** 988 (1953)
34. Feshbach, H., *Phys. Rev.*, **84,** 1206 (1951)
35. Bartlett, J. H., and Watson, R. E., *Proc. Am. Acad. Arts Sci.*, **74,** 53 (1940)
36. Feshbach, H., *Phys. Rev.*, **88,** 295 (1952)
37. Yennie, D. R., Wilson, R. N., and Ravenhall, D. G., *Phys. Rev.*, **92,** 1325 (1953)
38. Acheson, L. K., Jr., *Phys. Rev.*, **82,** 488 (1951)
39. Glassgold, A. E., *Scattering of High Energy Electrons by Nuclei* (Doctoral Thesis, Massachusetts Institute of Technology (1954) (Unpublished); *Phys. Rev.*, **94,** 757 (1954)
40. Bitter, F., and Feshbach, H., *Phys. Rev.*, **92,** 837 (1953)
41. Bodmer, A. R., *Proc. Phys. Soc.* (*London*), [A]**66,** 1041 (1953)

42. Yennie, D. R., Ravenhall, D. G., and Wilson, R. N., *Phys. Rev.*, **95,** 500 (1954)
43. Ravenhall, D. G., and Yennie, D. R., *Phys. Rev.*, **96,** 239 (1954); and *Phys. Rev.*, **98,** 277 (1955)
44. Schiff, L. I., *Phys. Rev.*, **98,** 277 (1955)
45. Elton, L. R. B., *Proc. Phys. Soc. (London)*, [A]**63,** 1115 (1950); [A]**65,** 481 (1952); and [A]**66,** 806 (1953)
46. Amaldi, E., Fidecaro, G., and Mariani, F., *Nuovo Cimento*, **7,** 757 (1950)
47. Guth, E., *Anz. Akad. Wiss. Wien. Math. naturw. Kl.*, **24,** 299 (1934)
48. McKinley, W. A., Jr., and Feshbach, H., *Phys. Rev.*, **74,** 1759 (1948)
49. Rose, M. E., *Phys. Rev.*, **73,** 279 (1948); **82,** 389 (1951)
50. Parzen, G., *Phys. Rev.*, **80,** 261 (1950); **80,** 355 (1950)
51. Smith, J. H., *Phys. Rev.*, **95,** 271 (1954)
52. Baranger, E., *Phys. Rev.*, **93,** 1127 (1954)
53. Yennie, D. R., Ravenhall, D. G., and Baranger, E., *Phys. Rev.*, **93,** 1128 (1954)
54. Smith, J. H., *The Scattering of High Energy Electrons by Heavy Nuclei* (Doctoral thesis, Cornell University, Ithaca, N. Y., 1951) (unpublished)
55. Thie, J. A., Mullin, C. J., and Guth, E. *Phys. Rev.*, **87,** 962 (1952)
56. Schiff, L. I., *Phys. Rev.*, **96,** 765 (1954)
57. Corben, H. C., *Phys. Rev.*, **94,** 787 (1954)
58. Lakin, W., and Kohn, W., *Phys. Rev.*, **94,** 787 (1954)
59. Mickelwait, A. B., and Corben, H. C., *Phys. Rev.*, **96,** 1145 (1954)
60. Wichmann, E., and Kroll, N. M., *Phys. Rev.* **96,** 232 (1954)
61. Wheeler, J. A., *Phys. Rev.*, **92,** 812 (1953)
62. Wilets, L., *Dan. Mat. Fys. Medd.*, **29,** No. 3 (1954)
63. Jacobsohn, B. A., *Phys. Rev.*, **96,** 1637 (1954)
64. Schwinger, J., *Phys. Rev.*, **75,** 651 (1949)
65. Smith, F. M., Birnbaum, W., and Barkas, W. H., *Phys. Rev.*, **91,** 765 (1953)
66. Rainwater, J., *Phys. Rev.*, **94,** 773 (1954)
67. Christy, R. F., and Keller, J. M., *Phys. Rev.*, **61,** 147 (1942)
68. Schawlow, A. L., and Townes, C. H., *Science*, **115,** 284 (1952)
69. Ford, K. W., and Hill, D. L., *Phys. Rev.*, **94,** 1630 (1954)
70. Townes, C. H., *Phys. Rev.*, **94,** 773 (1954)
71. Kroll, N. M., *Phys. Rev.*, **94,** 747 (1954)
72. Igo, G., and Wertheim, M. S., *Phys. Rev.*, **95,** 1097 (1954) (References to experimental work are given in this paper)
73. Brix, P., and Kopfermann, H., *Z. Physik*, **126,** 344 (1949); *Festschr. Akad. Wiss. Göttingen, Math-physik, Kl.* 17 (1951) (Other references here); *Phys. Rev.*, **85,** 1050 (1952)
74. Crawford, M. F., and Schawlow, A. L., *Phys. Rev.*, **76,** 1310 (1949)
75. Brix, P., and Frank, H., *Z. Physik*, **127,** 289 (1950)
76. Murakawa, K., and Ross, J. S., *Phys. Rev.*, **83,** 1272 (1951)
77. Brix, P., von Buttlar, H., Houtermans, F. G., and Kopfermann, H., *Nachr. Akad. Wiss. Göttingen Math.-physik. Kl.* 7 (1951)
78. Arroe, H., *Phys. Rev.*, **93,** 94 (1954)
79. Broch, E. K., *Arch. Math. Naturvidenskab*, **48,** 25 (1945)
80. Breit, G., Arfken, G. B., and Clendenin, W. W., *Phys. Rev.*, **77,** 569 (1950); **78,** 390 (1950)
81. Breit, G., *Phys. Rev.*, **86,** 254 (1952)
82. Humbach, W., *Z. Physik*, **133,** 589 (1952)
83. Wilets, L., Hill, D. L., and Ford, K. W., *Phys. Rev.*, **91,** 1488 (1953)

84. Feenberg, E., *Phys. Rev.*, **59,** 149 (1941); **59,** 593 (1941); and *Rev. Modern Phys.*, **19,** 239 (1947)
85. Brueckner, K., and Levinson, C., and Mahmoud, H., *Phys. Rev.*, **95,** 217 (1954)
86. von Weizacker, C. F., *Z. Physik*, **96,** 431 (1935)
87. Wilson, R. R., *Phys. Rev.*, **88,** 350 (1952) (References to experimental work here)
88. Ehrmann, J. B., *Phys. Rev.*, **81,** 412 (1951)
89. Feenberg, E., and Goertzel, G., *Phys. Rev.*, **70,** 597 (1946)
90. Jancovici, B. G., *Phys. Rev.*, **95,** 389 (1954)
91. Carlson, B. C., and Talmi, I., *Phys. Rev.*, **96,** 436 (1954)
92. Green, A. E. S., and Engler, N. A., *Phys. Rev.*, **91,** 40 (1953)
93. Townes, C. H., Foley, H. M., and Low, W., *Phys. Rev.*, **76,** 1415 (1949)
94. Rainwater, J., *Phys. Rev.*, **79,** 432 (1950)
95. Bohr, A., *Dan. Mat. Fys. Medd.*, **26,** No. 14 (1952)
96. Hill, D. L., and Wheeler, J. A., *Phys. Rev.* **89,** 1102 (1953)
97. Bohr, A., and Mottelson, B. R., *Dan. Mat. Fys. Medd.*, **27,** No. 16 (1953)
98. Goeppert-Mayer, M., paper on Nuclear Shell Theory, *Proc. Intern. Conf. of Theoretical Physics* (Kyoto and Tokyo, Japan, 1953), (Science Council of Japan, Tokyo, Japan, 970 pp., 1954)
99. Elliott, J. P., and Flowers, B. H., *Proc. Roy. Soc.* (*London*), [A] **229,** 536 (1955)
100. Alburger, D. E., and Pryce, M. H. L., *Phys. Rev.*, **95,** 1482 (1954)
101. Levinson, C., and Ford, K., *Phys. Rev.* (To be published)
102. Mack, J. E., *Rev. Modern Phys.*, **22,** 64 (1950)
103. Bohr, A., *Ph.D. Dissertation, Universitetits Institut for Teoretisk Fysik, Copenhagen: Rotational States of Atomic Nuclei* (Ejnar Munksgaards Forlag, Kobenhavn, Denmark, 55 pp., 1954)
104. Ford, K., *Phys. Rev.*, **90,** 29 (1953)
105. Szegö, G., *Orthogonal Polynomials* in *Colloquium Publications*, Vol. 23 (American Mathematical Society, Providence, R. I., 401 pp., 1939)
106. Goldhaber, M., and Sunyar, A. W., *Phys. Rev.*, **83,** 906 (1951)
107. Sunyar, A. W., *Phys. Rev.*, **98,** 653 (1955)
108. Huus, T., and Zupancic, C., *Dan. Mat. Fys. Medd.*, **28,** No. 1 (1953)
109. Temmer, G. M., and Heydenburg, N. P., *Phys. Rev.*, **96,** 426 (1954) (Other references there)
110. McGowan, F., and Stelson, P., *Phys. Rev.*, **99,** 112 (1955)
111. McClelland, C. L., Mark, H., and Goodman, C., *Phys. Rev.*, **93,** 904 (1954); **97,** 1191 (1955)
112. Hahn, B., and Hofstadter, R., *Phys. Rev.*, **98,** 278 (1955); Hahn, B., Hofstadter, R., Ravenhall, D. G., and Yennie, D. R., *Phys. Rev.* (To be published)
113. Downs, B. W., Ravenhall, D. G., and Yennie, D. R., *Phys. Rev.*, **98,** 277 (1955)
114. Yennie, D. R., Ravenhall, D. G., and Downs, B. W., *Phys. Rev.*, **98,** 277 (1955)
115. Coon, J. H., Graves, E. R., and Barschall, H. H., *Phys. Rev.*, **88,** 562 (1952)
116. Bratenahl, A., Fernbach, S., Hildebrand, R., Lieth, C., and Moyer, B., *Phys. Rev.*, **77,** 597 (1950)
117. Perlman, I., Ghiorso, A., and Seaborg, G. T., *Phys. Rev.*, **77,** 26 (1950)
118. Blaser, J. P., Boehm, F., Marmier, P., and Peaslee, D. C., *Helv. Phys. Acta*, **24,** 3 (1951)
119. Emmerich, W. S., *Phys. Rev.*, **98,** 1148 (1955)
120. Brenner, A., and Williams, R., *Mass. Inst. Technol. Prog. Rept. Lab. Nuclear Sci.*, p. 27 (1954)
121. Woods, R. D., and Saxon, D. S., *Phys. Rev.*, **95,** 576–77 (1954)

122. Saxon, D. S., *Elastic Scattering* (Report presented at Brookhaven Conference on Statistical Aspects of the Nucleus, January, 1955)
123. Gatha, K. M., and Riddell, R. J., Jr. *Phys. Rev.*, **86,** 1035 (1952)
124. Ford, K. W., *Phys. Rev.*, **95,** 1250 (1954)
125. Moszkowski, S. A., and Townes, C. H., *Phys. Rev.*, **93,** 306 (1954)
126. Johnson, M. H., and Teller, E., *Phys. Rev.*, **93,** 357 (1954)
127. Teller, E., and Wheeler, J. A., *Phys. Rev.*, **53,** 778 (1938)
128. Brueckner, K. (Personal communication)
129. Bohr, A., Froman, P. O., and Mottelson, B. R., *Dan. Mat. Fys. Medd.* (To be published)
130. Dresner, L., *Phys. Rev.* (To be published); Rasmussen, J. O., Jr., *Phys. Rev.* (To be published)
131. Christy, R., *Phys. Rev.*, **98,** 1205 (1955)
132. Redlich, M., *Phys. Rev.*, **95,** 448 (1954); *Phys. Rev.* (To be published)
133. True, W., *Phys. Rev.* (To be published)
134. Wigner, E., "Nuclear Masses and Binding Energies" (Paper presented at Univ. of Penna. Bicentennial Conf., Philadelphia, Penna., 1940); published in *Nuclear Physics* (Univ. of Pennsylvania Press, Philadelphia, Penna., 68 pp., 1941)
135. Swiatecki, W. J., *Proc. Phys. Soc.* (*London*), [A] **63,** 1208 (1950)
136. Born, M., and Yang, C. N., *Nature*, **166,** 399 (1950)
137. Gottfried, K., and Weisskopf, V. F., *Mass. Inst. Technol., Lab. for Nuclear Science, Prog. Rept.*, p. 27, Nov. 30, 1954
138. Brueckner, K., *Phys. Rev.* (To be published)
139. Gombas, P., *Acta Phys. Acad. Sci. Hungary*, **1,** 329 (1952); **2,** 223 (1952)
140. Gombas, P. (Personal communication)
141. Bohr, N., and Wheeler, J. A., *Phys. Rev.*, **56,** 426 (1939)

NUCLEAR RADIATION SHIELDING[1]

By E. P. Blizard

Oak Ridge National Laboratory, Oak Ridge, Tennessee

Preface

The building of nuclear radiation shields is a necessary part of preparing for most nuclear research. With the present emphasis on reactors and high-yield accelerators the shields are both thicker and more efficient by far than was the case fifteen years ago. Also, we are now much more conscious of the the dangers of radiation exposure and consequently take much greater pains to avoid them.

In spite of improved design, these larger shields are inevitably more expensive; they require greater space in buildings, which are themselves expensive; and they are inconvenient, for apparatus must be made to extend further between radiated and shielded locations. In addition, there are military applications for which the reactor and its shield must be mobile, light, and small. For these there is a strong incentive to develop the very best shield designs.

The changes are strongly noticeable throughout the laboratories of the world. The old shield walls of five-gallon water cans are nearly all gone. No longer is it possible to enter radiation areas without express permission of an operator. Shields are carefully checked for leaks or other inadequacies. There are federal regulations on permissible radiation levels outside radioactive materials as they are mailed or shipped. The philosophy that the shield is a simple adjunct which can be added nearly as an afterthought, and that it is cheaper to add another foot or two of concrete than to eliminate the need by careful design, is extant no longer. Instead, at least four handbooks and two textbooks are being written on the subject, and the material which is to fill these publications is much sought-after and largely heeded in modern design.

The present paper is in no sense designed to be a handbook but it is a report on the fundamental work which has been of most use in preparing the handbooks. The large body of work which has been done on the subject of radiation attenuation cannot possibly be described in a single review article, so only that which has been of use in the presently accepted shield design methodology will be treated and emphasis will be given to reactors, which present the greatest problem. Since no new physical phenomena are involved, interest in shielding lies in the end result. However, some of the work which must be done in the course of shielding research, such as the development of sensitive and special detectors and the invention of new mathematical techniques, will surely be more generally applicable. For example, methods of

[1] The survey of literature pertaining to this review was completed in March, 1955.

calculating attenuation of γ-rays and neutrons may apply to cosmic ray shower theory and vice versa.

The scope of the present treatment will include descriptions of the important radiation sources and of the individual attenuation processes. Following these are the calculations of attenuation in simple homogeneous shields as well as other problems in shield design, such as penetration after slant incidence, scattering, and the effects of voids in shields. Following this come some special methods for translating shield experiments into designs. Lastly, experiments and actual shield designs will be described briefly.

Introduction

Many modern shields, especially reactor shields, are required to attenuate by from 8 to 12 factors of ten. This fact alone sets the problem apart from most, for it means that the neutron or photon which penetrates the shield is extremely unusual. The average behavior of radiation may well be of little or no interest, for processes which are relatively uncommon may be just those for which the attenuation is least and the process may therefore dominate in penetration. An example of this lies in the prompt fission neutrons in a reactor. Most of these neutrons are born at about 1 Mev energy, and of course the behavior of the majority determines reactor criticality. On the other hand, most neutrons that escape from reactor shields are produced at energies in excess of about 7 Mev in spite of the fact that these constitute no more than about 2 per cent of all prompt neutrons. This fact comes about, of course, because of the general trend to lower cross sections with increased neutron energy.

The exact solution of the shielding problem is at present beyond the capabilities of even our best machines, except for the simplest cases. Approximate solutions based on semi-quantitative analysis, however, have been found for most problems. Analytic methods are required for calculation of most of the real situations, and they must be foreshortened for expedience. This is done by carefully examining the sources of radiation and the attenuation processes to determine which are most likely to be involved in the radiation which penetrates the shield. In addition to the more obvious mechanisms for shield penetration, there are special situations which arise from unusual designs. For example, a circulating fuel reactor will have delayed neutrons released in a heat exchanger and perhaps thereby activate a secondary coolant. If this is not taken account of in the design, the primary shield may well be nearly superfluous. For these reasons the first part of any design process consists of a careful examination of the radiation sources.

The Sources of Radiation

Since they are by far the most penetrating forms of radiations, only neutrons and γ-rays or x-rays are considered. The energy distribution is, of course, very important.

Prompt fission neutrons.—In the fission of U^{235} approximately 2.5 fast neutrons are released. For other fissionable isotopes the number varies

somewhat. The U^{235} thermal fission neutrons are distributed in energy according to an empirical formula suggested by Watt (1, 2):

$$N(E) = \sqrt{\frac{2}{\pi e}} \sinh \sqrt{2E}\, e^{-E} \qquad 1.$$

where $N(E)$ = number of neutrons per energy interval, Mev^{-1}, at energy E, Mev, per neutron produced, e = Naperian logarithm base, E = neutron energy, Mev.

The expression is not exact but appears to be accurate to about ± 10 per cent throughout the measured region from 0.075 to 17 Mev (1 to 5).

Delayed neutrons.—Delayed neutrons are not of importance in comparison with prompt neutrons except for those cases in which the reactor fuel is circulated out of the primary shield. They are released from certain fission products, each component being monoenergetic with a given radioactive half life. Hughes' collection of data (6, 7) is given in Table I.

TABLE I

DELAYED NEUTRONS

Half Life, sec.	Energy, kev	Absolute Yields per 10^4 Neutrons Emitted (prompt and delayed)		
		U^{235}	U^{233}	Pu^{239}
55.6	250	2.5	1.8	1.4
22.0	570	16.6	5.8	10.5
4.51	412	21.3	8.6	12.6
1.52	670	24.1	6.2	
0.43	400	8.5	1.8	11.9
Total		73.0	24.2	36.4

Prompt fission γ-rays.—In the fission of U^{235} prompt γ-rays are given off, some of which are quite energetic. These have been measured by Gamble (8, 9) to be distributed according to the following empirical formula:

$$N(E) = 8.2e^{-E} \qquad 2.$$

where $N(E)$ = number of photons per energy interval, Mev^{-1}, at energy E, Mev, per fission; E = energy of photon, Mev.

The expression above varies by as much as 30 per cent in places from the actual data. Gamble also reports the following interesting integrals which are obtained from his experimental data:

$$\int_{0.2}^{8\ \text{Mev}} N(E)\, dE = 7.59 \text{ photons/fission}$$

$$\int_{0.2}^{8\ \text{Mev}} EN(E)dE = 7.49 \text{ Mev/fission}$$

Fission product γ-rays.—The fission products are in many shielding problems the dominant source of γ-rays, although they are overshadowed as a source in a reactor core during operation because of their low energy. The most energetic common fission product γ-ray is from Rb^{88}, which emits a 2.8 Mev photon. The most successful fit to the fission product γ-emission data is that formulated by Way & Wigner (10):

$$\Gamma(t) = 1.26\, t^{-1.2}, \qquad 10 < t < 10^7 \text{ sec.} \qquad 3.$$

where $\Gamma(t)$ = γ-ray energy emission rate, Mev/sec., after one fission; t = time after fission, sec.

Two treatises are available which give the emission spectra as functions of reactor operation history for the total agglomeration of fission products. Moteff (11) has classed 24 nuclides according to energy and calculated the spectra, and Clark (12) has treated some 40 nuclides similarly except that he permitted each to retain its identity in the results of his calculation.

Secondary radiation sources.—On interaction with matter, neutrons cause secondary γ-rays to be emitted. These are either capture γ-rays or inelastic scattering γ-rays. Of the two, the former are generally the more important.

Capture γ-rays: A discussion of the neutrons capture process (96) and the concomitant release of capture γ-rays is out of place in this paper, except for a discussion of their importance in shielding. For this purpose, nuclides are classed according to the energy distribution and yield of their capture γ-rays as follows:

Class I: Following capture, the compound nucleus emits all or most of its excitation energy in a single transition, giving a predominant single hard γ-ray of energy equal or nearly equal to the neutron binding energy.

Class II: Several photons are given off per capture with the energy distributed between them so that the spectrum appears to cover the whole energy range up to the binding energy.

Class III: A charged particle is given off following capture, so that the capture γ-rays are weak or nonexistent.

In the first class there are many light elements, except that three light nuclides fall in the third class. In addition, the magic nuclei are in the first class, and, effectively, aluminum, iron, nickel, manganese, and copper fall into this category, although they do have multiple-photon emissions.

In the second class fall the more complicated heavy nuclei, although such intermediate elements as sodium, magnesium, silicon, phosphorus, sulphur, chlorine, potassium, and calcium are members.

The third class has two *bona fide* members, Li^6 and B^{10}. The former exhibits no capture γ-ray, and the latter only gives a single photon of 0.478 Mev in 93 per cent of the disintegrations (13). It is of interest to note, from a shielding point of view, that both these nuclides have large capture cross sections, which makes them useful for capture γ-ray suppressors, and they

are often added to shields just for this purpose. The third member of this class is N^{14}, which gives a proton and no capture γ-ray in 94 per cent of the captures. In other cases, it gives a total of 10.8 Mev in one, two, or more photons. Its capture cross section is low (1.7 barns) by comparison with lithium and boron. These properties mitigate the utility of nitrogen as a capture γ-ray suppressor, although in some special cases it may be useful in this respect.

Inelastic scattering γ-rays: Another important secondary source of γ-rays is the inelastic scattering of neutrons. This process is most important with heavy nuclei, for which the cross sections are high ($\sim$3 barns) and the thresholds for neutron energy are low ($\sim$200 kev for tungsten). Not enough experimental evidence is yet available to say with certainty just how these γ-rays are distributed in energy, but in general they would be expected to follow the same trend as the capture γ-rays. That is, the heavier nuclei will be expected to give more but softer photons than the lighter ones.

Interaction Processes

γ-rays.—It has been pointed out by Fano (14 to 16) and by Goldstein & Wilkins (17) that there are no less than 12 types of interaction of γ-rays with matter. Fortunately, only three of these need be studied in connection with shielding problems. The photoelectric effect dominates for low energy photons and high atomic number materials ($E \lesssim 0.15$ Mev for $Z=29$; $E \lesssim 0.5$ Mev for $Z=82$). Pair production is the dominant effect for high energy photons and high atomic number materials ($E>80$, 15, or 5 Mev for $Z=1$, 13, or 82, respectively). In the intermediate energy regions the Compton process is most important. Two excellent tabulations have been made of γ-ray cross sections by White (18) and by Davisson & Evans (19).

While a detailed discussion of the γ-ray interaction processes is left to the references, it is perhaps pertinent to mention the relative advantages from a shielding point of view of different materials. The cross sections per atom vary with atomic number for photoelectric, Compton, and pair-production processes, approximately as Z^5, Z, and $Z(Z+1)$, respectively. This means that on a weight basis the highest elements in the periodic table are best, but in the energy region in which the Compton process dominates, there is essentially no difference. An exception is hydrogen, for which $Z/A=1$, whereas for all other elements $Z/A \leqq \frac{1}{2}$. For low-energy γ-rays ($E \lesssim 0.1$ Mev) the weight advantage is very strong for high Z materials; for high energy ($E>5$ Mev) the advantage is definite but not so strong.

Neutrons.—The detailed cross section information which is needed for the calculation of neutron attenuation is not available. Nevertheless this pat excuse for lack of progress in neutron calculations is losing much of its original force. On one hand, our totality of cross section information obviously is increasing, and new techniques are being used for measurement in the energy region from 6 to 10 Mev (20), a most pertinent region which was barren for a long time. Also measurements of differential cross sections are beginning to appear (21 to 23). On the other hand, progress is being made in developing

the nuclear rationale on the basis of which predictions of differential cross sections are made. In addition to the many texts in the general field of nuclear physics, there has been a project at Nuclear Development Associates, Inc., under United States Atomic Energy Commission contract, for the collection, interpretation, and evaluation of fast-neutron experimental data in order to enable the prediction of cross sections in the region of interest for shielding (24). Unfortunately much of this work has been rendered obsolete by the newer "clouded crystal ball model" (25), but the latter will soon be applied to cross sections of interest in shielding.

An example of the filling in of experimental gaps by application of the theory is evident in the work of Goldstein (26) in deriving a complete picture of the oxygen cross section which he made preparatory to calculations of neutron penetrations in water (27).

As is implied above, it has been demonstrated that with fission sources the neutrons which penetrate thick shields have initial energies of the order of 8 Mev. This means that the cross section at this energy has particular significance. On this hypothesis, Welton & Albert (28) have shown that it is possible, using a single parameter, to describe the additional attenuation, introduced by lead and iron when slabs of these materials are added to a water shield. This parameter they called the "effective removal cross section." Subsequently many such cross sections have been measured at Oak Ridge National Laboratory, and a more definite definition has been given (29). A recent collection of removal cross section data by Chapman & Storrs (30) shows the close correspondence between the removal cross section and the total cross section for 8-Mev neutrons (Fig. 1). Roughly, it is found that the removal cross section, σ_{rem}, is about three-quarters of the total cross section:

$$\sigma_{rem} \cong 3/4\sigma_{\text{total, 8 Mev}} \qquad 4.$$

While this removal cross section applies well to slabs of material placed close to the source and followed by a thick (~120 cm.) water (or other hydrogenous) shield, other configurations are more common, e.g., those cases in which the material is distributed uniformly throughout the shield. While it is true that in general the cross section which applies in this case is about nine-tenths of that previously described, the situation is more complicated, and discussion is reserved for a later section.

The Attenuation of γ-Rays

Fundamental to all shielding problems is the calculation of the attenuation of radiation (neutrons or γ-rays) from a point isotropic or other simple source in an infinite homogeneous medium. This is of course only a start on the problem, for shields and their reactors are seldom homogeneous and never infinite. The effects of laminations, of boundaries, and of holes in the shield will remain after the simpler problem is solved.

The basic attenuation problem.—Given the attenuation coefficients it is a

simple matter to calculate the unscattered photon flux. Thus, for a point isotropic source in an infinite homogeneous medium, the uncollided photon number flux is:

$$N^0 = \frac{Se^{-\mu R}}{4\pi R^2} \qquad 5.$$

where S = source strength, photons per unit time; R = distance from source; μ = total linear absorption coefficient for γ-rays of the source energy in the medium.

It is because of those collisions in which photons are scattered and not absorbed that the usual calculation of γ-ray penetration is complicated. The

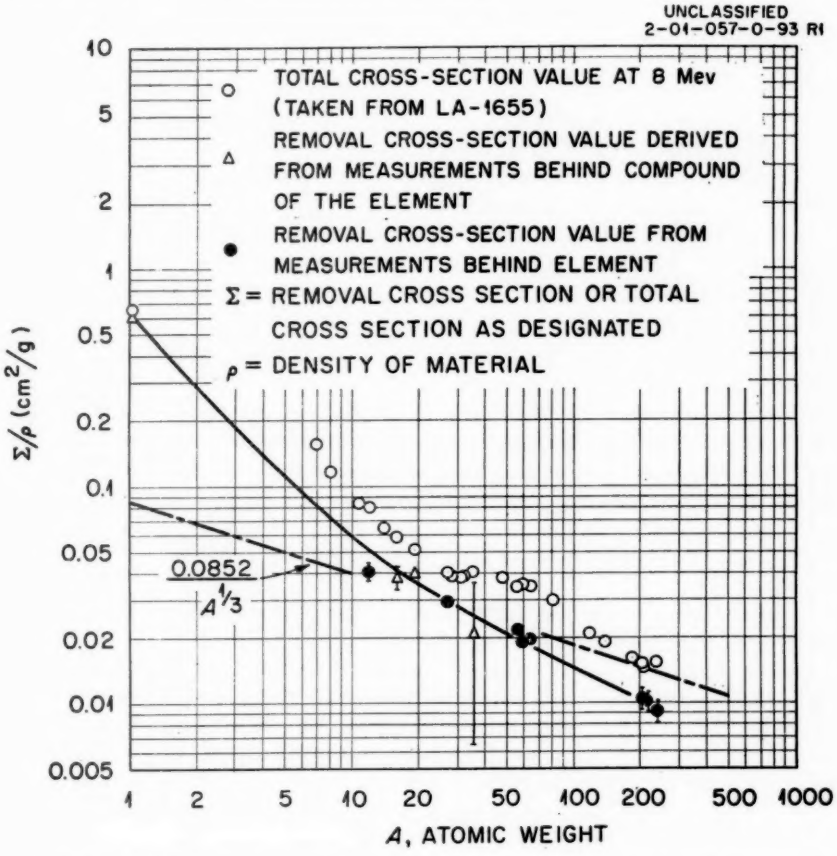

FIG. 1. Empirical mass attenuation coefficients for fast neutrons and comparable total coefficients for 8 Mev neutrons. (Total cross sections from *Los Alamos Scientific Report, LA-1655,* "Survey of Average Neutron Total Cross Sections from 3 to 13 Mev," by N. G. Nereson, S. Darden, E. Fryer, E. T. Jurney, O. Merrill, and M. M. Thorpe.)

totality of the complication is encompassed by the so-called buildup factor, which is the ratio of the actual intensity to that attributable solely to uncollided photons. Thus the photon number flux buildup factor is defined by the following equation:

$$N(R) = B(R)N^0(R) \tag{6.}$$

where N is the actual photon number flux for collided as well as uncollided photons.

It is common to define buildup factors for any of a number of measurable intensities, such as the energy flux, which is the product of the photon flux and photon energy integrated over all energies:

$$I(R) = B_E(R)I^0(R) \tag{7.}$$

where

$$I^0(R) = E_0N^0(R), \tag{8.}$$

$$I(R) = \int_0^{E<E_0} EN(R, E)dE + E_0N^0(R), \tag{9.}$$

E_0 = source energy per photon, assuming monoenergetic source; E = energy per photon of scattered radiation.

The dose, for which it is most common to calculate buildup factors, is the integral over all energies of the product of photon flux and energy and the energy absorption coefficient for air (or for tissue, which is about the same). This latter factor is the "poor geometry" attenuation coefficient and is variously defined, depending on the assumptions concerning secondary photons. The most common assumptions are that photoelectric and pair-production processes are genuine absorptions, i.e., that the fluorescent and annihilation radiations are absorbed almost at once and that the Compton-scattered photons are not. In this case the energy-absorption coefficient for source energy E_0 is:

$$\mu_a(E_0) = \mu_{\text{photo}}(E_0) + \mu_{\text{pair}}(E_0) + \int_{4\pi} \left(\frac{d\mu}{d\Omega}\right)_{\text{Compton}} \frac{E_0 - E}{E_0} d\Omega \tag{10.}$$

where $(d\mu/d\Omega)_{\text{Compton}}$ is the differential Compton cross-section per unit solid angle for scattering a photon of energy E_0 into a direction for which the scattered energy is E. The current practice is to define dose in terms of the rad, which is the amount of radiation which will deposit 100 ergs per gm. of material. There is no simple relationship between the dose as usually calculated for energy deposition in air and that for other materials. No great error is to be expected, however, in using air dose for tissue dose, since in both materials the Compton process dominates so that the energy depositions per gram will be about the same.

The calculation of buildup factors has been accomplished by approximations which yield extremely good results. The problem was first assayed by a number of different persons working independently, each group more or less unaware of the other's work. Perhaps the most notable feature of these early efforts is the "straight-ahead" approximation. In this, Compton scatterings

are assumed to degrade photons approximately correctly, but the angular deviation is ignored. This of course leads to an upper limit to penetration. The first such calculation was made by Grueling (31; see also 32). In addition to the "straight-ahead" assumption the Klein-Nishina formula for scattering cross section is replaced by a simpler function which allows separation of the pre- and postscattering energy variables. Grueling's choice for this latter approximation fits the slope and magnitude of the actual expression at the source energy. Others (33 to 37) have suggested different approximations which have met with varying degrees of success. These analytic approaches have by now been superseded in importance, particularly by the Spencer-Fano moments method (38, 39), their main contribution being the introduction of the linear approximation to the buildup factor, $B(R) \cong 1 + A\mu R$ where A is a factor of the order of unity. The approximation has since been shown to be crudely correct only for media which are primarily Compton scatterers, which is to say that it applies best to photon energies below the minimum in the total attenuation coefficient. This is, of course, not surprising since it is for this situation that the derivation was tailored.

The Spencer-Fano "moments" method (38, 39) of calculation of γ-ray attenuation, exploited so thoroughly by the groups at Nuclear Development Associates (17, 40) and the Bureau of Standards, has been by far the most prolific producer of attenuation data. This method therefore deserves a full description here. Unfortunately its complexity precludes this, but Goldstein & Wilkins (17) give a lucid and complete delineation of the method as well as most of the results.

The calculations are aimed at a calculation of the energy flux as a function of distance in an infinite homogeneous medium for certain simple sources or source distributions. Emphasis is put on accuracy at appreciable distances from the source, that is, from several to 20 mean free paths. The function which is of calculational interest is the angular energy flux,

$$I(\vec{r}, \vec{\Omega}, E) = EN(\vec{r}, \vec{\Omega}, E) \qquad 11.$$

where $N(\vec{r}, \vec{\Omega}, E)d\Omega dE dt dS$ is the number of photons of energy between E and $E+dE$, in solid angle $d\Omega$ about the direction $\vec{\Omega}$, passing in time dt through an element of surface dS located at $\vec{r}$ and perpendicular to $\vec{\Omega}$.

It is more convenient to use wavelength, λ, than energy and to describe the direction in terms of the cosine, ω, of the angle between photon direction and radius vector from the source. For the plane isotropic source, the transport equation is

$$\omega \frac{dI(x, \lambda, \omega)}{dx} + \mu(\lambda) I(x, \lambda, \omega) = \int_0^{\lambda} \int_{4\pi} I(x, \lambda', \omega') k(\lambda', \lambda) \frac{\delta(1 + \lambda' - \lambda - \cos\psi)}{2\pi} d\Omega' d\lambda' + S(\lambda, \omega)\delta(x) \qquad 12.$$

where x = distance from source plane; $k(\lambda', \lambda)$ = Klein-Nishina formula for Compton scattering; ψ = angle between Ω' and Ω (angle of scattering);

$S(\lambda, \omega)$ = source strength, photons per unit time per unit area of source plane. Of the two delta functions the first insures that the Compton relation between scattering angle and energy degradation is satisfied and the second insures that all the sources are in the plane $x = 0$.

The solution of this transport equation in a useful approximation has been adapted for use with the faster computing machines, and the SEAC at the Bureau of Standards was chosen for the work. The problem had to be reduced to manageable proportions and this was accomplished logically enough by concentrating the information to be obtained in the interesting spatial, angular, and energy regions. The angular energy flux is expanded first as a Legendre polynomial series:

$$I(x, \lambda, \omega) = \sum_{l=0}^{\infty} \frac{2l+1}{4\pi} I_l(x, \lambda) P_l(\omega) \qquad 13.$$

where

$$I_l(x, \lambda) = 2\pi \int_{-1}^{1} I(x, \lambda, \Omega) P_l(\omega) d\omega \qquad 14.$$

The zeroth moment, I_0, is the energy flux, and I_1 is the energy current density. If the transport equation (equation 12), is multiplied by $P_l(\omega)$ and an integration is carried out over all solid angles, a series of integro-differential equations is obtained which are satisfied by the coefficients I_l. Next it is noted that from a recursion formula for the Legendre polynomials it is possible to express ωI_l in terms of I_{l+1} and I_{l-1}, thus yielding a sequence of integro-differential equations in which the original direction variable ω does not appear.

The derivative in the transport equation is now eliminated by the introduction of spatial moments,

$$b_{nl}(\lambda) = \frac{\mu_0^{n+1}}{n!} \int_{-\infty}^{\infty} I_l(x, \lambda) x^n dx \qquad 15.$$

Thus multiplication of the equations which I_l satisfies by x^n and integration over all space yields, provided I_l satisfies certain convergence requirements, what Goldstein & Wilkins (17) describe as a "doubly indexed sequence of linear integral equations of Volterra type." Certain other simplifications are adopted, such as assuming monoenergetic sources and removing the delta function by transforming to spatial moments for the scattered flux alone. The integral equations are then solved for a chosen set of the moments. The desideratum is $I_0(x, \lambda)$, and this is obtained to good approximation from the $l = 0$ spatial moments up to about $n = 10$. The total necessary number of moments varies with the source geometry. It is necessary, in order to obtain a given moment b_{nl}, to first obtain $b_{n-1,\ l+1}$ and $b_{n-1,\ l-1}$. (The requirement is void when a negative index is indicated.) It is fortunate that in the case of the plane isotropic source about half the moments are identically zero owing to symmetry.

The reconstruction of the energy flux $I_0(x, \lambda)$ from the calculated mo-

ments must be carefully carried out, since for less than the complete set of moments the flux solution is not unique. Accordingly, the flux is expanded about a known function which is a reasonable approximation to the desired solution. For this function it is simplest to use the unscattered flux. Thus the total energy flux is equated to the product of the unscattered flux and a linear combination of appropriately chosen polynomials. Some polynomials which are well-suited for the expansion have been given by Spencer & Fano (38), and the appropriate coefficients are linear combinations of the spatial moments. The results of the work include dose buildup factors and energy spectra for the gamut of elements and photon source energies from 0.5 to 10 Mev. They have been compared with several experiments (41 to 45) and are found to agree extremely well.

A brief description of the results of Goldstein & Wilkins' calculations (17) is probably in order. For the lowest energy calculated, 0.5 Mev., the linear buildup factor is a fair approximation for an atomic number Z of between 30 and 40. For lower Z, the buildups are much higher, and for higher Z, much lower, as is to be expected on account of the strong Z-dependence of the photoelectric effect.

At 1 Mev, the linear buildup applies for elements with Z about 45 with the same, though not so drastic, changes with Z. At 2 Mev the linear buildup approximation is good only for large attenuations and $Z \sim 45$, and the photoelectric depression of buildup with increasing Z is much less evident, being strong only above about 40. At 4 Mev, in the low Z-region the trend is reversed (at large attenuations the buildup is maximum for $Z \sim 60$) because of the overriding importance of the variation of the Compton cross section slope in energy dependence. At 6 and 8 Mev there is a stronger maximum in the buildup factor at $Z \sim 70$ for large attenuations. For Z's greater than this the pair production cross section accounts for the lower buildup factor.

Taylor (46) has shown that it is possible to reproduce the buildup factor calculations of Goldstein & Wilkins (17) using a function which is the sum of two simple exponentials with three adjustable parameters which he has calculated to fit the original work. This is not merely interesting for the brevity of presentation it affords. The exponential form also makes integrations over sources which are distributed in space amenable to analytic attack.

Although the calculating machines were used to obtain the foregoing results, it has been possible to obtain some analytic expressions (47, 48, 49, 50) for the asymptotic trend in attenuation at very great penetrations. In general, the laws derived are the same as those of the "straight-ahead" approximation. It is also reassuring that for the case of lead the moment method and Spencer's semi-asymptotic calculation (48) for large attenuations "meet" with the same result.

An independent method for calculating γ-ray attenuation has been used by Peebles (50). In this work photons are classified according to the number of scatterings they have experienced, and the transport equation is solved successively for each component. The work would of course be prohibitive

if many scatterings were permitted and unreliable if too few were encompassed. The artifice by which this dilemma is circumvented is the division of the medium into many slabs, thin enough so that no more than three scatterings are likely, using the transmitted photons from one slab as the source for the next. The results of this method agree well with those from the moment method. It has not, however, enjoyed the wide acceptance of the latter, probably because the demonstration of its adequacy and reliability is somewhat more difficult. It does have the advantage, however, that angular distributions of photons are available from the results, and many useful calculations are presented for angles of incidence on the slab shield other than the normal.

Another technique for attenuation calculations is the stochastic, or Monte Carlo method (51, 52, 53). In this method, the histories of many particles (photons) are calculated, using the known cross sections and energy degradation laws. The probabilities for various events in the history (e.g., scattering through any angle, absorption, etc.) are known from the physical laws; particular events are chosen from equivalent possibilities in a random fashion so that if sufficient samples are taken the aggregate probability of shield penetration will be indicated by the fraction of histories in which penetration is the result. Since in most shields penetration is the rare exception, it is necessary to adjust the method so that the effort is concentrated on successful histories. If this is not done, either the work is prohibitive or the small penetration is not a reliable index of shield performance. To this end. photons are weighted according to their chance of penetration, and the calculations are concentrated on the most important histories. Unfortunately it is difficult to insure that the result is characteristic of the problem and not the chosen weighting function. The contribution of the method to the solution of the large attenuation problem has been essentially nil. On the other hand, it is extremely promising for special problems in which the geometry is complicated and the attenuation not great, e.g., for attenuations $\lesssim 10^4$. In this field it stands alone and promises to become more useful with current development. A significant success for the method is demonstrated in the recent work of Zerby (52) on the problem of attenuation of slant-incident γ-rays in two-region slab shields. The calculations agree very well with experiments by Kirn, Kennedy & Wyckoff (54), as well as Clifford *et al.* (55). The superiority of the Monte Carlo method for special problems is attested by the fact that Zerby's results include energy and directional distributions of the penetrating radiation.

An analytic calculation of the angular distribution of photons in a shield has not been carried out in many cases, but Spencer & Stinson (56) have calculated this quantity for Co^{60}-radiation in water. The moments method discussed above was applied, but more general polynomials were used which are solutions of third-order differential equations. The weighting function, instead of being the uncollided flux, is $(\mu_0 r)^l \exp(-\mu_0 r)$, where the power l is the previously mentioned Legendre index. Some experiments have been

performed at Oak Ridge National Laboratory (57) which seem to confirm the calculations. In addition, Certaine (58) has calculated the angular distribution of photons arising from plane isotropic and plane monodirectional sources. He has avoided the difficulty of slow convergence which the moments method exhibits for this calculation (attributable, for example, to a δ-function discontinuity in the angle ω in the first-scattered beam) by calculating first- and second-scattered photons separately. The analytic forms from the moment method for these components are then subtracted off, being replaced by the exact calculations. The calculations so performed are reported for several source energies and media and for penetrations up to 10 mean free paths.

Special γ-ray attenuation problems.—In practice the ideal conditions assumed in the foregoing discussion are seldom realized. As a consequence, various schemes are devised to obtain from the basic solutions reasonable estimates for the more difficult problems.

One complication is that the shield is always finite, and the solution is usually required in the region of the outer boundary. The effect of this termination is to remove the back-scattered radiation. Since this is seen intuitively to be low in number and energy, in view of the nature of the Compton scattering process, no correction is made with γ-rays for this effect. Measurements of γ-ray dose (59) in the region of the boundary of a water shield confirm this tenet. For materials of higher Z the effect would be even less.

Shields are not always made of a single element. The calculational methods such as the moments method can of course be applied to a homogeneous mixture of elements with cross sections from appropriately weighted contributions of the constituent elements. However, Goldstein & Wilkins (17) offer a convenient substitute method. They propose that the cross section of the mixture be approximated by that of some intermediate element for which the buildup factors are already calculated. It is demonstrated that for 2-Mev photons a 50 per cent by weight mixture of lead and water is well approximated by the element gadolinium for which $Z=64$. A moments method calculation for the mixture agrees to within a few per cent with the buildup for gadolinium up to 15 mean free paths.

If the shield is made up of successive layers of different materials the calculations by the moments method do not apply. Peebles' method (51) or a Monte Carlo method (52, 53) would, however, not be hampered by this feature, although no compilation of buildup factors for these cases is at hand or contemplated. (It would fill many handbooks.) The angular distributions of photons as calculated by Certaine (58) could be used to solve the problem of multilayered shields, since each region could be separately calculated, the leakage from one region serving as the source for the next. However, the complexity of the calculation is so great that such an effort is not warranted. Instead, rather simple rules of thumb are suggested.

For the case in which the last region is a fairly thick one (at least several mean free paths) it is reasonable to assume that the buildup is characteristic

of the material in the last layer and of the thickness in mean free paths of the whole shield. The defense of this assumption lies in the fact that, except for the case of quite low source energies, the harder scattered radiation is not greatly different in intensity relative to the unscattered component regardless of the atomic number of the medium. For this reason the harder built-up flux would be expected to be characteristic of the total shield attenuation. On the other hand, the softer built-up radiation is generated in rather a short distance, so that this, in which different Z materials differ the most, would be characteristic of the last layer.

The Attenuation of Neutrons

Until quite recently there was no counterpart for neutron attenuation calculations to the neat treatment of γ-rays by the Spencer-Fano moments method or any of its competitors. The reason for this lies largely in the uncertainties regarding cross sections which are only now beginning to clear. With the courage that stems from frustration, estimates in lieu of measurements are now being made (26) of the most likely differential cross sections for some elements found commonly in shields, and with these the moments method is now being applied to neutron attenuation calculations.

The basic attenuation problem.—As in the case of γ-rays, the fundamental calculation is for a point isotropic or other simple monoenergetic source in an infinite homogeneous medium. Again the physical dose is the quantity to be calculated, this being the energy deposited per unit weight of tissue. In the case of γ-rays the dose was rather closely related to the energy flux, that is, the convolution in energy and direction of photon flux and photon energy. The reason for this is that while the attenuation coefficient decreases with increasing energy, the average energy deposited per interaction increases strongly with photon energy so that the rate of energy deposition, or physical dose, closely corresponds to the energy flux. In the case of neutrons in tissue, the prime mechanism for absorption of energy is by elastic collision with protons. In the pertinent energy range of 2 to 10 Mev the cross section decreases nearly inversely with energy, whereas the average energy loss increases linearly with neutron energy. The result is that, unlike the γ-ray case, the neutron dose is roughly proportional to the number flux.

In the case of γ-rays the first attempts at analytic treatment of attenuation made use of the straight-ahead approximation, in which the energy degradation on interaction is treated correctly but angular deviation is ignored. For the case of attenuation of neutrons in hydrogen the same treatment has been applied, the justification being much the same as in the γ-ray case, namely that the significantly deviated neutrons are appreciably lower in energy and hence contribute little to the total transmission. Wigner (60, 61) has used this approximation to make an overestimate of the transmitted neutrons in a hydrogen shield. Young (62) has collected and compared much of this early work, demonstrating the feasibility of obtaining analytic solutions for specific assumptions regarding energy dependence of the hydrogen

cross section. Welton & Goertzel (63) have made some additional observations for the extension in which an isotropic scatterer is added to straight-ahead-scattering hydrogen, obtaining a form for the asymptotic distribution in energy as a function of distance. The straight-ahead approximation has been improved upon by Wick (64) who has derived expressions for the asymptotic form of attenuation, allowing some angular deviation of the neutrons. Welton (65, 66, 67) has extended this work and compared his results with experiments. This latter comparison, however, is somewhat clouded by the fact that Welton has used for his source a collimated plane distribution, whereas the experiments have been made with isotropic plane sources. Another rather more complete treatment by Holte (68, 69) has also shown the power of the Laplace and Fourier transform methods, comparing favorably with earlier experimental work. Tait & Biram (70) have calculated the neutron spectrum in a hydrogenous medium for the case of $1/v$ cross sections. They used the first two spherical harmonics and show this to give a reasonably accurate description of the spectrum.

Some of the early work on analysis of neutron attenuation by means of expansion in terms of the more familiar functions was carried out by Murray (71, 72, 73). He used the continuum theory for calculation of differential-scattering cross sections (74) and on the basis of this work was able to check by calculation a number of effective removal cross sections which had been measured at Oak Ridge National Laboratory (75).

The program of neutron attenuation computation at the Nuclear Development Associates, Inc. (NDA) (76, 77, 78), makes use of the Spencer-Fano moments method, with appropriate tailoring for the different cross sections. The first calculations were carried out on the SEAC, the computing machine at the National Bureau of Standards; later work was and will be calculated on the UNIVAC at New York University.

The first calculation (79) was for hydrogen, for which, of course, the cross section was well known. Aronson, in reporting the work, makes several interesting observations and comparisons. He verifies that the ~8-Mev neutrons in the fission spectrum are responsible for the penetrations to about 120 cm. (water equivalent hydrogen density), as is evident from the similarity in slopes in that region for a fission source and for an 8-Mev monoenergetic source. Comparison with a straight-ahead analytical calculation shows the latter to be only a slight overestimate. The comparison with Welton's (65) calculation was rather difficult because of the differences in hypotheses, but the two methods did not appear incontrovertibly to disagree, although the Welton buildup factors do seem to be lower at large penetrations.

The same method was used by Certaine & Aronson (80) of NDA to calculate the distribution of epithermal neutrons in water from a point isotropic fission source. The Goldstein oxygen data (26) and the Watt fission spectrum (1) were used. For this calculation direct comparison with experiment was possible since the work of Hill, Roberts, & Fitch (81, 82) was directly comparable. In so far as shielding theory is considered, the agreement is excellent.

It is interesting to note, however, that the neutron age, or one-sixth of the second spatial moment, was calculated to be 26 cm.², whereas the experiment gave 31 cm.². This discrepancy has been found before in other calculations (83) and implies that another experiment is in order. A calculation for 2.25-Mev neutrons by Volkin (84) gives 31.6 cm.², but that energy, while a mean for the fission spectrum, is not necessarily properly representative thereof for a calculation of the second spatial moment.

Of more direct interest to shielding are the subsequent calculations of penetration in water of monoenergetic (27) and fission (85) neutron sources. The calculations were carried out to 120 cm., which thickness is of considerable importance for many applications. The internal consistency and the agreement with measurements of Caswell (86) are impressive. For the low-energy end of the spectra an analytic treatment is used, and the spatial variation for these neutrons is taken to be that of the fast-neutron dose. For this analytical treatment, the calculation of energy variation amounts to that for the slowing down with a uniform distribution of sources, and this has a convenient analytic form because of the simplicity of the hydrogen slowing down, which of course predominates. The calculations again confirm the fact that the neutrons of about 8-Mev initial energy account for penetrations to 120 cm.

The removal cross section.—It has been observed (28) that the effect of insertion of thin slabs of materials into a water shield can be described in terms of a simple exponential attenuation factor. The material must be inserted near the source, and the thickness of water between source and detector must be greater than about 100 cm., 140 cm. being the usual distance chosen. Attenuation which is exactly exponential is characteristic of absorption processes alone. Of course in the case of fast neutrons other effects predominate, yet with a large thickness of water to filter out degraded or deflected neutrons a large fraction of the interactions are tantamount to absorption. These include all the inelastic scatterings and about half of the elastic scatterings. The equivalent absorption cross section which describes the effect of the inserted slab of material is called the effective removal cross section. It of course depends to some extent on the nature of the detector, the source (although a fission source is usually assumed, the concept has been developed independently and used by Moyer (87) for cyclotron shields), the thicknesses of water and sample, and the location of the latter within the shield. Fortunately it has been shown to be relatively independent of these factors within the limits described above, but an exact definition (29) has been used for purposes of uniformity and measurements are usually tailored as closely as possible to give the exactly defined quantity. Calculations by the moments method have recently been made by Goldstein & Aronson (88) to determine the equivalent removal cross section for elements added to a hydrogenous shield. These confirmed the validity of the concept and the approximations used heretofore.

Suppose a unit strength source of neutrons is located in an infinite water medium at some standard distance R_0 from a detector. The reading on the detector is then given by the kernel

$$G_0(R_0) = \frac{g_0(R_0)}{4\pi R_0^2} \qquad 16.$$

Now let there be inserted about the source a small sphere of the material whose removal cross section is to be measured. Its thickness (radius) is R_x, and the reading at R_0+R_x is now given by another kernel,

$$G(R_0 + R_x) = \frac{g_0(R_0)g_x(R_x)}{4\pi(R_0 + R_x)^2} \qquad 17.$$

The quantities $G_0(R_0)$, $G(R_0+R_x)$, R_0, and R_x are measured. From these can be found $g_0(R_0)$ and $g_x(R_x)$. $g_x(R_x)$ is assumed to be of exponential form, so that the macroscopic removal cross section is given by

$$\Sigma_x = \frac{\dfrac{dg_x(R_x)}{dR_x}}{g_x(R_x)} = \lim_{R_x \to 0} \frac{g_x(0) - g_x(R_x)}{R_x g_x(R_x)} = \lim_{R_x \to 0} \frac{1 - g_x(R_x)}{R_x} \qquad 18.$$

For measurement with R_x finite, as is of course necessary, the following is used:

$$g_x(R_x) = e^{-\Sigma_x R_x}$$

$$\Sigma_x = -\frac{1}{R_x} \log_e g_x(R_x)$$

Of course,

$$g_x(R_x) = \left(\frac{R_0 + R_x}{R_0}\right)^2 \frac{G(R_0 + R_x)}{G_0(R_0)} \qquad 19.$$

There are no point fission sources, but by irradiating a disk of uranium from the ORNL Graphite Reactor, the group at Oak Ridge National Laboratory have obtained a plane disk source which emits neutrons into an adjacent tank of water. At this facility, the so-called Lid Tank Shielding Facility (Fig. 2), many removal cross sections have been measured. For the slab geometry that is used there, transformations are required to interpret the data in terms of the exact quantities. For this, the kernels defined above are assumed to apply, the distance R_x being taken as the length in the slab measured along a ray between the detector and an element of the source. Integration of the kernel is then performed usually by some standard method (29, 30). It is found that the effective removal cross section does not in fact vary greatly with sample thickness up to thicknesses of five relaxation lengths (reciprocal macroscopic removal cross sections) and that the standard water thickness is not very critical, though care must be taken to avoid measurement of softer scattered radiation with large R_x and small R_0. In view of the near approach to equilibrium in the neutron spectrum it is possible to measure removal cross sections from thermal-neutron measurements, and these will be useful for predictions of fast-neutron dose attenuation. These cross sections have been shown to be additive for the case of several elements introduced together.

The foregoing applies to the case in which the material is added to a water shield in the region near the source. In many cases, however, the material

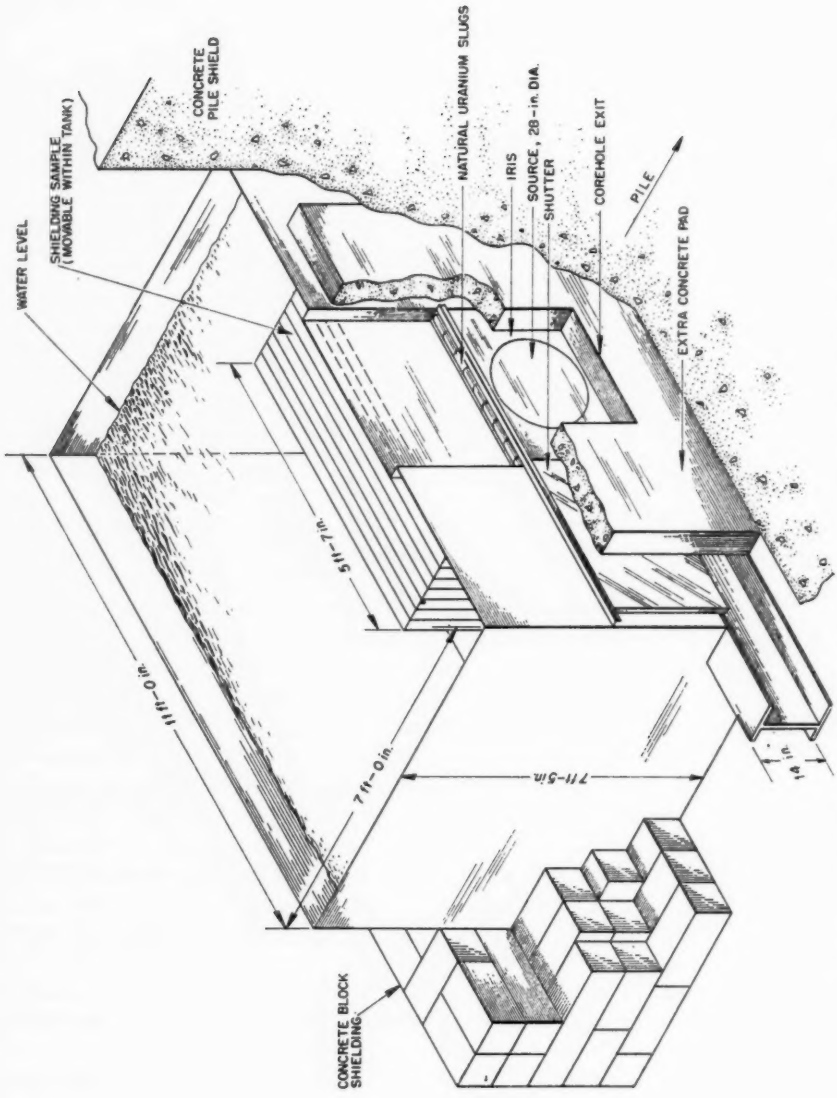

FIG. 2. Isometric view of Lid Tank Shielding Facility at Oak Ridge National Laboratory.

is added elsewhere. The most common other distribution is uniform. The effective removal cross section has been measured for distributed carbon by means of a saturated sugar solution, which is equivalent to water of normal density with about $\frac{1}{3}$ gm./cc. of carbon. For this measurement the removal cross section was nine-tenths of that for a slab of graphite next to the source. By comparing water and oil (CH_2) measurements it is possible to derive a similar quantity for oxygen, and this, too, appears lower for the distributed than for the close slab case. Attempts have been made to explain this difference, but none have been successful.

The concept of the effective removal cross section has been an extremely useful one, in that it affords a simple method of shield calculation which gives reasonably good answers and at the same time circumvents the expensive treatments by the moments method using a high-speed computing machine. In addition, of course, it is to be noted that the cross sections needed for the latter are mostly missing, whereas the removal cross sections are easily estimated if not already measured.

Up to this point it has been presupposed that the shield is largely water, or at any rate hydrogenous, and the other materials have been "added." At a sacrifice of exactness and some accuracy this concept can now be discarded, the attenuation being treated as exponential with the removal cross section defining the coefficient. There is, however, a limitation to this freedom which is paramount. For this method to apply, the attenuation of the fast neutrons must control the whole attenuation. The intermediate (circa 0.5 Mev) and lower neutrons must not be more penetrating than the fast neutrons from which they are produced; at least this must not be the case for the outermost regions of the shield. That this could be the case is evident from the behavior of a pure iron shield. For this the relaxation length of the fast neutrons is about 6 cm. The intermediate energy neutrons, on the other hand, are too slow to be further inelastically scattered, and too fast to be absorbed. Hence by a process of multiple elastic scatterings they diffuse outward, exhibiting a slowing down length in the neighborhood of 30 cm.

A more succinct way of putting the restriction is:

$$L_s < \frac{1}{\Sigma_x + \Sigma_y + \Sigma_z + \cdots} \qquad 20.$$

where $L_s^2 = 1/6\overline{r^2}$, $\overline{r^2}$ = second spatial moment of the slowing down density for a point source of neutrons of the controlling energy ($\sim$8 Mev), and the Σ's are the macroscopic removal cross sections of the different components of the shield material.

This requirement is easily met by the addition of hydrogen to a shield, and it is difficult to find shields without hydrogen which satisfy it. It is a matter of practical importance, too, for the best shields are those for which the fastest neutrons control, so the requirement should be met in any good shield design. It is obvious that diffusion at thermal or near-thermal energy

should not be appreciable either, but this requirement is met satisfactorily by almost all materials, so that it is never necessary for this purpose to add materials with high thermal-neutron absorption cross sections.

Because the total cross section of hydrogen varies so strongly with energy, any removal cross section ascribed to this element will be a function of R_0, which defines the amount of hydrogen in the shield. (Other hydrogenous materials are treated by rather obvious substitutions.) As a consequence, the hydrogen attenuation is usually treated separately, using either a measured attenuation kernel (89) or one of the NDA calculations.

Integration methods of neutron shield design.—Data on which to base neutron shield design appear either in the form of integral measurements for certain simple source distributions, such as the Lid Tank disk, or as a collection of removal cross sections which may be used in conjunction with hydrogen attenuation data. There are two general methods for using this information.

The Uniform Kernel Method: The simplest method to use is the homogeneous or kernel method (90, 91) for which the basic assumption is that there exists a unique attenuation kernel which describes the dose at every point in the shield (and on its surface) for each element of source and which is a function only of the separating distance. The conditions attendant upon this assumption are never actually met in practice. For example, the reactor core is never made of the same material as the shield, although their properties as regards fast-neutron attenuation may not differ much. The shield itself is seldom homogeneous and never infinite, and this introduces an error, for clearly the kernel is then a function of position as well as separation distance. Nevertheless, for fast neutrons at least, the kernel method gives reasonable results.

The method is used to predict the dose in one situation on the basis of a measurement in another. First it is necessary to determine the kernel itself or some basic form which serves to define the kernel. Suppose an infinite plane is uniformly endowed with sources of strength unity per unit area. The dose at a distance z from it is given by a simple integration:

$$D_{Pl}(z, \infty) = \int_{\text{plane}} G(R)ds = 2\pi \int_z^\infty G(R)RdR \qquad 21.$$

and

$$G(z) = -\frac{1}{2\pi z}\frac{d}{dz} D_{Pl}(z, \infty) \qquad 22.$$

For a finite disk source of radius a,

$$D_{Pl}(z, a) = \int_z^{\sqrt{z^2 + a^2}} G(R)RdR \qquad 23.$$

It is possible to relate the infinite plane result to a sum of disk source results by means of judicious choice of the integration limits. Thus

$$D_{Pl}(z, \infty) = \sum_{\nu=0}^{\infty} D_{Pl}(\sqrt{z^2 + \nu a^2}, a) \qquad 24.$$

and

$$G(z) = \sum_{\nu=0}^{\infty} B(\sqrt{z^2 + \nu a^2}) \qquad 25.$$

where

$$B(z) = -\frac{1}{2\pi z} \frac{dD_{Pl}(z, a)}{dz}$$

These relations are easily verified by writing down the integrals for the summands as indicated by equation 23.

It is also possible to show that for a spherical shell coated with unit strength source per unit area the dose is related to doses from plane sources as follows:

$$D_{sph}(b, a) = \frac{a}{b} \{D_{Pl}(b - a, \infty) - D_{Pl}(b + a, \infty)\} \qquad 26.$$

where a = radius of sphere, and b = distance from sphere center to detector.

By other similar relations, but often with approximations, it is possible to relate the dose in a given geometry to many others. This method is often used when full-scale experiments are available and when the reactor-shield complex is not too inhomogeneous.

The method suffers most in that it does not properly take into account the relative thicknesses of different shield layers for other than a point or plane source. The next method to be discussed attempts to do this.

The Method for Inhomogeneous Shields: Ascoli (92) has suggested a method of shield design in which the attenuation kernel is taken to be the product of an inverse square in the distance and an exponential whose exponent is the integrated number of relaxation lengths along the ray connecting source and detector. Thus,

$$G(R) = \frac{1}{4\pi R^2} exp\left(-\int_{ray} \Sigma_r(x, y, z)\, ds\right) \qquad 27.$$

where $\Sigma_r(x, y, z)$ = macroscopic effective removal cross section, assumed to vary arbitrarily with position in reactor and shield, and ds = element of length along the source-detector ray.

Simon (93) has demonstrated a convenient form for the dose in spherical geometry using Ascoli's kernel, for the case in which the macroscopic removal cross section of the shield is a function solely of the radial distance from reactor core center. This method has in general proved more flexible than the uniform kernel method, although the latter, when applicable, is much easier to use. Simon has also demonstrated a calculational method for determining dose from secondary radiation such as capture γ-rays from slowed-down fast neutrons. This is a logical extension of the Simon-Ascoli method.

The weakness in the Simon-Ascoli method lies in the question of whether

the number of relaxation lengths along the straight ray is a true index of the attenuation. In general, a line integral of the same integrand along another path is smaller than that along the ray. While there must be some penalty (in the sense that attenuation is a penalty on the radiation) ascribed to curvature (or bending) of the path of integration, it is quite clear that the Ascoli kernel must be in some sense an underestimate for other than homogeneous shields. In practice the method appears to give quite good results, for the apparent reason that most shields are nearly homogeneous for fast neutrons. When the method is applied to γ-rays it also can be expected to give nearly correct results, for in this case the degradation accompanying deflection puts a rather severe penalty on an appreciably curved path of integration.

It is important to note that both this method and the kernel method of shield design are equally applicable to γ-ray attenuation problems. They were devised, however, to apply to neutrons, for which there has been available until quite recently no more sophisticated analytical treatment. In the absence of microscopic data other than the removal cross sections these have been essentially the only methods.

Shields Which Have Been Built

The Brookhaven reactor shield (94) is one of the first shields to be designed and built with the post-war attention to cost. It has in general proved quite satisfactory, although its γ-ray attenuation is somewhat lower than was expected, a fact attributed to the large piece size of the steel aggregate that was used.

Another shield in which careful design was invested is that for the Materials Testing Reactor in Idaho. For this case a barytes aggregate portland concrete was used. This was the first application of an Ascoli-type kernel for shield design, antedating the work of Ascoli, who formalized the method and described its general applicability.

In general, it can be said that it is possible to design reactor and accelerator shields with a fair degree of confidence, but such special problems as voids in shields and unusual geometries, scattering, etc. are not sufficiently well understood to afford a rationale for their solution. There is a considerable amount of experimental data on ducts through cyclotron shields (95) but no universal theory connects the results.

LITERATURE CITED

1. Watt, B. E., "Energy Spectrum of Neutrons from Fissions Induced by Thermal Neutrons," *U. S. Atomic Energy Commission Document, AECD-3073* (1951, date declassified); based on *Los Alamos Scientific Lab. Rept., LA-718 (1948)* (Classified)
2. Watt, B. E., *Phys. Rev.* **87,** 1037 (1952)
3. Bonner, T. W., Ferrell, R. A., and Rinehart, M. C., *Phys. Rev.*, **87,** 1032 (1952)
4. Hill, D. L., *Phys. Rev.*, **87,** 1034 (1952)
5. Nereson, N., *Phys. Rev.*, **85,** 600 (1952)

6. Hughes, D. J., *University of Chicago, Metallurgical Lab. Rept., CF-3596* (1946) (Classified)
7. Hughes, D. J., Dabbs, J., Cahn, A., and Hall, D., *Phys. Rev.*, **73,** 111 (1948)
8. Gamble, R. L., "Fission Gamma-Ray Spectrum" (Physics Div. Semiannual Prog. Rept. for Period Ending September 10, 1953) *Oak Ridge Natl. Lab. Rept., ORNL-1620*, p. 15 (1953)
9. Francis, J. E., and Gamble, R. L., "Prompt Fission Gamma Rays" (Physics Div. Semiannual Prog. Rept. for Period Ending March 10, 1955) *Oak Ridge Natl. Lab. Rept., ORNL-1879* (1955)
10. Way, K., and Wigner, E. P., *Phys. Rev.*, **73,** 1318 (1948)
11. Moteff, J., "Fission Product Decay Gamma Energy Spectrum" (Aircraft Nuclear Propulsion Project) *General Electric Rept., APEX* 134 (1953)
12. Clark, F. H., *Decay of Fission Product Gammas, NDA-27-39* (Nuclear Development Associates, Inc. Rept., 1954)
13. Ajzenberg, F., and Lauritsen, T., *Revs. Mod. Phys.*, **24,** 321, esp. 351 (1952)
14. Fano, U., "Gamma-Ray Attenuation," (*Reactor Handbook*, Technical Information Service) *U. S. Atomic Energy Commission Document, RH-1*, p. 753 (1953) (Classified); *U. S. Atomic Energy Commission Document, AECD-3645* (August, 1955) (Unclassified version)
15. Fano, U., *Nucleonics*, 11(8), 8 (1953)
16. Fano, U., *Nucleonics*, 11(9), 55 (1953)
17. Goldstein, H., and Wilkins, J. E., Jr., "Calculations of the Penetration of Gamma Rays" (Technical Information Service) *U. S. Atomic Energy Commission Document, NYO-3075* (1954); previously issued by Nuclear Development Associates, Inc., as *NDA-15C-41*
18. White, G. R., "X-ray Attenuation Coefficients from 10 Kev to 100 Mev," *Nat. Bur. Standards Rept., NBS-1003* (1952)
19. Davisson, C. M., and Evans, R. D., *Revs. Mod. Phys.*, **24,** 79 (1952)
20. Nereson, N., and Darden, S., *Phys. Rev.*, **94,** 1678 (1954)
21. Jurney, E. T., Arnold, G. P., Schafer, W. D., Swickard, E. O., and Zabel, C. W., "Inelastic Collision and Transport Cross Sections for Some Light Elements," *Los Alamos Scientific Lab. Rept., LA-1339* (1951)
22. Jurney, E. T., and Zabel, C. W., *Phys. Rev.*, **86,** 594 (1952)
23. Walt, M., and Beyster, J. R., *Phys. Rev.*, **98,** 677 (1955)
24. Feld, B. T., Feshbach, H., Goldberger, M. L., Goldstein, H., and Weisskopf, V. F., *Final Report of the Fast Neutron Data Project, Rept. NYO-636* (Nuclear Development Associates, Inc., 1951)
25. Feshbach, H., Porter, C., and Weisskopf, V. F., *Neutron Reactions and the Formation of the Compound Nucleus, Rept. NDA-15B-4, NYO-3076* (Nuclear Development Associates, and Massachusetts Institute of Technology, 1953)
26. Goldstein, H., *Fast Neutron Data for Oxygen, Rept. NDA-15C-15* (Nuclear Development Associates, Inc., 1953)
27. Aronson, R., Certaine, J., and Goldstein, H., *Penetration of Neutrons from Point Isotropic Monoenergetic Sources in Water, Rept. NDA-15C-60, NYO-6269* (Nuclear Development Associates, Inc., 1954)
28. Albert, R. D., and Welton, T. A., *Westinghouse Electric Corp., Atomic Power Division Rept., WAPD-15* (1950) (Classified)
29. Blizard, E. P., *Oak Ridge Nat. Lab. Rept., CF-54-6-164* (1954) (Classified)
30. Chapman, G. T., and Storrs, C. L., *Oak Ridge Natl. Lab. Rept., ORNL-1843* (1955) (Classified); unclassified version to be issued later

31. Greuling, E., *Appendix A* in Bernstein, S., Preston, W. M., Wolfe, G., and Slattery, R. E., *Oak Ridge Natl. Lab. Rept., MonP-172*, p. 23 (1946) (Classified)
32. Nordheim, L. W., "Physics Division Report for Month Ending June 30, 1946," *Oak Ridge Natl. Lab. Rept., MonP-130*, p. 7
33. Bethe, H. A., *General Electric Nucleonics Project Report* (*Knolls*), *A-4251* (Classified) (1947)
34. Hirschfelder, J. O., Magee, J. L., and Hull, M. H., *Phys. Rev.*, **73,** 852 (1948)
35. Foldy, L. L., and Osborn, R. K., *Phys. Rev.*, **81,** 395, 400 (1951)
36. Bethe, H. A., Fano, U., and Karr, P. R., *Phys. Rev.*, **76,** 538 (1949)
37. Fano, U., *Phys. Rev.*, **76,** 739 (1949)
38. Spencer, L. V., and Fano, U., *Phys. Rev.*, **81,** 464 (1951)
39. Spencer, L. V., and Fano, U., *J. Research Natl. Bur. Standards*, **46,** 446 (1951)
40. Goldstein, H., and Aronson, R., *Status Report on Calculations of Gamma-Ray Penetrations, NDA-15C-1, NYO-3079* (Nuclear Development Associates, Inc., Rept., 1953)
41. White, G. R., *Phys. Rev.*, **80,** 154 (1950)
42. Dixon, W. R., *Phys. Rev.*, **85,** 498 (1952)
43. Elliot, J. O., Farrar, R. T., Myers, R. D., and Ravilious, C. F., *Phys. Rev.*, **85,** 1048 (1952)
44. Hayward, E., *Phys. Rev.*, **86,** 493 (1952)
45. Roys, P. A., Shure, K., and Taylor, J. J., *Phys. Rev.*, **95,** 911 (1954)
46. Taylor, J. J., *Application of Gamma Ray Build-up Data to Shield Design, Atomic Power Division Rept., WAPD-RM-217* (Westinghouse Electric Corporation, 1954)
47. Wick, G., *Phys. Rev.*, **75,** 738 (1949)
48. Spencer, L. V., "Penetration and Diffusion of x-Rays: Calculation of Spatial Distributions by Semi-Asymptotic Methods," *Natl. Bur. Standards U. S., Rept. NBS-1726* (1952)
49. Fano, U., *J. Research Natl. Bur. Standards*, **51,** 95 (1953)
50. Peebles, G. H., *Gamma-Ray Transmission Through Finite Slabs, R-240* (RAND Corporation Rept., 1952); previously issued as *Rept. RM-653*, Parts I (1951); II (1952)
51. Berger, M. J. (Five papers on applications of the Monte Carlo and moments methods were received too late for review; To be published by *National Bureau of Standards*, and subsequently by *Physical Review*.)
52. Zerby, C. D., "Preliminary Report on the Penetration of Composite Slabs by Slant Incident Radiation," *Oak Ridge Natl. Lab. Rept., CF-54-9-120* (1954)
53. Shor, S. W. W., *Nuclear Shielding Studies: V. Computation of Radiation Shield Thickness by the Monte Carlo Method, Technical Rept. No. 32* (Laboratory for Nuclear Science and Engineering, Massachusetts Institute of Technology, 1950)
54. Kirn, F. S., Kennedy, R. J., and Wyckoff, H. O., "Oblique Attenuation of Gamma-Rays from Cobalt-60 and Cesium-137 in Polyethylene, Concrete and Lead, *Natl. Bur. Standards Rept., NBS-2125* (1952)
55. Clifford, C. E., Blosser, T. V., and Watson, F. N., *Oak Ridge Natl. Lab.* (Private communication)
56. Spencer, L. V., and Stinson, F., *Phys. Rev.*, **85,** 662 (1952)
57. Blizard, E. P., Maienschein, F. C., Peelle, R. W., and Love, T. A., "Angular

Distribution of Photons from a Co^{60} Source in Water," *Oak Ridge Natl. Lab. Rept.* (To be published)

58. Certaine, J., *Angular Distribution of Photons from Plane Monoenergetic Sources, NDA-15C-10, NYO-3074* (Nuclear Development Associates, Inc., 1953)
59. Hungerford, H. E., *Oak Ridge Natl. Lab. Rept., ORNL-1611* (1954) (Classified)
60. Wigner, E. P., "Protection Against Radiation" (*Univ. Chicago Rept., CH-137* (No date)
61. Wigner, E. P., and Young, G., *Oak Ridge Natl. Lab. Rept., MonP-283* (1947) (Classified)
62. Young, G., *Oak Ridge Natl. Lab. Rept., MonP-293* (1947) (Classified)
63. Welton, T. A., and Goertzel, G., "Asymptotic Distribution of Neutrons from a Point Source in a Medium Containing Hydrogen and an Isotropic Scatterer," *Oak Ridge Natl. Lab., U. S. Atomic Energy Commission Rept., AECD-2796* (1949; declassified in 1950)
64. Wick, G. C., *Phys. Rev.*, **75**, 738 (1949)
65. Blizard, E. P., and Welton, T. A., *Oak Ridge Natl. Lab. Repts., ORNL-1133*, Parts I and II (1952) (Classified)
66. Blizard, E. P., and Welton, T. A., *Reactor Science and Technology*, **1**, No. 3, p. 15 (1951); *U. S. Atomic Energy Commission Rept., TID-73* (Classified)
67. Welton, T. A., and Blizard, E. P., *Reactor Science and Technology*, **2**, No. 2, p. 73 (1952), *U. S. Atomic Energy Commission Rept., TID-2002* (Classified)
68. Holte, G., *Arkiv Fysik*, **2**(48), 523 (1951)
69. Holte, G., *Arkiv Fysik*, **3**(14), 209 (1951)
70. Tait, J. H., and Biram, M. B., "The Calculation of the Spectrum of Neutrons at Points in a Semi Infinite Hydrogenous Medium, Whose Free Surface Is Irradiated by Monoenergetic Neutrons Falling Normally onto It," *British Atomic Energy Research Establishment Rept., A.E.R.E.T/M 92* (1953)
71. Murray, F. H., "Approximate Calculation of the Neutron Flux from a Plane Source in an Infinite Medium Where the Nuclear Cross Sections Vary with the Energy and with the Distance from the Source, for Energies above 5 Mev," *Oak Ridge Natl. Lab. Rept., ORNL-218* (1948)
72. Murray, F. H., *Oak Ridge Natl. Lab. Rept. ORNL-424* (1949) (Classified)
73. Murray, F. H., "An Approximate Calculation of the Neutron Flux in a Thick Shield Containing Some Heavy Elements, with the Aid of Certain Recurrent Relations Between the Coefficients in a Legendre Series Expansion," *Oak Ridge Natl. Lab. Rept., ORNL-748* (1950)
74. Murray, F. H., "Notes on the Calculation of the Attenuation of Neutrons Through Thick Shields," *Oak Ridge Natl. Lab. Rept., CF-53-11-64* (1953)
75. Murray, F. H., *Oak Ridge Natl. Lab. Rept., CF-53-12-60* (1953) (Classified)
76. Certaine, J., *A Solution of the Neutron Transport Equation, Introduction and Part I, NDA-15C-43, NYO-3081* (Nuclear Development Associates, Inc., Rept., 1954)
77. Certaine, J., *Integral Term for Elastic Scattering of Particles, NDA-15C-12* (Nuclear Development Associates, Inc., Rept., 1953)
78. Certaine, J., *A Solution of the Neutron Transport Equation, Part III, NYO-6270* (Nuclear Development Associates, Inc., Rept., 1954)
79. Aronson, R., *Neutron Penetration in Hydrogen, NDA-15C-39* (Nuclear Development Associates, Inc., Rept., 1954)
80. Certaine, J., and Aronson, R., *Distribution of Fission Neutrons in Water at the*

Indium Resonance Energy, NDA-15C-40 (Nuclear Development Associates, Inc., Report, 1954)

81. Hill, J. E., Roberts, L. D., and Fitch, T. E., "The Slowing Down Distribution from a Point Source of Fission Neutrons in Light Water", *Oak Ridge Natl. Lab. Rept., ORNL-181* (1948)
82. Hill, J. E., Roberts, L. D., and Fitch, T. E., *J. Appl. Phys.*, **26**, 1013 (1955)
83. Zweifel, P. F., and Hurwitz, H., Jr., (Address given at Shielding Information Meeting, Knolls Atomic Power Lab., May 13–14, 1954) *Technical Information Service Rept., WASH-174* (Classified)
84. Volkin, H. C., *J. Appl. Phys.*, **25**, 83 (1954)
85. Aronson, R., Certaine, J., Goldstein, H., and Preiser, S., *Penetration of Neutrons from a Point Isotropic Fission Source in Water, NDA-15C-42, NYO-6267* (Nuclear Development Associates, Inc., Rept., 1954)
86. Caswell, R. S., Gabbard, R. F., Doering, W. P., and Padgett, D. W., *Phys. Rev.*, **94**, 786 (1954)
87. Moyer, B. J., University of California (Private communication)
88. Goldstein, H., and Aronson, R., *Effective Removal Cross Sections Theory, TID-2015*, p. 147 (1954) (Classified)
89. Maienschein, F. C., "Attenuation by Water of Swimming Pool Reactor Radiations," *Oak Ridge Nat. Lab. Rept., ORNL 1891* (1955)
90. Blizard, E. P., *Oak Ridge Nat. Lab. Rept., CF-51-10-70*, Parts I and II, Revised (1952) (Classified)
91. Blizard, E. P., "Reactor Leakage for Shielding Calculations," *Oak Ridge Natl. Lab. Rept., CF-53-7-170* (Revised) (1953)
92. Ascoli, G., Appendix XV in *U. S. Atomic Energy Commission Document, ANP-52*, 196 (1950) (Classified)
93. Simon, A., Chapter III-B-1 in *Oak Ridge Natl. Lab. Rept., ORNL-1575*, 67 (1954) (Classified)
94. Pratt, W. W., Fox, M., Kouts, H. J., and Rand, A. C., *Brookhaven Natl. Lab. Rept., BNL-145* (1951) (Classified)
95. Crawford, J. W., and Kintner, E. E., "Experiments to Determine the Effect of Ducts on the Attenuation of Neutrons and Gamma Rays in the M.I.T. Cyclotron Shield," *Neutron and Gamma Ray Shielding Group and Electronic Nuclear Instrumentation Group Quarterly Prog. Rept., April–June, 1950*, p. 10
96. Mittelman, P. S., and Liedtke, R. A., *Nucleonics* **13**(5), 50 (1955)

NUCLEAR REACTIONS OF INTERMEDIATE ENERGY HEAVY PARTICLES[1]

By D. C. Peaslee

Department of Physics, Purdue University, Lafayette, Indiana

Introduction

Heavy-particle reactions at intermediate energies have been an important part of nuclear physics since its early days, but lately this sub-field has taken on special interest. The impetus for recent developments derives largely from experiment, with theoretical interpretation still in the process of following after the fact. Since activity in this field appears to be scarcely, if at all, past its peak, the present review can be only a sort of interim report. Enough progress has already been made, however, so that a survey of the present position seems worth while.

The general tenor of recent studies has been that the statistical model (1, 2, 3) of nuclear reactions is of less universal validity than has usually been assumed. Whether this also reflects a failure of the compound nucleus model (3) seems largely a matter of semantics. The original formulation of the concept (3) contained two distinct parts: the notion that the incident particle amalgamated into a compound state by relatively rapid (10^{-20} sec.) sharing of the incident energy among all the nucleons in the nucleus; and that at lower energies were to be found individual, isolated "resonances" or quasi-stationary (eigen-) states of the compound system. The first picture of rapid diffusion of excitation energy through the nucelus is essentially a classical one; according to the correspondence principle, this can be represented quantum mechanically only as a sum over many eigenstates. For an individual resonance level, no such classical picture is permissible: it is simply an eigenstate of energy E, with time dependence given by a multiplicative factor $\exp(-iEt/\hbar)$. It is not possible to make any measurement of time-dependent processes, like the diffusion of energy, on this state alone. The classical, energy-sharing picture of the compound nucleus applies only at high enough excitation that the compound nucleus is represented mathematically as a sum over many individual eigenstates.

In the original formulation (3) this sum was not performed explicitly, but intuitive arguments were used to predict the expected results of such a summation: the incident energy would be rapidly divided among all the nucleons, and

> for some time afterwards ($\gg 10^{-21}$ sec.) no single particle will possess sufficient kinetic energy to leave the nucleus. The possible subsequent liberation of a proton or an α-particle or even the escape of a neutron from the intermediate compound system will therefore imply a complicated process in which the energy again happens to be concentrated on some particle at the surface of the nucleus . . . breaking up of this

[1] The survey of literature pertaining to this review was concluded in March, 1955.

intermediate system by the ejection of a material particle, or its passing with the emission of radiation to a final stable state, must in fact be considered as separate competing processes which have no immediate connexion with the first stage of the encounter. (3).

Subsequent theoretical investigation (4, 5) has made it clear that the idea of resonant eigenstates of the compound system can be developed to the point of providing a complete mathematical framework for describing any nuclear process. In exactly the same sense that any nonpathological function can be expanded in a Fourier series with appropriate coefficients, any nuclear process can be represented as occurring through a series of resonant states, again with appropriate coefficients. In this mathematical sense, therefore, the compound nucleus (eigenstate) model has universal validity.

Unfortunately, but necessarily, any such mathematical framework does not of itself contain any physical information about the nucleus: this must be inserted in the guise of the resonant-state expansion parameters. For comparison with measurements not made at an individual resonance (which is perforce the case except for the lowest energies or lightest nuclei) some average must be taken over the many contributing eigenstates. The simplest way of doing this is to assume no correlation between neighboring eigenstates. This leads to a "statistical model" with exactly the properties originally envisioned for the nonresonant compound nucleus (3): complete independence of the formation and decay processes of the compound system, and relatively long lifetime of the compound system relative to the time for passage of a nucleon across the nucleus. It is this aspect of the compound nucleus model, which we may call the statistical assumption, that recent experiments have shown to be not entirely adequate.

To avoid confusion resulting from the too-inclusive term "compound nucleus model," we shall in accordance with the above discussion distinguish between the "eigenstate decomposition" and the "statistical assumption." The eigenstate decomposition has general validity and is particularly suited to the description of isolated resonances; the eigenstates involved are those of the compound system. The resonance parameters that describe a particular state of a physical nucleus are not given by the decomposition procedure, which is just a mathematical formality. There is no physical theory at present capable of predicting the parameters of a particular isolated resonance in a heavy nucleus, so that these parameters are inserted into the resonance formula from comparison with experiment.

On the other hand, less detailed knowledge is required for prediction of experimental results involving an average or sum over many contributing eigenstates. One need only be able to specify some average values of the resonance parameters and the gross energy dependence of these averages. Various postulates may be introduced at this point: in lieu of experimental information, the "statistical assumption" of complete randomness in neighboring eigenstates (1) seems natural; recent measurements suggest the applicability at even the lowest energies (6 to 9) of what may be called the

"optical assumption," at least as far as elastic and total cross sections are concerned.

We may also distinguish between an "assumption," which is a way of summing over many eigenstates of the compound system, and a "model," which is the classical picture corresponding to this type of summation. Thus the "statistical assumption" leads to the "statistical model" (which has often loosely been called the compound nucleus model), and the "optical assumption" to the "optical model." The optical model presents a picture that is the opposite extreme from the statistical model: the incident particle does not share its energy with the other nucleons very rapidly. There is a strong probability that it[2] will re-emerge elastically. Energy sharing begins as a quite individual process, in which one target nucleon is excited by collision, the primary collision products make secondary collisions, etc. The resulting cascade process eventually distributes the energy among all the nucleons to form the type of state assumed in the statistical model, provided that none of the particles escapes from the nucleus before the energy distribution is complete. In the optical model such escape is much more likely than in the statistical model, and the distribution of the escaping products will depend on the way in which the cascade is initiated. For example, a $(p, 2p)$ process in the optical model could be attributable to a single p-p collision inside the nucleus, with both products escaping; the cross section might be appreciably higher than for an $(\alpha, 2p)$ process, even with the same intermediate nucleus at the same excitation energy. Thus the optical model can also account for reaction cross sections; the calculations become quite laborious, however, and "Monte Carlo" methods must be used (11).

The simplest application of the optical model is to the elastic scattering and total cross sections of a nucleus: here the model is equivalent to a simple effective potential well with real and imaginary parts, the latter to account for absorption (i.e., anything but elastic scattering). This potential well has had an interesting history: in the earliest days of nuclear theory, through about 1935, the potential well was used almost exclusively; reactions were considered, with some exceptions (12), to proceed by "direct" or optical model type collisions. The experiments showing large absorption of slow neutrons (13) could even be interpreted by this model, which gives a $1/v$ law. But the experiments soon afterward showed epithermal resonance absorption of neutrons (14 to 20), and the optical model was completely displaced by the statistical compound nucleus (3). Now refined experiments show the necessity of taking seriously again the optical model; it is fortunate

[2] By "it" is meant the incident particle or any other particle of identical type, energy, and other parameters, which could be produced in the nucleus by exchange. Throughout the discussion exchange processes will not be introduced explicitly, since they are cumbersome to express and do not affect qualitative or first-order conclusions. Also it will not be necessary to distinguish whether the entities constructed under the optical assumption are actual individual nucleons or groups of nucleons with single-particle behavior (10).

that in the meanwhile theory has progressed to the point where the statistical assumption can be relinquished without disturbing the basic notion of decomposition according to eigenstates. Recent use of the optical model began with high energy reactions at 100 Mev. (11, 21, 22). For a time it was thought that the statistical model would dominate the elastic and total cross sections at lower energies, but measurements show that the optical model is valid down to the lowest energies, in which region a special form of it was applied even in the heyday of the statistical model (23).

The earlier supposed region of validity of the statistical model for elastic and total cross sections would have provided a convenient definition of "intermediate energy" for purposes of the present discussion. Lacking this, we take an arbitrary range of about 0 to 65 Mev. incident energy. The lower limit indicates the extreme range over which the optical model for nuclear reactions applies; the upper limit is arbitrary and not well-defined but is approximately at a minimum in the density of experimental data.

The discussion below divides naturally into four parts: (*a*) formulation of the eigenstate decomposition; (*b*) discussion of the statistical and optical models; (*c*) comparison with experiment on elastic and total cross sections, being mostly concerned with the optical model; (*d*) comparison with experiment on nuclear reactions, where both optical and statistical aspects appear, resulting in a situation at present complicated and obscure.

One may finally ask, what is the generic relationship of the eigenstate decomposition to various classically visualizable models, such as the optical and statistical? An ideal logical treatment of nuclear reactions would deduce from the force laws between nucleons all the parameters of the eigenstate decomposition. Since this is at present impossible, a successful classical model serves as a means of specifying the average behavior of the resonance parameters, thereby providing conditions that must be met by any ultimate deductive approach.

The Eigenstate Decomposition (5, 24, 25)

A single stage of a nuclear reaction comprises the collision of two (complex) particles and the subsequent re-emission of two particles with conservation of energy, angular momentum, and parity. Each possible different assignment of quantum numbers to the two-particle system constitutes a "channel." We denote the set of channel quantum numbers by c, adding explicitly such quantum numbers s, l, . . . as may be required in particular cases. The set c includes the number of nucleons in each "particle," the internal energy state of each particle, their intrinsic spins and parities, their relative orbital angular momentum, the total angular momentum of the system. A reaction starting from a given entrance or initial channel c can yield products in a large number of exit (final) channels c'. The cross section for the reaction $c \rightarrow c'$ can be written

$$\sigma_{cc'} = \frac{(2l_c + 1)\pi}{k_c^2} \left| S_{cc'} \right|^2 \qquad 1.$$

where k_c, l_c are the wave number and orbital angular momentum of relative motion in the entrance channel, and $S_{cc'}$ is a coefficient dependent on the total energy E of the reaction; it is in principle different for each pair cc'. The square array of coefficients $S_{cc'}$ composes the scattering matrix for the system; it is the natural quantity to discuss in theoretical considerations of reactions.

The definition of channels already contains implicitly the idea that at wide separations of the two particles in a channel there are no interactions between the particles that will disturb their internal arrangement—i.e., no nuclear interactions. This is made more precise by assigning a channel radius a_c to each channel, outside of which the particles behave as free. For separations $r_c > a_c$ the only potentials acting are the "long-range" centrifugal and coulomb repulsions associated with the relative motion of the centers of gravity of the particles. The channel radius a_c cannot be chosen smaller than the range a of nuclear forces between the two "particles"; choosing it larger is inconvenient because the description of nuclear reactions will then involve quantities not intrinsic to the nucleus—e.g., the distance $(a_c - a)$. Although the radius a_c presumably varies from one channel to another, the usual simplifying assumption has been that

$$a_c \approx a \qquad 2.$$

for all channels, where a is some sort of effective nuclear radius.

The introduction of the channel radii a_c is the basic step in obtaining the eigenstate decomposition: they define a spatially-bounded region. Whatever the forces acting inside this region, its boundedness alone limits the system to (an infinite number of) eigenstates at discrete energies E_λ. These energies are real, since the idealized system bounded in every channel cannot decay. The eigenstates are functions of the system as a whole, so that each eigenstate affects every channel. We can define a (real) coefficient $\gamma_{\lambda c}$, which is essentially the amplitude of the λth eigenstate in the cth channel. The region external to a_c is mathematically simple to handle, since it requires only the solution of the two-body wave equation with long-range potentials. The connection between internal and external regions is established through the usual continuity of the wave function and its first derivative at a_c.

Any wave function in the interior region can be expanded in terms of the eigenstates, since they form a complete set. This applies to physically realistic wave functions with outgoing waves in many channels but incoming waves in only one channel, even though the eigenstates themselves are defined for a stationary system with standing waves in every channel. Thus the scattering matrix element $S_{cc'}$ can be expressed in terms of the internal eigenstates, in particular in terms of their energies E_λ and channel amplitudes $\gamma_{\lambda c}$. The formulas given below for this expansion follow in a schematic way the treatment of Thomas (25).

The general element of the scattering matrix is

$$S_{cc'} = e^{-i(\phi_c+\phi_{c'})}\left[\delta_{cc'} + 2iP_c^{1/2}(R^{-1}XR)_{cc'}P_{c'}^{1/2}\right]$$

$$R_{cc'} = \sum \frac{\gamma_{\lambda c}\gamma_{\lambda c'}}{E_\lambda - E} \qquad X = \frac{1}{(1/R) - L} \tag{3.}$$

$$L_{cc'} = \delta_{cc'}(S_c + iP_c)$$

The quantities R and X are square matrices of the same order as $S_{cc'}$, and the $L_{cc'}$ constitute a diagonal matrix in this same representation, since $\delta_{cc'}$ is the Kronecker symbol. The quantities S_c, P_c, and ϕ_c are all characteristic of the two-body motion in the region external to a_c and enter equation 3 through fitting of the wave function and its derivative at this boundary. The argument of the exterior wave function at the channel radius is $\rho = k_c a_c$; and if $F(\rho)$ and $G(\rho)$ are the regular and irregular radial functions of the external region at this point,

$$\begin{aligned} L &= S + iP = \frac{\rho}{O}\left(\frac{dO}{d\rho}\right) \\ O &= F + iG \\ \phi &= \tan^{-1} F/G. \end{aligned} \tag{4.}$$

The subscripts c can be added for each channel.

The contributions of the internal region to $S_{cc'}$ are all contained in the matrix $(R^{-1}XR)$, which is algebraically more complicated than the "exterior" parts of equation 3. The complication would be reduced if R and X commuted, as would be the case if $L=0$. The noncommutativity of R and X can be approximately accounted for (25) by writing

$$R^{-1}XR \approx \bar{X} = \frac{1}{(1/\bar{R}) - L} \tag{5.}$$

For elastic scattering $1/\bar{R}$ is essentially the function f of the schematic treatment (26), and

$$\bar{R}_{cc} = \sum_\lambda \frac{\gamma_{\lambda c}\gamma_{\lambda c}}{E_\lambda - E + (\Delta_\lambda' - (i/2)\Gamma_\lambda')} \tag{6.}$$

The physical interpretation of the quantities in equation 6 becomes apparent on substituting equations 6 and 5 into equation 3 and reducing to the special case of a one-level formula. Then

$$(1/\bar{R} - L)^{-1} = \frac{\gamma_{\lambda c}^2}{E_\lambda - E + (\Delta_\lambda' - (i/2)\Gamma_\lambda') - \gamma_{\lambda c}^2 L_c} \tag{7a.}$$

$$S_{cc} = e^{-2i\phi_c}\left[1 + \frac{2iP_c\gamma_{\lambda c}^2}{E_\lambda - E + (\Delta_\lambda' - S_c\gamma_{\lambda c}^2) - (i/2)(\Gamma_\lambda' + 2P_c\gamma_c^2)}\right] \tag{7b.}$$

This is to be compared with the customary form

$$S_{cc} = e^{-2i\phi_c}\left[1 + \frac{i\Gamma_{\lambda c}}{(E_\lambda + \Delta_\lambda) - (i/2)\Gamma_\lambda - E}\right] \tag{8.}$$

The comparison shows that half-width of the incident channel c is

$$\Gamma_{\lambda c} = 2P_c\gamma_{\lambda c}^2 \tag{9.}$$

and that Γ_λ' is what is called the absorption half-width, being the sum over

all channels open to the state λ except the incident channel:

$$\Gamma_\lambda' = \sum_{c' \neq c} \Gamma_{\lambda c'} \qquad 9a.$$

The total half-width of the state λ is

$$\Gamma_\lambda = \Gamma_\lambda' + \Gamma_{\lambda c} = \sum_{c'} \Gamma_{\lambda c'} \qquad 9b.$$

Similar considerations hold for the energy level shifts Δ. These shifts are of no interest to the subsequent discussion and will be absorbed into the definition of E_λ; the resulting slight energy dependence of E_λ can be ignored here.

For nonelastic ($c' \neq c$) processes, we have to write

$$\overline{R}_{cc'} = \sum_\lambda \frac{\gamma_{\lambda c}\gamma_{\lambda c'}}{E_\lambda - (i/2)\Gamma_\lambda - E} \approx X' \qquad 10.$$

since in first approximation the contribution of the L matrix in the denominator of X' is of the form $(\gamma_{\lambda c} L \gamma_{\lambda c'}) = 0$, as L has values only in single channels and has no cross terms between channels. Since $R_{cc'}$ must be symmetric in c and c', equation 10 contains Γ_λ instead of Γ_λ' in this approximation.[3]

The strength function.—The various experimental cross sections in units of $(2l_c+1)\pi/k_c^2$ are

$$\begin{aligned} &\text{elastic:} && \sigma_{cc} = |1 - S_{cc}|^2 \\ &\text{reaction:} && \sigma_{cc'} = |S_{cc'}|^2, \quad c \neq c' \\ &\text{absorption:} && \sigma_{ca} = \sum_{c' \neq c} |S_{cc'}|^2 = 1 - |S_{cc}|^2 \\ &\text{total:}^4 && \sigma_c = \sigma_{cc} + \sigma_{ca} = 2[1 - \text{Re}\,\{S_{cc}\}] \end{aligned} \qquad 11.$$

In case of a single dominant level in $\overline{R}$ the expressions in equation 11 reduce to the familiar Breit-Wigner forms (27). In the present discussion we are interested in the opposite extreme, where an average must be taken over many levels. If the levels themselves are not closely enough spaced to be indistinguishable, the experimental indefiniteness of the incident energy E is assumed sufficient to effect the average over many levels. The advantage of the form of equation 6, and in principle of equation 10, is that the validity of its average is not restricted to a certain range of Γ_λ/D_λ, where D_λ is the average spacing of the levels λ. Consider the diagonal term $\overline{R}_{cc}$, which is sufficient for calculation of the most readily measured cross section, the total σ_c: in equation 6 replace Σ_λ by $\int(dE_\lambda/D_\lambda)$ and call the quantity $\gamma_{\lambda c}^2/D_\lambda = s_c(E_\lambda)$ the "strength function" of the levels at E_λ. Then[5]

[3] A second approximation (25) indicates that, in equation 10, $\gamma_{\lambda c}$ should be replaced by $\gamma_{\lambda c}/(1-\overline{R}_{cc}L_c)$ and correspondingly for $\gamma_{\lambda c}$.

[4] Re = real part of; Im = imaginary part of.

[5] Equation 12 is very similar in form to the Kronig-Kramers dispersion formula for the scattering of light (27a). The amplitude for forward scattering of particles of orbital momentum l_c by the compound nucleus mechanism only (no potential scattering) is

$$a_0(E) = \frac{(2l_c+1)}{k_c} P_c(E) R_{cc}(E) \qquad 12a.$$

$$\overline{R}_{cc}(E + i\Gamma'/2) = \int \frac{s_c(E_\lambda)dE_\lambda}{E_\lambda - (E + i\Gamma'/2)} \qquad 12.$$

Here Δ_λ' has been absorbed into E_λ, and $\Gamma' = \langle\Gamma_\lambda'\rangle_{av}$ is now regarded as a constant. Equation 12 is a Stieltjes transform that can be applied for $\Gamma'/D \ll 1$ as well as $\Gamma'/D \gg 1$. It also has the inverse,

$$s_c(E) = \frac{1}{\Gamma \to 0^+} \lim \ \mathrm{Im}\ \{\overline{R}_{cc}(E + i\Gamma/2)\} \qquad 13.$$

Equation 13 appears to be of potential usefulness in reducing measurements on the gross energy behavior of nuclear cross sections. The most straightforward quantity to measure is the total cross section σ_c. This does not directly yield $\mathrm{Im}\{\overline{R}_{cc}\}$, but any simple model that can be devised to fit the measured $\mathrm{Re}\{S_{cc}\}$ will also yield indirectly an expression for $\mathrm{Im}\{\overline{R}_{cc}\}$, which can then be converted by equation 13 to a corresponding function $\gamma^2/D(E)$. It may then be possible to interpret the behavior of this function in terms of a model of nuclear structure.

For example, the optical model indicated by analysis (28) of low energy (0 to 3 Mev.) neutron measurements (6 to 9) yields the specific form for $l=0$:

$$\overline{R}_{cc}(E) = 1/f = \frac{1}{Z \cot Z}$$

If the individual resonance levels λ are well separated, the average cross section for compound nucleus formation can be written

$$\begin{aligned} \sigma_c(c) &= (2l_c + 1)\pi/k_c^2 \int \frac{\Gamma_{\lambda c}\Gamma}{(E - E_\lambda)^2 + (\Gamma/2)^2} \frac{dE_\lambda}{D_\lambda} \\ &= (2l_c + 1)2\pi^2/k_c^2 P_c(E_\lambda)\{s_c(E_\lambda)/D_\lambda\} \end{aligned} \qquad 12b.$$

Substituting equations 12a and 12b into equation 12 would yield

$$\begin{aligned} a_0(E) &= \frac{P_c(E)}{2\pi^2 k_c} \int \frac{[k_{c'}^2/P_c(E')]\sigma_c(E')dE'}{E' - E} \\ &\approx \frac{k_c}{2\pi^2} \int \frac{\sigma_c(E')dE'}{E' - E} \end{aligned} \qquad 12c.$$

which is exactly analogous to the Kronig-Kramers relation.

Equation 12c cannot actually be correct, although of a very suggestive form. It implies a separate dispersion relation of the Kronig-Kramers type for every individual value of l_c, against the existence of which general arguments can be given (27b). The failure of equation 12c can be traced to the failure of equation 12b, which is a relation like equation 32 below and can be valid only for regions of "weak coupling" where $s_c(E)$ is small. For any l_c regions of weak and strong coupling both occur over an energy range of a few Mev, so that the integrand in equation 12c is seriously in error. It is perhaps of interest to note that in spite of the failure of 12c, equation 12 is generally valid and does seem to imply a sort of dispersion relation for individual l_c. This relation is not exactly of the Kronig-Kramers type, for there is only an implicit relation between the integrand $s_c(E')$ and the compound formation cross section $\sigma_c(E')$ which can be made explicit just in weak coupling regions.

$$Z^2 = \frac{2Ma^2}{\hbar^2}\left[(E + V_0) + iW/2\right] \qquad 14.$$

where M is the mass of the neutron, and $-(V_0+iW/2)$ is the effective square well potential in the nucleus. Now since

$$Z^{-1}\tan Z = \sum_{p=1}^{\infty} \frac{2}{(p - 1/2)^2\pi^2 - Z^2} \qquad 15.$$

equation 14 is equivalent to

$$\overline{R}_{cc}(E) = \sum_{p=1}^{\infty} \frac{(\hbar^2/Ma^2)}{E_p - (E + iW/2)}$$

$$E_p = \frac{\pi^2\hbar^2}{2Ma^2}(p - 1/2)^2 - V_0 \qquad 16.$$

and by equation 13 the corresponding strength function is

$$s(E) = \left\langle \frac{\gamma_{\lambda c}^2}{D_\lambda} \right\rangle_{av} = 1/(2\pi)\sum_p \frac{W(\hbar^2/Ma^2)}{(E_p - E)^2 + (W/2)^2} \qquad 17.$$

The quantity $\gamma_{\lambda c}^2$ can be regarded (at least near its maxima) as the relative probability that the state λ in the internal region consists of the incident nucleon moving in an effective potential provided by the target nucleus in its ground state. If D_λ is assumed to be constant, the resonances in equation 17 show that the single-particle configuration is not uniformly distributed among the internal states but shows a definite concentration about energies characteristic of the shell model. This implies that single-particle wave functions may be a useful first approximation to some nuclear configurations, as the success of the shell model has already emphasized. If in equation 17 $W\to 0$, the single-particle picture would be a perfect approximation for those states with $\lambda = p$; if at the other extreme $W\to\infty$, the single-particle configuration would be uniformly distributed among all the nuclear states λ and hence would probably not be a very useful starting point for describing any state. The situation in equation 17 is described as "intermediate" (29).

Compound nucleus formation.—Of the directly measurable cross sections in equation 11 only the total cross section σ_c can be simply related to the strength function $s(E)$, because only σ_c is linear in $\overline{R}$. The other cross sections all involve $|\overline{R}|^2$, which can be evaluated only by making a particular choice for the form of $\overline{R}$, such as equation 16. To avoid this restriction, we try to use general, semiquantitative arguments based on a time-dependent picture of the reaction, as in Figure 1 (30). The incident particles arrive as wave packets at the boundary of the interior region, represented for convenience as a plane. Fitting of the wave function and its derivative at the surface results (on a one-channel picture) in two outgoing wave packets for each one falling on the surface: one outgoing packet in the exterior region of intensity $|S_{cc}|^2 \leqq 1$ relative to the incident intensity, and a packet transmitted to the interior region with relative intensity $T_c = 1 - |S_{cc}|^2$ to assure

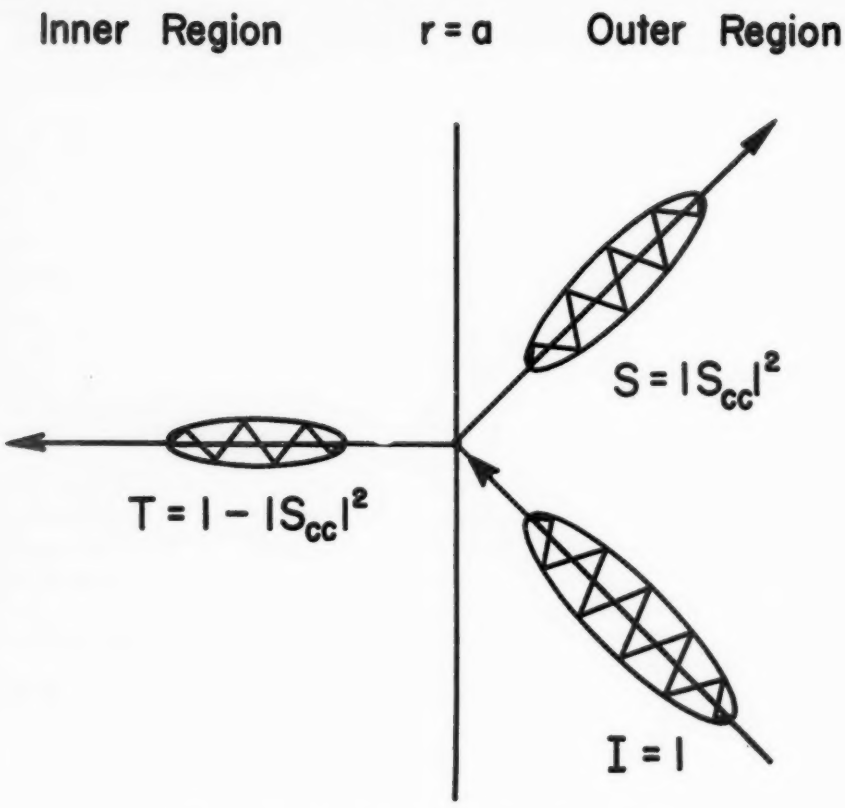

FIG. 1. Wave packets at the surface of a nucleus.

conservation of particles. The wave function of the transmitted packet in the interior (compound nucleus) region can be written

$$\psi_T = \sum_\lambda a_{T\lambda}\psi_\lambda e^{-iE_\lambda t/\hbar} \qquad 18.$$

where E_λ are the characteristic, real energies associated with ψ_λ. The coefficients $a_{T\lambda}$ are arranged so that at time $t=0$ the wave function ψ_T represents the nucleus in a state where all the excitation energy is localized in a single particle, incident at the border of the interior region. As time passes, the various terms of equation 18 progressively depart from their original phase relations, producing two effects: the transmitted wave packet moves with a higher velocity than in the exterior region, corresponding to a real potential $V=-V_0$. More important, the simple wave packet representing a single particle in a potential well gradually disappears. The individual ψ_λ contain strong admixtures of configurations where the excitation energy is distributed among many nucleons; the emergence of these other configurations

with time (the $a_{T\lambda}$ are fixed to make them cancel at $t=0$) corresponds to "absorption" of the simple one-particle state.

This process is not irreversible, however, because the E_λ are real and discrete, having an average spacing D. The coefficients $a_{T\lambda}$ are large only for E_λ in the region of E, the actual energy of the reaction; for the relatively narrow range of importance about E, we can take $D(E)=\text{const}$. Under this assumption, the terms in equation 18 must all return to their original relative phases after a time no greater than t_0, where (30)

$$t_0 D/\hbar = 2\pi. \tag{19.}$$

The motion of the wave packet in the interior region is thus periodic; after each interval t_0, the single particle in a potential well reappears at the nuclear surface. The probability of penetrating this surface is the same in either direction, namely $T_c = 1 - |S_{cc}|^2$.

The description above is entirely in terms of a one-channel nucleus. If more channels are available for emission from internal state, the one-particle picture is subject to continuous decay at a mean rate

$$1/\tau = \Gamma'/\hbar. \tag{20.}$$

Here Γ' is again the "absorption half width," $\Gamma' = \Gamma - \Gamma_c$, where Γ is the total half width and Γ_c that for the channel under consideration. The probability that the internal state will survive a single cycle is

$$w = e^{-t_0/\tau} = e^{-2\pi\Gamma'/D}. \tag{21.}$$

Thus (31) the probability that the original particle can escape after one cycle is wT_c; the probability that it will be irrevocably absorbed is $(1-w)$. These probabilities maintain the same relative magnitudes throughout any number of cycles, so that the probabilities P_e and P_a of elastic re-emission and absorption are

$$\begin{aligned} P_e/P_a &= wT_c/(1-w) = T_c/A \\ A &= (e^{2\pi\Gamma'/D} - 1) \\ P_e + P_a &= 1. \end{aligned} \tag{22.}$$

Absorption can occur only through the compound state.

The total cross section for forming the compound state, in units of $(2l_c+1)\pi/k_c^2$, is

$$\sigma_c(C) = 1 - |S_{cc}|^2 = T_c. \tag{23.}$$

The corresponding elastic scattering and absorption cross sections are

$$\begin{aligned} \sigma_{cc}(C) &= T_c\left[\frac{T_c}{A+T_c}\right] \\ \sigma_{ca} &= T_c\left[\frac{A}{A+T_c}\right]. \end{aligned} \tag{24.}$$

The notation (C) indicating compound state can be dropped from σ_{ca}. The compound elastic scattering $\sigma_{cc}(C)$ must be combined with the elastic scattering at the surface in Figure 1, $\sigma_{cc}(S)$, also called (28) the "shape elastic"

scattering. Because of the random nature of the compound elastic scattering, it is completely incoherent with the surface elastic scattering, and

$$\sigma_{cc} = \sigma_{cc}(S) + \sigma_{cc}(C). \tag{25.}$$

The expression in equation 11 for σ_{cc} can be decomposed into two incoherent parts by considering averages of S_{cc} over energy ranges small in comparison with the slow change of $s(E)$ but large with respect to D. If $\langle S_{cc}\rangle$ is such an average of S_{cc}, then

$$\begin{aligned}\sigma_{cc} &= \langle |\, 1 - S_{cc}|^2\rangle \\ &= \langle |\, \{1 - \langle S_{cc}\rangle\} + \{\langle S_{cc}\rangle - S_{cc}\}\,|^2\rangle \\ &= \langle |\, 1 - \langle S_{cc}\rangle|^2\rangle + \langle |\, \langle S_{cc}\rangle - S_{cc}|^2\rangle \\ &= |\, 1 - \langle S_{cc}\rangle|^2 + \{\langle |\, S_{cc}|^2\rangle - |\, \langle S_{cc}\rangle|^2\}.\end{aligned} \tag{26.}$$

The cross term between $1-\langle S_{cc}\rangle$ and $\langle S_{cc}\rangle - S_{cc}$ vanishes on the average, so that the two parts of the final expression are incoherent and can be assigned (28) to $\sigma_{ce}(S)$ and $\sigma_{ce}(C)$, respectively. The appearance of $\langle S_{cc}\rangle$ in $\sigma_{cc}(S)$ implies that this same quantity should appear in equation 23, or

$$T_c = 1 - |\, \langle S_{cc}\rangle|^2. \tag{27.}$$

The last quantity can be calculated from the integral in equation 12 for $\overline{R}_{cc}$, so that we have avoided direct computation of $|\overline{R}_{cc}|^2$. Evaluation of $|\overline{R}_{cc}|^2$ for a specific form similar to equation 16 leads to the same results (25).

It should be emphasized that compound nucleus formation here does not imply that the statistical assumption is valid, in which random phase relations are assumed among the $a_{T\lambda}$ in equation 18. The reaction cross sections $\sigma_{cc'}$, for example, may be strongly influenced by the disposition of the $a_{T\lambda}$; that is, they will depend on the way in which the compound state is formed. Taking the time-dependent picture literally, we may say that only near the middle of a cycle of length t_0 will the compound state decay randomly into the various possible channels c'; near the ends of the cycle the decay is weighted heavily in favor of channels c'' where the nuclear configuration is not very different from that in c. Thus on the average over a cycle decay into channels c'' will be somewhat favored. The failure of the statistical assumption is also apparent in the compound elastic cross section $\sigma_{cc}(C)$: if we put $T_c \approx 2\pi P_c/D$ (see below) in equation 24, we have for $\Gamma'/D \ll 1$

$$\sigma_{cc}(C) \approx 2\pi \frac{\Gamma_c^2}{D(\Gamma' + \Gamma_c)} = \frac{2\pi\Gamma_c^2}{D\Gamma} \tag{28.}$$

This is the usual expression (26) for the compound elastic cross section averaged over widely separated resonances. The statistical assumption implies that the form of equation 28 should be valid independent of Γ'/D, while equation 24 shows that as Γ'/D becomes large, $\sigma_{cc}(C)$ falls off much more rapidly than in equation 28. That is, there exists an average destructive interference in the compound elastic scattering from overlapping levels.

At energies E far from the "giant resonances" of $s(E)$ given by equation 17 there is an approximate, simple relation between T_c and s_c. When E is

not near a pole of expression 17, we can get an approximate value for the integral in equation 12 by taking only the contributions from the pole in the denominator, neglecting the poles of s_c itself. Then

$$R_{cc}(E) \approx \pi i s_c(E) \tag{29.}$$

$$T_c = 1 - |\langle S_{cc}\rangle|^2 = 1 - |1 + 2iP_c\overline{R}_{cc}|^2 = 4\pi P_c s_c(1 - \pi P_c s_c) \approx 2\pi(\Gamma_c/D) \tag{30.}$$

where the term in s_c^2 is dropped because all quantities are supposed to be small. This is the expression used in equation 28 above. It also brings out the relation to the intuitive concept of the "sticking probability" that appears in the older literature (1, 32, 33). The sticking probability ξ_c for any channel is defined to be $0 \leq \xi_c \leq 1$ such that in units of $(2l_c+1)\pi/k_c^2$

$$\sigma_c(C) = P_c\xi_c = T_c. \tag{31.}$$

Comparison with equation 30 shows that in the present case

$$\xi_c \approx 2\pi s_c(E). \tag{32.}$$

Equation 31 is a general equivalence between the sticking probability ξ_c and the transmission coefficient T_c: they are equal at incident energies high enough for the particles in the incident channel to collide under classical conditions. Of course T_c is a function of s_c at all energies, but only in the "weak coupling" region between the giant resonances can the relation readily be made explicit, as in equation 32.

The effect of the "optical assumption" of equation 17 for $s_c(E)$ upon the individual reaction cross sections $\sigma_{cc'}$ has not yet recieved much study. Evaluation of an expression of the form

$$\overline{R}_{cc'} \simeq \int \frac{(s_c s_{c'})^{1/2} dE_\lambda}{E_\lambda - i\Gamma_\lambda/2 - E} \tag{33.}$$

would be required. Even without detailed considerations it seems likely that $\overline{R}_{cc'}$ will turn out not to be in accord with the pure statistical assumption, but that reactions may display a strong "memory" of the way in which they are produced.

Angular distributions.—The angular distribution of products from a nuclear reaction will in principle tell something about the degree of validity of the statistical assumption. The angular distribution of the reaction $c \to c' \neq c$ can be written (34)

$$\frac{d\sigma_{cc'}}{d\Omega} = \frac{1}{(2s+1)k_c^2} \sum_{\substack{J_1 l_1 l_1' \\ J_2 l_2 l_2'}} i^{-l_1+l_1'+l_2-l_2'} S^{*J_1}_{cs l_1; c's' l_1'} S^{J_2}_{cs l_2; c's' l_2'} K(J_1 l_1 l_1' J_2 l_2 l_2' ss'; \theta) \tag{34.}$$

where s is the channel spin (sum of the intrinsic spins of the two particles), l is the orbital momentum, J is the total angular momentum of the system. The function $K(\theta)$ is a purely geometrical factor containing the angular dependence. If we use equation 10 in the defining equation 3 for S, the quantity S^*S is of the form

$$\sum_{\lambda_1,\lambda_2} \frac{\gamma^{J_1}_{cs l_1 \lambda_1} \gamma^{J_1}_{c's' l_1' \lambda_1}}{E_{\lambda_1} - E - (i/2)\Gamma_{\lambda_1}} \cdot \frac{\gamma^{J_2}_{cs l_2 \lambda_2} \gamma^{J_2}_{c's' l_2' \lambda_2}}{E_{\lambda_2} - E - (i/2)\Gamma_{\lambda_2}} \cdot \tag{35.}$$

Under the statistical assumption the signs of the γ's are randomly distributed, so that in the summations in equations 34, 35 the only terms that occur always with the positive sign are those for which $l_1=l_2$, $l_1'=l_2'$, $J_1=J_2$, $\lambda_1=\lambda_2$. These terms are accordingly much larger than the remaining terms with random signs, which latter are hence neglected in the statistical approximation. Then

$$\frac{d\sigma_{cc'}}{d\Omega}\sim\sum_{\lambda ll'J}\frac{(\gamma^{J}_{cs l\lambda})^2(\gamma^{J}_{cs' l'\lambda})^2}{(E_\lambda-E)^2+(1/2\Gamma_\lambda)^2}K(Jll'Jll'ss';\theta). \tag{36.}$$

The angular functions K with equal indices appearing in equation 36 have the property (35, 36) that they can be expressed as functions of $\cos^2\theta$ only and so are symmetric about $\xi=90°$. The absence of such symmetry in an observed reaction (e.g., the presence of forward peaking) may thus be taken as an indication that the statistical assumption leading to equation 36 is not entirely valid for that reaction. Of course, under the optical approximation there are strong correlations among the $\gamma_{cs l\lambda}$, so that highly asymmetric $d\sigma_{cc'}/d\Omega$ may result. It should perhaps again be emphasized that the presence of a nonisotropic angular distribution does not rule out the statistical assumption, which is incompatible only with a nonsymmetric distribution.

For elastic processes the surface scattering angular distribution has the elementary form (28)

$$\frac{d\sigma_{cc}(S)}{d\Omega}=\frac{1}{4k_c^2}\left|\sum_l(2l+1)P_l(\cos\theta)\{1-\langle S_{cc}\rangle\}\right|^2. \tag{37.}$$

The angular distribution of the compound elastic scattering is not easy to compute and has never been evaluated in full detail. The difficulty arises from the fact that in equation 35 c', s', $l_1'=c$, s, l_1, so that positive definite coefficients are obtained without the necessity of setting $\lambda_1=\lambda_2$, $J_1=J_2$. The sum over λ_1, λ_2, therefore becomes more complicated than in the nonelastic reaction; similar considerations are responsible for the fact that $\sigma_{cc}(C)$ in equation 24 is much less than in equation 28 for $\Gamma'/D\gg1$. Fortunately, the question of the angular distribution of $\sigma_{cc}(C)$ is of practical importance only at the very lowest energies, for at moderate energies $\Gamma'/D\gg1$, and $\sigma_{cc}(C)$ becomes negligible.

The Optical and Statistical Models

The eigenstate decomposition has the virtue of providing a mathematically complete description of nuclear reactions and leads most naturally to rigorous and simple expressions for isolated resonances. On the other hand, it does not seem so ideally suited for the description of nonresonant processes and is on the whole rather formal. To obtain somewhat more immediate insights into nuclear behavior, physical models of various types are helpful. They always involve oversimplifications and cannot claim the general validity of the eigenstate decomposition, but a successful model frequently provides a basis for intuitive interpretation and prediction.

Two extreme models will be described here: the optical and the statistical. The optical and statistical approximations of the preceding section are usually determined by the requirement that they reproduce the results of these models. The optical and statistical models are opposite extremes in a general sense: the optical model assumes a maximum of coherence among nuclear phenomena, the statistical model assumes a minimum, or total incoherence. This distinction is maintained at all points where the notions of coherence versus incoherence have any meaning: e.g., in the relative phases of competing reactions, in the relative sign of neighboring γ_λ, etc.

The optical model.—The optical model in its simplest form represents the nucleus as a static potential well without internal structure; the only refinement is that the potential may have both real and imaginary parts, to allow for absorption as well as elastic scattering. Under this definition the shell model and the usual degenerate Fermi gas treatment of nuclear binding energy are also examples of the optical model. The success of the optical model at these lowest energies may make its applicability to low-energy nuclear reactions somewhat less surprising. Although the optical model in nuclear physics antedates the proposal of the compound nucleus, the relation of its parameters to the basic two-body nuclear forces has been studied only recently (37, 38, 39).

To obtain this relation, it is convenient to regard the ground state nuclear wave function as a product of independent-particle wave functions. Such product functions form a complte set and can serve as a basis for description:

$$\psi^0 = \phi_1{}^0(r_1)\phi_2{}^0(r_2) \cdots \phi_A{}^0(r_A) \qquad 38.$$

Here the $\phi_j{}^0$ are all normalized over the volume of the nucleus. For simplicity, all complicating effects are neglected, such as antisymmetrization and linear combinations of different sets of ϕ_n, nucleon spin and isotopic spin components, etc. Consider now the elastic scattering of an incident nucleon by a nucleus in its ground state, again neglecting exchange effects. The first-order scattering amplitude in the Born or perturbation approximation is

$$a_1 \sim \int \psi^{0*} \sum_{j=1}^{A} V(r - r_j) e^{-i\Delta k \cdot r} \psi^0 d^{3A} r = V^{00}(k_f, k_i) \qquad 39.$$

where $V(r-r_j)$ is the potential acting between the incident nucleon (r) and the jth nucleon in the nucleus; $\Delta k = k_f - k_i$ is the impulse given to the scattered nucleon by the nucleus. The scattering amplitude is

$$a_1 \sim \sum_j \rho_j(\Delta k) V(\Delta k)$$

$$V(\Delta k) = \int V(r) e^{-i\Delta k \cdot r} d^3 r \qquad 40.$$

$$\rho_j(\Delta k) = \int e^{-i\Delta k \cdot r_j} \left| \phi_j{}^0(r_j) \right|^2 d^3 r_j$$

and if the average density of a nucleon in the nucleus is

$$\rho = 1/A \sum_{j=1}^{A} |\phi_j^0(r)|^2,$$

$$a_1 \sim A\rho(\Delta k) V(\Delta k) = V^{00}(k_f, k_i) \tag{41.}$$

Next consider the second-order perturbation approximation. In the intermediate state the nuclear wave function ψ^{m_j} can differ from ψ^0 by having the jth nucleon in the mth excited state with wave function $\phi_j^m(r_j)$. The scattered nucleon goes to an intermediate plane wave state denoted by k_m. The corresponding matrix element is

$$V^{m_j 0}(k_m, k_i) = \rho_j^m(k_m - k_i) V(k_m - k_i)$$

$$\rho_j^m(k) = \int \phi_j^{m*}(r_j) e^{-ik \cdot r_j} \phi_j^0(r_j) d^3 r_j \tag{42.}$$

and the scattering amplitude is

$$a_2 \sim \sum_{k_m} \frac{V^{00}(k_f, k_m) V^{00}(k_m, k_i)}{E_{k_m} - E} + \sum_{k_m, m_j \neq 0} \frac{V^{0m_j}(k_f, k_m) V^{m_j 0}(k_m, k_i)}{E_m - E} \tag{43.}$$

The first term of equation 43 represents double scattering of the incident nucleon with the target nucleus remaining in its ground state throughout; we can argue that this term is larger than the second by a factor of order A.

If in the second term of equation 43 we neglect the dependence of the denominator on the state ϕ_j^m and replace E_m by some appropriate $\bar{E}_{k_m}$ dependent only on k_m,

$$\sum_{m_j \neq 0} \frac{V^{0m_j}(k_f, k_m) V^{m_j 0}(k_m, k_i)}{E_m - E} \approx \frac{V(k_f - k_m) V(k_m - k_i)}{\bar{E}_{k_m} - E} \times \sum_m \rho_j^m(k_f - k_m) \rho_j^m(k_m - k_i)$$

$$= \frac{V(k_f - k_m) V(k_m - k_i)}{\bar{E}_{k_m} - E} \rho_j(\Delta k) \tag{44.}$$

where the last step follows from the definition 42 by closure. Then with $\Sigma \rho_j(\Delta k) = A\rho(\Delta k)$, the scattering amplitude becomes

$$a_2 \sim \sum_{k_m} \frac{A\rho(k_f - k_m) A\rho(k_m - k_i) V(k_f - k_m) V(k_m - k_i)}{E_{k_m} - E}$$

$$+ \sum_{k_m} \frac{A\rho(\Delta k) V(k_f - k_m) V(k_m - k_i)}{\bar{E}_{km} - E} \tag{45.}$$

Although the terms in equation 45 differ slightly, ρ is of order unity for moderate Δk, and $\bar{E}_{k_m}$ is not expected to differ radically from E_{k_m}, as is confirmed by sample calculations. Thus the second term of equation 45 is small relative to the first by a factor of order $A/A^2 = 1/A$ and can be neglected for large A, where in practice "large A" seems to be of order 10.

This argument is an example of the statement that the optical model assumes a maximum of coherence in all nuclear processes. In the elastic scattering matrix element V^{00} the factor A arises because of coherent scattering from each of the A nucleons in the nucleus.

The two-step inelastic process $V^{0m_j} V^{m_j 0}$ is incoherent in the sense that after the step $0 \to m_j$, the only step that leads back to ψ^0 is $m_j \to 0$, and not $m_{j'} \to 0$, $j' \neq j$. These remarks can be extended to the scattering amplitude of

any order, a_n. The largest term in a_n is the coherent one, where at each stage the target nucleus remains in its ground state. The next largest term is that in which one target nucleon is excited to a state ϕ_j^m and ultimately returned to ϕ_j^0. Even if all the other steps involve coherent scattering, the step in which $\phi_j^m \rightarrow \phi_j^0$ can occur only through scattering of the incident nucleon by the jth nucleon in the target and is thus reduced by a factor of order $1/A$ in comparison with the coherent term.

Interactions among the target nucleons have not been explicitly introduced here. The expansion $a_1, a_2 \cdots a_n \cdots$ is in terms of the number of scatterings n of the incident nucleon; each amplitude a_n implicitly includes the interactions among target nucleons to all orders.

If we retain only the dominant terms in a_n, of order A^n, the perturbation expansion becomes just that for scattering of the incident nucleon by the effective potential

$$-V_0(r) = \int \sum_j \rho_j(r_j) V(r - r_j) d^3 r_j \qquad 46.$$

The negative sign is inserted in equation 46 as a matter of definition, to make V_0 intrinsically positive for attractive forces; $-V_0(r)$ is the real part of the nuclear optical potential. The imaginary part is determined by estimating the mean free path of the incident nucleon for inelastic collision with one of the target nucleons in the nucleus. This mean free path is of the form

$$\lambda = 1/\langle \sigma f_{ex} \rangle \rho \qquad 47.$$

where ρ is the nucleon density, σ is the total cross section for nucleon-nucleon collision and f_{ex} is a reduction factor attributable to the exclusion principle. The brackets indicate an average over all momentum states of the nucleons in the target. If the incident nucleon energy is low, most of its inelastic collisions with target nucleons will be forbidden because at least one of the collision products would have to go into a momentum state that is already occupied. The effective cross section for inelastic collisions is thus substantially reduced by a factor f_{ex}. As the incident energy becomes large, $f_{ex} \rightarrow 1$, but the total nucleon-nucleon cross section decreases; and at low energies σ is large but $f_{ex} \rightarrow 0$. Thus, as a function of incident nucleon energy, λ passes through a flat minimum somewhere between 20 to 50 Mev. Values of λ calculated by this model are shown in Figure 2 (40).

The imaginary part of the optical well is simply calculated from λ. If the optical potential is $V = -(V_0 + iW)$, the wave number of the incident nucleon in the nucleus is

$$K = \sqrt{\frac{2M}{\hbar^2}\{(E + V_0) + iW\}} = k' + i/2\lambda \qquad 48.$$

A plane wave e^{ikz} falls off in intensity by a factor e in a distance λ. Knowing V_0 and λ, we can determine the effective W by equation 48. At present W appears to be only of order 1 to 2 Mev. at the lowest incident energies, rising

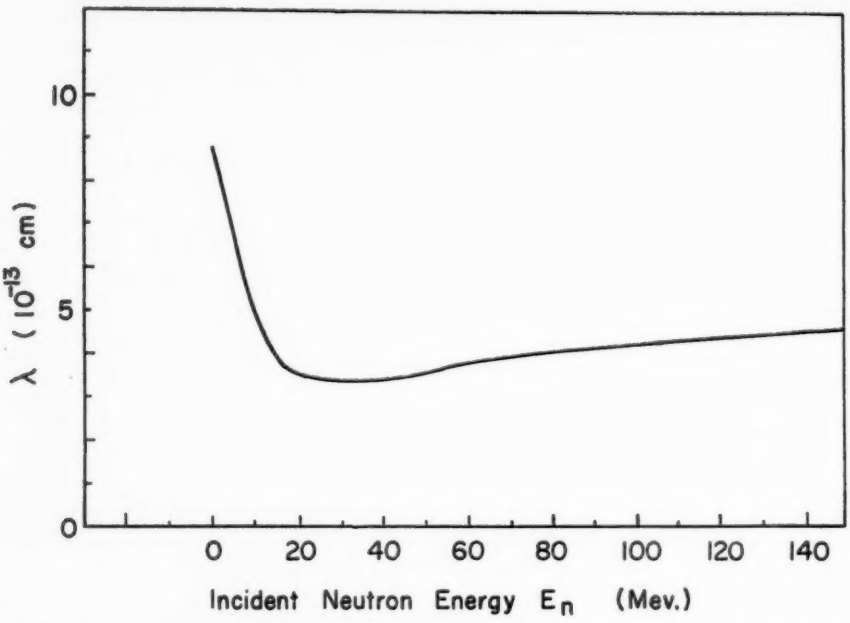

FIG. 2. Mean free path λ as a function of neutron incident energy, after (40). Note added in proof: More recent calculations suggest that this curve is only qualitatively correct.

to a fairly constant value of ~10 Mev. for incident nucleon energies $\gtrsim 10$ Mev.

The nucleon-nucleon potential $V(r-r_j)$ in equation 46 is not yet well known, and detailed experimental knowledge of the nucleon-nucleon scattering amplitude $a(\boldsymbol{k}_i, \boldsymbol{k}_f)$ seems likely to become available sooner than an adequate theory for $V(r)$. It is possible to express V_0 in terms of $a(\boldsymbol{k}_i, \boldsymbol{k}_f)$ with a validity equivalent to that of the Born approximation, but it is not now clear how to proceed from $a(\boldsymbol{k}_i, \boldsymbol{k}_f)$ to V_0 otherwise. Consider a single elastic scattering of the incident nucleon, regarding the target nucleons as fixed at positions $\boldsymbol{r}_j$: the sum of the scattering amplitudes from all the nucleons in the nucleus with phase factors for their different positions is

$$\sum_{j=1}^{A} e^{i\Delta \boldsymbol{k}\cdot\boldsymbol{r}_j}\, a(\boldsymbol{k}_i, \boldsymbol{k}_f) \qquad 49.$$

Taking the expectation value of this for the nuclear ground state, we have

$$a_1 = \sum_j \rho_j^*(\Delta k) a(\boldsymbol{k}_i, \boldsymbol{k}_f) = \rho(\Delta k) a(\boldsymbol{k}_i, \boldsymbol{k}_f) \qquad 50.$$

If equation 50 is now regarded as the first-order scattering from an effective optical potential $V(r)$, then with

$$U=2MV/\hbar^2$$

$$U/4\pi = \frac{1}{(2\pi)^3}\int e^{i\boldsymbol{\Delta k}\cdot\boldsymbol{r}}\rho(\boldsymbol{\Delta k})a(\boldsymbol{k}_i,\boldsymbol{k}_f)d^3(\Delta k) \qquad 51.$$

where a minus sign has been absorbed by the convention in equation 46.

At first sight the range of validity of equation 51 may appear limited. The amplitude $a(\boldsymbol{k}_i, \boldsymbol{k}_f)$ is complex, and the calculated U will also be; but equation 51 is an inversion of the Born-approximation type, which has the well-known defect of yielding a purely real scattering amplitude for any real potential. It might therefore appear that only the real part of U in equation 51 can be given a physical interpretation. Actually, the situation is somewhat better than this, and the imaginary part of U is also significant, at least to first order. According to equation 48, if $k'\lambda \gg 1$,

$$k'^2 + ik'/\lambda \approx \frac{2M}{\hbar^2}(E+V_0) + i\left(\frac{2M}{\hbar^2}\right)W \qquad 52.$$

With $\sigma f_{ex}=\sigma'$ for the effective collision cross section in the nucleus equation 47 gives

$$k'\sigma'\rho = \left(\frac{2M}{\hbar^2}\right)W \qquad 53.$$

For any scatterer (41)

$$k'\sigma' = 4\pi \operatorname{Im}\{\alpha_0\} \qquad 54.$$

where α_0 is the forward scattering amplitude. Thus

$$\begin{aligned}\left(\frac{2M}{\hbar^2}\right)W/4\pi &= \operatorname{Im}\{\alpha_0\}\,\rho(r)\\ &= \operatorname{Im}\{\alpha_0\}\,(2\pi)^{-3}\int e^{i\boldsymbol{\Delta k}\cdot\boldsymbol{r}}\rho(\boldsymbol{\Delta k})d^3(\Delta k)\end{aligned} \qquad 55.$$

which is a form similar to $\operatorname{Im}\{U\}$ in equation 51.

To make this similarity more explicit, consider (42) a polynomial expansion of $a(\boldsymbol{k}_i, \boldsymbol{k}_f)$

$$a(\boldsymbol{k}_i,\boldsymbol{k}_f) = \alpha_0 + i(\boldsymbol{k}_i\cdot\boldsymbol{k}_f - k^2)\,\alpha_1 + \cdots + i^n(\boldsymbol{k}_i\cdot\boldsymbol{k}_f - k^2)\alpha_n + \cdots \qquad 56.$$

where the α's would be real if the Born approximation were valid. It is convenient to use the quantity $(\boldsymbol{k}_i\cdot\boldsymbol{k}_f)-k^2=(\boldsymbol{k}_i\cdot\boldsymbol{\Delta k})=-1/2(\boldsymbol{\Delta k})^2$ as the expansion parameter instead of the more immediate $(\boldsymbol{k}_i\cdot\boldsymbol{k}_f)$, because then α_0 is the forward scattering amplitude. Corresponding to equation 51, we have

$$\begin{aligned}U/4\pi &= u_0 + u_1 + \cdots + u_n + \cdots\\ u_n(r) &= \frac{\alpha_n}{(2\pi)^3}\int e^{i\boldsymbol{\Delta k}\cdot\boldsymbol{r}}(i\boldsymbol{k}_i\cdot\boldsymbol{\Delta k})^n\rho(\boldsymbol{\Delta k})d^3(\Delta k)\\ &= \alpha_n(\boldsymbol{k}_i\cdot\boldsymbol{\nabla})^n\rho(r)\\ &= \alpha_n\left(\frac{\boldsymbol{p}_i\cdot\boldsymbol{\nabla}}{\hbar}\right)^n\rho(r)\end{aligned} \qquad 57.$$

The higher (nonspherical) terms in $a(\boldsymbol{k}_i, \boldsymbol{k}_f)$ can thus be represented as optical potentials that are velocity-dependent and related to the various gradi-

ents of the nuclear density distribution, rather than to the density ρ itself, as for the spherically symmetric part.

According to the discussion above the real and imaginary parts of u_0 in equation 57 are both significant, at least if the imaginary part is not too large. How to interpret the imaginary parts of u_n has not been studied, but so far not much application has been made of u_n with $n \neq 0$.

Spin-orbit coupling.—Similar remarks of course hold for the spin-orbit coupling effective on the incident nucleon in the nucleus. The nucleon-nucleon scattering amplitude contains a term which is, to lowest order, of the form (43, 44)

$$a_{ls} = i\alpha_{ls}\sigma \cdot (\boldsymbol{k}_i \times \boldsymbol{k}_f) \tag{58.}$$

where $\boldsymbol{\sigma}$ is the spin operator of the incident nucleon. The form of equation 58 is the only scalar that can be constructed from the vectors $\boldsymbol{k}_i$, $\boldsymbol{k}_f$ and the pseudo-vector $\boldsymbol{\sigma}$; α_{ls} will be real in the Born approximation. Then the optical spin-orbit potential is

$$\begin{aligned} U_{ls}(r)/4\pi &= \frac{i\alpha_{ls}}{(2\pi)^3}\int e^{i\Delta \boldsymbol{k}\cdot\boldsymbol{r}}(\boldsymbol{\sigma}\cdot\boldsymbol{k}_i \times \boldsymbol{k}_f)\rho(\Delta k)d^3(\Delta k) \\ &= \alpha_{ls}\boldsymbol{\sigma}\cdot(\boldsymbol{k}_i \times \nabla)\rho(r) \\ &= \hbar^{-1}\alpha_{ls}\boldsymbol{\sigma}\cdot\boldsymbol{p}_i \times \boldsymbol{r}(1/r\,\partial\rho/\partial r) \\ &= \hbar^{-1}\alpha_{ls}\boldsymbol{\sigma}\cdot\boldsymbol{L}(1/r\,\partial\rho/\partial r) \end{aligned} \tag{59.}$$

showing the usual dependence on the derivative of the (assumed spherically symmetric) density distribution.

Reactions on the optical model.—The optical model can also be used to some extent for calculating inelastic scattering and reaction cross sections, although its applicability in the simplest form will be limited by the details of the nuclear wave functions involved. Consider an extreme case of inelastic scattering, where the final state of the nucleus has the wave function ψ^{m_j}, with only one (independent) nucleon in an excited state, as would occur in an ideal shell model. Then the arguments used in equations 43, 44, and 45 would indicate that the matrix element to first order in the inelastic process, but corrected for all coherent multiple scattering before and after the inelastic event, is

$$M \sim \int \psi^{m_j *}\phi_f^* V(r - r_j)\phi_i \psi^0 d^{3A} r_j dr \tag{60.}$$

where ϕ_i, ϕ_f are the initial and final wave functions of the incident nucleon in the effective optical potential $-(V_0 + iW)$. As with equation 49, the multiple-scattering effects are included ϕ_i, ϕ_f; the calculation of the inelastic process can be carried to higher orders in $V(r - r_j)$ by using some technique (e.g., coupled equations) that does not rely on an expansion in powers of $V(r - r_j)$ but still permits the use of ϕ_i, ϕ_f.

In actual nuclei the final nuclear state will always be more complicated than ψ^{m_j}, especially when it is an eigenstate ψ_λ. The wave function can be written

$$\psi_\lambda = a_{\lambda m_j}\psi^{m_j} + \sum_{m'} \psi^{m'} \qquad 61.$$

where the $\psi^{m'}$ are more complicated configurations not to be reached from ψ^0 by the one-step process described by equation 60. The contributions of "direct" inelastic scattering to the total cross section will thus be $|a_{\lambda m_j}|^2 \times |M|^2$, and there will be additional contributions from more complicated processes. The most complicated processes will be of a statistical character, as opposed to the optical nature of the direct process. There will of course be intermediate paths from ψ^0 to some of the less complex $\psi^{m'}$ that are not well described by either the one-step or statistical extremes.

The angular distribution of optical processes described by equation 60 tends to show forward peaking, which becomes more pronounced with increasing incident energy, while the statistical processes must yield angular distributions symmetric about 90°. Thus the measurement of inelastic angular distributions gives at least a qualitative indication of the relative magnitude of $|a_{\lambda m_j}|^2$. If the distribution has strong forward peaking, the initial and final nuclear wave functions are very "similar," differing mainly by the arrangement of one nucleon; if the distribution is predominantly symmetric, the initial and final nuclear configurations are relatively "dissimilar."

The same considerations can be applied to reactions, such as (n, p) or (p, n), where the initial and final nuclear wave functions can differ by only one orbital. The prime example of this type of "optical" treatment of nuclear reactions has of course been the "stripping" reactions, mainly (d, p) and (d, n) [see (45) for references]. The stripping contribution to the (d, p) reaction is calculated for that part of the final nuclear wave function which consists of the target nucleus in its ground state plus one neutron in an excited state. The general success of the stripping calculations in comparison with experiment is an indication that most low-lying nuclear states are well described by such a shell model picture; the occasional appearance of a relatively symmetrical (d, p) angular distribution suggests that some levels do not have much of this simple character.

The statistical model.—The statistical model can be most clearly described for reactions other than elastic scattering. In terms of Figure 1 it assumes that the transmitted wave packet is immediately absorbed and never reconstituted: the incident energy is instantly and randomly distributed among all the configurations ψ_λ that may be present. From this random distribution eventually occurs the decay that produces the reaction. The previous discussion of Figure 1 may make this assumption seem a little unrealistic, but the statistical model is supposed to represent one extreme form of the compound nucleus. It has perhaps not always been clear that the "compound nucleus" concept does not necessarily imply the statistical model. In the statistical model the phases of the ψ_λ present in any nuclear wave function are random and remain so with time in a time-dependent picture. There is hence no interference between separate ψ_λ in the decay process. The rate of

decay into any channel c' is an average over that for the ψ_λ with E_λ in the neighborhood of E. In terms of equation 10 the signs of $\gamma_{\lambda c}$ and $\gamma_{\lambda c'}$ are assumed totally uncorrelated, so that

$$|\overline{R}_{cc'}|^2 = \sum_{\lambda,\lambda'} \left(\frac{\gamma_{\lambda c}\gamma_{\lambda c'}}{E_\lambda - E - (i/2)\Gamma_\lambda}\right)\left(\frac{\gamma_{\lambda' c}\gamma_{\lambda' c'}}{E_{\lambda'} - E - (i/2)\Gamma_\lambda}\right)$$
$$\approx \sum_\lambda \frac{\gamma_{\lambda c}^2\gamma_{\lambda c'}^2}{(E_\lambda - E)^2 + (\Gamma_\lambda/2)^2} \qquad 62.$$

A secondary assumption is generally made, either explicitly or implicitly, that the $\gamma_{\lambda c}^2$ show no gross energy dependence on E_λ. This is not absolutely necessary: $\gamma_{\lambda c}$ could be assumed to have random sign fluctuations but to have a magnitude correlated with E_λ. Such an assumption is rather artificial, however, and it seems more in the spirit of the extreme statistical model to take $\gamma_{\lambda c}$ independent of energy except for random fluctuations.

The statistical model refers only to the compound nucleus, and for elastic scattering the compound nucleus contribution is given by a form like 62 with $c' = c$. In this case the primary statistical assumption of random signs for $\gamma_{\lambda c}$ and $\gamma_{\lambda' c}$ is of no consequence, since only positive quantities $\gamma_{\lambda c}^2$ occur. The only relevant statistical assumption is the secondary one that $\gamma_{\lambda c}^2$ is independent of E_λ. This leads to the "continuum model" (46), in which the total nuclear cross section for compound nucleus formation (with incident neutrons) is a monotonically decreasing function of the incident energy (equation 68).

Under the statistical assumption all nuclear cross sections can be determined from the general quantum mechanical requirement of reciprocity or detailed balance (1). The primary statistical assumption implies a complete separation of the production and decay processes for the compound nucleus. The compound system is formed and remains throughout its lifetime in a chaotic state, the properties of which depend only on the excitation energy and not on the mode of formation. The probability of forming the compound nucleus through the entrance channel c is T_c (equation 23). If we could produce the same compound nucleus through channel c' (this is generally impossible in practice, since at least one of the particles in c' will be in an excited state), the probability of formation would $T_{c'}$, calculable in exactly the same way as T_c. One aspect of reciprocity is the fact that the transmission coefficient of any channel is identical in both directions, for decay and formation of the compound nucleus. Thus the relative probability of decay through any channel c' is $T_{c'}$.

To obtain the cross section for any nuclear reaction, we must take account of competition among the many possible decay channels for the compound nucleus (1). In general, we only wish to distinguish the kind of particle (n, p, α, etc.) emitted and its energy; many channels c' will be lumped together under this crude classification. We perform this summation over many channels by introducing $\omega_{c'}(E_x)$, the density of channels for particle c' per unit excitation energy E_x of the residual nucleus. Then the relative probabil-

ity of emitting particle c' in the range of channel kinetic energy $dE_{c'} = -dE_x$ is

$$T_{c'}\omega_{c'}(E_x)dE_{c'} \tag{63.}$$

To normalize these probabilities, we compute the "total transmission"

$$I_i = \sum_{c'} \int_0^{E(C)-B_{c'}} T_{c'}\omega_{c'}(E_x)dE_{c'} \tag{64.}$$

where $E(C)$ is the energy of the compound nucleus and $B_{c'}$ is threshold energy for the channel c'. The cross section for the reaction $c \rightarrow c'$, with c' in the energy range $dE_{c'}$ is then

$$\begin{aligned} d\sigma_{cc'} &= \frac{\pi}{k_c^2} \sum_l (2l+1)T_c^l \left\{ \frac{T_{c'}}{T_t}\, \omega_{c'}(E_x) \right\} dE_{c'} \\ &= \sigma_c(C) \left\{ \frac{T_{c'}}{T_t} \omega_{c'}(E_x) \right\} dE_{c'} \end{aligned} \tag{65.}$$

In this expression the $\sum_l$ is explicit for the entrance channel only. For the exit channel the sum over all l is already implied:

$$T_{c'} = \sum_l (2l+1)T_{c'}^l = \frac{k_{c'}^2}{\pi}\, \sigma_{c'}(C) \tag{66.}$$

Inserting equation 66 in equation 65 yields

$$\begin{aligned} \sigma_{cc'} &= \sigma_c(C) \left\{ \frac{k_{c'}^2 \sigma_{c'}(C)}{F} \right\} \omega_{c'} dE_{c'} \\ F &= \sum_{c'} \int_0^{E(C)-B_{c'}} k_{c'}^2 \sigma_{c'}(C) \omega_{c'}(E_x) dE_{c'} \end{aligned} \tag{67.}$$

If we now make the secondary assumption that $T_{c'}^l$ varies with energy only because of factors external to the nuclear radius a, then $T_{c'} = \text{const} \times P_{c'}^l$. The resultant $\sigma_{c'}(C)$ have the classical form (47)

$$\sigma_{c'}(C) \approx \pi(a + k_{c'}^{-1})^2 \left[1 - \frac{zZe^2/(a + k_{c'}^{-1})}{E_{c'}} \right] \tag{68.}$$

where zZe^2 is the product of particle charges in channel c'. These forms can be refined by calculating the wave mechanical $P_{c'}^l$ explicitly (47).

Level densities.—Actual calculation of $\sigma_{cc'}$ depends on the level density function $\omega(E_x)$. This has been estimated by statistical mechanical procedures (2, 32, 48 to 51); various authors differ somewhat in the details, but the gross features are always the same. The nucleus is regarded as a Fermi gas of independent particles. The level density ω of this system and its excitation energy E_x are both expressed in terms of a parameter T, which by analogy is called the "temperature" of the nucleus. Of course the levels of the nucleus are not those of independent particles, but the interactions between nucleons are not expected to alter the average level densities. The dominant term of the level density is the exponential

$$\omega \sim e^{S(E_x)} \tag{69.}$$

where S is the "entropy," and $1/T=\partial S/\partial E_x$ (T is in energy units so that Boltzmann's constant does not appear explicitly). All treatments also conclude that the dominant dependence of S should be

$$S \sim (AE_x)^{1/2} \qquad 70.$$

where A is the number of nucleons in the nucleus. The nuclear "temperatures" expected for incident particle energies up to 50 Mev. range roughly over $T \approx 1-4$ Mev. (50).

The calculation of ω appears to be one of the more satisfactory features of the theory of nuclear reactions. Given a nucleus in a statistical state, the formulae 65 to 70 presumably apply (49, 50). The discrepancies with experiment seem more likely to be attributable to nonrealization of the statistical conditions than to serious errors in the expressions for ω.

Comparison with Experiment: Elastic and Total Cross Sections

Total neutron cross sections.—The first experiments failing to verify the predictions of the statistical model were the total cross section measurements for neutrons in the range 0 to 3 Mev. (6 to 9). The cross sections did not always fall monotonically with increasing neutron energy, and the energy variation followed a smooth pattern with A. Figure 3 represents[6] a three-dimensional plot of σ_n against E_n and A. The major features of this plot are reproduced by an optical model (28) in which the nucleus is replaced by a square potential well of radius and depth

$$\begin{aligned} a &= r_0 A^{1/3}, & r_0 &= 1.45 \times 10^{-13} \text{ cm.} \\ V &= -V_0(1+i\zeta), & V_0 &= 42 \text{ Mev.}, \ \zeta = 0.03 \end{aligned} \qquad 71.$$

The cross sections calculated with parameters 71 are shown in Figure 4. The letters S, P, D, $\cdots$, denote the orbital angular momenta of the neutrons responsible for the corresponding peaks in the cross section. The agreement between Figures 3 and 4 is generally quite striking and lends strong support to the model and to the (approximate) parameters in equation 71.

It is, in fact, possible to deduce the values of V_0 and $W=\zeta V_0$ from the known parameters of nucleon-nucleon forces. A detailed treatment using U_0 of equation 57 for the near-ground states of a nucleus (52) indicates a value of V_0 on the order of 35 Mev.; and the calculation of W from equations 47 and 48 (53) leads to $W \approx 2$ Mev. at low-incident energies. The value of r_0 in equation 71 is rather larger than 1.2×10^{-13} cm. indicated by electromagnetic experiments, but a recent analysis (54) has indicated that a better fit to the neutron data at about 4 Mev. is obtained by taking

$$\begin{aligned} a &= r_0 A^{1/3} + b_n \\ r_0 &= 1.26 \times 10^{-13} \text{ cm.}, \qquad b_n \approx 0.7 \times 10^{-13} \text{ cm.} \end{aligned} \qquad 72.$$

which is much more consistent with the electromagnetic measurements.

The angular distributions of elastic neutron scattering have been measured at $E_n=1$ Mev. (54). The calculated angular distributions are somewhat

[6] In both Figures 3 and 4 the energy scale is in units of $(ka)^2=2Mr_0^2A^{2/3}E_n/\hbar^2$.

uncertain because of the difficulty with the compound elastic cross section. In spite of the flexibility allowed by this uncertainty, the agreement between theory and experiment is somewhat less satisfactory than for the total cross sections. The calculations have been based on the convenient but unrealistic model of a square well with perfectly sharp edges; allowing some smear of the boundary region of V_0 might appreciably alter the calculated angular distribution. This has been found in the case of elastic proton scattering at $E_p = 18$ Mev. (see below), but corresponding calculations for low-energy neutrons have not been reported.

Separate measurements of the neutron absorption cross section in this low energy range have been reported only in a preliminary fashion (55) and do not agree particularly well with the model parameters used for the total cross sections. Here again edge effects may be of importance.

Reduced widths and strength function.—An independent means of checking the optical model at low energies is through direct measurement of Γ_n for a number of isolated resonances and the calculation of $\langle \Gamma_n/D \rangle$ or hence $s(E)$. Such measurements have been collected in the region near $A \sim 150$ (56) and near $A \sim 50$ (57). The experimental quantity plotted against A is $\langle \Gamma_n^0 \rangle / \langle D \rangle$, where $\Gamma_n^0 = \Gamma_n/(E_n)^{1/2}$ to remove the energy-dependent factor present in P_n but not in $s(E)$. In both regions $\langle \Gamma_n^0 \rangle / \langle D \rangle$, shows a maximum as a function of A: a pronounced peak at $A \sim 52$, and a less well-defined one at $A \sim 160$ to 165. Fitting these maxima to formula 17, we have

$$\frac{2MV_0}{\hbar^2} a^2 = (p - 1/2)^2 \pi^2$$
$$a = r_0 A^{1/3} + b_n \qquad 73.$$

where $p = 3$, 4 for $A = 52$, 160 to 65. If V_0 is a constant, the ratio b_n/r_0 is determined by the A's for $p = 3$ and $p = 4$ and turns out to be

$$b_n/r_0 \approx 0.6 \qquad 74.$$

which is compatible with equation 72. From the absolute A values of the maxima, it follows that

$$r_0^2 V_0 = 67 \text{ Mev.} \times 10^{-26} \text{ cm.}^2 \qquad 75.$$

so that $V_0 = 40$ to 47 Mev. as r_0 varies in the range 1.3 to 1.2×10^{-13} cm. The peaks of $\langle \Gamma_n^0 \rangle / \langle D \rangle$ as a function of A should be proportional in width to $\zeta = (W/V_0)$ and in height to $1/\zeta$. Although the estimates of ζ made by these means from present data may be unreliable, they show some discrepancies: the apparent peak height at $p = 4$ is better fitted by $\zeta \approx 0.05$ than by $\zeta = 0.03$ as in equation 71; the peak height of $p = 3$ seems on the other hand to require $\zeta < 0.02$. The widths of both peaks suggest values on the order of $\zeta \sim 0.1$. These fluctuations may be in part attributable to the fact that the shape of the nuclear well is badly approximated as a well sharply cut off at radius a (58). Information about ζ as also provided in principle by the values of $\langle \Gamma_n^0 \rangle / \langle D \rangle$ at the minima between the peaks. These minimum values should be approximately proportional to ζ and are expected at $A \approx 25$, 95, 240 (28).

Energy dependence of optical potentials.—Measurements of neutron cross

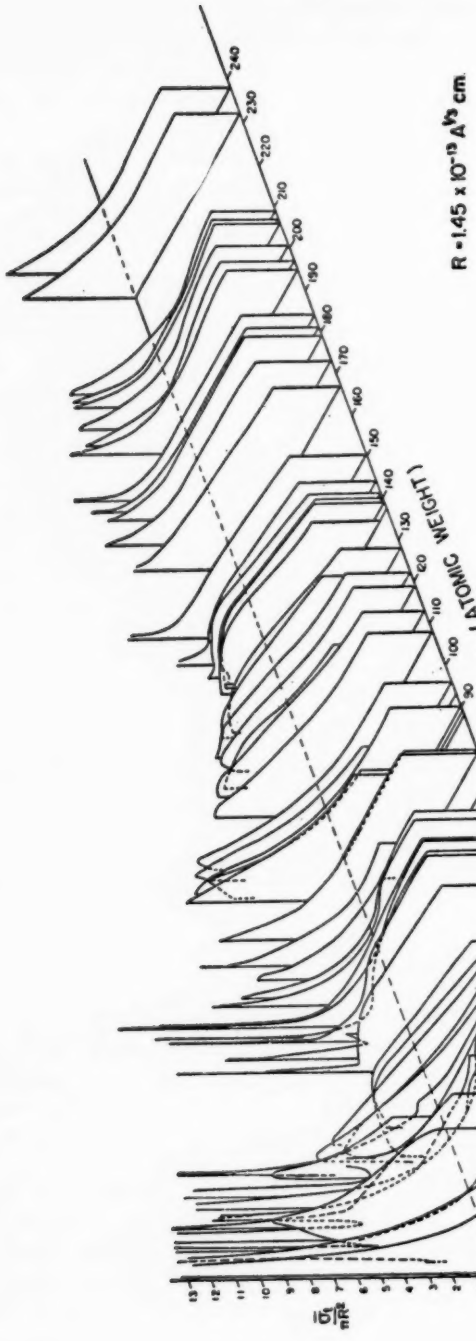

FIG. 3. Observed total neutron cross sections [Barshall *et al.*, reported in (28)]: $\sigma_t = \sigma_c$ of the text, $1/\lambda = k_c$ of the text.

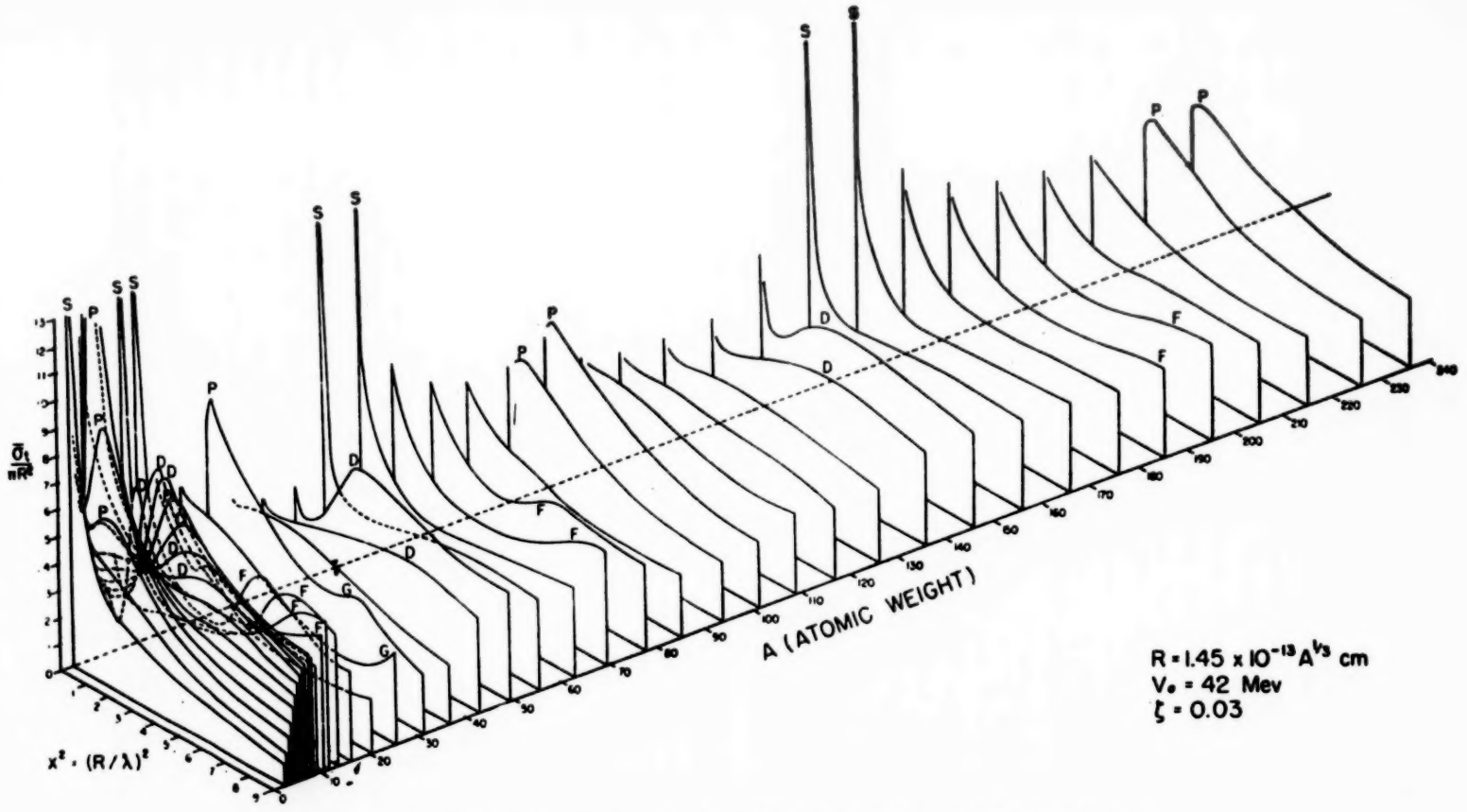

FIG. 4. Calculated total neutron cross sections (28): $\sigma_t = \sigma_c$ of the text, $1/\lambda = k_c$ of the text.

sections at incident energies $\gtrsim 3$ Mev. are rather sporadic but give some indication of the variation with energy of the optical model parameters, V_0 and W. Angular distributions of elastically-scattered neutrons $E_n = 4.1$ Mev. (59) appear to require for an optical model fit (60) about the same V_0 and a as in equation 71, but with a considerably larger ζ, say of order 0.1 .At this energy the compound elastic scattering is considered to be negligible for most nuclei, so that the calculated angular distribution is based on $\sigma_e(S)$ alone. A large value of ζ is also suggested by the relatively smooth angular distributions reported at $E_n = 3.7$ Mev. (61).

There is some coverage of neutron cross sections up to $E_n \approx 20$ Mev. (62 to 69). Fits to the total and absorption cross section as a function of A, and to the angular distributions (70) from C, Al, Cu, Sn, and Pb have been made at $E_n = 14$ Mev. (71) with the parameters

$$\begin{aligned} V_0 &= -(42 + 11i) \text{ Mev.} && r \leqq 1.22A^{1/3} \\ &= -36 \text{ Mev.} && 1.22A^{1/3} \leqq r \leqq 1.22A^{1/3} + 0.74 \\ &= 0 && r > 1.22A^{1/3} + 0.74 \end{aligned} \qquad 76.$$

where r is in units of 10^{-13} cm. There is a gap in the measurements from about 20 to 40 Mev; but for selected targets the total cross sections for neutrons have been observed over the range 40 to 100 Mev. (72, 73, 74). When plotted against a logarithmic energy scale (75), these cross sections show pronounced and systematic fluctuations. No completely consistent analysis has been made of these curves of the whole energy range from 0 to 100 Mev., but an optical model analysis has been made of the high energy end (76).

It is not yet possible to draw more than rather qualitative conclusions about the energy dependence of V_0 and λ (or W). It appears that as E_n ranges from 0 to 100 Mev., the magnitude of V_0 decreases from ~ 40 to ~ 20 Mev.; the decrease appears at present to be fairly uniform, although this is uncertain. The behavior of λ at low energies is very striking, and can be very crudely represented by

$$\lambda \approx (3.5 + 20e - E/2) \times 10^{-13} \text{ cm.} \qquad 77.$$

where E is the incident nucleon energy in Mev. The coefficient 3.5 in equation 77 is slightly energy-dependent and increases gradually by a factor of about 1.5 as E ranges up to 100 Mev. (See Figure 2.) The strongly energy-dependent part of λ represents the great increase at low energies effected by the exclusion principle.

Proton scattering.—Angular distribution measurements have also been reported for elastic proton scattering (77 to 85). Such charged particle measurements should in principle be capable of higher precision than those with neutrons. They have an additional advantage in the interference with Coulomb scattering, which provides an absolute calibration of the nuclear scattering amplitude. Proton elastic scattering therefore seems best suited to reveal finer details of the effective nuclear potential well. It has already shown, for example, that the well cannot have the physically unrealistic sharp edge. A striking feature of the experimental angular distributions for

$E_p = 18$ to 22 Mev. on medium and heavy elements is the extremely low differential cross sections in the backwards directions (82, 83). Exact calculations on a square well model for Cu (87) were unable to reproduce this low backscattering, although the square well model is not in such serious disagreement for a light nucleus like Al (83), where the backscattering is relatively high. On the other hand, the use of rounded corners at the edge of the potential well (88), according to the formula

$$V = \frac{-(V_0 + iW)}{1 + e^{(r-a)/b}} \qquad 2b \approx 0.7 \times 10^{-13}\text{cm}. \qquad 78.$$

gives much better agreement with the experimental results for Ni and even for a heavy element like Pt. The comparison of the square and rounded edge models for Pt is shown in Figure 5.

A qualitative interpretation of the dependence on potential shape may be found in terms of the optical model. In the crudest form of the optical model (Fig. 6a) the rays pass without deviating through the region of the potential, and the entire cross section is computed from their change of phase on this passage. No account is taken of refraction and reflection at the edges of the potential. It is not difficult to take refraction also into account, as shown in Figure 6b for an attractive potential. The refractive effect is a

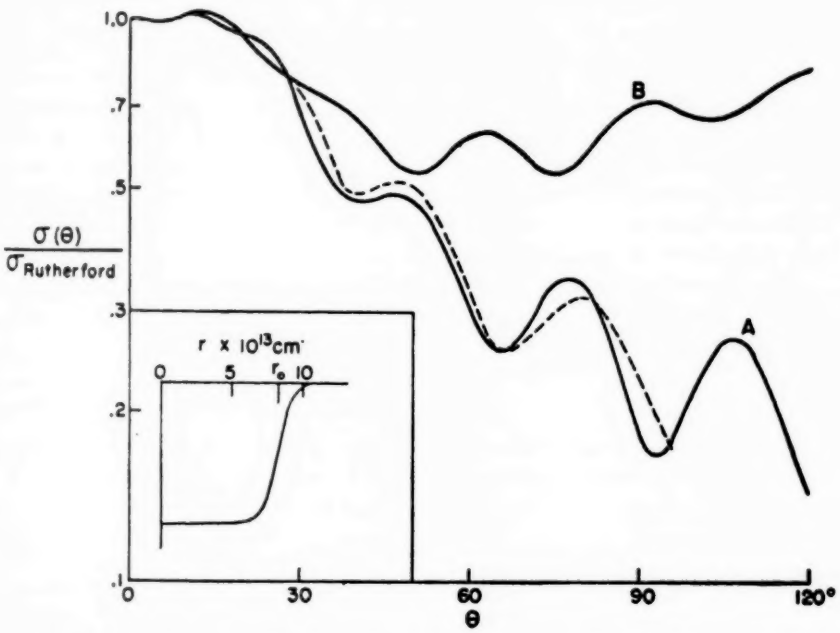

FIG. 5. Calculated elastic scattering of 22 Mev. protons on Pt (88): curve A is for a potential of the shape shown, curve B for a comparable square well with sharp edges. The dashed line shows the experimental curve (82).

maximum for a potential with sharp edges, and even in this case it is generally insufficient to give any substantial backscattering, as suggested in Figure 6b. The major contributions to backscattering must come from the neglected reflections at the front and back surfaces of the potential. At $E_p = 18$ to 22 Mev. the optical mean free path λ is near its minimum, so that for a large nucleus only reflection at the back surface need be considered; reflected waves from the front surface will be substantially absorbed and can be in first approximation neglected. The reflection coefficient of a surface is known to be a maximum if this surface is sharp, and to decrease to zero for an infinitely diffuse surface. The difference between curves A and B in Figure 5 is thus attributed to the difference in reflection coefficients of the sharp versus the diffuse back surface of the nucleus.

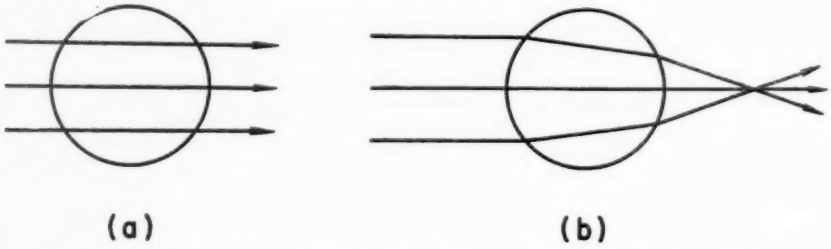

FIG. 6. Optical model (a) without refraction or reflection at the boundaries; (b) with refraction, without reflection.

Light nuclei, on the other hand, are small enough to be fairly transparent, so that the backscattering is the result of multiple internal reflections in the nucleus including both front and back surfaces. For such multiple-reflective processes the properties of the individual surfaces are apparently less critical, so that the backscattering with rounded potential edges may be to some extent reproduced by square edges as well.

The general validity of the optical approach in treating these phenomena is nicely borne out by comparison (Fig. 7) of the positions of successive maxima and minima throughout the periodic table (82). The angular position θ of any particular maximum or minimum varies as

$$\theta \sim A^{-1/3} \qquad 79.$$

usually within the experimental error. This is roughly in accordance with the diffraction theory from an optical sphere (neglecting Coulomb interference), for which the maxima and minima are defined by

$$ka \sin \theta/2 = \text{const} \qquad 80.$$

If θ is not too large, $\sin \theta/2 \approx \theta/2$; since $k = (2ME_p/\hbar^2)^{1/2}$ is a constant for the experiments, and $a = r_0 A^{1/3}$, equation 80 is equivalent to the proportionality 79. The curves in Figure 7 also show a systematic dependence on A of the backscattering (relative to Rutherford scattering); it is large in the lightest elements (Be, C) and progressively diminishes, becoming small in the

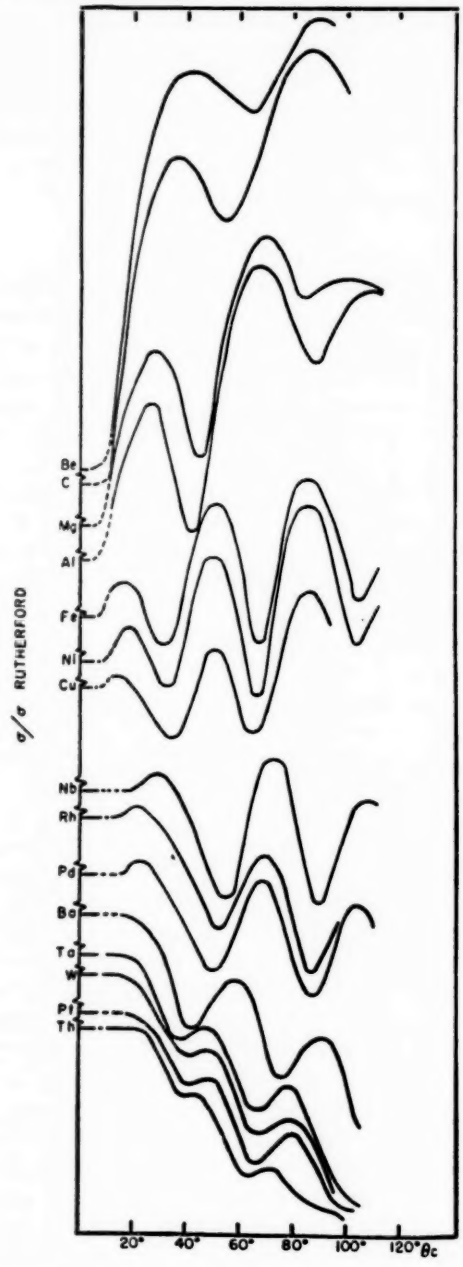

FIG. 7. Elastic scattering of 22 Mev. protons relative to Rutherford scattering throughout the periodic table (82).

heaviest elements (Pt, Th). This behavior illustrates graphically the reduction of backscattering from any but the back surface of the nucleus as the nuclear dimensions become large.

Spin-orbit coupling.—The calculated angular distributions for 20 Mev. protons and 14 Mev. neutrons have sharper minima than are observed even in experiments with good angular resolution. This may be attributed (71) at least in part to the presence of a spin-orbit term

$$\sigma \cdot \boldsymbol{L} V_{ls}(r) \qquad 81.$$

in the optical potential. In any scattering process the vector $\boldsymbol{L}$ will be perpendicular to the scattering plane formed by the incident and emergent particle direction. If we quantize σ along the direction of $\boldsymbol{L}$, the spin-orbit coupling 81 will not flip the spin direction during the scattering process. The total scattering cross section is the sum of separate, noninterfering cross sections for "spin up" and "spin down" particles. Because of the potential 81, however, the spin up and spin down particles encounter slightly different potentials in the nucleus, so that the cross section curves for the two varieties of spin are not identical. In particular, they will in general have their minima at neighboring but not identical angles, so that the composite total cross section will have broader and shallower minima than occur for a calculation with a single potential.

More details of this spin-orbit coupling would presumably be revealed if polarization (i.e., double scattering) measurements should become possible in this energy region. The polarization should show a striking dispersion curve as the angle of observation passes through one of the minima in the scattering cross section. It is unfortunate that the most interesting polarization effects occur in the regions of minimum absolute cross sections. The only direct measurements of polarization so far have been with neutrons at $E_n = 0.4$ Mev. (89). According to Figure 4, p-wave scattering should be predominant at this energy in the vicinity of $A = 100$, so that spin-orbit coupling could be observed. The measurements indicate a spin-orbit potential of the same sign and approximate magnitude as that in the shell model; a more precise statement is not possible at present.

Complex particles.—The optical model should also be relevant for the elastic scattering of more complex particles, although to date there is very little experimental information on this subject (90, 91, 92). The only optical-type analysis (93) has been approximate but indicates that the model is applicable to α-particle scattering. Two interesting features result from this analysis: the imaginary part W of the optical potential for α-particles increases rapidly with incident energy up to $E_\alpha = 40$ Mev.; and the magnitude of W attains much larger values than for neutrons and protons. Using the quoted (93) values $W_0 = 30$ Mev. for $E_\alpha = 40$ Mev., $\theta = 60°$, we obtain an optical mean free path for the α-particle of $\lambda_\alpha \approx 0.6 \times 10^{-13}$ cm. This value may be a little too small: to judge from the published curves (93), a choice of $V_0 \approx 40$ Mev. in harmony with neutron and proton scattering would lower

W_0 to around 20 Mev., and the mean free path would increase to $\lambda_\alpha \approx 1.0 \times 10^{-13}$ cm. These mean free paths are roughly in accord with a very simple picture. If the four nucleons in an α-particle do not interfere with each other in passing through the nucleus, the probability that any one of them will be absorbed is four times as great as for a single nucleon. Since absorption of any nucleon from the α-particle means its destruction as an entity, its mean free path for "optical absorption" would be

$$\lambda_\alpha \approx 1/4\lambda \qquad 82.$$

The average energy of translation per nucleon in a 40 Mev. α-particle is 10 Mev., at which energy $\lambda \approx 3.6 \times 10^{-13}$ cm., so that the observed λ_α are consistent with equation 82. The rapid decrease of W for α energies below 40 Mev. (93) reflects the increase of λ with decreasing energy. Of course a more refined consideration is needed, especially on the question of how to take the binding energy of the α-particle into account.

It would be desirable in this connection to have experiments from which to establish directly the appropriate potentials V_h and W_h for the heavy particles h. Cyclotron measurements of the angular distribution in elastic α-scattering on heavy elements (92) do not show a very strong structure of peaks and valleys because of damping by the large absorption coefficient and the relatively narrow spacing of the pattern for so large a value of kR. Elastic α-scattering from light elements is more promising; Al shows a well resolved peak structure in the elastic $d\sigma/d\Omega$ for 20 Mev. α's (94).

Comparison with Experiment: Nuclear Reactions

Under "reactions" we include every process except elastic scattering. As indicated in the section on Optical and Statistical Models, there are at least two extreme approaches to the interpretation of nuclear reactions, the respective optical and statistical models. Unfortunately, a successful model of nuclear reactions is not at present available: the predictions of the statistical model (1), though simple and general and thoroughly worked out, show substantial deviations from recent detailed measurements. The optical model, on the other hand, has not yet been completely explored theoretically, especially in its application to reactions. It has the difficulty that it will certainly involve the knowledge of more specific and variable parameters than enter into the statistical model. Almost entirely open at present is the further question of whether any simple scheme can be found for combining the optical and statistical models in cases (presumably the great majority) where the true situation lies somewhere between these extremes. In the absence of a reliable and well-implemented model for nuclear reactions, the discussions of the present section will be of a rather qualitative and preliminary character.

The optical and statistical components of a given reaction have different angular and energy distributions. The optical components always tend to asymmetric distributions peaked in the forward direction (95, 96, 97), es-

pecially at high energies: since only a few target nucleons at most are involved in a "direct" reaction of this type, the forward momentum of the incident particle produces forward peaking of the reaction products. The angular distribution of the statistical component, on the other hand, is symmetrical about 90°.

Optical effects on the energy distribution of reaction components are a little more varied. There is first of all the tendency to reaction products of high energy, produced in a "knock-on" process without much sharing of energy with other nucleons in the nucleus. In addition, the exceptional transparency of nuclear matter in the region a few Mev. above the energetic threshold enhances "leakage" of nucleons in this energy region. Thus even if the knock-on processes leave behind a certain amount of excitation energy in the nucleus, this energy will tend to leak out as low-energy nucleon emission before being shared among all the nucleons to establish the statistical state. Optical effects thus modify the energy distribution expected from the statistical model by emphasizing both high and low energies.

Angular distributions from individual levels.—Among low-lying levels and light nuclei are some fortunate cases where the reaction products corresponding to a single energy level of the residual nucleus can be resolved. Then only the angular distribution is a matter for consideration and provides an immediate, qualitative evaluation of optical versus statistical components for the reaction. The part of the distribution with forward-and-back symmetry can be labeled "statistical," and the forward-peaked component "optical." This is a very crude method of distinction and is probably subject to refinement but may serve as a zeroth approximation. The angular distribution of 10 Mev. (p, p') scattering to the first excited state (1.38 Mev.) of Mg^{24} provides an opportunity for this type of analysis (84). In this case the optical ("direct collision") component approaches the statistical ("compound nucleus") in intensity. These relative intensities appear to vary quite widely from one reaction to another: the inelastic scattering of 10 Mev. protons to the first excited states of C^{12} (84), N^{14} (85), and Ne^{20} (86) appears to be largely symmetrical, while that to excited states in A (86) and Fe^{56} (98) shows an appreciable forward asymmetry.

A crude interpretation of this variation is in terms of the "similarity" or its absence between the wave functions of the ground and excited levels of the residual nucleus. As mentioned in the section on Optical and Statistical Models, the optical inelastic reaction is essentially the part that occurs by rearrangement of only one nucleon in the transition from initial to final nuclear states. Thus if these states are very similar, the optical component will be large; it will be small if they are dissimilar, i.e., described by wave functions that differ mainly by several single-particle orbitals.

A type of reaction that should proceed predominantly through the optical component is inelastic deuteron scattering (d, d'). In the statistical model the loosely-bound deuteron is very unlikely to hold together through a reaction; in the optical model it is comparable to a single nucleon in inelastic

scattering, although somewhat more liable to absorption in passing through the nucleus. This reaction has been reported on C (91, 99), where the 4.4 Mev. and 9.6 Mev. levels have been observed, but not that at 7.5 to 7.6 Mev. This would suggest that the two observed levels are similar to the ground state, the one at 7.5 Mev. dissimilar. This is confirmed by the inelastic scattering of high energy (96 Mev.) protons on C (100). The conditions of a fast incident particle on a small nucleus seem considerably to favor optical over statistical processes: again only the 4.4 and 9.6 Mev. levels appear, and the 7.5 Mev. level is absent. The optical component of the 0 to 1.38 Mev. transition in Mg^{24} also reveals itself in (d, d') scattering (101).

The same distinction of similar versus dissimilar configurations may be useful in considering some (d, p) and (d, n) reaction results. These reactions are generally considered to proceed mainly by "stripping" which is calculated on a purely optical basis (95), and shows the usual forward peaking. If, however, the components of initial and final nuclear states that differ by only one nucleon orbital form a relatively small fraction of the initial and final configurations, the simple stripping calculation will not be very applicable. The statistical contribution to the reaction might then be dominant, leading to a p or n distribution symmetrical about 90°. Recently (d, p) angular distributions more in accord with statistical than with stripping theory have been reported (102, 103) in B and Ni, although the stripping peaks are found in a majority of cases so far investigated (45). It is of interest to note that the one reported case of symmetry (in fact, isotropy) in (d, n) angular distributions (104) occurs for $B^{11}(d, n)C^{12*}$ leading to the 7.5 Mev. state of C^{12}, while the reactions leading to the ground, 4.4 Mev., and 9.6 Mev. states all show stripping peaks.

Individual nuclear levels are also singled out in isomeric state excitation by inelastic (neutron) scattering (105, 106, 107). Since the isomeric and ground states are well described by the simple shell model, they might be expected to be very similar in the sense of the present discussion. The same is true of the levels above the isomeric state that feed it by cascade gamma emission after the inelastic scattering. One would therefore expect to see appreciable forward peaking in the inelastically scattered neutrons. Isomeric states are not favorable for coincidence measurements, but the recent extension (108) to inelastic scattering to low, nonisomeric states makes neutron angular distributions not inconceivable. The excitation functions measured are in general agreement with statistical theory (36, 109); it is not known, however, to what extent these differ from excitation functions that could be calculated on the optical model. It can also be argued that the angular distribution would be a more sensitive means of detecting a mixture of optical and statistical components than the excitation functions.

Charged particle yields.—Reaction measurements on medium and heavy nuclei at moderate excitations and higher cannot distinguish individual levels in the residual nucleus. In this case the optical model is most conveniently represented in terms of individual free nucleons in a Fermi well. The reaction

is envisioned as a "Monte Carlo" process (11), in which energy is transferred by nucleon-nucleon collisions, taking into account the exclusion principle. Some of these knock-on nucleons will escape directly from the nucleus; these constitute the "optical component" of the reaction, with characteristic high energies and forward angular distribution. The nucleons that do not escape but fall below the binding energy threshold B of about 8 Mev. contribute their excitation energy ($\lesssim B$) to the statistical mode, since they have no appreciable chance of escaping during the energy distribution process. This model has been used satisfactorily at high incident proton energies of 300 to 400 Mev. (110) and $\lesssim$100 Mev. (111); the extension of the optical domain down to zero incident energy implies that such a Monte Carlo approach should be useful for reactions at any energy. Its chief drawback is the numerical labor involved in obtaining specific results for any particular reaction; but this is characteristic of the optical model.

At intermediate energies the reactions that display the knock-on optical component most clearly are those involving the emission of charged particles, particularly from heavy elements. Because of the Coulomb barrier the kinetic energy of escaping charged particles must generally exceed the barrier energy $B_Z = zZe^2/a$. On the statistical model, however, the average kinetic energy available for emission is of order T, where T is the nuclear temperature in Mev. For heavy nuclei $T \sim 1$ Mev., $B_Z \gtrsim 10$ Mev., so that $T \ll B_Z$. The emission of charged particles relative to neutrons is reduced by a factor of order $f_c/f_n \sim e^{-B_Z/T} \ll 1$ for heavy elements. For light elements B_Z is smaller and T is larger, so that f_c/f_n may not be extremely small; even for heavy elements this ratio is mitigated somewhat by Coulomb barrier penetration, which means that B_Z is replaced by an effective $B_Z' < B_Z$. The f_c/f_n calculated from the statistical model can still be as small as, say, 10^{-6}. The knock-on processes generally yield particles with energies $E \gtrsim B_Z$ and do not discriminate strongly between neutrons and charged particles. Thus a yield of charged particles substantially in excess of the small statistical f_c/f_n is evidence for the optical component.

The first experimental evidence of this type was provided by γ-induced reactions (112) at 17 Mev., where the $(\gamma, p)/(\gamma, n)$ ratio around $Z = 50$ was of order 10^2 times the statistical f_c/f_n. Subsequent studies with (n, p) reactions (113, 114) induced by 14 Mev. neutrons showed similar results. The proton yield ratio Y_p (observed)/Y_p(statistical) shows a systematic increase with Z, averaging around 1 for lighter elements and approaching 10^4 for the heaviest elements. This corresponds to the fact that Y_p (statistical) falls off rather sharply as Z increases past $Z \sim 40$, while the observed cross sections fall off much more slowly because of the knock-on particles. The large Y_p (obs.)/Y_p (stat.) ratio does not necessarily imply that this optical component is very large: it could amount in some cases to only a few per cent of the total reaction cross section and still make for a large ratio, since Y_p (stat.) is so exceedingly small.

The optical or direct component appears very graphically in measure-

ments of inelastic protons from (p, p') processes at 30 Mev. (115, 116). The authors point out that three features of the observations indicate a strong optical component: the p' energy distribution is more uniform and hence has a higher average value than that predicted statistically; the p' angular distribution has a definite forward bias at all energies; the total p' yield is an order of magnitude larger than the statistical calculation allows. This factor of increase in the cross section applies even to the protons emitted at 135° to the incident beam, implying (116) that these protons are mainly the result of a small Monte Carlo cascade. The model is used of direct collisions in the "rim" of the nucleus, with a black interior where the statistical model holds. A consistent optical picture would be quite similar in effect, though not identical: the incident and struck nucleon wave functions should be those of free particles throughout the entire volume of the nucleus. Since, however, the effective nucleon potential at 10 to 30 Mev. excitation has a large imaginary component, these free-particle wave functions will have a radial dependence rather like $\sinh(r/\lambda)$ and will tend to be concentrated mostly near the nuclear surface.

The cross sections for production of α-particles by (n, α) at 14 Mev. (114) shows the same qualitative features as the (n, p) cross section. The ratio Y_α (observed)/Y_α (statistical) increases from $\sim$1 at low Z to $\sim 10^4$ at the highest Z. The explanation again presumably involves a direct collision process. This seems to imply that α-particles have a definite if transitory existence as sub-groups in the nucleus. This is already implied by equation 81: at very low energies the nucleon mean free path is extremely long, which makes for the validity of the shell model; the mean free path λ_α before an α-particle grouping dissociates may be only one-fourth as long, but this can still be several times the nuclear radius.

Of course the Y_α (obs). may represent only a small fraction of the total reaction yield from neutron bombardment and still exceed by orders of magnitude the calculated Y_α (stat.). The knock-on α-particles must come from regions near the edge of the nucleus, for after collision they have high kinetic energies and extremely short mean free paths.

The inadequacy of the statistical model is also indicated by measurements of relative reaction yields as a function of the incident particle. According to the statistical model a given yield ratio like f_p/f_n should depend only on the excitation energy of the nucleus and not on its mode of formation. Studies of the ratio between (p, pn) and $(p, 2n)$ yields (117, 118) as compared with (n, p) cross sections (114) indicate that the tendency for proton emission is enhanced by an order of magnitude or more if the incident particle is a proton instead of a neutron. This contradicts the statistical model, but is at least qualitatively in accord with the optical model: the incident proton is predominantly emitted after one or a few inelastic collisions in the nucleus, so that (p, pn) is greatly enhanced. With incident neutrons re-emission of the incident particle is equally predominant but does not contribute to (n, p).

Inelastic energy distributions.—Detailed studies of the energy distribution

resulting from inelastic proton scattering at 18 Mev. (119) have shown two discrepancies with the statistical model: not only are the scattered protons concentrated too much at high energies, but they are also excessively abundant at low energies. These deviations are usually expressed with reference to the statistical predictions. If the statistical formula 67 is assumed correct and equations 69 and 70 inserted, we have

$$\ln \sigma_{pp'} - \ln \sum_l (2l+1) T_{p'}{}^l + \text{const.} = \ln \omega(E_x) \sim E_x{}^{1/2} \qquad 83.$$

Here the constant on the left hand side involves quantities like F and $\sigma_c(C)$ of equation 67 which do not vary in the experiments considered. Figure 8 shows the experimental points for Cu at 60° and 150° relative to the incident beam. For comparison is shown a curve varying as $E_x{}^{1/2}$. Although the scale factor and zero position of the $E_x{}^{1/2}$ curve are not determined, there can be little doubt that the experimental points for low energy of the emitted protons (plotted as ϵ in Fig. 8) follow a curve of different shape from $E_x{}^{1/2}$. A good approximation to the experimental points at low energy is in fact a simple linear variation as E_x or as ϵ.

The deviation of the measured points at high ϵ from the curve in Figure 8 is qualitatively just as expected from single collisions in the optical model: the products, either knock-ons or the incident proton of slightly degraded energy, have much higher energies than probable in the statistical model. This "high-energy tail" of the distribution should have a predominantly forward direction on the single-collision model; this is borne out in Figure 8 and in similar measurements on other elements throughout the periodic table (119). There seems to be no difficulty about associating the high-energy tail with a "direct collision" optical component.

The low-energy (in terms of ϵ) portion of Figure 8 is more difficult to understand. It does not appear to show significant variation with angle and is therefore not associated with single collisions. If the linear dependence on E_x is expressed in the form

$$\omega \sim e^{E_x/T} \qquad 84.$$

the associated "temperature" T is on the order of 1 Mev. for all elements studied; it decreases only slightly from Al to Pt and has certainly nothing of the $T \sim A^{-1/2}$ character suggested by equation 70. Furthermore, the dependence of equation 84 on E_x should more properly be replaced (119) by a dependence on ϵ,

$$\omega \sim e^{-\epsilon/T} \qquad 85.$$

This is seen by comparing the curves of (log ω-const) at low ϵ for different incident energies E_p. Figure 9 shows the comparison for $E_p = 18$ and $E_p = 16$ Mev. The values of the constant in equation 83 should be essentially the same in both cases, so that Figure 9 actually compares log ω for the two cases. It appears that ω is a function of ϵ alone, not of $E_x = (E_p - \epsilon)$.

No satisfactory explanation is yet available for the anomalous behavior

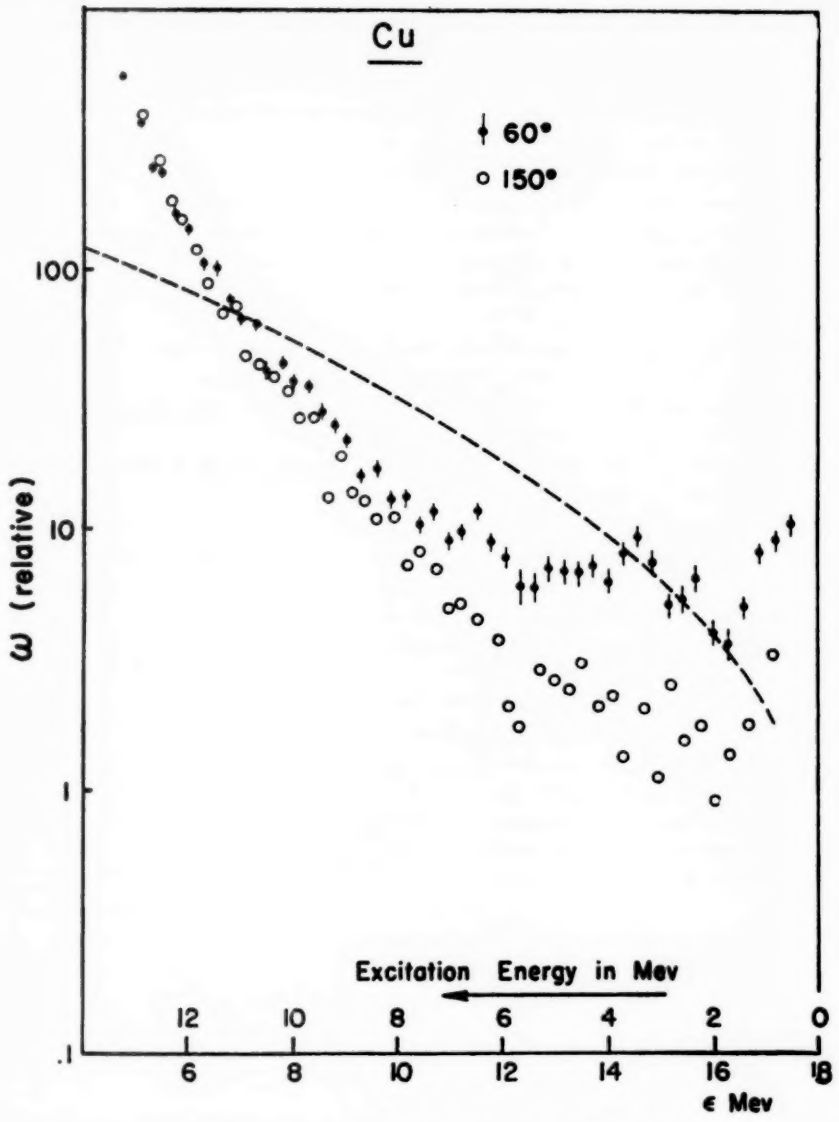

FIG. 8. Inelastic proton scattering from Cu (119). The dotted line varies as $E_x^{1/2}$.

described by equation 85. The preceding discussion, however, has emphasized the necessity for considering optical or direct-collision components as major contributions to nuclear reactions. It is tempting to look for interpretations of equation 85 along the same general lines. For example, the validity

of the optical model down to the very lowest energies implies that all reactions should be calculated by following a Monte Carlo scheme until none of the residual nucleons can escape because their kinetic energies above the top

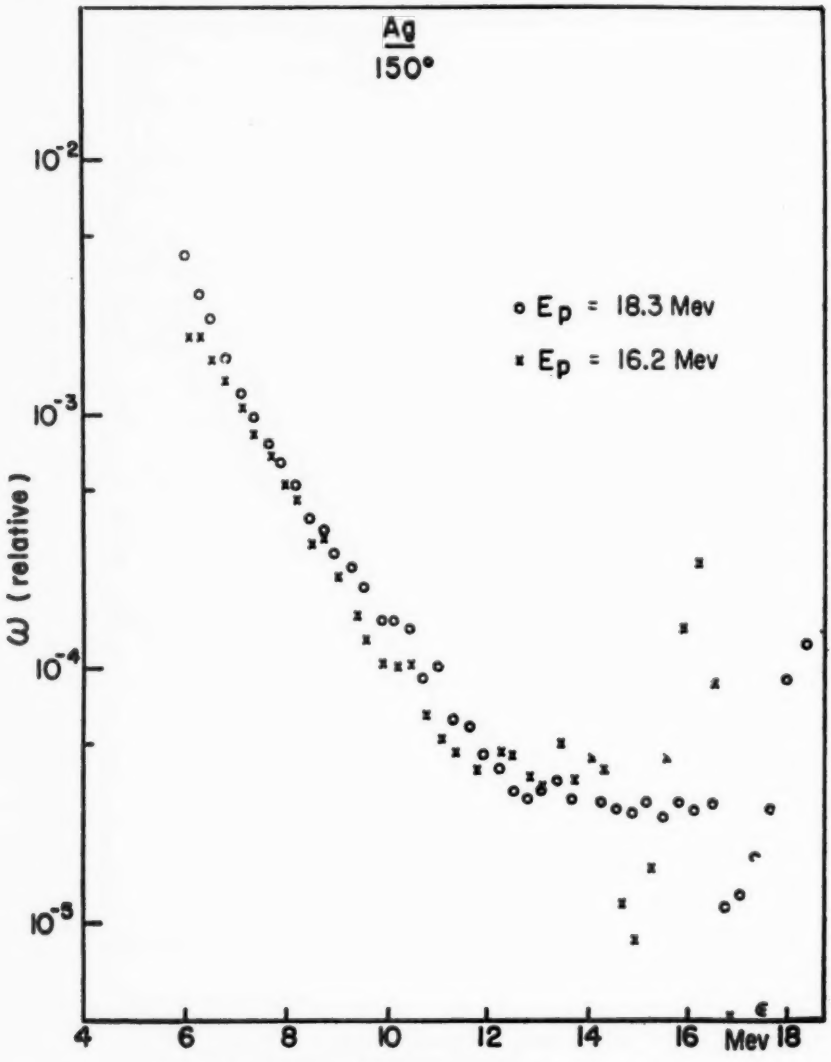

FIG. 9. Comparison of inelastic proton scattering from Ag at $E_p = 16$ and 18 Mev. (119).

of the Fermi well are all below the nucleon binding energy B. Only the energy of these residual nucleons will evenutally be randomly distributed and contribute to the statistical component of the reaction. During the proc-

ess of degradation in the nucleus, the nucleons pass through an energy region where they have still enough energy to escape as free particles, and their mean free path in the nucleus becomes very long because of the Pauli principle. The nucleons are therefore especially likely to escape through this transparent "window" during the cascade process. This escape will have the qualitative features of equation 85: it is a function of the particle energy above the top of the Fermi well or hence above the threshold for emission; it is a gross feature of nuclear matter regarded in the optical approximation and should be much the same for any nucleus; it happens during a cascade process after several collisions and therefore does not show a strong forward angular dependence.

An extremely crude estimate of the window effect is obtained by noting that when the mean free path of a nucleon is $\lambda \ll a$, the nuclear radius, the probability of escape from the nucleus is $\sim\lambda$. If for λ we insert equation 77, the dominant term in the nucleon escape probability will have the form 85. Actually, the constants in equation 77 do not seem quite appropriate to yield equation 85; but a much more careful calculation is required, including the modifications necessary in equation 77 for protons. Because of the lower average binding energy for protons the exponential in equation 77 should probably be dominant up to higher energies. For very heavy elements, however, the region where equation 85 applies would be practically lost because of the high Coulomb barrier. Something of the sort indeed seems to be happening for Pt (119).

The emission of neutrons from (p, n) (120) and (n, n') (121 to 125) reactions induced in the same energy range appears to show the same type of behavior in the regions of low ϵ. In the absence of the Coulomb barrier, the domain of equation 77 is of order $\epsilon \approx 0$ to 4 Mev. for neutrons as compared with $\epsilon \approx 5$ to 8 Mev. for protons (119). The neutron results are complicated by the possible presence of appreciable $(2n)$ emission. There is also preliminary evidence (126) for a forward peaked high-energy tail in the neutron distribution, resulting from direct collisions.

It should be noted that even the statistical state of the nucleus, left behind after all the cascade particles have escaped, will be subject to the window effect. Particle emission from a statistical state occurs only through fluctuations that concentrate much of the available energy on a single particle. When this happens, however, the favored particle may be regarded as beginning a new cascade, during which it is especially likely to escape at energies where λ is long.

Ideal statistical conditions.—Under what conditions, if any, will the statistical model be strictly valid? If the total excitation energy in residual particles after the cascade is sufficiently high, then there will be vacancies at all energies in the levels of the Fermi well and the effect of the exclusion principle will be much reduced. If, for example, the nuclear temperature is as high as 7 Mev. (127), the nucleon mean free path will be very short at all low and intermediate energies. The window effect will be absent, and the condi-

tions should be suitable for maintenance of a statistical energy distribution with the gradual boiling off of particles. These conditions are found in nuclear stars in emulsion initiated by cosmic rays or bombardment by particles from high energy accelerators. After subtraction of the knock-on tracks as indicated by a Monte Carlo calculation (110), the remaining tracks can be interpreted satisfactorily in terms of the statistical model (49, 50). In some of these cases an excessive number of low-energy charged particles have been observed (49, 128), which might indicate that the temperature is not always high enough to eliminate the window effect.

A possible interpretation of equation 84 in thermodynamic language appropriate to the statistical model involves the idea of a phase change in nuclear matter (129, 130). Then $T \approx 1$ Mev. is the characteristic temperature at which nuclear matter "melts"; it will be the temperature observed for all partially melted nuclei, regardless of E_x and A. The full implications of this notion have yet to be worked out; for example, the extent of its equivalence with the Monte Carlo picture of nuclear reactions is unknown. A comparison suggests that the "melting" should be regarded as a process in momentum space rather than coordinate space.

LITERATURE CITED

1. Weisskopf, V. F., and Ewing, D. H., *Phys. Rev.*, **57**, 472 (1940)
2. Weisskopf, V., *Phys. Rev.* **52**, 295 (1937)
3. Bohr, N., *Nature*, **137**, 344 (1936)
4. Kapur, P. L., and Peierls, R., *Proc. Roy. Soc.* (*London*), **166**, 277 (1938)
5. Wigner, E. P., and Eisenbud, L., *Phys. Rev.*, **72**, 29 (1947)
6. Barschall, H. H., *Phys. Rev.*, **86**, 431 (1952)
7. Miller, D. W., Adair, R. K., Bockelman, C. K., and Darden, S. E., *Phys. Rev.*, **88**, 83 (1952)
8. Walt, M., Becker, R. L., Okazaki, A., and Fields, R. E., *Phys. Rev.*, **89**, 1271 (1953)
9. Okazaki, A., Darden, S. E., and Walton, R. B., *Phys. Rev.*, **93**, 461 (1954)
10. Eden, R. J., and Francis, N. C., *Phys. Rev.* (In press)
11. Goldberger, M. L., *Phys. Rev.*, **74**, 1268 (1948)
12. Harkins, W. D., and Gans, D. M., *Phys. Rev.*, **46**, 397 (1934)
13. Amaldi, E., D'Agostino, O., Fermi, E., Pontecorvo, B., Rasetti, F., and Segrè, E., *Proc. Roy. Soc.* (*London*), **149**, 522 (1935) (Earlier references cited there)
14. Bjerge, T., and Westcott, C. H., *Proc. Roy. Soc.* (*London*), **150**, 709 (1935)
15. Artsimovitch, L., Kourtschatov, I., Missovski, L., and Palibin, P., *Compt. rend.* **200**, 2159 (1935)
16. Moon, P. B., and Tillman, J. R., *Nature*, **135**, 904 (1935)
17. Szilard, L., *Nature*, **136**, 950 (1935)
18. Fermi, E., and Amaldi, E., *Ricerca sci.*, **6**(2), 544 (1935)
19. Frisch, O. R., Hevesy, G., and McKay, H. A. C., *Nature*, **137**, 149 (1935)
20. Halban, H. v., and Preiswerk, P., *Compt. rend.*, **202**, 133 (1936)
21. Serber, R., *Phys. Rev.*, **72**, 1114 (1947)
22. Fernbach, S., Serber, R., and Taylor, T. B., *Phys. Rev.*, **75**, 1352 (1949)
23. Bethe, H. A., *Phys. Rev.*, **57**, 1125 (1940)
24. Teichmann, T., and Wigner, E. P., *Phys. Rev.*, **87**, 123 (1952)
25. Thomas, R. G., *Phys. Rev.*, **97**, 224 (1955)
26. Feshbach, H., Peaslee, D. C., and Weisskopf, V. F., *Phys. Rev.*, **71**, 1451 (1947)
27. Breit, G., and Wigner, E., *Phys. Rev.*, **49**, 519 (1936)

27a. Kronig, R. de L., *J. Opt. Soc. Amer.*, **12**, 547 (1926)

27b. Gell-Mann, M., Goldberger, M. L., and Thirring, W. E., *Phys. Rev.*, **95**, 1612 (1954)

28. Feshbach, H., Porter, C. E., and Weisskopf, V. F., *Phys. Rev.*, **96**, 448 (1954)
29. Lane, A. M., Thomas, R. G., and Wigner, E. P., *Phys. Rev.* (In press)
30. Weisskopf, V. F., *Helv. Phys. Acta*, **23**, 187 (1950)
31. Porter, C. E., in Taylor, A. E., and Wood, E., *Phil. Mag.*, **44**, (1953)
32. Bethe, H. A., *Revs. Mod. Phys.*, **9**, 69 (1937)
33. Konopinski, E. J., and Bethe, H. A., *Phys. Rev.*, **54**, 130 (1938)
34. Blatt, J. M., and Biedenharn, L. C., *Revs. Mod. Phys.*, **24**, 258 (1952)
35. Wolfenstein, L., *Phys. Rev.*, **82**, 690 (1951)
36. Hauser, W., and Feshbach, H., *Phys. Rev.*, **87**, 366 (1952)
37. Watson, K. M., *Phys. Rev.*, **89**, 575 (1953)
38. Francis, N. C., and Watson, K. M., *Phys. Rev.*, **92**, 291 (1953)
39. Francis, N. C., and Watson, K. M., *Phys. Rev.*, **93**, 313 (1954)
40. Morrison, C. G., Muirhead, H., and Rosser, W. G. V., *Phil. Mag.*, **44**, 1326 (1953)

41. Lippmann, B., and Schwinger, J., *Phys. Rev.*, **79,** 469 (1950)
42. Kisslinger, L. S., *Phys. Rev.* (In press)
43. Takeda, G., and Watson, K. M., *Phys. Rev.*, **94,** 1087 (1954)
44. Wolfenstein, L., and Ashkin, J., *Phys. Rev.*, **85,** 947 (1952)
45. Huby, R., *Progr. Nuclear Phys.*, **3,** 177 (1953)
46. Feshbach, H., and Weisskopf, V. F., *Phys. Rev.*, **76,** 1550 (1949)
47. Blatt, J. M., and Weisskopf, V. F., *Theoretical Nuclear Physics* (Wiley, New York, N. Y., 864 pp., 1952)
48. Sneddon, I., and Touschek, D., *Proc. Cambridge Phil. Soc.*, **44,** 391 (1948)
49. LeCouteur, K. J., *Proc. Phys. Soc.* (*London*), **63,** 259 (1950)
50. Lang, J. M. B. and LeCouteur, K. J., *Proc. Phys. Soc.* (*London*), **67,** 586 (1954)
51. Bloch, C., *Phys. Rev.*, **93,** 1094 (1954)
52. Brueckner, K. A., Levinson, C. A., and Mahmoud, H. M., *Phys. Rev.*, **95,** 217 (1954)
53. Emmerich, W. S., *Bull. Am. Phys. Soc.*, **30**(1), 9 (1955)
54. Walt, M., and Barschall, H. H., *Phys. Rev.*, **93,** 1062 (1954)
55. Walt, M., and Barschall, H. H., in Feshbach, H., Porter, C. E., and Weisskopf, V. F., *Phys. Rev.*, **96,** (1954)
56. Carter, R. S., Harvey, J. A., Hughes, D. J., and Pilcher, V. E., *Phys. Rev.*, **96,** 113 (1954)
57. Bollinger, L. M., Cotè, R., and LeBlanc, J., *Bull. Am. Phys. Soc.*, **30**(1), 23 (1955); (and Private communication)
58. Scott, J. M. C., *Phil. Mag.*, **45,** 441 (1954)
59. Walt, M., and Beyster, J. R., in Friedman, F. L., and Weisskopf, V. F., *Kgl. Danske Videnskag Selskab* (in special anniversary volume for N. Bohr) (In press)
60. Friedman, F. L., and Weisskopf, V. F., *Kgl. Danske Videnskab Selskab* (in special anniversary volume for N. Bohr) (In press)
61. Whitehead, W. D., and Snowdon, S. C., *Phys. Rev.*, **92,** 114 (1953)
62. Coon, J. H., Graves, E. R., and Barschall, H. H., *Phys. Rev.*, **88,** 562 (1952)
63. Goodman, L. S., *Phys. Rev.*, **88,** 686 (1952)
64. Nereson, N., and Darden, S., *Phys. Rev.*, **89,** 775 (1953)
65. Day, R. B., and Henkel, R. L., *Phys. Rev.*, **92,** 358 (1953)
66. Henkel, R. L., Cranberg, L., Jarvis, G. A., Nobles, R., and Perry, J. E., *Phys. Rev.*, **94,** 141 (1954)
67. Cook, C. F., and Bonner, T. W., *Phys. Rev.*, **94,** 561 (1954)
68. Nereson, N., and Darden, S., *Phys. Rev.*, **94,** 1678 (1954)
69. Smith, J. R., *Phys. Rev.*, **95,** 730 (1954)
70. Coon, J. H., in Culler, G., Fernbach, S., and Sherman, L., *U. S. Atomic Energy Commission Document, UCRL-4436* (January, 1955)
71. Culler, G., Fernbach, S., and Sherman, N., *U. S. Atomic Energy Commission Document, UCRL-4436* (January, 1955)
72. Taylor, A. E., and Wood, E., *Phil. Mag.*, **44,** 95 (1953)
73. Ragent, B. I., and Linlor, W. I., *Phys. Rev.*, **92,** 835 (1953)
74. Hillman, P., Stahl, R. H., and Ramsey, N. F., *Phys. Rev.*, **96,** 115 (1954)
75. Barschall, H. H., *Am. J. Phys.*, **22,** 517 (1954)
76. Taylor, T. B., *Phys. Rev.*, **92,** 831 (1953)
77. Burkig, J. W., and Wright, B. T., *Phys. Rev.*, **82,** 451 (1951)
78. Baker, C. J., Dodd, J. N., and Simmons, D. H., *Phys. Rev.*, **85,** 1051 (1952)

79. Gugelot, P. C., *Phys. Rev.*, **87,** 525 (1952)
80. Goldman, L. M., *Phys. Rev.*, **89,** 349 (1953)
81. Burcham, W. E., Gibson, W. M., Hossain, A., and Rotblat, J., *Phys. Rev.*, **92,** 1266 (1953)
82. Cohen, B. L., and Neidigh, R. V., *Phys. Rev.*, **93,** 282 (1954)
83. Dayton, I. E., *Phys. Rev.*, **95,** 754 (1954)
84. Fischer, G. E., *Phys. Rev.*, **96,** 704 (1954)
85. Freemantle, R. G., Prowse, D. J., and Rotblat, J., *Phys. Rev.*, **96,** 1268 (1954)
86. Freemantle, R. G., Prowse, D. J., Hossain, A., and Rotblat, J., *Phys. Rev.*, **96,** 1270 (1954)
87. Chase, D. M., and Rohrlich, F., *Phys. Rev.*, **94,** 81 (1954)
88. Woods, R. D., and Saxon, D. S., *Phys. Rev.*, **95,** 577 (1954)
89. Adair, R. K., Darden, S. E., and Fields, R. E., *Phys. Rev.*, **96,** 503 (1954)
90. Farwell, G. W., and Wegner, H. E., *Phys. Rev.*, **95,** 1212 (1954)
91. Freemantle, R. G., Gibson, W. M., and Rotblat, J., *Phil. Mag.* **45,** 1200 (1954)
92. Wall, N. S., Rees, J. R., and Ford, K. W., *Phys. Rev.* (In press)
93. Izumo, K., *Progr. Theoret. Phys.* (*Japan*), **12,** 549 (1954)
94. Bleuler, E. (Private communication)
95. Butler, S. T., *Proc. Roy. Soc.* (*London*), **208,** 559 (1951)
96. McManus, H., and Sharp, W. T., *Phys. Rev.*, **87,** 188 (1952)
97. Austern, N., Butler, S. T., and McManus, H., *Phys. Rev.*, **92,** 350 (1953)
98. Schrank, G., Gugelot, P. C., and Dayton, I. E., *Phys. Rev.*, **96,** 1156 (1954)
99. Keller, K. K., Niedner, J. B., Wang, C. F., and Shull, F. B., *Phys. Rev.*, **81,** 481 (1951)
100. Strauch, K., and Titus, W. F., *Phys. Rev.*, **95,** 854 (1954)
101. Greenlees, G. W., *Proc. Phys. Soc.* (*London*), **68,** 97 (1955)
102. Pratt, W. W., *Phys. Rev.*, **93,** 816 (1954)
103. Pratt, W. W., *Phys. Rev.*, **94,** 1086 (1954)
104. Grave, A., *Phil. Mag.*, **45,** 1205 (1954)
105. Francis, A. E., McCue, J. J. G., and Goodman, C., *Phys. Rev.*, **89,** 1232 (1953)
106. Ebel, A. A., and Goodman, C., *Phys. Rev.*, **93,** 197 (1954)
107. Martin, H. C., Diven, B. C., and Taschek, R. F., *Phys. Rev.*, **93,** 199 (1954)
108. Kiehn, R. M., and Goodman, C., *Phys. Rev.*, **95,** 989 (1954)
109. Margolis, B., *Phys. Rev.*, **93,** 204 (1954)
110. Bernardini, G., Booth, E. T., and Lindenbaum, S. J., *Phys. Rev.*, **88,** 1017 (1952)
111. Jackson, J. D., *Phys. Rev.*, **95,** 651 (1954)
112. Hirzel, O., and Wäffler, H., *Helv. Phys. Acta*, **20,** 373 (1947)
113. Wäffler, H., *Helv. Phys. Acta*, **23,** 239 (1950)
114. Paul, E. B., and Clarke, R. L., *Can. J. Phys.*, **31,** 267 (1953)
115. Eisberg, R. M., and Igo, G. J., *Phys. Rev.*, **93,** 1039 (1954)
116. Eisberg, R. M., *Phys. Rev.*, **94,** 739 (1954)
117. Cohen, B. L., Newman, E., Charpie, R. A., and Handley, T. H., *Phys. Rev.*, **94,** 620 (1954)
118. Cohen, B. L. (Reported at Brookhaven Conference on Statistical Aspects of the Nucleus, Upton, L. I., New York, *BNL 331* (12) Jan., 1955)
119. Gugelot, P. C., *Phys. Rev.*, **93,** 425 (1954)
120. Gugelot, P. C., *Phys. Rev.*, **81,** 51 (1951)
121. Stelson, P. H., and Goodman, C., *Phys. Rev.*, **82,** 69 (1951)
122. Whitmore, B. G., and Dennis, G. E., *Phys. Rev.*, **84,** 296 (1951)

123. Graves, E. R., and Rosen, L., *Phys. Rev.*, **89**, 343 (1953)
124. Whitmore, B. G., *Phys. Rev.*, **92**, 654 (1953)
125. O'Neill, G. K., *Phys. Rev.*, **95**, 1235 (1954)
126. Rosen, L. (Reported at Brookhaven Conference on Statistical Aspects of the Nucleus, Upton, L. I., New York, *BNL 331* (C21) Jan., 1955)
127. Kind, A., and Patergnani, E., *Nuovo cim.*, **10**, 1375 (1955)
128. Silver, E. G., and Waniek, R. W., *Phys. Rev.*, **95**, 586 (1954)
129. Weisskopf, V. F., *Proc. Am. Acad. Arts Sci.*, **82**, 360 (1953)
130. Trainor, L. E. H. (Private communication)

NUCLEAR PARTICLE DETECTION (CLOUD CHAMBERS AND BUBBLE CHAMBERS)[1]

By William B. Fretter

Department of Physics, University of California, Berkeley, California

Introduction

The first photographs of the tracks of nuclear particles in a cloud chamber were obtained by C.T.R. Wilson (1) in 1911. A year later (2) Wilson published photographs of tracks of α-particles, β-particles, and the electrons produced by a beam of x-rays passing through his chamber. In these pictures, Wilson set a standard of quality for cloud-chamber photographs that has not often been excelled and described techniques of measurement that are still of great importance. The development of cloud chambers has made possible many discoveries in nuclear physics and has provided visual proof of the existence of various types of nuclear particles. A collection of some of the most important and beautiful cloud chamber pictures has been made by Gentner, Maier-Leibnitz & Bothe (3) and by Rochester & J. G. Wilson (4) in which they trace the growth of knowledge of nuclear physics through the years since 1911, demonstrating clearly the importance of the cloud chamber technique.

Cloud chambers, when operated under suitable conditions, can provide information on the charge, momentum, velocity, lifetime, direction of motion, and interaction properties of nuclear particles, as well as the total number of such particles existing at a given time within the useful volume of the chamber. Cloud chambers have been operated at low, atmospheric, and high pressure, in balloons 100,000 ft. above the earth, in mines hundreds of feet below the surface of the earth, on mountain tops for cosmic ray research, and in the beams of particles created by accelerators. They are versatile and adaptable, but inevitably have their limitations. The invention in 1952 of the bubble chamber by Glaser makes available still another instrument for the detection of nuclear particles. Bubble chambers have important applications in connection with high-energy accelerators. They can be operated on a cycle of a few seconds, can be made with various liquids, including liquid hydrogen, and have many detection properties in common with cloud chambers.

This article will review the developments in cloud-chamber and bubble-chamber technique that have been made since 1951. The excellent book by J. G. Wilson (5) and the article by Das Gupta & Ghosh (6) describe the classical work on expansion cloud chambers in some detail. Snowden has written a review article (7) on diffusion cloud chambers that contains much valuable material, and Glaser has published several articles on bubble chambers that will be referred to in the latter part of this paper.

[1] The survey of literature pertaining to this review was completed in April, 1955.

UNIVERSITY OF MICHIGAN LIBRARIES

The three instruments, expansion cloud chambers, diffusion cloud chambers, and bubble chambers have much in common in their characteristics as particle detectors. They have, or can be made to have, the same order of magnitude of physical size, and thus the time required for a particle to cross any one is about the same, and the instruments are useful in measuring particles of comparable lifetime. All three chambers can be used for momentum and ionization measurements under the proper experimental conditions. They are useful only when the flux of particles is relatively low, i.e., less than about one particle per cm.^{2} per sec. Although the dead time, or resetting time of these instruments varies considerably, they are all very much longer than are those for counters. These instruments are particularly useful in exploratory experiments where the nature of the particles is not known, and they indicate clearly whether one or several particles traversed the detector. These chambers can all be used to observe nuclear interactions in nearly pure elements, and information on details of the interaction is obtainable.

There are, of course, important differences in properties and uses of these devices. The resetting time for an expansion chamber is much longer than for diffusion or bubble chambers. The time resolution of the bubble chamber is much better than for cloud chambers, especially if the bubble chamber contains an organic liquid. These considerations are important in the use of particle detectors in connection with an accelerator. Both the diffusion chamber and the bubble chamber can be operated with fillings of hydrogen at relatively high density, whereas it is inconvenient to operate an expansion cloud chamber with high pressure hydrogen. A disadvantage of the diffusion chamber is that the sensitive layer is not more than 3 in. thick and cannot be made vertical for observation of cosmic rays. The expansion chamber and bubble chamber are not seriously limited in size, shape, or orientation, but the bubble chamber appears to be difficult to use as a counter-controlled chamber to detect cosmic rays. The diffusion chamber and the bubble chamber are particularly useful for detection of accelerated particles and provide information on the interaction of elementary particles.

Expansion Cloud Chambers

The double-chamber technique.—An important development in the past few years has been the increasing use of two or more cloud chambers, one placed above the other, in cosmic-ray work, to allow observation of nuclear particles under various conditions. It seems likely that such techniques will be useful in accelerator work. A double-chamber apparatus was used by Street (8) and later by Fretter (9) at the suggestion of Hazen, to determine the mass of μ-mesons. A cloud chamber placed in a magnetic field provided information on the momentum of the particle, while the second chamber, which contained a series of lead plates, provided information on the range of the particle. This technique has been extended by Brode and his students (10 to 15), who also used a triple-chamber apparatus (Fig. 1). Two cloud

chambers were used to determine the momentum of a particle by its deflection in a magnetic field between the chambers, and a third chamber containing plates was used to determine the range. This apparatus had the advantage of using a permanent magnet to supply the magnetic field, and thus was not dependent on a source of D.C. power. It was installed in an airplane to investigate the nature of the cosmic ray particles at high altitude. Physicists in Russia (16) have also used the double cloud-chamber technique for measurement of the mass of cosmic ray particles.

The multiple chamber technique has been very useful in experiments on the unstable particles produced in high-energy nuclear interactions. Leighton (17, 18, 19) constructed a pair of cloud chambers between which material

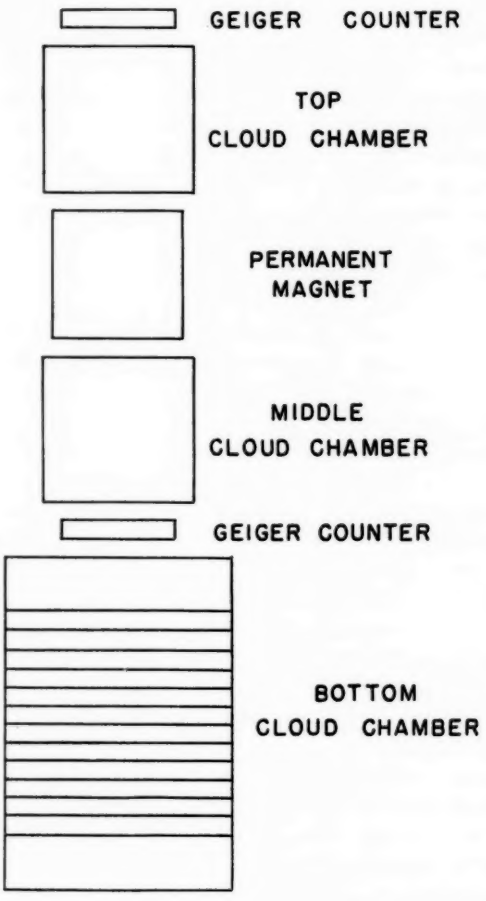

FIG. 1. Triple cloud chamber arrangement for momentum and range measurements.

UNIVERSITY OF MICHIGAN LIBRARIES

could be placed. These chambers were both in a magnetic field, and observations were made on particles created in or traversing the material between the chambers. Each chamber was rectangular in shape, approximately 33 cm. wide, 19 cm. high, and 12 cm. illuminated depth, and the magnetic field was 5000 gauss. Such an arrangement of chambers seems to produce less distortion near the absorbing material than would have been present if a single cloud chamber with a plate mounted in it had been used.

A similar but larger cloud-chamber apparatus has been constructed by the C.I.T.[2] group (20) and installed in a 48-in. magnet. This apparatus is very flexible, with provision for four chambers, one above the other, or a combination of two chambers without plates and one larger chamber with plates. A typical arrangement is to have two chambers, each 20.5 cm. high, 56 cm. wide, and 20 cm. illuminated depth above a larger chamber 46 cm. high, 56 cm. wide, and 20 cm. illuminated depth. The magnetic field is about 8000 gauss.

Two very large cloud chambers, one in a magnetic field and the other containing plates have been used by a group at the École Polytechnique (21). This apparatus (Fig. 2) is installed at the Pic du Midi (2850 m.) and has been used for the study of charged and neutral unstable particles. The illuminated region of the upper chamber is 68 cm. high, 64 cm. wide, and 30 cm. deep. A magnetic field of 2600 gauss is provided by a pair of water-cooled coils using 200 kw. The field is uniform to 2 per cent over the useful region of the chamber. The lower chamber has an illuminated volume of 68 cm. by 64 cm. by 40 cm., and contains 15 copper plates, each 1 cm. thick. The tracks of particles traversing both chambers cannot be seen in the interval of 40 cm. between the chambers, but no trouble is encountered in following tracks from one chamber to the next. The apparatus is triggered on penetrating showers. Six cameras are used to photograph the chambers; two of these are centered on the top and bottom chambers, while the others are at the sides, to make stereoscopic measurements possible. The great advantage of this apparatus has been that because of its large size, accurate measurements of momentum and range of particles stopping in the lower chamber yield precision values of the mass of these particles. In addition, there is sufficient material in the lower chamber so that there is a fairly good chance that the secondaries coming from the decay of unstable particles will also stop in the chamber. Measurements of mass have been made on 19 protons for calibration (22). The mean standard deviation for these values is $\pm 150 m_e$, indicating that the spurious curvature in the upper chamber was less than 150 m.$^{-1}$.

Another double chamber apparatus has been built by the Princeton group (23) and operated at mountain altitude. They have observed an S-particle that stopped in the lower chamber, and sent a secondary back into the upper chamber, giving an excellent measurement of the momentum of the secondary particle.

[2] C.I.T. here refers to California Institute of Technology.

It has become increasingly apparent that cloud chambers must be developed that are capable of precision measurements. The double chamber work, and the work of Thompson (24, 25) and his students have been along these lines. Thompson's cloud chamber is particularly good as regards thermal turbulence. He has also made a careful study of the errors involved in reduction of the film measurements, and advocates the use of dummy tracks and angles to verify the methods used.

The ionization-momentum compromise.—It has long been believed that accurate measurements of ionization and momentum on the same track were mutually exclusive. Measurements of ionization involve the counting of droplets along the track, and require that the track be diffuse enough so that the droplet images do not overlap. It was also customary to separate the positive and negative ion columns to determine the condensation efficiency. Difficulties in measurement of the position of a diffuse track, and distortions attributable to the electric field usually combined to make momentum measurements quite uncertain.

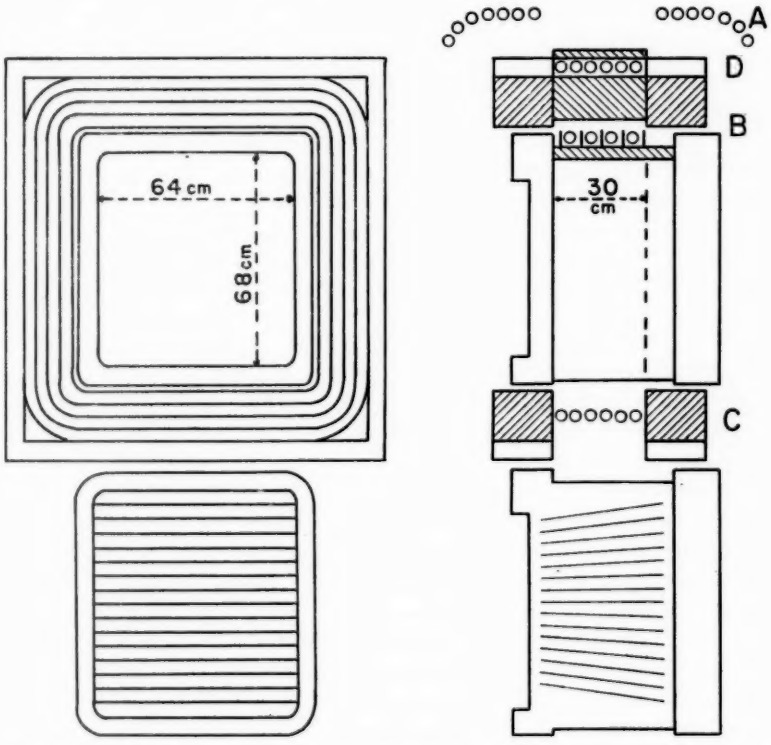

FIG. 2. Double cloud chamber apparatus used at Pic du Midi for studies of particles in penetrating showers. Counter trays for selection of events are shown at A B C D.

UNIVERSITY OF MICHIGAN LIBRARIES

A new approach to this problem has been made by Cowan (26) and by Fretter & Friesen (27). Instead of splitting the track to observe condensation efficiency, these experimenters calibrated the minimum ionization level in each picture of interest by observing tracks at or near the minimum. The gas in the chamber was either a mixture of helium and argon, or pure helium. In these gases the ions diffuse quickly enough and the ionization is small enough that ionization measurements can be made readily, and momentum measurements are very little affected.

Cowan adopted the procedure for ionization measurements of dividing the track into cells and counting the droplet images stereoscopically, thus eliminating any background correction. Fretter & Friesen follow this procedure and have made a study of the errors involved in measurement of ionization in this way. In a sample of 41 protons they find a mean probable error on an individual measurement of $\pm 120 m_e$. It was found that accurate temperature control of the chamber was required for precision momentum measurements. Fretter & Friesen maintained side-to-side differences of temperature of less than 0.02°C., and a top-to-bottom gradient of about 0.3°C. They photographed against the background of a highly polished black back plate, on which the required fiducial lines were scribed. They have also published (27) a description of their method of making corrections for conical projection and nonuniformity of the magnetic field.

The use of calibration tracks, often high energy electrons, in the measurement of ionization makes it necessary to know the ionization-velocity relation with some accuracy, particularly in the region where the density effect is important. An experiment by Ghosh, Jones & Wilson (28) has shown that the ionization of high-energy μ-mesons agrees well with that predicted by current theories, but that confirmation of specific theoretical details awaits additional experimental data. In this work, the writers used conventional methods of drop counting in oxygen, splitting the tracks to determine the condensation efficiency. The momenta of the particles were measured in an auxiliary apparatus.

Recent advances in experimental technique.—Several rather large cloud chambers for multi-plate applications have been developed. Such a chamber, designed for use in cosmic rays, is described in detail, together with much of the required auxiliary equipment, by Lovati *et al.* (29). This chamber has dimensions 50 cm. $\times$60 cm. $\times$15 cm. illuminated depth, and is constructed so that it can support a large weight of plates. It uses a conventional rubber diaphragm and velvet supported on a hole plate. The large plate chamber used by the École Polytechnique group (21) has a unique system of auxiliary rubber diaphragms that are collapsed to provide a rapid expansion.

The largest expansion chamber constructed to date was built at MIT by a group headed by Bridge & Rossi (30). This chamber, which is 60 in. wide, 48 cm. high and has 18 in. illuminated depth, contains 17 plates of $\frac{1}{2}$ in. steel. Because of its unusual size, many difficult technical problems had to be overcome, but the chamber has operated satisfactorily at the cosmotron.

The expansion is by means of a solid piston sealed by a rubber ring 4 in. wide around the edges. Four expansion valves are used and the expansion time is 35 msec., adequate for use at the cosmotron. Greater speed could be obtained by decreasing the weight of the piston, adding more valves, or expanding into a vacuum, and provision has been made for these possibilities, but fast expansion times in large chambers sometimes cause serious shock-wave difficulties. The front glass is 1.25 in. thick, tempered. It deflects 0.85 in. during an expansion at the operating pressure of 20 cm. Hg. The plates are 2 in. apart at the front of the chamber and are slanted to converge 15.5 ft. in front of the chamber. The chamber is illuminated by two flash lamps at each side, each dissipating 10,000 joules, backed by parabolic cylinder reflectors. Three cameras are used, one in the center and two at 30° from the center, and the lenses are used at a mean magnification of 1/17.6, with stop f/22. The chamber was fabricated of aluminum castings, coated on the inside with natural rubber. Typical operating conditions with a mixture of argon and helium are to have three slow expansions and a total dead time of 5 to 7 min. Such a chamber may be very useful in the study of *S*-particles, since the ranges of the known secondary particles are short enough to permit observation of a relatively large number of the secondaries.

It has long been known that in rubber diaphragm chambers, background that is produced behind the velvet during an expansion comes into the chamber on subsequent compression. It has been found by Blumenfeld, Booth & Lederman (31) that a clearing field applied behind the velvet baffle has an important effect in reducing the fog produced in this way. Such a clearing field appears to be particularly important when the cloud chamber is being operated in the beam of an accelerator, where ionization levels are high.

Expansion cloud chambers have the disadvantage of a rather long dead time, made necessary by the slow return to equilibrium conditions after a fast expansion, and thus do not take advantage of the frequent pulses available at an accelerator. A fast recycling cloud chamber was developed by Gaerttner & Yeater (32) using momentary over-compression of the filling gas to evaporate the droplets to a size where they could be removed by a clearing field. With this chamber, operation at a repetition period of 5 sec. was possible. The coil providing the magnetic field was also pulsed with current from a condenser power supply. A cloud chamber using over-compression has been operated (33) by Kessler & Lederman in the 125 Mev π^--meson beam of the Columbia cyclotron, and a one-minute cycle was possible.

Another approach to this problem has been made by Emigh (34) with a fast-compression cloud chamber. Instead of over-compressing the chamber, Emigh re-compressed the gas quickly enough so that the transfer of heat from walls to gas and back again was substantially reduced over that occurring in a conventional chamber. In this way a repetition time of 10 sec. was obtained. This technique is simpler mechanically than the over-compression technique, and the chamber used is a rubber diaphragm type. Both these techniques

UNIVERSITY OF MICHIGAN LIBRARIES

have been used in conjunction with accelerators, but there is no reason why they would not be suitable for use in other applications.

If an apparatus is used that takes pictures at a fast rate, it is necessary to make provisions for analyzing the pictures quickly. Instruments for rapid measurement of the curvature of cloud chamber tracks have been made by Gaerttner & Yeater (35) and by Emigh (36). These instruments are useful when the cloud chamber is not very deep, or the lens is quite far away, so that conical projection corrections are negligible. If this is not the case, the time required to make the geometrical measurements and the corrections for an individual track is very much longer than that necessary for the curvature measurement alone.

The distortions of tracks in cloud chambers attributable to thermal currents and expansion irregularities are a serious cause of error in the measurement of momentum. A study of thermal distortions has been made by Carter & Street (37), who used a collimated x-ray beam to provide a reference column in ions in their chamber. This technique should be useful in providing a continuous check on distortions. Carter & Street were also able to make measurements on drop growth and sensitive time with the pulsed x-ray beam.

It is possible to operate a cloud chamber in such a way that the ionization produced in the chamber produces the triggering pulse (38 to 42). The gas used must be such that the electrons do not attach appreciably, and are collected at an electrode to give a triggering pulse. The positive ions move relatively slowly, and provide condensation centers after the chamber has expanded. Brown (43) has investigated cosmic-ray nuclear interactions in gases by means of such a chamber.

Burhop has reported (44) the construction and operation of a high-pressure expansion chamber 22.5 cm. in diameter that contains argon at 100 atm. The density of the argon at this pressure is 0.18 g./cm.$^{-3}$, and the chamber can be used for studies of either cosmic rays or accelerated particles. High-pressure expansion chambers suffer from the disadvantage of long recovery time, usually about 15 min., but have the advantages of good stopping power, large sensitive volume, and long sensitive time. Burhop describes the chamber in detail and discusses measurements made, including track width, δ-rays, scattering, and curvature of tracks in a magnetic field. In such a chamber with a magnetic field of 7000 gauss the error in momentum determination caused by the scattering of a particle of mass 200 electron masses is of the order of 25 per cent.

Valuable information on the techniques of cloud chamber operation can be found in a series of articles written by those who lectured at the 1953 Varenna summer school of physics. These articles were written with cosmic-ray applications primarily in mind, but the results should also be valuable in the detection of particles coming from machines.

Blackett (45) discussed the general problem of the precision of momentum measurement in a magnetic field cloud chamber, taking into account the

diffusion of the ions and the consequent uncertainty of the position of the track and the uncertainty attributable to scattering. He found that the relative importance of these errors depends on the momentum to be measured and the pressure in the chamber, other conditions remaining constant, and that an optimum pressure of the gas can be calculated if the momentum to be measured is known. Blackett also investigated the effect of the expansion time, light delay time, and resetting time of a cloud chamber on its efficiency for detecting nuclear events. He demonstrated that if the chamber is large the resetting time so limits the rate of picture-taking that operation of the chamber at sea level yields as many nuclear events as would be found by operation at mountain altitude. For smaller chambers, or for those with short resetting time, mountain sites are advantageous.

The use of cloud chambers for the estimation of lifetime of particles was discussed (46) by Newth. The statistical analysis (47, 48) of the data on the life span of particles observed in a cloud chamber can yield values of the mean life only if care is taken to avoid bias in the selection of data. Newth analyzed the various factors of importance such as the necessity of allowing for the identification of the particular particle in calculating the potential path length in the chamber, and the possibility of working with mixtures of particles.

Newth also wrote an article (49) on the design and operation of magnet cloud chambers. The design of the magnet, particularly the power-versus-field characteristics, and the desirability of including iron in the magnetic circuit were illustrated by various examples of cloud chamber magnets now in use. The Jungfraujoch apparatus which consists of a large cloud chamber in a magnetic field was described in some detail, and problems of photography and temperature control outlined. Temperature gradients in this chamber give rise to serious convective distortion, and attempts have been made to compensate for these in momentum measurements.

The measurement of cloud chamber tracks was discussed by Barker (50). The determination of the momentum of a track in a cloud chamber from measurements on a film involve a number of complicated operations if the momentum is to be determined accurately and the error estimated. Corrections must be made for the conical projection of the track in the chamber onto the film, the dilation of the gas, the nonuniformity of the magnetic field, and the interlocking effect of the conical projection and the nonaxial component of the field. The errors include lens distortions, the curvature introduced by the front glass, the gaseous convection error, and the error in actual curvature measurement on the film.

A detailed review (51) of the problems involved in the use of multiplate chambers was made by Peyrou. With a multiplate chamber, if techniques of lighting and expansion are good, accurate measurements of ranges of particles can be made, and estimates of energies can be obtained from measurements of angles of scattering in successive plates.

UNIVERSITY OF MICHIGAN LIBRARIES

Diffusion Cloud Chambers

Introduction.—The theory of diffusion cloud chambers, first discussed by Langsdorf (52), was extended by Shutt (53) and summarized by Snowden (54) in his general review article. Bevan (55) has measured the optimum and limiting conditions for downward diffusion cloud chambers and has in general verified the theory given by Shutt. Succi & Tagliaferri (56) have applied the theory specifically to the operation of a chamber containing air at atmospheric pressure.

A diffusion cloud chamber operates by the diffusion of a condensible vapor from a warm region where it is not saturated to a cold region where it becomes supersaturated, and provides the proper condition for growth of droplets around ions, just as in an expansion cloud chamber.

The vapor density increases with temperature, while the gas density decreases with temperature. A given mixture of gas and vapor may thus have a density that increases, or decreases with temperature, depending on the temperature range and the constituents. It is important to maintain a density gradient in the chamber, such that the density of the mixture at the top is less than that at the bottom, to prevent convection turbulence. Most diffusion chambers in current use are arranged for downward diffusion. The top is warm, and the vapor is introduced there, while the bottom is cold. Upward diffusion chambers have not been used extensively because of the difficulty of maintaining stable conditions near the cold surface, which in this case must be at the top. We will confine our attention to downward diffusion chambers and will present some results of the theory as they apply to the use of diffusion chambers in nuclear particle detection.

Shutt predicted (53) that chambers containing heavy gases such as air or argon would be useful only up to two or three times atmospheric pressure. He calculated the temperature gradient required for operation under various conditions, and showed that, with dry ice temperature at the bottom of the chamber, the top of a chamber containing air at 3 atm. must be at a temperature in excess of 293°K. If the temperature at the top is higher than this value, two difficulties arise. First, the sensitive region tends to become unstable and turbulent, and second, the background fog increases rapidly. On the other hand, Shutt showed that chambers containing light gases such as hydrogen, deuterium, and helium, were unsuitable for use at atmospheric pressure but became useful at pressures of 20 to 30 atm. The possibility of constructing a high-pressure hydrogen chamber for use with high-energy accelerators was immediately exploited by Shutt and his collaborators (57).

Shutt (53) has considered the effect of the heat produced by the condensation of the drops and the mechanism for its removal. He finds that heat is exchanged between the gas and walls by a process of convection, but calculates that the required motion of the gas near the walls is quite small, and concludes that this small amount of motion explains the excellent stability of the gas in diffusion cloud chambers. Such stability is important in reducing

the effect of thermal tubulence on the curvature of tracks in a magnetic field.

With these introductory remarks, we proceed to a review of the experimental work on diffusion chambers. Chambers operated near atmospheric pressure will be considered first, then a low-pressure chamber, and finally the high-pressure chambers and their use with high-energy accelerators.

Atmospheric pressure diffusion chambers.—The first atmospheric pressure chamber was operated by Langsdorf (52), but it was not until Cowan (58) and Nielsen, Needels & Weddle (59) constructed chambers of great mechanical simplicity and ease of operation that the instrument showed substantial promise as a nuclear particle detector. Such chambers are now widely used in elementary physics laboratories and demonstrations of particle tracks. Nielsen (59) experimented with an upward diffusion chamber using propanol in helium at atmospheric pressure but obtained better tracks in downward diffusion chambers. These observers were able to get sensitive regions from 2 to 3 in. high, and no experimenter has been able to do much better than this in either high-pressure or low-pressure chambers.

The application of diffusion cloud chambers to quantitative experiments with nuclear particles has various complications. The fact that the sensitive region is horizontal and relatively thin restricts their use in cosmic ray research. For detection of particles coming from accelerators, particular attention must be given to the ion load imposed upon the chamber when a burst of fast particles traverses it. Cowan (58) first considered this problem in connection with synchrotron exposures, and concluded with that a properly synchronized sweep-field voltage pulse in the chamber, it would recover in 3 or 4 sec. Usually the picture repetition rate must be slower than this, to allow charging of the condenser bank that supplies the energy for the photographic flash. The depletion of vapor by heavily ionizing tracks is a serious problem in most diffusion chambers, and causes gaps in tracks to occur.

Lovati & Succi (60) describe a diffusion chamber constructed for use with a magnetic field for experiments in nuclear physics. The experimental arrangement is shown in Figure 3 and is fairly typical of chambers of this kind. The magnetic field is 1000 gauss, the cooling of the bottom is done by a mechanical refrigerator, and methyl alcohol is used as the vapor. The chamber has a diameter of 35 cm. and a height of 18 cm., and is photographed stereoscopically. Chambers such as these should be useful in investigations of the products of radioactive decay, especially in experiments where large numbers of photographs are required to observe unusual events.

A very large chamber was constructed by Relf & Powell (61) to be used in observations on the structure of extensive air showers of cosmic rays, and with the 6 Bev proton accelerator at Berkeley. This chamber was 8 ft. long, 4 ft. wide, and 5 in. deep, contained air at atmospheric pressure, and methyl alcohol for the vapor. The many difficult problems of construction and operation of such a large chamber were solved and it was possible to

UNIVERSITY OF MICHIGAN LIBRARIES

operate the chamber successfully for 540 hr. out of a continuous 720 hr. run. The vapor source consisted of a set of eight narrow trays suspended just under the top glass. The alcohol was heated by contact with copper tubing through which warm water was passed. The cooling of the bottom plate was provided by a spray of cold alcohol on the lower side of the bottom plate. The alcohol was cooled by contact with solid CO_2, over which it flowed before entering the gear pump. Twelve-hundred pounds of dry ice were consumed every 24 hr. The chamber was illuminated by four flash tubes, each charged

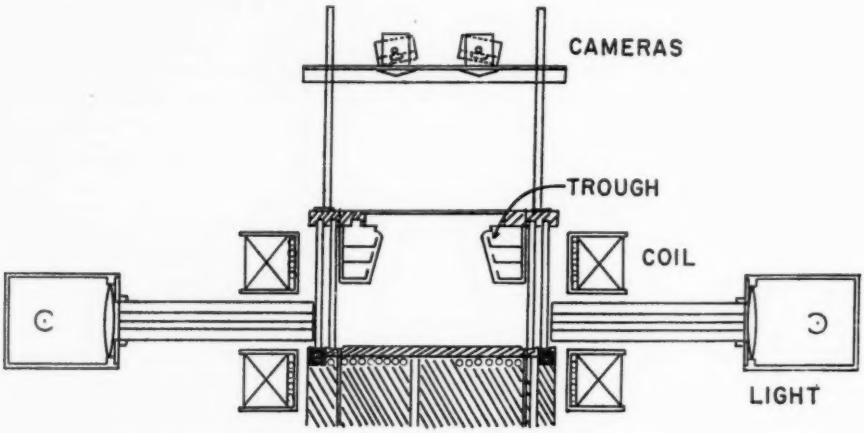

FIG. 3. Diffusion cloud chamber for use at atmospheric pressure.

with 1000 μf. at 1.5 kv. The viewing light was a water-cooled 1000 w. commercial mercury arc. Those who saw the chamber in operation can testify to the beauty of the tracks that constantly formed, fell, and disappeared from view.

This chamber was used in a study (62) of cosmic ray air showers at sea level to determine the density distribution of shower particles. In such an experiment it suffices to photograph the tracks end-on, or at small angles to the vertical, because only the total number of tracks per unit area is required, not the details of individual tracks. Relf found that the lateral distribution of the shower particles followed the Molière distribution in all but one example. A detailed report on this work appears in a University of California Radiation Laboratory Report (63).

The utility of multiplate expansion chambers for various experiments in which considerable amounts of heavy material are needed in a beam of particles leads to the question of whether it is possible to put plates in a diffusion chamber. Various experimenters have tried this, but none has published an extensive report on his results. It seems, however, to be possible to operate a diffusion chamber with plates if they do not unduly disturb the temperature gradient in the gas. Plates of plastic materials or glass, or

metallic plates with coatings of plastic to reduce the heat conduction into the gas, have been tried with some success. Further work along these lines is clearly needed if the atmospheric pressure diffusion chamber is to compete with high pressure chambers in nuclear physics research.

A diffusion cloud-ion chamber has been used by Block, Brown & Slaughter (64) for the detection of nuclear interactions. The chamber consisted of a glass cylinder 16 in. in diameter and 9 in. high filled with argon and amyl alcohol vapor at 1.4 atm. The ion chamber was placed in the sensitive volume, and consisted of six 1/16 in. stainless steel rods arranged in a hexagonal cylindrical array 3 in. in diameter and 9 in. long, together with a central wire of 1/16 in. stainless steel. The central wire was grounded, and the array of rods was maintained at −1200 volts. As in the expansion ion-cloud chambers, the electrons were collected to provide the pulse that triggered the flash lamps after track formation. The pulse height was used to select nuclear events.

Low-pressure diffusion chambers.—For the detection of low-energy β-particles it is sometimes desirable to use a cloud chamber containing gas at low pressure, and if the events to be observed are rare, the use of a diffusion chamber is indicated. A low-pressure helium diffusion cloud chamber has been constructed and operated by Choyke & Nielsen (65). Mass stability considerations indicate that for a downward diffusion chamber filled with helium and ethanol, at atmpspheric pressure, the maximum permissible top temperature is about −20°C. At reduced pressures of helium the top temperature must be even lower, and in order to obtain a sufficiently thick sensitive region the bottom temperature must be maintained well below dry ice temperature. Choyke & Nielsen constructed a chamber using liquid nitrogen as coolant. A diagram of this chamber is shown in Figure 4. The bottom temperature was maintained at about −130°C. Heated double windows surrounding the chamber were necessary to prevent formation of condensation and frost. With helium in the chamber, operation was obtained in a pressure range of 75 cm. to 15 cm. Hg. At atmospheric pressure a sensitive depth of 3 cm. was obtained, but, when the pressure was reduced to 15 cm. Hg, to reduce the rate of fall of the droplets it was necessary to lower the top temperature considerably, and the resulting thickness of the sensitive layer was only about 1 cm. Photographs of tracks in helium at 15 cm. Hg were obtained. In this chamber it was not necessary to apply an electric clearing field.

High-pressure diffusion cloud chambers.—When a light gas such as hydrogen or helium is used in a downward diffusion cloud chamber and the bottom of the chamber is maintained at dry ice temperature, stability of the gas-vapor mixture occurs only when the pressure of the light gas is maintained at several times atmospheric pressure. Diffusion chambers operating at about 25 atmospheres pressure, first discussed by Shutt (53, 57) have become one of the most important tools of high-energy nuclear physics. Such chambers can be operated in connection with the large proton synchrotrons and

UNIVERSITY OF MICHIGAN LIBRARIES

can accept each pulse of particles accelerated. They provide information on the interactions of the fundamental particles with each other, rather than on the complex interactions of particles with heavier nuclei. The techniques of analysis of events and scanning of the photographs obtained are related both to previously-known expansion-chamber techniques and the photographic emulsion techniques.

Shutt and his collaborators have published several papers describing their apparatus and the experiments performed with it. The most detailed description of the apparatus appears in a paper (66) by Fowler *et al.* They have built two high-pressure diffusion chambers, one 16 in. in diameter operated in a 10,500 gauss magnetic field, and the other 6 ft. long, 11 in. wide, without magnetic field. A cross-section of the magnetic field chamber is shown in Figure 5. It is conical rather than cylindrical in shape so that it

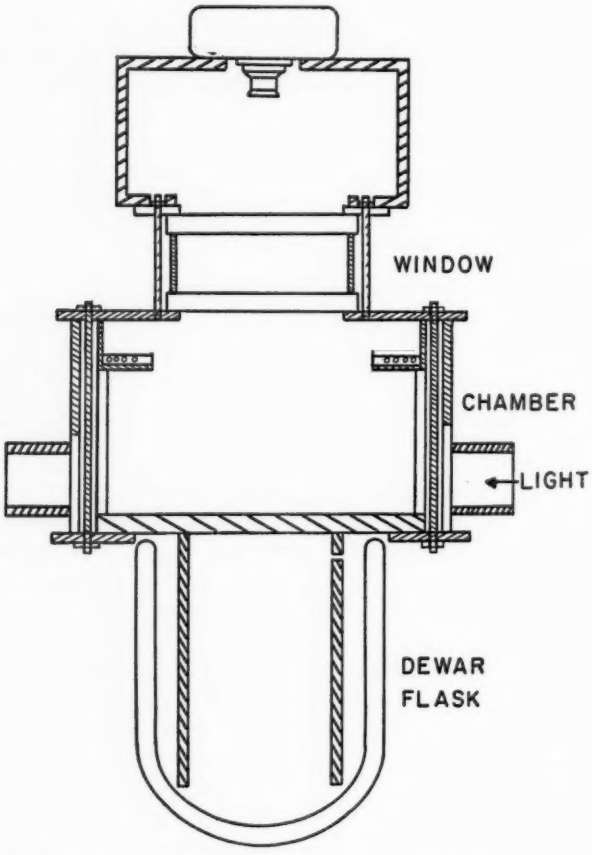

FIG. 4. Diffusion cloud chamber for use at low pressure.

can be fitted into the conical hole in the magnet pole piece. The magnet is pulsed, since the equipment is designed for use with the Brookhaven National Laboratory cosmotron, and the chamber is made of inconel, a nickel alloy of high electric resistivity, to keep induced currents low. The chamber will operate either with H_2 at 300 lb./in.^{2} or with He at 225 lb./in.^{2}, and methyl alcohol as the vapor. The bottom is cooled by a noninductively-wound copper cooling coil through which trichlorethylene is pumped at dry ice temperature. An electric clearing field of 500 volts is provided by means of a graphite plate suspended by threads just above the sensitive region. It is necessary to remove the oxygen impurity from the filling gas to prevent motion of the paramagnetic gas in the changing magnetic field.

The timing of the cloud chamber operation relative to the cosmotron is shown in Figure 6. The time between passage of the beam and flashing of the lights is normally set at 0.11 sec. Operation of this chamber at the cosmotron typically yields about 5000 pictures per day.

The long high-pressure cloud chamber built at Brookhaven is shown in

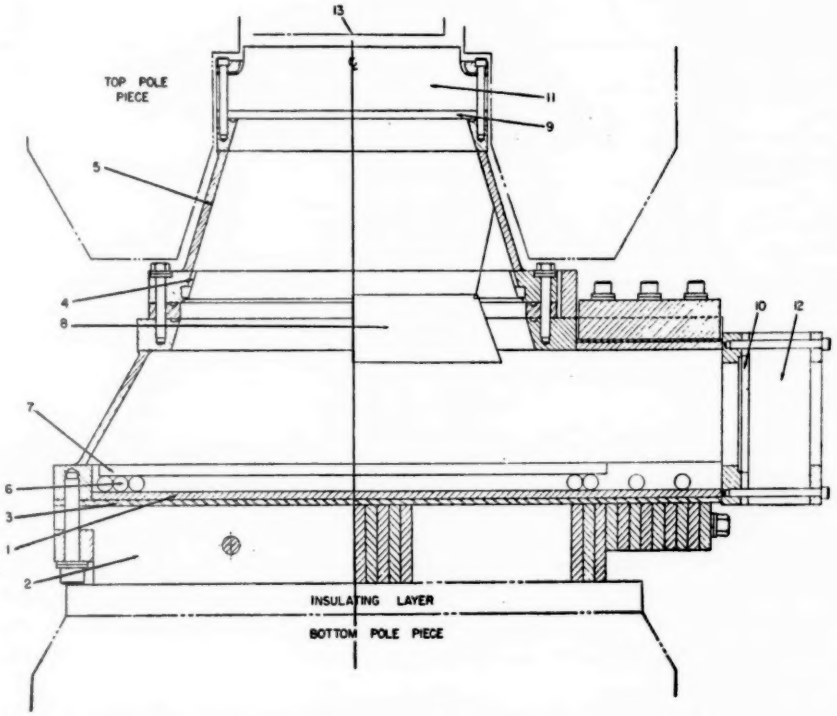

FIG. 5. High-pressure diffusion chamber for use in magnetic field (Brookhaven). The right hand side shows a section through one side window used for illumination. The left hand side shows a section at right angles to the first.

Figure 7. More nuclear events are recorded in it than in the magnetic field chamber, since over four times as much gas is exposed to the beam. The shell of the cloud chamber has a cylindrical shape, but the top of the cylinder is modified to provide a window. The window consists of a single long Allite sheet $\frac{1}{4}$ in. thick, supported by thick Lucite blocks to withstand the pressure. Allite plastic is used because it is not attacked by alcohol, but it is not available in large thick blocks. Methanol vapor is supplied to the chamber from thermally-insulated trays to which heat may be applied. A sweeping field is provided with electrodes mounted just above the sensitive region. The beam enters the chamber through end covers of $\frac{1}{8}$ in. steel. The problem of photographing this large chamber was rather difficult, and involves the use of mirrors mounted inside the chamber.

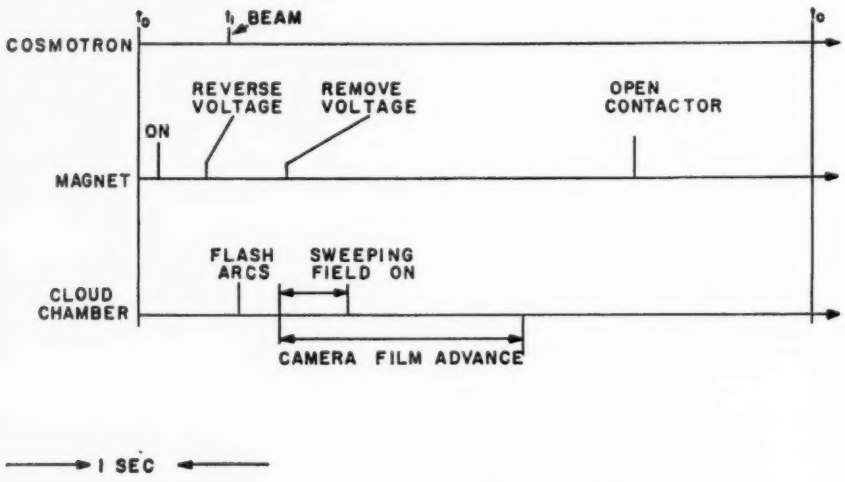

FIG. 6. Cycle of operation of cosmotron, chamber magnet, and diffusion chamber.

An integral part of the long chamber equipment is a novel scanning device. A special projector was built in which the image plane and the film plane are tipped to produce a distorted image in which the chamber length is compressed. The length is compressed to 18 in., while the width remains full size. This device saves 75 per cent in scanning time because of the smaller area to be scanned and, in addition, has the advantage of magnifying small angular deflections of lengthwise tracks, making them easier to detect. The beam particles also show up strongly against the randomly oriented background tracks.

The problem of background in cloud chambers near high-energy accelerators is a serious one. Cloud chambers are indiscriminate devices, sensitive to ionizing particles coming from all directions, and it has usually been necessary to supply substantial shielding in addition to that required by the

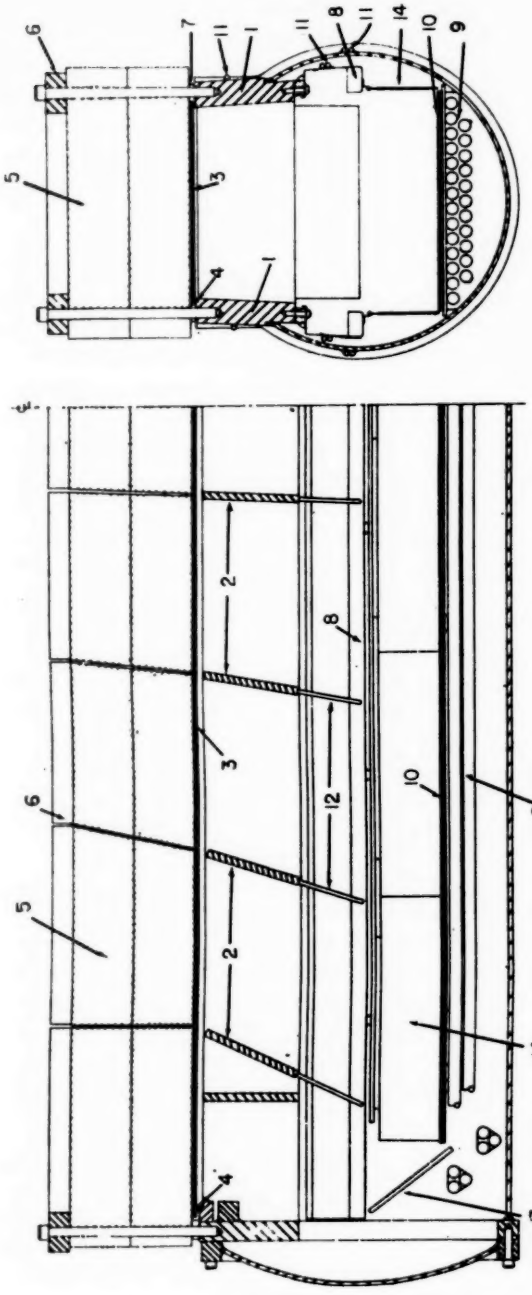

FIG. 7. Long high-pressure diffusion chamber (Brookhaven). At the right a transverse section through the center is shown. At the left one-half of a lengthwise section is shown, the other half being symmetrical.

machine itself. Cloud chamber pictures that have many background tracks are difficult to scan, and events are often missed, or spurious chance events are observed. The diffusion chambers at the cosmotron are operated inside a shielding house made of iron-oxide loaded concrete shielding blocks 3 ft. thick, with a 6 in. steel roof. The beam from the machine is deflected and cleaned of low-energy particles by an analyzing magnet. Since the acceleration period is nearly one second long, the presence of low-energy particles in the diffusion chamber is avoided by the procedure of plunging a target into the beam late in the cycle. Generally no more than 10 to 20 beam particles per pulse can be scanned and analyzed reliably.

The Brookhaven group emphasizes the importance of adequate scanning time and procedures. The problem is quite similar to those encountered in nuclear emulsion work, where the scanning and analysis time is far greater than the exposure time. At Brookhaven, between 100 and 300 pictures can be scanned per man-day, depending on the care with which the work is done, and the amount of cross-checking required. The analysis of events observed is estimated to take 20 or more man-days per cosmotron day.

High-pressure diffusion chambers have been built by Snowden & Bevan (67) for use with the Harwell cyclotron. The first of these was a 9 in.-diameter chamber originally built to withstand 4 atm. pressure, and later (55) modified for 11 atm. Bevan has made an extensive series of measurements with this chamber to determine the optimum and limiting conditions for its operation, and has compared the results with the theory worked out by Shutt (53). Temperature measurements were made with thermocouples in good thermal contact with the well-lagged side of the cloud chamber, and care was taken to allow the gas and the walls to come into temperature equilibrium. Shutt predicted that the vertical temperature distribution required for tracks to be formed in a gas at temperatures below 260° K. depends with good approximation on a single parameter:

$$\beta_a = \mu_0 P^{5/3} (n_0 \tau Z)^{4/3} D_0^{-1/3}$$

where μ_0 = viscosity of the gas at 273° K., D_0 = diffusion coefficient of the vapor within the gas at N.T.P. and one atmosphere pressure, P = pressure in atmospheres, n_0 = number of ions per cm.^{3} per sec. which would be produced in air at N.T.P. by the mean radiation intensity within the chamber, τ = number of atoms per molecule of gas, and Z = atomic number of the gas.

Taking into account the formation of neutral condensation nuclei, and estimating other factors in the equation, Bevan finds the parameter

$$B_a = \mu_0 D_0^{-1/3} P^{1/3} [n_0 \tau Z P + 14.5 \exp (0.116t)]^{4/3}$$

where t°C. is the highest temperature of vapor within the chamber. Bevan makes a plot of the minimum temperature gradient required for track formation against the corresponding values of B_a for various gases, pressures, ion loads, and trough (liquid) temperatures, and shows that data lie quite well on a single curve. He also discusses the effect of trough temperature and its effect on instability in the chamber and the formation of neutral vapor-

molecule aggregates. It is generally advisable to employ the lowest trough temperature consistent with other operating conditions. An extreme case was observed when the temperature of the alcohol in the trough was raised to the boiling point. Fine streamers of descending rain were observed to be produced within the sensitive region, probably resulting from the evolution of large numbers of neutral condensation nuclei from the boiling liquid.

A larger high-pressure chamber constructed at Harwell is described by Snowden (67). It has a diameter of 18 in., is designed for a pressure of 25 atm., and can be placed in a Helmholtz coil system that gives a magnetic field of 13,000 gauss. The beam of 150 Mev protons from the Harwell cyclotron is admitted into the chamber through a $1\frac{1}{2}$ in. diameter hemispherical window made of 0.005 in. stainless steel. The bottom of the chamber is cooled by acetone sprayed by a pump from a series of jets situated below the base of the chamber. The acetone is maintained at a temperature of $-70°C.$ by a heat exchanger immersed in methyl alcohol and solid carbon dioxide. The chamber has thick plastic windows for viewing and illumination, each of double construction to eliminate condensation effect. Excellent photographs (54) have been obtained with this chamber, illustrating the effect of good beam collimation on the background observed in the chamber.

A high-pressure diffusion cloud chamber similar to the Brookhaven magnet chamber has been constructed (68) for use at the Columbia University Nevis Cyclotron. Since the ion load was rather high, it was necessary to maintain a 8°C./cm. temperature gradient over the sensitive layer. This was provided by a 400 watt heater in the chamber wall 1.4 in. above the top of the sensitive layer. The top was kept at 12°C. A Helmholtz coil magnet mounted in a soft iron shell produced a uniform magnetic field in the chamber. The slow mesons studied in this experiment were accompanied by a rather large background, and it was necessary to wait 10 sec. between pictures to allow the chamber to recover.

A 36 atm.-diffusion cloud chamber (69) has been constructed for use with the 184 in. cyclotron and with the bevatron at Berkeley. This chamber has several unique features, including the high pressure of the filling gas, the intense magnetic field, and some unusual constructional details. It is shown in Figure 8. The chamber was designed to fit into the existing cloud chamber magnet (70) which is capable of supplying a pulsed magnetic field of 21,000 gauss on an 11-sec. cycle, with a duration of the full field of about 0.2 sec. The upper portion of the chamber duplicates the upper pole piece formerly used. The chamber is cooled by acetone circulating at dry ice temperature. The glass (C) through which the photograph is taken is much smaller than the 19 in. chamber diameter and thus need not be very thick to withstand the pressure. The chamber is illuminated through $\frac{5}{8}$ in.-thick Astrolite windows, cast especially for the purpose and machined to the inside radius of the chamber.

In operation the usable sensitive volume extends to within 0.5 in. of the bottom, and is from 2 to 2.5 in. high and 10 in. diameter. The clearing field

of −900 volts is grounded about 4 sec. before the beam pulse. The chamber has been used with a magnetically analyzed beam of 4.5 Bev negative pions from the bevatron. Optimum conditions are to have about 15 mesons per pulse on an 11 sec. cycle.

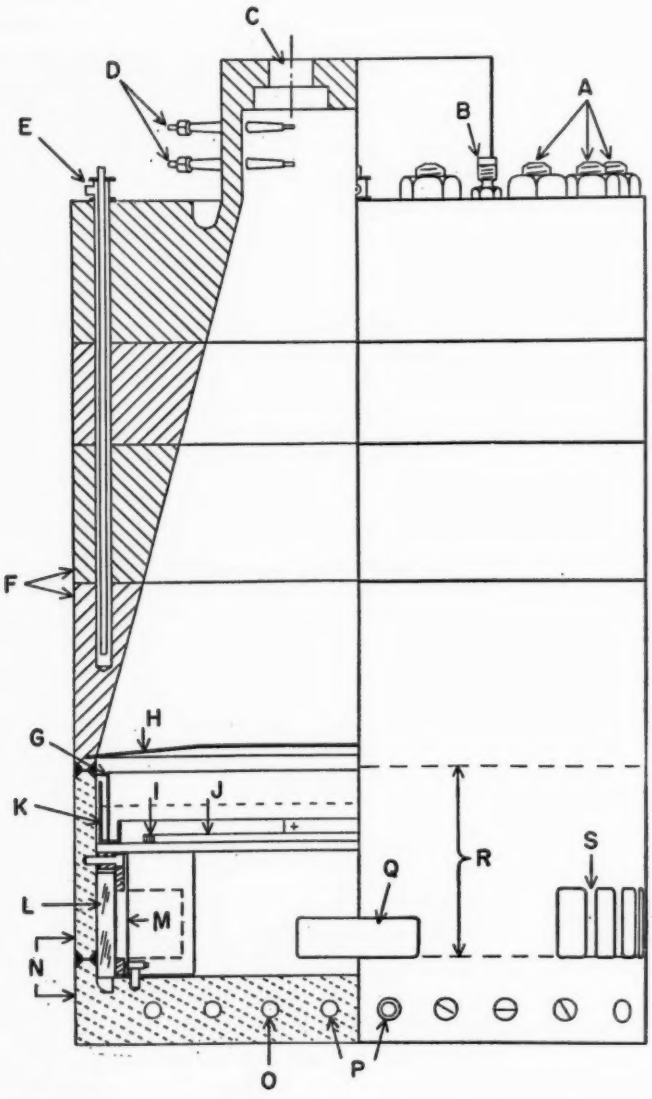

FIG. 8. High-pressure diffusion chamber used at bevatron. Some features: C: viewing ports and camera ports; F: upper pole assembly; I: clearing field support; J: clearing field wires; K: copper alcohol tray; L: cast astrolite windows; O: acetone channel.

To illustrate the use of high-pressure diffusion cloud chambers as nuclear particle detectors, several experiments will be described. The work of the Brookhaven group is certainly the best illustration of the utility of the technique. Their first paper (71) describes a measurement of π^--p scattering made in a beam of pions from the Columbia University Nevis cyclotron. 5600 pictures taken during one day's operation were examined, corrections made for π-μ decays, and a cross-section of 3 millibarns for the scattering of 60-Mev negative pions by hydrogen was obtained. A similar experiment (72) performed using positive pions yielded not only a total cross-section of 20 ± 4 millibarns, but also an angular distribution of the differential scattering in the center of mass system. This work was summarized and additional data presented, together with a description of the apparatus (73) and the results obtained when the chamber was filled with helium. The techniques used in the operation of the chamber in connection with the cyclotron are discussed in some detail. The problem of the background remained a serious one, in spite of substantial amounts of shielding and a steering magnet. The chamber was operated without a magnetic field, and thus the slow electron background was quite evident. In a strong magnetic field these particles are bent into small circles and are thus not such a problem, although they may create holes in tracks because of local depletion of vapor.

The first work of the Brookhaven group with the high pressure diffusion chamber at the cosmotron was reported (74) in 1953, when they described a V°-particle produced by a 1.5-Bev negative pion incident on a proton. A later paper (75) discusses in detail the application of the method to the investigation of the production of various heavy unstable particles by negative pions. This work illustrates the utility of a high pressure hydrogen diffusion chamber in the study of unstable particles. The reactions observed in the gas are presumably pion-proton reactions, and the presence of other nucleons does not complicate the analysis of the event. Out of 26,000 photographs, six events interpretable as production in the gas were observed. Two of these involved the production of a pair of neutral V-particles, one event appeared to be the production of a pair of heavy charged unstable particles. The others were single events. It is of interest to know whether these particles are always produced in pairs, and the properties of the diffusion chamber enter decisively into the discussion. The advantages of the diffusion chamber with an accelerator are the essentially pure hydrogen (the alcohol makes up a very small fraction of the gas present) and the collimated horizontal beam. The disadvantage is the thin sensitive region, and if neutral particles are produced at a large angle to the incoming beam, they may leave the sensitive region before they decay. The length of track of the secondary particles available for measurement may be rather short unless the plane of the decay is oriented parallel to the sensitive region. Thus accurate momentum measurements may be limited by the length of track. On the other hand, an observed pair, with both particles coplanar with the point where the pion disappeared in interaction with the proton, is a most convincing piece of

evidence that production in pairs does exist. Before the invention of the bubble chamber, no other instrument could have provided such reliable evidence.

Another piece of information gained in this experiment was the cross-section for production of heavy unstable particles by 1.5 Bev π^--mesons. This was found to be about 1 millibarn.

Further work along this line has been done by Walker (76), who has observed two additional cases of double production of neutral V-particles in the Brookhaven apparatus. Walker took advantage of the known energy of the incident π^--mesons to show that the pair production of V°-particles sometimes probably involved an intermediate step, with a very short-lived particle decaying into the observed Λ°-particle. Such an intermediate step had been suspected by the Brookhaven group also (77).

A second experiment performed by the Brookhaven group concerned meson production in n-p collisions (78). The magnetic field diffusion cloud chamber was placed in the external neutron beam emerging at 0° from a carbon target struck by the circulating proton beam of the cosmotron at a time when the protons had energies of 2.2 Bev. A lead collimator in the cosmotron shield defined a beam 1 in. $\times$ 2 in. in size, and was followed by a magnet to remove charged particles. It was necessary in this experiment to determine the energy spectrum of the neutron beam, as well as to observe the reactions caused when an n-p collision occurred. Momentum measurements on the particles produced, together with analysis of the event taking into account the ionization density of the tracks, made it possible to determine that the median energy of neutrons was 1.7 Bev and that the spectrum spread from 1.0 Bev to 2.2 Bev, rising gradually toward the upper value. A large amount of useful information was obtained from the 20,000 photographs including the ratio of double meson production to single meson production, which was found to be 20 times as great as that predicted by Fermi's theory. Studies were made of the angular distribution of the particles produced, which show rather definite asymmetries in the center-of-mass system. No hyperons or K-particles were observed to be produced in n-p collisions.

It is difficult to imagine either the preceding experiment, or the following, also done by the Brookhaven group, having been performed with any instrument other than a high pressure hydrogen-filled diffusion cloud chamber. The hydrogen bubble chamber, to be discussed in a later section of this report, may be as useful in the future, but at the time the experiments were done, the diffusion chamber was unique in its field. It was used to observe the π^--p interactions at 1.4 Bev (79) which produce various types of unstable particles, including π-mesons. The magnet chamber was used to provide information on the momentum of the particles, but pictures of the long chamber were also analyzed to get cross-section data. There were 147 interactions observed with magnetic field and 323 interactions without field. The total cross-section was found to be 34.6 ± 2.7 millibarns, the elastic cross-

section 10.0 ± 0.8 millibarns. Results on angular distributions were also obtained. About 28,000 cosmotron pulses were photographed with the magnet chamber and 14,000 in the long chamber. Such a large number of photographs can be taken in a little over a week of cosmotron time, but take many months for a large group of scanners and physicists to scan and analyze.

Experiments performed with the Columbia diffusion chamber include a measurement of the rest mass energy of negative pions (80) and a study of internal pair formation of mesic γ-rays produced in pion-hydrogen reactions (68). In these experiments slow negative pions stop in the gas and interact with the protons in the gas. The photographs of the chamber gave accurate information on the momentum of the particles produced and permitted study of the distribution in angle and energy of the electron pairs.

Bubble Chambers

The most extraordinary development in particle detectors in recent years is the invention of the bubble chamber by Glaser (81 to 86). In a series of papers remarkable for their clarity, Glaser outlined how he recognized the need for a particle detector that would do a certain job, and how he conceived the idea for a bubble chamber. Cloud chambers, even high-pressure diffusion cloud chambers, have the basic disadvantage that the density of material in the chamber is low compared to 1 g./cm.^{3}. Emulsions have density of that order of magnitude, but consist primarily of silver and bromide, elements of complex nuclear structure. There was a clear need for a detector similar to a cloud chamber in which tracks of particles could be seen or photographed, but whose sensitive volume might be filled with a hydrogen-rich medium of high density. Glaser had the idea that such an instrument could be made by taking advantage of the instability of superheated liquids against bubble formation just as a Wilson cloud chamber uses the instability of supercooled vapors against droplet formation. He reasoned (81) that the passage of ionizing particles through such a superheated liquid might cause local ionization centers which could create condensation nuclei for the formation of bubbles. It is well-known that liquids can be superheated but that, unless the container is very clean and the quantity rather small, the liquid quickly goes into rapid boiling. Glaser suspected that the triggering mechanism for boiling might be ionizing cosmic rays which pass through the superheated liquid, and that the waiting time for small containers was long simply because of the small number of cosmic rays traversing them per unit time.

The first experiment was made with diethyl ether at 130°C. and 20 atm. pressure. In the presence of a radioactive source, the liquid in a small glass tube always boiled as soon as the pressure was released, but if the source was removed, the time between the pressure release and the onset of boiling ranged from 0 to 400 sec., averaging 68 sec. This is to be compared with the average time of 34 sec. between traversals of the tube by a cosmic-ray particle. There thus seemed to be a possibility of the detection of ionizing radiation by such an instrument.

In the development of the bubble chamber Glaser worked out a theory (83, 84) based on the hypothesis that two or more charges formed in the region of an incipient bubble would encourage the bubble growth because of electrostatic repulsion. If n charges exist in each bubble, the resulting condition for observation of microscopic bubbles is that

$$P_\infty(T) - P > P_n(T) = \frac{3}{2}\left(\frac{4\pi}{n^2e^2}\right)^{1/3}[\sigma(T)]^{4/3}[\epsilon(T)]^{1/3}$$

P_∞ = normal saturated vapor pressure at temperature T, P = actual applied pressure on the system, e = electronic charge, $\sigma(T)$ = surface tension at temperature T, and $\epsilon(T)$ = dielectric constant at temperature T.

To find the temperature at which a bubble chamber will operate, one plots $P_n(T)$ and $P_\infty(T)$ on the same graph for various values of n and obtains the intersections of the two curves. For diethyl ether the predicted and measured temperatures agree to within 10°C. if n is between 2 and 10. Actually the approximations made are not good if n is as small as 2 or 3.

It is not at all clear that the postulate of charges in bubbles explains bubble growth. The bubbles may start from local heating of the liquid resulting from the energy loss of the particle "like the plunge of a hot needle" (86). The formula derived by Glaser is, however, empirically useful in predicting chamber behavior. Generally the proper operating pressure is found (85) to be roughly two-thirds of the critical pressure and the operating temperature is in the region about two-thirds of the way from the normal boiling temperature to the critical temperature.

The next question was whether the particle left a track or a series of bubbles as it traversed the superheated liquid. Glaser reported in 1953 (82, 83) success in photographing tracks of penetrating cosmic ray particles. The bubble chamber consisted of a heavy-walled cylindrical Pyrex bulb 3 cm. long and 1 cm. inside diameter. The bulb was maintained at a temperature variable between 138°C. and 143°C., but constant to 0.5°C. by means of a temperature bath of mineral oil. The ether was under pressure of 300 lbs./in.^{2} until a valve was released, at which time it dropped to atmospheric pressure and became superheated. The liquid normally remained quiet for several seconds, after which eruptive boiling occurred. The chamber was placed in a vertical cosmic ray telescope, which triggered a flash-tube and camera arrangement if a particle passed through during the waiting time. Several photographs of tracks of cosmic ray particles were obtained in this way, and the important potentialities of this nuclear particle detector became apparent. Glaser found that the bubbles grew extremely rapidly, and that it was necessary to wait only a few microseconds before the bubbles were sufficiently large to photograph. Thus photographs of tracks could be taken very quickly after the passage of the particle, and pre-existing motion of the liquid would not cause appreciable distortion of the track, as it often does in cloud chambers.

Glaser tried other experiments with this small glass chamber (84, 85, 86). He took photographs of the chamber with a high-speed motion picture camera at 3000 frames per sec. that showed clearly the formation of the track, the growth of the bubbles, and the initiation of eruptive boiling. These pictures showed that the bubbles grow to 2 mm. in diameter in about 300 microseconds, and that tracks could not be identified after 20 milliseconds. Since the eruptive boiling produces an audible sound, an attempt was made to use the sound to trigger the lights, and thus to see chamber-controlled tracks. A phonograph pick-up was placed in contact with the bulb to detect the sound. Unfortunately the speed of sound in the liquid limited the response time of the triggering apparatus to about 100 microseconds, whereas the bubbles for best results must be photographed in 5 microseconds. Glaser also tried to trigger the lights using scattered light from the droplets, but obtained rather poor-quality pictures using this technique.

One important result found was that the number of bubbles per centimeter depended on the temperature of the chamber, the number increasing rapidly with the temperature. The possibility of measuring and controlling the bubble density became apparent, since for a minimum ionization track in ether, the bubble density is about 25 per cm., and the bubbles are only .02 cm. in diameter if the photography is quick enough.

The practicability of a bubble chamber containing ether led to the question as to whether it would be possible to operate such a chamber using liquid hydrogen. A bubble chamber containing pure hydrogen would have the obvious advantage of simplicity in interpretation of the collisions with protons without contaminating elements. The first liquid hydrogen chamber was constructed by Hildebrand & Nagle (87), using techniques similar to Glaser's, but at liquid hydrogen temperature. The hydrogen was contained in a glass bulb of volume 3 $cm.^3$ and could be observed by eye through the unsilvered Dewar flasks that surrounded the apparatus. The temperature of the chamber was maintained above the temperature of hydrogen boiling at atmospheric pressure by means of a small heater, such that the hydrogen was in equilibrium with its vapor at a pressure of 3 atm. When the pressure in its chamber was reduced to 1 atm., and in the absence of radiation other than cosmic radiation, the hydrogen remained superheated for periods up to 70 sec. before boiling, with an average waiting period of 22 sec. The presence of a radioactive source caused immediate triggering of boiling. Although no track photographs were reported, the results closely paralleled those of Glaser with ether, and the potentialities of liquid hydrogen were clearly indicated. A similar experiment with liquid nitrogen was successful also.

The early experiments on bubble chambers were all done in very clean, small, glass bulbs, to avoid the presence of condensation centers at the walls that might initiate boiling. It soon became clear that for practical use as nuclear particle detectors, larger chambers were necessary. The construction of large clean chambers of glass to operate at relatively high pressures posed a difficult technical problem, but in chambers fabricated of glass and metal

with gaskets, boiling always started at some point before the required degree of superheat could be attained.

That this difficulty might be overcome was suspected in some work done at the University of California Radiation Laboratory (88) under the direction of L.W. Alvarez. The first photographs of tracks in a hydrogen bubble chamber were observed by J. Wood, even though long periods of superheat were not attained. The chamber was 1½ in. in diameter and made of glass, thus somewhat larger than previous chambers. The Berkeley physicists were disappointed at first in their inability to obtain the long periods of superheat found by previous workers, but track photographs showed that such conditions were not required in the successful operation of a large bubble chamber. If the chamber is expanded more rapidly than the rate of growth of bubbles that form on the surface, the required superheat can be maintained for a long enough time to permit the practical use of the chamber.

Further work using gasketed chambers, where long times of superheat cannot be obtained, has been done by the Berkeley group (89, 90) using liquid hydrogen and by Glaser (84, 85) using organic liquids. Hildebrand at Chicago has obtained beautiful tracks (91) with a chamber containing liquid pentane by placing it in a beam of π-mesons from the Chicago synchrocyclotron. It is now clear that larger chambers can be constructed of metal and glass and gaskets, and that there is no obvious upper limit to the size of a bubble chamber.

A 4-in.-diameter liquid hydrogen bubble chamber has been constructed at Berkeley (89) and used in the 4 Bev π^--meson beam of the bevatron. Contrary to the previous technique of immersing the chamber in pressurized liquid hydrogen, the 4-in. chamber is placed in thermal contact with the bath by means of a copper suspension block that supports the chamber from the bottom of a reservoir containing liquid hydrogen. A diagram of the apparatus is shown in Figure 9. Heat loss by radiation is minimized by a liquid nitrogen cooled jacket that partially surrounds the chamber. The chamber itself is formed of a brass cylinder 2 in. long, 4 in. inner diameter, with glass viewing windows sealed to each end by lead "O"-rings. A half-inch diameter stainless steel tube in thermal contact with the side of the bath leads from the chamber to the expansion and filling systems. The chamber is maintained at about 70 lbs./in.^{2} by a pressure-regulated supply of hydrogen attached to this tube through a .030 in. orifice which restricts the flow from the supply during an expansion. The expansion piston, which moves to produce the expansion, is 2 in. in diameter and has a 5 in. stroke. It was important to provide a heat exchanger for the hydrogen gas in the expansion line. The heat exchanger consists of several tufts of copper wool soldered to the inside of the expansion tube, which is in good thermal contact with the reservoir of liquid hydrogen.

Prior to the expansion of the chamber the pressure of the chamber is determined by the pressure of the regulated supply of hydrogen gas, and the piston is locked in the compressed position. About 50 milliseconds before the beam of particles is pulsed through the chamber the piston is released. The

piston then moves under the pressure of the hydrogen, the pressure in the chamber is thereby reduced, and the liquid hydrogen becomes superheated. About 5 milliseconds after the particles pass through the chamber, the light is flashed and the photograph of the tracks is taken. Light-field illumination was used at first with the stroboscopic light illuminating a ground-glass plate but dark-field illumination has proved to be more satisfactory.

It is to be noted that the bubbles in liquid hydrogen grow very much more

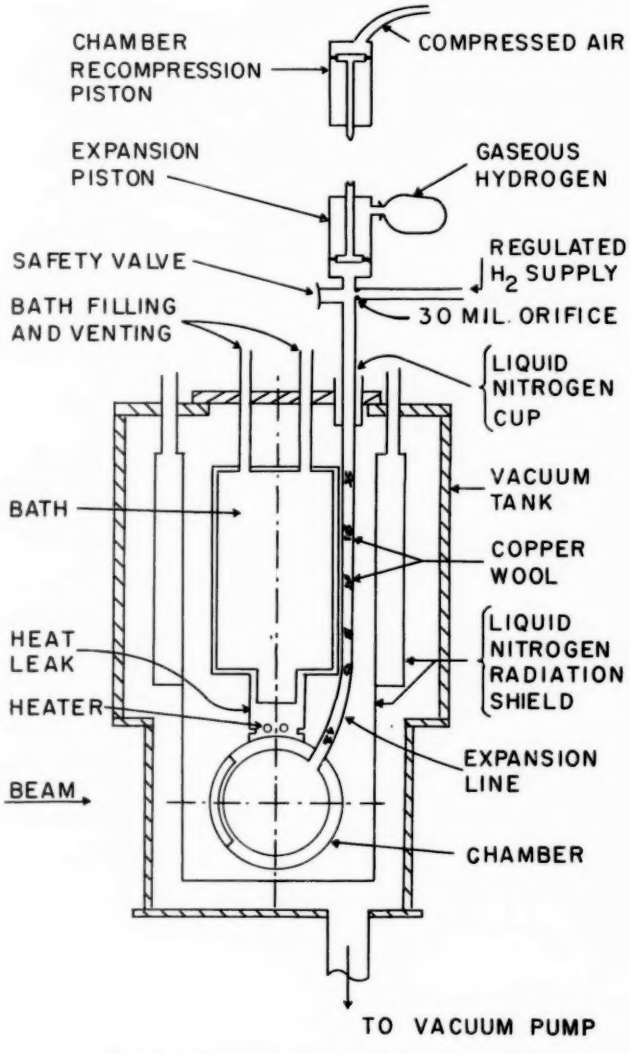

FIG. 9. Liquid hydrogen bubble chamber.

slowly than in ether, where growth times are of the order of microseconds. In liquid hydrogen the bubbles grow approximately as $r=0.1t^{1/2}$, where r is the radius of the bubble in mm., and t the age in milliseconds. The slow growth of bubbles in liquid hydrogen may be explained by the low thermal conductivity, which limits the flow of heat toward the growing bubble.

The 4-in. diameter chamber is normally run at a repetition rate of 5 cycles per minute to correspond to the bevatron pulse rate, although it can be operated at 10 c.p.m. The heater shown in Figure 9, which provides the heat necessary to maintain the chamber at the proper temperature, requires

PLATE I. Stereoscopic photograph of a nuclear event in a liquid-hydrogen bubble chamber. A 4 Bev π^--meson enters at the top, strikes a proton, and makes a four-prong star. Plate set at 90° orientation from normal. Top of photograph is at reader's left.

5 to 10 watts in normal operation. The liquid hydrogen loss rate is 2 to 3 liters per hr., with about 25 liters each of liquid hydrogen and nitrogen required to cool the system initially.

The 4-in. liquid hydrogen chamber has been used in studies of π^--p interactions at 4 Bev. Various examples of nuclear interactions have been observed, including the production of V-particles and the multiple production of mesons, as indicated by a 4-prong star (Plate I).

The success of the 4-in. liquid hydrogen bubble chamber has led the Berkeley group to design a larger chamber that can be placed in a magnetic field. In hydrogen chambers, the deflection of a particle attributable to scattering in the hydrogen is negligible in comparison to its deflection in a magnetic field. Such an instrument should prove to be exceedingly valuable in the study of fundamental particle interactions, especially in the study of short-lived heavy mesons and hyperons. If the technique of bubble-counting can be worked out for measurements of ionization, the instrument will be even more useful.

A large bubble chamber containing diethyl ether has been built by Glaser (85) and put into operation at the cosmotron. After preliminary experiments with a fabricated chamber 2 in. in diameter and 1 in. thick, Glaser constructed a chamber with a sensitive volume of $6\times3\times2$ in. The body of the chamber is made of one piece of dural, polished on the inside, and the windows are made of tempered glass sealed with teflon gaskets. At one end of the chamber the 2×3 in. inside cross-section is flared out to a circular cross-section with a gasket ring 5 in. in diameter. A teflon diaphragm backed by silicone rubber is clamped to this ring and forms a movable wall of the chamber. The position of the diaphragm is controlled by compressed nitrogen which can be released to expand the chamber. The entire chamber is heated in a thermostatically-controlled oven and operated at about 157°C., with *iso*-pentane in the chamber at a pressure of 350 lbs. in.^{2}.

The 6-in. chamber becomes sensitive to minimum ionizing particles 3.5 milliseconds after the expansion is initiated, and remains sensitive for about 10 milliseconds. For operation at the cosmotron, the chamber is expanded 4 milliseconds before the beam arrival and the lights are flashed 90 microseconds after the arrival of the first hundred protons. Glaser notes particularly the temperature sensitivity of the chamber and states that for a minimum ionizing particle the bubble count goes from 8 per cm. at 155°C. to 24 per cm. at 157°C.

Such a bubble chamber has good stopping power, and the pictures taken in the 2 Bev proton beam were rich in π-μ-electron events. Glaser also is planning a larger bubble chamber for accelerator work.

Precise information about the sensitive time of Glaser's 2-in. chamber was obtained (85) by exposing it to pulses of x-rays. The total number of bubbles in the chamber was estimated to be zero for radiation bursts earlier than 3.6 milliseconds after the expansion began, 20 for bursts at 3.7 milliseconds, 20,000 at 4.9 milliseconds, and 20,000 for bursts occurring until 12.0 milli-

seconds after which the bubble count rapidly drops to zero. Apparently there is some time interval during the cycle in which wall boiling evolves vapor just fast enough to keep up with the expansion process, maintaining a sufficiently low pressure to provide the necessary superheat for track formation.

The sharp increase in the number of bubbles found between 3.7 milliseconds and 4.9 milliseconds provides information on the lifetime of bubble nuclei. Apparently all bubble nuclei disappear after about one millisecond, and the average lifetime may be much shorter. Such a short life has two effects. It reduces the background of unwanted "old" tracks that are always to be found in the vicinity of a large accelerator. On the other hand, the short lifetime of bubble nuclei makes the possibility of counter-controlled expansions for cosmic rays quite remote, since expansion of the chamber in such a short time after the passage of a particle does not seem feasible. The technical difficulties involved in the operation of bubble chambers are mostly concerned with the maintenance of the proper temperature conditions. Rather elaborate temperature regulation is required for the oven surrounding Glaser's 6-in. chamber.

The precision of the measurement of magnetic curvature in chambers containing organic liquids, where the bubble growth time is of the order of microseconds, will be limited by optical problems such as differences in refractive index, and also possibly by multiple scattering. In the hydrogen chambers, where the photography time is several milliseconds, noticeable distortions of tracks have been observed that may have their origin in convective motions in the liquid. In hydrogen, scattering should not be important; however, slow electrons scatter enough so that they are easily distinguishable from fast particles when there is no magnetic field.

Photography

The techniques of photography of cloud chambers and bubble chambers are quite similar, and recent developments in these methods can be applied to both types of instruments. The problems of drop photography were discussed by Wilson (5) and reviewed by Newth (49). The size of the image of a single drop may be determined either by the diameter of the central disk of the optical diffraction pattern formed by the lens aperture on the film, or by the properties of the emulsion such as grain size and turbidity. In very fast emulsions the latter are dominant, and typical diameters of drop-image size range from 20 to 30 microns. The drop images used by Cowan (26), are 27 μ in diameter, and Wilson & Newth take 20 μ as a reasonable value. Fretter & Friesen (27) and a group at Imperial College (45) have worked, however, with drop images only 12 μ in diameter and thus can use higher values of the object/image ratio. Linagraph Ortho film has a resolving power of 95 lines/mm., whereas Linagraph Pan has 70 lines/mm. and actually appears to be much more grainy than the Ortho. Kodak Linagraph Ortho and Ilford 59GI appear to be the best films for giving small drop diameters.

The almost universal use of Xenon-filled flash tubes and the development of the films mentioned above have made possible great improvement in cloud chamber photography. The films are very sensitive in the blue; Linagraph Ortho has a blue speed of 400, green speed of 125, while Linagraph Pan has a blue speed of 640 and a green speed of 125. The light from Xenon flash tubes is predominantly in the blue. These films were designed for high-contrast photography, which is also desirable for cloud-chamber work.

Many cloud chamber experiments do not require resolution of individual droplets in the track, and requirements on the film and lighting are less stringent if this is the case. The photographic background for track photography has usually been black velvet, but considerable success has been attained in the use of black mirrors for background. In diffusion chambers, where the background surface is horizontal, black dye in a pool of alcohol has been used. For vertical expansion chambers, highly polished black anodized aluminum pistons have been satisfactory (27), particularly when the light beam comes very close to the piston.

Luminescent Chamber

A new method of photographing tracks of ionizing particles has been described by Zavoiskii *et al.* (92) in which the tracks occur in luminescent substances and are photographed by means of a sensitive electron-optical converter. In such a "luminescent chamber" photographs of tracks of relativistic particles and of stars produced by neutrons have been obtained. The luminescent material used was sodium iodide or cesium iodide crystals activated with thallium. The light from the track of an ionizing particle is projected by a lens on the photocathode of the electron-optical converter (evidently a form of iconoscope connected to a television-type viewing screen) and on the screen of the converter it is possible to see tracks of particles above the natural noise background. In practice, synchronizing pulses obtained from photomultipliers viewing the same crystal were used to obtain the photographs of a particular event.

Such a luminescent chamber is continuously sensitive, and motion pictures may be made of the tracks, but the thermal noise of the iconoscope is reduced if it is pulsed. The time discrimination of the luminescent chamber is very much better than that of any other type of particle detector. Zavoiskii hopes to use the instrument to study luminescent processes taking place in the time duration of from 10^{-12} to 10^{-14} sec. It may also be possible to identify particles by using the dependence of the density of darkening of the film as a function of residual range.

LITERATURE CITED

1. Wilson, C. T. R., *Proc. Roy. Soc.* (*London*), [A]**85**, 285 (1911)
2. Wilson, C. T. R., *Proc. Roy. Soc.* (*London*), [A]**87**, 277 (1912)
3. Gentner, W., Maier-Leibnitz, H., and Bothe, W., *An Atlas of Typical Expansion Chamber Photographs* Pergamon Press, London, England, 199 pp., 1954)
4. Rochester, G. D., and Wilson, J. G., *Cloud Chamber Photographs of the Cosmic Radiation* (Pergamon Press, Ltd., London, England, 128 pp., 1952)

5. Wilson, J. G., *The Principles of Cloud-Chamber Technique* (Cambridge University Press, Cambridge, England, 131 pp., 1951)
6. Das Gupta, N. N., and Ghosh, S. K., *Rev. Mod. Phys.*, **18,** 225 (1946)
7. Snowden, M., in *Progress in Nuclear Physics*, **3** (Frisch, O. R., Ed., Academic Press, Inc., New York, N. Y., 1953)
8. Street, J. C., *J. Franklin Inst.*, **227,** 765 (1939)
9. Fretter, W. B., *Phys. Rev.*, **70,** 625 (1946)
10. Brode, R. B., *Rev. Mod. Phys.*, **21,** 37 (1949)
11. Retallack, J. G., and Brode, R. B., *Phys. Rev.*, **75, 1716** (1949)
12. Merkle, T. C., Goldwasser, E. L., and Brode, R. B., *Phys. Rev.*, **79,** 926 (1950)
13. Goldwasser, E. L., and Merkle, T. C., *Phys. Rev.*, **83,** 43 (1951)
14. Rosen, A. Z., *Phys. Rev.*, **93,** 211 (1954)
15. Ballam, J., and Lichtenstein, P. G., *Phys. Rev.*, **93,** 851 (1954)
16. Azimov, S., Birger, N., Dobrotin, N., Zhdanov, G., Kokurin, Y., and Slavatinskii, S., *Doklady Akad. Nauk, SSSR*, **78,** 447 (1951) [Translated in *Guide Russ. Sci. Period. Lit.* (Brookhaven), **4,** 339 (1951)
17. Leighton, R. B., Wanlass, S. D., and Anderson, C. D., *Phys. Rev.*, **89,** 148 (1953)
18. Alford, W. L., and Leighton, R. B., *Phys. Rev.*, **90,** 622 (1953)
19. York, C. M., Leighton, R. B., and Bjornerud, E. K., *Phys. Rev.*, **95,** 159 (1954)
20. van Lint, V. A. J., Trilling, G. H., Leighton, R. B., and Anderson, C. D., *Phys. Rev.*, **95,** 295 (1954)
21. Gregory, B., Lagarrigue, A., Leprince-Ringuet, L., Muller, F., and Peyrou, C., *Nuovo cimento*, **11,** 292 (1954)
22. Fretter, W. B., Gregory, B. P., Johnston, R., Lagarrigue, A., Meyer, H., Muller, F., and Peyrou, C., *Phys. Rev.*, **92,** 1583 (1953)
23. Hodson, A. L., Ballam, J., Arnold, W. H., Harris, D. R., Rau, R. R., Reynolds, G. T., Treiman, S. B., *Phys. Rev.*, **96,** 1089 (1954)
24. Kim, Y. B., Burwell, J. R., Huggett, R. W., and Thompson, R. W., *Phys. Rev.*, **96,** 229 (1954)
25. Thompson, R. W., "Hyperons and Heavy Mesons: The Uncharged Particles," in *Progress in Cosmic Ray Physics*, **3** (Wilson, J. G., Ed., North Holland Publishing Co., Amsterdam, Holland) (Interscience Publishers, New York, N. Y., In press)
26. Cowan, E. W., *Phys. Rev.*, **94,** 161 (1954)
27. Fretter, W. B., and Friesen, E. W., *Rev. Sci. Instr.* **26** (July, 1955)
28. Ghosh, S. K., Jones, G. M. D. B., and Wilson, J. G., *Proc. Phys. Soc.* (*London*), **67,** 331 (1954)
29. Lovati, A., Mura, A.. Tagliaferri, G., and Terra, L., *Nuovo cimento*, **8,** 713 (1951)
30. Bridge, H. (Private communication)
31. Blumenfeld, H., Booth, E. T., and Lederman, L. M., *Rev. Sci. Inst.*, **25,** 1220 (1954)
32. Gaerttner, E. R., and Yeater, M. L., *Rev. Sci. Instr.*, **20,** 588 (1949)
33. Kessler, J. O., and Lederman, L. M., *Phys. Rev.*, **94,** 689 (1954)
34. Emigh, C. R., *Rev. Sci. Instr.*, **25,** 221 (1954)
35. Gaerttner, E. R., and Yeater, M. L., *Rev. Sci. Instr.*, **20,** 526 (1949)
36. Emigh, C. R., *Rev. Sci. Instr.*, **25,** 567 (1954)
37. Carter, R. S., and Street, J. C., *Rev. Sci. Instr.*, **25,** 627 (1954)
38. Cohen, M. J., *Phys. Rev.*, **75,** 1329 (1949)
39. Hodson, A. L., Loria, A., and Ryder, N. V., *Phil. Mag.*, **41,** 826 (1950)

40. Fireman, E. L., and McHaney, G. M., *Rev. Sci. Instr.*, **21,** 813 (1950)
41. Lewis, H. W., Brown, W. W., Seevers, D. O., and Hones, E. W., *Rev. Sci. Instr.*, **22,** 259 (1951)
42. Loria, A., *Nuovo cimento*, **11,** Suppl. 2, 319 (1954)
43. Brown, W. W., *Phys. Rev.*, **93,** 528 (1954)
44. Burhop, E. H. S., *Nuovo cimento*, **11,** Suppl. 2, 343 (1954)
45. Blackett, P. M. S., *Nuovo cimento*, **11,** Suppl. 2, 264 (1954)
46. Newth, J. A., *Nuovo cimento*, **11,** Suppl. 2, 290 (1954)
47. Bartlett, M. S., *Phil. Mag.*, **44,** 249 (1953)
48. Bartlett, M. S., *Phil. Mag.*, **44,** 1407 (1953)
49. Newth, J. A., *Nuovo cimento*, **11,** Suppl. 2, 297 (1954)
50. Barker, K. H., *Nuovo cimento*, **11,** Suppl. 2, 309 (1954)
51. Peyrou, C., *Nuovo cimento*, **11,** Suppl. 2, 322 (1954)
52. Langsdorf, A., *Rev. Sci. Instr.*, **10,** 91 (1939)
53. Shutt, R. P., *Rev. Sci. Instr.*, **22,** 730 (1951)
54. Snowden, M., in *Progress in Nuclear Physics* (Frisch, O. R., Ed., Academic Press Inc., New York, N. Y., and Butterworth-Spring, London, England, 1953)
55. Bevan, A. R., *J. Sci. Instr.*, **31,** 45 (1954)
56. Succi, C., and Tagliaferri, G., *Nuovo cimento*, **9,** 1092 (1952)
57. Miller, D. H., Fowler, E. C., and Shutt, R. P., *Rev. Sci. Instr.*, **22,** 280 (1951)
58. Cowan, E. W., *Rev. Sci. Instr.*, **21,** 991 (1950)
59. Nielsen, C. E., Needels, T. S., and Weddle, O. H., *Rev. Sci. Instr.*, **22,** 673 (1951)
60. Lovati, A., and Succi, C., *Nuovo cimento*, **11,** 163 (1954)
61. Relf, K. E., and Powell, W. M., *Rev. Sci. Instr.*, **25,** 1182 (1954)
62. Relf, K. E., *Phys. Rev.*, **97,** 172 (1955)
63. Relf, K. E., and Powell, W. M., *Univ. Calif. Radiation Lab. Rept. UCRL-2412*, November, 1953
64. Block, M. M., Brown, W. W., and Slaughter, G. G., *Phys. Rev.*, **86,** 583 (1952)
65. Choyke, W. J., and Nielsen, C. E., *Rev. Sci. Instr.*, **23,** 307 (1952)
66. Fowler, W. B., Shutt, R. P., Thorndike, A. M., and Whittemore, W. L., *Rev. Sci. Instr.*, **25,** 996 (1954)
67. Snowden, M., and Bevan, A. R., *J. Sci. Instr.*, **30,** 3 (1953)
68. Sargent, C. P., Cornelius, R., Rinehart, M., Lederman, L. M., and Rogers, K. (Private communication)
69. Elliott, J. B., Maenchen, G., Monethrop, P. H., Oswald, L. O., Powell, W. M., and Wright, R. W., *Univ. Calif. Radiation Lab. Rept. UCRL-2865* (1955)
70. Powell, W. M., *Rev. Sci. Instr.*, **20,** 403 (1949)
71. Shutt, R. P., Fowler, E. C., Miller, D. H., Thorndike, A. M., Fowler, W. B., *Phys. Rev.*, **84,** 1247 (1951)
72. Fowler, E. C., Fowler, W. B., Shutt, R. P., Thorndike, A. M., and Whittemore, W. L., *Phys. Rev.*, **86,** 1053 (1952)
73. Fowler, E. C., Fowler, W. B., Shutt, R. P., Thorndike, A. M., and Whittemore, W. L., *Phys. Rev.*, **91,** 135 (1953)
74. Fowler, W. B., Shutt, R. P., Thorndike, A. M., and Whittemore, W. L., *Phys. Rev.*, **91,** 1287 (1953)
75. Fowler, W. B., Shutt, R. P., Thorndike, A. M., and Whittemore, W. L., *Phys. Rev.*, **93,** 861 (1954)
76. Walker, W. D., *Proc. 5th Rochester Conf. on High Energy Physics*, p. 148 (Physics Dept., Univ. of Rochester, Rochester, N. Y., 1955)

77. Fowler, W. B., Shutt, R. P., Thorndike, A. M., and Whittemore, W. L., *Phys. Rev.*, **98,** 121 (1955)
78. Fowler, W. B., Shutt, R. P., Thorndike, A. M., and Whittemore, W. L., *Phys. Rev.*, **95,** 1026 (1954)
79. Eisberg, L. M., Fowler, W. B., Lea, R. M., Shephard, W. D., Shutt, R. P., Thorndike, A. M., and Whittemore, W. L., *Phys. Rev.*, **97,** 797 (1955)
80. Cornelius, R. C., Sargent, C. P., Rinehart, M. C., Lederman, L. M., and Rogers, K., *Phys. Rev.*, **92,** 1583 (1953)
81. Glaser, D. A., *Phys. Rev.*, **87,** 665 (1952)
82. Glaser, D. A., *Phys. Rev.*, **91,** 496 (1953)
83. Glaser, D. A., *Phys. Rev.*, **91,** 762 (1953)
84. Glaser, D. A., *Nuovo cimento*, **11,** Suppl. 2, 361 (1954)
85. Glaser, D. A., *Phys. Rev.*, **97,** 474 (1955)
86. Glaser, D. A., *Sci. American*, **192,** 46 (Feb., 1955)
87. Hildebrand, R. H., and Nagle, D. E., *Phys. Rev.*, **92,** 517 (1953)
88. Wood, J. G., *Phys. Rev.*, **94,** 731 (1954)
89. Stevenson, M. L. (Private communication)
90. Parmentier, D., Schwemin, A., Alvarez, L., Crawford, F., and Stevenson, M. L., *Bull. Am. Phys. Soc.*, **29,** 8, *Abstr. U12* (1954)
91. Hildebrand, R. H., in *Proceedings of the 1954 Glasgow Conference on Nuclear and Meson Physics* (Pergamon Press, Ltd., London, England, and New York, N. Y., 352 pp., 1955)
92. Zavoiskii, E. K., Smolkin, G. E., Plakov, A. G., and Butslov, M. M., *Doklady Akad. Nauk. S.S.S.R.*, **100,** 241 (1955)

DESIGN COMPARISON OF REACTORS FOR RESEARCH[1]

By L. B. Borst

Department of Physics, New York University, University Heights, N. Y.

Survey

Nuclear reactors for research (1 to 7) may be compared by several criteria: neutron flux, neutron energy, capacity, cost, fuel, moderation, coolant, and safety.

Fast and intermediate neutron energy reactors will not be discussed, since for research purposes only one fast reactor has been built ("Clementine" at Los Alamos), and this has been dismantled. Fast reactors may well find utility for breeding and power. Argonne National Laboratory's E.B.R. at Arco, Idaho is considered as its name states: it is an Experimental Breeder Reactor. The United Kingdom's "Zephyr" is a low-power fast reactor for study of the behavior of fast reactor assemblies.

Generally speaking, unenriched uranium reactors are large and costly for their flux, but their large size gives a research capacity unequalled by the high intensity enriched fuel units. The total investment transcends private financing, so that without exception these are government-owned reactors.

Using graphite moderation (with unenriched fuel) the multiplication factor for an infinitely large system is about 1.10, so that leakage must be minimized and the size must be large. A twenty-foot dimension is usually considered minimum which corresponds roughly to 400 tons of moderator. The sequence in this group is given in Table I.

TABLE I

Graphite Moderated Unenriched Research Reactors

Reactor	Date	Flux (cm^{-2} sec^{-1})	Power (kilowatts)
CP-1 Chicago	1942	4×10^{6}	0.1
CP-2 Argonne	1943	10^{8}	0.2
X-10 Oak Ridge	1943	10^{12}	4,000
GLEEP Harwell	1947	3×10^{10}	100
BEPO Harwell	1948	10^{12}	4,000
BNL Brookhaven	1950	5×10^{12}	28,000

The investment and research capacity of such reactors necessarily imply a large and well-integrated research program. Graphite as a moderator is

[1] The survey of literature pertaining to this review was completed in February, 1955.

well-adapted to large-scale production of plutonium or power, in the United States using water as a coolant, in England and France using air or a compressed gas as a coolant.

Beryllium as a moderating material has found no extensive use. Cost and biological hazard have restricted its use primarily to incidental use as a reflector material. Deuterium and hydrogen are superior moderators, and research reactors for the forseeable future will use them. Slowing-down lengths for fission neutrons are: 5.7 cm. for H_2O and 11.0 cm. for D_2O, compared to 19 cm. for graphite and 9.9 cm. for Be. Characteristic sizes of water or deuterium moderated reactors are materially reduced, and with them investment and research capacity.

Among the early reactors were CP-3 and NRX, both based upon D_2O moderation and unenriched uranium. Characteristic dimensions are 6 to 10 ft., corresponding to several tons of heavy water, or an investment for heavy water alone in the million dollar range. Table II summarizes this family.

TABLE II

HEAVY WATER UNENRICHED RESEARCH REACTORS

		Flux (cm^{-2} $sec.^{-1}$)	Coolant	Power (kilowatts)
CP-3 Argonne	1944	10^{12}	Circulated moderator	300
NRX Chalk River	1947	7×10^{13}	H_2O	40,000
ZOE Chatillon France	1948	3×10^{10}	Circulated moderator	10
JEEP Kjeller, Norway	1951	10^{12}	Circulated moderator	300
SLEEP Stockholm, Sweden	1954	10^{12}	Circulated moderator	300
P-2 Saclay, France	1952	4×10^{12}	Nitrogen gas 10 atm.	1,500

The use of enriched uranium makes the problem of establishing a chain reaction simple. The multiplication factor for an infinite medium is in the vicinity of 2, so that a significant fraction of neutrons may be permitted to escape. The nuclear design then changes from a near infinite region (surrounded by a reflector as a neutron economizer) to a near point source surrounded by an extended nonreproducing reflector. Characteristic dimensions for H_2O are about 1 ft. and for D_2O, 2 to 3 ft.

The construction cost for enriched reactors will no longer depend upon the quantity of moderator, but rather upon the cooling and control system and particularly upon the extent and nature of the experimental facilities. The total investments involved may be reduced to a scale permitting private financing. However, by comparison with unenriched uranium the research capacity is severely limited, and a balance must be found between research capacity, flux, power, material requirements, and cost. The remainder of the discussion will be directed to an analysis of these parameters.

A list of enriched research reactors is given in Table III.

TABLE III

ENRICHED RESEARCH REACTORS

	Date	Flux ($cm^{-2}sec^{-1}$)	Fuel (gm.)	Coolant	Power (kilowatts)
LOPO Los Alamos	1944			Conduction	.001
HYPO Los Alamos	1944	10^{11}		H_2O	6
SUPO Los Alamos	1951	2×10^{12}	870	H_2O	45
LITR Oak Ridge	1950	10^{13}	3000	H_2O	2,000
CP-3′ Argonne	1950	4×10^{12}	4000	Convective circulation D_2O	300
Swimming Pool Oak Ridge	1951	10^{12}	3000	Convective circulation H_2O	100
MTR Idaho Falls	1952	5×10^{14}	4000	H_2O	30,000
NCRR Raleigh	1953	4×10^{11}	848	H_2O	10
CP-5 Argonne	1954	2×10^{13}	1700	Forced circulation D_2O	1,000

The costs of these various units are difficult to compare. HYPO and SUPO are reported to cost about $500,000, presumably including the building. LITR is $1,000,000 in a minimum-cost enclosure. The Oak Ridge Swimming Pool is estimated at $250,000 of which about one-half is for the reactor. CP-3′ is difficult to evaluate since it is a modification of CP-3 which was built under war-time conditions. The MTR has a construction cost of $18,000,000 of which perhaps $12,000,000 can be charged to the reactor.

The North Carolina State reactor represents a cost of $120,000 for reactor, $380,000 for building and $120,000 for laboratory auxiliaries. CP-5 is estimated to cost $2,500,000 of which perhaps one half is chargeable to the reactor.

UTILITY OF RESEARCH REACTORS

Research reactors seem to require no salesmanship, since most institutions would be pleased to own one. When the more concrete question of finances and utility are raised, answers are not as well-defined.

Industrial interests in research reactors stem from the numerous technological problems confronting groups studying atomic power. Other uses involve the development of new products and processes and the study of fundamental science which may lead to other future products.

University interests seem to fall into four categories: (*a*) training of nuclear engineers; (*b*) engineering research similar in objective to industrial research objectives; (*c*) fundamental pure scientific studies in the fields of physics, chemistry, metallurgy, and biology; and (*d*) medical studies both fundamental and clinical. The balance between these interests will largely govern the choice of reactor type and power.

In addition, convenience is a strong determining factor in the evaluation

of the use to which a reactor will be put. Industrial reactors can usually be located on an industrial site where access is adequate and there is sufficient isolation.

In the case of the urban university, selection of a site and appropriate design can be transcendent considerations. The selection of an isolated site which will permit latitude in selection of power, flux, and design will restrict use by professors and students because of time lost in transportation and inability to arrange appropriate class schedules. The choice of a campus site will have grave repercussions on the choice of design, permissible operating levels, and the varieties of research which can be conducted.

Various university groups advocate each of the three principal designs: water boiler, swimming pool, and CP-5.

Groups representing the engineering viewpoint generally favor the swimming pool. They cite the pedagogical value of being able to see all parts of the operating reactor and of being able to see the glow from the chain reaction. In this respect the swimming pool is clearly superior. In addition, the desire on the part of engineers to test or to irradiate large specimens can be easily- and well-satisfied by this design. Among the various universities this is numerically the strongly-favored design.

One university group (Massachusetts Institute of Technology) favors the CP-5 design for a flux of 10^{13} cm.$^{-2}$ sec.$^{-1}$ on the basis particularly of safety and stability considerations. It would have the largest active volume of the three types and would therefore support the largest research load.

The water boiler was the first type of reactor completely described in the open literature. In addition, because of its inherent stability and safety it was selected by North Carolina State College for construction. It most nearly approaches the point neutron source, has a small fuel requirement, and consequently a small power output for a given flux. It, therefore, has advantages as a neutron source over the other designs. Such a source is useful for neutron research, for medical neutron therapy and for irradiation of small samples.

Statutory Restrictions (United States)

The United States Atomic Energy Act of 1946 contained enabling clauses concerning reactors for medical and pure research. A policy clause enjoined the Commission to support fundamental research on a broad basis. Use of enriched uranium or plutonium in research reactors was subject to strict control. Among restrictions was the requirement that

> no applicant will be enabled to obtain an amount (of fissionable material) sufficient to construct a bomb or other military weapon . . . The Commission shall not distribute any material to any applicant, and shall recall any distributed material from any applicant who is not equipped to observe or who fails to observe such safety standards to protect health and to minimize danger from explosion or other hazard to life or property as may be established by the Commission.

The Atomic Energy Act of 1954 makes the same general statements, but permits specific additional arrangements particularly by way of licensing procedures. Among other licensing provisions are the following:

Sec. 53e. Each license issued pursuant to this section shall contain and be subject to the following conditions—

(6) special nuclear material shall be distributed only on terms as may be established by rule of the Commission, such that no user will be permitted to construct an atomic weapon;

(7) special nuclear material shall be distributed only pursuant to such safety standards as may be established by rule of the Commission, to protect health and to minimize danger to life or property; and

(8) the licenses will hold the United States and the Commission harmless from any damages resulting from the use or possession of special nuclear material by the licensee.

Sec. 104. Medical Therapy and Research Development.

a. The Commission is authorized to issue licenses to persons applying therefore for utilization facilities for use in medical therapy. In issuing such licenses the Commission is directed to permit the widest amount of effective medical therapy possible with the amount of special nuclear material available for such purposes to impose the minimum amount of regulation consistent with its obligations under this Act to promote the common defense and security and to protect the health and safety of the public.

b. The Commission is authorized to issue licenses to persons applying therefore for utilization and production facilities involved in the conduct of research and development activities leading to the demonstration of the practical value of such facilities for industrial or commercial purposes. In issuing licenses under this subsection, the Commission shall impose the minimum amount of such regulations and terms of license as will permit the Commission to fulfill its obligations under this Act to promote the common defense and security and to protect the health and safety of the public and will be compatible with the regulations and terms of license which would apply in the event that a commercial license were later to be issued pursuant to section 103 for that type of facility. In issuing such licenses, priority shall be given to those activities which will, in the opinion of the Commission lead to major advances in the application of atomic energy for industrial or commercial purposes.

c. The Commission is authorized to issue licenses to persons applying therefore for utilization and production facilities useful in the conduct of research and development activities of the types specified in section 31 and which are not facilities of the type specified in subsection 104b. The Commission is directed to impose only such minimum amount of regulation of the license as the Commission finds will permit the Commission to fulfill its obligations under this Act to promote the common defense and security and to protect the health and safety of the public and will permit the conduct of widespread and diverse research and development.

At the time of writing, the U. S. Atomic Energy Commission is establishing uniform licensing procedures (*a*) for production and utilization facilities, (*b*) for special nuclear materials, and (*c*) for operators. In connection with the production and utilization facilities applicant, he will first be issued a Construction Permit which will permit him to execute his project. Such a

Construction Permit would be directly convertible to an Operating License.

In summary, judging from the number of institutions (more than ten) discussing reactor projects with the Commission, no serious impediment is to be expected for the competent institution with a valid program and a willingness to accept financial liability in the event of an accident.

Available Reactor Types

Water boiler.—The water boiler (8 to 12) consists of a vessel containing a light water solution of a suitable uranium salt, usually nitrate or sulfate. The enrichment of the uranium made available by the Atomic Energy Commission is nominally 90 per cent U^{235}. The optimum hydrogen-uranium ratio is about 400 to 1, although there seems good reason to go to a higher ratio.

Following Los Alamos design, the vessel is spherical. It is kept nearly full of liquid, so that unusually large changes in density will discharge solution from the sphere into a high-capacity condenser from which the solution will return by gravity after an appropriate delay.

The cooling system consists of a cooling coil immersed in the uranium solution. Light water circulates through this coil. At Los Alamos this is a closed cycle, the heat being dissipated in a cooling tower. At Raleigh an open cycle is used, the water being released to sewer after suitable hold-up.

The choice of anion is difficult. Nitrates are very soluble and are not seriously corrosive to stainless steel. Sulfates are less soluble, subject to peroxide precipitation, and are corrosive in stainless steel. Sulfur has a lower absorption cross-section for thermal neutrons than nitrogen and should therefore be superior in neutron economy. The principal difficulty with nitrates is that they are thermodynamically unstable and subject to serious radiation damage from the heavily-ionizing fission products. Free nitrogen is therefore a by-product. This must be collected or discharged, and replaced by periodic addition of nitric acid.

Water is decomposed by fission fragments at a rate of 0.5 moles/kwhr., so that a mixture of hydrogen and oxygen (containing nitrogen, perhaps, along with water vapor and spray) is continuously emitted. These gases purge volatile fission products from the liquid. The gases must be held below their explosive concentrations and recombined under controlled conditions. Dilution gas must be circulated over the surface of the solution and through de-mister, condensor, catalyst bed, heat exchanger, and circulation pump. Argon, air, and oxygen have been used as sweep gases. At a power level of 35 kw. (SUPO) 0.3 cu.ft./min. of gas is evolved. To assure dilution below the explosive limit ten- to one-hundredfold dilution is indicated. At Los Alamos 4 cu.ft./min. is the circulation rate. Nitrogen gas accumulates so that it must be continuously or intermittently discharged. The system is operated normally at slightly below atmospheric pressure. At Raleigh, North Carolina, because sulfate is used, there is no accumulation of nitrogen.

Increase in temperature reduces the efficiency of the chain reaction, so that a negative temperative coefficient of $2 \times 10^{-4}\, \Delta k/k$ per degree centigrade

is observed. From cold to hot operation requires 1.2 per cent excess reactivity. This has a very strong stabilizing effect.

Under high-power operating conditions, gas bubbles will always be present in the solution. The addition of an increment in reactivity will raise the power and heat the solution, raising the vapor pressure of water in the bubbles and thereby reducing the density of the solution. Again stability is conferred.

A sudden increase in reactivity if small will result in a rapid power and temperature rise with slight increase in bubble size. If the change is appreciable, the solution may reach its boiling point and eject a fraction of the fuel and moderator from the system.

If the critical condition is overestimated, about 1.5 per cent can be absorbed in temperature effect. Additional reactivity may be absorbed in bubble formation. The kinetics of the system will, however, depend upon a relation involving the velocity of sound and the reactor period. The latter depends upon the prompt neutron generation time, which will vary with size, composition, and reflector.

As previously mentioned a large fraction of the fission neutrons escape from the vessel. The vessel is therefore surrounded by a reflector consisting of beryllium, graphite, or other suitable moderators. At Los Alamos the inner layer is beryllium oxide, the outer, graphite. At North Carolina, graphite is used throughout.

Whenever air is exposed to neutrons, argon-41 is generated. This 2 hr. beta-gamma emitter is a serious nuisance around reactor structures. Since commercial graphite has a density of 1.6, whereas the crystal lattice has a density 2.25, it is 40 per cent void (most of which is interconnected) and acts as a radioargon generator. Ventilation is usually provided to maintain the reactor shield and reflector slightly below room pressure so that there is a reliable flow from the experimental area into the reactor shield.

Swimming pool reactor.—The principal operating example of the swimming pool is the Bulk Shielding Facility at Oak Ridge, Tennessee (13 to 17). It is in principle an extremely simple installation, consisting of a large deep tank of water in which a matrix of fuel assemblies is suspended. These elements consist of parallel plates 3×24 in. fabricated from a uranium-aluminum alloy encased in pure aluminum. These plates are brazed into assemblies consisting of from 5 to 10 plates having a roughly square exterior. These fuel assemblies engage a grid so that the final matrix is roughly square and contains from 16 to 25 assemblies. The reactor size is therefore 12 to 15 in. square and 24 in. high.

The water in the swimming pool serves three simultaneous functions: (*a*) moderator, (*b*) coolant, and (*c*) shield. In addition, surrounding water may serve as a reflector. A beryllium or graphite reflector may be substituted if desirable with appreciable reduction in the required fuel.

Natural convection through the fuel plate serves to remove heat generated. A limit to this mode of heat removal seems to be about 100 kw. total

power. For the higher power levels proposed for future reactors a forced circulation system will be required. Present plans involve 1000 kw. dissipation.

The ultimate in flexibility is achieved in this design, since the shape of the fuel matrix can be accommodated to the particular needs of the experiment. Samples can be inserted and removed by long-handled manipulators. As constructed at Oak Ridge, the reactor is supported from a movable bridge so that it can be translated within the tank.

Reactors planned at Michigan and Penn State are directed toward more general research functions than the Bulk Shielding Facility. The tank structure is therefore more elaborate and permits access to the exterior of the tank. To accommodate neutron beams, the tank wall is perforated, and to reduce the beam length, the tank wall is constructed of massive concrete similar to other reactor shields.

Without question this type of reactor is the most flexible reactor available. To balance this flexibility a carefully selected and trained crew is required.

Small excursions of reactivity can be absorbed by temperature rise. The prompt neutron generation time in light water is 6×10^{-5} sec. Neutron multiplication can therefore occur with a time constant short compared to the time for conduction and transfer of heat to coolant. Perhaps 10 msec. is the shortest time constant which may be considered safe. This period in a light water assembly would be equivalent to 1.3 per cent in excess reactivity. 1 to 2 per cent is usually considered the maximum acceptable excess reactivity.

These values are modified by the presence of a reflector of beryllium or carbon, since neutrons escaping to the reflector moderate more slowly and diffuse back to the fuel region. They therefore constitute a group of very short-period delayed neutrons which will appreciably retard the kinetic behavior of the reactor. A 4 per cent reactivity change does not seem excessive.

The effects of radiation upon the water in the lattice are those of decomposition and activation. At full power, bubbles consisting of hydrogen and oxygen as in the case of the water boiler are seen to rise from the swimming pool assemblies. Quantitatively the problem is less severe since only γ-rays and neutrons escape the fuel element, the fission fragments being trapped in the aluminum. Reasonable room ventilation is adequate to disperse these gases at 100 kw. At 1000 kw. a hood may be required over the fuel region, and a strong air stream would carry dissociation products away.

Corrosion products and soluble constituents of the concrete tank as well as impurities in the water will absorb neutrons so that the pool will eventually become radioactive. This activity has not been found to be excessive at the Bulk Shielding Facility.

CP-5.—The new research reactor at Argonne National Laboratory, designated CP-5, is a high-flux (2×10^{13}cm.$^{-2}$sec.$^{-1}$) reactor optimized for low power (1000 kw.) operation and experimental availability (18, 19). This is achieved by using heavy water as a moderator and coolant with swimming

pool type fuel elements. Forced circulation D_2O cooling is used. An array of seventeen fuel assemblies are spaced to permit insertion of control strips between rows in a tank containing seven tons of heavy water. This tank is surrounded by an additional graphite reflector approximately a foot thick.

As a central facility for a National Laboratory, extensive research facilities are incorporated. An installation of this magnitude is beyond the financial ability of most institutions. Extensive design work is required to take care of items which are minor effects in the other two designs. For example, (*a*) heat dissipation in the graphite reflector requires a separate cooling system; (*b*) heat will be generated near the inner face of the shield and must be removed; (*c*) a circulating helium system with recombiner must be installed to avoid possible explosion and loss of heavy water.

Reduction of the operating criteria would materially reduce the investment and considerably simplify the system. The inventory of heavy water would not be appreciably affected, however.

The great advantage to this design is that D_2O is a superior moderator, having good moderating power and extremely small neutron absorption. If minimum uranium and extraneous absorbers are used, neutrons will diffuse for a long time before absorption. The thermal flux will be high for a given power. Epithermal neutron fluxes will however not be significantly improved. Unfortunately flux depression attributable to presence of a sample is extreme for the very reason that little absorber is normally present.

The prompt generation time between creation and absorption of a neutron is estimated to be a millisecond. This is exceedingly long compared to that in light water. Using the previous criterion of a ten millisecond period as the minimum permissible, the reactor can respond to a 10 per cent excursion in reactivity without dangerous consequences.

Selection of Design

The choice of a reactor design will depend upon a number of considerations: available funds, research program, location, safety, etc. Each group evaluates these various features in a different manner and arrives at a different solution. For campus use where available space is limited, safety must be a major consideration. While no simple statement defines these problems, a few generalizations can be made.

Thermal reactors cannot detonate in the manner of a bomb. No consideration need be given to shock wave damage nor to thermal radiation. Only under the most severe test conditions has it been possible to destroy a reactor and to liberate the contained fission products. Hazards from thermal reactors are therefore the release of fission products. Present thinking emphasizes the containment of these fission products in the immediate neighborhood of the reactor, and the protection of nearby people from severe exposure.

The General Electric Company Reactor at West Milton, CP-5, and the Duquesne Light Company power plant near Pittsburgh have established

precedents. Each of these units is located within a hermetically-sealed building so designed as to take any possible pressure change without failure.

Low-leakage buildings are incorporated at Penn State and at Michigan, and will probably become integral features of any urban or campus reactor. In addition, the incorporation of shielding into these buildings is being considered, so that if all contained fission products are uniformly distributed over the interior of the building, persons in the course of normal activities outside the building will not be dangerously exposed during a period of, say, one hour, necessary to rope off the area.

These two extraordinary provisions are gaining acceptance in lieu of the older reactor safeguard formula. This formula has gained general acceptance as a reasonable criterion for isolation of a reactor. It is

$$r = 0.01\sqrt{P}$$

where r=radial distance in miles, and P=average power in kw. For a 1000 kw. reactor this is 0.3 mile or 1700 ft., for a 100 kw. reactor it is 0.1 mile or 530 ft. Responsible workers will feel more comfortable when this formula is met than when it is violated.

The maximum power is therefore an exceedingly important parameter in the selection of a reactor. Research space and extensive facilities will almost inevitably increase the power for a given flux. While well-defined fluxes are significant for given fields of research, some degree of ingenuity is appropriate to minimize the flux and hence the power for a given type of work.

Present experience demonstrates that a flux of 2×10^{12} cm.$^{-2}$sec.$^{-1}$ can be obtained from a water boiler operating at 40 kw., 10^{12} cm.$^{-2}$sec.$^{-1}$ from a swimming pool at 100 kw. using natural circulation, and 10^{13} cm.$^{-2}$sec.$^{-1}$ from a CP-5 at 600 kw. If fluxes of 10^{13} cm.$^{-2}$sec.$^{-1}$ are required, present water boiler designs may not be considered. However, for a flux of 10^{12} cm.$^{-2}$sec.$^{-1}$ the water boiler represents the smallest power output.

An additional advantage of small power output is that it minimizes refueling. Assuming a 50 per cent duty cycle (more than most universities could afford), refueling at 5 per cent burnup would be required once in ten years for the 30 kw. water boiler and 100 kw. swimming pool, but would be required twice a year for CP-5. The investment in equipment necessary for periodic refueling is by no means trivial.

Separate and distinct from the problem of runaway are the problems of normal operation. In simplicity of operation the swimming pool excels. CP-5 with its two cooling systems and recombination system is intermediate, and the water boiler which involves an extremely active recombination system is most troublesome. Parenthetically it may be remarked that in the water boiler it is quite possible to segregate fission products continuously and thereby reduce the hazard of a severe accident.

The development of leaks in the water boiler recombination system is a very real operating problem. It does not, however, represent the type of hazard which would endanger the public. By maintaining reduced pressure

in the system it is possible to detect leaks before fission products are allowed to escape. The reactor may be shut down while these fission products are allowed to decay.

Detection and location of leaking fuel assemblies in the swimming pool and CP-5 are problems requiring consideration. Likewise these do not represent dangerous situations, and means can be devised after failure and detection for their correction.

An additional operating problem is the question of how heavily to load the reactor beyond its critical loading. Experiments almost always increase leakage or introduce poisons, thereby increasing the fuel requirement for steady state operation. Experimental facilities must be so designed that sudden removal of equipment or introduction of moderator such as water, carbon, etc., will not exceed the range of control within which the reactor will automatically compensate. This problem is present in any experimental reactor.

A distinction between the three designs arises when xenon poisoning is considered. In solid fuel reactors excess reactivity must be provided to override the accumulated Xe^{135} after high power operation. The required excess at 10^{12} cm.$^{-2}$sec.$^{-1}$ flux is 0.4 per cent at 10^{13} cm.$^{-2}$sec.$^{-1}$, 2 per cent. In the water boiler, xenon is continuously removed, so that negligible excess reactivity is required for xenon override.

A further distinction arises in connection with flux distribution. The fuel elements for solid fuel reactors are quantized, the last element probably adding about 2 per cent in reactivity. As a fuel load is burned, the control rods must be continuously removed with a resultant continuous variation in the flux distribution. Addition of new elements will markedly change rod positions and flux distributions. In a liquid fuel reactor additional fuel may be added from time to time to compensate for burnup without appreciable effect upon the flux distribution.

In summary at a flux of 10^{12} cm.$^{-2}$sec.$^{-1}$ the water boiler and swimming pool are competitive in cost and performance, the swimming pool being simpler and more flexible, the water boiler representing lower power and greater safety, but being more complicated to operate. At 10^{13} cm.$^{-2}$sec.$^{-1}$ flux the water boiler is presumed to be impractical. The choice between swimming pool and CP-5 will be dictated by the evaluation of versatility, simplicity, safety, and cost. CP-5 will certainly be the more expensive (even excluding the cost of heavy water).

Problems external to the reactor itself involve shielding, ventilation, heat rejection, emergency cooling, and instrumentation. In most cases these are independent of reactor type.

Shielding involves an appreciable fraction of the cost of the installation and requires design evaluation. For small reactor size and large shield thickness the shield cost will vary approximately with the cube of the shield thickness. Neutron beam intensities will vary approximately inversely as the square of the shield thickness. Both considerations as well as building size

encourage the use of high efficiency shielding materials (see "Nuclear Radiation Shielding" by E. P. Blizard, pages 73–98, in this volume).

Ordinary concrete (150 lb./ft.^{3}) would be required in a thickness of about 8 ft. Concrete loaded with Barytes ($BaSO_4$) can be poured with a density of 215 lb./ft.^{3}. Such material was used at North Carolina State College and is being used at Pennsylvania State University. Breazeale, at the latter institution, reports a cost of $180.00 per cubic yard in place. At Argonne National Laboratory, the Bookhaven-type shield consisting of iron punchings, limonite (hydrated ferric oxide), and portland cement was used. A shield thickness of 4.5 ft. has proved more than sufficient. The cost of such a mix will depend largely on the current price of selected scrap iron.

Shielding should be adequate not only for biological reasons but also to minimize instrument background. A well-shielded, carefully-supervised research reactor can have an instrument background as low as twice or at most a few times cosmic-ray background. To accomplish this, careful attention must be given to details of construction to avoid and eliminate thin spots. Constant vigilance must be maintained to control the background contribution of each experiment.

Ventilation of the shield is required to prevent radioargon from entering the experimental area. (Oxygen-19 is another radioactive product of neutron irradiation of air, although its short half life of 29 sec. usually insures decay before release.) The product of flux times air volume is a good measure of radioargon production, since decay is usually negligible. Consequently free-air volumes in the high flux region should be minimized. A thermal column and graphite reflector pose serious problems. In CP-5 the graphite reflector is in a helium atmosphere—another complication. At North Carolina the flux is not sufficiently high to cause great concern. No straightforward solution to this problem exists.

Ventilation air is conventionally discharged from a tall stack. Acceptable A^{41}-concentration for an infinite cloud is 10^{-12} curies per cubic centimeter (10^{-3} μc./l). In these types of reactors the infinite cloud is not always a valid model, since, because of decay, an infinite cloud can never be formed. A comparable finite cloud calculation considers zero wind velocity and an ever expanding sphere of gas corrected for argon decay and abrorption. At a discharge rate of 10,000 cu. ft./min. there is a tenfold error in assuming the infinite cloud case. Other radio isotopes produced by bombarding air such as A^{37}, O^{19}, O^{15}, N^{13}, C^{14} are found to be no significant problem in comparison to the A^{41} problem.

Several thousand cubic feet per minute are usually required to assure negative pressure within the shield under most severe conditions of open experimental ports. With this quantity of air it is sometimes possible to remove heat generated from γ-ray absorption in the reactor structure. The conversion of a building with appreciable air flow to a hermetically sealed building must be assured in the case of an accident and must be completely automatic. This can be accomplished by a trigger mechanism actuated by a radiation meter within the building.

The rejection of heat is usually accomplished by a stream of water. In the swimming pool this only need be a cooling coil immersed in the pool. At North Carolina an open circuit is used involving once-through circulation of tap water through a hold-up and monitoring system to drain. A positive device must prevent back siphoning.

Closed cycles are probably preferable since they eliminate one means of losing control over active materials. Heat can be transferred from the primary system, passing through the reactor, to a secondary system which can be cooled in a spray tower. If large amounts of air are required to dilute radioargon, there is no reason why heat should not be directly transferred to this air stream through finned exchangers. A high temperature stack discharge will assist in diluting the effluent.

After sudden termination of the chain reaction, heat continues to be generated from the decay of fission products and from fission resulting from delayed neutrons. The power output will fall within a few seconds to 10 per cent of the operating power. After 10 min. it will fall to 3 per cent and thereafter diminish roughly as t^{-1}. The heat capacity of most reactors will take care of the first few minutes, but a small cooling stream must be continued for a long period. An extremely reliable source of energy must be provided which is not subject to interruption under extreme conditions. Gravity flow from a head tank is often used.

Control systems can become excessively elaborate but cannot be simplified beyond a certain point. Reactor shutdown must be certain under any combination of circumstances. For this reason systems are duplicated to achieve statistical independence. More than one type is usually required, operating by as diverse principles as possible. Numerous sensing elements are connected to what is called the "scram" circuit any one of which can shut the reactor down. A minimum set of signals might be these:

Neutron flux (by two or three different elements)
Gamma flux
Power failure
Fuel or Moderator temperature
Coolant temperature rise
Structural temperatures
Ventilating air activity
Cooling water activity
Room air activity
Coolant flow
Ventilating air flow
Reactivity (reactor period)
Seismograph

Other signals are required for particular types. For the water boiler measurements might include solution level, catalyst temperature, purge air flow, hydrogen gas concentration. For the swimming pool, they might be water level, water activity, motion of bridge. For CP-5 they might be helium pressure, catalyst temperature, etc. The circuits used must be of the fail-safe variety under any foreseeable set of conditions.

Conditions during reactor start-up are usually considered to be most critical, since most reactors when in steady state operation show remarkable ability to respond to changes of operating conditions. Start-up, however is a different matter. The power level sometimes changes by a factor of 10^8 to 10^9 and must be controlled when it approaches operating levels. Reduction of the range of power to 10^6 to 10^7 can sometimes be accomplished by incorporating permanent neutron sources in the reactor structure. A reactor using heavy water moderator has an abundant supply of photoneutrons, so start-up is a problem only at initial operation or after replacing fuel.

Instruments are now available with ranges up to 10^8 and are eminently appropriate for start-up. The most satisfactory instrument so far developed is the period meter. This indicates the reactor period independently of power level. This is accomplished by differentiating the log of an ionization current.

Two schools of reactor start-up seem to exist. One relies heavily upon instruments to bring the reactor to criticality. Under these conditions the reactor can be brought into operation in 5 to 10 min. The other school relies more heavily upon the operator and provides mechanical limits on the rate of addition of reactivity. Following this procedure usually involves half an hour and sometimes more to establish the chain reaction.

Design Evaluation

After the design is well developed, in the United States it is necessary to prepare a report for review by the Atomic Energy Commission Advisory Committee on Reactor Safeguards.

In* the terms of the Atomic Energy Act of 1946, the responsibility for safety of reactors lies with the Atomic Energy Commission. The Advisory Committee on Reactor Safeguards is a committee of the Commission, and we report to the General Manager, giving him our opinion as to the hazards and problems of reactors and all nuclear assemblies, except weapons. The general manager or his appropriate deputy takes whatever action he deems desirable, taking into consideration the advice which our committee has given.

Please note that this committee is advisory. We have no power to initiate any design. We have no power to change any design, nor to approve or disapprove the operation of a reactor. We advise the general manager or his deputy.

As a matter of practical operation, the committee is asking that all proposals be brought to its attention just as soon as the problems and the probable hazards connected with this reactor can be forseen and the concept of the reactor which is desired can be reduced to a few sketches, diagrams, and notes. At the time this preliminary information is brought to the attention of the committee, an attempt is made to list all of the problems which can be foreseen which must be settled and data which must be obtained before any valid evaluation of the hazards can be made.

Finally, a formal hazards summary report is submitted to the committee for its final judgment and recommendations. If we have done this job properly, when the hearing and study and consideration of this hazards summary report is made, there will be no major problems left to be solved. This is because, we hope, we have agreed

* C. R. McCullough, February 17, 1953 P. 24 AECU 2900 (see 6).

what the problems are in our preliminary meeting; and you go back and work out the answers to these questions so that when we come together at our final meeting, there is already a basis of agreement.

Items to be covered are given under item 04 *Hazard Summary Report* of Chapter 8401 *Reactor Safety Determination* of the A. E. C. Manual.

a. The Reactor and Its Operation:

1. Description of the reactor, including associated facilities, and of the proposed site.

2. Detailed plan of normal operation.

3. Plan for control of the experiments which will be performed in the reactor, including the limitations which will be placed on the experiments.

4. The normal schedule of chemical processing and disposal of reactor products.

5. The normal methods of disposal of radioactive or poisonous effluents—gases, liquids and solids.

6. Description of safety mechanisms of the reactor.

7. For mobile power plant application, a detailed analysis of the compatibility of the reactor design, operating, and safety characteristics with established specifications for power systems falling within the category of the intended reactor use.

b. Hazards:

1. An enumeration of all potentially hazardous features, including the effects of fire in or near the facility housing the reactor.

2. Experimental information, calculations, assumptions, etc., used in evaluating hazards enumerated.

3. Steps taken to minimize risk.

4. Extent of release of radioactive material and damage to be expected, if failure should occur.

c. Hazard to Surrounding Area in the Event of Failure and in Normal Operation:

1. Meteorological data relating to the possible atmospheric dissemination of radioactive material and possible extent of hazards to population and industries in the event of failure. Methods proposed for the control of stack gases and the possibilities of the correlation of reactor operation with meteorological conditions.

2. Hydrological data on the area, the expected drainage of liquids in the case of a major accident, and the distribution of activities in the drainage system under such conditions.

3. Data on local earthquakes, including their intensities and nature of damage which could occur in the event of earthquakes of various intensities.

d. Make-up of Surrounding Area:

1. Distribution of population within possible hazard radius of the proposed location.

2. List of vital industrial, national defense, and public service installations within possible hazard radius of the proposed location.

Reactor Construction

In the United States a construction license must be negotiated with the Atomic Energy Commission defining the project restrictions and arrangements under the Atomic Energy Act of 1954.

The manner in which research projects are often carried out at universities is for the university to function as the architect-engineer. Under this

scheme the members of the engineering school or maintenance department supervise design, the maintenance department then places numerous contracts for excavation, building construction, and the installation of various equipment. The reactor and instruments are fabricated in shops and installed by members of the academic and service staffs. Initial tests and operation are in the hands of the academic staff. North Carolina and Penn State have been carrying out their projects in this manner.

During the past year there has been widespread industrial interest in the field, and it is possible to obtain specific industrial contracts for any part or all of a reactor project. The University of Michigan is carrying out its project by retaining an engineering firm to prepare complete plans. These were then issued for lump sum construction bids. At bid opening there were 34 bidders, many of whom submitted bids on the project as engineered but also submitted alternate designs. The University of Utah submitted general specifications to several concerns and requested lump sum bids upon a design to be specified.

Under present circumstances it is certainly quicker and probably cheaper to contract design and construction rather than to retain the functions of architect-engineer. During construction, well-defined arrangements should be in effect concerning inspection. This will differ from contract to contract. An outside inspector can be retained, a university representative can be used or the prime contractor can be given the inspection function. Under present circumstances there is little likelihood of voluntary introduction of defective materials.

Certain of the items have functions completely outside the understanding of normal industry. The shield, for instance, is a massive concrete structure and any construction man knows it will not fall down. Insisting that there be no voids or faults running any appreciable distance from inside to outside is quite unintelligible and is likely to be misunderstood. Use of a radium source and counter during concrete placement can often save extensive correction at a later date.

Construction men usually take the attitude that if it isn't right the first time it can always be changed. It is usually extremely hard to convince them of the consequences of alterations or failures after initial reactor operation.

Initial Operation

Upon completing construction in the United States a final Atomic Energy Commission review will be made of the structure, design changes, changes in proposed methods of operation, and facilities for fuel accountability, health-safety, and security. The construction license will presumably be converted to special materials and utilization facility operating licenses. Unless the reactor has an operating prototype of which it is a direct copy, special tests may be required at an Atomic Energy Commission site or possibly in the proposed installation. Fuel would then be made available and the reactor will be ready to operate.

No requirements are known concerning the presence of experienced personnel during start-up. A proposal to start up a new reactor in a populated area without the supervision of an experienced person would have doubtful merit.

In any event it is generally considered desirable to itemize in advance and in detail the sequence of start-up operations. Such a document is valuable in anticipating equipment needs and in showing flaws in the order of events or inadequate data to enable a rapid evaluation of unexpected results. Independent review of the proposed procedures is an invaluable method of informing the crew in advance and in obtaining perspective.

The following operations are generally a reasonable way of proceeding:

I. Testing of complete system without fuel
   a. for leaks
   b. for instrument response, polarity, etc.
   c. safety circuits, all shut down signals
II. Cautious loading of fuel with periodic measurement of multiplication of artificial source
   a. observe steady state neutron density
   b. observe transient on removing source
   c. predict criticality by independent extrapolations
III. Prepare reactor as though to operate at full power
   a. close shielding
   b. check level setting of safety circuits
IV. Establish criticality at nominal power
V. Obtain two or three independent calibrations of power indicator
   a. foil calibration
   b. ion chamber comparison to known source, neutrons and gammas
   c. fission counter or chamber
VI. Check safety systems by reactor operation
VII. Calibrate control system
VIII. Measure reactivity change with temperature, pressure etc.
IX. Measure reactivity effects of various experimental arrangements, reflector position etc.
X. Simulate various emergencies to check predictions
XI. Check out cooling system at low power
XII. Raise power in stages repeating above as necessary
XIII. Establish operating power and repeat all calibrations
XIV. Review power operating procedures to confirm their pertinence
XV. Train operating crew for routine operations.

While this list appears formidable, it can be carried out in an unexpectedly short time.

The greatest danger is that self-applied pressure will accelerate the pace to a dangerous degree. The crew must therefore be carefully watched to prevent undue fatigue. Under such conditions data are often taken more rapidly than they can be organized and interpreted. This is highly undesirable. At each stage data should be reviewed and completely understood before proceeding to the next stage.

The safe period of reactor operation is now over and the reactor is ready for routine operation. It must be remembered that accidents have never occurred with an inexperienced crew operating a new and uncalibrated reactor. The real dangers in reactor operation come when the operation is routine, the response of the reactor is familiar, and everything is under control. In a university environment, particularly, there is a tendency to avoid the routine and take short cuts, and it is this virtue of the research scientist, making him outstanding in his field, which can constitute a significant and real danger to the installation.

Probably the most effective accident preventive is to be found in a sound and well-conceived operating organization which carries real responsibility and authority.

LITERATURE CITED

GENERAL

1. Goodman, C., Ed., *Science and Engineering of Nuclear Power* (Addison-Wesley Press, Cambridge, Mass., 2 vols., 820 pp., 1947)
2. Murray, R. L., *Introduction to Nuclear Engineering* (Prentice-Hall Inc., New York, N. Y., 418 pp., 1954)
3. Stephenson, R., *Introduction to Nuclear Engineering* (McGraw-Hill Book Co., New York, N. Y., 387 pp., 1954)
4. Glasstone, S., and Edlund, M. C., *Elements of Nuclear Reactor Theory* (D. Van Nostrand Co., New York, N. Y., 416 pp., 1952)
5. Hughes, D. J., *Pile Neutron Research* (Addison-Wesley Publishing Co., Cambridge, Mass., 386 pp., 1953)
6. Grigorieff, W. W., Ed., *Proceedings University Research Reactor Conference, AECU-2900*, (Tech. Information Service, Atomic Energy Commission, Oak Ridge, Tenn. 221 pp., 1954)
7. Benedict, M., *Nuclear Reactors for Research* (Massachusetts Institute of Technology, Cambridge, Mass., 34 pp., 1954)

WATER BOILER

8. "An Enriched Homogeneous Nuclear Reactor," *Rev. Sci. Instr.* **22**, 489 (1951)
9. Beck, C. K., *Nucleonics*, **8**, 5 (Dec., 1950)
10. Murray, R. L., *Nucleonics*, **10**, 52 (Dec., 1952)
11. Busey, H. M., *Nucleonics*, **12**, 9 (May, 1954)
12. King, L. D. P., *Nucleonics*, **11**, 25 (Sept., 1953)

SWIMMING POOL

13. Breazeale, W. M., *Chem. Eng. Progr.*, **50** (12), 6 (1954)
14. Breazeale, W. M., *Nucleonics*, **10**, 56 (Nov., 1952)
15. Breazeale, W. M., *Nucleonics*, **12**, 73 (Feb., 1954)
16. Widdoes, L. C., *Chem. Eng. Progr.*, **50**, (11) 213 (1954)
17. Richardson, L. A. and Gillan, G. K., *Eng. News-Record*, **154**, 47, 48 (April 7, 1955)

CP-5

18. Untermeyer, S., *Nucleonics*, **12**, No. 1, 12 (Jan., 1954)
19. Weills, J. T., *Chem. Eng. Progr.*, **50** (I) 213 (1954)

INDUSTRIAL APPLICATIONS (MASS SPECTROMETRY)[1]

By Clifford E. Berry and J. K. Walker
Consolidated Engineering Corporation, Pasadena, California

Introduction

Historically, the earliest applications of mass spectrometry were naturally involved with the study of the properties of matter per se, and this field, which we may term the scientific field, continues at a high level of activity. In the early 1940's, however, applications of an industrial or technical nature were developed, in which the investigator was concerned with deducing the composition of a particular sample from its mass spectrum. Because of the rapidity and specificity of mass spectrometric methods, these technical applications have come to be widely used and accepted in many industries; this is true in particular in the petroleum and chemical industries.

At the present time, many hundreds of instruments are in use in such applications throughout the world. A variety of types of instruments are commercially available, both in this country and abroad, and, in addition, many workers have constructed their own instruments to satisfy special requirements.

In this paper we shall attempt to summarize recent advances in the art and to point out some of the current problems. The subject matter naturally divides into the following categories: (*a*) high-molecular weight mass spectrometry; (*b*) process monitoring; (*c*) mass spectrometry of solids; (*d*) automatic reduction of spectral data. In general, the references include only work reported since 1952, although in a few instances of historical importance earlier work is cited.

High Molecular Weight Mass Spectrometry

The first major application of industrial mass spectrometry was in the analysis of mixtures of light hydrocarbons, for which relatively pure calibrating materials were available or easily prepared, and for which interpretation of spectra was simple. There has been a continuing effort by numerous workers in the field to extend the molecular weight range, until at the present time hydrocarbon type analyses of materials in the gasoline, kerosene, and light gas oil boiling ranges have become standard (1 to 4). These procedures will not be discussed here; rather, we will consider the recent extension of these techniques to the heavy gas oil, lubricating oil, and wax ranges, and to materials other than hydrocarbons.

Before proceeding to the detailed discussion, it should be pointed out that

[1] The survey of literature pertaining to this review was concluded in January, 1955.

the main difficulties at present associated with high molecular weight mass spectrometry are not instrumental (except for some problems of stability) but rather are primarily concerned with the lack of pure calibrating materials and with the difficulties of interpretation of spectra.

In the present state of the art, it is not possible to analyze for individual compounds in complex mixtures of heavy materials, and because of the astronomical number of possible isomers this may never be realized except in very limited cases. Thus, the investigator must resort to analysis by compound type, and must utilize chemical or physical separation of groups of components of a mixture in combination with mass spectrometry to obtain useful information. The mass spectrometer, nonetheless, offers a powerful tool for determining the distribution of hydrocarbons in such complex mixtures not only according to mass but also by nuclear structural types.

Qualitative analysis of heavy gas oil.—Composition of the heavy gas oil range of petroleum still remains a challenge in the oil industry. A combined chromatographic, ultraviolet absorption and mass spectrometric technique, reported by Lumpkin & Johnson (5), has been developed for the identification and qualitative analysis of compound types, using the method of structural correlation of mass spectra previously reported by Kinney & Cook (6). Briefly, this method consists of a systematic correlation of nuclear spectral ions. It is found that unusually abundant ions are formed for the predominant nucleus plus a finite number of substituted groups, e.g, in substituted aromatic compounds the nucleus is represented by the benzene ring $C_6H_5^+$, where the substitutions are $n(CH_2)$, and where n is equal to 1, 2, or 3.

Numerous polynuclear or condensed ring compounds can be positively identified and their distribution qualitatively determined. The hydrocarbon nuclei consist primarily of the type C_nH_{2n-a}, where a is an even number. Similarly, several substituted thiophene and condensed aromatic-thiophene type compounds can be identified in the heavy gas oil.

Information such as this is extremely valuable to the refining industry, where the problem of sulfur removal determines in many cases what products can be produced. If the general structure, quantity, and weight distribution is known, refining procedures can be used to reduce the sulfur to hydrogen sulfide gas for subsequent removal.

Lubricating oil type analyses.—Applying the principles used in gasoline type analyses, Clerc *et al.* (7) found that the hydrocarbons in lubricating oils could be classified as alkanes, noncondensed cyclopentanes, noncondensed cyclohexanes, condensed cycloalkanes, monoaromatics, and naphthalenes. In order to perform this quantitative analysis it is necessary to identify only a relatively small number of discrete mass numbers. Certain mass groups are selected so that the fragment ions in the mass spectra are the same for any one type regardless of the number of carbon atoms or of the number of rings in the molecular structure. The alkanes include all molecules of the structure C_nH_{2n+2}. The noncondensed cycloalkanes classify the following groups as one:

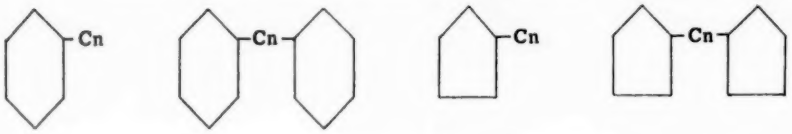

Cyclohexanes Cyclopentanes

The condensed cycloalkanes include all molecules with two carbon atoms common to two or more ring structures:

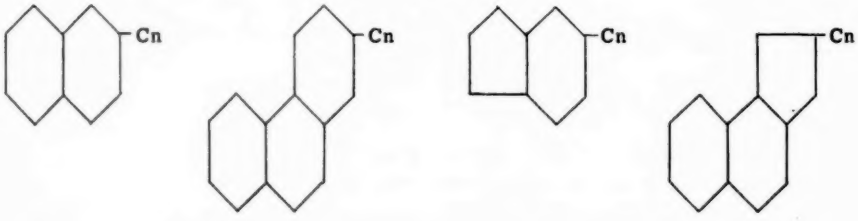

The monoaromatics and naphthalenes are distinguished from these groupings by the following characteristic molecular types:

monoaromatics	*naphthalenes*
C_nH_{2n-6}	C_nH_{2n-12}
C_nH_{2n-7}	C_nH_{2n-12}
C_nH_{2n-8}	
C_nH_{2n-9}	

Quantitative analyses are made on these lubricating oils by comparing the sum of the various nuclear ions to the total ionization of the sample in the C_4 to C_{11} region. This procedure eliminates the need for accurate sample metering and normalizes slight operating variables in the mass spectrometer. The assumption is made that all hydrocarbons produce equal ion intensities in the region of C_4 to C_{11}, which is not the case for individual pure hydrocarbons but holds for narrow boiling petroleum fractions of any one type. The characteristic mass groupings used in the type analysis of lubricating oils are shown in Table I.

A calibration matrix based on an average of 29 alkanes, 4 noncondensed cyclopentanes, 12 noncondensed cyclohexanes, 17 condensed cycloalkanes, 5 monoaromatic concentrates, and 2 naphthalene concentrates is given in Table II. The calibration coefficients are tabulated as a percentage of the total C_4 to C_{11} ion intensity. With few exceptions, the accuracy of the determination is ± 10 per cent in the high concentration range. Checks made on pure hydrocarbons show similar agreement with the exception of the isomers containing highly branched aliphatic substitution on the ring structures. Olefins determined by this procedure are grouped with the noncondensed cycloalkanes.

TABLE I

IONS CHARACTERISTIC OF LUBRICATING OIL HYDROCARBONS*

Type	Mass Numbers Summed
Alkanes	70, 71, 84, 85, 99, 113
Noncondensed Cyclopentanes	69, 83, 97, 111, 125, 139
Noncondensed Cyclohexanes	83, 97, 111, 125, 139, 153
Condensed Cycloalkanes	67, 81, 95, 109, 121, 122, 123, 135, 136, 137, 149, 150, 151
Monoaromatics	77, 78, 90, 91, 92, 104, 105, 106, 117, 118, 119, 129, 130, 131, 132, 133, 143, 144, 145, 146
Naphthalenes	128, 141, 142, 155, 156

* From Clerc *et al.* (7).

Synthetic blends of the various hydrocarbons in the lubricating oil and wax range, analyzed before and after dewaxing and urea extraction, are tabulated in Tables III and IV.

Hydrocarbon type analysis of waxes.—In addition to the spectral correlations for hydrocarbon type analyses, O'Neal (8) has described a technique for determining the distribution of structural types by carbon number. In the case of wax, the isoalkanes may be differentiated from the normal alkanes and cycloalkanes. The normal alkanes exhibit sizeable molecular ions (C_nH_{2n+2}), but contribute only a few ions of the C_nH_{2n+1} and C_nH_{2n} type. The isoalkanes on the other hand, make essentially no contribution to the C_nH_{2n+2} spectral peaks, but display relatively large C_nH_{2n-1} and C_nH_{2n} peaks. This effect is shown graphically in Figure 1 and illustrates the po-

TABLE II

CALIBRATION MATRIX*

Mass Numbers†	Alkanes	Noncondensed Cycloalkanes		Condensed Cycloalkanes	Monoaromatics	Naphthalenes
		Cyclopentanes	Cyclohexanes			
70	*35.8*	14.4	9.3	2.7	5.1	3.6
69–139	9.7	*33.4*	35.0	9.4	10.1	8.4
83–153	5.9	21.7	*30.0*	5.5	5.5	6.1
67	1.2	5.2	7.3	*50.6*	7.1	5.1
77	0.1	0.3	0.4	3.2	*40.7*	4.7
128	1.7	0.4	0.2	0.1	2.8	*41.2*
C_6–C_{11}	100	100	100	100	100	100

* From Clerc *et al.* (7).

† The actual mass numbers summed are those listed in Table I.

TABLE III

HYDROCARBON TYPE ANALYSIS OF LUBRICATING OIL RAFFINATE*

Hydrocarbon Type	Wax-Oil Composition (%)		Dewaxed Oil (%)	Wax (%)
	Expt.	Calc.		
Alkanes	37	37	10	27
Noncondensed Cycloalkanes	40	40	33	7
Condensed Cycloalkanes	21	22	21	1
Monoaromatics	2	1	1	0
	100	100	65	35

* From Clerc *et al.* (7).

tential for determining both of these types, as well as the cycloalkanes, for each molecular carbon number. An example of the distribution of these hydrocarbon types found in a petroleum wax is shown in Figure 2 where the concentrations of the various types are plotted against carbon number of the hydrocarbon molecules. The relative accuracy of determination of the normal alkanes in the molecular weight range of the paraffinic waxes is shown in Figure 3. A synthetic blend of the normal alkanes is plotted and compared to the mass spectrometer determination; an agreement of approximately 1 per cent is found throughout the molecular weight range.

Of primary concern in the development of hydrocarbon type analyses of this kind is the possibility of utilizing waste products and products of low demand which are prevalent as by-products in a modern refinery. At the present time gasoline and lubricating oils are the desired marketable products; a knowledge of the molecular structure of the waste products often

TABLE IV

HYDROCARBON TYPE ANALYSIS UREA EXTRACTION PRODUCTS OF A PARAFFIN WAX*

Hydrocarbon Type	Charge		Products	
	Expt.	Calc.	Reactive	Un-Reactive
	(%)	(%)	(%)	(%)
Alkanes	87	88	85	3
Noncondensed Cycloalkanes	13	12	5	7
Condensed Cycloalkanes	0	0	0	0.3
Monoaromatics	0	0	0	0.1
	100	100	90	10

* From Clerc *et al.* (7).

sheds some light on the means by which they can be upgraded. It is not difficult to conceive of the time when this type of analysis can be used to schedule the complete operation of a refinery on the basis of a few simple analyses performed on the original crude oil.

Organic chemical analyses.—Development of high-temperature inlet systems in mass spectrometry has overcome the limitations of low sample vapor pressure in organic chemical analyses; the one remaining limitation in this field is that of chemical stability at elevated temperatures. McLafferty (9) has reported on a number of applications of high temperature mass spectrometry, particularly in the field of aromatic chemicals. In the course of his work he has accumulated spectra for 1800 compounds in the following general groups: (*a*) halogenated hydrocarbons, (*b*) polyhydric alcohols and amines, (*c*) substituted organic acids, (*d*) metallic halides, (*e*) metallo-organic compounds, (*f*) siloxanes, (*g*) organo-phosphorous chemicals, and (*h*) alkaloids.

Process Monitoring

The most important industrial use of the mass spectrometer is as a laboratory tool to which are brought individual samples for analysis. There is, however, growing interest in another mode of operation, in which a sample is piped to the instrument for continuous analysis. Such operation is obviously desirable in many applications, e.g., in studying pilot plant operation where rapid changes must be followed. In addition, it opens the way for automatic control of a process by end-point analysis, in contrast to the present widely-used control of the process parameters.

Instruments designed for industrial use in continuous analysis differ from laboratory instruments in certain respects; in particular, (*a*) there must be a means for obtaining continuously a representative sample from high-pressure, high-temperature streams, (*b*) the instrument must be small, in-

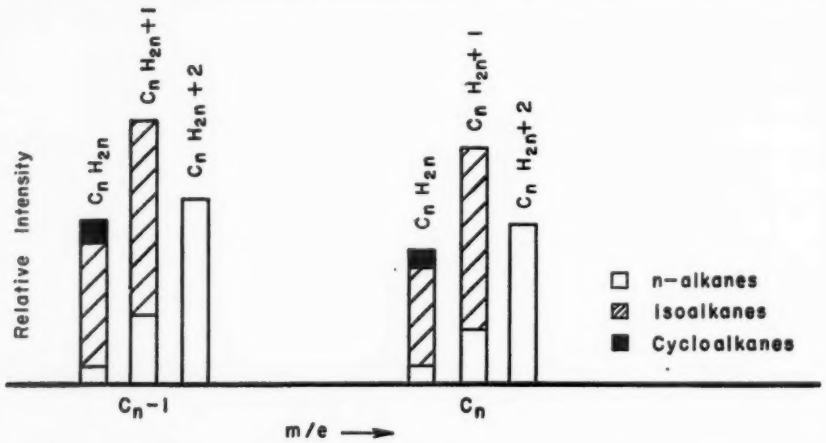

FIG. 1. Relationship of hydrocarbon type to specific mass [O'Neal (8)].

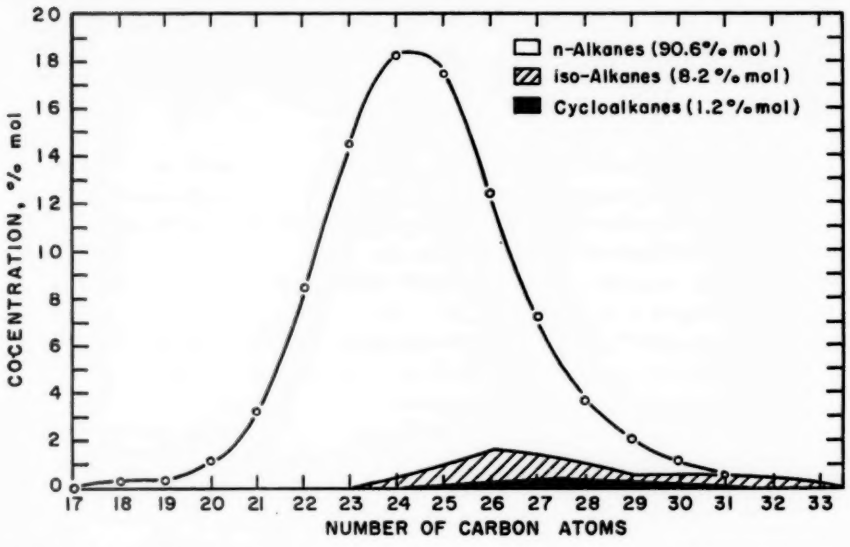

FIG. 2. Composition of a paraffin wax from mass spectrometer analysis [O'Neal (8)].

expensive, and reliable, and (*c*), for many applications, the instrument must be enclosed in an explosion-proof housing.

Of these requirements, (*a*) has been satisfactorily solved (10), the items listed under (*b*) are relative and are in some respects matters of opinion, and (*c*) has not been accomplished but appears to be mainly a matter for good engineering design. Notwithstanding the considerable efforts now being

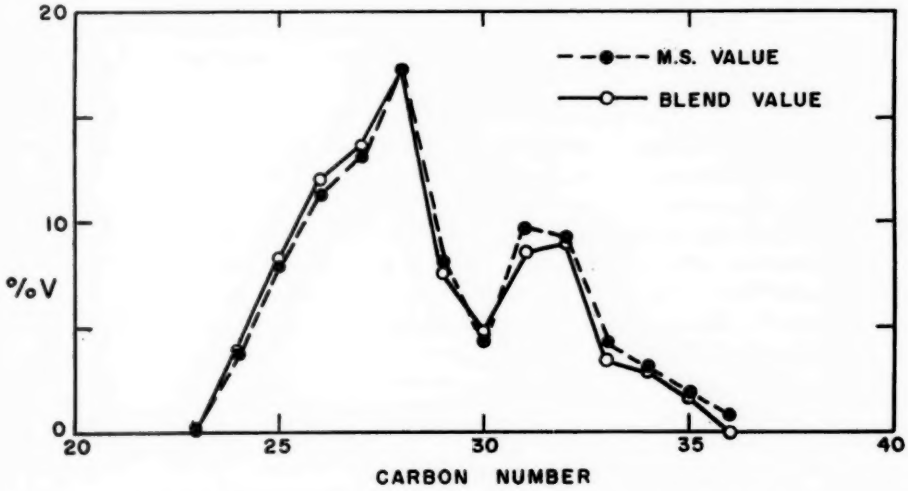

FIG. 3. Mass spectrometer analysis of a synthetic wax [O'Neal (8)].

expended in this field, it is only fair to state that actual installations of equipment are few and are largely of an exploratory nature.

In this section we will consider first some of the instrumentation aspects and, second, some typical applications.

Instrumentation.—The first mass spectrometers used for process monitoring on a continuous basis were those developed by Nier *et al.* (11) for use during the war in the separation of uranium isotopes at the gaseous diffusion plants. These instruments were used to monitor certain constituents of the process stream in order to maintain purity. The instruments utilized conventional 60° magnetic sector analyzers with a radius of 3 in., and with a resolving power of about 70.

Robinson *et al.* (10), in 1950, described an experimental instrument for use in refinery pilot plant studies. This utilized a 160° magnetic analyzer with a $2\frac{1}{2}$ in. radius, having a resolving power of 70. The instrument was housed in a vapor-tight (not explosion-proof) housing, and contained many automatic features, such as periodic standardization by a reference sample. Two of these instruments were built for use in exploring the possibilities of continuous process monitoring; their use has been described by Lanneau (12).

Next, several smaller experimental instruments were constructed in collaboration between Consolidated Engineering Corporation and Esso Laboratories, by modifying commercial mass spectrometer leak detectors for higher resolving power (about 20) and for semi-automatic operation. The results of work with these instruments have also been reported by Lanneau (12).

Following this early work, a number of instrument developments have been reported since 1952, all of which are aimed primarily at the problem of satisfying the requirements set forth above for process monitoring. In practically all cases, these developments involve exploitation of various new ideas for mass separation as contrasted with the classical single-focusing magnetic analyzer.

Jernakoff (13), Morgan *et al.* (14), and Lanneau *et al.* (15) in a series of papers, have described an instrument based on the "ion resonance" (Omegatron) principle, which employs a radiofrequency electric field at right angles to a fixed magnetic field. Ions having a cyclotron resonance frequency equal to the frequency of the applied electric field gain energy continuously and spiral out to a collector. All other ions fail to gain sufficient energy and are not collected. While this device has potentially high efficiency, since it requires no slits or baffles limiting collection of desired ions, it has also a fundamental limitation in that the ionizing and analyzing regions are inseparable. Therefore, an extremely low background pressure is required in order to ensure a sufficiently high sample-to-background ratio. With this device, resolving power of the order of 90 has been reported (14).

Wilson & Gifford (16) have reported the development of a 180° magnetic analyzer having a radius of only 2 cm. and a resolving power of 20. Aside

from its small size the instrument is of fairly conventional nature. Walker *et al.* (17) have reported the performance of this instrument.

Wherry & Kerasek (18) have described an instrument based on the radiofrequency mass spectrometer first developed by Bennett (19). In this device which requires no magnetic field, ions are injected at the end of a tube containing a series of transverse grids. By applying a radiofrequency voltage to certain of the grids and properly proportioning static electric fields, ions of a selected mass can be made to gain more energy in traversing the tube than ions of any other mass. The use of a potential barrier in front of the collector then selects the desired ions.

Although numerous papers on this type of mass spectrometer appeared prior to that of Wherry & Kerasek, Wherry's instrument is apparently the first in which adequate resolving power (of the order of 100) together with both satisfactory intensity and analytical accuracy were achieved.

Another radiofrequency nonmagnetic analyzer, related to the one just described, was reported by Donner (20). This is based on the linear accelerator, but is operated in reverse—that is, as a decelerator. Ions are shot through a series of grids, the spacing of which becomes progressively smaller. Alternate grids are connected together, and between the two sets thus formed a radiofrequency potential is applied. Ions of the correct mass lose a maximum of energy as compared with either heavier or lighter ions, and are separated at the end by a parallel plate electrostatic analyzer. The resolving power of this device is of the order of 100.

McLaren & Wiley (21) have described a linear time-of-flight mass spectrometer, based on the early work of Stephens (22), in which short pulses of ions are shot into a drift tube at a radiofrequency repetition rate. Since all ions have the same energy, their velocities vary inversely as the square root of the mass, so that resolution in time and space occurs as the pulses traverse the drift tube. The sequence of separated pulses is collected and observed on a cathode-ray oscillograph, which gives a continuous display of the spectrum or any portion thereof. Resolving power of the order of 100 has been reported.

Robinson & Hall (23) have reported the development of a small mass spectrometer utilizing the perfect-focusing properties of crossed electric and magnetic fields (cycloidal analyzer), which is based on the early work of Bleakney & Hipple (24). In this device, ions are injected into the region of crossed fields through a slit and, after traversing one complete loop of a cycloid, are brought to a focus at a point which depends only on their mass, and which is independent of their initial direction or velocity. Using an analyzer with a focal distance of 1.1 in., a resolving power of 150 has been obtained.

Several of the devices just described have become available commercially (14, 16, 23), and it is anticipated that others of the group may become available in the future. It is plain that a wide range of techniques is being applied in devising means for separating ions; however, at the present time

there appears to be no clear advantage of one approach over the others. Moreover, in the opinion of the writers, the cost and complexity of a mass spectrometer appear to be fairly independent of the form of mass separation used, but rather to depend mainly on the overall specifications of the instrument, e.g., mass range, recording speed, flexibility, etc.

Applications.—Various types of instruments other than mass spectrometers are currently being applied to the continuous measurement of certain properties of process streams. Among these instruments are nondispersive infrared analyzers, ultraviolet analyzers, refractometers, thermal conductivity analyzers, and others. In general, most of these devices are nonspecific, and often implicit in their use is the assumption that the composition of the mixture being analyzed is virtually constant except for the component of interest. In a great many cases this is sufficiently true, and devices of this sort, because of their simplicity, are naturally chosen.

On the other hand, many problems exist where several constituents of a process stream must be monitored, or where several constituents may change as well as the ones of interest. In these cases the mass spectrometer, because of its specificity and flexibility, is the only presently available tool.

The overall requirements for mass spectrometers for such applications have been given earlier. In addition to these general requirements, the instruments require certain features such as automatic programming to permit cyclic recording of only those mass numbers in the spectrum which are of interest in a particular problem, and automatic sample switching to permit several process streams to be cyclically recorded on the same instrument. It is also likely that in the future simple analog computers will be required for some problems, in order to present the spectral information in the most useful form.

Typical applications reported in the petroleum, petrochemical, and chemical fields, are: (*a*) monitoring the ethane content of a "de-ethanizer" column (10); (*b*) monitoring the complete composition of hydrocarbon gas streams from reforming pilot units and fluid cracking units (12); (*c*) monitoring the C_5-content of the overhead stream from a butane stabilizer column (12); (*d*) as a key-constituent monitor for light gas streams from ethylene recovery plants (12); (*e*) monitoring feed stock, intermediate stream compositions, and final product purity in a Wulff-process plant for producing high-purity acetylene or ethylene or both from natural gas (17); (*f*) monitoring an argon stream for trace quantities of O_2 and N_2;[2] (*g*) monitoring an ethylene stream for trace quantities of O_2;[2] (*h*) monitoring the purity of ethylene oxide;[2] and (*i*), continuously measuring the composition of the atmosphere in vacuum furnaces, particularly in the vacuum refining of titanium.[2]

Besides these truly industrial applications, a number of applications have been reported where the ability of this type of instrument to follow

[2] These particular applications are known to the writers through private communications; no publications exist as yet.

dynamic chemical processes has been of importance. These include such problems as study of metabolic gas exchange in growing plants (25), measurement of certain properties of human respiratory systems (26), and study of automotive combustion gases (27). It is to be expected that advances in instrumentation techniques will permit many more such diverse applications in the future.

Analysis of Solids

Mass spectrometer ion sources capable of producing ions from solid materials have been known for many years. Although numerous ionizing processes have been employed, probably the most important are these: (*a*) vaporization of a sample through heating, following by electron bombardment of the vapors; (*b*) direct emission of ions from a heated filament coated with the compound to be analyzed; and (*c*) generation of ions in a spark discharge drawn between a sample electrode and another electrode, or between two electrodes of the sample.

All of these techniques have been used (and are being used) for scientific studies, particularly in applications concerned with the accurate measurement of isotopic weights and abundances. Unfortunately, no commercially available instruments have appeared; this is mainly because of the uncertain state of the art, insofar as ionizing solid samples is concerned, when compared with the simplicity and versatility of the ion sources used for analyzing samples of materials which can be vaporized at room temperature or at slightly elevated temperatures.

The difficulties inherent in the various methods of ionizing solid samples may be simply stated. In method (*a*) (vaporization and electron bombardment) different constituents of the sample evaporate at different rates, so that in principle it is necessary to evaporate the entire sample, and to integrate the abundance of each ion species in time, in order to arrive at the sample composition. In method (*b*) (direct emission of ions) the efficiency of ionization of a given sample constituent depends on the difference between its ionization potential and the work function of the emitting surface; thus, there is a wide range of efficiencies for different materials, and the method is found useful for only about half of the elements in the periodic table. In addition, the rate of ionization of a given constituent depends on the composition of the mixture. In method (*c*) (spark discharge) all materials present in the sample are ionized with efficiencies equal within an order of magnitude. However, the problem of using sensitive electrometer circuits in the vicinity of high-voltage high-frequency sparks has not been overcome. Furthermore, the spark produces ions of a wide range of energies, requiring both a velocity- and direction-focusing analyzer; finally, the fluctuations in the ion current caused by fluctuations in the spark require long-term averaging.

Notwithstanding these difficulties, the use of the mass spectrometer in determining the composition of alloys has long appeared attractive, particularly because the mass spectrum of an alloy is simpler and should permit easier interpretation than the emission spectrum, for example. Also, certain

elements which do not produce lines in an emission spectrum should be observable in a mass spectrum.

Probably the first serious attempt to devise an instrument for alloy analysis was that of Gorman *et al.* (28), who used a spark source in a Dempster double-focusing analyzer. In order to overcome the fluctuations in the spark, they measured not the ion current at a given mass, but rather the ratio of that current to a fixed fraction of the total unresolved ion current. In typical analyses of certain stainless steels, limits of detectability of minor constituents of the order of 0.1 per cent were reported. Unfortunately, this work has not been continued.

A more recent application has been that of Hannay (29, 30), who used a spark source in a Mattauch double-focusing analyzer for measuring the impurities in a nearly pure germanium. By using careful calibration techniques in combination with photographic detection, he was able to determine, within an order of magnitude, impurities as low as one part in ten million, and to measure surface contaminations of the order of one-tenth of a monolayer.

Before leaving this section, one powerful technique which shows great promise in certain applications will be mentioned; this is the technique of isotope dilution (31). This method is suited to the determination of the amount of a particular element present in a heterogeneous sample, provided that this element exists in more than one isotopic form and provided that samples of the element in question are available with the normally rarer isotope substantially enriched. Briefly, the procedure consists of adding a known weight of the enriched material to a known weight of the unknown, effecting an isotopic equilibrium, and extracting an arbitrary amount of the element in question (not necessarily a pure extraction). Comparison of the isotope ratios of the original material, the added material, and the extracted material, together with the weights used, provides a close determination of the amount of the element originally present.

It should be pointed out that with any of the methods of ionization of solid samples previously mentioned, the inherent limitations become second- or higher-order effects when isotope ratios are measured, so that these limitations are not pertinent to the isotope dilution method. On the other hand, the use of this method to determine the entire composition of a sample would be extremely tedious, and at the present time is limited by the nonavailability of enriched samples of all of the elements which it might be desired to measure.

Automatic Reduction of Spectral Data

The use of the mass spectrometer in determining chemical composition of mixtures of substances is based on the fact that a properly designed instrument produces a spectrum of a mixture which is a linear superposition of the spectra of the constituents of the mixture. The instrument is thus used as an empirical device, being calibrated with unit amounts of the pure materials expected in a given mixture. Because of the linear superposition

property, the calculation of a mixture spectrum involves, in the general case, the solution of a set of linear simultaneous equations.[3]

The data reduction techniques used since the inception of industrial mass spectrometry have gone through four distinct phases: (*a*) manual reading of the recorded spectrum, and computation using a desk calculator; (*b*) manual reading, followed by analog computation; (*c*) manual reading, followed by automatic digital computation; (*d*) automatic digital recording, followed by automatic digital computation.

The main factor influencing this sequence of techniques has been the desire to reduce the time required to complete an analysis. This is important for two reasons; first, by reducing man hours, the costs of analysis are reduced, and, second, by reducing elapsed time, closer control of the process involved is achieved. The latter factor is particularly important in pilot plant work.

It should be understood, of course, that the later techniques have not replaced the earlier ones completely, and that the technique chosen by any laboratory depends on such factors as the availability of computing equipment and the sample load.

In performing a mass spectrometric analysis using techniques (*a*), (*b*), or (*c*), there are three well-defined steps: first, the spectrum is recorded, second, the recorded spectrum is read and tabulated, and, third, the tabular values are subjected to computation. By the time phase (*c*) had been reached, advances in the mass spectrometer and in high-speed digital computers made it apparent that the most fruitful area for reducing both elapsed time and man hours lay in the area of reading and tabulating the recorded spectra. Thus, recent efforts have been directed mainly at this aspect.

Two systems have been reported recently which automatize the gathering of spectral information in digital form. The first of these (32), developed by Consolidated Engineering Corporation[4] is comprised basically of (*a*) a program unit which sequentially selects a series of predetermined mass numbers, (*b*) a converter for digitizing the magnitude of the ion current at each selected mass number, and (*c*) an output device which may consist of an electric typewriter, or a card or tape punch. The output device records in digital form a code giving the mass number, a code giving the scale factor for the reading, and the ion current reading itself. Thus, all necessary information for an automatic calculation is obtained. The analog-digital converter used in this scheme employs a self-balancing digital potentiometer which provides digital output in the form of electrical contact closures.

The other system which has been reported (33) is a joint development

[3] In certain cases, the coefficient matrix of the set may be essentially triangular, or even diagonal (e.g., in a mixture of the rare gases, where the spectra of the individual constituents do not overlap).

[4] This device is sold under the trade name "SpectroSADIC" and is referred to by this name in most of the literature.

of the Atlantic Refining Company and the Physics Research Corporation.[5] This system starts out with a program unit essentially the same as the Consolidated system. The analog-digital converter, however, is radically different, consisting of a cathode ray tube containing a coded mask. The output signal of the mass spectrometer deflects the electron beam in the tube so that a particular line of the code is picked out, and a sweep of the beam along this code line produces a series of pulses representing the digital value of the original ion current signal. In order to obtain sufficient dynamic range, a logarithmic amplifier is used between the mass spectrometer and the converter, and the antilog is obtained during subsequent computation. The final portion of this system is a small, general-purpose digital computer. Although the system is basically designed so that the mass spectrometer and computer work simultaneously on a given sample, it is possible to store digital spectral information on punched tape for later use.

Dudenbostel & Priestley (34) have discussed the use of such systems, and give the time savings gained over two previous methods of handling data. They show that a more than fourfold reduction in man hours per sample has resulted from completely automatic operation as compared with manual reading and analog computation [phase (*b*) above].

The systems just discussed find their greatest usefulness in laboratories where routine analysis of a great many similar samples is required. However, in nonroutine work, or in work of an exploratory nature, complete rather than partial spectra are needed, so that these devices become less useful. On the other hand, automatic digital presentation of complete spectra appears highly desirable, particularly in high-molecular-weight work, where datum points at as many as 600 mass numbers may be required for a single sample. For this reason a number of laboratories are working on devices for digitizing an entire spectrum.[6] Unfortunately, none of these devices has materialized at this writing, and no publications have been made.

Turning to the computational problem per se, from a mathematical standpoint the solution of a set of simultaneous equations offers no difficulty, and a high-speed digital computer can be coded to solve a given set of equations in a variety of ways.[7] Difficulties arise, however, in the areas of (*a*) instrument instability or long-term drift in spectra, resulting in both random and systematic errors in analysis, and (*b*) choice of the "best possible" method of treating the redundancy of data which generally arises.

Barnard & Fox (35) have discussed the possible criteria to apply in deciding how best to use the redundant data. They point out three possible

[5] Now a part of Marchant Research, Inc.

[6] Various private communications.

[7] Since a given set of calibrating data is used as long as possible (often for many months) there is no point in performing for each analysis a direct solution of the set of equations; rather, it is common practice to invert the matrix comprised of calibration data, so that subsequent analyses merely require the multiplication of a vector by a square matrix.

methods, which are summarized below:

(*a*) From the original data, only enough rows of coefficients are chosen to form a square matrix, which can then be solved exactly. The results are checked in the unused rows, and final *ad hoc* adjustments are made in the results so as to distribute the residuals in a reasonable manner. Obviously, considerable judgment is required, as the criterion of adjustment is not clear-cut.

(*b*) All of the original data are used, by linearly combining certain rows (perhaps in a weighted manner) so as to form a square matrix. This method also requires judgment in that it is not clear, *a priori*, which rows should be combined and what weights if any should be used.

(*c*) All of the data are used in a least squares solution, in which the rows are initially weighted on the assumption that all are equally reliable. Thus, no *a posteriori* judgment or adjustment is required.

In comparing methods (*a*) and (*c*), Barnard & Fox found little difference in results on analyses run shortly after calibrations were made, and slight preference for method (*c*) for analyses made at a later time. However, these studies were made with mixtures involving relatively small redundancy of data. In general, for highly redundant systems method (*c*) might be expected to give higher average accuracy, although the accuracy for those constituents of the mixture which contribute only at a few points of the spectrum will suffer because of the redistribution of errors inherent in the method.

It is clear that this is a difficult problem, requiring much empirical study. It is to be hoped that the rapid mathematical experimentation now possible with modern computing machines will permit clarification of the difficulties.

LITERATURE CITED

1. Brown, R. A., Doherty, W., and Spontak, J., Consolidated Engineering Corp., *Mass Spectrometer Group Rept. 84* (1950)
2. Brown, R. A., Melpolder, F. W., and Young, W. S., *Petroleum Processing*, **7**, 204 (1952)
3. Lumpkin, H. E., Thomas, B. W., and Elliott, A., *Anal. Chem.*, **24**, 1389 (1952)
4. Melpolder, F. W., Brown, R. A., Young, W. S., and Headington, C. E., *Ind. Eng. Chem.*, **44**, 1142 (1952)
5. Lumpkin, H. E., and Johnson, B. H., *Anal. Chem.*, **26**, 1719 (1954)
6. Kinney, I. W., Jr., and Cook, G. L., *Anal. Chem.*, **24**, 1391 (1952)
7. Clerc, R. J., Hood, A., and O'Neal, M. J., *Anal. Chem.* (In press)
8. O'Neal, M. J., *Application of High Molecular Weight Mass Spectrometry to Oil Constitution* (Paper No. 2, Presented at Institute of Petroleum, Hydrocarbon Research Group, Conf. on Applied Mass Spectrometry, London, England, (October, 1953)
9. McLafferty, F. W., *Analytical Applications of High Temperature Mass Spectrometry to Chemistry* (Presented at 2nd Annual Meeting, ASTM Committee E-14 on Mass Spectrometry, New Orleans, Louisiana, May, 1954)
10. Robinson, C. F., Washburn, H. W., Berry, C. E., and Perkins, G. D., *Instruments*, **24**, 221 (1951)
11. Nier, A. O., Abbott, T. A., Pickard, J. K., Leland, W. T., Taylor, T. I., Stevens, C. M., Dukey, D. L., and Goertzel, G., *Anal. Chem.*, **20**, 188 (1948)

12. Lanneau, K, P., *Ind. Eng. Chem.*, **45,** 2381 (1953)
13. Jernakoff, G., *High Frequency Ion Resonance Mass Spectrometry* (Presented at Pittsburgh Conf. on Analyt. Chem. and Appl. Spectroscopy, Pittsburgh, Pennsylvania, March, 1952)
14. Morgan, W. A., Jernakoff, G., and Lanneau, K. P., *An Ion Resonance Mass Spectrometer for Industrial Applications* (Presented at 125th Nat. Am. Chem. Soc. Meeting, Chicago, Illinois, September, 1953)
15. Lanneau, K. P., *Performance and Application of an Ion Resonance Mass Spectrometer* (Presented at 2nd Annual Meeting, ASTM Committee E-14 on Mass Spectrometry, New Orleans, Louisiana, May, 1954)
16. Wilson, G., and Gifford, A. P., A New Monitoring Mass Spectrometer (Presented at Pittsburgh Conf. on Analyt. Chem. and Appl. Spectroscopy, Pittsburgh, Pennsylvania, March, 1953)
17. Walker, J. K., Gifford, A. P., and Nelson, R. H., *Ind. Eng. Chem.*, **6,** 1400 (1954)
18. Wherry, T. C., and Kerasek, F. W., *Performance of the Non-magnetic RF Mass Spectrometer Tube* (Presented at 2nd Annual Meeting, ASTM Committee E-14 on Mass Spectrometry, New Orleans, Louisiana, May, 1954)
19. Bennett, W. H., *J. Appl. Phys.*, **21,** 143 (1950)
20. Donner, W., *An RF Linear Decelerator Mass Spectrometer* (Presented at 2nd Annual Meeting, ASTM Committee E-14 on Mass Spectrometry, New Orleans, Louisiana, May, 1954)
21. McLaren, I. H., and Wiley, W. C., *A New Time-of-Flight Mass Spectrometer,* (Presented at 1st International Instrument Congress and Exposition, Philadelphia, Pennsylvania, September, 1954)
22. Stephens, W. E., *Bull. Am. Phys. Soc.*, **21,** 22 (1946)
23. Robinson, C. F., and Hall, L. G., *A New Development in Process Control Mass Spectrometers* (Presented at 2nd Annual Meeting, ASTM Committee E-14 on Mass Spectrometry, New Orleans, Louisiana, May, 1954)
24. Bleakney, W., and Hipple, J. A., *Phys. Rev.*, **53,** 521 (1938)
25. Brown, A. H., Nier, A. O., and Van Norman, R. W., *Plant Phys.*, **27,** 320 (1952)
26. Bartels, J., Severinghaus, J. W., Forster, R. E., Briscoe, W. A., and Bates, D. V., *J. Clin. Invest.*, **33,** 41 (1954)
27. Walker, J. K., and O'Hara, C. L., *Anal. Chem.*, **27,** 825 (1955)
28. Gorman, J. G., Jones, E. J., and Hipple, J. A., *Anal. Chem.*, **23,** 438 (1951)
29. Hannay, N. B., *Rev. Sci. Instr.*, **25,** 644 (1954)
30. Hannay, N. B., and Ahearn, A. J., *Anal. Chem.*, **26,** 1056 (1954)
31. Inghram, M. G., "Stable Isotope Dilution as an Analytical Tool," *Ann. Rev. Nuclear Sci.*, **4,** 81 (1954)
32. Rock, S. M., Berry, C. E., and Sink, R. L., *Automatic Conversion of Mass Spectra to Digital Form* (Presented at Pittsburgh Conf. on Analyt. Chem. and Appl. Spectroscopy, Pittsburgh, Pennsylvania, March, 1952)
33. Young, W. S., Ramser, J. H., Brown, R. A., Melpolder, F. W., Carrick, G. R., Spontak, J., and Headington, C. E., *A Mass Spectrometer-Digital Computer Combination for Automatic Analysis* (Presented at Pittsburgh Conf. on Analyt. Chem. and Appl. Spectroscopy, Pittsburgh, Pennsylvania, March, 1952)
34. Dudenbostel, B. F., and Priestley, W., *Anal. Chem.*, **26,** 1275 (1954)
35. Barnard, G. P., and Fox, L., *Application of Digital Computing Methods to Mass Spectrometry Analysis* (Paper No. 18, Presented at The Inst. of Petroleum, Hydrocarbon Research Group, Conf. on Appl. Mass Spectrometry, London, England, October, 1953)

RADIATION CHEMISTRY

By F. S. Dainton

Department of Physical Chemistry, University of Leeds, Leeds, England

The first review of Radiation Chemistry in the *Annual Review of Nuclear Science* was by Magee (1) and, since he not only covered the work published during 1953 but also included in his survey certain important publications which appeared prior to 1953, this article will be largely confined to advances made during the period February, 1954 to January, 1955 inclusive. During this period, a second, posthumous edition of Lea's valuable monograph (2) has appeared, the proceedings of an Informal Conference on Physical and Chemical Aspects of Basic Mechanisms in Radiology (3) held during May seventh to ninth, 1953 have been issued, and also the usual *Annual Report* (4) has been pulished. A notable event had been the appearance of Volume I of *Radiation Research*, a new journal which seems likely to attract many articles on Radiation Chemistry.

In a review of this kind it is not possible to mention every paper which has actual or potential relevance to the main subject, nor have I attempted to do this. It has seemed to me to be preferable to restrict the discussion to systems in which the absorption of high energy radiations has resulted in a detectable chemical change or in which physical changes have been observed which can be directly related to chemical changes with some certainty. For example reference to radiation damage to metals and crystals, other than ice, will be omitted, whereas changes in the physical and chemical properties of amorphous, glassy, or partly crystalline, long chain organic compounds, including polymers, will be treated. Likewise, biological systems will only be discussed where their properties throw new light on the radiation chemistry of water; and all *in vivo* systems will be passed over.

The central problem of Radiation Chemistry is to identify the spatial and temporal characteristics of each step which takes place between the passage of the initial charged particle and the formation of the reaction products; and the general line of attack is as follows. First, the final products must be identified and their "G values" determined, i.e. the number of molecules of each product formed per 100 ev energy absorbed by the whole system as a consequence of the absorption of the radiation. When the dependences of the G values on various parameters such as dose rate, concentrations of reagents or other added substances, temperature, pH, and other factors are known, it is generally possible to make useful deductions about the nature of the immediate chemical antecedents of the products, and occasionally it is possible to estimate the lifetime and spatial distribution of these precursors. The next step is to test these hypotheses by other means which may include such diagnostic chemical procedures as the addition of "radical catchers" or "scavengers" and by physical observations such as spectroscopic and magnetic measurements. If the postulated intermediates can be gener-

ated by means not involving ionising radiation then radiomimetic and other studies can be made which often afford useful information about the intermediates; examples of this will be given. The chemically significant intermediates are often atoms or free radicals which may have originated from the breakdown of excited molecules or from molecular ions in spontaneous or charge-transfer processes; and it is a requirement that the parent species and its distribution should be consistent with the theoretical physicists' picture of the process of energy loss of the absorbed radiation and with the experimental physicists' information about their properties, as derived from, say, mass-spectroscopic data and the properties of ions in gases. For his part the theoretician can help the chemist by provision of a great range of information, for example concerning the electronic states of the molecules, the dipole-relaxation characteristics of the solvent, energy and charge transfer cross sections, and time scales of processes. Considerations of this kind have, with one exception, determined the classification adopted in this review; the exception is the Radiation Chemistry of Water and Aqueous Systems which has commanded the attention of chemists to a greater extent than any other subject and which will be dealt with separately.

Sources, Energy Absorption, and Physical Dosimetry

No major innovation in types of sources, either internal or external, has taken place. A convenient, simple Co^{60} γ-ray source which permits samples of varying sizes to be irradiated at intensities up to 3,000 r/min. and at temperatures from liquid air to several hundred degrees C. has been described by Firestone & Willard (5). Sr-Y^{90} sources of β-particles are likely to find wide application. They have already been used by Hardwick (6) in studies on aqueous solutions and by Dainton, Ivin & Sheard (7) for initiating polymerisation in liquid sulphur dioxide. In view of the increased interest in heavy particle radiation it is not surprising that the notorious difficulties in using Po^{210} as an α-particle source have been overcome for both external and internal sources. For the former, Miller & Wilkinson (8) deposited polonium on a platinum disc and covered the surface with thin mica, whilst for the latter the same workers used a solution of polonium sulphate containing $\sim$5 mc. per ml. prepared by dissolving in 1N H_2SO_4 the hydroxide which had been coprecipitated with $Nd(OH)_3$ from nitric acid solution. The properties of these sources have been carefully investigated by these authors. The Pt foil technique has also been used by McDonell & Hart (9), and the group at the Institut du Radium (10) have prepared satisfactory internal sources by dissolving in acid polonium peroxide which had been anodically deposited on gold immediately before. Pile radiation has been used by many workers, and some irradiations have been carried out by recoil particles from (n,α) reactions such as $B^{10}(n,\alpha)Li^7$ and $Li^6(n,\alpha)T^3$ (9). All these sources are likely to be used extensively in the future.

Machine accelerated ions have several desirable features, particularly in connection with dosimetry, and amongst those used during 1954 have been

cyclotron 28 and 35 Mev He ions (11). At the other end of the energy scale the cheap and easily monitored glow discharge anode system (12), in which positively charged gaseous ions with an energy of 600 ev. enter the solution, obviously has its utility for producing conditions somewhat analogous to those obtaining at the end of a particle track.

In chemical processes proceeding via an intermediate produced at a rate proportional to the intensity of the radiation and disappearing at a rate proportional to the square of its own concentration, data concerning the lifetime of the intermediate and its reactivity with other molecules can be obtained by using either intermittent radiation of variable flashing time, or single high intensity pulses. In photochemistry these techniques, referred to as the rotating sector technique and flash photolysis have long been used. In radiation chemistry the analogous techniques have only just begun to be applied. Controlled intermittency of γ-rays was first achieved by Hart & Matheson (13) by fixing the substance to be irradiated on a rotating wheel, so that it was carried through the beam from an 80c. Co^{60} source, and by Dainton & Rowbottom (14), who kept the sample fixed in position and arranged for mechanical alternate insertion and withdrawal of a 650 mc. Co^{60} source. A better arrangement is that adopted by Spinks *et al.* (15) who interrupted the narrow beam from a 1100c. Co^{60} γ-ray source by a 1 in 3 sector cut from a solid steel cylinder 12 in. long and 6 in. in diameter and rotated about its figure axis at controlled rates varying from circa 6000 to 6 rpm. Controlled pulsed radiation has not yet been applied.

There has been continuing activity in the perennial problem of physical dosimetry and cognate problems, such as backscatter of high energy electrons (16), straggling (17), the determination of W (=energy to create an ion pair in mixed as well as in pure gases) (18), the spatial distribution of the energy dissipation by high energy x-rays (19), and improvements in the calculations for the energy loss per unit length of track (20) conveniently designated by Zirkle (21) as L.E.T. (linear energy transfer). The interest of radiation chemists in this problem has been focused on absolute determinations of the energy absorbed in aqueous systems irradiated by photons or fast electrons. Such determinations may be made by direct calorimetry, in the manner described by Lazo, Dewhurst & Burton (22) for CO^{60} γ-rays, or indirectly by power input or ionisation methods. The power-input method has been used for high energy (1 and 2 Mev) cathode rays with full and careful corrections for backscatter, window absorption, and bremsstrahlung. Both of these methods have been applied and yield G values for the oxidation of ferrous sulphate in air-saturated 0.8 N H_2SO_4 solution of 15.8 ± 0.3 (22) and 15.6 ± 0.5 (23) respectively. These values are in gross disagreement with values obtained prior to 1954 by the ionisation method, including the careful work of Miller (24), who found a constant yield of 20.3 for dose rates up to 10^5 r/min. using x-radiation of energy between 1.5 and 2.25 Mev. Lower values of G had been obtained by the ionisation method, e.g. 16.7 [Hochanadel & Ghormley (25)], and during 1954 several others have appeared which are

listed below in Table I. The varying values of W_{air} given in column three, emphasise that the good agreement is more apparent than real. It is not possible to say that this important discrepancy has been fully accounted for.

TABLE I

G-VALUES IN THE OXIDATION OF FERROUS SULPHATE

Radiation	G	Value of W_{air} used	Reference
24.5 Mev x-rays	15.9±0.4	32.5	(26)
Co^{60} γ-rays	15.9±0.4	32.5	(26)
1 Mev x-rays	15.9±0.5	34.3	(27)
200 kvp x-rays	16.2±0.8	35.0	(28)
Ra and Co^{60} γ-rays	20.8	32.5 (probably)	(60)

It may well be that the value of W_{air} for high energy electrons should be larger than the 32.5 ev commonly used. Internal α- or β-particle sources present fewer problems, and good agreement between the results for the molecular hydrogen yield and the ferrous oxidation yield has been obtained by workers in Edinburgh (8), Paris (10), and Chicago (9).

CHEMICAL DOSIMETRY*

A chemical reaction of known G value which is readily reproducible, independent of intensity, and not very temperature-dependent can be used as an accurate dosimeter and, once calibrated for the radiation to be used, has many advantages. Reactions which meet these requirements usually possess G values less than 20 and are, therefore, of little value for the measurement of small doses, for which the use of electronic devices is preferable. The employment of chain reactions provides the necessary magnification but also generally requires much more stringent conditions to achieve the reproducibility; moreover the G values of many chain reactions are intensity dependent. The requisite sensitivity can sometimes be attained by calorimetric or tracer analytical methods. Thus Rødstam and Svedberg (29) claim that by using Fe^{59} as a tracer the ferrous sulphate actinometer can be used to measure doses in the range from 0 to 100 r with an accuracy of 2 r; and Suttle (30) has shown that the bromoform-crystal violet system will give a detectable colour with a dose as small as 5 r. An aqueous solution of an indicator in contact with a low molecular weight chlorinated hydrocarbon can also serve as a stable and reliable actinometer (31).

* Note added in proof: Ehrenberg & Sacland (149) have determined $G_{E_c} \cdots (O_2, 0.8)$ for various particle radiations resulting from the interaction of pile neutrons with various elements, thereby enabling a most valuable extension of the utility of the ferrous sulphate dosimeter.

Actinometry can be used to best advantage in integral dosimetry for large doses when the dose-rate is fluctuating, e.g. in a pile under variable operating conditions. Recently Hart and co-workers (32, 33) have suggested that the measurement of molecular products, the G values of which are around unity, would be suitable and have recommended two methods. The first method is to measure manometrically the total gas ($=2H_2+O_2$) evolved from aqueous potassium iodide solution; and the second method is to measure the ferric ion formed when an acidified solution of ferrous and cupric sulphates is irradiated. Both methods can be adapted to the measurement of neutron fluxes by the addition of boric acid to the solution. The second method is interesting in that it relies on the cupric ion being reduced by hydroperoxy radicals,

$$Cu^{++} + HO_2 \rightarrow Cu^{+} + H^{+} + O_2 \qquad 1.$$

the resultant cuprous ion reducing any ferric ion in the system according to

$$Cu^{+} + Fe^{+++} \rightarrow Cu^{++} + Fe^{++} \qquad 2.$$

so that any net oxidation of ferrous ion which is observed is attributable only to the "molecular" hydrogen peroxide generated. This method only measures the hydrogen peroxide yield provided $G_H = G_{OH}$. In passing, it should be noted that the agreement concerning the values for the ferrous sulphate system using Po^{210} α-particles extends the utility of this reaction as an actinometer to 5.3 Mev α-particles.

Primary Processes

The year under review has seen steady progress in the acquisition of new experimental data relevant to the general problem of the processes which occur within about 10^{-7} sec. after a molecule has been traversed by a fast charged particle. In the particular case of liquid water the advantages and shortcomings of the two competing theories of the primary processes in this medium have become more clearly delineated. This latter point will be discussed in the section on aqueous solutions.

Mass spectrometry continues to provide useful information concerning the formation and stability of molecular ions in the gas phase. In addition to data concerning molecular ionisation potentials obtained [see, for example (34)], ionisation potentials of radicals have been measured (35) and some progress has been made in the experimental study of dissociative electron capture (36). Perhaps the results of most obvious significance to radiation chemistry are those of Lindholm (37) who has studied the positive ions formed when CO_2, H_2O, H_2S, NH_3 CH_4, and N_2O are bombarded with atomic ions (A^{++}, Kr^{++}, Ne^{+}, F^{+}, A^{+}, Kr^{+}, O^{+}, Cl^{+}, Br^{+}, C^{+}, P^{+}, S^{+}, Se^{+} Zn^{+}, B^{+}, and H_2O^{+}) which have been accelerated through 500 ev. Large collision cross-sections were obtained for resonance transfer only, i.e. when the recombination energy of the atomic ion coincided with the appearance potential of the fragments of the target molecule. In water vapour H_2O^{+}

and OH^+ are the predominant species: the former is usually in excess of the latter, but the ratio $[OH^+]/[H_2O^+] \geqq 1$ for Kr^{++}, Ne^+, and F^+. In H_2S, the radical ion SH^+ is always formed in greater amounts than H_2S^+. Collinson (4) has drawn attention to the particular relevance of these studies to the conditions at the end of α-particle tracks and suggested that OH^+ may occupy a role in these systems of hitherto unsuspected importance which might account for the known greater ease of carrying out oxidation by α-rays than by β- or γ-rays.

A detailed survey of the mass-spectral data of a large number of organic compounds has been made by Pahl (38), who has shown that there is a systematic variation of the "average fracture quotient," $\overline{Q}_B$, with the number of bonds in a molecule, Z_B. $\overline{Q}_B$ is defined as

$$\frac{1}{Z_B} \frac{\sum I_B}{\sum I_M}$$

where I_B is the intensity of appearance of a positive ion resulting from a bond fracture and I_M is the intensity of appearance of the undecomposed molecular ions. Substituent effects are clearly apparent in this work but whether structural influences are significant at higher electron energies is doubtful, although Leder & Marton (39) have shown that the energy loss of 30 kev electrons in thin films of the oxides of certain elements differs from that of the sulphides.

To detect and identify free radicals in irradiated systems, paramagnetic resonance measurements may be used. For example, free radicals on the nitrogen atoms have been identified by Combrisson & Uebersfeld (40) in amino acids irradiated with a dose of circa 10^7 r gamma radiation; and the same authors have observed a resonance spectrum in irradiated plastics, which also display a post-irradiation decay of the absorption. The results obtained for ice and solid solutions of ice and certain other substances are especially interesting and will be referred to later.

Essex (41) has shown that the extents to which the processes of (*a*) ion recombination, (*b*) dissociative electron attachment, (*c*) dissociation without electron capture, and (*d*) dissociation accompanying ionisation, each contribute to the observed chemical change can often be determined in gas phase reactions by studying the effect on the yield of clearing fields of various strengths in conjunction with a Loeb Electron Filter. In the cases of ammonia decomposition and hydrogen chloride synthesis ion recombination plays a large part, but this is not true for the α-ray-induced decomposition of nitrous oxide for which process (*c*)

$$e^- + N_2O \rightarrow e^- + N_2 + O \qquad 3.$$

plays a large part. In addition to these processes, charge transfer between ions, e.g. $X^+ + Y^- \rightarrow X + Y$ or between ions and atoms, e.g. $A^+ + B \rightarrow A + B^+$ may be important. In a recent discussion (42), D.R. Bates has pointed out that the application of Landau & Zener's method to interionic transfer leads

to the conclusion that the transfer coefficient is a maximum, not when the transfer is thermoneutral but when it is exothermic by a few electron volts.

In the last few years the notion that an appreciable fraction of the chemical change may be derived from excitation has received increasing support and there are signs that attempts are being made to identify the excited levels involved, to investigate their stability towards dissociation and reagents, and to learn about inter- and intramolecular energy transfer phenomena [see for example (1) pp. 174–79]. The absorption coefficients of water in the vacuum ultraviolet have been measured by Watanabe & Zelikoff (43), who assign the diffuse band with a maximum at 1650 Å to excitation to a level which is assumed to undergo predissociation to $H_2(^1\Sigma g^+)$ and O (^{1}D). The presumption that this transition occurs to any extent under secondary electron impact in aqueous systems might form the basis of an alternative explanation of the "molecular" yield of hydrogen and its remarkable insensitivity to solute type or concentration. Another excited level which may play a part in the radiation chemistry of water is the long-lived linear triplet state, the existence of which has been proposed on theoretical grounds by Niira (44). Other evidence for excited species in irradiated water will be presented later but at this point it is useful to reflect that if all the energy not employed in ionisation is used in excitation then the molecules so produced give rise to much less chemical change than would be expected. There are at least two possible reasons for this. The first is that if chemical reaction attributable to the formation of the excited molecules is preceded by their dissociation, the dissociative process may be inefficient because of the "cage" effect. Evidence for this effect in solution photochemistry is steadily accumulating. Thus Lampe & Noyes (45) have shown that the quantum yield for the photodissociation of molecular iodine in organic media is always less than unity, and that it decreases with the molecular weight of the solvent and increases with rise of temperature. Likewise Taube *et al.* (46, 47) have shown that in the photodissociation of the halogens and of hydrogen peroxide in aqueous solution there is considerable primary recombination. Evidence for a similar effect is also provided by activity retention measurements in carbon tetrachloride (48). A second reason might be that the excited molecules are deactivated or that the excitation energy is emitted as light. The former explanation is rendered unlikely by the attainment of a limiting value of the measured radical yield at quite low solute concentrations. The objection to the latter is that even if light is emitted (49), which has been disputed (50), it occurs at very short wave lengths where the extinction by the medium is high and therefore the excitation is likely to persist, until finally a molecule is dissociated.

Another suggestion which has been made (51) is that slow secondary electrons might excite optical levels of solute molecules. However this is a "direct" effect which would lead to a concentration dependence of the chemical yield and is therefore not germane to the general problem of the role of excitation in "indirect" action.

If excited species are involved in the primary act, problems of energy, transfer become important, Considerable progress has been made in this field from investigations of scintillation and "protection" effects in multicomponent systems. These systems together with studies of intramolecular energy transfer will be reserved for later discussion. For the present purpose it will suffice to note that intermolecular transport of electronic energy requires an overlap of energy levels of acceptor and donor, whether it proceeds by a "photon cascade" or an "exciton" mechanism.

Gaseous Inorganic Systems

Essex (41) has revised his published and unpublished data on the effect of clearing fields on the decompositions of ammonia, nitrous oxide, and azomethane and on the hydrogen-chlorine reaction when induced by α-particles, drawing attention to the fractions of the total chemical change associated with each of four primary processes for each of the reactions investigated. Sr-Y^{90} β-particles have been used to initiate the decomposition of carbon dioxide gas at room temperature (52). In pure carbon dioxide only small amounts of carbon monoxide and oxygen are formed, because of the existence of a very rapid back reaction. If 0.2 mole per cent of nitrogen dioxide is added the rate of the radiolysis increases fivefold and the initial G value is about 10. The mechanism is not discussed but presumably the following reactions are involved

$$CO_2 \xrightarrow{\beta^-\sim\sim} CO + O \text{ (forward reaction)} \quad 4.$$
$$CO + O + M \rightarrow CO_2 + M \text{ (back reaction)} \quad 5.$$
$$NO_2 + O \rightarrow NO + O_2 \quad 6.$$

the nitrogen dioxide retarding the back reaction by withdrawing oxygen atoms from the system. Nitrogen dioxide has been shown to undergo decomposition into nitrogen, oxygen, and nitric oxide (53) when subjected to pile radiation. The presence of N_2O in the products is regarded by the authors as evidence for the formation in the primary act of nitrogen atoms which can react with nitrogen dioxide in three different ways [reactions 7(a), 7(b), and 7(c)].

$$N + NO_2 \rightarrow (a)\ 2NO, \quad \text{or} \quad (b)\ N_2O + O, \quad \text{or} \quad (c)\ N_2 + O_2 \quad 7.$$

The kinetics of the decomposition of ammonia (54, 55) in electric discharges have been studied. Nitrogen ($G\sim0.8$) and hydrazine ($G\sim2.5$) are formed, but some of the hydrogen atoms produced in the primary act reduce the hydrazine back to ammonia by the sequence of reactions

$$H + NH_2 \rightarrow NH_3 \text{ third body or wall process} \quad 8.$$
$$H + N_2H_4 \rightarrow NH_3 + NH_2 \quad 9.$$

and, accordingly, the yield of hydrazine can be increased by coating the reaction vessel wall with platinum which catalyses the combination of hydrogen atoms. The authors consider that only relatively low excited states of

ammonia are involved in this primary act, possibly even below optically attainable levels.

Dorfman & Hemmer (56) have found that tritium β-particles bring about the combination of hydrogen and oxygen at 25°C. The G value is about 10 for the tritium-oxygen reaction and 13 for the hydrogen-oxygen reaction, and it is doubtful whether chains are involved. No hydrogen peroxide was detected in the products.

Reactions of Organic Compounds

Pure compounds.—A compilation of data concerning the radiation decomposition of pure organic compounds has appeared (57). McDonell & Newton (58) have reported that when air-free liquid normal and branched chain alcohols are irradiated with 28 Mev helium ions autoreduction and autoxidation occur, and hydrogen and saturated hydrocarbons appear in the products, together with aldehydes, ketones and glycols. The results can be explained by assuming that either the C—C or the C—H links adjacent to the carbinol group are usually severed, whereas the hydroxyl group is rarely detached. This hypothesis differs from that proposed by Coleby *et al.* (59) to account for indirect action by x-rays on methyl alcoholic solutions of steroids where it is supposed that hydroxyl radicals are formed; but it is in line with the mass-spectral data for alcohols reviewed by Pahl (38).

Solutions of DPPH.—Some very interesting results have been obtained by investigating the bleaching of dilute solutions of the stable free radical DPPH (α,α'diphenylpicrylhydrazyl) in chloroform and methyl acetate. Chapiro *et al.* (60), using Ra γ-rays, 1.2 Mev x-rays, 190 kev x-rays, and 37 kev x-rays, observed that in the first stages the reaction proceeds smoothly, but after 80 to 90 per cent destruction of DPPH secondary reactions make their appearance. Above a certain value of the concentration, which depends on the dose rate, the initial rate of destruction of DPPH is independent of its concentration and proportional to the dose rate, but below this value the rate decreases and tends to become dependent on the dose rate. The mechanism adopted for this reaction is that originally proposed by Dainton & Miller (61) for single solute indirect action and is summarised

	Rate	
$S \longrightarrow\!\!\!\!\sim\!\!\!\!\sim\!\!\!\!\rightarrow R$	$G_R I$	10.
$2R \rightarrow X$	$k_{11}[R]^2$	11.
$R + h \rightarrow R{-}h$	$k_{12}[R][h]$	12.

where S denotes solvent, R the radical formed from it which reacts with DPPH (represented by h) to produce R—h and X is the unknown stable product or products formed by the interaction of pairs of R radicals. Two extreme concentration ranges may be distinguished. At high concentrations where reaction 11 plays a negligible part, the rate $= G_R I$, where G_R is the radical yield and I the dose rate in units of 100 ev. The values of G_R obtained were high and dependent on the quality of the radiation. Thus taking

$G_{F^{e+3}}$ as 21 (it was measured as 20.8 for 1.2 Mev x-rays and 21.2 for 37 kev x-rays using ionisation methods) the values of G_R in chloroform were very large, of the order 50(1.2 Mev γ-rays), 150(190kv x-rays), and 10^3(37kv x-rays) and for methyl acetate using γ-rays G_R was 16.5. At low concentrations where $k_{11}[R] \gg [k_{12}h]$ the rate is much less than in the high concentration range and the rate expression is $k_{12}[h](G_R I/k_{11})^{1/2}$. The authors define a critical solute concentration $[h]_c = (40 G_R I k_{11})^{1/2}/k_{12}$, corresponding to a critical stationary radical concentration $[R]_c = k_{12}[h]_c/40k_{11}$, which is arbitrarily chosen such that only 2.5 per cent of the radicals are not reacting with the DPPH. The observed values of $[h]_c$ depend on both the radiation intensity and quality, an effect which the authors ascribe to radical distribution influences. This point is taken up fully by Chapiro (62) in a later publication, the essence of his argument being that since $k_{12}/k_{11}^{1/2}$ increases with I, the concentration of DPPH to capture 97.5 per cent of the primary radicals (i.e. $[h]_c$) has to be larger at lower intensities where there are fewer secondary electron tracks per unit volume and the initial distribution of the radicals is therefore to be regarded as highly inhomogeneous. Chapiro adopts a model for this system similar to that proposed by Magee & Samuel (63) for water, and supposes that shortly after an electron has passed there will exist two groups of radicals, the first group in high local concentration in small clusters and the second group forming a "continuous background" of lower concentration. The decay of the concentration of radicals in the first group will depend on k_{11}, k_{12} and $[h]$ but, except in the unlikely event of an appreciable number of clusters from one track coinciding with those of another, will be unaffected by the radiation intensity. By contrast the radicals in the continuous background derived from one track will mingle with those of others, and since the radicals undergo mutual destruction (reaction 11), the time constant of their decay will be intensity dependent. This treatment suggests that the observed value of $[h]_c$ will comprise two terms, $[h]_c^\circ$ appropriate to the clusters, and $[h]_b = (40 I G_R k_{11})^{1/2}/k_{12}$ because of the continuous background. This, admittedly oversimplified, treatment thus qualitatively accounts for the observed constancy of $[h]_c$ at low intensities, and its increase with I at high intensities tending to a limiting value of $(40 I G_R k_{11})^{1/2} k_{12}$ when the intensity is so high that there is almost complete overlap of the radicals from different tracks. This approach lends itself to the definition of a "homogeneity factor" $= [h]_c/[h]_b$, which is unity for a uniform distribution.

This approach is a very interesting one and should be applied further. In so doing it should be borne in mind that the homogeneity factor deduced from experiments made in this manner will depend on the nature of the solute if the latter reacts by a chain reaction. It has already been pointed out (64) that if the radicals in the clusters initiate a chain reaction of lifetime greater than the lifetime of the radicals in the absence of a solute, then radical activity will have a greater time to diffuse away from the track. Chemical measures of homogeneity are clearly only measures of "radical reactivity" distribution.

Mixtures.—An increasing amount of work has been carried out on two-component systems. Burton & Manion (65) have indicated that in a mixture of *A* and *B*, protection of *A* by *B*, by energy transfer, will not occur if the accessible energy levels of *B* lie above those of *A*. Under these circumstances *B* may sensitise the radiolysis of *A*. A case in point, studied by Burton & Patrick (66), is the slight sensitisation of the rearrangement decomposition of propionaldehyde by benzene-d_6, a result which in view of the known stability of benzene to radiation ($G_{H_2} = \sim 10^{-2}$), might at first sight have seemed surprising. However benzene does protect aliphatic hydrocarbons against decomposition by electron bombardment, and the argument had previously been advanced (67) that this protection involved energy transfer. The possibility also existed that the benzene acted as a sink for hydrogen atoms which are intermediates for the hydrocarbon decomposition, presumably via a reaction of the type

$$H + C_6H_6 \rightarrow H_2 + \text{residue.} \qquad 13.$$

By studying the isotopic composition and total yields of the hydrogen gas evolved from different mixtures of *cyclo*-hexane and benzene-d_6 under 1.5 Mev electron bombardment when reaction 14 should occur,

$$H + C_6D_6 \rightarrow HD + \text{residue} \qquad 14.$$

Burton & Patrick (67) have shown that radical reactions of this type occupy a subsidiary role in the protection mechanism, which is mainly by energy transfer. Maddock (68) has suggested that, if the fluorescence efficiency of solutes is a measure of the efficiency of energy transfer from solvent to solute molecules, then good scintillators in benzene solution might be expected to give marked protection to benzene against radiolysis. Burton & Patrick (69) have found this not to be the case; neither anthracene nor *p*-terphenyl protect, and *m*-terphenyl exerts only a slight protective action. The mechanism of energy transfer from exicted solvent to solute molecules in organic systems has been carefully re-examined by Birks (72) who rejects the "exciton" (70) and "sensitised fluorescence" (71) theories because both theories require a degree of electronic coupling which does not exist in organic systems. Instead he suggests a "photon cascade" mechanism, in which the solvent molecules in high electronic states fluoresce with a delay time of $\sim 10^{-11}$ sec., the emitted photon being strongly absorbed by neighbouring molecules which in turn fluoresce. At each stage some thermal degradation of energy occurs until the magnitude of the quantum reaches the normal fluorescence value for the first excited level of the solvent or reaches a value at which it can excite the fluorescence of the solute. A merit of this theory is that it readily accounts for the observation that the efficiency of the scintillator is a function of the fluorescing power of the solvent, e.g. *p*-terphenyl is much less efficient in "nonfluorescent" solvents such as paraffin oil, hexane, etc.

The γ-ray induced chlorination of aromatic compounds has been investigated and has possible commercial application since, compared with photochemical chlorination, nuclear addition is favoured (73).

Systems containing alkyl monohalides.—The interrelation between the phenomena observed following light absorption, γ-ray absorption, and radiative neutron capture by alkyl halides has been again emphasised in a series of papers by Hamill & Williams (74). The quantum yields of iodine formation at 3260 and 2537 Å, and also the G value for iodine when 50 kvp x-ray are used show the same dependence on structure, namely, an increase with the number of C—H groups. This result is in keeping with the reaction sequence

$$RR'CHCH_2I \xrightarrow{h\nu,\ X} RR'\dot{C}HCH_2 + I \qquad 15.$$

$$RR'\dot{C}HCH_2 + RR'CHCH_2I \rightarrow RR'CHCH_3 + RR'\dot{C}CH_2I \qquad 16.$$

$$RR'\dot{C}CH_2I \rightarrow RR'C{=}CH_2 + I \qquad 17.$$

where the radical emerging from reaction 15 is "hot." This scheme also accounts for the equivalent amounts of alkane and alkene which are formed and can readily be extended to include attack on the solvent by "hot" radicals. The authors consider that radiative neutron capture gives effectively one atom-radical pair. Retention of halogen reactivity by the parent halide then depends on whether recombination occurs within the cage or after diffusion from the cage. In the latter case addition of solutes reactive either to the halogen atom or the alkyl radical will decrease the retention, and this effect is observed when inactive halogens or halo-olefines are the solutes.

The known reactivity of methyl radicals with iodine

$$CH_3 + I_2 \rightarrow CH_3I + I \qquad 18.$$

can be used to detect minute amounts of them if the I_2 is radioactive. If is found that when dilute solutions ($\sim 10^{-2}M$) of methyl iodide or acetic acid in various hydrocarbons containing $10^{-4}M I_2^{131}$ are subjected to γ-irradiation, CH_3I^{131} is produced. The only consistent explanation of these and related phenomena is that the solute captures an electron ejected from the hydrocarbon lying in the tracks of the secondary electrons, and that the capture is dissociative

$$CH_3I + e^- \rightarrow CH_3 + I^- \qquad 19.$$

The concentration dependence of the methyl iodide yield suggests that the methyl halide is competing for electrons with solvent hydrocarbon cations.

Polymerisation.—A large number of unsaturated compounds can be polymerised or copolymerised by ionising radiation, frequently under milder conditions than are otherwise necessary. Thus, vinyl chloride is polymerised in the vapour phase (75), styrene and ethylene oxide can be polymerised in an electric discharge (76), ethylene can be polymerised by Co^{60} γ-rays at room temperature under pressures of from 250 to 1600 lbs. per sq. in. or copolymerised with sulphur dioxide to form the polysulphone (77), perfluoro compounds including C_3F_6, $(CF_2{:}CF)_2$, $CF_2{:}CF.CN$ and $(CF_3)_2C{:}CF_2$ form

the addition polymers (78) ,and even pure benzene gives small amounts of a soluble, low molecular weight yellow polymer when irradiated with 1.5 Mev electrons (79). Acrylamide can be polymerised either in aqueous solution (80, 82) or in the solid state (81). The kinetics of the former reaction are very simple (82); the rate is proportional to the monomer concentration and the square root of the dose rate, unless certain chain terminating agents are added. No chain transfer occurs even with hydrogen peroxide, and there is good evidence that all the available radicals are utilized in initiation. The solid state polymerisation displays unusual kinetics which are consistent with the hypothesis that the initiating radicals may be derived from either monomer or polymer molecules, that polymer chains undergo mutual termination, and that each member of a terminating pair may be derived from the same or from different tracks. An interesting feature of the reaction is that the crystallinity of the solid as judged by x-ray reflection intensities decreases steadily throughout the reaction, although the external appearance remains crystalline; a clear case of pseudomorphism. *N*-vinyl pyrrolidone in aqueous solution can be polymerised by γ-rays even when the system is frozen (78).

Liquid phase radiation-initiated polymerisations generally have kinetic features very similar to the same reaction initiated by light or thermal catalysts. Thus the Trommsdorff effect has been observed in the γ-ray bulk polymerisation of styrene and methyl methacrylate (83), and the γ-ray emulsion polymerisation of styrene is faster than the bulk polymerisation. The kinetics of the bulk polymerisation of styrene are still not entirely settled. Chapiro & Wahl (84) have extended the previous work of the French school and find that from 0.29 to 410 r per min. the rate is proportional to $I^{0.48}$ and the degree of polymerisation of $I^{-0.46}$. Ballantine (85) consider that the intensity exponent of 0.5 for the rate may extend to 1150 r per min. However the earlier results of Manowitz (86) which, taken with Chapiro's data, suggest that the exponent falls below 0.5 at high dose rates, when taken by themselves suggest a first power dependence on intensity. The former conclusion is more in accord with theoretical expectations, since at very high intensities not all the primary radicals may be utilised in initiation, in which case the intensity exponent would be expected to be less than 0.5 (87).

One substance which has a very large negative free energy of polymerisation to form polymethylene (88) but which has so far resisted polymerisation by catalysts or ionising radiation is cyclopropane (89).

Breakdown of polymers and large molecules.—Macromolecular solids have long been known to undergo changes of physical properties during irradiation. As an example of this may be cited the conductivity induced in polythene (90), polystyrene (91), and polytetrafluoroethylene (92) by x-irradiation. It would be expected that the radiation would result in radical formation, which has been confirmed by paramagnetic resonance measurements (40), and that in solids these radicals would persist, their persistence being manifested in post-irradiation decay phenomena, which have also been observed. In solids which are permeable to or which dissolve oxygen it is likely

that irradiation in an oxygen atmosphere would result in oxidation, probably with peroxide formation. Fats irradiated with x-rays or electrons do behave in a manner explicable in these terms (93). The detailed chemistry of the changes undergone by assemblies of long chain molecules is however still very imperfectly understood. The questions which arise are these: (*a*) What bonds are broken in the primary act; is the main chain severed or are side groups detached? (*b*) Are the radicals so formed mobile, and, if so, is this migration by mass transfer (i.e. diffusion), by energy transfer, or by bond rearrangement, and what is the influence on this mobility of additives, which are either mixed or chemically incorporated with the polymer molecules? (*c*) Can the radicals undergo mutual destruction and step-wise degradation? (*d*) Can a radical in one chain react with neighbouring chains, and, if so, what type of reaction occurs and does it lead to cross-linking? and finally (*e*) If any of these processes do occur, what are the factors which influence them? Fortunately the techniques of polymer chemistry are now sufficiently developed to enable fairly clear answers to be given to some of these questions. Thus elastic properties, solubility, softening point, and viscosity of the soluble fraction can inform about cross-linking; x-ray reflections about crystallinity; spectra about characteristic groupings; mass-spectrometric analysis of volatile products about the bonds broken; and so on. While all the data cannot be discussed here, a selection of the salient findings is given below; the literature for 1954 is given by subjects in the references (94 to 107).

The melting point of solid paraffins subjected to pile radiation at first falls and then rises suddenly, the system becoming infusible and insoluble in common organic solvents at a dose which is approximately inversely proportional to the length of the paraffin chain (97). These facts are taken to mean that cross-linking of the hydrocarbon chains occurs and that the energy required to form one cross-link, later shown to be $\sim$24 ev, is independent of chain length. Hydrogen gas is evolved and the hydrogen : carbon ratio decreases during irradiation. Since for each cross link formed one molecule of hydrogen should be liberated, whereas for each severing of a main chain one molecule of hydrogen should be absorbed, the ratio of cross-linking to main chain scission can be calculated, provided the amount of unsaturation which develops can also be measured. For polythene, which Charlesby considers to behave like a pure hydrocarbon, measurements of the sol fraction indicate that this ratio is about 3. The data on ethane, propane, and butane obtained by Honig & Sheppard (113) and Lind & Bardwell (114) for α- and *d*-bombardment suggest that similar processes are occurring in these cases. Cross-linking also occurs in the olefines and acetylenes (98) but to a lesser extent the further the double bond lies from the end of the molecule. Loss of unsaturation has also been observed when an electric discharge is passed through *n*-hexadecene-1 (99).

There is little doubt that cross linking is the major factor responsible for the considerable changes in physical properties of polythene, but some

of the earlier views (115a) concerning the mechanism have been shown to need revision. Thus Lawton *et al.* (103) have shown that as much as 15 per cent of the gas evolved on electron bombardment consists of C_2, C_3, and C_4, saturated and unsaturated, hydrocarbons, and that the efficiency of the cross-linking depends on the average molecular weight of the sample (102). Furthermore Dole (105, 106) has found by bromine absorption measurements that from 70 to 80 per cent of the hydrogen evolution is associated with the development of unsaturation and only 20 to 30 per cent with cross linking. Infrared spectroscopic measurements show that the unsaturation which develops is that of the *trans*-vinylene group

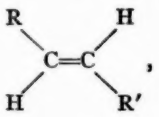

but that unsaturation present before irradiation, attributable to vinylidene groups

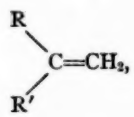

disappears. For each vinylidene group disappearing only about 3.6 molecules of hydrogen are produced, and these facts have led Dole to suggest that in the primary act free radicals are produced at random along a polymer chain, but that these radicals are capable of migration (presumably by displacement of H atoms in the opposite direction) along the chain until a vinylidene group is reached. The radical will then be localised by transforming the vinylidene group into a resonance stabilised allylic radical which slowly reacts to produce a cross-link, possibly involving the formation of a *trans* vinylene group. Such migration of reactivity may also be the explanation of Alexander & Charlesby's claim (96) that an aromatic ring incorporated in dodecane exerts its maximum protection against cross linking the closer it is to the centre of the chain, and, therefore, the shorter the average distance over which this migration has to occur. However these authors prefer to regard the migration as one of energy transfer.

The behaviour under pile radiation of cellulose (111), rubber (112), siloxanes (109), polystyrene (94), polyvinyl acetate (94), polyvinyl alcohol (94), gutta-percha (94), neoprene (94), nylon (94), and polyethylene terephthalate (115b) have been interpreted by Charlesby as evidence for cross-linking, but more detailed investigation by Todd (107) shows that for polyethylene terephthalate the cross-linking is inappreciable and the main effect is one of degradation, possibly accompanied by branching. Little (108) has confirmed Todd's findings and has also shown that the main effect in nylon is one of methyl substitution rather than cross-linking. Miller, Lawton &

Balwit (95) have drawn attention to the broad classification that cross-linking occurs only if the polymer contains at least one α-hydrogen atom; examples are polymethylene, polyethylene, and $(\cdot CH_2—CH(X)\cdot)_n$ where $X = R$, COOH, COOMe, $CONH_2$, COMe, OR; and degradation predominates in polymers containing the base mole $(CH_2—C(Me)\,Y\cdot)$. Y = Me, C_6H_5, COOH, COOMe, $CONH_2$. For those polymers in the second group, the degradation is often accompanied by decomposition of the side chain (110).

Ice, Water, and Aqueous Solutions

Most of the characteristics of the radiation chemistry of predominantly or wholly aqueous systems can be accounted for by a primary act which may be written

$$H_2O \text{—}\sim\sim\text{→} \alpha H + \beta OH + \gamma H_2 + \delta H_2O_2 \qquad 20.$$

and in the past the aim of experimental investigations has been to determine the values of the coefficients α, β, γ and δ for different qualities and dose rates of radiation, for different solutes and solute concentrations and other experimental variables; to discover whether these species are the only ones formed and in particular whether H and OH are actually formed or are merely a convenient way of representing the chemical behaviour of other entities such as H_2O^-, H_2O^+ and H_2O^*; and finally to adduce evidence concerning the spatial distribution of the primary products. The present position has been admirably summarised by Allen (116) and by Dewhurst, Samuel & Magee (117). Any acceptable theory of the primary act must not only account for the firm conclusions reached by the experimentalists but also provide an intrinsically satisfactory mechanism of the formation of the primary products. During 1954 some considerable advances have been reported and are discussed below.

Magnetic and isotopic studies.—The paramagnetic resonance spectra of ice and deuterated ice irradiated with total doses of the order 10^5 to 10^6r have been measured at 4° and 77°K. by Smaller, Matheson & Yasaitis (118). At 77°K. ice gives a doublet and deuterated ice a triplet structure, suggesting the presence of hydrogen ($i = \frac{1}{2}$) and deuterium ($i = 1$) atoms respectively. However, the separation of the doublet (= 85 Mc/s) is much less than the theoretical value (= 1420 Mc/s) for a free atom, a discrepancy which is not easily explained. In ice containing hydrogen peroxide at 77°K., the doublet attributable to hydrogen is weakened, but a new one appears of lower separation which is probably attributable to the OH radical; a result which suggests that the reaction

$$H + H_2O_2 \rightarrow H_2O + OH \qquad 21.$$

can occur at these temperatures. The hyperfine structure of atomic hydrogen has also been observed in the spectrum of pure phosphoric acid, and approximately 5 M H_2SO_4 and $HClO_4$, at 77°K. to which a dose of the order of 10^7r of γ-rays had been given (119).

Grossweiner & Matheson (120) have extended their previous work (121)

on the luminescence of ice excited by 50 kev x-rays and tritium β-rays. In a most elegant investigation they measured the fluorescence spectrum, the kinetics of its "build up" to the steady state, the dependence of the steady state intensity on the dose rate, and the effects of temperature and small amounts of salts. In addition the x-ray-induced thermoluminescence, which is suppressed by H_2O_2, NaCl, and HCl, was studied. The authors regard the luminescence as resulting from release of the electrons from their traps followed by migration to and radiative capture by other impurity centres. The release is thought to be attributable either to thermal activation of a single site or to reaction between adjacent species; for the latter the reaction

$$OH + H^- \rightarrow H_2O + e^-$$

is suggested.

Whilst the evidence for free hydroxyl radicals is regarded as secure, the evidence presented by Dainton & Collinson (122) has been effectively questioned by Fiquet & Bernas (123), who have shown that the infrared absorption band at 2,200 cm.$^{-1}$, assigned by Collinson & Dainton to *C—D* vibrations is shown by polyacrylonitrile and polymethacrylonitrile prepared in deuterium-free systems, and even by the product obtained by anionic polymerisation of acrylonitrile and propionitrile. No definite assignment for this band can be given. However Collinson (124) has found, by mass-spectrometric and ionisation methods respectively, that polyacrylonitrile prepared by irradiation of dilute solutions in deuterium oxide or tritiated water do contain chemically-bound deuterium and tritium. Thus, whilst it is likely that atoms are formed in the primary act and do inititate polymerisation, the infrared evidence is unreliable.

Kelly, Rigg & Weiss (125) have shown that, when de-aerated acidified ferrous sulphate solution enriched in deuterium oxide is irradiated, the isotopic composition of the evolved hydrogen cannot be accounted for merely by supposing that hydrogen-water exchange is catalysed by hydrogen atoms. In oxygen-saturated solution, or solutions containing ceric ion, where the hydrogen atoms are likely to be oxidised, the separation factor decreases but does not become unity, and the authors consider that the separation arises from the interaction of excited water molecules, in a reaction which is normally responsible for the molecular yield.

Reaction studies.—A feature of 1954 has been the increased attention paid to heavy particle radiations and to studies of the relative magnitudes of the "molecular" yields of hydrogen and hydrogen peroxide and their dependence (if any) on the experimental variables. Considerable differences exist between the methods of presentation of results. Allen (116) and many other workers assume that H, OH, H_2 and H_2O_2 are the only products, thereby interrelating the coefficients in equation 20. He postulates three equations designated *F*, *R*, and *E*

$$\left.\begin{array}{l} 2H_2O \rightarrow H_2 + H_2O_2 \quad (F) \\ H_2O \rightarrow H + OH \quad (R) \\ 2H_2O \rightarrow 2H + H_2O_2 \quad (E) \end{array}\right\} \text{ whence } \left\{\begin{array}{ll} G_{H_2} = F;\ G_{H_2O_2} = F + E & 22. \\ G_H = R + 2E;\ G_{OH} = R & 23. \\ G_{-H_2O} = 2(F + E) + R & 24. \end{array}\right.$$

but Hart prefers the formulation 1, 2, and 3.

$$\left.\begin{array}{ll} H_2O \rightarrow H + OH & (1) \\ H_2O \rightarrow \tfrac{1}{2}H_2 + \tfrac{1}{2}H_2O_2 & (2) \\ H_2O \rightarrow H + \tfrac{1}{2}H_2O_2 & (3) \end{array}\right\} \text{ whence } \left\{\begin{array}{rl} G_{H_2} = \tfrac{1}{2}G_2;\ G_{H_2O_2} = \tfrac{1}{2}(G_2 + G_3) & 23. \\ G_H = G_1 + G_3;\ G_{OH} = G_1 & 22. \\ G_{-H_2O} = G_1 + G_2 + G_3 & 24. \end{array}\right.$$

To avoid confusion and to leave open the questions (*a*) whether H, OH, H_2, and H_2O_2 are the only products and (*b*) whether yields are truly independent of the nature and concentration of the solute, we shall use the following symbols. $G^M_{H_2}$ and $G^M_{H_2O_2}$ for the "molecular" yields of hydrogen and hydrogen peroxide as determined in an experiment the conditions of which may be specified by additional fairly obvious parenthetical subscripts. Thus $G^M_{H_2O_2(\gamma, O_2, Fe^{+2}0.8)}$ would be that part of the yield of H_2O_2 per 100 ev as measured in an oxygen saturated, 0.8 *N* H_2SO_4 solution of ferrous ion using γ-rays, not due to the reaction of HO_2 radicals. Whenever high energy light particle radiation is used, $G_{Fe^{3+}}$ (O_2, 0.8) will be taken as 15.5. Radical yields of H (G^R_H) and OH (G^R_{OH}) will be similarly qualified by a subscript. This method of presentation has the advantage of being dissociated from stoichiometric equations of the type of 22, 23, and 24 which suggest modes of origin for the primary products.

(*a*) Heavy particle radiation: Air-free aqueous solutions of acetic acid bombarded with 35 Mev helium ions give rise to hydrogen peroxide and succinic acid, the concentration of each of the products approaching a limiting value (126). Analysis of the gaseous products formed when sealed ampoules containing aqueous solutions are placed in the Chatillon pile (127) has shown that the permanent gas is largely hydrogen and oxygen, the amount of the latter being greater than that from pure water except in the cases of ferrous sulphate, benzene, phenol, and benzoic acid as solutes. The composition of the condensable gases is dependent on the functional groups in the organic solute. Irradiation under bismuth or cadmium shields indicates that the water decomposition is mainly attributable to the neutron component of the pile radiation.

Much work has been done with Po^{210} α-rays, with good agreement between different investigators (8, 9, 10). Values of $G_{Fe^{+3}(O_2,\ 0.8,)}$ of 5.94 ± 0.1(8), 6.2 ± 0.2(9), and 6 (10a) have been obtained and should be compared with 5.2 and 4.2 for the internal sources based on the $B^{10}(n, \alpha)Li^7$ and $Li^6(n, \alpha)T^3$ reactions respectively (9). The hydrogen yields are generally in excellent agreement being $G_{H_2(Fe^{+2},O_2,0.8,Po\alpha)} = 1.56(8)$, 1.57 (9); $G_{H_2(NaPO_2,Po\alpha,O_2)} = 1.8$ (10 c); $G_{H_2(Po\alpha)}$ for many dilute solutions = 1.7 to 1.9 (10) and for pure water 1.8 (10d). The remarkably constant value of G_{H_2} irrespective of whether oxidation, reduction, or polymerisation is occurring in the system supports the idea that the hydrogen is produced by a mechanism which does not involve hydrogen atoms as intermediates.[1]

[1] In two papers (8, 9) concerned with ferrous sulphate solution values of $G_H{}^R$ and $G_{H_2O_2}$ are either given or can be calculated and the agreement is good; thus $G_{H_2O_2}{}^M = 1.74$ and 1.74; $G_H{}^R = 0.77$ and 0.70.

$G^M_{H_2O_2}$ generally decreases with solute concentration, e.g. at 2×10^{-4} M sodium phosphite $G^M_{H_2O_2}=0.9$ and it decreases to zero at 5×10^{-3} M, the oxidation yield of the solute showing a corresponding rise so that $G_{H_2O_2}+G_{PO_4}^{\equiv}$ is constant at ~1.1. Of particular significance is that fact that chloride ion inhibits the formation of H_2O_2, and that in 0.4 M HCl to which H_2O_2 has been added, irradiation with Po^{210} α-rays leads to complete destruction of the H_2O_2 (10b). It therefore seems possible that hydroxyl radicals are intermediates in the formation of molecular H_2O_2, and that other solute —OH reactions can compete effectively. Anta & Haissinsky (10a) find that G for ceric reduction is 3.24 independent of the dose rate. Using the value $G_{H_2O_2}\sim1$ they conclude that reduction of Ce(IV) by hydroxyl radicals must be taking place. However, if Hart & Miller's values of $G_{H_2O_2}$ are accepted it is not necessary to assume the occurrence of this reaction.

(*b*) β-particles, x- and γ-rays: The results reported in the period reviewed

TABLE II

RADICAL ($G_H{}^R$, $G_{OH}{}^R$) AND MOLECULAR ($G_{H_2}{}^M$, $G_{H_2O_2}{}^M$) YIELDS* IN AQUEOUS SYSTEMS IRRADIATED BY X- OR γ-RAYS PUBLISHED IN 1954

[$G_{Fe^{+3}(O_2,\ 0.8)}=15.5$ throughout]

Radiation	Reference Number	System	$G_{H_2O_2}{}^M$	$G_{H_2}{}^M$	$G_H{}^R$	$G_{OH}{}^R$
Co^{60}	134	O_2-sat KBr	0.76	0.41	2.8	2.1
Co^{60}	128	KI, KBr at own pH KNO_2(pH 11), $NaAsO_2$(pH 10.4)	—	0.44	—	—
Co^{60}	128	Same at 0.4 M H_2SO_4	—	0.385	—	—
Co^{60}	128	Same at 1.0 M H_2SO_4		0.37		
Co^{60}	129	Air-sat KBr soln. 0.4 M H_2SO_4	0.78	0.39	3.68	2.90
Co^{60}		Air-sat KBr soln 0.01 N H_2SO_4	0.75	0.42	2.76	2.11
Co^{60}	130	Acid Ce(IV) sat with H_2 or CO	—	—	2.52	2.52
Co^{60}	8	0.4 M H_2SO_4, $FeSO_4$	—	0.425	—	—
Co^{60}	8	KBr (own pH)	—	0.51	—	—
Co^{60}	131	O_2 sat, HCOOH solution pH 0.32	0.86	0.265	3.59	2.40
Co^{60}	131	O_2 sat, HCOOH solution pH 2.10	0.81	0.35	3.47	2.56
Co^{60}	131	O_2 sat, HCOOH solution pH 2.70	0.52	0.42	3.02	2.83
Co^{60}	131	O_2 sat, HCOOH solution pH 6.81	0.48	0.41	2.98	2.84
Co^{60}	131	O_2 sat, HCOOH solution pH 11.58	0.53	0.44	3.10	2.92
Co^{60}	132	O_2 sat[HCOOH] = 10^{-4} M	—	0.32	—	2.58
Co^{60}	132	O_2 sat[HCOOH] = 10^{-2} M	—	0.43	—	2.82
Co^{60}	132	O_2 sat[HCOOH] = 1 M	—	0.43	—	3.44
200 kev, p, x	28†	$FeSO_4$, 0.4 M H_2SO_4		0.52	3.63	3.63

* The values in this table are those given by the authors multiplied by the appropriate factor to reduce to a common value $G_{Fe^{+3}(O_2,\ 0.8)}=15.5$.

† Assuming $G_H=G_{OH}$; $G_{H_2}{}^M=G_{H_2O_2}{}^M$.

are presented in Table II. With one exception (28) the value of $G^M_{H_2O_2}$ exceeds that of $G^M_{H_2}$ in the same system. In the formic acid-oxygen system, Hart (131) has demonstrated that as the pH is increased to 4, $G^M_{H_2O_2}$ decreases to zero whilst $G^M_{H_2}$ and G^R_{OH} increase to values of 0.45 and 2.82 respectively. This pH effect is a most important result and points to the necessity of studies of the effect of changes of acidity in other systems.

It is now certain that a number of solutes which do not themselves react with hydrogen peroxide can nevertheless influence the yield of this product in both air-free and air-saturated solutions. The case of bromide ion has been particularly well-investigated by Sworski (129), who found that in 0.01 N H_2SO_4 solution, $G_{H_2O_2}$ decreases from 1.16 when [KBr] = 1μM. to 0.69 when [KBr] = 10 mM. Dainton & Sutton (133) reported a similar influence of ferrous sulphate on $G^M_{H_2O_2}$ over the limited range of concentrations for which measurements of the H_2O_2 yields are possible in this system. It seems probable that the "molecular" hydrogen peroxide is formed via at least one hydroxyl radical as an intermediate and that solutes which react very rapidly with OH will materially reduce the apparent value of $G^M_{H_2O_2}$. Since Fe^{++} performs this function, other solutes which react with OH more rapidly than ferrous ion should be more effective. The special case of a solute which can react with both H and OH is particularly interesting, since at low concentration in air-free water it should capture all the hydrogen atoms and hydroxyl radicals which are responsible for initiating the back reaction (written in equation 27)

$$H + OH + x(H_2 + H_2O_2) \rightarrow (2x + 1)H_2O \quad x > 1 \qquad 27.$$

and thus enable hydrogen and hydrogen peroxide to accumulate; whereas at high concentrations it should begin to compete effectively with the H_2O_2-forming reaction, written formally as

$$2OH \rightarrow H_2O_2, \qquad 28.$$

and thus cause the yield of H_2O_2 to decrease. Hence the observed yield of H_2O_2 in air-free water should increase from zero, pass through a maximum value, and finally decline as the concentration of the solute is increased. One such solute is acrylamide (82).

This sensitivity of $G^M_{H_2O_2}$ is in marked contrast to the behavior of $G^M_{H_2}$ which is independent of pH in the range of from 4 to 12 (131), of temperature (128), and of most solutes (128). The total hydrogen yield is naturally dependent on the solute; for example the initial yield of hydrogen is increased by iodide ion in acid solution. This is possibly caused by the oxidation of iodide ion by H_2^+, i.e.

$$H + H^+ + I^- \rightarrow H_2 + I \qquad 29.$$

However as the reaction proceeds, iodine accumulates, reaction 30 can proceed, and G_{H_2} decreases to $G_{H_2}{}^M$.

$$H + I_2 \rightarrow HI + I \qquad 30.$$

According to Hochanadel & Ghormley (134) the hydrogen yield in oxygen saturated water is raised from 0.20 to 0.41 by potassium bromide because the removal of hydroxyl radicals by bromide ion prevents the reaction

$$OH + H_2 \rightarrow H_2O + H \qquad 31.$$

Combining this result with measurement of the peroxide yields and with Sworski's data, radical and molecular yields can be calculated.

Careful work on air-saturated acidified ferrous sulphate solution containing millimolar chloride reveals a temperature coefficient of 0.04 ± 0.03 per degree for the yield of ferric ion which Schwarz (135) considers to result from extraneous causes, although it should be noted that a coefficient of 0.026 has been obtained by other investigators (133). Vermeil & Cottin (136) have found that in air-free acidified solutions of *n*-butanol, cyclohexane, or cyclohexanol (RH in equation 32) there is no oxidation of ferrous ion, but there is complete reduction of ferric ion, an effect which is caused by the occurrence of the reactions

$$\cdot OH + H - R \rightarrow H_2O + R\cdot \qquad 32.$$

$$R\cdot + Fe^{3+}OH^- \rightarrow ROH + Fe^{++} \qquad 33.$$

When benzene is present, there is an equilibrium with approximately equivalent amounts of ferrous and ferric ion present and it must be concluded, as had previously been demonstrated by Baxendale & Magee (137), that the phenyl radical can also oxidise ferrous ion

$$C_6H_5\cdot + Fe^{++} + H^+ \rightarrow C_6H_6 + Fe^{+++} \qquad 34.$$

The initial reduction yield in these systems is about 7, which exceeds all the values of G_{OH} given in the table, and strongly suggests that the ferric ion is also being reduced by H atoms. It would be most interesting to measure the hydrogen yields in this system.

Complete reduction of ferric ion is also obtained even in aerated solution when it is complexed with *ortho*-phenanthroline either in the mononuclear blue form (138) or the dinuclear buff-coloured form (139). Both reactions are complex, but the G values are high and it seems likely that H, OH, and HO_2 can all reduce the solute, that hydrogen peroxide may also do so somewhat slowly, and that the ligand itself may be attacked. Reduction also seems to occur in deaerated solutions of methylene blue, co-enzyme I, nicotinamide methochloride, and cytochrome-C protected from OH attack by sodium benzoate or alcohol (140), and in the inactivation of bacteriophage (141).

Barron (142) has surveyed the processes involved in solutions of biologically significant solutes where oxidation is generally the more important, and after-effects often exist. Further examples of these behaviour types have been reported (143). Such oxidations frequently have a valuable specific character; thus Phillips (144) has shown that sugar alcohols are oxidised by

1.5 Mev electrons to the aldo-sugar. Other oxidative reactions include the x-ray degradation of polymethacrylic acid (145), the inactivation of yeast alcohol dehydrogenase (146), and the liberation of acid from chloral hydrate and chloroform solutions (15). These last reactions are chain processes involving mutual termination, and sector experiments indicate lifetimes of the orders 0.1 and 1.0 sec. respectively.

An elegant study of the γ-ray and photochemically-induced exchange of oxygen between water vapour and oxygen (147) has revealed the existence of a chain reaction above pH 9 which requires for its interpretation the assumption that hydroxyl radicals undergo electrolytic dissociation to H^+ and O^- with a K_a of about 10^{-9}.

The primary act.—The only purely theoretical paper published during 1954 is by Laidler (148), who has discussed the potential energy diagrams for the ground and excited states of water and its molecular ions. He concludes that the H_2O^- ion dissociates into $2H+O^-$ rather than into $H+OH^-$, a result which is contrary to the findings of electron swarm experiments and the appearance of H^- at low electron energies in the mass-spectrometer.

The physical measurements on ice and frozen aqueous solutions (118 to 121) leave little doubt that hydroxyl radicals and hydrogen atoms are formed, and it is also probable that even in ice the hydrogen atoms have a degree of mobility which enables them to react with hydrogen peroxide. The presence of hydrogen and hydrogen peroxide in the products when solutes are present in air-free water which react with either H or OH is clear evidence that, as proposed by Allen many years ago the latter can initiate the reaction 27. The new data reported this year are consistent with equation 20, but there is still little certainty about its detailed mechanism. Weiss' results (125) suggest (but do not prove) that the bimolecular interaction of excited molecules may result in direct formation of H_2 and H_2O_2, but it seems clear that $G^M_{H_2O_2}$ is generally greater than $G^M_{H_2}$ and very much more sensitive to the presence of solutes, being decreased by solutes which are known to be reactive to OH. The inequality, $G^M_{H_2O_2} > G^M_{H_2}$, is explicable on the radical diffusion theory of Samuel & Magee (63) concerning the spatial distribution of the primary act equally well as on the older theory, provided it is assumed that the diffusion of hydrogen atoms is more rapid than that of OH radicals; but if this assumption is made it is difficult to account for the solute dependence of $G^M_{H_2O_2}$ when $G^M_{H_2}$ is so remarkably constant. The larger molecular yield obtained with heavy particle rays and their similar solute dependence are arguments in favour of the precursors of the molecular hydrogen peroxide being very reactive and simulating the behaviour of hydroxyl radicals to a degree which lends support to the view that they are hydroxyl radicals. In this case the observations of Hart that $G^M_{H_2O_2}$ decreases rapidly with increased pH may perhaps be interpreted in terms of his proposal that the hydroxyl radical dissociates. One might envisage the reactions $2O^- \rightarrow O_2^{=}$ and $O^- + OH \rightarrow HO_2^-$ as much less likely than $2OH \rightarrow H_2O_2$ and have a negligible

$G^{M}_{H_2O_2}$ in alkaline solution containing a reactive substrate for hydroxyl radicals.

On the exclusively theoretical side many interesting points have been made by Platzmann (3) of which only the major one can be mentioned here. Since the gaseous reaction

$$e^- + H_2O \rightarrow H + OH^- \qquad 35.$$

is slightly endothermic, the corresponding reaction in solution can only occur provided that some of the hydration energy of OH^- is made available. The necessary dipole relaxation takes time and a thermalised electron is therefore free to diffuse for periods of the order of 10^{-11} seconds. Thus the hydrogen atoms may be produced at sites even more remote from the hydroxyl radicals than Lea (2) supposed. If this is correct it is easier to see why $G^{M}_{H_2O_2} > G^{M}_{H_2}$ but it is also more difficult to account for solute influences.

LITERATURE CITED

1. Magee, J. L., *Ann. Rev. Nuclear Sci.*, **3,** 171 (1954)
2. Lea, D. E., *Actions of Radiations on Living Cells*, 2nd ed. (Cambridge University Press, Cambridge, England, 416 pp., 1955)
3. *Basic Mechanisms in Radiobiology II Physical and Chemical Aspects* (Magee, J. L., Kamen, M. D., and Platzman, R. L., Ed., National Research Council, Washington, D. C., 145 pp., 1953)
4. *Ann. Repts. on Progr. Chem.* (*Chem. Soc. London*), **50,** 63 (1954)
5. Firestone, R. F., and Willard, J. E., *Rev. Sci. Instr.*, **24,** 904 (1953)
6. Hardwick, T. J., (Private communication)
7. Dainton, F. S., Ivin, K. J., and Sheard, D. R., *Trans. Faraday Soc.* (In press)
8. Miller, N., and Wilkinson, J., *Trans. Faraday Soc.*, **50,** 690 (1954)
9. McDonell, W. R., and Hart, E. J., *J. Am. Chem. Soc.*, **76,** 2121 (1954)
10. (a) Anta, M. C., and Haissinsky, M., *J. chim. phys.*, **51,** 33 (1954)
    (b) Anta, M. C., and Haissinsky, M., *J. chim. phys.*, **51,** 401 (1954)
    (c) Cottin, M., *J. chim. phys.*, **51,** 404 (1954)
    (d) Anta, M. C., and Lefort, M., *J. chim. phys.*, **51,** 29 (1954)
    (e) Lefort, M., *J. chim. phys.*, **51,** 351 (1954)
11. McDonell, W. R., and Newton, A. S., *J. Am. Chem. Soc.*, **76,** 4651 (1954)
12. Hickling, A., and Linacre, J. K., *J. Chem. Soc.*, 3595 (1952); 711 (1954)
13. Hart, E. J., and Matheson, M. S., *Discussions Faraday Soc. No. 12*, 169 (1952)
14. Dainton, F. S., and Rowbottom, J., *Trans. Faraday Soc.*, **49,** 1160 (1953)
15. Freeman, G. R., Van Cleave, A. B., and Spinks, J. W. T., *Can. J. Chem.*, **32,** 322 (1954); Hummel, R. W., Van Cleave, A. B., and Spinks, J. W. T., *Can. J. Chem.*, **32,** 522 (1954)
16. Hayward, E., and Hubbel, J. H., *J. Appl. Phys.*, **25,** 506 (1954); Sternglass, E. J., *Phys. Rev.*, **95,** 345 (1954); Müller, R. H., *Phys. Rev.*, **93,** 891 (1954); Johns, H. E., Hunt, J. W., and Fedoruk, S. *Brit. J. Radiol.*, **27,** 443 (1954)
17. Warner, C., and Rohrlich, F., *Phys. Rev.*, **93,** 406 (1954)
18. Bortner, T. E., and Hurst, G. S., *Phys. Rev.*, **93,** 1236 (1954); Erskine, G. A., *Proc. Roy. Soc.* (*London*), [A]**224,** 362 (1954)
19. Brysk, H., *Phys. Rev.*, **96,** 419 (1954)
20. Boag, J. W., *Natl. Bur. Standards Report No. 2903*, (1953); *Radiation Research*, **1,** 323 (1954)
21. Zirkle, R. E., *J. Cellular Comp. Physiol.*, **39,** Suppl. 1, 75 (1952)
22. Lazo, R. M., Dewhurst, H. A., and Burton, M., *J. Chem. Phys.*, **22,** 1370 (1954)
23. Saldick, J., and Allen, A. O., *J. Chem. Phys.*, **22,** 438 (1954)
24. Miller, N., *Nature*, **171,** 688 (1953)
25. Hochanadel, C. J., and Ghormley, J. A., *J. Chem. Phys.*, **21,** 880 (1953)
26. Cormack, D. V., Hummel, R. W., Johns, H. E., and Spinks, J. W. T., *J. Chem. Phys.*, **22,** 6 (1954)
27. Weiss, J(erome), Bernstein, W., and Kuper, J. B. H., *J. Chem. Phys.*, **22,** 1593 (1954)
28. Farmer, F. T., Rigg, T., and Weiss, J., *J. Chem. Soc.* (*London*), 3248 (1954)
29. Rødstom, G., and Svedberg, T., *Nature*, **171,** 512 (1953)
30. Suttle, J. F., *U. S. Atomic Energy Commission Report No. LA-1615* (1954)
31. Taplin, G. V., and Douglas, C. H., *U. S. Patent*, 2,682,510
32. Hart, E. J., and Gordon, S., *Nucleonics*, **12** (4), 40 (1954)
33. Hart, E. J., and Walsh, P. D., *Radiation Research*, **1,** 342 (1954)

34. Franklin, J. L., and Field, F. H., *J. Am. Chem. Soc.*, **76**, 1994 (1954); and McDowell, C. A., and Cox, B. C., *J. Chem. Phys.*, **22**, 946 (1954)
35. Lossing, F. P., Ingold, K. U., Henderson, I. H. S., *J. Chem. Phys.*, **22**, 6218 (1954); Waldron, J. D., *Trans. Faraday Soc.*, **50**, 102 (1954)
36. Gutbier, H., Neuert, H., *Z. Naturforsch.*, **9a**, 335 (1954)
37. Lindholm, E., *Z. Naturforsch.*, **9a**, 535 (1954)
38. Pahl, M., *Z. Naturforsch.*, **9b**, 188 (1954)
39. Leder, L. B., and Marton, L., *Phys. Rev.*, **95**, 1345 (1954)
40. Combrisson, J., and Uebersfeld, J., *Compt. Rend.*, **238**, 1397 (1954)
41. Essex, H., *J. Phys. Chem.*, **58**, 42 (1954)
42. Conference on *The Physics of Ionised Gases* held at University College, London, England, April, 1953
43. Watanabe, K., and Zelikoff, M., *J. Opt. Soc. Amer.*, **43**, 753 (1953)
44. Niira, K., *J. Phys. Soc. Japan*, **7**, 193 (1952)
45. Lampe, F. W., and Noyes, R. M., *J. Am. Chem. Soc.*, **76**, 2140 (1954)
46. Rutenberg, A. C., and Taube, H., *J. Am. Chem. Soc.*, **72**, 5561 (1950); **75**, 763 (1953)
47. Hunt, J. P., and Taube, H., *J. Am. Chem. Soc.*, **74**, 5999 (1952)
48. Hamill, W. H., and Williams, R. R., *J. Chem Phys.*, **22**, 53 (1954)
49. Richards, E. W. T., *Proc. Phys. Soc.* (*London*), [A]**67**, 922 (1954)
50. Miller, N., *Discussions Faraday Soc., No. 12*, 46 (1952)
51. Weiss, J., *Nature*, **174**, 78 (1954)
52. Hogan, A. J., *U. S. Atomic Energy Commission Report, SO-3255*, (1954); abstract given in *Nuclear Science Abstracts*, **8**, (21), Abstract No. 6426 (1954)
53. Harteck, P., and Dondes, S., *J. Chem. Phys.*, **22**, 953 (1954)
54. Suzuki, M., and Miyami, H., *J. Chem. Soc. Japan*, **75**, 813 (1954) (In Japanese and not available to the author in English)
55. Devins, J. C., and Burton, M., *J. Am. Chem. Soc.*, **76**, 2618 (1954)
56. Dorfman, L. M., and Hemmer, B. A., *Phys. Rev.*, **94**, 754 (1954); *J. Chem. Phys.*, **22**, 1555 (1954)
57. Tolbert, B. M., and Lemmon, R. M., *U. S. Atomic Energy Commission Report UCRL-2704* (1954)
58. McDonell, W. R., and Newton, A. S., *J. Am. Chem. Soc.*, 4651 (1954)
59. Coleby, B., Keller, M., and Weiss, J., *J. Chem. Soc.* (*London*), 66 (1954)
60. Chapiro, A., Boag, J. W., Ebert, M., and Gray, L. H., *J. chim. phys.*, **50**, 468 (1953)
61. Dainton, F. S., and Miller, N., *Proc. XIIIth Intern. Congr. Pure and Appl. Chem., London, 1947;* see also Dainton, F. S., *Ann. Rept. Progr. Chem.*, **45**, 31–32 (1948)
62. Chapiro, A., *J. chim. phys.*, **51**, 165 (1954)
63. Magee, J. L., and Samuel, A. H., *J. Chem. Phys.*, **21**, 1080 (1953)
64. Dainton, F. S., and Collinson, E., *Discussions Faraday Soc. No. 12*, 212, 226, (1952)
65. Burton, M., and Manion, W. P., *J. Phys. Chem.*, **56**, 560 (1952)
66. Burton, M., and Patrick, W. N., *J. Phys. Chem.*, **58**, 424 (1954)
67. Burton, M., and Patrick, W. N., *J. Phys. Chem.*, **58**, 421 (1954)
68. Maddock, A. G., *Discussions Faraday Soc., No. 12*, 124 (1952)
69. Burton, M., and Patrick, W. N., *J. Chem. Phys.*, **22**, 1150 (1954)
70. Bowen, E. J., *Proc. Phys. Soc.* (*London*), [A]**62**, 26 (1949)
71. Franck, J., and Livingston, R. S., *Revs. Mod. Phys.*, **21**, 505 (1949)

72. Birks, J. B., *Phys. Rev.*, **94**, 1567 (1954)
73. Harmer, D. E., Anderson, L. C., and Martin, J. J., *Chem. Eng. Progr. Symposium Ser., No. 11*, 253 (1954)
74. Hamill, W. H., and Williams, R. R., Jr., *J. Chem. Phys.*, **22**, 53 (1954); *Radiation Research*, **1**, 158 (1954); Cochran, E. L., Hamill, W. H., and Williams, R. R., Jr., *J. Am. Chem. Soc.*, **76**, 2145 (1954); Hamill, W. H., Williams, R. R., Jr., Cochran, E. L., and Roy, J. C., *J. Am. Chem. Soc.*, **76**, 3274 (1954)
75. Mund, W., van Meersche, M., and Momigny, J., *Bull. soc. chim. Belges*, **62**, 645 (1954)
76. Otozai, K., Kume, S., Nagai, S., Yamamoto, T., and Fukushima, S., *Bull. Chem. Soc. Japan*, **27**, 476 (1954)
77. Lewis, J. J., Martin, J. J., and Anderson, L. C., *Chem. Eng. Progr.*, **50**, 249, (1954); also *U. S. Atomic Energy Commission Report, 1943-17-P* (1954)
78. Ballantine, D. S., *U. S. Atomic Energy Commission Report, B.N.L.-294* (1954); *B.N.L.-317* (1954)
79. Burton, M., and Patrick, W. N., *J. Am. Chem. Soc.*, **76**, 2626 (1954)
80. Schulz, R., Renner, G., Henglein, A., and Kern, W., *Makromol. Chemie*, **12**, 20 (1954)
81. Mesrobian, R. B., Ander, P., Ballantine, D. S., and Dienes, G. J., *J. Chem. Phys.*, **22**, 565 (1954); *Phys. Rev.*, **94**, 1413 (1954); Henglein, A., and Schulz, R., *Z. Naturforsch.*, **9b**, 617 (1954)
82. Collinson, E., Dainton, F. S., and McNaughton, G. S., *J. Chim. Phys.* (In press)
83. Ballantine, D. S., Colombo, P., Glines, A., and Manowitz, B., *Chem. Eng. Progr., Symposium No. 11*, **267** (1954)
84. Chapiro, A., and Wahl, P., *Compt. Rend.*, **238**, 1803 (1954); Chapiro, A., Magat, M., Sebban, J., and Wahl, P., *Contribution à la cinetiques des polymerisations vinyliques* (Paper presented at *Intern.* Symposium on Macromolecular Chemistry, Milan, Italy, Sept., 1954)
85. Ballantine, D. S. (Personal communication)
86. Manowitz, B., Horrigan, R. V., and Bretton, R. H., *U. S. Atomic Energy Commission Report B.N.L.-141* (1951)
87. Dainton, F. S., and Collinson, E., *Discussions Faraday Soc., No. 12*, 212, p. 224 (1952)
88. Dainton, F. S., Devlin, T. R. E., and Small, P. A., *Trans. Faraday Soc.*, **51**, (1955)
89. Ivin, K. J. (Private communication); Small, P. A. (Private communication)
90. Fowler, J. F., and Farmer, F. T., *Nature*, **173**, 317 (1954)
91. Fowler, J. F., and Farmer, F. T., *Nature*, **174**, 800 (1954)
92. Fowler, J. F., and Farmer, F. T., *Nature*, **174**, 136 (1954)
93. Hannan, R. S., and Shepherd, H. J., *Brit. J. Radiol.*, **27**, 36 (1954); Hannan, R. S., *Food Sci. Abstr.*, **26**, 121 (1954)

Breakdown of macromolecules (References 94 to 115b)

(1) General reviews

94. Charlesby, A., *Nucleonics*, **12**, (6), 18 (1954)
95. Miller, A. A., Lawton, E. J., and Balwit, J. S., *J. Polymer Sci.*, **14**, 503 (1954)
96. Alexander, P., and Charlesby, A., *Nature*, **173**, 578 (1954)

(2) Pure hydrocarbons

97. Charlesby, A., *Proc. Roy. Soc.* (*London*), [A]**222**, 60 (1954)

98. Charlesby, A., *U.K. Atomic Energy Authority Report, A.E.R.E., M/R-1415* (1954)
99. Boelhouwer, C., and Waterman, H. I., *Research*, **7**, (56) (1954)

(3) Polythene (Polyethylene)

100. Anon., *Chem. Eng. News*, **32**, 1342 (1954)
101. Baskett, A. C., and Miller, C. W., *Nature*, **174**, 364 (1954)
102. Lawton, E. J., Balwit, J. S., and Bueche, A. M., *Ind. Eng. Chem.*, **46**, 1703 (1954)
103. Lawton, E. J., Zemany, P. D., and Balwit, J. S., *J. Am. Chem. Soc.*, **76**, 3437 (1954)
104. Ballantine, D. S., Dienes, G. J., Manowitz, B., Ander, P., and Mesrobian, R. B., *J. Polymer Sci.*, **13**, 410 (1954)
105. Dole, M., and Keeling, C. D., *J. Am. Chem. Soc.*, **75**, 6082 (1953)
106. Dole, M., Keeling, C. D., and Rose, D. G., *J. Am. Chem. Soc.*, **76**, 4304 (1954)

(4) Polyethylene terephthalate, Nylon, Siloxanes, Poly methyl methacrylate, cellulose and rubber

107. Todd, A , *Nature*, **174**, 613 (1954)
108. Little, K., *Nature*, **173**, 680 (1954)
109. Charlesby, A., *Nature*, **173**, 679 (1954)
110. Alexander, P., Charlesby, A., and Ross, M., *Proc. Roy. Soc.* (*London*), [A]**223**, 392 (1954)
111. Charlesby, A., *U.K. Atomic Energy Authority Report, A.E.R.E., M/R-1342* (1954)
112. Charlesby, A., *Atomics*, **5**, 12 (1954)
113. Hornig, R. E., and Sheppard, C. W., *J. Phys. Chem.*, **50**, 119, 144 (1946)
114. Lind, S. C., and Bardwell, D. C., *J. Am. Chem. Soc.*, **48**, 1575, 2335 (1926)
115a. Charlesby, A., *Proc. Roy. Soc.* (*London*), [A]**215**, 187 (1952)
115b. Charlesby, A., *Nature*, **171**, 167 (1953)
116. Allen, A. O., *Radiation Research*, **1**, 85 (1954)
117. Dewhurst, H. A., Samuel, A. H., and Magee, J. L., *Radiation Research*, **1**, 62 (1954)
118. Smaller, B., Matheson, M. S., and Yasaitis, E. L., *Phys. Rev.*, **94**, 202 (1954)
119. Livingston, R., Zeldes, H., and Taylor, E. H., *Phys. Rev.*, **94**, 725 (1954)
120. Grossweiner, L. I., and Matheson, M. S., *J. Chem. Phys.*, **22**, 1514 (1954)
121. Grossweiner, L. I., and Matheson, M. S., *J. Chem. Phys.*, **21**, 1654 (1952)
122. Dainton, F. S., and Collinson, E., *Discussions Faraday Soc., No. 12*, 212, p. 221 (1952)
123. Fiquet, F., and Bernas, A., *J. chim. phys.*, **51**, 47 (1954)
124. Collinson, E. (To be published)
125. Kelly, P., Rigg, T., and Weiss, J., *Nature*, **173**, 1130 (1954); *Chemistry & Industry*, 1291 (1954)
126. Garrison, W. M., Hayward, H. R., and Weeks, B. M., *Radiation Research*, **1**, 97 (1954)
127. Rolin, M., *J. chim. phys.*, **51**, 35 (1954)
128. Schwarz, H. A., Losee, J. P., and Allen, A. O., *J. Am. Chem. Soc.*, **76**, 4693 (1954)
129. Sworski, T. J., *J. Am. Chem. Soc.*, **76**, 4687 (1954)
130. Johnson, E. R., and Weiss, J(erome), *J. Chem. Physics*, **22**, 752 (1954)
131. Hart, E. J., *J. Am. Chem. Soc.*, **76**, 4198 (1954)

132. Hart, E. J., *J. Am. Chem. Soc.*, **76,** 4312 (1954)
133. Dainton, F. S., and Sutton, H. C., *Trans. Faraday Soc.*, **49,** 1011 (1953)
134. Ghormley, J. A., and Hochanadel, C. J., *J. Am. Chem. Soc.*, **76,** 3351 (1954)
135. Schwarz, H. A., *J. Am. Chem. Soc.*, **76,** 1587 (1954)
136. Vermeil, C., and Cottin, M., *J. chim. phys.*, **51,** 24 (1954)
137. Baxendale, J. H., and Magee, J. L., *Discussions Faraday Soc., No. 14,* 160 (1953); *Trans. Faraday Soc.*, **51,** 205, (1955)
138. Amphlett, C. B. (Private communication)
139. Lefort, M., *J. chim. phys.*, **50,** 580 (1953)
140. Stein, G., and Swallow, A. J., *Nature,* **173,** 937 (1954)
141. Alper, T., and Ebert, M., *Nature,* **173,** 987 (1954)
142. Barron, E. S. G., *Radiation Research,* **1,** 109 (1954)
143. For example, Conway, B. E., *Nature,* **173,** 579 (1954); Weiss, J., and Scholes, G., *Nature,* **173,** 267 (1954); Jayson, G. G., Scholes, G., and Weiss, J., *Biochem. J.* (*London*), **57,** 886 (1954)
144. Phillips, G. O., *Nature,* **173,** 1044 (1954)
145. Alexander, P., and Fox, M., *Trans. Faraday Soc.*, **50,** 605 (1954)
146. Barron, E. S. G., *Arch. Biochem. and Biophys.*, **48,** 149 (1954)
147. Hart, E. J., Gordon, S., and Hutchinson, D. A., *J. Am. Chem. Soc.*, **75,** 6165 (1954)
148. Laidler, K. J., *J. chem. phys.*, **22,** 1740 (1954)
149. Ehrenberg, L., and Saeland, E., *Chemical Dosimetry of Radiation Giving Different Ion Densities. An experimental determination of G values for* Fe^{3+} *oxidation. Joint Establishment for Nuclear Energy Research Publication No. 8* (Kjeller per Lillestrøm, Norway)

MASS SPECTRA AND THE CHEMICAL SPECIES PRODUCED BY THE IMPACT OF LOW ENERGY ELECTRONS[1,2]

By Morris Krauss, Austin L. Wahrhaftig, and Henry Eyring
Department of Chemistry, University of Utah, Salt Lake City, Utah

The nature of the processes important in radiation chemistry have been discussed in several recent review articles. The excellent review by Magee (1) in Volume 3 of this series, concerned primarily with the mechanisms and principles of radiation chemistry, lists 13 references to recent reviews and symposia on radiation chemistry or closely allied fields. The conference sponsored by the National Research Council, Committee on Nuclear Science, Subcommittee on Radiobiology, at Highland Park (May, 1953) was concerned with the basic mechanisms in radiobiology. The proceedings of this informal conference (2) present an excellent picture of the present problems in the field.

It is generally agreed that the major chemical effects of high-energy ionizing radiation are produced by the low-energy secondary electrons. Hence, a complete discussion of "Chemical Species Produced by the Impact of Low Energy Electrons" would be another review of radiation chemistry. This article is rather arbitrarily limited to a review and discussion of certain topics in mass spectra with special emphasis on matters of interest in radiation chemistry.

In the mass spectrometer, one observes the ions produced by the impact of single electrons of known energy upon isolated molecules. The pressure is sufficiently low so that, except in rare cases, no intermolecular reactions occur. The primary process and the subsequent reactions under these simple conditions are discussed first; the effects of intermolecular collisions are then briefly reviewed.

A number of books and reports of symposia on mass spectrometry have appeared in the last several years. The 1951 Faraday Society Discussion on Hydrocarbons (3) contains several articles on the ionization and dissociation of molecules by electron impact. The NBS Symposium on Mass Spectroscopy (4) was primarily concerned with problems in precision mass spectroscopy (mass measurement) and with instrumentation. Ewald & Hintenberger (5) are also concerned primarily with instrumentation, mostly for precision mass spectrography. *Modern Mass Spectrometry* by Barnard (6) is an excellent general text on mass spectrometry with many references. Half of the book is devoted to instrumentation, the remainder to applications

[1] The survey of literature pertaining to this review was completed in December, 1954.

[2] The preparation of this review was assisted by the U. S. Atomic Energy Commission.

with emphasis on experimental techniques. In the short monograph on *Mass Spectrometry* by Robertson (7), there is more discussion of the theory of the ionization process, and also an interesting chapter on the study of free radicals. Two conferences were held by the Mass Spectrometry panel of The Institute of Petroleum (London), in 1950 and 1953. The conference reports (8, 9) include excellent, very complete bibliographies. The basic references for the quantum mechanical discussion of the electron impact process are the treatises by Mott & Massey (10) and by Massey & Burhop (11). As is usually the case, the reasonably exact calculations on very simple systems only give an indication as to the nature of the situation in the much more complex systems discussed in this review. There is a monograph on *Negative Ions* by Massey (12).

Lastly, there is the truly overwhelming collection of mass spectral data assembled by the American Petroleum Institute (13), in which is tabulated the mass spectra of approximately 900 compounds, mostly hydrocarbons but including some amines, alcohols, and many other types of compounds.

Ionization Probability Curves

The primary processes described by Magee (1) which result in the formation of ions can be thoroughly studied in the mass spectrometer. The information most often desired is the efficiency of ion production or the ionization probability curve, the dependence of ion current upon bombarding electron voltage. The minimum electron voltage at which an ion appears, the appearance potential, is of fundamental importance in the determination of bond energies, ionization potentials, and other quantities. No standard procedure of measurement has yet been developed. The major difficulty in the determination of appearance potentials is the interpretation of the curvature at the threshold of ionization-probability curves attributable to the thermal energy spread of the bombarding electrons. Various empirical methods have been devised to overcome this difficulty; the important ones are (*a*) initial break (14), (*b*) linear extrapolation (15), (*c*) extrapolated difference (16), and (*d*) critical slope (17). A number of comparative discussions and experiments (18 to 23) appear in the literature, but it is felt that no definitive statement can be made merely by an inter-comparison of these conventional methods.

The retarding potential difference method of Fox *et al.* (24, 25), in which the ions measured are formed by nearly monoenergetic electrons of known energy, has alleviated this difficulty. The reduction of the effects of the electron energy spread allows a detailed study of the structure of ionization probability curves. Ionization probability curves in the rare gases are found to be linear in excess electron energy near the threshold. The doublet separations of Kr^+ and Xe^+ are determined in good agreement with spectroscopic values when it is assumed that the curve resulting from two or more ionization processes is a linear superposition of the linear ionization probabilities for the processes (26). Deviations from linearity in the curves are

ascribed to auto-ionization[3] (27) from excited states of the atom which lie above the ionization limit.

Wigner, in a study of two-body reactions, has shown that analysis of the long range interaction of the resultant particles is sufficient to derive the energy dependence of the cross section at the threshold (28). Wannier has extended this work to ionization by electron impact and has derived a threshold law which varies as the 1.127th power of the excess electron energy (29). An application of the Born & Oppenheimer approximation by Bates *et al.* (30) gives a linear threshold law. The ionization probability curve for He^+ over an 8 ev energy range is linear (31). Over a small energy region near threshold the scatter of experimental points precludes any definite conclusion.

Wannier, in a private communication to Hickam *et al.* (31), reports that in the case of double ionization the threshold law varies approximately as the square of the excess electron energy. However, they found that the doubly-ionized rare gases, Ne^{++}, A^{++}, Kr^{++}, and Xe^{++} exhibit linear ionization probability curves. The considerable curvature found by earlier investigators near the ionization threshold indicates the inability to resolve structural details attributable to the electron energy spread (32, 33, 34). Clarke has obtained an ionization probability curve for Xe^{++} which apparently confirms Wannier's prediction (35). The electron spread employed in this work was considerably larger than Hickam's and may account for the contradictory results. It is not felt that excitation to excited vibrational levels as proposed by Clarke (35) would account for the curvature found for NO as the overlap of the vibrational eigenfunctions should decrease rapidly for the higher excited vibrational states of the ion.

Very pronounced deviations from linearity were observed in the ionization probability curves for Zn, Cd, and Hg (36). Earlier interpretations of the structure of the Hg curve by Lawrence (37) and Nottingham (38) were rejected by Hickam as inapplicable to Zn and Cd. He postulates auto-ionization from optically-forbidden states which, unlike optically-allowed transitions, are excited by electron impact with a maximum in the probability close to threshold (11).

The interpretation of these curves and the more complicated ones which arise from polyatomic molecules require some *a priori* knowledge of the variation of the cross section with excess electron energy. The work, thus far, has not been conclusive although the evidence for the linear law presented by Fox *et al.* is impressive. The predictions of Bates *et al.* and Wannier disagree very widely for the threshold dependence for the further ionization of singly-charged ions, and an experimental investigation may help resolve this very important question. In addition, there may be a lower limit on the reso-

[3] Auto-ionization is the formation of an ion by excitation of an atom or molecule to an excited electronic state lying above its lowest ionization potential with subsequent radiationless transition to the ion with the ejected electron carrying off the excess of energy.

solution of the breaks in ionization probability curves. Wigner shows theoretically that a cusp exists in the probability for a process already in progress at the threshold of a new process (28). Such an interdependence may exist in the three-body ionization problem.

Morrison has shown that a linear dependence of the probability of ionization on excess electron energy results in the second derivative of the ionization efficiency curve having the shape of a reversed Boltzmann curve (39). An experimental study of various molecules (40) employing automatic recording devices (41) for the first and second derivatives produced qualitative agreement.

Morrison qualitatively discusses the many factors producing fine structure. He postulates competition between electronic processes contrary to Fox *et al.* and discusses the effects on the curves. No clear-cut decision is evident on the basis of the curves presented by Morrison, as it is difficult to decide what fraction of the structure in his second derivative curves is real. The curves obtained by the more direct technique of Fox *et al.* are relatively free of instrumental complications.

Fox *et al.* have not yet applied their method to the determination of breaks in ionization efficiency curves of the fragment ions. Many investigators have observed breaks occurring in the ionization efficiency curves of fragment ions utilizing the more conventional apparatus and methods for the determination of the appearance potentials (42, 43, 44). Clarke (35) has identified two breaks in the N^+ curve obtained from electron impact of N_2 which correspond very closely with the spectroscopic values for the energy separation of the ^4S_u from the ^2D_u and ^2P_u levels of N. A value of 9.8 ev is then deduced for the dissociation energy of N_2.

The ionization probability curves for CO, N_2, C_3H_6, and C_6H_6 have also been reported and interpreted using the assumptions of Fox *et al.* (45). Reasonable agreement is obtained with the spectroscopic data available. The results for the polyatomic molecules indicate that the presence of low-lying states strongly influences appearance potentials obtained by the critical slope or linear extrapolation methods. The discrepancy between the electron impact and spectroscopic ionization potentials for benzene observed in earlier studies has been shown not to be real (45, 46). The energy levels resulting from simple ionization in the paraffins are spaced approximately 0.5 ev apart near the ground state and should be resolvable (47, 48). Honig's (17) indirect deduction that a square-law dependence on the excess energy holds for a large number of hydrocarbons may be explained by the above results.

McDowell & Cox (49) have determined that the ionization potentials of CH_3F and C_2H_5F are very close to those of CH_4 and C_2H_6, respectively. This supports Mulliken's (50) view that the nonbonding fluorine orbitals do not interact appreciably with the C—H and C—C orbitals.

The possibility of obtaining accurate values of the inner ionization

potentials will offer a firmer basis to the Lennard-Jones & Hall semi-empirical theory of these ionization potentials (47). Hall has pointed out these are needed to resolve certain ambiguities which arise when second neighbor interactions are included (51). A group orbital modification has been developed and applied by Hall (52, 53) and by Franklin (54) to the prediction of a large number of ionization potentials. In a study of the ionization potentials of substituted acetylenes serious disagreement was found with the spectroscopic value for the ionization potential of propyne (55). Internally consistent results were found for the group orbital calculations of the ionization potentials of the substituted acetylenes if the electron impact value was used. A more recent measurement (56) of the ionization potentials of propyne and 2-butyne is in agreement with the results obtained by Franklin & Field. The charge distribution for states of the parent ion reached by vertical ionizations is certainly related to the molecular cracking pattern (57), although for the patterns produced by high-energy electrons, of, say, 50 to 75 ev, a statistical model seems to be more applicable. The ionization of molecules by charge exchange from collision with atomic ions provides a means of introducing a definite amount of energy corresponding to the recombination energy of the atomic ions. Lindholm has studied the mass spectra of H_2S (58), CO_2, H_2O, and NH_3 (59) which result from collision with a number of different atomic ions. The resulting spectra are analyzed in terms of the electronic structure of the molecules and the cross-section for charge exchange. Charge exchange collisions involving low energy ions of N_2 and O_2 have been studied by Potter and the results discussed in terms of the electronic states of the molecules and ions (60).

Kinetic Energy of Fragment Ions

Hagstrum (61) has considered the various processes resulting from electron impact and discusses the efficiency of dissociation processes as a function of electron energy and kinetic energy of the fragments. This information is necessary for the complete specification of an ionization process. In a review, he lists (62) the various investigations of the kinetic energy of product ions done prior to 1951 and reports on his studies of the kinetic energies of all ions observed from the dissociative ionization processes in CO, N_2, NO, and O_2. The range of kinetic energies observed in the fragment ions is satisfactorily explained by Franck-Condon transitions from the ground state of the molecule to various attractive and repulsive states of the ion.

McDowell & Warren (42) observed that the half-width of the ion beam at the collector slit is increased for ions with initial kinetic energy. The ions in the mass spectrum of methane and the CH_2^+, CH^+, and C^+ ions from CH_3CN are formed without appreciable kinetic energy.

Hipple (63) has found that all the lower-mass ($m/e < 16$) ions in *n*-butane have appreciable kinetic energy as was indicated by the appearance potential studies of Stevenson & Hipple (64). Direct quantitative information on the

kinetic energies of ions found in the mass spectra of polyatomic molecules, however, is very scanty. The papers by Kandel (65, 66) are discussed in this review in the section on bond dissociation energies.

Satellite peaks in the mass spectrum of benzene were found to possess high kinetic energy and high appearance potentials (67) and were described as resulting from the dissociation of doubly charged ions into two singly-charged fragments. Mohler *et al.* have quantitatively studied the kinetic energies of the satellite peaks in 13 hydrocarbons and CH_3CF_3 and find that the energies range from 1.5 to 3.4 ev (68).

Negative Ions

A discussion of many appearance potential and abundance studies of negative ions has been presented by Marriott & Craggs (69). The experimental difficulties are reviewed with special reference to measurements at low electron energies (0 to 2 ev). Pritchard has reviewed the determination of electron affinities by electron impact measurements (70). He notes that negative ion abundances usually average only a hundredth of that of positive ions. The precise determinations of the appearance potentials of such low-intensity peaks is difficult. The abundances of negative ions from halogen containing compounds are much higher. Ahearn & Hannay show that the magnitudes of the negative ion peaks from SF_6 are considerably larger than a typical peak such as O^- from CO (71). They also observed secondary resonance captures of slow electrons produced by primary ionization processes, with ion currents beyond 2 ev for SF_6^- and SF_5^- varying linearly with the square of the pressure. Craggs, McDowell & Warren observed that the halomethanes form negative ions by both resonance capture and an ion pair process, while negative ions from molecules like cyanogen and methyl cyanide are formed largely by resonance capture (72). Thorburn (73) has re-determined the appearance potentials of O^+ and O^- in view of the discrepancy of previously reported values (62, 74). The results disagree with the values determined by Hagstrum, and dissociative processes are suggested leading to O^--ion in the ground state. Studies of the electron detachment cross-section of O^--ions formed by thermal and electron bombardment sources support this interpretation of the dissociative processes (75).

Relatively large C_2H^- and H^- peaks have been detected in acetylene, methane, and ethane (76). The C^-, CH^-, and CH_2^- ions are detected in low intensity in methane and ethane, but no indication of CH_3^- is found in agreement with the results of Smith (14). The electron affinities of Se and S were deduced from the appearance potentials of Se^- and S^- from H_2Se and H_2S (77). Appearance potential measurements for resonance capture in HBr and HCl and for dissociative capture to give Cl^- and Br^- have been reported (78). The ions O^- and SO^- have been detected in the mass spectra of SO_2 and the electron affinity of SO determined from the difference in the appearance potentials of O^- and SO^- (79).

Detection of Radicals

The detection of free radicals by mass spectrometry was first achieved by Eltenton (80, 81). Robertson has pointed out the suitability of low-energy electrons for the detection of free radicals and calculates that the minimum detectable ratio of radicals to stable molecules is from 1 in 10^4 to 1 in 10^6 (82, 83). Short-lived intermediates in flames have been observed (81, 84). Robertson (85) and Foner & Hudson (86) have studied the production of HO_2 from atomic hydrogen and molecular oxygen. The work done at the National Research Council laboratories in Ottawa on free radicals is reviewed by Lossing, Ingold & Henderson (87). Reaction of radicals on the walls of the ionization chamber has been detected (88), and LeGoff *et al.* have discussed the possible inability to detect reactive radicals (89). The use of molecular beam methods has been suggested by Dunning (90) to eliminate such surface effects.

Hipple & Stevenson have measured the ionization potentials of CH_3 and C_2H_5 radicals (91) and that of CH_2 was determined by Langer & Hipple (92). More recent work on the CH_3 and CH_2 radicals which included the determination of the appearance potentials of the fragment ions is presented later in Table I. The ionization potentials of the methyl, allyl, and benzyl radical have been measured by Lossing, Ingold & Henderson (93). The observed ionization potential of the allyl radical is .9 ev lower than the value predicted by Evans & Szwarc (94). McDowell has noted that the observed value may be in error (95). The ionization potential of the benzyl radical is also in doubt (96).

Adiabatic Correlation

A correlation must exist between the electronic states of the parent molecule, molecule-ion, and the fragment ions and radicals. In molecules of high symmetry, such correlations impose restrictions upon the possible decomposition reactions, which may be derived by considerations involving the symmetry of the activated complex. McDowell has applied adiabatic correlation rules to the interpretation of the mass spectra of a number of molecules including ammonia, methane, and the methyl halides and cyanide (97, 98). A similar study was made by Laidler for H_2O (99) employing the electron impact data of Mann, Hustrulid & Tate (100). Laidler deduced that the OH^--ions are not produced by a primary reaction in the radiation chemistry of water vapor. These studies have applied the method of Shuler (101) in whose paper the earlier references may be found. A review by Laidler & Shuler on elementary reactions involving excited electronic states discusses the construction of potential energy surfaces employing semiquantitative theoretical and experimental data (102). Such studies require improved experimental data (as from monoenergetic electron beam studies) and more theoretical information as to the nature and position of excited energy levels in order to reach definitive conclusions. They represent the

beginnings of an effort to correlate mass spectral data with other information on the electronic states of small polyatomic molecules as was done earlier by Hagstrum for several diatomic molecules (62).

Some additional features of the methane mass spectrum will be discussed from this viewpoint as a greater literature exists on this molecule than on any other. The experimental data of various investigators (Table I) are

TABLE I

APPEARANCE POTENTIALS AND BREAKS IN IONIZATION EFFICIENCY CURVES FOR IONS FROM METHANE, METHYL, AND METHYLENE

	*	†	Potentials				
			CH_4^+	CH_3^+	CH_2^+	CH^+	C^+
CH_4	(14)	a	13.2 ±0.4	14.5 ±0.4	15.8 ±0.5 23.0 ±0.8	23.4 ±0.6	26.8±0.8
	(103)	b	13.0 ±0.2	14.4 ±0.3	20.0 ±0.3	24.3 ±0.5	—
	(104)	a	13.04±0.02	14.57±0.05	—	—	—
	(105)		13.3 ±0.3	14.5 ±0.3	16.5 ±0.3 21.5 ±1.0	22.5 ±0.5 27.0 ±1.0	21.5±1. 29.5±1.
	(42)	c	13.12±0.02	14.39±0.02	15.30±0.5 20.1 ±0.1	22.4 ±0.1 26.2 ±0.2	26.2±0.2
	(106)	a	13.10±0.1	14.30±0.1	15.5 ±0.2	23.4 ±0.2	27.0±0.2
	(108)	a	13.1 ±0.2	14.3 ±0.2	15.6 ±0.2	23.0 ±0.5	26.9±0.2
CH_3	(106)	a	—	9.85±0.1	15.30±0.1	16.2 ±0.2	17.8±0.2
	(107)	a	—	10.11±0.1	15.29±0.08	—	—
	(107)	b	—	10.04±0.12	15.41±0.15	15.58±0.3	—
CH_2	(106)	a	—	—	11.90±0.1	17.1 ±0.2	18.0±0.2

* References. See LITERATURE CITED.

† Method of determination of appearance potential

a. Initial break

b. Linear Extrapolation

c. Extrapolated difference in voltage

not in agreement on the appearance potentials of the less abundant ions. The agreement on the fine structure of the ionization efficiency curves is very poor. The heat of sublimation of graphite is deduced to be of the order of 130 kcal./mole from the electron impact studies (106) whereas more direct determinations yield a value of 170 kcal./mole (109, 110).

The $^2T_2(T_d)$ electronic state[4] of CH_4^+ must be unstable with respect to some nontotally symmetric vibration in accordance with the Jahn & Teller

[4] The nomenclature is that of Mulliken as applied by McDowell.

theorem (111). Van Vleck has suggested that the CH_4^+ ion ground state might have a structure of V_d symmetry (112). McDowell (98) points out the $[pt_2]$ orbital will then split and give $[\pi e]$ and $[zb_2]$ orbitals. However, the resulting E state is still degenerate and will be unstable with respect to at least one nonsymmetric vibration. Thus, there might be three adiabatic ionization potentials for methane arising from the $[pt_2]$ orbital in addition to the one from the $[sa_1]$ orbital.

Consistency relations lead Langer, Hipple & Stevenson (106) to assume that identical CH_3^+ ions, $^1A_1'$ (D_{3h}), are formed from CH_4 molecules and CH_3 radicals under electron bombardment. The value of $D(CH_3^+—H)$ is then found to be 1.2 ev or about one-fourth that of $D(CH_3—H)$. A similar bond weakening was deduced from the unexpectedly large difference in the mass spectrometric ionization potentials of CH_4 and CD_4 (113). This suggests a significant difference between the vertical and adiabatic ionization potentials[5] of methane.

Two effects will result from the lower symmetry of the CH_4^+ ion. The resultant shift of the potential minima will, on vertical ionization, result in large excitation of the vibrational levels in the ions, CH_4^+ and CD_4^+, which, in view of the large vibrational quanta in these molecules, might explain the large differences in the appearance potential. There will also occur a weakening of some bond or bonds as a result of the electronic reorganization.

Langer *et al.* conclude that at the first appearance potential of CH^+ in CH_4

$$CH_4 + e \rightarrow CH^+ + 3H + 2e$$

with the CH^+ ion in its $^1\Sigma^+$ ground state. However, they surmise from a study of the C^+-appearance potentials that the common state of formation from CH_2 and CH_3 radicals is the $^1\Pi$ state with the processes represented by

$$CH_3 + e \rightarrow CH^+ + H_2 + 2e$$

$$CH_2 + e \rightarrow CH^+ + H + 2e$$

The high values deduced for $D(C^+—H)$ in the study of Langer *et al.* and for $D(CH—H)$ by Waldron suggests the alternative that CH^+ is formed in its $^3\Pi$ state. This violates the spin conservation rules in the formation of CH^+-ion from the $CH_3^+(^1A'_1)$ ion and requires the assumption that the formation of excited CH^+ proceeds from excited states of the CH_2^+ and CH_3^+ ions. The proposed scheme is illustrated schematically in Figure I for the CH_2^+ dissociation. The ground state of CH_2^+ may be either $^2A_1$ or $^2B_1$ as the electronic structure of the radical is still uncertain (114, 115). There are six states above the ground state which correlate with the $^1\Pi$ and $^3\Pi$ states of CH^+. The first appearance of CH^+ will result from transition to a

[5] The vertical ionization potential is the energy required for ionization of a molecule with no change in the interatomic distances whereas the adiabatic ionization potential is the energy difference between the equilibrium configurations of molecule and ion.

potential curve, correlating with the $^3\Pi$ state, which is attractive but whose minimum is appreciably displaced from that of the neutral radical such that vertical ionization will cause dissociation at the observed appearance potential.

A similar condition may be assumed for CH_3 dissociation as $^1E''$ or

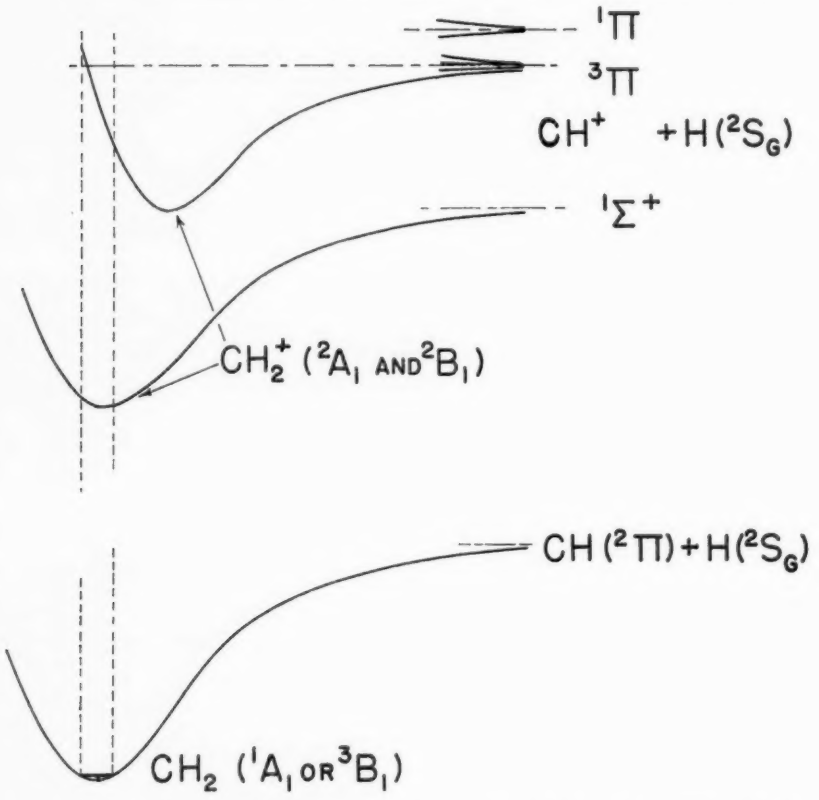

FIG. I. Schematic potential curves for ionization-dissociation of the CH_3 radical.

$^3E''$ states will correlate with $^1\Pi$ or $^3\Pi$, respectively. No difference has been found between the ionization potentials of CH_3 and CD_3 (93), indicating that the minimum of the ground state of the ion is not displaced with respect to the minimum of the radical. Thus, dissociation probably occurs from an excited state. With the assumption that the CH^+-ion is formed in the $^3\Pi$ state, about 0.5 ev lower than the $^1\Pi$ state, one obtains more reasonable values for $D(C^+—H)$ and $D(CH—H)$.

QUASI-EQUILIBRIUM THEORY

A theory of the mass spectra of polyatomic molecules, obtained by applying absolute reaction rate theory for isolated systems to the dissocia-

tion of the parent molecule-ions, has been presented by Rosenstock *et al.* (116). This theory was developed in an attempt to explain the major observations of the mass spectra of polyatomic molecules of the size of propane and larger observed in the gaseous state. Then, the correlation rules described in the previous section impose few restrictions; the discussions in this section frequently apply only to such molecules. The above authors conclude that all valence electrons in the molecule must have approximately equal probabilities of removal, yet the energy excess over that required to give the ion in its lowest state must be free to rapidly travel about in the molecule (116 to 119). Radiationless transitions offer a mechanism by which such energy transfer can occur.

In normal, chemically-stable molecules formed from light atoms, there is a gap of several ev between the energy of the ground state and the excited states. When an electron is removed from a molecule, the resulting ion will, in general, no longer have an isolated lowest state. The electronic state of the ion with its odd electron can no longer be described simply in terms of localized orbitals, but use must be made of molecular orbitals extending over the entire molecule (48). No detailed knowledge exists as to the nature of the potential surfaces for any polyatomic ion, especially for ions containing over 10 atoms. One might argue that as the complexity of the molecular system increases the probability that the removal of one electron places it in a highly repulsive state decreases. Experimentally, it was found that the vast majority of fragment ions collected in the mass spectrometer are formed with small (less than 0.4 ev) amounts of kinetic energy (120) and hence do not arise by dissociation from strongly repulsive states. Consistency in bond energy calculations indicates that much less kinetic energy is imparted to the most abundant ions. Appearance potential measurements indicate that the formation of the more abundant ions, constituting over 90 per cent of any mass spectrum, requires from zero to at most four ev over the vertical ionization potential of the parent molecule (64). In an ion such as $C_3H_8^+$ with 19 valence electrons, the average spacing between electronic states is of the order of one millivolt while the room-temperature vibrational energy is about 1/2 volt. The various potential surfaces will differ greatly in their dependence on nuclear coordinates, so there will be a very large number of intersections, at many of which the probability of transition will be large. Following vertical ionization, there will be some transformation of the initial excess of electronic energy (over the ion ground state) into vibrational energy in 10^{-13} sec. This energy will circulate around the molecule until sufficient energy has concentrated in some one of the several energetically possible reaction coordinates to give reaction. Vibrational energy transfer about the molecule will also be expedited by the radiationless transitions.

A means of calculating the unimolecular breakup of such an ion is now required. Usual reaction rate theory applies to systems in thermal equilibrium (121). In the analogous theory for the decomposition of an isolated system (116), the basic assumptions are that the energy can circulate about the various degrees of freedom of the system randomly and rapidly compared

to the rate of reaction, and that the fraction of states giving rise to any reaction is such a small fraction of the total states accessible to the system with the given energy that the rates for the several reactions possible are independent of each other. Instead of the usual expressions for "sum over states" or partition functions for the normal and activated complex states, expressions for the density of energy levels for these states are required. For an isolated system, the result is

$$k'(E) = \int_0^{E-\epsilon_0} \frac{\rho\ddagger(E, \epsilon_0, \epsilon_t)}{\rho(E)} \frac{1}{h} d\epsilon_t,$$

where $\rho(E)$ is the density of energy levels for the system with total energy E, and $\rho\ddagger(E, \epsilon_0, \epsilon_t)$ is the density of energy levels for the system in the activated complex configuration with ϵ_0 activation energy and ϵ_t translational energy in the reaction coordinate. It has been shown by Magee (122) that the expression for $k'(E)$, integrated over all energies for a thermal distribution, yields $k'(T)$. If the system is represented by a collection of harmonic oscillators, then the above simplifies to

$$k'(E) = \left(\frac{E - \epsilon_0}{E}\right)^{N-1} \prod_{j=1}^{N} \nu_j \Big/ \prod_{i=1}^{N-1} \nu_i\ddagger$$

Analogous expressions have been derived (123); it is believed that this derivation gives a better insight into the physical situation. In the calculations to date, a slightly more general expression, where the system is represented by a collection of harmonic oscillators plus internal rigid rotors, has been used. A very large number of electronic states is assumed in order to obtain the necessary radiationless transitions and then is neglected in the rate calculations. This is equivalent to the approximation that reaction occurs when essentially all of the energy of the ion is in the form of vibrational energy and that only a small, essentially constant number of electronic states is involved in the several reactions. An alternative viewpoint is that the approximation by which one separates electronic and vibrational energy is not applicable to a system where the lifetime in an electronic state is not long compared to the time for a nuclear vibration. The nuclei must have some sort of motion, for which the simplest approximation will be a set of "average" normal modes. While the forces between atoms are not linear functions of any set of coordinates, they certainly do not change either discontinuously or by orders of magnitude. Lacking more exact knowledge, the ion is represented by one electronic state of some large degeneracy in which the density of states is given by conventional formulae in terms of the "average" nuclear motions. The large degeneracy, which may be a function of energy, is the same for the normal and the activated states of the ion and so does not affect the rates.

The reaction scheme, with calculated rates for all reactions, permits the calculation of the "cracking pattern" of a parent ion of a given energy. It is then necessary to sum or integrate over-all parent ion energies, using an appropriate energy distribution. Most ions will acquire at least a small

amount of vibrational energy from the vertical ionization. Very few ions obtain enough energy to end in strongly repulsive states. Since nothing further is known, an energy probability function that gives agreement with experiment is selected. An average parent ion energy of about 5 ev was found necessary in the calculations next described.

The only detailed applications of the theory are to propane and 2,2-dideuteropropane (124). The assumed reaction scheme for the dideuteropropane is shown in the following scheme:

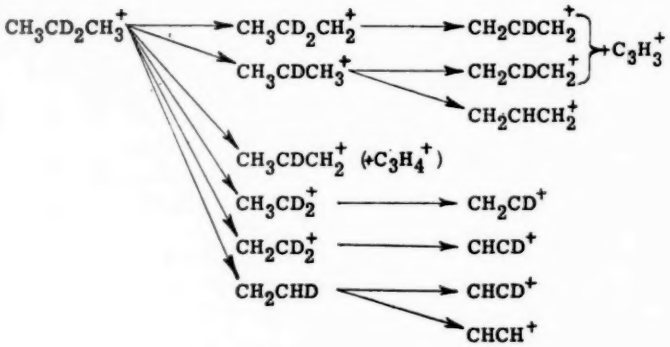

A similar scheme was used for propane. Many assumptions are obviously involved in the selection of this set of reactions. For instance, only a few of the possible H—D interchanges have been considered; the minimum that would give all the important peaks. The single carbon fragments, totaling 1.2 per cent of total ionization, have been ignored.

The results of the calculations are given in Table II. Much better agreement with the data could be obtained by several recalculations, slightly modifying the assumed frequencies and the initial energy distribution of the parent ions. It is believed the present calculation serves the purpose of demonstrating that the main features of a mass spectrum can be explained in terms of the theory. The calculations for the dideuteropropane were completely determined by the assumptions made for propane and the usual rules for calculating changes in zero point energy and vibrational frequencies on deuterium substitution.

Metastable ion peaks were first shown by Hipple, Fox & Condon (125, 126) to be the result of ions dissociating after acceleration but before magnetic analysis in the mass spectrometer. Such ions appear at nonintegral masses, M^*, given by $M^* = M^2/M_0$, where M_0 is initial mass accelerated and M is the fragment mass analyzed. Measurements by Hipple (127) led to values of the order of 10^{-6} seconds for the half-lives of such ions.

In the theory now under discussion, there is nothing special in any way about the so-called "metastable ions." It is merely an accident of conventional mass spectrometer design that ions having a reaction rate constant of about 10^6 sec^{-1} appear in part as metastable ions (116, 119, 124). The

TABLE II

CALCULATED AND OBSERVED MASS SPECTRA FOR PROPANE AND 2,2-DIDEUTEROPROPANE

m/e	Propane			2,2-Dideuteropropane		
	ion	R.A * Calc.	R.A.† Obs.	ion	R.A. Calc.	R.A.† Obs.
46				$CH_3CD_2CH_3$	10.8	12.9
45				$CH_3CD_2CH_2$	1.7	1.9
44	$CH_3CH_2CH_3$	12.4	12.5	CH_3CDCH_3	2.5	3.5
43 (+40)‡	$CH_3CH_2CH_2$ CH_3CHCH_3	10.9	10.5	CH_3CDCH_2 (C_3H_4)	4.0	4.3
42 (+40/39)	CH_3CHCH_2 (C_3H_4)	5.9	2.0	CH_2CDCH_2 (C_3H_3)	4.3	4.0
41 (+39)	CH_2CHCH_2 (C_3H_3)	7.1	9.4	CH_2CHCH_2	0.6	1.3
31				CH_3CD_2	22.2	28.5
30				CH_2CD_2	20.8	19.8
29	CH_3CH_2	19.9	30.7	CH_2CHD	15.3	9.1
28	CH_2CH_2	25.9	19.0	CH_2CD	10.2	8.0
27	CH_2CH	12.9	10.3	CHCD	6.1	3.1
26	CHCH	5.0	1.8	CHCH	1.6	0.6
$39.2 = 41^2/43$		0.02	0.05§	$(C_3H_7^+ \rightarrow C_3H_5^+ + H_2)$		
$25.1 = 27^2/29$		0.14	0.08	$(C_2H_5^+ \rightarrow C_2H_3^+ + H_2)$		
$24.1 = 26^2/28$		0.03	0.01	$(C_2H_4^+ \rightarrow C_2H_2^+ + H_2)$		

* Both calculated and observed relative abundances (R. A.) are normalized to total ionization equal 100.

† Schissler, D. D., Thompson, S. D., and Turkevich, J. (131).

‡ Ion masses and corresponding ions in parenthesis assumed to result from decomposition of ion with which it is grouped.

§ American Petroleum Institute (13).

metastable ion intensities listed in Table II were calculated with the same rate equations as were used in the rest of the calculations. The time interval during which observable metastable ions would be formed was calculated from the known geometry and voltages in the mass spectrometer.

Fox & Langer (44) compare the appearance potentials for the formation of metastable ions with the appearance potentials for the corresponding reactant ions and product ions. They find that where the reactant ion and product ion have significantly different appearance potentials, the appearance potential of the metastable ion peak is the same as the value for the product ion. The one exception, in isobutylene, must be attributable to lack of mass spectrometer sensitivity, which they demonstrated had led to similarly inconsistent results with *n*-butane. While their discussion assumes

that a metastable ion peak results from ions excited to some particular state different from the main group of ions, their data are consistent with the interpretation given in the preceding paragraph.

Negative metastable ions have been reported by Donnally & Carr (128) in the mass spectrum of $C_2H_5PO_2Cl_2$. The measured half-lives were 1.9 and 4.8×10^{-6} sec., determined by measurements over the time interval 2.5 to 5 μsec.

Much information regarding the reactions of the parent ion in the mass spectrometer has been obtained from a study of deuterated molecules. All of the deuterated methanes have been studied (129, 130, 131). It is found that deuterium substitution increases the amount of hydrogen loss, but the deuteriums come off in smaller amount. The first observation results from the larger amount of energy circulating in the molecule since in a simple bond rupture the zero point energy of the parent ion will be lowered more than that of the activated complex by deuterium substitution (116). The difference in change in zero point energy, when two competing processes in one ion are compared, will make a hydrogen atom more easily removable than a deuterium atom. Schissler, Thompson & Turkevich (131) also give and discuss the mass spectra of ethane and four deuteroethanes. The two-carbon fragment ion spectra for the mono- and dideuteroethanes are well interpreted in terms of the two rules just given. The empirical weighting factors for increased probability of C—H bond break and for decreased probability of C—D bond break, listed in Table III, give excellent agreement with experiment.

TABLE III

WEIGHTING FACTORS FOR C—H AND C—D BOND RUPTURE RELATIVE TO THE NONDEUTERATED MOLECULE

Factor*	Molecule				
	CH_3D	CH_2D_2	CHD_3	C_2H_5D†	CH_3CHD_2†
a	1.23	1.48	1.80	1.09	1.15
b	0.55	0.65	0.76	0.60	0.80

From Schissler, Thompson & Turkevich (131).

* a—factor for C—H bond rupture.
b—factor for C—D bond rupture.

† For two-carbon fragment ions only.

This method of calculating the effect of deuterium substitution was not satisfactory for the C_2 fragments from 1,1,1-trideuteroethane, or for the single-carbon fragments from any of the partially deuterated ethanes. In an attempt to elucidate the nature of the processes occurring, Schissler *et al.* also obtained spectra at much lower electron voltages, thereby greatly limit-

ing the number of possible reactions. With this very useful mode of attack it was found that 13 volt electrons, which give only the fragment ion $C_2H_4^+$ from C_2H_6, remove H_2, HD, and D_2 in relative amounts 0.04, 0.70, and 0.25, respectively, from CD_3CH_3. This is contrary to the simple rules previously given. Energetically, one would expect to lose only HD so as to be left with $CH_2{=}CD_2^+$ rather than $CH_3{-}CD^+$ or $CH{-}CD_3^+$ (64). We believe that the loss is practically always of hydrogen (or deuterium) from adjacent carbon atoms to give ethylene ion directly, but that the activation energy for the process

$$CH_3{-}CD_3^+ \rightarrow CH_2D{-}CHD_2^+$$

is slightly less than the activation energy for the process

$$CH_3{-}CD_3^+ \rightarrow CH_2{=}CD_2^+ + HD$$

so that H—D exchange occurs before dissociation in some fraction of the molecules. Also, when CH_3CD_3 is bombarded with 17-volt electrons, masses 18, 17, 16, and 15 can only result from simple C—C bond rupture and must be assigned to the ions CD_3^+, CHD_2^+, CH_2D^+ and CH_3^+. The relative abundances found are 7.2, 2.5, 2.1, and 7.1. This indicates that an H—D exchange occurs in approximately one-third of the parent ions before this reaction. The relative probability of H_2, HD, and D_2 loss in the competing reaction would then have to be calculated taking into account this exchange reaction and also the fact that in the loss of a diatomic (or polyatomic) fragment the effect of deuterium substitution both on the activated complex and on the normal ion must be considered. To the extent the quasi-equilibrium theory previously given applies to a molecule as small as ethane, the fact that loss of D_2 is more probable than H_2 implies that the activated complex for this reaction is a "tight" four-membered ring complex. Evidence for a similar four-membered ring activated complex in the thermal dehydrobromination of ethyl bromide is presented in a recent paper by Friedman, Bernstein & Gunning (132). The data of Schissler *et al.*, particularly the single carbon fragment ions, are also discussed by Flynn & Hulburt (133). They point out that the peaks at $m/e = 14.5$ and 13.5, with 0.50 and 0.03 per cent of total ionization, respectively, must be attributable to $C_2H_5^{++}$ and $C_2H_3^{++}$. To obtain a consistent scheme for the mass spectrum of C_2H_5D it is necessary to assume that the $m/e = 14$ peak, representing 1.24 per cent of total ionization, is actually attributable to CH_2^+ (0.34 per cent) and $C_2H_4^{++}$ (0.90 per cent). They also conclude that the $C_2H_4^+$ ions have the ethylene structure, but that the doubly-charged ions are $CH_3{-}CH^{++}$. This discussion of data obtained with 75 volt electrons does not contradict the discussions given previously based upon data obtained with 13.0 and 17.5 volt electrons, when double ionization is not energetically possible.

Schissler *et al.* also give data for 2-deuteropropane and 2,2-dideuteropropane, but do not discuss the spectra in detail. Their data was used in the detailed study of propane described previously in this paper. Other deuterated propanes have been prepared by Condon (134), but the mass spectra

and infrared spectra indicated that the isotopic purity was not high. The study of deuterium-substituted molecules is an extremely powerful method in deducing the nature of the breakdown reactions. Because there are then fewer ions formed having the same mass but different structures, it is very desirable to study the highly-deuterated molecules, as $CD_3CH_2CD_3$. However, since the major peaks of less deuterated compounds often coincide with the smaller peaks of the compound under investigation, it is essential that the highest possible isotopic purity be obtained.

The mass spectra of all the monodeutero C_1 through C_4 paraffins have been discussed in some detail by Stevenson & Wagner (135) and the mass spectra of the propanes and butanes containing C^{13} also have been discussed by Stevenson (136). A theoretical basis for the observations is obtained by considering the dissociation of a molecule, ABA, and its isotopically substituted counterpart, ABA'. Then, in the set of reactions

$$ABA + e \rightarrow A + BA^+ + 2e \qquad 1.$$

$$ABA' + e \rightarrow A + BA'^+ + 2e \qquad 2.$$

$$ABA' + e \rightarrow A' + BA^+ + 2e \qquad 3.$$

Stevenson concludes that if A' is the "heavier" isotope of A, reaction 2 is more probable than reaction 3 because of the greater zero point energy of the product ion in 3. We believe that the important quantity is the zero point energy in the activated complex, not in the product ion; however, in this case where a bond is simply broken, the two quantities are essentially the same. In comparing the probabilities of reactions 2 and 3 with 1, Stevenson discusses the effect of varying zero point energy upon the amplitude of oscillation in the ground state, following the scheme he found quantitatively applicable in discussing H_2 and D_2 (137). While in a molecule such as H_2, with only a very restricted number of electronic states, the zero point amplitude is very important, in a larger molecule the energy distribution in the parent ion will be essentially determined by the transition probabilities to the large number of excited electronic states and will be largely independent of isotopic substitution. The zero point energy of the parent ion will enter in setting the zero for the excess energy that is available for causing reaction. The finding of $C^{13}H_3^+$ in the mass spectrum of propane-2-C^{13} and *iso*-butane-2-C^{13} may be explained in terms of a quasi-equilibrum dissociation taking place in two steps. Then, the intermediate will be a hydrogen-deficient ion on which the hydrogens will be extremely mobile, so that a statistical arrangement of the hydrogens (and deuteriums, if present) on the carbons will be obtained.

A large fraction of the mass spectra listed in the massive American Petroleum Institute compilation (13) include ions that can only be formed by rearrangement in the parent ion. In 3,3-diethyl pentane, the largest peak, 57 or $C_4H_9^+$, comprising 39 per cent of the total ionization involves a rearrangement.

A general discussion of such rearrangement peaks was given by Langer

(138). Three possible mechanisms are proposed: (*a*) Isomerization of the parent molecule-ion prior to dissociation, (*b*) Shift of hydrogen atoms during dissociation, and (*c*) Breakdown of directed bonds between atoms so that more or less random combinations of atoms are possible as fragments. He points out that (*a*) may frequently be excluded, as mass peaks required by the necessary isomerization are not found. The "randomization" of the excited molecule (*c*) can not be simply excluded, since if it were true there is no way to determine how the atoms would recombine. The shift of hydrogens, (*b*), is adequate to explain all observed rearrangement peaks in hydrocarbon mass spectra. Langer & Johnson (139) find support for the idea of statistical rearrangement of ionic fragments or randomization in the excited molecule ion in a study of C^{13}-labeled *neo*-pentane. Happ & Stewart (140) find only simple hydrogen shift occurs in the rearrangement giving the major mass peak, $m=60$ or CH_3COOH, from *n*-butyric acid. Momigny also finds it necessary to include only hydrogen migration to explain rearrangement peaks in the mass spectra of several benzene derivatives (141). It is stated that the mass spectrum of *s*-triazine contributes to the idea that the individual atoms lose their identity in the process of fragmentation (142). However, 78 per cent of the total ionization is in the parent ion and fragments obtainable by simple bond break and another 21 per cent requires only the shift of one hydrogen atom. Only 0.9 per cent requires more extensive rearrangement of the $(—NCH—)_3$ ring to give C_2^+ and C_2H^+ fragments.

A number of deuterated normal butanes have been synthesized and the mass spectra determined by McFadden (143). In addition to the 2-deuterobutane previously described by Stevenson & Wagner (135), the 1,1,1-trideutero, 1,1,1,3,3-pentadeutero, and 1,1,1,2,2,3,3-heptadeutero compounds were prepared. From the mass spectra obtained with 80 volt electrons, it was determined that the reaction scheme was more complicated than expected. We believe that a detailed discussion will require the obtaining of complete mass spectra at reduced electron voltages. Even more necessary will be the use of the new techniques described in the previous section of this report to obtain highly precise appearance potentials for each of the several similar reactions that replace one gross reaction when deuterium atoms are introduced into the molecule. Several qualitative conclusions can be drawn from the presently available data on the deuterobutanes. A peak at mass 49 which can only be $C_3D_6H^+$, obtained from $CD_3CD_2CD_2CH_3$ with the ratio of mass 50 to 49 of 20.3 to 3.1 indicates an H—D exchange in approximately one-seventh of the parent ions before the C—C bond break. Similarly, the existence of a peak at mass 33, $C_2HD_4^+$, from $CD_3CH_2CD_2CH_3$, implies an H—D exchange, that must be between carbon atoms 2 and 3. Similar arguments require that H—D exchanges take place between carbon atoms 1 and 3 and also between carbon atoms 1 and 4. The interpretation of these rearrangement peaks as impurity peaks is excluded by the nonexistence of other peaks of the impurity required.

Bond Dissociation Energies

The present detailed knowledge of bond dissociation energies of hydrocarbons, originating with the work of Stevenson (144) is one of the major accomplishments of the application of the mass spectrometer to studies of molecular structure. Only certain special aspects of the method will be discussed here. At the appearance potential of an ion formed by simple bond break,

$$R_1R_2 + e \rightarrow R_1^+ + R_2 + 2e,$$
$$A(R_1^+) = D(R_1 - R_2) + I^e(R_1) + E$$

where D is the dissociation energy of the indicated bond, I^e denotes the ionization potential, and E represents any excess energy, either electronic or kinetic, given to the ion and neutral fragment. In the first application of the "indirect method" in which the difference in appearance potentials for the same ion from two different compounds is obtained and combined with thermal data to yield a bond energy, Stevenson assumed that in similar reactions, terms in E would be similar and hence cancel (144). From the agreement between five "indirect" and two "direct" determinations Stevenson more recently has concluded that in many cases the excess energy term, E, is negligible (145). Stevenson finds $D(CH_3-H) = 4.42 \pm .04$ ev. It is improbable that the energy going into vibrational and electronic excitation of the products at the appearance potential is much larger than the .04 ev probable error.

In general, Stevenson (145) finds that in

$$R_1 - R_2 + e \rightarrow R_1^+ + R_2 + 2e,$$

the equality

$$A(R_1^+) = I^e(R_1) + D(R_1 - R_2)$$

holds if and only if $I^e(R_1) < I^e(R_2)$. If $I^e(R_1) > I^e(R_2)$, then $A(R_1^+)$ is greater than the sum on the right. This relationship is frequently called Stevenson's rule by other workers in this field. It was also stated by Wallenstein *et al.* (117). It is implicit in the quasi-equilibrium theory of mass spectra previously described in this review. In the activated complex for the dissociation of $R_1-R_2^+$ into fragments R_1 and R_2, the bond joining R_1 and R_2 will be essentially a one electron bond. As for H_2^+, there will be two electronic states for the parent ion correlating with the two states for the separated fragments, $R_1^+ + R_2$ and $R_1 + R_2^+$, the lower state attractive, the upper state repulsive (146). If $I^e(R_1) < I^e(R_2)$, then the state correlating with $R_1^+ + R_2$ will be attractive and dissociation will take place with no kinetic energy in the fragments. The state correlating with $R_1 + R_2^+$ will be of much higher energy—at least several volts—at normal internuclear distances in the parent ion and should result in high kinetic energy in the product ion. Since, in general, appearance potentials do not correspond to excitation to such

excited states (119), nor are most ions found with kinetic energy, the mode of formation of R_2^+ must usually be successive reactions, as

$$R_1 - R_3 + e \rightarrow R_1 - R_2^+ + 2e$$

$$R_1R_2^+ \rightarrow R_3^+ + R_4, \qquad I^a(R_3) < I^a(R_4)$$

$$R_3^+ \rightarrow M + R_3^+, \qquad I^a(R_2) < I^a(M)$$

where M will in general be an olefin. Then, $A(R_2^+) - A(R_3^+)$ in the mass spectrum of R_1R_2 will yield the activation energy for the last reaction written. This is in agreement with the ideas expressed by Stevenson in his last papers (145, 147, 148).

Heats of formation of ions and radicals as obtained by combining mass spectral and thermal data have been calculated by Franklin & Lumpkin (149), by Franklin & Field (150), and by Field (151, 152). Field assumes that the breakup of a molecule under electron bombardment is a quasi-equilibrium stepwise process so that the neutral fragments accompanying any ion are the ones most easily formed. He then calculates heats of formation of ions and radicals resulting from two successive reactions as well as from simple reactions and so obtains bond energies not obtainable under the more restrictive approach of Stevenson. We are in general agreement with the procedure followed by Field, but differ on some details; further data are necessary.

An extensive listing of appearance potentials in aromatic hydrocarbons is given by Field & Franklin (153). Ionization potentials are compared with those calculated by Franklin using the group orbital method of Hall. There is evidence that ionization with loss of a methyl radical from the xylenes, trimethylbenzene, and the methylethylbenzenes leads not to the expected phenyl ion but to the more stable benzyl ion. Various correlations of ionization potentials with rates of aromatic substitution reactions are made. The difficulties and possibilities in applying electron impact data to organic reactions in solution are considered.

The detailed study of normal C_4—C_6 alkane mass spectra has led Stevenson to several unexpected conclusions regarding the structure of the ions and radicals formed at the appearance potential (147). He concludes that

$$n\text{-}C_6H_{14} + e \rightarrow s\text{-}C_3H_7^+ + s\text{-}C_3H_7 + 2e$$

and that s-$C_3H_7^+$ is also obtained from C_3H_8, n-C_4H_{10}, and n-C_5H_{12}. However, the n-C_3H_7 radical is believed to be formed along with $C_4H_9^+$ from n-C_7H_{16} and along with $C_5H_{11}^+$ from n-C_8H_{18}. Also, it is concluded that the $C_4H_9^+$ obtained from n-C_5H_{12}, n-C_7H_{16}, and n-C_8H_{18} has the secondary structure, but that in the case of the last compound, the C_4H_9 radical obtained at the same time has the n or primary structure. It is concluded that normal alkyl ions are not formed as dissociation products in alkane mass spectra, but that n-propyl mercaptan and n-propyl chloride do give n-$C_3H_7^+$ on electron impact. While these conclusions are only based upon

the resulting consistency in values calculated for various dissociation energies and ionization potentials, the simple assumption that the ion and radical obtained in $R_1\text{-}R_2+e\rightarrow R_1^+ + R_2 = +2e$ have the structures given by simple break is excluded. The time for these dissociations must be long in terms of vibrational periods so that the hydrogens can find themselves in the correct positions to form the required new bonds as the initial bonds are broken in the activated complex.

The difficulties in obtaining meaningful appearance potentials have been discussed in the previous section of this report. Stevenson, using the "initial break" method has consistently obtained results indicating that his data are appreciably better than he claims; see, for example, the agreement shown in his Table II (see 145). Other workers have frequently been less successful and so have tried to use a more objective method of finding the appearance potential. Since bond energy calculations involve only appearance potential differences it might seem that the errors in the linear extrapolation method or the critical slope method would cancel out. This is definitely not true for the linear extrapolation method. Ionization efficiency curves for productions vary so in fine structure near the appearance potentials that errors of 0.5 ev or 12 kcal. are easily possible even though results reproducible to 0.1 ev or less are obtained.

The studies of Stevenson just described lead to an insight into the processes occuring at the appearance potential. The determination of the proper explanation for the fine structure in ionization probability curves is a problem for the immediate future. It is frequently postulated that a break represents the start of a new reaction producing the ionic species. An alternative explanation is that the breaks correspond to the inner ionization potentials of the parent molecule (48).

The kinetic energy of fragment ions at the appearance potential has been determined in several cases by Kandel (65). He finds the total excess kinetic energy associated with the formation of CH_3^+ ion from C_2H_6, C_3H_6, and $C_6H_5CH_3$ to be 0.70 volts, 1.99 volts, and 0.40 volts, respectively. Calculations of bond energies, assuming the CH_3^+ is formed by simple bond break from a repulsive state, leads to values consistent with other studies. This is clearly not in accord with the general idea of quasi-equilibrium dissociation. While ethane might be excluded as being too small for that theory to apply, propane and toluene certainly are of sufficient size. At least some dissociation yielding small fragments does proceed directly from repulsive states rather than by successive breakdown. However, the peaks with $m/e \leqq 15$ only constitute a small fraction of the total ionization, about 1 per cent for propane.

Kandal (66) has also studied the mass spectrum of nitromethane in detail, determining the cracking pattern for 70 volt electrons and the appearance potentials and kinetic energy excess for all important ions; C^+, CH_3^+, and O^+ are formed with kinetic energy. The important fragment ions can be explained by equilibrium dissociation, stepwise in the case of $m/e=14(CH_2^+)$ and $m/e=13(CH^+)$. A low value for the appearance poten-

tial of $m/e = 30$, NO^+, requires that this be a rearrangement peak with CH_3O the neutral fragment.

Appearance potentials and mass spectra have been determined for a number of aliphatic amines by Collin (154, 155, 156) and the C—N bond energies have been calculated. Appearance potentials for several cyclic hydrocarbons and heterocyclic molecules have been reported and discussed by Hissel (157).

The ideas of the authors of this review regarding the quasi-equilibrium nature of the dissociation of polyatomic molecules under electron impact have been emphasized in the last two sections. This theory has several limitations. It certainly does not apply to small molecules, as H_2O and CH_4, probably only in part to C_2H_6. Even for C_3H_8, it does not apply to the single carbon fragments since CH_3^+ is formed with kinetic energy. Three exceptions to Stevenson's rule have been noted by Field (152), in propylene, methyl fluoroform, and methylcyclopropane. These are all cases of molecules of sufficient symmetry that there might well be sets of noninteracting electronic states, one set yielding R_1^+, one R_2^+, from $R_1R_2^+$. We think that while ionization to repulsive states and multiple ionization yield specific mass peaks, most ions—over 90 per cent in most mass spectra—result from quasi-equilibrium decomposition. Perfluoro compound mass spectra are entirely different from those of the corresponding hydrocarbons (158). In aromatic molecule ions such as benzene, there again might well be groups of noninteracting attractive electronic states, such as give rise to fluorescence in the case of molecules. By limiting the amount of electronic excitation converted into vibrational energy, such grouping of states into bands will increase the yield of parent ions.

Intermolecular Reactions

In the mass spectrometer, approximately 10^{-5} sec. elapses between the formation of the parent ions and the final collection of the parent and fragment ions. In a gas at one atmosphere, about 10^4 collisions will occur in this time as noted by Magee, Table II (1). As a consequence, the reactions of charge exchange, charge neutralization, and collisional deactivation will greatly change the decomposition reactions of the parent ion. Also ions can be produced by collisions of the type

$$A + B^* \rightarrow A^+ + B + e$$

if $E(B^*) > I^z(A)$. A striking example of this is the change in the apparent value of W, the energy in ev required to form an ion pair in a gas, with purity. A fraction of a per cent of impurity in helium lowers the value of W from 46.0 to 30. ev (159). Thus, the several attempts to explain the apparent lack of correlation between W and I^z for the rare gases and other molecules were in error; the expected correlation exists if the gas is pure so that ions cannot be formed by the reaction above.

The calculations on propane (119) indicate that over 50 per cent of the

ion reactions occurring in the mass spectrometer are completed in 10^{-9} sec. To that extent, the ions initially produced by secondary electrons of energy over about 25 ev should be similar to those produced in the mass spectrometer. However, the final products obtained from the ions formed by an electrical discharge in a gas or by ionizing radiation certainly do not result merely from simple charge neutralization. In the reactions $A^+ + e \rightarrow A$ and $B^+ + C^- \rightarrow BC$, the energy of charge neutralization will invariably be at least twice the amount necessary to cause dissociation. In accordance with the calculations for positive ion dissociation, such excited molecules even if quite large will probably dissociate before they are deactivated by collision. The fragments will then react further to yield the final products.

The secondary electrons produced by ionizing radiation can introduce energy into a system both by ionization and by excitation. The relative importance of these two paths in leading to chemical reaction is presently in dispute. One interesting approach to the determination of the importance of radicals is that of Gevantman & Williams (160), who use radioactive iodine as a scavenger in the radiolysis of alkanes. They find a complementary relation to the mass spectra of the compounds.

By appropriate modification to permit operation at higher pressures, a mass spectrometer can be used to study secondary reactions between ions and molecules. The work with the parabola spectrograph of Henglein & Ewald (161), while for high energy ions, is an important step in this direction.

In liquids, still less direct relationship will exist between mass spectra and radiation chemistry. Mass spectral data should be useful in yielding information about the amount of excess electronic energy imparted to the ions. However, only a negligible fraction of the ions formed will decompose before collision. Radiationless conversion of electronic energy to vibrational energy which is rapidly removed by collision will probably take the ion to its lowest state without decomposition. Chemical reaction will then result from dissociation following charge neutralization (162).

LITERATURE CITED

1. Magee, J. L., *Ann. Rev. Nuclear Sci.*, **3**, 171–92 (1953)
2. Magee, J. L., Kamen, M. D., Linschitz, H., and Platzman, R. L., *Physical and Chemical Aspects of Basic Mechanisms in Radiobiology* (National Academy of Sciences-National Research Council Publication 305, 145 pp., 1953)
3. *Discussions Faraday Soc., No. 10*, 339 pp., (1951)
4. *Nat'l. Bur. Standards, U. S., Circ. 522*, 273 pp., (1953)
5. Ewald, H., and Hintenberger, H., *Methoden und Anwendungen der Massenspektroskopie* (Verlag Chemie, Weinheim, Germany, 288 pp., 1952)
6. Barnard, G. P., *Modern Mass Spectrometry* (Institute of Physics, London, England, 326 pp., 1953)
7. Robertson, A. J. B., *Mass Spectrometry* (John Wiley & Sons, Inc., New York, N. Y., 135 pp., 1954)
8. *Mass Spectrometry* (Institute of Petroleum, London, England, 205 pp., 1952)
9. *Applied Mass Spectrometry* (Institute of Petroleum, London, England, 333 pp., 1954)
10. Mott, N. F., and Massey, H. S. W., *Theory of Atomic Collisions*, 2nd ed. (Clarendon Press, Oxford, England, 388 pp., 1949)
11. Massey, H. S. W., and Burhop, E. H. S., *Electronic and Ionic Impact Phenomena*, (Clarendon Press, Oxford, England, 669 pp., 1952)
12. Massey, H. S. W., *Negative Ions*, 2nd ed. (University Press, Cambridge, England, 136 pp., 1950)
13. *Catalog of Mass Spectral Data*, Am. Petroleum Inst. Research Project 44 (Carnegie Institute of Technology, Pittsburgh, Pennsylvania, 1947)
14. Smith, L. G., *Phys. Rev.*, **51**, 263–75 (1937)
15. Vought, R. M., *Phys. Rev.*, **71**, 93–101 (1947)
16. Warren, J. W., *Nature*, **165**, 810–11 (1950)
17. Honig, R. E., *J. Chem. Phys.*, **16**, 105–12 (1948)
18. Waldron, J. D., and Wood, K., *Mass Spectrometry*, 16–26 (Institute of Petroleum, London, England, 205 pp., 1952)
19. Morrison, J. D., *J. Chem. Phys.*, **19**, 1305–8 (1951)
20. Morrison, J. D., and Nicholson, A. J. C., *J. Chem. Phys.*, **20**, 1021–23 (1952)
21. Mariner, T., and Bleakney, W., *Phys. Rev.*, **72**, 807–14 (1947)
22. Foner, S. N., Kossiakoff, A., and McClure, F. T., *Phys. Rev.*, **74**, 1222 (1948)
23. Neuert, H., *Angew. Chem.*, **65**, 454–59 (1953)
24. Fox, R. E., Hickam, W. M., Kjeldaas, T., Jr., and Grove, D. J., *Phys. Rev.*, **84**, 859–60 (1951)
25. Fox, R. E., Hickam, W. M., Kjeldaas, T., Jr., and Grove, D. J., 211–6, *Natl. Bur. Standards, U. S., Circ. 522*, 273 pp. (1953)
26. Fox, R. E., Hickam, W. M., and Kjeldaas, T., Jr., *Phys. Rev.*, **89**, 555–58 (1953)
27. White, H. E., *Introduction to Atomic Spectra*, 394–98 (McGraw-Hill Book Company, Inc., New York, N. Y., 457 pp., 1934)
28. Wigner, E. P., *Phys. Rev.*, **73**, 1002–9 (1948)
29. Wannier, G. H., *Phys. Rev.*, **90**, 817–25 (1953)
30. Bates, D. R., Fundaminsky, A., Leech, J. W., and Massey, H. S. W., *Trans. Roy. Soc. (London)*, [A]**243**, 93–143 (1951)
31. Hickam, W. M., Fox, R. E., and Kjeldaas, T., Jr., *Phys. Rev.*, **96**, 63–65 (1954)
32. Bleakney, W., *Phys. Rev.*, **36**, 1303–8 (1930)
33. Stevenson, D. P., and Hipple, J. A., *Phys. Rev.*, **62**, 237–40 (1942)

34. Dibeler, V. H., Mohler, F. L., and Reese, R. M., *J. Research Natl. Bur. Standards*, **38**, 617–20 (1947)
35. Clarke, E. M., *Can. J. Phys.*, **32**, 764–74 (1954)
36. Hickam, W. M., *Phys. Rev.*, **95**, 703–5 (1954)
37. Lawrence, E. O., *Phys. Rev.*, **28**, 947–61 (1926)
38. Nottingham, W. B., *Phys. Rev.*, **55**, 203–19 (1939)
39. Morrison, J. D., *J. Chem. Phys.*, **21**, 1767–72 (1953)
40. Morrison, J. D., *J. Chem. Phys.*, **22**, 1219–23 (1954)
41. Morrison, J. D., *J. Chem. Phys.*, **21**, 2090–91 (1953)
42. McDowell, C. A., and Warren, J. W., *Discussions Faraday Soc., No. 10*, 53–65 (1951)
43. Neuert, H., and Clasen, H., *Z. Naturforsch.*, **7a**, 410–16 (1952)
44. Fox, R. E., and Langer, A., *J. Chem. Phys.* **18**, 460–64 (1950)
45. Fox, R. E., and Hickam, W. M., *J. Chem. Phys.*, **22**, 2059–63 (1954)
46. Omura, I., *Bull. Research Inst. Appl. Electronics*, **6**, 15–20 (1954)
47. Lennard-Jones, J., and Hall, G. G., *Proc. Roy. Soc.* (*London*), [A]**205**, 541–52 (1950)
48. Lennard-Jones, J., and Hall, G. G., *Trans. Faraday Soc.*, **48**, 581–84 (1952)
49. McDowell, C. A., and Cox, B. C., *J. Chem. Phys.*, **22**, 946 (1954)
50. Mulliken, R. S., *Phys. Rev.*, **47**, 413–15 (1935)
51. Hall, G. G., *Trans. Faraday Soc.*, **50**, 319–22 (1954)
52. Hall, G. G., *Trans. Faraday Soc.*, **49**, 113–18 (1953)
53. Hall, G. G., *Proc. Roy. Soc.* (*London*), [A]**213**, 102–13 (1952)
54. Franklin, J. L., *J. Chem. Phys.*, **22**, 1304–11 (1954)
55. Franklin, J. L., and Field, F. H., *J. Am. Chem. Soc.*, **76**, 1994–97 (1954)
56. Coats, F. H., and Anderson, R. C., *J. Am. Chem. Soc.*, **77**, 895–6 (1955)
57. Thompson, R., *Applied Mass Spectrometry*, 154–57 (The Institute of Petroleum, London, England, 333 pp., 1954)
58. Lindholm, E., *Proc. Phys. Soc.* (*London*), [A]**66**, 1068–70 (1953)
59. Lindholm, E., *Applied Mass Spectrometry*, 191–96 (The Institute of Petroleum, London, England, 333 pp., 1954)
60. Potter, R. F., *J. Chem. Phys.*, **22**, 974–79 (1954)
61. Hagstrum, H. D., 193–99, *Natl. Bur. Standards. U. S., Circ. 522*, 273 pp. (1952)
62. Hagstrum, H. D., *Rev. Mod. Phys.*, **23**, 185–203 (1951)
63. Hipple, J. A., *J. Phys. Chem.*, **52**, 456–62 (1948)
64. Stevenson, D. P., and Hipple, J. A., *J. Am. Chem. Soc.*, **64**, 1588–94 (1942)
65. Kandel, R. J., *J. Chem. Phys.*, **22**, 1496–99 (1954)
66. Kandel, R. J., *J. Chem. Phys.*, **23**, 84–87 (1955)
67. Hustrulid, A., Kusch, P., and Tate, J. T., *Phys. Rev.*, **54**, 1037–44 (1938)
68. Mohler, F. L., Dibeler, V. H., and Reese, R. M., *J. Chem. Phys.*, **22**, 394–97 (1954)
69. Marriott, J., and Craggs, J. D., *Applied Mass Spectrometry*, 173–84 (Institute of Petroleum, London, England, 333 pp., 1954)
70. Pritchard, H. O., *Chem. Revs.*, **52**, 529–63, (1953)
71. Ahearn, A. J., and Hannay, N. B., *J. Chem. Phys.*, **21**, 119–24 (1953)
72. Craggs, J. D., McDowell, C. A., and Warren, J. W., *Trans. Faraday Soc.*, **48**, 1093–99 (1952)
73. Thorburn, R., *Applied Mass Spectrometry*, 185–90 (Institute of Petroleum, London, England, 333 pp., 1954)

74. Lozier, W. W., *Phys. Rev.*, **46**, 268–76 (1934)
75. Hasted, J. B., *Proc. Roy. Soc.* (*London*), [A]**222**, 74–83 (1954)
76. Bailey, T. L., McGuire, J. M., and Muschlitz, E. E., Jr., *J. Chem. Phys.*, **22**, 2088–89 (1954)
77. Neuert, H., *Z. Naturforsch.*, **8a**, 459–62 (1953)
78. Gutbier, H., and Neuert, H., *Z. Naturforsch.*, **9a**, 335–37 (1954)
79. Neuert, H., and Rosenbaum, D., *Naturwissenschaften*, **41**, 85–86 (1954)
80. Eltenton, G. C., *J. Chem. Phys.*, **10**, 403 (1942)
81. Eltenton, G. C., *J. Chem. Phys.*, **15**, 455–81 (1947)
82. Robertson, A. J. B., *Mass Spectrometry*, 47–60 (Institute of Petroleum, London, England, 205 pp., 1952)
83. Robertson, A. J. B., *Discussions Faraday Soc.*, **14**, 115 (1953)
84. Foner, S. N., and Hudson, R. L., *J. Chem. Phys.*, **21**, 1374–82 (1953)
85. Robertson, A. J. B., *Applied Mass Spectrometry*, 112–20 (Institute of Petroleum, London, England, 333 pp., 1954)
86. Foner, S. N., and Hudson, R. L., *J. Chem. Phys.*, **21**, 1608–9 (1953)
87. Lossing, F. P., Ingold, K. U., and Henderson, I. H. S., *Applied Mass Spectrometry*, 102–11 (Institute of Petroleum, London, England, 333 pp., 1954)
88. Ingold, K. U., and Lossing, F. P., *J. Chem. Phys.*, **21**, 1135–44 (1953)
89. LeGoff, P., Robertson, A. J. B., Eltenton, G. C., and Lossing, F. P., Discussion in *Applied Mass Spectrometry*, 120–24 (The Institute of Petroleum, London, England, 333 pp., 1954)
90. Dunning, W. J., *Mass Spectrometry*, 96–98 (Institute of Petroleum, London, England, 205 pp., 1952)
91. Hipple, J. A., and Stevenson, D. P., *Phys. Rev.*, **63**, 121–26 (1943)
92. Langer, A., and Hipple, J. A., *Phys. Rev.*, **69**, 691 (1946)
93. Lossing, F. P., Ingold, K. U., and Henderson, I.H.S., *J. Chem. Phys.*, **22**, 621–25 (1954)
94. Evans, M. G., and Szwarc, M., *J. Chem. Phys.*, **19**, 1322–23 (1951)
95. McDowell, C. A., *Applied Mass Spectrometry*, 124–5 (Institute of Petroleum, London, England, 333 pp., 1954)
96. Farmer, J. B., Henderson, I.H.S., McDowell, C. A., and Lossing, F. P., *J. Chem. Phys.*, **22**, 1948 (1954)
97. Mc Dowell, C. A., *Trans. Faraday Soc.*, **50**, 423–30 (1954)
98. McDowell, C. A., *Applied Mass Spectrometry*, 129–53 (Institute of Petroleum, London, England, 333 pp., 1954)
99. Laidler, K. J., *J. Chem. Phys.*, **22**, 1740–45 (1954)
100. Mann, M. M., Hustrulid, A., and Tate, J. T., *Phys. Rev.*, **58**, 340–47 (1940)
101. Shuler, K. E., *J. Chem. Phys.*, **21**, 624–32 (1953)
102. Laidler, K. J., and Shuler, K. E., *Chem. Revs.*, **48**, 153–224 (1951)
103. Koffel, M. B., and Lad, R. A., *J. Chem. Phys.*, **16**, 420–22 (1948)
104. Mitchell, J. J., and Coleman, F. F., *J. Chem. Phys.*, **17**, 44–55 (1949)
105. Geerk, J., and Neuert, H., *Z. Naturforsch.*, **5a**, 502–4 (1950)
106. Langer, A., Hipple, J. A., and Stevenson, D. P., *J. Chem. Phys.*, **22**, 1836–44 (1954)
107. Waldron, J. D., *Trans. Faraday Soc.*, **50**, 102–6 (1954)
108. Branson, H., and Smith, C., *J. Am. Chem. Soc.*, **75**, 4133–38 (1953)
109. Hoch, M., Blackburn, P. E., Dingledy, D. P., and Johnston, H. L., *J. Phys. Chem.*, **59**, 97–99 (1955)

110. Chupka, W. A., and Inghram, M. G., *J. Phys. Chem.*, **59**, 100–4 (1955)
111. Jahn, H. A., and Teller, E., *Proc. Roy. Soc.* (*London*), [A]**161**, 220–35 (1937)
112. Van Vleck, J. H., *J. Chem. Phys.*, **1**, 219–38 (1933)
113. Lossing, F. P., Tickner, A. W., Bryce, W. A., *J. Chem. Phys.*, **19**, 1254–58 (1951)
114. Niira, K., and Oohata, K., *J. Phys. Soc. Japan*, **7**, 61–65 (1952)
115. Duchesne, J., and Burnelle, L., *J. Chem. Phys.*, **21**, 2005–8 (1953)
116. Rosenstock, H. M., Wallenstein, M. B., Wahrhaftig, A. L., and Eyring, H., *Proc. Natl. Acad. Sci. U. S.*, **38**, 667–78 (1952)
117. Wallenstein, M. B., Wahrhaftig, A. L., Rosenstock, H. M., and Eyring, H., *Symposium on Radiobiology*, 70–93 (Nickson, J. J., Ed., John Wiley and Sons, Inc., New York, N. Y., 465 pp., 1952)
118. Wallenstein, M. B., *The Ionization and Dissociation of Molecules by Electron Impact* (Doctoral thesis, Univ. of Utah, Salt Lake City, Utah, 1951)
119. Rosenstock, H. M., *Absolute Rate Theory for Isolated Systems and the Mass Spectra of Polyatomic Molecules* (Doctoral thesis, Univ. of Utah., Salt Lake City, Utah, 1952)
120. Washburn, H. W., and Berry, C. E., *Phys. Rev.*, **70**, 559 (1946)
121. Glasstone, S., Laidler, K. J., and Eyring H., *The Theory of Rate Processes* (McGraw-Hill Book Company, Inc., New York, N. Y., 611 pp., 1941)
122. Magee, J. L., *Proc. Natl. Acad. Sci. U. S.*, **38**, 764–70 (1952)
123. Slater, N. B., *Proc. Roy. Soc.* (*London*), [A]**194**, 112–31 (1948)
124. Kropf, A., *The Isotope Effect and Metastable Ions in the Mass Spectra of Polyatomic Molecules* (Doctoral thesis, Univ. of Utah, Salt Lake City, Utah, 1954) (To be published)
125. Hipple, J. A., and Condon, E. U., *Phys. Rev.*, **68**, 54–55 (1945)
126. Hipple, J. A., Fox, R. E., and Condon, E. U., *Phys. Rev.*, **69**, 347–56 (1946)
127. Hipple, J. A., *Phys. Rev.*, **71**, 594–99 (1947)
128. Donnally, B. L., and Carr, H. E., *Phys. Rev.*, **93**, 111–14 (1954)
129. Evan, M. W., Bauer, N., and Beach, J. Y., *J. Chem. Phys.*, **14**, 701–7 (1946)
130. Dibeler, V. H., and Mohler, F. L., *J. Research Natl. Bur. Standards*, **45**, 441–44 (1950)
131. Schissler, D. O., Thompson, S. O., and Turkevich, J., *Discussions Faraday Soc., No. 10*, 46–53 (1951)
132. Friedman, H. L., Bernstein, R. B., Gunning, H. E., *J. Chem. Phys.*, **23**, 109–12 (1955)
133. Flynn, J. H., and Hulbert, H. M., *J. Am. Chem. Soc.*, **76**, 3396–3400 (1954)
134. Condon, F. E., *J. Am. Chem. Soc.*, **73**, 4675–78 (1951)
135. Stevenson, D. P. and Wagner, C. D., *J. Chem. Phys.*, **19**, 11–16 (1951)
136. Stevenson, D. P., *J. Chem. Phys.*, **19**, 17–21 (1951)
137. Stevenson, D. P., *J. Chem. Phys.*, **15**, 409–11 (1947)
138. Langer, A., *J. Phys. Chem.*, **54**, 618–29 (1950)
139. Langer, A., and Johnson, P., *Rearrangement Peaks in the Mass Spectrum of Terminally C^{13}-Labeled Neopentane* (Paper presented at *Symposium on Isotopes in Petroleum Chemistry*, Amer. Chem. Soc., Chicago, Ill., September, 1950)
140. Happ, G. P., and Stewart, D. W., *J. Am. Chem. Soc.*, **74**, 4404–8 (1952)
141. Momigny, J., *Bull. soc. roy. sci. Liège*, **22**, 541–60 (1953)
142. Judson, C. M., Francel, R. J., and Weicksel, J. A., *J. Chem. Phys.*, **22**, 1258–59 (1954)

143. McFadden, W. H., *The Mass Spectra of Deuterated Butanes* (Doctoral thesis, Univ. of Utah, Salt Lake City, Utah, 1954) (To be published)
144. Stevenson, D. P., *J. Chem. Phys.*, **10**, 291–94 (1942)
145. Stevenson, D. P., *Discussions Faraday Soc., No. 10*, 35–45 (1951)
146. Eyring, H., Walter, J., and Kimball, G. E., *Quantum Chemistry* (John Wiley & Sons, Inc., New York, N. Y., 394 pp., 1947)
147. Stevenson, D. P., *Trans. Faraday Soc.*, **49**, 867–78 (1953)
148. Schissler, D. O., and Stevenson, D. P., *J. Chem. Phys.*, **22**, 151–52 (1954)
149. Franklin, J. L., and Lumpkin, H. E., *J. Am. Chem. Soc.*, **74**, 1023–26 (1952)
150. Franklin, J. L., and Field, F. H., *J. Chem. Phys.*, **21**, 2082–83 (1953)
151. Field, F. H., *J. Chem. Phys.*, **20**, 1734–39 (1952)
152. Field, F. H., *J. Chem. Phys* , **21**, 1506–10 (1953)
153. Field, F. H., and Franklin, J. L., *J. Chem. Phys.*, **22**, 1895–1904 (1954)
154. Collin, J., *Bull. soc. roy. sci. Liège*, **20**, 707–10 (1951)
155. Collin, J., *Bull. soc. roy. sci. Liège*, **21**, 446–56 (1952)
156. Collin, J., *Bull. soc. chim. Belges.*, **62**, 411–27 (1953)
157. Hissel, J., *Bull soc. roy. sci. Liège*, **21**, 457–63 (1952)
158. Dibeler, V. H., Reese, R. M., and Mohler, F. L., *J. Chem. Phys.*, **20**, 761 (1952)
159. Bortner, T. E., and Hurst, G. S., *Phys. Rev.*, **93**, 1236–41 (1954)
160. Gevantman, L. H., and Williams, R. R., Jr., *J. Phys. Chem.*, **56**, 569–74 (1952)
161. Henglein, A., and Ewald, H., 205–10, *Natl. Bur. Standards, U. S., Circ. 522*, 273 pp., (1952)
162. Burton, M., and Patrick, W. N., *J. Phys. Chem.*, **58**, 421–30 (1954)

RADIOCHEMICAL SEPARATION TECHNIQUES

By H. L. Finston and John Miskel
Brookhaven National Laboratory, Upton, Long Island, New York

Introduction

A survey has been made of the recent literature,[1] covering the fields of nuclear physics, nuclear chemistry, radiochemistry, and analytical chemistry with respect to new separation techniques in general and to application of separation techniques to the particular problems facing the investigator working with radionuclides. The problems of separation of radionuclides, except for the special cases of Szilard-Chalmers and recoil separation, are essentially the problems of analytical chemistry. The analytical chemistry literature has been carefully scrutinized, and suggestions are made as to the application of procedures which may not have been used for radiochemical separations. The increased application of γ-counting (both of solids and solutions) has obviated in some cases the necessity for preparing a sample in a gravimetric form previous to counting. This presents the possibility of applying standard analytical procedures, such as colorimetry, polarography, etc., to the problem of yield determination.

The separation procedures have been divided into four general classes: precipitation, solvent extraction, volatilization, and chromatography. Miscellaneous chemical methods, such as "carrier-free" procedures and nongravimetric yield determinations, have been included in the appropriate major class. In addition, the application of instruments such as γ-ray spectrometers and α pulse-height analyzers to the identification of radionuclides is discussed.

To facilitate the use of this chapter as a reference source for radiochemical separations, the material and references discussed in each section have been arranged in tabular form wherever possible.

Precipitation

The use of precipitation reactions for isolating specific elements or groups of elements is, of course, the technique most familiar to radiochemists. In addition to the more conventional precipitation methods, precipitations from homogeneous solutions and precipitations in the presence of complexing agents, for example EDTA (ethylenediamine tetra-acetic acid), which have been developed primarily by the analytical chemist are discussed. The precipitation onto ion exchange columns is mentioned as a rather new technique which may have some useful application, and plating procedures are also included under this heading.

Complexones.—The usefulness of metal chelates in radiochemical separa-

[1] January, 1953 to January, 1955.

TABLE I

STABILITY OF EDTA CHELATE COMPLEXES*

pH	4.00	6.50	8.65	11.00
	Cr	Ni	Ni	Co
	Cu	Cu	Co	Ni
	Ni	Co	Cu	Cu
	Pb	Zn, Cd	Zn, Cd	Zn, Cd
	Co	Ca	Ca	Ca
			Mg	Mg
			Sr	Sr
			Ba	Ba

* *Tech. Bull. No. 2. The Versenes*, Bersworth Chemical Company, Framingham, Mass. (1951).

tions has long been recognized, and the application of reagents which form insoluble compounds with metal cations, such as 8-hydroxyquinoline (oxine), cupferron, α-nitroso-β-napthol, etc., are commonplace. In recent years a number of new aminopolycarboxylic acids have come into widespread use, and of these, EDTA is, in the opinion of Belcher (1), perhaps the most important reagent ever applied in analytical chemistry. These compounds (the complexones) have the special property of forming water-soluble chelates with a large number of metallic ions, and the chelation is preferential. Table I shows the order of chelation of some of the common metals at various pH's in order of decreasing strength of complex from top to bottom.

The uses of the complexones in analysis may be divided into four categories: (*a*) masking action, (*b*) colorimetric analyses, (*c*) titrimetry, and (*d*) polaragraphy. Of these, only the masking action in precipitation reactions is of primary interest in the field of radiochemical separations. The influence of oxine on the complexes formed between EDTA and various metallic ions has been studied. The results summarized in Table II indicate the specificity which may be obtained using a general precipitant in con-

TABLE II

IONS PRECIPITATED BY OXINE IN THE PRESENCE OF EDTA*

Acetic Acid-Ammonium Acetate Buffer	Sodium Acetate-Ammonium Hydroxide Buffer
Mo^{6+}	Al^{3+}
W	Fe^{3+}
U^{6+}	Cu^{+}
V^{5+}	Cu^{++}

* Prible, R., and Malat, M., *J. Coll. Czech. Chem. Comm.*, **15**, 121 (1950).

junction with the complexones. Some recent applications of complexones in conjunction with precipitation from homogeneous solution have been reported and are reviewed in that section.

Precipitation from homogeneous solution.—When a precipitate is formed by addition of a reagent to a solution, even though very dilute reagent may be added with vigorous stirring, there is often considerable coprecipitation and occlusion as a result of local supersaturation. Subsequent digestion of the precipitate may not materially decrease the amount of "normally nonprecipitating" ion or radical present in the precipitate. When the precipitating ion or radical can be formed in the solution by the gradual hydrolysis or oxidation of a parent compound, the liquid phase remains homogeneous and the absence of concentration gradients results in greatly reduced coprecipitation, or occlusion, or both of foreign ions.

The gelatinous nature of hydroxide precipitates, such as ferric hydroxide, which tends strongly to cause coprecipitation and occlusion, early led to the application of homogeneous precipitation techniques to these substances by analytical chemists in order to obtain more compact and pure precipitates. In many cases, radiochemical procedures take advantage of the occlusion and coprecipitation accompanying these gelatinous precipitates as a means of "scavenging" a solution of unwanted activities. On the other hand, there are often situations in which the scavenging process is undesirable and the use of a homogeneous technique may be advantageous.

A most satisfactory method for increasing the pH of a solution in a homogeneous manner is by the hydrolysis of urea at 90° to 100°C. The hydrolysis can be stopped at any desired pH by cooling the solution; the maximum pH which can be reached depends upon the concentration of ammonium salt in the solution. Other effective methods for increasing the pH of a solution are by hydrolysis of acid amides, such as acetamide, and of trichloracetates.

The application of neutralization reactions is not limited to precipitation of basic salts, since many other precipitates can be formed by neutralization of an acid solution. The precipitation of acid-soluble salts may also be accomplished by the slow homogeneous hydrolysis of urea. Gordon & Firsching (2) have precipitated barium chromate from acid solution by raising the pH in this manner, while Heyn & Schupak (3) have used the hydrolysis of ammonium peroxydisulfate to lower the pH in order to precipitate barium sulfate from a solution containing the barium complexed by ethylenediamine. The hydrolysis of esters of inorganic acids and the oxidation or reduction of a parent compound to yield the desired precipitating ion extends the scope of the homogeneous technique beyond the limitations of neutralization reactions. Elving & Zook (4) precipitate $PbSO_4$ with dimethyl sulfate. The separation of americium from lanthanum by the fractional precipitation of lanthanum oxlate with dimethyl oxalate is reported by Herman (5). A recent application of this technique involving a gradual oxidation (6) is the precipitation of $Fe(OH)_3$ from a versene complex at a fixed pH (3.0 to 3.2)

by oxidation with H_2O_2 at room temperature. An example of homogeneous precipitation involving reduction is the precipitation of thorium iodate (7) with the iodate produced by reduction of periodate with ethylene glycol. The latter is produced upon the hydrolysis of β-hydroxyethyl acetate. The homogeneous precipitation of metal sulfides by use of thioacetamide as a source of sulfide has been studied by Flaschka (8). The sulfide precipitates obtained in this manner have the usual advantages of homogeneous precipitates in that they are dense, coarsely crystalline, and easily filtered. The use of EDTA in combination with thioacetamide has also been investigated by

TABLE III

ELEMENTS PRECIPITATED WITH THIOACETAMIDE IN ACID SOLUTION*

Element	Max. normality of acid			Remarks
	HCl	H_2SO_4	HNO_3	
Antimony (III)	1	—	—	
Arsenic (III)	1	6	1	As_2S_3 incompletely ppt. from HAc sol'n.
Arsenic (V)	6	6	—	
Bismuth	1	—	2	
Cadmium	1	6	—	
Copper	2	6	0.5	
Germanium	—	6	—	
Lead	0.1	—	0.3	Ppt. slow from hot neutral or weak acid. Rapid from acid sol'n made ammoniacal
Mercury	0.2	0.5	0.5	
Selenium				Mixture of S and Se ppts. from hot or cold acid solution
Tin	1			

* Reproduced from *Chemist-Analyst*, 44, 5 (1955) (Courtesy J. T. Baker Chemical Company).

Flaschka (9). This combination allows for increased specificity in sulfide precipitations resulting from the masking effect of the EDTA for some ions. Excess Ca^{++} can be used to demask an EDTA-metal complex when desired. Tables III and IV summarize the results obtained with thioacetamide.

Precipitation on ion exchange columns.—Precipitation reactions in which the source of the precipitating agent is a pretreated ion exchange resin have recently been performed and may have some application for radiochemical analysis. For example, this technique has been applied to the precipitation of BiOCl on Dowex 1,[2] which had been pretreated with hydrochloric acid to convert the resin to the chloride form (10). The columns were prepared by

[2] Dowex-1 is a strongly basic anion exchange resin of the quaternary amine type.

TABLE IV

ELEMENTS PRECIPITATED WITH THIOACETAMIDE IN NEUTRAL OR BASIC SOLUTION

Element	Solution	Remarks
Bismuth	Ammoniacal	Bi_2S_3 ppt. in presence of tartrate or EDTA
Cadmium	KCN or ammoniacal	Prolonged boiling and excess thioacetamide required. EDTA prevents or delays CdS ppt. Excess Ca allows ppt. to form in presence of EDTA.
Copper	Ammoniacal	Rate of ppt. influenced by EDTA. Prolonged boiling required for complete ppt.
Cobalt	Ammoniacal+NH_4^+	Coarse ppt. forms after incubation period. CoS shows no colloidal tendency. EDTA masks ppt'n. Ca demasks.
Iron	Ammoniacal	Acid Fe (III) solutions are reduced by thioacetamide. FeS ppts. on addition of ammonia. No ppt. in presence of EDTA.
Lead	Neutral, or ammoniacal	PbS ppts. slowly from neutral or weakly acid sol'ns. Rapid ppt'n from acid sol'n made ammoniacal.
Mercury	Neutral, or ammoniacal	HgS precipitates in cold. Not affected by EDTA.
Nickel	Ammoniacal+NH_4^+	Coarse ppt. forms after incubation period. NiS shows no colloidal tendency. EDTA masks ppt'n. Ca demasks.
Silver	Ammoniacal or neutral	Ppt. forms at once in cold sol'n. EDTA has no effect
Thallium (I)	Ammoniacal	Ppt. forms readily, even in presence of EDTA
Thallium (III)	Ammoniacal	Slightly acid Tl (III) solution forms Tl_2S after addition of ammonia.
Tin (II)	Ammoniacal tartrate	SnS forms on heating. EDTA masks ppt'n. Ca unmasks.
Tin (II)	Stannite	SnS forms, hot or cold
Tin (IV)	Ammoniacal tartrate	EDTA has no effect
Zinc	Ammoniacal	A cold sol'n allowed to stand 1/2 to 3/4 hr., then heated gives easily filterable ppt. after long incubation period.

equilibration of the resin with 6 N HCl, followed by washing with water to remove excess acid. The washing was continued until the effluent gave no test for chloride. The sample, in a minimum volume of 1 to 2 N HNO_3, formed a white precipitate of BiOCl at the top of the column which migrated evenly down the column upon washing with water. This suggests the possibility of an equilibrium of the type,

$$R\text{—}Cl + BiO^+ = R^+ + BiOCl$$

which, if so, affords a convenient technique for multiple reprecipitation and consequently a very pure precipitate. Bismuth and thorium were separated in this manner; thorium was completely recovered in the eluant, and greater than 99 per cent of the bismuth was retained on the column. Sr^{90} and Y^{90} were also separated in a similar manner. An equilibrium mixture of Sr^{90} and Y^{90} was passed through a Dowex-1 column which had been pretreated with hydroxide ion. The Sr^{90} was eluted with water, the Y^{90} remaining on the column as yttrium hydroxide. An aluminum absorption curve of the strontium fraction (Fig. 1) showed no more Y^{90} present than that corresponding to the natural growth in the time interval between the separation and the measurement. The yttrium was removed from the column by elution with 1 M HCl. An analysis of the decay curve of the yttrium fraction (Fig. 2) indicated less than 1 per cent Sr^{90} contamination.

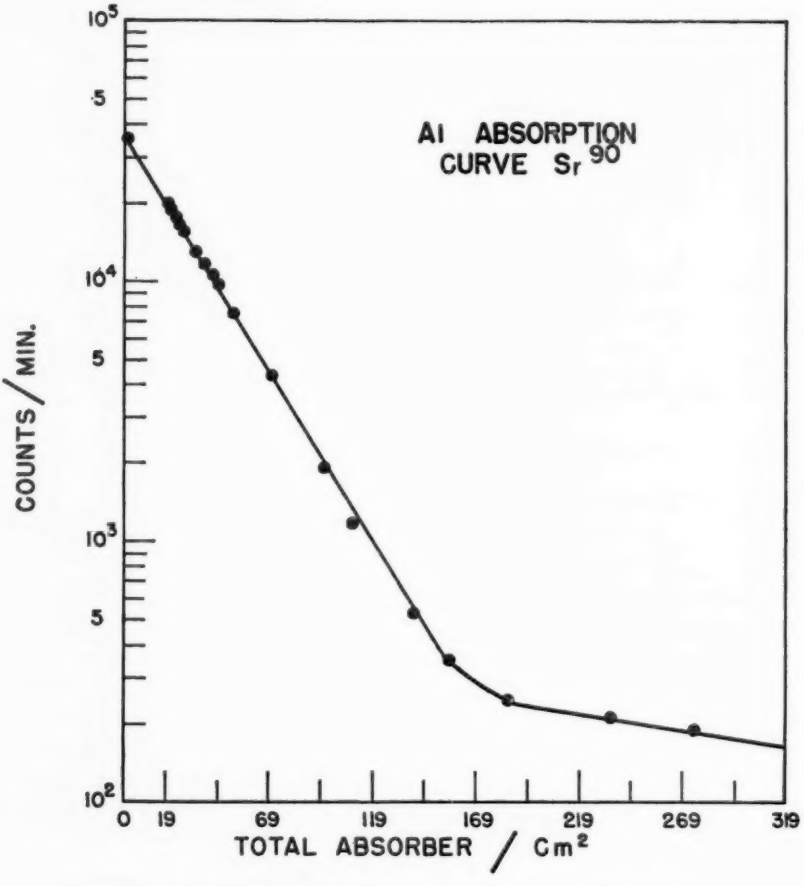

FIG. 1. Aluminum absorption curve of the strontium fraction.

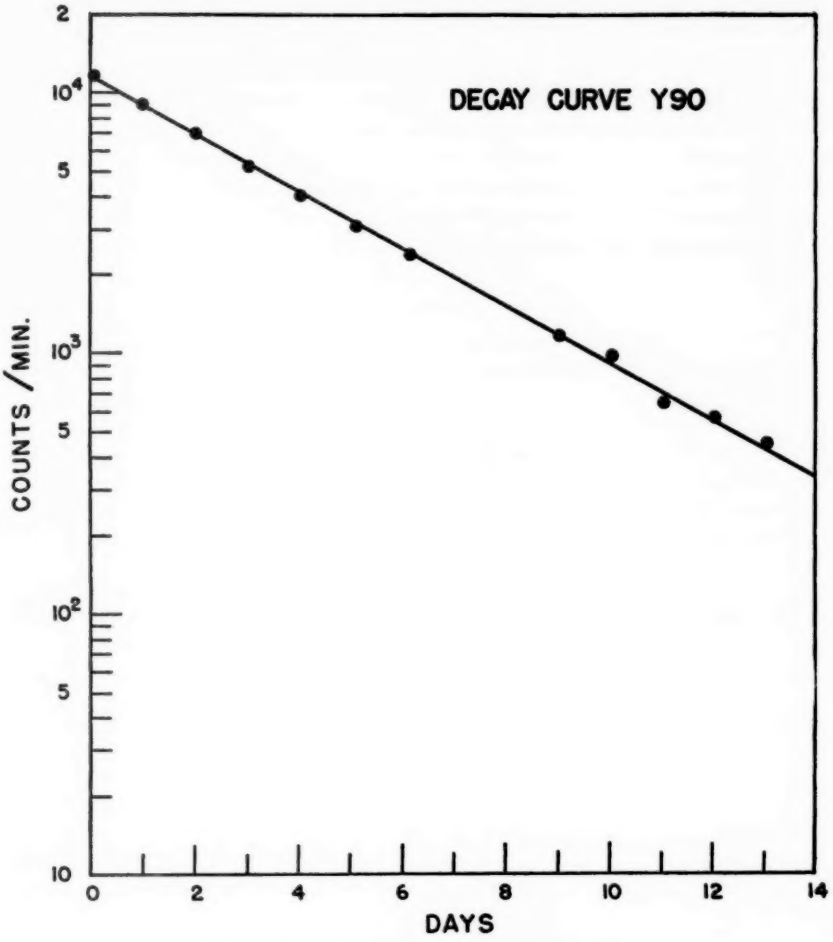

FIG. 2. Decay curve of the yttrium fraction.

Komlev & Tsimbalista (11) performed similar precipitation separations on alumina columns. By pretreating a column with silver ion, they have removed iodide, bromide, and chloride from solution. They also have employed sulfide-treated columns to remove bismuth and cadmium, and iodide-treated columns for separation of silver, mercury, and lead.

Precipitation separations.—A new analogue of cupferron, 2-fluorenyl cupferron, has been prepared and used successfully in the quantitative determination of iron (12). The compound has many characteristics in common with cupferron: it forms precipitates with many cations, and is as sensitive as neocupferron for the determination of iron. The qualitative characteristics of the fluorene analogue are given in Table V.

Sircar and his co-workers have tested the thiosemicarbazones of eight aldehydes and five ketones as reagents for some metallic cations at different pH ranges (13). In some cases results were obtained which may be of interest in the field of separations chemistry and are summarized in Table VI. Precipitation separations, other than those previously described, are summarized in Table VII.

The necessity for routine analysis of long-lived fission products has focused attention on the need for simpler, yet reliable, procedures for radiometric determinations of Cs^{137}, Zr^{95}, and Sr^{90}. Another nuclide of importance, although not a fission product, is P^{32} which is widely used as a tracer and beta-standard. Improved procedures for these nuclides are summarized in Table VIII.

TABLE V

PRECIPITATIONS WITH 2-FLUORENYL CUPFERRON

Cation	Solution	Precipitate
Sb^{+++}	Acid (HCl)	Light yellow
Ba^{++}	Neutral	White
Bi^{+++}	Sl. Acid (HCl)	White
Cd^{++}	Sl. Acid (HCl)	White
Ca^{++}	Basic (NH_4OH)	White
Cr^{+++}	Sl. Acid (HCl)	Dirty-white
Co^{++}	Neutral; sl. basic (NH_4OH)	Red-brown
Cu^{++}	Acid (HCl); neutral	Dirty-white
Fe^{+++}	Acid (HCl)	Red-brown
Pb^{++}	Neutral	White
Mn^{++}	Sl. Acid (HCl)	Dirty-white
Hg^{+}	Sl. Acid (HCl)	White
Hg^{++}	Neutral	White
Ni^{++}	Sl. Acid (HCl)	Yellow-green
Ag^{+}	Neutral	White
Sr^{++}	Neutral	White
Th^{++++}	Neutral	White
Sn^{++}	Neutral	White
Sn^{++++}	Neutral	White
Zn^{++}	Sl. Acid (HCl)	White

Electro- and chemical plating.—A number of review articles on electrochemical analysis have been published since 1951, including a comprehensive monograph by Lingane (39) published in October 1953. The book discusses principles, methods, and apparatus of electroanalysis, controlled potential electrolysis, internal electrolysis, as well as electrographic analysis, potentiometric titrations, coulometric analysis, and conductometric analysis. The latter four techniques are of interest to the radiochemist only insofar as they

offer other than gravimetric methods for yield determinations. Among the other review articles are a shorter and less comprehensive review by Lingane (40), and a recent review article by DeFord (41) which covers the theory of electroanalysis, controlled potential separations, mercury cathode separations, internal electrolysis and constant current electrolysis, and the techniques of electro-oxidation and reduction and coulometric titrations.

Ishibashi & Fujinga (42) have published a review on the principles and methods of controlled-potential electrolysis, and Palmer & Vogel (43) have described an electronic device for regulation of the cathode at the desired potential, with respect to a standard reference electrode, to ± 1 millivolt.

TABLE VI

PRECIPITATIONS WITH THIOSEMICARBAZONES

Aldehyde or Ketone	Ion	pH	Color of Precipitate	Observations*
Vanilline	Hg^{+}	5.89	light yellow	soluble in alcohol and acetone
Benzaldehyde	Hg^{++}	5.89	light yellow	quantitative, soluble in alcohol
	Cu^{+}	3.4–7	green gel	quantitative
	Cu^{++}	3.4–7	green gel	quantitative
Anisaldehyde	Hg^{+}	5.89	yellow precipitate	insoluble in alcohol, dil acids and dil NH_4OH
	Hg^{++}	5.89	yellow precipitate	same as above
	Cu^{++}	3.4–7	green precipitate	soluble hot alcohol
Resorcyl-aldehyde	Hg^{++}	3.4–7	yellow precipitate	quantitative, soluble in hot alcohol

* In addition to the precipitation reactions, it was noted that Co formed highly-colored complexes with some of the reagents investigated allowing the detection of 1 part in 10^8.

Some recent applications of controlled potential electrolysis are reported in Table IX.

Irvine (49) and his group at MIT are studying the deposition behavior of millimolar solutions of Tl and Cd at a mercury cathode. They have found that the potential at which half of the element is deposited agrees closely with the polarographic half-wave potential; the presence of other ions in the mercury, specifically moderate amounts of Cu and Bi, does not affect the deposition behavior of Cd.

The use of a micro-mercury cathode consisting of a rigid metal cathode plated with mercury is reported by Hahn (50). This technique was developed for use with small volumes of solution where the conventional mercury pool cathode was unsatisfactory because of the limited mercury surface in contact with the solution, the inherent difficulty in minimizing spray losses, and the problem of achieving efficient stirring. The cathode used by the author

TABLE VII

Precipitation Separations

Element	Reagent	Remarks	Ref.
Barium	CO_3	Ba precipitated from NH_4OH-EtOH solution. Solubility loss of 0.005% when 3.04 gm. of barium are precipitated.	14
Cadmium	2-(*o*-Hydroxyphenyl)-benzoxazole	Precipitation is complete in the pH range 11–12. Tartrate employed to complex heavy metals.	15
	Triphenylmethyl-arsonium Iodide	Quantitative in the range of 1–100 mg. Cd. Interfering ions are Sb, Bi, As, Cu, Pb, Hg, and Ag.	16
	Quinoline-8-carboxylic acid	Excess reagent added to acid solution and pH adjusted by making the solution alkaline to bromthymol blue.	17
	Reinecke's salt (diamine tetrathiocyanate-chromium (III))	Forms an insoluble salt in 0.1 to 1.0 N mineral acid, with a complex cadmium-bithiourea cation.	18
Cesium, Potassium, Rubidium, and Ammonium Ion	Sodium tetra-phenyl boron	Precipitate made from slightly acid solution. Mg, Ca, Al, Fe, Co, Ni, Mn, SO_4, PO_4 do not interfere.	19
Copper	*p*-Anisidine	As little as 0.688γ detected in aqueous solution containing SCN^- or I^-. pH = 6.8–6.9.	20
Germanium	240 gm. NH_4Cl + 14 gm. Tartaric acid + 13 gm. $BaCl_2 \cdot 2H_2O + H_2O$ to make 1 liter	Very insoluble precipitate. Up to 5 mg. is completely precipitated from basic solution.	21
	1% 3,4-dihydroxyazobenzene in ethanol and hydrochloric acid	Precipitation is complete.	22
Mercury	Phenylboric acid	The precipitate was dried at 70°C. and weighed in vacuo.	23
	2-(O-Hydroxyphenyl)-benimidazole	Hg can be determined with an accuracy of −0.3% in the range of 10–80 mg. Ferric ion is the main interference.	24
	Adipic acid	Hg is precipitated from an aqueous solution at pH 2.8 by the addition of saturated adipic acid solution. There is no interference from Pb, Ag, or Tl.	25
Platinum Group	P-Iodoaniline	Precipitates Pa, Pt and Os at pH 4.	26
	Strychnine	Dense precipitates formed with Pa, Pt, Ir, Os.	26
	Brucine	Reacts like strychnine	26
	2 Mercaptabenzothiole	Pt and Pd precipitate in the cold; the remainder react upon heating.	26
Silver	1,2- 3-benzotriazole	10–100 mg. Ag precipitated quantitatively in the presence of EDTA. There is no interference from metals, and Cl^-, Br^-, and F^- do not interfere. Iodide forms a precipitate with Ag.	27
Thorium	Benzenephosphonic acid	pH 0.5–1. Dry at 150°C. to constant weight factor = 0.38796%.	28
	Iodate	40% HNO_3 solution; 10% oxalic acid. Ti, Zr, Bi are not precipitated.	29
	2.4-Dichlorophenoxyacetic acid	Ca, Ba, Sr, Mg, Zn, etc., and earths do not interfere.	30
	Phenylglycine-e.c.-carboxylic acid	Neutral solution. As little as 1 mg. Th can be precipitated.	31
Zirconium	Benzilic acid	Quantitatively precipitated 10–60 mg. Zr from 50 ml. solution containing 15 ml. 12 N, HCl. The precipitate is ignited to ZrO_2.	32

TABLE VIII

TABLE VIII

IMPROVED RADIOMETRIC DETERMINATIONS

Nuclide	Precipitate	Carriers	Conditions	Remarks	Contamination (in per cent)	Precision	Ref.
Ca^{137}	Cesium phosphotungstate	3 mg. Ca 0.5 mg. Ru	Precipitated with 1 ml. 0.05 0.05 *M* phosphotungstic acid from 5*N* HNO_3	Precipitate mounted on Al disc	Ce 0.1 La Zr 0.2 Ru	Quant.	33
	Cesium (or Potassium) Dipicrylaminate	5 mg. Cs	Precipitated from neutral solution with 2 ml. 3% Magnesium dipicrylamine reagent	The sample was first scavenged by Fe $(OH)_3$, $Y(OH)_3$, and $SrCO_3$ precipitations		−6%	34
Zr^{95}	Zirconium mandelate	5 mg. Zr^4	Precipitated from dilute HCl solution with 5 ml. 16% mandelic acid reagent	Preliminary separation as the barium fluozirconate	Ce—.08 to 1.85 Sr—0.22 to 2.25 Nb—0.07 to 0.26		35
Sr^{90}	Strontium Oxalate	10 mg. Sr	Precipitated from ammoniacal solution with 10 ml. saturated ammonium oxalate	Precipitate mounted on Al disc	Ce—0.5 Ru—0.16 Cs—0.05 Zr, Nb—0.04 Y—0.14	Quant.	36
	Strontium Carbonate	10 mg. Sr	Precipitated from ammoniacal solution with 3M ammonium carbonate	Approximately 60% chemical yields	Compares favorably with fuming HNO_3 procedure		37
P^{32}	Bismuth Phosphate	50 mg. PO_4	dilute HNO^3 acid 20 ml. 0.3 M $Bi(NO_3)_3$ in 5M HNO_3	Rapid procedure	SO_4, Pb, PB^4, Cd	Good	38
	Magnesium Ammonium Phosphate	10 mg. PO_4 stoichiometric amt. of Mg.	Ammonium hydroxide added to an acid solution	Rapid procedure	All soluble cations other than Na, K, NH_4	Good	38
	Ammonium Phosphomolybdate	The procedure followed is given in *Scott's Standard Methods of Chemical Analysis*, N. H. Furman, Ed., p. 694, D. Van Nostrand and Company, New York (1939)		Good results were obtained under proper conditions. The precipitate is finely divided and difficult to filter			38

consisted of a silver foil 1.5×2 cm. bent into a semicircular shape and coated on both sides with 0.3 to 0.5 gm. of mercury. Stirring is accomplished by the evolution of gases during electrolysis, and spray losses are minimized by use of a tall, narrow, cylindrical cell. The anode consisted of a length of 12 gauge platinum wire. Solutions containing iron or copper and aluminum, uranium or zirconium in 3–5 ml. of 0.5 to 1.0 N H_2SO_4 were electrolyzed to determine the

TABLE IX

CONTROLLED POTENTIAL ELECTROLYSIS

Element	Voltage vs Sat Calomel Electrode	Conditions	Remarks	Ref.
Antimony	−0.3	Sulfate-citrate solution 50–70°C.	N_2H_4 or NH_2OH used to prevent anodic oxidation	48
Bismuth	−0.2	Sulfate-citrate solution 50–70°C.		48
Bismuth	−0.4	Tartrate solution		46
Copper	−0.3	Tartrate solution		46
Copper	−0.22, −0.3	HCl solution	Isolated anode	47
Lead	−0.5, −0.6	Tartrate solution		46
Silver	−0.24	Ammoniacal solution	O_2 bubbled through solution. Copper present	44
Tin	−0.6, −0.65	Tartrate solution		46
Tin	−0.6	Sulfate-citrate solution 50–70°C.	N_2H_4 or NH_2OH used to prevent anodic oxidation	48
Zinc	−1.4	Ammoniacal+NH_4Cl	20 to 40 min.	45

cathode efficiency. In all cases the iron or copper was plated quantitatively while at least 98 per cent of the foreign ions remained in solution.

Bock & Hockstein (51) have made a detailed investigation of the deposition of about 20 different elements into a mercury cathode. The anode consisted of 0.08 mm. platinum wire wound into a flat spiral of 30 mm. diameter, and the mercury cathode had a surface area of 50 cm.^{2} All the electrolyses were carried out at room temperature. Their results are summarized in Table X. Chemla & Pauly (52) have employed electrodeposition into a mercury cathode to separate Na^{22} carrier-free from a magnesium target. They used a plating cell of unique design which permitted the continual stripping of the sodium, from the mercury cathode, as it was deposited. The electrolysis was carried out at an applied potential of 24 volts and a current of 130 milliamperes. A yield of 95 per cent was obtained in 10 hr. The cell construction is shown in Figure 3.

TABLE X

ELECTRODEPOSITION INTO MERCURY CATHODE

Element	Initial Amount (gm.) (volume 150 ml.)	N H_2SO_4	Time (hours)	Per cent remaining* in aqueous phase
Arsenic	1.0	0.1	1.5	0.3
Antimony	0.1	1.5	1.5	5.5
Bismuth	1.0	0.5	1.5	0.003
Cadmium	1.0	0.1	1.5	0.01
Chromium				
Cr^{III}	1.0	0.1	1.5	0.06 (Cr^{III})
$Cr_2O_7^{=}$	1.0	0.5	1.5	0.005 (Cr^{VI}) 19.6 (Cr^{III})
Cobalt	1.0	0.1	1.5	0.04
Copper	1.0	0.1	1.5	0.001
Gallium	0.1	0.05	1.5	0.6
Germanium	0.1	0.1	1.5	47.9
Indium	1.0	0.1	1.5	0.008
Iron	1.0	0.1	1.5	0.002
Manganese†	0.5	0.1	1.5	0.06 (Mn^{VII}) 1.5 (Mn^{II})
Molybdenum	0.1	0.1	1.5	0.35
Nickel	1.0	0.1	1.5	0.04
Rhenium	0.1	0.1	1.5	55.9
Selenium	1.0	0.1	1.5	0.3
Tellurium	0.1	0.1	0.25	3.3
Thallium	1.0	0.1	1.5	0.01
Tin	1.0	1.5	1.5	0.2
Zinc	1.0	0.1	1.5	0.02

* In general, plating from more dilute acid solution and for somewhat longer times increased the amount deposited.

† Approximately 0.5 per cent of the manganese appeared on the anode as MnO_2.

SOLVENT EXTRACTION

In the last few years, considerable emphasis has been placed on the application of new solvents to solvent extraction separations (See Table XI) and on the development of extraction apparatus. The β-diketones and the butyl phosphates appear to have widespread use as extracting media.

The use of solvent extraction for rare-earth separations has also been investigated. Fischer and his co-workers (53) have studied the extraction of the various rare earths from a concentrated $LiNO_3$, rare-earth nitrate aqueous solution into both diethyl ether and pentanone. The separations obtained are comparable with those from fractional crystallization methods but the

over-all distribution coefficient, (RE)org./(RE)aq. is quite small ($\sim 10^{-3}$). Similar separation factors for rare earths have been obtained by Spedding (54) at Iowa State College using tributylphosphate as the extraction medium. Although the present rare-earth-extraction procedures do not appear to be useful for radiochemical separations, they may be of interest for obtaining pure rare earths for target materials and are, therefore, included in Table XII.

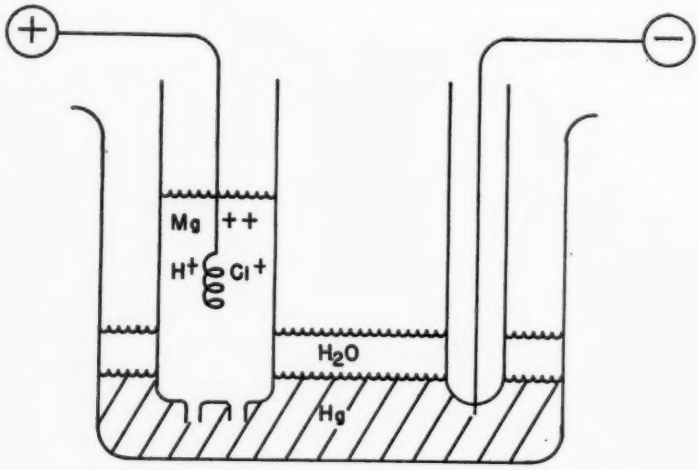

FIG. 3. Electrolysis cell for carrier-free separation of Na^{22}.

The use of fused salts for removal of fission products from molten U-Bi alloys has been the subject of recent study. Bareis, Wiswall & Winsche (76) have used a KCl—LiCl eutectic at 450°C. as an extraction medium. They have obtained distribution coefficients of the order of 10 for various rare earth tracers.

VOLATILIZATION DISTILLATION

Volatilization has been applied extensively to radioactive materials as a means of separation. One of the advantages of volatility separations is the great reduction in the bulk of material that can be obtained when the desired activity is not isotopic with the target material; in fact, in many cases it is possible to obtain "carrier-free" products.

Volatilization separations for "carrier-free" materials are carried out, in general, in essentially the same manner as for macro amounts of material. However, to increase the speed of separation and the yield of "carrier-free" substances, inert-gas sweeping is often employed. For example, Davis (77) has separated approximately 10^5 atoms of 35-day A^{37} from 3900 liters (approximately 3×10^{23} molecules) of CCl_4 by sweeping the CCl_4 with 4000 liters of helium and then removing the argon from the helium with a charcoal trap.

Another useful property of volatilization methods is the possibility for very rapid separations. By means of a "flash-distillation," Campbell (78) was able to isolate an 0.33 second state of Ge^{73} from a solution of its parent As^{73}. Similarly, Spiess (79) has volatilized astatine from a mixture of astatine and polonium on a platinum ribbon. The separation required less than 0.5 sec. As much as 10 gm. of bismuth has been separated from 10 mg. of uranium

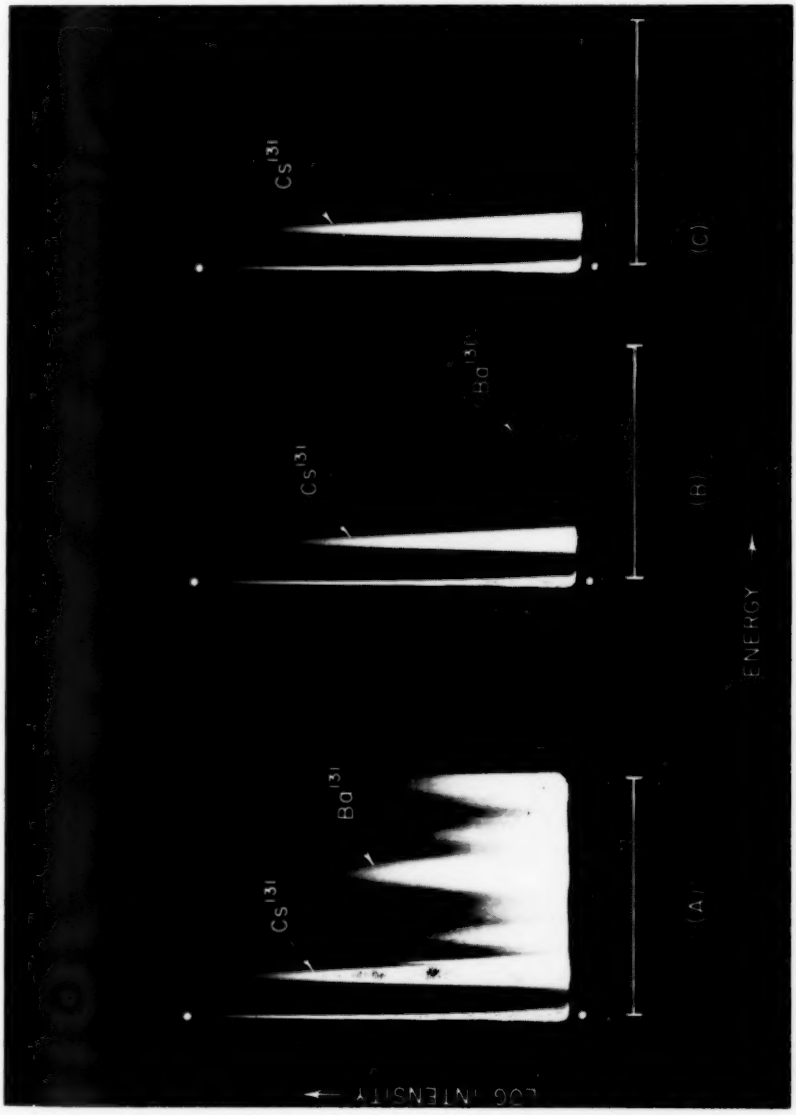

FIG. 4. Gray-wedge analysis of Ba^{131}-Cs^{131} separation.

TABLE XI

Separation by Solvent Extraction

Element	Probable Chemical Form	Solvent System (before mixing)		Dist. Coeff. (Nonaq.)/(Aq.)	Remarks	Ref.
		Aqueous Phase	Nonaqueous Phase			
Aluminum	Al^{III}	pH 9.7–10.0, Al^{III} 0.015*M*	butyric acid in $CHCl_3$ (~1:5)	~9	Fe^{III} and Be^{III} also extract	55
	Al^{III}	pH 4.42 Al^{III} 0.015*M*	acetylacetone*	~9	See ‡	56
	Al(acetylacetonate)	pH 4.8, 0.068M F^-	0.015*M* Al (acetylacetonate) in acetylacetone*	0.031	See ‡	56
Beryllium	Be^{II}	pH 9.3–9.7	butyric acid in $CHCl_3$ (~1:5)	~11	Fe^{III} and Al^{III} also extract	57
	Be^{II}	pH 9.3–9.7, Na EDTA	butyric acid in $CHCl_3$ (~1:5)	~11	Fe^{III} and Al^{III} do not extract!	55
	Be^{II}	pH 1.51~3×10^{-3}*M* Be	acetylacetone*	19	See ‡	56
Chromium	Cr^{III}	pH −0.3	acetylacetone*	19	See ‡	56
	Cr^{III}	pH 5.6	acetylacetone*	70	See ‡	56
Cobalt	Co^{III}	0.25 gm. α-nitroso-β-naphthol in 100 ml. 5% HAc.	benzene	~50	Carrier-free cobalt separated. Aqueous solution requires 1 hr. mixing before extraction will be complete.	58
	Co^{III}	pH −0.7	acetylacetone*	—	See ‡. probably similar to Cr^{III}	56
Copper	Cu(acetylacetonate)	pH 6.00	0.004*M* Cu (acetylactonate) in acetylacetone*	7.3	See ‡	56
	Cu^I	pH 4.4–7.5 $NH_2OH\cdot HCl$ and 2,2-diquinolyl.	*n*-amyl alcohol	—	Extraction "quantitative" for microgram amounts of Cu.	59
Gallium	Ga^{III}	3*M* HCl	tributyl phosphate	1700		60
	Ga^{III}	1*M* HCl	tributyl phosphate	20		60
	Ga(acetylacetonate)	pH 3.3→4.8	.00086*M* Ga (acetylacetonate) in acetylacetone*	28	See ‡	56
Germanium	Ge^{IV}	11*M* HCl	benzene	260	Distribution Coefficient: $(As^{5+}) \leqq 0.003$.	61

* Nonaqueous phase equilibrated, before mixing, with mineral acid, or base, of same molality as in aqueous phase.

† Butyl phosphate mixture was: 82% *n*-dibutyl phosphate
18% mono-*n*-butyl phosphate.

‡ Acetylacetone extracts Cu, Zn, Be, Fe, Al, Ga, Mn, In, Zr, V, Cr, and Co. Steinbach (SE9) gives extraction coefficients as a function of pH for each of these elements and also suggests separation procedures for various pairs. CO^{II}, Mg^{II}, Hg^{II}, Ni^{II}, and Na^I acetylacetonates do not extract into acetylacetone.

TABLE XI—(*continued*)

Element	Probable Chemical Form	Solvent System (before mixing)		Dist. Coeff. (Nonaq.)/(Aq.)	Remarks	Ref.
		Aqueous Phase	Nonaqueous Phase			
Hafnium	Hf^{IV}	pH 1.3	0.1*M* oxine in $CHCl_3$	1	Larger distribution coefficient at different pH	62
Indium	In^{III}	1*M* HNO_3, 3% H_2O_2	0.06*M* mixed butyl† phosphates	>19	Carrier-free In	63
	In^{III}	1*M* HNO_3, 3% H_2O_2	0.6*M* mixed butyl phosphate in *n*-butyl ether	>19	Carrier-free In	63
	In(acetylacetonate)	pH 3.85→4.43	0.0046*M* (In acetylacetonate) in acetylacetone*	>100	See ‡	56
Iron	Fe^{III}	pH 1.19→4.0, 0.025*M* Fe^{III}	acetylacetone*	>100	See ‡	56
	Fe^{III}	pH 10→10.5	butyric acid in $CHCl_3$ (~1:5)	~9	Al^{III} and Be^{III} also extract	55
Lanthanum	La^{III}	pH 6.5	0.1*M* oxine in $CHCl_3$	1		62
Manganese	MnO_4^-	4*N* NaOH, 5*M* MnO_4^-	pyridine*	8000		64
Niobium	Nb^V	1*M* HNO_3	0.6*M* mixed butyl phosphates in *n*-butyl ether‡	>19	Carrier-free Nb	63
	Nb^V	11*M* HCl	diisopropyl ketone*	9.0	No Ta interference	65
	Nb^V	3.7*M* HCl, 0.4*M* HF	diisopropyl ketone*	0.047		66
	Nb^V	3.9*M* HNO_3, 0.4*M* HF	diisopropyl ketone*	0.0043	$K_{Ta}/K_{Nb}=880$	66
	Nb^V	4.5*M* H_2SO_4, 0.4*M* HF	diisopropyl ketone*	0.12		66
	Nb^V	4.6*M* $HClO_4$, 0.4*M* HF	diisopropyl ketone*	0.031		66
	Nb^V	11*M* HCl	10% tribenzylamine in $CHCl_3$	72.6	$K_{Nb}/K_{Ta}=1900$	67
	Nb^V	2*M* HCl	8% tribenzylamine in $CHCl_3$	0.003		67
	Nb^V	8*M* HCl	methyl dioctylamine in xylene	—	No K reported. Overall yield of Nb in procedure low.	68
	Nb^V	6*M* HCl, 0.05*M* $(COOH)_2$	diisobutylcarbinol*	~.17		73
	Nb^V	6*M* HCl, 0.05*M* $(COOH)_2$, 4*M* H_2SO_4	diisobutylcarbinol*	~5		73
Protactinium	Pa^V	6*M* HCl	5% methyldioctylamine in xylene	19		73
	Pa^V	6*M* HCl	0.5*M* TTA in xylene	7.7		73
	Pa^V	6*M* HCl	diisopropylcarbinol*	999	Presence of 10 mg. Nb carrier, as oxalate, reduced K to 0.008	73
Rhenium	ReO_4	4*M* NaOH, 3.8*M* ReO_4^-	pyridine*	255		64
Samarium	Sm^{III}	pH 5.7	0.1*M* oxine in $CHCl_3$	1		62

TABLE XI—(*continued*)

Element	Probable Chemical Form	Solvent System (before mixing)		Dist. Coeff. (Nonaq.)/(Aq.)	Remarks	Ref.
		Aqueous Phase	Nonaqueous Phase			
Tantalum	Ta^{V}	11*M* HCl	10% tribenzylamine in $CHCl_3$	0.038	$K_{Nb}/K_{Ta}=1900$	67
	Ta^{V}	2*M* HCl	8% tribenzylamine in $CHCl_3$	0.0005		67
	Ta^{V}	3.7*M* HCl, 0.4*M* HF	diisopropyl ketone*	4.3		66
	Ta^{V}	3.9*M* HNO_3, 0.4*M* HF	diisopropyl ketone*	3.8	$K_{Ta}/K_{Nb}=880$	66
	Ta^{V}	4.5*M* H_2SO_4, 0.4*M* HF	diisopropyl ketone*	19		66
	Ta^{V}	4.6*M* $HClO_4$, 0.4*M* HF	diisopropyl ketone*	9.0		66
Technetium	TcO_4^-	4*M* NaOH, $\sim 4\times10^{-6}$*M* TcO_4^-	pyridine*	778		64
	TcO_4^-	$\sim 10^{-6}$*M* tetraphenyl As^+	$CHCl_3$	~100	Carrier-free Tc from mixed fission prod.	69 70
Thorium	Th^{IV}	3*M* HNO_3, 3*M* $Ca(NO_3)_2$, 0.3*M* Th^{IV}	20% *n*-butyl phosphate 80% *n*-butyl ether	9.97		71
	Th^{IV}	3*M* HNO_3, 3*M* $Ca(NO_3)_2$, 0.6*M* Th^{IV}	20% *n*-butyl phosphate 80% *n*-butyl ether	2.78		71
	Th^{IV}	pH 3.1	0.1*M* oxine in $CHCl_3$	1		62
	Th^{IV}	—	TTA in benzene	—	Carrier-free Th^{231} (UV) sep.	72
Uranium	UO_2^{II}	pH 1.3, $\mu=2.00$	0.5*M* TTA in benzene	1		74
	UO_2^{II}	pH 1.3, $\mu=2.00$, 0.5*M* F^-	0.5*M* TTA in benzene	0.71		74
	UO_2^{II}	pH 1.3, $\mu=2.00$, 10.0*M* HF	0.5*M* TTA in benzene	0.17		74
	UO_2^{II}	pH 1.3, $\mu=2.00$, 0.11*M* SO_4	0.5*M* TTA in benzene	0.0085		74
	UO_2^{II}	pH 2.6	0.1*M* oxine in $CHCl_3$	1		62
Vanadium	VO^{II}	0.019*M* VO^{II}, pH 2.13→4.19	acetylacetone*	2.3	See ‡	56
Yttrium	Y^{III}	1*M* HNO_3, 3% H_2O_2	0.6*M* mixed butyl phosphate‡ in *n*-butyl ether	>19	Carrier-free Y	63
Zinc	Zn^{II}	pH 5.8→6.8, $\sim 3\times10^{-4}$*M* Zn^{II}	acetylacetone*	~1.5	See ‡	56
Zirconium	ZrO^{II}	1*M* HNO_3, 3% H_2O_2	0.06*M* mixed butyl phosphate‡ in *n*-butyl ether	>19		63
	Zr(acetylacetonate)	1*M* HNO_3, 3% H_2O_2	0.06*M* mixed butyl phosphate‡ in *n*-butyl ether	>19		63
	ZrO^{II}	pH 2.4→4.0	0.001*M* Zr (acetylacetonate) in acetylacetone*	2.3	See ‡	56

TABLE XII

RARE EARTH SEPARATION BY SOLVENT EXTRACTION

Solvent System (before mixing)		Separation*		Ref.
Aqueous Phase	Nonaqueous Phase	Elements Compared	Separation Factor†	
200 gm. RE/liter	Tributyl Phosphate	Nd/Pr	12.5	54
200 gm. RE/liter	Tributyl Phosphate	Sm/Nd	15	54
200 gm. RE/liter	Tributyl Phosphate	Gd/Sm	11	54
200 gm. RE/liter	Tributyl Phosphate	Ce/La	14	54
400 gm. RE/liter	Tributyl Phosphate	Nd/Pr	14	54
400 gm. RE/liter	Tributyl Phosphate	Sm/Nd	18	54
400 gm. RE/liter	Tributyl Phosphate	Gd/Sm	13	54
400 gm. RE/liter	Tributyl Phosphate	Ce/La	15	54
500 gm. RE/liter	Tributyl Phosphate	Pr/Ce	15	54
RE Nitrates‡	Diethyl Ether	Pr/La	2.25	75
Re Nitrates	Diethyl Ether	Nd/La	3.47	75
Re Nitrates	Diethyl Ether	Sm/La	8.92	75
Re Nitrates	Diethyl Ether	Em/La	10.7	75
Re Nitrates	Diethyl Ether	Gd/La	14.5	75
RE Nitrates	Diethyl Ether	Tb/La	19.1	75
RE Nitrates	Diethyl Ether	Dy/La	28.1	75
RE Nitrates	Diethyl Ether	En/La	32.4	75
RE Nitrates	Diethyl Ether	Yb/La	50.2	75
RE Nitrates	Pentanone	Ce/La	2.14	75
RE Nitrates	Pentanone	Pr/La	3.02	75
RE Nitrates	Pentanone	Nd/La	3.63	75
RE Nitrates	Pentanone	Sm/La	4.08	75
RE Nitrates	Pentanone	Gd/La	3.55	75
RE Nitrates	Pentanone	Dy/La	4.17	75
RE Nitrates	Pentanone	Ho/La	5.02	75
RE Nitrates	Pentanone	Er/La	5.89	75
RE Nitrates	Pentanone	Tm/La	6.31	75
RE Nitrates	Pentanone	Yb/La	6.03	75
RE Nitrates	Pentanone	Lu/La	5.50	75

* Extraction coefficient for (total RE)org./(total RE)aq. approximate 10^{-3}.

† Separation Factor refers to nonaqueous phase.

‡ RE Nitrates are dissolved in ~20% $LiNO_3$ solution.

by vacuum distillation of the bismuth at 800°C. The separation required less than 1 hr. and greater than 99.99 per cent of the Bi was volatilized (80).

CHROMATOGRAPHY—ION EXCHANGE

A complete review of inorganic chromatography which includes the ap-

TABLE XIII

Ion Exchange Separation

Element	Separated from	Resin		Sol'n	Eluant*	Remarks	Ref.
		Type	Treatment				
Aluminum	Iron	IR 120			(a) 0.1*N* KI followed by 0.15*N* KCl and 0.2*N* HCl (*b*) 2*N* HCl	Fe^{+++} reduced to Fe^{++} and eluted by (a) (*b*) elutes Al	83
Americium	Curium	Dowex 50	87°C.		0.4*M* lactic acid pH 4.0	Approx. 2 hr. $C_{Am}/C_{Cm}=1.19$; Cross-contamination ~2%	84
Americium	Curium	Dowex 50			0.1*M* tartaric acid pH 4.0	Rm. Temp. approx. 16 hr. $C_{Am}/C_{Cm}=1.30$; Cross-contamination ~0.2%	84
Cadmium	Uranium	IR 120			(*a*) 0.5*N* oxalic (*b*) 1*N* HCl	(*a*) elutes U (*b*) elutes Cd Initially Cd/U = $1/10^4$	85
Cobalt	Iron	Dowex 1			(*a*) 5*M* HCl (*b*) 0.5*M* HCl	(*a*) elutes Co (*b*) elutes Fe	86
Curium	Americium	Dowex 50			0.1*M* tartaric acid pH 4.0	Rm. Temp. approx. 16 hr. $C_{Am}/C_{Cm}=1.30$; Cross-contamination ~0.2%	84
Curium	Americium	Dowex 50	87°C.		0.4*M* lactic acid pH 4.6	Approx. 2 hr. required $C_{Am}/C_{Cm}=1.19$; Cross-contamination ~2%	84
Hafnium	Zirconium	Dowex 50			0.45*M* HNO_3 + 0.09*M* citric acid	Zr elutes first	85
Iridium	Other Platinum Metals	Dowex 50			(*a*) 0.05*M*–0.5*M* HCl (*b*) 2*M* HCl (*c*) 4–6*M* HCl	Pt passes through (*a*) elutes Pd (*b*) elutes Rh (*c*) elutes Ir	86
Iron	Aluminum	IR 120			(*a*) 0.1*N* KI followed by 0.15*N* KCl and 0.2*N* HCl (*b*) 2*N* HCl	Fe^{+++} reduced to Fe^{++} and eluted by (*a*) (*b*) elutes Al	83
Iron	Cobalt	Dowex 1			(*a*) 5*M* HCl (*b*) 0.5*M* HCl	(*a*) elutes Co (*b*) elutes Fe	86

* When more than one eluant is used, letter gives order of use. Remarks column then indicates which elements are eluted.

Element	Separated from	Resin		Sol'n	Eluant*	Remarks	Ref.
		Type	Treatment				
Neptunium	Uranium and Fission Products	IR 120		dil. HNO_3	1–2*M* HNO_3	Orig. soln. treated with SO_2, then LaF_3 scavenge. LaF_3 fumed with H_2SO_4, then dissolved in dil. HNO_3.	89
Neptunium	Uranium and Fission Products	IR 120		dil. HNO_3	1–2*M* HNO_3	Orig. soln. oxidized with hot HNO_3. Np in eluate free from most f.p. and U.	89
Neptunium	Uranium and Fission Products	IR 120			(*a*) HCl (*b*) complexing agent	(*a*) elutes f.p. (*b*) elutes Np	89
Palladium	Other Platinum Metals	Dowex 50			0.05→0.5*M* HCl	Pt passes thru; Pd stripped by eluant.	88
Phosphorus	Sulfur	Nalcite HCR	$FeCl_3$ passed thru col. to convert to Fe^{+++} form. 2*N* NH_4OH passed thru converts to $Fe(OH)_3$	$PO_4^{\equiv}$		Col. specific for phosphate. Phosphate removed with dil. NaOH. P^{32} removed carrier free	90
Platinum	Other Platinum Metals	Dowex 50		$HClO_4$, all trace halides removed.		Pt passes through column.	88
Potassium	Sodium	Dowex 50				K+~0.3% Na	91
Radium	Barium	Dowex 50			0.32*M* ammonium citrate pH 5.6	Ba/Ra approx. 4440/1 99% Ra obtained with 1% Ba	92
Rare Earths							
Rare Earths	Uranium	IR 120			(*a*) 1*N* oxalic (*b*) 5*N* HCl	(*a*) elutes U (*b*) elutes R.E. Initially; RE/U ~1/10^6	93
Europium	Pr and Sm	IR 120				Pr, n.d.; Sm, n.d.	94
Europium	Terbium	IR 120			0.25*M* citrate pH 3.50	C_{Eu}/C_{Tb} = 1.7	95
Europium	Terbium	IR 120			1.00*M* citrate pH 2.46	C_{Eu}/C_{Tb} = approx. 1.2	95
Europium	Terbium	IR 120			0.026*M* EDTA pH 3.62	C_{Eu}/C_{Tb} = 3.5	95
Europium	Terbium	IR 120			0.20*M* lactate pH 6.00	C_{Eu}/C_{Tb} = 1.8	95
Europium	Terbium	Dowex 50	87°C.		0.03*M* glycolate pH 4.00	C_{Eu}/C_{Tb} = 2.0	95

TABLE XIII—(*continued*)

Element	Separated from	Resin		Sol'n	Eluant*	Remarks	Ref.
		Type	Treatment				
Europium	Terbium	Dowex 50	87°C.		0.50*M* malate pH 3.25	$C_{Eu}/C_{Tb}=1.5$	95
Gadolinium	Tb and Eu	Dowex 50				Tb, n.d.; Eu, n.d.	94
Neodymium	Pm and Pr	Dowex 50				Pm, n.d.; Pr, n.d.	94
Praseodynium	Nd	Dowex 50				Nd, n.d.	94
Promethium	Sm and Nd	Dowex 50				Sm, n.d.; Nd. approx. 0.01%	94
Samarium	Eu and Pm	Dowex 50				Eu, approx. 0.3%; Pm, n.d.	94
Samarium	Europium	Dowex 50	87°C.		0.25*M* citrate pH 3.50	$C_{Sm}/C_{Eu}=1.15$	95
Samarium	Europium	Dowex 50	87°C.		1.00*M* citrate pH 2.46	$C_{Sm}/C_{Eu}=1.13$	95
Samarium	Europium	Dowex 50	87°C.		0.026*M* EDTA pH 3.62	$C_{Sm}/C_{Eu}=1.60$	95
Samarium	Europium	Dowex 50	87°C.		0.20*M* lactate pH 6.00	$C_{Sm}/C_{Eu}=1.28$	95
Samarium	Europium	Dowex 50	87°C.		0.30*M* glycolate pH 4.00	$C_{Sm}/C_{Eu}=1.28$	95
Samarium	Europium	Dowex 50	87°C.		0.50*M* malate	$C_{Sm}/C_{Eu}=1.15$	95
Terbium	Y and Gd					Y approx. 0.15% Gd, n.d.	94
Yttrium	Terbium	Dowex 50		approx. 5*M* $HClO_4$	5*M* $HClO_4$	Tb not detectable	94
Rhodium	Other Platinum Metals	Dowex 50			(*a*) 0.05*M*–0.5*M* HCl (*b*) 2*M* HCl	Pt passes thru, Pd elutes with (*a*) Rh elutes with (*b*)	88 91
Sodium	Potassium	Dowex 50	(12% cross linked-400 mesh)			Na clean of K	96
Technetium	Molybdenum	IRA 400 IRA 120	Resin in perchlorate form	NH_4TcO_4 Mo as Molybdate, 10% NaOH	(*a*) 10% NaOH (*b*) 0.5*M* NH_4CNS	(*a*) elutes Mo (*b*) elutes Tc Trace Ag and Co remain on column	96
Uranium	Rare Earths	IR 120			(*a*) 1*N* oxalic (*b*) 5*N* HCl	(*a*) elutes U (*b*) elutes R.E. Initially, R.E. approx. 10^{-6} of U	93
Uranium	Cadmium	IR 120			(*a*) 0.5*N* oxalic (*b*) 1*N* HCl	(*a*) elutes U (*b*) elutes Cd; Initially; Cd/U approx. $1/10^4$	85
Zirconium	Hafnium	Dowerx 50			0.45*M* HNO_4+0.09*M* citric acid.	Zr elutes first	87

plications of paper chromatography has been published by Wells (81), and another review article by Weil (82) deals exclusively with paper chromatography. The specific separations which have been reported in the recent literature are summarized in Tables XIII and XIV.

TABLE XIV

PAPER-CHROMATOGRAPHIC SEPARATIONS

Elements Separated	Chemical State	Solution	Developer	R_f*	Remarks	Ref.
Cobalt	Co^{++}			0.61		97
Copper	Cu^{++}			0.92		97
Nickel	Ni^{++}			0.98		97
Lead	Pb^{++}			0.40		97
Mercury	Hg_2^{++}			0.72		97
Silver	Ag^{+}			0.54		97
Bismuth	Bi^{+++}			0.62		97
Copper	Cu^{++}			0.15		97
Lead	Pb^{++}			0.31		97
Mercury	Hg^{++}			0.84		97
Arsenic	As^{+++}			0.64		97
Antimony	Sb^{+++}			0.80		97
Tin	Sn^{++}			0.98		97
Arsenic	$AsO_4^{\equiv}$		80 ml. EtOH, 20 ml. H_2O,	0.83		98
	$AsO_3^{\equiv}$		5 gm. CCl_3COOH, 0.3	0.68		98
Phosphorus	$PO_4^{\equiv}$		ml. 14*N* NH_4OH	0.82		98
	$P_2O_7^{=}$			0.61		98
	PO_3^{-}			0.86		98
Arsenic	$AsO_4^{\equiv}$		40 ml. isopropyl alcohol	0.40		98
	$AsO_3^{\equiv}$		20 ml. isobutyl alcohol,	0.40–0.49		98
Phosphorus	$PO_4^{\equiv}$		39 ml. H_2O, 1 ml. 14*N*	0.39		98
	$P_2O_7^{=}$		NH_4OH	0.28		98
	PO_3^{-}			0.49		98
Molybdenum	Mo^{+++}	dil HCl	*n*-butanol saturated with 2*N* HNO_3 and 2*N* HCl		Mo separated from Co, Cr, Cu, Fe, Mn, Ni, U and V	99
Copper	Cu^{++}	dil HNO_3	*n*-butanol saturated with			99
Iron	Fe^{+++}		0.5*N* HNO_3 and 2% benzoyl acetone			99
Sodium	Na^{+}	chloride	80% E+OH, 20% H_2O		10 to 20 hr.	100
Magnesium	Mg^{++}					100
Iron	Fe^{+++}	chloride	20 ml. butanol, 10 ml.		Fe travels with liquid	100
Rhodium	Rh^{+++}		12*N* HCl		front	100
Palladium	Pd^{++}	HNO_3-HCl	butanol equilibrated with			100
Rhodium	Rh^{+++}		1*N* HCl			100
Cobalt	Co^{+++}	chloride	5% HCl 5% H_2O in ace-			100
Iron	Fe^{+++}		tone			100
Copper	Cu^{++}	chloride	butanol equilibrated with		Approximately 20 hr.	100
Zinc	Zn^{++}		1*N* HCl			100
Protactinium	Pa^{V}	dil HNO_3	20% 16*N* HNO_3 in ether			100
Uranium	UO_2^{++}					100

* R_f is the ratio of the distance traveled by the ion to the distance traveled by the solvent front.

TABLE XV

SUMMARY OF SEPARATION PROCEDURES

Element	Tables	Element	Tables
Aluminum	II, XI, XII	Neptunium	XIII
Americium	XIII	Nickel	I, IV, V, X, XIV
Antimony	III, V, IX, X	Niobium	XI
Argon	*	Palladium	XIII, XIV
Arsenic	III, X, XIV	Phosphorus	VIII, XIII, XIV
Astatine	*	Platinum	VII, XIII
Barium	I, V, VII	Polonium	*
Beryllium	XI	Potassium	VII, XIII
Bismuth	*, III, IV, V, IX, X, XIV	Protactinium	XI, XIV
Cadmium	I, III, IV, V, VII, X, XIII	Rare Earths	XI, XII, XIII
Calcium	I, V	Radium	XIII
Cesium	VII, VIII	Rhenium	X, XI
Chromium	I, V, X, XI	Rhodium	XIII, XIV
Cobalt	I, IV, V, X, XI, XII, XIV	Rubidium	VII
Copper	I, II, III, IV, V, VI, VII, IX, X, XI, XIV	Selenium	III, X
		Silver	IV, V, VII, IX, XIV
Curium	XII	Sodium	XIII, XIV
Gallium	X, XI	Strontium	I, V, VIII
Germanium	*, III, VII, X, XI	Tantalum	XI
Hafnium	XI, XIII	Technetium	XI, XIII
Indium	X, XI	Tellurium	X
Iridium	XIII	Tallium	IV, X
Iron	II, IV, V, X, XI, XIII, XIV	Thorium	V, VII, XI
		Tin	III, IV, V, IX, X
Lanthanum	XI, XII	Uranium	*, II, XI, XIII, XIV
Lead	I, III, IV, V, IX, XIV	Vanadium	II, XI
Magnesium	I	Wolfram	II
Manganese	V, X, XI, XIV	Yttrium	XI, XIII
Mercury	III, IV, V, VI, VII, XIV	Zinc	I, IV, V, IX, X, XI, XIV
Molybdenum	II, X, XIV	Zirconium	VII, VIII, XI, XIII

* See discussion of volatilization.

INSTRUMENTAL ANALYSIS

The recent advances in the design of spectrometers for α-, β-, and γ-radiations have made practical the routine use of these instruments as analytical tools for radiochemistry. Their use enables, in many cases, the course of a separation to be monitored for a specific isotope or element without resort to ordinary analytical chemical methods, and, indeed, the analysis is often far more sensitive than the chemical analytical method. Alpha pulse height analysis, for example, is used extensively in the laboratories at Hanford and Berkeley both as a means of identification and of quantitative analysis.

Connally & Leboeuf (101) and Salmon (102) have described the general principles of β- and γ-scintillation spectrometry and the applications of these techniques to radiochemical analysis.

The "Grey-wedge" pulse height analyzer, developed by Bernstein, Chase & Schardt (103, 104) is most convenient for making routine use of β- and γ-radiations for analysis. This device utilizes a photographic method for recording the spectral data and is equivalent in performance to a 50-channel electronic analyzer. The γ-spectra obtained in the course of the separation of carrier-free Cs^{131} from a Ba-Cs mixture is reproduced in Figure 4. Picture A was made with the irradiated $BaCO_3$ sample before the start of separation; picture B was taken after two cycles of a Ba-Cs separation procedure; and picture C is of the final separated Cs^{131} source. There is no evidence of barium γ-radiation in C.

LITERATURE CITED

1. Belcher, R., *Chem. Chem. Mnfr.* (1953)
2. Gordon, L., and Firsching, F. H., *Anal. Chem.*, **26,** 759 (1954)
3. Heyn, A. H. A., and Schupak, E., *Anal. Chem.*, **26,** 1243 (1954)
4. Elving, P. J., and Zook, W. C., *Anal. Chem.*, **25,** 502 (1953)
5. Herman, J. A., "Separation of Americium from Lanthanum by Fractional Oxalate Precipitation from Homogeneous Solutions," *AECD-3637; Los Alamos Sci. Lab. Rept., LAMS-1625* (Oct., 1953)
6. McNevin, W. M., and Dunton, M. L., *Anal. Chem.*, **26,** 1246 (1953)
7. Stine, C. R., and Gordon, L., *Anal. Chem.*, **25,** 1519 (1953)
8. Flaschka, H., *Chemist-Analyst*, **44,** No. 1, 2 (March, 1955)
9. Flaschka, H., *Z. Anal. Chem.*, **137,** 107 (1952)
10. Samos, G., and Finston, H. L. (Private communication)
11. Komlev, A. I., and Tsimbalista, L. I., *Zhur, Anal. Khim.*, **8,** 217 (1953)
12. Oesper, R. E., and Fulmer, R. E., *Anal. Chem.*, **25,** 908 (1953)
13. Sircar, S. S. G., and Satpathy, S., *J. Indian Chem. Soc.*, **31,** 450 (1954)
14. Tucker, H., "Precipitation of Barium Carbonate," *Mound Lab. Rept. MLM-931,* 15 pp. (Dec. 16, 1954)
15. Walter, J. I., and Freiser, H., *Anal. Chem.*, **24,** 984 (1952)
16. Dwyer, F. P., and Gibson, N. A., *Analyst*, **75,** 201 (1950)
17. Majumdar, A. K., *J. Indian Chem. Soc.*, **22,** 309 (1945)
18. Rulfs, C. L., Pryzbylamicy, E. P., and Skinner, C. E., *Anal. Chem.*, **26,** 408 (1954)
19. Geilman, W., and Gebauer, W., *Z. Anal. Chem.*, **139,** 161 (1953)
20. Batalin, A. Kh., *Zhur. Anal. Khim.*, **8,** 182 (1953)
21. Shrauzer, G. N., *Mikrochim. Acta*, 124, (1953)
22. Tehakinan, A., and Benillard, P., *Compt. rend.*, **233,** 1, 112 (1951)
23. Halzbecker, Z., *Chem. Listy*, **46,** 20 (1952)
24. Walter, J. L., and Freiser, H., *Anal. Chem.*, **25,** 127 (1953)
25. Plank, J., *Acta Chim. Acad. Sci. Hungary*, **5,** 387 (1953)
26. Ryan, D. E., *Analyst*, **79,** 707 (1954)
27. Cheng, K. L., *Anal. Chem.*, **26,** 1038 (1954)
28. Banks, C. V., and Davis, R. J., "Analytical Applications of Thorium with Benzenephosphoric Acid," *Ames Lab. Rept., ISC-52,* 21 pp. (Sept. 1954)

29. Tillu, M. M., and Anthanole, V. T., *Anal. Chim. Acta*, **11**, 62 (1954)
30. Dotta, S. K., and Banarjee, G. I., *Indian Chem. Soc.*, **31**, 397 (1954)
31. Dotta, S. K., and Banarjee, G. I., *Indian Chem. Soc.*, **31**, 149 (1954)
32. Klingenberg, J. L., Vlanne, P. N., and Mendel, M. G., *Anal. Chem.*, **26**, 754 (1954)
33. Mizzan, E., "Phosphotungstate Precipitation Method of Analysis of Radioactive Cesium in Solution of Long-Lived Fission Product Activities," *PDB-128*, Chalk River Project, Canada, 14 pp., (July 16, 1954)
34. Hahn, R. B., and Barker, R. C., "Determination of Radioactive Cesium in Fission Products," *U. S. Atomic Energy Commission Document, AECU 2903*, 13 pp. (1954)
35. Hahn, R. B., and Skonieczny, R. F., "The Determination of Radioactive Zirconium in Fission Products," *U. S. Atomic Energy Commission Document, AECU-2908*, 20 pp. (1954)
36. Mizzan, E., "Rapid Determination of Strontium Activity in Mixed Fission Product Solution," *PDB-122*, Chalk River Project, Canada, 10 pp. (June, 1954)
    Product Solution," *PDB-122*, 10 pp. (June 1954)
37. Turk, E., "A Modified Radiochemical Strontium Procedure," *Argonne Natl. Lab. Rept., ANL-5184*, 8 pp. (Dec. 1953)
38. Hahn, R. B., and Anderson, R. L., "Radiochemical Methods for the Determination of Phosphorus-32," *U. S. Atomic Energy Commission Document, AECU-2910*, 12 pp. (1954)
39. Lingane, J. J., *Electroanalytical Chemistry* (Interscience Publishers, New York, N. Y., 448 pp., 1953
40. Lingane, J. J., "Innovations in Electroanalytical Chemistry," *27th Annual Priestly Lectures* (Pennsylvania State College, State College, Pa., 1953)
41. DeFord, D. D., *Anal. Chem.*, **26**, 135 (1954)
42. Ishibashi, M., and Fujinga, T., *J. Japan Chem.*, **1**, 155 (1953)
43. Palmer, J. F., and Vogel, A. I., *Analyst*, **78**, 428 (1953)
44. Diehl, H., and Buttes, J. P., *Analyst*, **77**, 268 (1952)
45. Foster, D. G., *Anal. Chem.*, **25**, 669 (1953)
46. Lingane, J. J., and Jones, S. L., *Anal. Chem.*, **23**, 1798 (1951)
47. Foster, D. G., *Anal. Chem.*, **25**, 1557 (1953)
48. Dean, J. A., and Reynolds, S. A., *Anal. Chem. Acta*, **11**, 390 (1954)
49. Irvine, J., Merritt, G., Jr., and Funkhouser, J., "Chemistry of the Fission Elements Group," *U. S. Atomic Energy Commission Document, AECU-2404*, Massachusetts Inst. Technol., 13 pp.; (Jan., 1953) *J. Electrochem. Soc.* (To be published)
50. Hahn, R. B., *Anal. Chem.*, **25**, 1749 (1953)
51. Bock, R., and Hockstein, K. G., *Z. Anal. Chem.*, **138**, 339 (1953)
52. Chemla, M., and Pauly, J., *Bull. soc. chim. France*, **20**, 432 (1953)
53. Fischer, W. G., Braune, G., Deitz, W., Juberman, O., Krause, G., Niemann, K., and Siekemeir, G., *Angew. Chem.*, **66**, 317 (1954)
54. Bochinski, J., Smutz, M., and Spedding, F., "Separation of Individual Rare Earths by Liquid-Liquid Extraction from Multicomponent Monazite Rare Earth Nitrates. Undiluted Tributyl Phosphate and Concentrated Aqueous Rare Earth Nitrate Systems at Low Acid Concentrations," *Ames Lab. Rept., ISC-438*, 34 pp. (May 27, 1953)

55. Banerjee, S., Sundaram, A. K., and Sherma, H. D., *Anal. Chim. Acta*, **10**, 256 (1954)
56. Steinbach, J. F., *Acetylacetone as an Analytical Extraction Agent* (Doctoral thesis), 127 pp., NYO-6347, University of Pittsburgh, Pittsburgh, Pa. (1953)
57. Sundaram, A. K., and Banerjee, S., *Anal. Chim. Acta*, **8**, 526 (1953)
58. Dick, J. L., and Kurbatov, M. H., *J. Am. Chem. Soc.*, **76**, 5245 (1954)
59. Guest, R. J., "Use of 2,2-Diquinolyl in the Colorimetric Determination of Copper in Minerals and Ores," *NP-4457*. Dept. of Mines and Tech. Surveys, Mines Branch, Ottawa, Canada, 15 pp. (Dec. 9, 1952)
60. Bennet, W., and Irvine, J. W., Progr. Rept. Mass. Inst. Technol., Feb., 1953 (Unpublished)
61. Green, M., and Kafalas, J. A., *J. Chem. Phys.*, **22**, 760 (1954)
62. Dyrssen, D., and Dahlberg, V., *Acta Chem. Scand.*, **7**, 1186 (1953)
63. Scadden, E. M., and Ballou, N. E., *Anal. Chem.*, **25**, 1602 (1953)
64. Goishi, W., and Libby, W. F., *J. Am. Chem. Soc.*, **74**, 6109 (1952)
65. Hicks, H. G., and Gilbert R. S., "Extraction of Niobium into Di-Isopropyl Ketone from Hydrochloric Acid Solution," *MTA-33*, Livermore Research Lab., California Research and Developement Co., Livermore, Calif. 8 pp. (April 22, 1953)
66. Stevenson, P. C., and Hicks, H. G., *Anal. Chem.*, **25**, 1517 (1953)
67. Ellenburg, J. Y., Leddicotte, G. W., and Moore, F. L., *Anal. Chem.*, **26**, 1045 (1954)
68. Douglas, D. L., Mewherter, A. C., and Schuman, R. P., *Phys. Rev.*, **92**, 369 (1953)
69. Tribalate, S., and Beydon, J., *Anal. Chim. Acta*, **8**, 22 (1953)
70. Mizzan, E., "Technetium Studies," *PDB-101*, Chalk River Project, Canada, 18 pp. (Oct. 8, 1953)
71. Anderson, M. R., "Distribution of Thorium Nitrate Between Water and a Mixture of Butyl Phosphate and Butyl Ether," *ISC-116, Ames Lab. Rept.*, 23 pp. (July 1, 1950) (Declassified Nov. 25, 1953)
72. Freedman, M. S., Jaffey, A. H., Wagner, F., Jr., and May, J., *Phys. Rev.*, **89**, 302 (1953)
73. Moore, F. L., "Separation of Protactinium and Niobium by Liquid-Liquid Extraction," *ORNL-1675 Oak Ridge National Lab. Rept.* 20 pp. (Feb. 15, 1954) (Declassified June 16, 1954)
74. Day, R. A., Jr., and Powers, R. M., *ORO-117*, Emory University, Emory, Georgia, 13 pp. (1953)
75. Fischer, W., Braune, G., Dietz, W., Jubermann, O., Krause, G., Niemann, K., and Siebemeir, G., *Angew. Chem.*, **66**, 317 (1954)
76. Bareis, D., Wiswall, R. H., Jr., and Winsche, W. E., *Nucleonics*, **12**, No. 7, 16 (1954)
77. Davis, R., *Phys. Rev.*, **97**, 766 (1955)
78. Campbell, E. C., and Nelson, F. (Private communication)
79. Spiess, F. N., *Phys. Rev.*, **94**, 1292 (1954)
80. Samos, G., and Finston, H. L. (Private communication)
81. Wells, R. A., *Quart. Rev. Chem. Soc.*, **7**, 307 (1953)
82. Weil, H., *Can. Chem. Processing*, **38**, 68 (1954)
83. Kakihana, H., and Kojima, S., *Japan Analyst*, **2**, 421 (1953)
84. Glass, R. A., "Chelating Agents Applied to Ion Exchange Separations of

Americium and Curium," *UCRL-2521*, Radiation Lab., Univ. of California, Berkeley, Calif., 11 pp. (Mar. 23, 1954) (Declassified May 12, 1954)
85. Dizdar, Z., *Bull. Inst. Nuclear Sci., Boris Kidrich (Belgrade)*, **2**, 85 (1953)
86. Helwig, H. L., Ashikawa, J. K., Clokie, H., and Smith, E. R., "Separation of Iron and Cobalt on Synthetic Resins," *UCRL-2296*, Radiation Lab., Univ. of California, Berkeley, Calif. 6 pp. (Aug. 5, 1953)
87. Benedict, J. T., Schumb, W. C., and Coryell, C. D., *J. Am. Chem. Soc.*, **76**, 2036 (1954)
88. Stevenson, P. C., Franke, A. A., Borg, R., and Nervik, W., "The Separation of the Four Platinum Group Metals, Palladium, Rhodium, Iridium and Platinum," *UCRL-2329*, Radiation Lab. Rept., Univ. of California, Berkeley, Calif., 3 pp. (Aug. 24, 1953)
89. Johansson, G., *Svensk Kem. Tidskr.*, **65**, 79 (1953)
90. McIsaac, L. D., and Voigt, A., "A New Technique for the Separation of Radiophosphorus from Sulfur," *ISC-271, Ames Lab. Rept.* 33 pp. (June 1952)
91. Arons, W. L., and Solomon, A. K., "The Separation of Sodium from Potassium by Means of Ion-Exchange Chromatography," *U. S. Atomic Energy Commission Document, AECU-2661*, Biophysical Laboratory, Harvard Medical School, Cambridge, Mass., 16 pp. (1952)
92. Power, W. H., Kirby, H. W., McCluggage, W. C., Nelson, G. D., and Payne, J. H., "Separation of Radium and Barium by Ion-Exchange Elution," *MLM-833, Mound Lab. Rept.*, 33 pp. (April 15, 1953)
93. Dolar, D., and Draganic, Z., *Bull. Inst. Nuclear Sci., Boris Kidrich (Belgrade)*, **2, 77** (1953)
94. Freiling, E. C., and Bunney, L. R., *J. Am. Chem. Soc.*, **76**, 1021 (1954)
95. Mayer, S. W., and Freiling, E. C., *J. Am. Chem. Soc.*, **75**, 5647 (1953)
96. Hall, N. F., and Johns, D. H., *J. Am. Chem. Soc.*, **75**, 5787 (1953)
97. Tewari, S. N., *Kolloid-Z.*, **133**, 132 (1953)
98. Volmar, Y., Ebel, J. P., and Bassili, Y. F., *Bull. soc. chim. France*, **20**, 1085 (1953)
99. Pollard, F. H., McOmie, J. F. W., Stevens, H. M., and Maddock, J. G., *J. Chem. Soc.*, 1338 (1953)
100. Lederer, M., *Anal. Chim. Acta*, **8**, 134 (1953)
101. Connally, R. E., and Leboeuf, M. B., *Anal. Chem.*, **25**, 1095 (1953)
102. Salmon, L., "Some Analytical Aspects of Gamma Spectroscopy," *AERE c/m 206*, Atomic Energy Research Establishment, Harwell, Berks, England, 15 pp., (May 29, 1954)
103. Bernstein, W., Chase, R. L., and Schardt, A. W., *Rev. Sci. Instr.*, **24**, 437 (1953)
104. Chase, R. L., "Coincidence Gray Wedge Pulse Height Analyzer BNL Model EHI-501-Description and Instructions for Use," *BNL 263 (T-42), Brookhaven Natl. Lab. Rept.*, 14 pp. (Nov. 1953)

THE FUNDAMENTALS OF RADIOAUTOGRAPHY[1]

By William P. Norris and Lois A. Woodruff

Division of Biological and Medical Research, Argonne National Laboratory, Lemont, Illinois

INTRODUCTION

A photographic emulsion, using essentially the radioautographic technique, enabled Becquerel (1) to discover the radioactivity of uranium in 1896. A further impetus to the use of photographic emulsions came in 1911 when Reinganum (2) found that the path of an α-particle was recorded as a row of developed silver grains. Since that time a large quantity of literature describing the effects of ionizing particles on emulsions has accumulated in the field of nuclear physics. Today, this work has resulted in the development of sensitive emulsions especially designed to respond to ionizing particles and many of the details of the response mechanism have been explained. The early work in this field was reviewed by Shapiro (3). More recently pertinent reviews have been written by Webb (4), Yagoda (5), Beiser (6), and Goldschmidt-Clermont (7).

As a wide variety of artificially radioactive isotopes have been available for experimentation during the last eight years, there has been rapid progress in the development of techniques for radioautography. This effort has been concentrated toward applications in biological sciences; however, there has been considerable interest in other areas—notably, mineralogy and metallurgy. Limitations of this review make it impracticable to mention all the recent papers dealing with applications of the method. The authors have attempted to restrict discussion to those aspects of fundamental importance in the successful utilization of the radioautographic technique.

GENERAL ASPECTS OF RADIOAUTOGRAPHY

Radioautography is a technique whereby an ionization-sensitive emulsion is placed in intimate contact with a specimen in order to determine the location of its radioactive components. The basis of the technique is extraordinarily simple. Inspection of Figure 1, using only geometrical considerations, shows that the degree to which the image corresponds to the radioactive inclusion depends, in varying amount, on all the following: (a) specimen thickness, (*b*) emulsion thickness, (*c*) width of the separating gap, and (*d*) range of the ionizing particle. So long as the ionizing particle has a finite range in the emulsion, it is evident that the size of the image will always exceed that of the original. The planning and interpretation of a radioautographic study must also take into account the other properties of the incident ionizing

[1] Work performed under the auspices of the U. S. Atomic Energy Commission. The survey of literature pertaining to this review was completed in December, 1954.

radiations, the characteristics of the emulsion, and the overall influence exerted by experimental conditions.

It is possible to divide radioautographs into two categories: (*a*) contrast and (*b*) high-resolution. In contrast radioautography the emulsion densities become high enough to allow densitometric measurements. Where the specimen is thicker than the range of the ionizing particles, the measured densities bear a direct relationship to the total radiation dosage at the specimen surface (8). Since no attempt at high resolution is ordinarily made in contrast

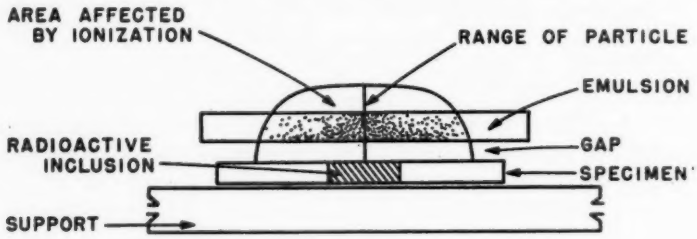

FIG. 1. Illustration of geometric relationships in radioautography.

radioautography, coarse grained, fast emulsions (such as No-screen x-ray film) are often used.

High-resolution radioautography may be subdivided depending on whether it is desired to view (*a*) the tracks of individual particles or (*b*) the distribution of silver grains. This choice is limited to β-emitters, since α-particles will inevitably produce a track in any of the usable emulsions. Ordinarily it is undesirable to expose the emulsion to the point where densitometry or unaided visual examination is possible, since unnecessarily high grain densities tend to obscure tracks or to make grain counting difficult. In high-resolution radioautography, the superimposed emulsion and specimen are viewed microscopically and it is evident that distortion of either is to be avoided. Representatives examples of these radioautographic types are shown in Figures 2 to 5.

EMULSIONS FOR RADIOAUTOGRAPHY

Emulsions are dispersions of small silver halide (silver bromide) crystals in gelatin. Their response characteristics vary with (*a*) silver bromide concentration, (*b*) size of the silver bromide grains, and (*c*) variations in compounding procedures and the presence or absence of trace amounts of reagents which may function as sensitizers or desensitizers. Being the most dense component, the silver bromide content exerts the major influence on the path length, or range, of an ionizing particle in the emulsion. In a given emulsion type, sensitivity varies directly with grain size (6). Unfortunately, the details of methods of sensitization used by emulsion manufacturers are not available. Some insight into the subject of emulsion sensitization can be gained from the discussions of Mees (13, Chap. 11, 12) and Yagoda (5, Chap. 4).

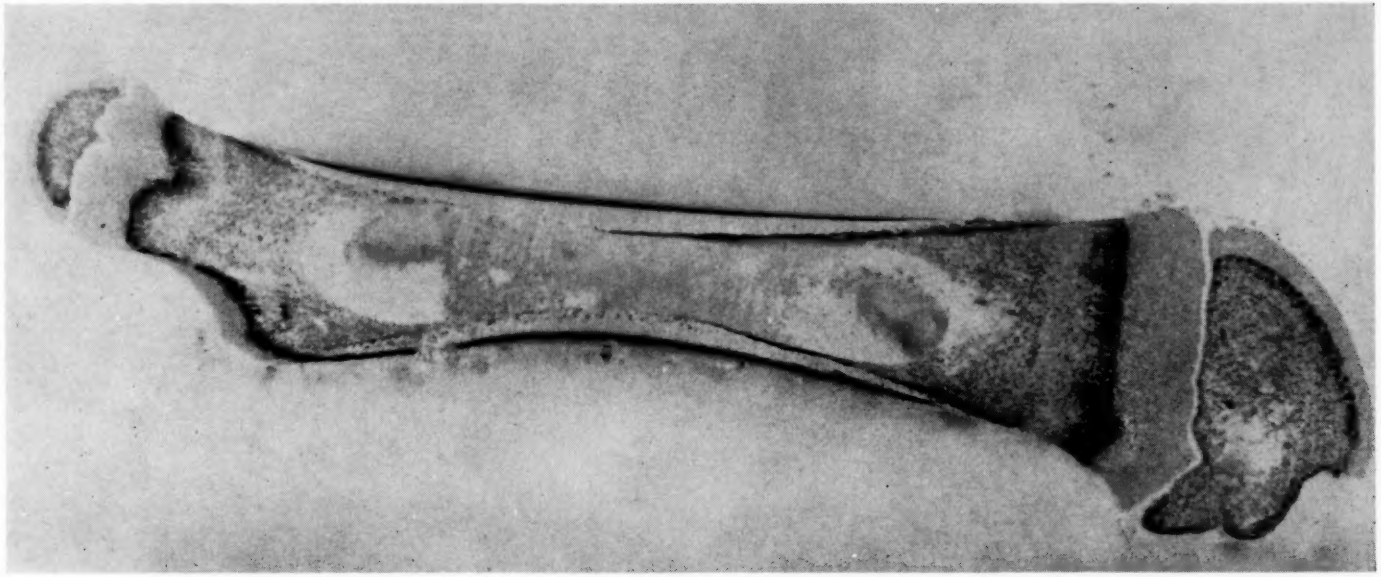

FIG. 2. Contrast radioautograph showing the distribution of injected Ca^{45} in the femur of a young pig. No-Screen x-Ray Film (full scale). [Courtesy Comar, Visek, Lotz & Rust (9).]

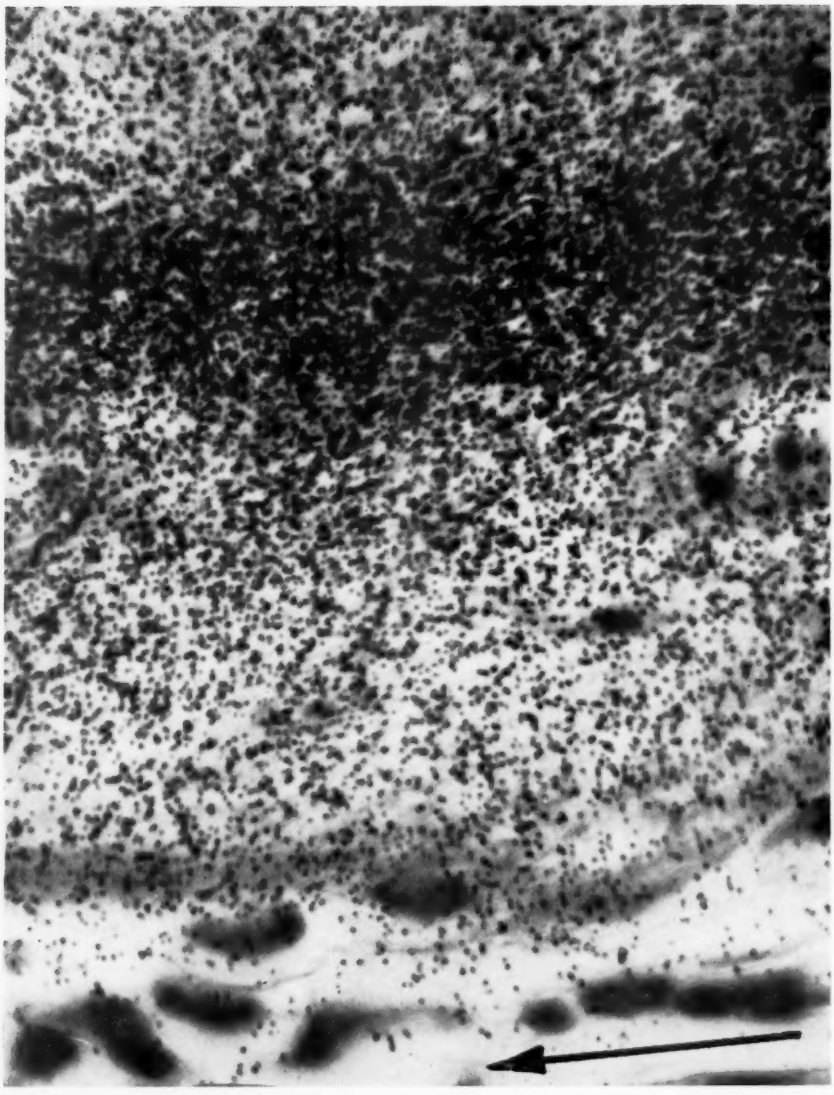

FIG. 3. High-resolution radioautograph showing the distribution of developed grains about a linear deposit of Ca^{45} in rat femur. Eastman Kodak Permeable Base Stripping Film. (×1832) [Courtesy Arnold & Jee (10).]

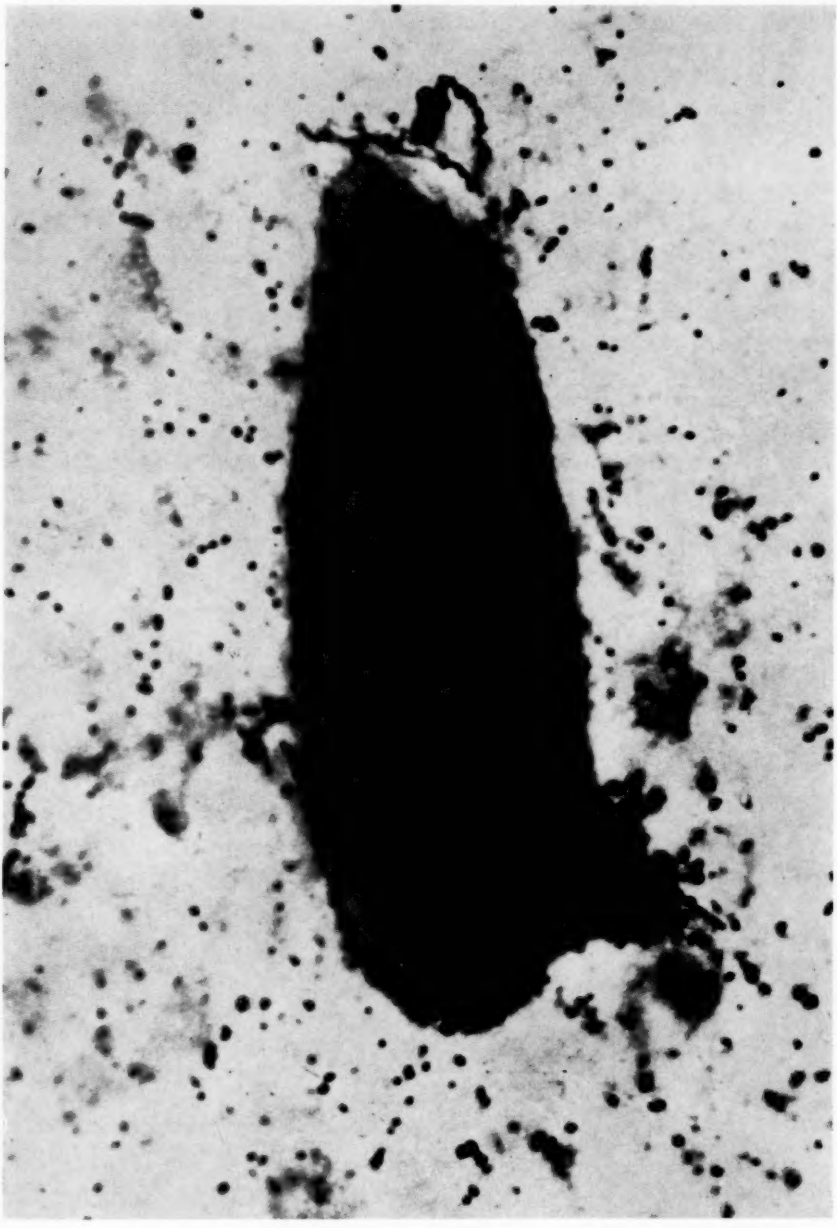

FIG. 4. Beta-track radioautograph of *Paramecium caudatum* containing P^{32} and embedded in Ilford G-5 liquid emulsion. The present authors estimate the magnification at approximately 450×. [Courtesy King, Harris & Tkaczyk (11).]

Several physicists have made their own emulsions. The descriptions of the processes used serve to illustrate the relatively minor departures in technique which may influence emulsion sensitivity (14).

Nuclear and x-ray type emulsions have usually been used in radioautography. The x-ray emulsions which have been utilized have larger grains and are appreciably faster.

Nuclear emulsions are characterized by their high content of silver bromide and small grain size—factors which enhance their usefulness in high-resolution radioautography. They are manufactured in the United States by the Eastman Kodak Company, and in England by Kodak Limited and by Ilford Limited. The essential chemical composition and physical characteristics of nuclear emulsions, quite regardless of type or manufacturer, are very similar (Tables I and II).

Nuclear and x-ray emulsions for radioautography may be obtained in various forms: mounted on glass plates, or on cellulose acetate sheets or rolls; as emulsions which may be stripped from these supports; or in gel form which, when melted at about 40°C., may be applied directly to the specimen surface. If desired, emulsions may be obtained with a thin coating of gelatin which protects against scratches and abrasions. The manufacturers may, when practicable, modify the form in which these emulsions are supplied.

FIG. 5. Alpha track radioautograph showing Pu^{239} in a rabbit femur. Eastman Kodak Permeable Base Stripping Film (×160). [Woodruff & Norris (12).]

The water content of emulsions varies with the relative humidity as shown in Table III.

PHYSICAL PRINCIPLES

Mechanism of Emulsion Response

The theory of the mechanism by which a grain of silver bromide is rendered developable was first expounded by Gurney & Mott (15), and later modified by Mitchell (16, 17, 18). According to the Gurney-Mott theory, a process which results in the dissipation of energy within the emulsion may

TABLE I

Emulsions for Radioautography

Mfg.	Type	Form as usually supplied	Emulsion* thickness μ	Mean AgBr grain diam. μ	Sensitivity† (Max. β energy in Mev)	Safe Light
Eastman Kodak Co.	NTA	on 0.05″ Glass base	10, 25	0.25	0.009	Wratten Series 0
	NTB	on 0.06″ Glass base	10, 25	0.25	.025	Wratten Series 2
		Stripping emulsion with 10 μ cellulose ester impermeable base	10			
	NTB2	on 0.06″ Glass base	10, 25	0.25	0.2	Total darkness ‡
	NTB3	on 0.06″ Glass base	25	0.25	All	Total darkness‡
	Autoradiographic permeable base (5μ) stripping film		5	0.25	0.015	Wratten Series 2
	Type A‖	Autoradiographic plate on .06″ glass base or as Industrial x-ray film	25	—	—	—
	No-Screen‖	x-ray film or autoradiographic plate on 0.06″ glass base	25	8	—	—
	Type K	Industrial x-ray film	—	—	—	—
Kodak Ltd.§	V.1001	x-ray stripping emulsion with 10μ gelatin base on glass plates	12	1.5	—	Wratten 6B or Series 1
	Autoradiographic stripping emulsion with 10μ gelatin base—on glass plate		4	0.15	~0.1	Wratten Series 1
Ilford	C2	In gel form or on .05″ glass base	10, 25	0.2	.03	Ilford "S" #902
	B2			0.4	.07	Ilford "S" #902
	E1			0.2	None	Ilford "S" #902
	G5			0.3	All	Ilford "S" #902

* In many cases, thicker emulsions are available. Thicknesses in excess of 25μ are not listed because of their limited usefulness in radioautography.

† Sensitivity is defined in terms of the maximum β-particle energy which produces a recognizable track in the emulsion.

‡ These emulsions may be somewhat less satisfactorily used with a Wratten Series 2 filter and a 15 watt bulb at distances of 4 ft. or more.

§ Types NT-1a, NT-2a and NT4 are no longer available.

‖ The autoradiographic plate is similar to, but not identical with, the x-ray film both in sensitivity level and in emulsion composition.

TABLE II

COMPOSITION OF DRY NUCLEAR EMULSIONS USEFUL IN RADIOAUTOGRAPHY*

	East Kodak Co.	Kodak, Ltd.	Ilford†
	gm/cm³		
Ag	1.70	1.97	2.025
Br	1.22	1.44	1.465
I	0.054	0.036	0.057
C	0.34	0.27	0.30
H	0.043	0.038	0.049
O	0.17	0.16	0.20
S	—	—	0.011
N	0.11	0.080	0.073

* Dried to constant weight at 110°C.
† For Type G5, Br = 1.496, I = 0.026.

raise the energy states of some electrons of the bromine atoms to vacant states in the conductance bands of the crystals. These electrons migrate rapidly, at a rate which is nearly temperature-independent, to "sensitivity specks," presumably sites of impurities or imperfections in the crystal, where they are held, rendering the site negatively charged. Positively charged silver ions then migrate in to neutralize the charge and produce an atom of reduced silver. The process repeats until a "latent image," an aggregate of several reduced silver atoms, is formed at the sensitivity speck. The latent image provides the catalytic stimulus which allows the grain containing it to be developed.

The process of latent image formation is accompanied by the liberation of

TABLE III

MOISTURE CONTENT OF NUCLEAR EMULSIONS USEFUL IN RADIOAUTOGRAPHY UNDER VARIOUS HUMIDITY CONDITIONS

Relative humidity in per cent	Eastman Kodak	Kodak Limited	Ilford Limited
	per cent weight		
0	—	—	1.41
30	—	1.3	2.06
50	2.2	2.6	2.65
60	—	—	2.95
70	4.0	3.5	3.70
85	—	—	5.17

bromine from the crystal. Under conditions of high intensity exposure, the local concentrations of this oxidizing agent may reach the point at which the latent image is destroyed. This mechanism of reversal is called solarization (13, Chap. 7).

The primary process of latent image formation is considered to be reversible. Webb (19) and Beiser (20) proposed that this reversibility results from the thermal ejection of electrons followed by loss of the newly-formed silver ion. When the number of silver atoms at the sensitivity speck is small the deposit is quite unstable and has been called an "unstable subimage." Hoerlin & Hamm (21) estimated the mean lifetime of these subimages to be approximately ten seconds.

The passage of an ionizing particle through a silver bromide grain, requiring in the neighborhood of only 10^{-14} sec., is the equivalent of a high intensity exposure when its specific energy loss is high. In this case, all the sensitivity specks may become negatively charged and electrons will be repelled because of electrostatic forces. The neutralization of the negatively charged sensitivity speck is a relatively slow process, since it depends upon the rate of diffusion of silver ions in the crystal. Thus, otherwise available electrons may be lost and the efficiency of energy utilization reduced. The influence of specific energy loss on the nature of the latent image produced has been beautifully demonstrated by Hoerlin & Hamm (21). Under high intensity exposures, such as the traversal of a grain by an α-particle, the latent images in a single grain were small and numerous. As the specific energy loss diminished, the latent image centers became fewer and larger.

Although direct analytical evidence is not available to demonstrate it, there is little doubt that the latent image consists of metallic silver (13, Chap. 4). As in physical development, the silver bromide may be removed from an emulsion without removing the latent image. Further, the chemistry of the latent image is essentially that of free silver (22, Chap. 3).

Specific Energy Loss

Only charged particles are capable of causing ionization and thus of blackening an emulsion. In considerations of emulsion response in radioautography, only α- and β-particles are of interest.[2] Gamma- and x-radiations exert their effects on emulsions indirectly by means of secondary β-particles produced when the primary photons undergo photoelectric absorption or Compton scattering. Because of the long distances which photons may travel before undergoing absorption, they produce inferior radioautographs and their probability of registering in the emulsion is low.

When an energetic particle traverses matter it loses energy, most of which

[2] Exceptions may occur where the specimen is bombarded with particles which cause nuclear reactions. For example, Mayr, *et al.*, (23) used the alpha tracks produced by neutron bombardment of boron, [$B^{10}(n, \alpha)Li^7$], for the radioautographic detection of small quantities in tissue.

goes into production of ions, as a function of the square of its charge, ze, its energy which is a function of its velocity, v, the number of atoms of stopping material per cc., N, the mean atomic number of the stopping material, Z, and its mean ionization potential, I (24). Smith (25) and Webb (4) used the following equation to calculate the average energy loss per unit distance, $-dE/dx$ (in Mev./cm.), as a function of particle energy

$$-dE/dx = \frac{4\pi e^4 z^2 N}{mv^2}\left\{Z\left[\ln\left(\frac{2mv^2}{I}\right) - \ln(1-\beta^2) - \beta^2\right] - C_k\right\} \qquad 1.$$

where m is the mass of the electron, $\beta = v/c$ (c is the velocity of light), and C_k is a correction term applied only when v is approaching the K electron velocities of the stopping atoms and is large with respect to those of the other orbital electrons. When v is less than about 5×10^9 cm./sec. the relativistic correction terms involving β nearly cancel and may be omitted. The function of equation 1 is plotted in Figure 6 to show the rate of energy loss of α- and β-particles in a typical nuclear emulsion. This curve illustrates that, as the energy of the particle increases, its rate of energy loss decreases to a mini-

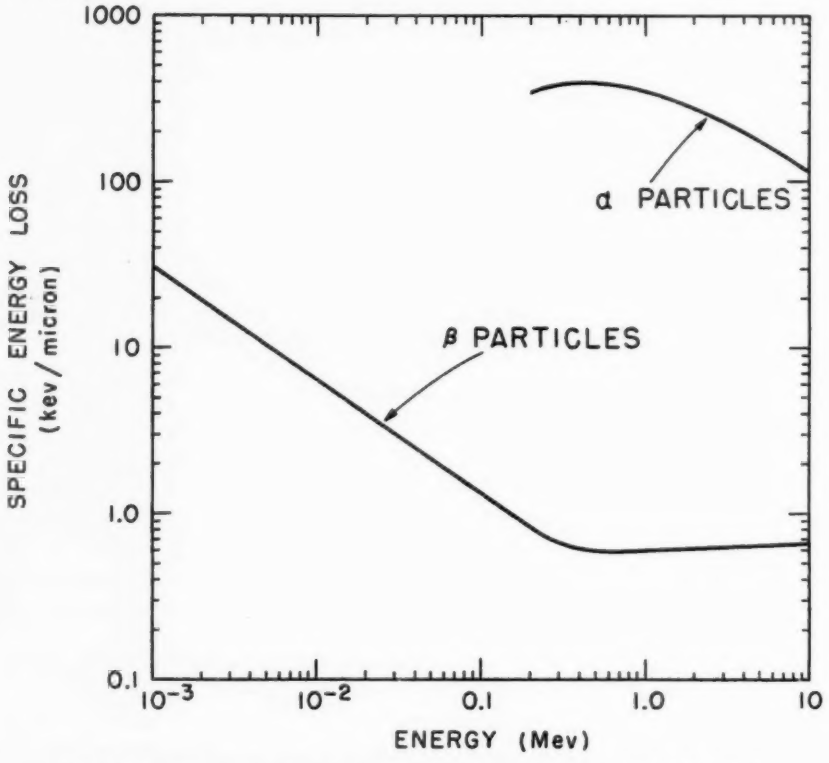

FIG. 6. Specific energy loss in nuclear emulsions as a function of particle energy. [Values taken from Herz (26) and Bogaardt (27).]

mum value (minimum ionization) which is then approximately independent of particle energy. Alpha particles, being doubly charged, will reach a minimum ionization value which is four times that of a singly charged particle. Thus the most dense ionization occurs near the termination of a particle track, and grain density in an emulsion may be expected to be highest at this point.

Particle range and emulsion stopping power.—The range of particles in nuclear emulsions is of interest from theoretical and practical aspects of radioautography. The theoretical range-energy relationship, referring to equation 1, is given by the expression

$$R = \int_0^E (dE/(dE/dx)) \qquad 2.$$

Beta particles at minimum ionization travel in an approximately straight path, but as the particle loses energy its track becomes progressively more tortuous. Cork (28) states that at high energies (above perhaps 0.5 Mev.) the range of β-particles in matter varies almost linearly with energy; while at low energies range is more nearly proportional to the square of the energy. Direct measurements of the total curved length of path of β-particles in nuclear emulsions have been made up to energies of 250 kev. (26, 29, 30, 31). Herz (31) determined both the depth of penetration and the curved track length of monoenergetic electrons in NT2a emulsion exposed in the electron microscope. His results, which were compatible with previously published data showed that, between electron energies of 25 to 80 kev., the ratio of curved length of track to depth of penetration is 1.4.

Mees (13, Chap. 8) converted the experimental values of electron ranges in aluminum, reported by Glendenin (32), into ranges in nuclear emulsions, thereby extending the curve obtained by direct observation (Fig. 7).

The range of α-particles in nuclear emulsions is known with great accuracy, the extent of disagreement being around 1 to 2 per cent. Steigert *et al.* (33) reported range-energy relationships for α-particles in NTA emulsions and compared the experimental results with values calculated using theoretical considerations. Their data (Fig. 7) agree closely with other reported values (34 to 37).

Stopping power is defined as the ratio of the particle range in air to the particle range in the emulsion. For a given emulsion the numerical value assigned to its stopping power is a function of the type of particle and its energy. Stopping power has been reported by Lattes, Fowler & Cuer (37), for α-particles, to vary from 1500 to 2000 with increasing particle energy. For α-particles produced by naturally radioactive elements, the best mean value is about 1600, corresponding to an energy of about 5 Mev.

Sensitivity

The sensitivity of an emulsion has been defined in terms of the lowest rate of energy loss which is recognizable as a track. However, as discussed

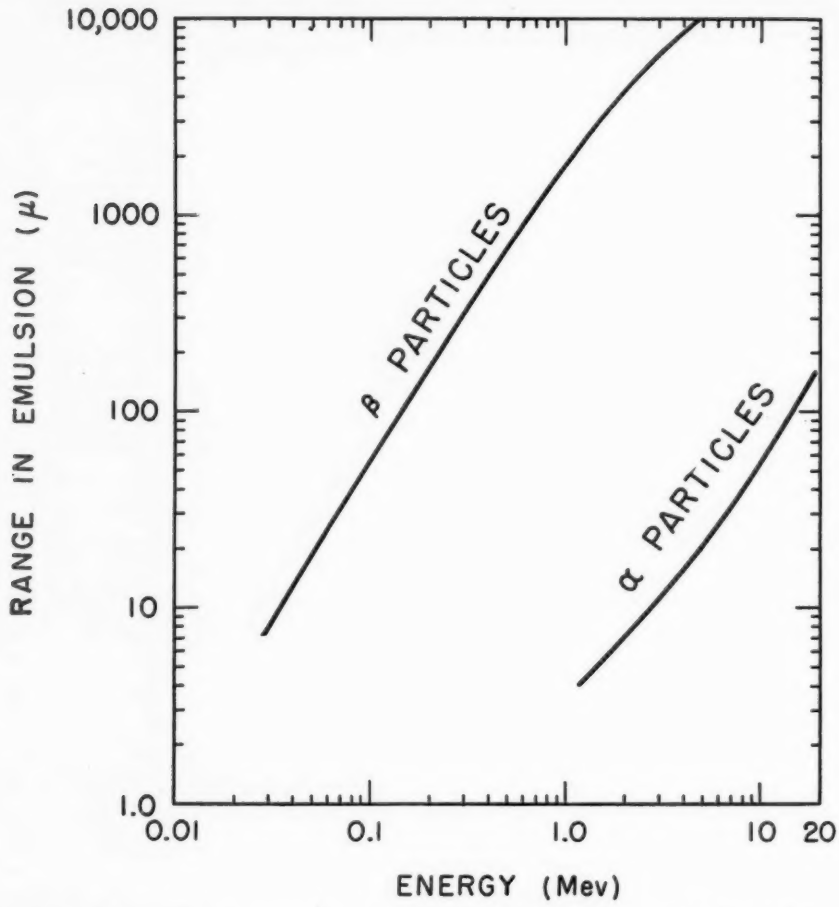

FIG. 7. Range in nuclear emulsion as a function of particle energy. [Values taken from Ross & Zajac (29, 30), Steigert, Toops & Sampson (33), and Rotblat (34).]

by Webb (4), sensitivity is described more quantitatively by the number of ion pairs required to induce developability of a single grain. With a 1 Mev. β-particle, which has the minimum rate of energy loss for electrons, sensitivity requires that 35 ion pairs/0.3μ diameter grain produce a developable latent image. Since the amount of energy dissipated per grain is a function of the grain diameter, sensitivity will vary according to grain size.

According to Yamakawa (38), 5.8 ev are required to produce one ion pair in silver bromide. Previously Van Heerden (39) obtained a value of 7.6 ev. Webb (40) and Hoerlin (41) using different methods, estimated that a minimum of ten reduced silver atoms per grain is required to induce developability under the best conditions.

In sensitive emulsions, with rates of energy loss less than four times the minimum value, grain density in the track is directly proportional to the rate of energy loss (42). At higher values of specific energy loss, saturation effects prohibit the relationship. Della Corte *et al.* (43, 44, 45) have expressed the probability of a grain being rendered developable in terms of the average length of gaps between developed grains and the gap length corresponding to one grain.

According to these definitions, emulsions which do not register the paths of β-particles above a given energy as recognizable tracks are insensitive below the equivalent specific energy loss value. In this case, it is the random variations in rate of energy loss and the probability of multiple hits during the lifetime of the unstable subimage which render occasional grains developable. With marginal sensitivity only the terminal portion of the path may register as a track, starting from that point where the rate of energy loss equals or exceeds the limiting sensitivity of the emulsion.

Temperature influence on sensitivity.—Since the diffusion of silver ions in the silver bromide grains is the rate-limiting factor in the response mechanism, the process is temperature-dependent. Beiser (6) states that most nuclear emulsions attain maximum sensitivity at about 20°C. Dollmann (46) and Lord (47) have shown that the grain density in proton tracks in Ilford C2 emulsions is highest when exposed at about 20°C. Ilford G5 exhibited maximum grain density at 0°C. (47). Track grain densities were diminished at temperatures both higher and lower than the optimum. Beiser (6) concluded that the decrease in grain density above the optimum temperature is caused by the increased rate of thermal ionization of the silver atoms of the latent image. Lord (47) found the sensitivity of Ilford G5 emulsion to be zero at −200°C. Dilworth (48) had previously utilized the reduced sensitivity at low temperatures to allow intermittent recording of ionizations. The data of these authors show that the number of grains per track may be altered by 10 to 20 per cent by changing the temperature from 0° to 20°C. Thus emulsion sensitivity should be stated in terms of the temperature of exposure. Specific information does not seem to be available; however, it is assumed that values for emulsion sensitivity represent the maxima, presumably attained at around 20°C.

Emulsion Response

Speed and sensitivity are terms often used synonymously. However, speed is more properly used to denote the rate of increase of optical density as a function of total exposure. In emulsions of similar grain size, speed may be used as an indication of relative sensitivity.

The density of an exposed and processed emulsion is defined as the logarithm of the ratio of the intensity of the incident light, I_0, to the transmitted light, I. ($D = \log I_0/I$.) The normal fog density of unexposed emulsions may be expected to range from 0.04 to 0.4 according to Cobb & Solomon (49). These authors found a value of 0.06 for NTB nuclear emulsion and 0.2 for

Eastman No-screen x-ray film. Measurements of background density include, in addition to silver grains from fog and stray ionizations, the contributions of the gelatin and associated supporting material. The conditions of storage and processing exert a considerable influence on background density.

Berriman *et al.* (50) state that a density of 0.5 above background is the reasonable upper limit likely to be used in radioautography. Dudley (51) published curves relating the number of monoenergetic β-particles required to produce a given density in various emulsions to the energy of the incident

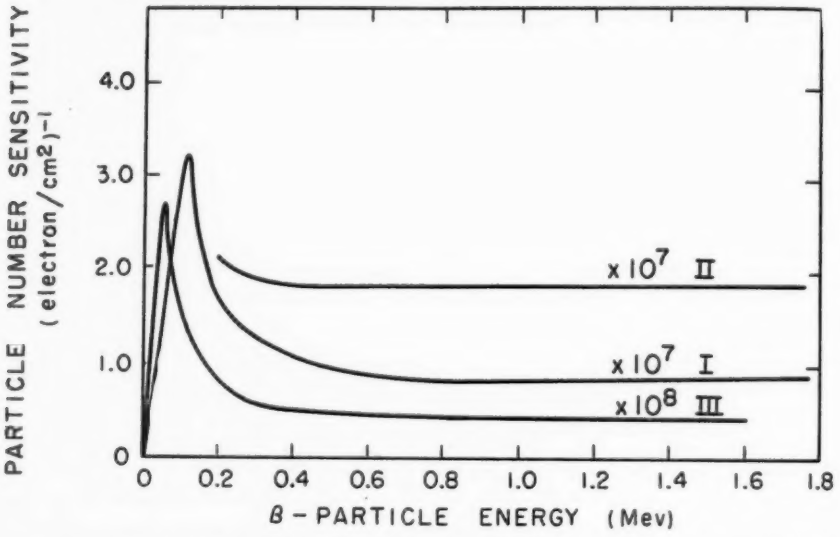

FIG. 8. Number of β-particles/cm.^{2}, as a function of particle energy required to produce a density of 0.3 above background. Curve I: Eastman Kodak No-Screen x-Ray Film, single coated, perpendicular incidence, Curve II: Eastman Kodak No-Screen x-Ray Film, single coated, diffuse incidence. Curve III: NTB Stripping Film, perpendicular incidence. [Values from Dudley (51).]

particle. Because of their angular distribution in the emulsion, diffusely incident particles were more efficient, by approximately a factor of two, than those perpendicularly incident when the range of the particles in the emulsion appreciably exceeded its thickness. Typical results obtained by Dudley for Eastman No-screen x-ray film and for NTB nuclear emulsion are given in Figure 8. At low electron energies, the apparent rise in speed with particle energy is caused by the increasing energy dissipated per particle in the emulsion. Beyond the point where particle range exceeds emulsion thickness, the increased number of particles required is the result of the reduction in specific energy loss.

Similar results were reported by Lamerton & Harriss (52) who found the ratio of the grain yields (developed grains/incident electron) for diffusely

/perpendicularly incident P^{32} electrons to be 0.8/0.5 or 1.6 in Kodak Limited Autoradiographic stripping emulsion.

The dependence of emulsion response on β-particle energy and the angle of particle incidence makes it difficult to give any simple formulation for the density produced by a given number of incident particles. Berriman *et al.* (50) found that an exposure to approximately 10^9 betas/cm.^{2} was required to give a density of 0.5 above background in Kodak Limited Autoradiographic plates 4μ thick. This value is in substantial agreement with Dudley's results using NTB stripping film. With single-coated Eastman No-screen x-ray film, Dudley found that roughly one-twentieth as many betas/cm.^{2} were required as with NTB emulsion to produce the same density (see Figure 8). Wainwright *et al.* (53) using a value of 6×10^6 betas/cm^2 as a suitable total exposure, published a nomograph relating specimen counting rate and isotope half life to required exposure time. No statement of emulsion type was made, but calculations are presumed to be based on the response of No-screen x-ray film.

When emulsions are exposed to the action of light, it is well known that the relationship between total exposure and emulsion density is not linear. This is usually referred to as reciprocity law failure. However, this is not the case in exposures to ionizing particles. For some time it has been recognized that when emulsions are exposed to x-rays a linear relationship between total exposure and emulsion density is obtained. Bell (54, 55), in 1936, demonstrated this relationship for both γ- and x-radiations over wide ranges of exposure intensities. Since the effect of these radiations on emulsions is produced by secondary electrons, it follows that this same linear relationship is to be expected with β-particles. This must also hold for α-particles where, under ordinary conditions, the probability of rendering a grain developable is almost one.

This linear relationship between emulsion blackening and total exposure to monoenergetic β-particles has been demonstrated by Dudley (51) to obtain over a considerable range of particle energies (0.03 to 1.2 Mev.). Similar results were obtained by Berriman *et al.* (50), Cobb & Solomon (49), and Lamerton & Harriss (52). The latter obtained their results by counting grains and found, using P^{32} ($E_{max}=1.7$ Mev.) and S^{35}($E_{max}=0.167$ Mev.), that the grain yield (or the density increment per electron) was higher with S^{35} electrons—a result in accord with prediction based on the specific energy loss of the electrons.

According to the theory of latent image formation, as discussed earlier, it would appear that the slope of the line relating density to exposure should be somewhat dependent upon exposure intensity when there exists a fair probability of a grain undergoing multiple hits within the mean lifetime of the unstable subimage. The authors have found no reference to this subject in the literature of radioautography. It is probable that, at the intensities usually employed, this is not an important consideration.

The slope of the curve relating total exposure to emulsion density, under

otherwise fixed conditions, will vary depending on the rate of latent image fading under the conditions of exposure. The factors which influence latent image fading will be considered in more detail later. When the rate of latent image fading is appreciable, it imposes a limitation on the useful length of radioautographic exposure time since an equilibrium condition will be established in which the rate of fading will equal the rate of latent image formation. Since fading of the latent image proceeds as an exponential function of time (56, 57), the useful length of exposure, for practical purposes, is twice the latent image half life. In this case 75 per cent of the maximum equilibrium density will have been reached. Andresen *et al.* (58) encountered such a situation in measurements of the grain yield from C^{14}. In their work, the grain yield tended to decrease over an exposure period of four days and was attributed to fading of the latent image. Herz (26) reported 30 per cent fading in one week in Kodak Limited Autoradiographic stripping emulsion kept under recommended conditions.

FACTORS WHICH INFLUENCE THE LATENT IMAGE

The rate of fading of the latent image has been demonstrated to vary widely depending on the characteristics of the emulsion (59). Under otherwise constant conditions, fading seems to proceed more rapidly with smaller latent images (56). Albouy & Faraggi (60) found that fading proceeded faster in the region of minimum ionization than in the terminal region of high specific ionization.

Effects of Chemicals

Chemical reactions in great variety may be possible when an emulsion is placed in contact with the specimen. The previous comments concerning sensitizing and desensitizing agents for emulsions are of interest here, particularly with reference to biological specimens where the chemical composition is complex. It is conceivable that the chemicals associated with the specimen may alter the sensitivity of the emulsion either locally or generally.

The occurrence of positive and negative artifacts, attributable to direct chemical action, has already been established. Positive artifacts are areas blackened by chemical or mechanical action. A negative artifact refers to the absence of an image attributable to inhibition or reversal of emulsion response by chemical action. Although chemical interferences in radioautography have been recognized more abundantly in connection with the formation of positive artifacts, ample evidence is available to indicate that the negative artifact presents an equally severe problem. Various authors have emphasized the importance of control processes to detect artifacts. Comprehensive information concerning reagents which cause artifacts in radioautography is not available; only a few have been studied and reported in any detail.

Water content of the emulsion.—The water content of the emulsion has

been demonstrated to affect the rate of latent image fading. Beiser (6) noted that the curve of rate of latent image fading as a function of relative humidity reported by Albouy & Faraggi (61) is very similar to the curve of absorbed water content versus relative humidity reported by Mees (13, Chap. 3). It is strongly implied that the rate of fading is an exponential function of the moisture content of the emulsion. The observation that emulsion sensitivity is reduced at high relative humidities is probably the result of the increased rate of fading of the latent image.

Albouy & Faraggi (61) suggested that fading occurs by the oxidation of the silver atoms of the latent image by oxygen in the presence of water

$$2Ag + O + H_2O \rightarrow 2Ag^+ + 2OH^- \qquad 3.$$

Consideration of this equation makes evident the fact that fading will proceed more rapidly at low pH values and will be repressed under alkaline conditions.

Atmospheric oxygen.—Mather (62) demonstrated that a 90 per cent reduction in the rate of fading of proton tracks in Eastman NTB and Ilford C2 emulsions could be achieved by storing the plates under vacuum. Beiser (6) suggested that the residual 10 per cent fading in Mather's experiment resulted from thermal agitation of electrons which occasionally results in oxidation of atoms of the latent image. Mather found that the rate of fading was also increased by increasing humidity and temperature. Beiser (56) has shown that under otherwise fixed conditions the rate of fading in air is an exponential function of the reciprocal of the absolute temperature.

Albouy & Faraggi (61) showed conclusively that oxygen is responsible for much of the fading produced by storing nuclear emulsions in contact with the atmosphere. In their experiments Ilford C2 emulsions stored in air for 50 days before development lost about 25 per cent of the initial number of grains. In pure oxygen more than 50 per cent were lost, while storage in nitrogen resulted in a loss of about 6 per cent. These results refer to rates of surface fading in thick emulsions, and the fading observed in the interior of the emulsion amounted to considerably less. The observation that the process proceeds from the surface leaves little doubt that diffusion of oxygen into the emulsion is the rate limiting factor. With the thin emulsions ordinarily used in radioautography, one should not observe significant differences between the surface and interior rates of fading.

Hydrogen peroxide.—It is unlikely that there is any appreciable difference in the mode of action of hydrogen peroxide and that of water or oxygen or both (61). The response of fast emulsions, such as No-screen x-ray film, to traces of hydrogen peroxide is different from that of nuclear emulsions in that positive artifacts are produced (5, Chap. 1). This effect is also pH-dependent with production of false images proceeding more readily on the alkaline side. It would appear that this phenomenon is related to the observation that hydrogen peroxide in alkaline solution is a weak developing agent for these faster films.

Fading of the latent image in nuclear emulsions by hydrogen peroxide has been advantageously utilized to remove accumulated background grains prior to usage (63, 64). This was accomplished by storing the emulsion over 3 per cent hydrogen peroxide in a closed container for 4 hr. at 25°C. Sensitivity was restored by drying the emulsion over $CaCl_2$ for from 1 to 2 hours.

Pseudo-photographic effects attributable to hydrogen peroxide have been reported when specimens were placed next to emulsions for radioautography. Churchill (65) found that hydrogen peroxide produced in the oxidation of fresh scratches and abrasions of metallic surfaces caused the image of the scratch to be reproduced on x-ray film. Other work has indicated that hydrogen peroxide or organic peroxides may be evolved from certain woods (66), and rock specimens (67). Ansheles found the effects localized in the regions of cracks and fissures through which peroxides were presumably evolved to the emulsion surface. Other materials which appear to produce pseudo-photographic effects by evolution of hydrogen peroxide are Canada balsam, sealing wax, and resins (5, Chap. 1).

Miscellaneous reagents.—Other chemicals in great variety either are known to affect photographic and nuclear emulsions or have been implicated indirectly. In general, the action of oxidizing agents may be expected to inhibit image formation or to cause fading of the latent image. Reducing agents will ordinarily cause fogging. As indicated in the preceding discussion, whether a given compound will function as an oxidizing or as a reducing agent may be expected to be a function of the emulsion, pH conditions, temperature, and the presence or absence of incidental reagents which may catalyze or inhibit the reaction.

Interferences may also be produced by reagents which form insoluble salts when reacted with silver bromide. The most widely recognized compound in this class is hydrogen sulfide.

Severe difficulties with chemical anomalies have occurred in radioautography of biological specimens. Boyd & Board (68) demonstrated that normal fresh or frozen rat tissue produced images, by direct chemical action on NTB emulsions, with distinctive patterns which closely resembled radioautographs. Later Board (69), working with guinea pig tissues, showed that the emulsion reducing materials were stable at 60°C., dialysable, and "inhibited" by iodoacetic acid. Since Board found that solutions of glutathione and cysteine produced blackening of NTB emulsion, he suggested that sulfhydryl compounds were primarily responsible. Everett & Simmons (70) found that rat tissue also contained water soluble, nondialysable substances which reduced emulsions, but that the water-extracted tissues caused no blackening. They concluded that sulfhydryl compounds were not the only responsible agent, and supported this contention by demonstrating that those areas in rat skin which were stained with sulfhydryl specific reagents did not coincide exactly with areas of chemical reduction.

Everett & Simmons found Bouin's solution to be a satisfactory fixative which did not contribute to the darkening of emulsions. However, Doniach

& Pelc (71) reported that tissues fixed in Bouin's fluid exhibited negative artifacts. It would appear that fixatives containing mercury or copper salts are undesirable since Board (69) stated that these materials desensitize NTB emulsion. There is no general agreement as to which tissue fixation techniques are most compatible with emulsion methods for radioautography.

It is difficult to distinguish between chemical reduction and valid grain radioautographs. Bourne (72) contended that chemical fogging of an emulsion may be recognized by the fact that fogging will spread outward from the specimen surface as a function of the rate of diffusion of the interfering substance in the emulsion. Therefore, microscopic examination should reveal fog grains only near the specimen surface. Everett & Simmons (70) were unable to distinguish between positive artifacts and valid radioautographs by this method. However, it would appear that whether or not such differentiation is practicable would depend to a considerable extent on emulsion thickness, time of exposure, and the rate of diffusion of the interfering substance.

Miscellaneous Artifacts

Artifacts caused by agents other than chemical have been observed. When an emulsion is stripped from its support enough light may be produced through static discharges, especially under low humidity conditions, to produce blackening (73).

Silver bromide grains may be rendered developable by the application of excessive or uneven pressures, as in scratches or abrasions, or in attempts to improve contact between specimen and emulsion (74). Doniach & Pelc (71) found that the pressure exerted by stripping emulsions drying on a specimen sometimes produced blackening, especially in the region of the edges of the sections. Bartell & Brockway (75) reported that the sensitivity of untreated Kodak lantern slides increases from the center to the edges and that emulsion sensitivity is increased by mechanical disturbances such as cutting, handling and packing. It is well known that one of the early obstacles to the preparation of very thick emulsions on glass for nuclear research arose from the extreme pressures produced on drying the emulsion which often pulled slivers of glass from the base.

Fluorescence and photoluminescence phenomena in the specimen may also cause artifacts (76). Yagoda (5, Chap. 1) mentioned artifacts produced by fluorescence of certain compounds, particularly petroleum products, under the impact of β-radiation. Boyd & Board (68) differentiated between chemical and fluorescence artifacts by interposing thin glass cover slips between the specimen and the emulsion.

TECHNICAL CONSIDERATIONS

Specimen Preparation

Space does not permit detailed discussion of methods for the preservation and preparation of specimens for radioautography. In general, as at-

tempts are made to increase the detail and resolution of radioautographs, the quality of the specimen must increase and its thickness decrease. It is necessary to produce a smooth, flat surface which will give intimate contact with the emulsion.

As indicated earlier the specimen should not contain or evolve chemicals which produce artifacts by reacting with the emulsion. Many workers have attempted to coat the specimen with protective films to prevent chemical effects, but the results have been equivocal. Everett & Simmons (70) tested thin coatings of Duco cement, silicone (Dri Film), Geon resin, Permamount, Formvar, and cellophane. Only the cellophane covering, which was 27μ thick, prevented histochemical reduction of Ansco Bulk Emulsion A. Blundell & Rotblat (77) recommend use of a 1 per cent solution of Perspex (methyl methacrylate) in chloroform. Eidinoff *et al.* (78) report satisfactory results when suspensions of microorganisms in water were dried on Formvar-coated nuclear emulsions. MacDonald *et al.* (79) found that celloidin in methyl alcohol had no effect on emulsions, but that celloidin in ether-alcohol produced darkening of Eastman Type M emulsion. Using the wet-process method, Gomberg (80) obtained best results using vinyldene chloride (Saran 2000) in methyl ethyl ketone for tissue specimens and a 90:10 copolymer of vinyl chloride and vinyl acetate (Vinylite VYNS, Bakelite Corp.) in methyl ethyl ketone for metal specimens mounted in bakelite. Eastman Kodak produces an NTB stripping emulsion with an impermeable cellulose ester base which was utilized by Boyd & Williams (73). Holt & Warren (81) preferred to use an 18μ air gap instead of an "impermeable" coating. The preparation and properties of thin films of a number of likely materials were reviewed by Chapman-Andresen (82).

When the specimen contains soluble radioactive compounds, measures must be taken to prevent leaching or translocation. Williams (83) demonstrated leaching of plutonium from tissue sections when they were immersed in water according to the radioautographic technique described by Evans (84). Yagoda (5, Chap. 1) states that if polished sections of pitchblende, which frequently contain inclusions of metallic silver, are etched with nitric acid, polonium may be brought into solution and deposited electrochemically on the silver inclusions.

Freeze-drying (81) and frozen sectioning (85) methods have been utilized to reduce leaching in biological studies. Asboe-Hansen (86) and Russell *et al.* (87) treated tissues with basic lead acetate in an effort to insolubilize sulfates and phosphates. In histochemical studies of specific insoluble compounds, such as labelled desoxyribonucleic acid (DNA), soluble radioactive materials have been removed by extensive washing of the sections (88, 89).

Apposition of Emulsions

A number of methods and modifications of methods for bringing emulsions into contact with specimens have been described. These may be divided into two general categories: (*a*) methods in which the specimen and

emulsion are not permanently apposed, and (*b*) methods in which specimen and emulsion are permanently joined together. These techniques have been reviewed in detail by Fitzgerald *et al.* (90), and Gross *et al.* (91).

Where the specimen and emulsion are kept separate, there is the advantage that the two may be processed separately and problems of the effects of developers on the specimen or of histological processing on the emulsion do not arise. However, in high-resolution work, problems exist in accurately realigning the specimen and the emulsion. Holt & Warren (81) marked the specimen slide with radioactive ink to improve the precision of realignment. Buie *et al.* (92), and Williams (83) described methods in which the specimen was mounted on a flexible glass cover slip secured at one end to the glass base holding the emulsion. With this sytem the specimen may be removed from the emulsion and the two processed separately while retaining their orientation.

Specimens may be permanently affixed to emulsions using either the mounting method of Evans (84, 93) and Endicott & Yagoda (94) in which the specimen is floated into position on top of the emulsion, the liquid emulsion technique of Bélanger & LeBlond (95) and Bélanger (96) in which melted emulsion is painted directly over the specimen (97), or the stripping film technique of Pelc & Howard (98) in which the emulsion is stripped from its base, floated on water, and transferred into position overlaying the specimen (10, 99). Stieff & Stern (100) have described a method of dry-mounting Eastman impermeable base stripping film. With finely divided specimens such as microorganisms or rock powders the specimens may be distributed upon the emulsion (100) or incorporated into liquid emulsions (11, 101).

Gomberg (80) and Towe, Gomberg & Freeman (102) described a "wet-process" method in which the emulsion is produced by precipitation of silver bromide in celloidin ($CdBr_2$ impregnated) covering the specimen. This method has been applied both to the study of biological materials and metals.

With permanently-mounted specimen-emulsion systems, the problem of maintaining orientation is simplified. The main disadvantage is that both emulsion and specimen are subjected to all processing and staining procedures. Doniach & Pelc (71) found that eosin, used in counterstaining of tissues, caused dissolution of developed silver grains.

Exposure of Emulsions

In the exposure of the emulsion, many of the factors previously mentioned may exert a considerable influence. Most workers have chosen a temperature around 5°C. with calcium chloride as a desiccant. (In a closed container at 5°C. $CaCl_2$ produces an equilibrium condition which results in a constant relative humidity of 39.8 per cent.) This temperature appears to have been chosen in an effort so minimize fogging, but, as pointed out earlier, the sensitivity of the emulsion may also be reduced. It is not clear whether

the advantages gained in reduced fogging outweigh the disadvantages of reduced emulsion sensitivity.

There is a practical limit to the duration of exposure which is imposed by the half life of the isotope involved, the accumulation of background fog, and, in addition, by the rate of fading of the latent image under the conditions of exposure. Fading of the latent image during exposure may be nearly eliminated by storage in an inert atmosphere, such as dry nitrogen or carbon dioxide (103).

Perhaps the greatest difficulty in predicting exposure times, even when the radioactive content of the specimen is well known, arises when the degree of inhomogeneity of the radioactive deposits is unknown. Therefore, it is usually necessary to use a series of graded exposures. Where the variations in concentration are large, optimum exposures in one area may be suboptimum in others; or it may be necessary to overexpose some regions in order to demonstrate perceptible concentrations elsewhere.

Processing

Developers are weak reducing agents, maintained at pH values from around 7 to more than 11 depending upon the formulation, which in themselves are incapable of effectively reducing silver bromide. However, the presence of the elemental silver of the latent image catalyzes the reduction of silver bromide so that grains containing latent images are reduced to grains of silver. Della Corte *et al.* (43) have shown that this catalytic action may extend to as many as four adjacent silver bromide grains, an observation of some interest in connection with quantitation by grain counting.

Apparently the number and size of the silver specks comprising the latent image will affect the speed of reduction of the grain. Beiser (6) states that with densely ionizing particles, such as alphas, the tracks are visible after "moderate" development and background fog is reduced. However, only strong development utilizes the full sensitivity of the emulsion and is required to register weakly ionizing particles.

Fixing baths containing reagents such as sodium thiosulfate are used to remove residual silver bromide. This reagent tends to dissolve metallic silver and its use must be carefully controlled. Mees (13, Chap. 17) states that the solubilization of silver in thiosulfate solutions is increased by the presence of oxygen and with decreasing pH. Where large amounts of silver salts accumulate in the fixer there may be some tendency for surface phenomena to occur—particularly the deposition of elemental silver on the surface of the emulsion (6, 74).

The processing of emulsions is highly responsive to temperature, which is ordinarily maintained at some constant value between 10° and 20°C. Howard & Pelc (104) reported artifacts similar to weak radioautographs when developing temperatures exceeded 18°C. Doniach & Pelc (71) observed that severe distortion, termed reticulation, occurred as a result of sudden temperature changes during processing.

Distortion of Emulsion

When unsupported nuclear emulsions are placed in water (as with some applications of stripping emulsions) they swell so that the surface area may increase by as much as 40 per cent. When mounted on a firm base and dried to 50 per cent relative humidity the emulsion is thinner than it was originally and is under appreciable tension. Since development allows interim relaxation before the emulsion is finally dried for examination, there is opportunity for it to fail to preserve its orientation with the specimen. This type of distortion is aggravated by changes in pH and tonicity (105).

Emulsions fastened to glass supports become thicker when immersed in water, although their lateral dimensions are not observed to change significantly (105). With thicker emulsions, it has been observed that some lateral distortion is introduced by unequal drying at the surface. When silver bromide, which comprises about 45 per cent of the volume of the emulsion, is removed in processing, the thickness is reduced to about one-third of the original value (106).

EXAMINATION AND INTERPRETATION

General Examination

In high-resolution radioautography the specimen and the developed emulsion are ordinarily examined microscopically as a unit. Whereas artifacts produced by mechanical means usually have an easily recognizable appearance, those caused by chemical action are often indistinguishable from a true radioautograph.

The limiting factor in the recognition of a radioautograph is the number of background grains per unit area of emulsion. Coates (107) has shown that the number of fog grains per unit area increases as a function of development time, and that the fog grain distribution is entirely random.

Pelc & Howard (98), who used Kodak Limited Autoradiographic stripping film, state that fog grain density should not exceed from 4 to 6 grains/$100\mu^2$, in which case 10 grains/$100\mu^2$ above background can be accepted as a radioautograph. Andresen *et al.* (58), using the same emulsion, obtained a mean value of 4.2 grains/$100\mu^2$ with a range from 0.35 to 21 grains/$100\mu^2$. They found no perceptible increase in background grain density with exposure times up to 30 days. The random nature of fog grain distribution established by Coates and further illustrated by Andresen *et al.* shows that a radioautographic grain count in the region of the background density can only be stated in terms of the probability function.

Beiser (108) has shown, by means of artificial fog diagrams (equivalent in size to 1500× magnification), that when the background grain density exceeds 0.5 grains/$100\mu^2$ ability to recognize electron tracks exhibiting low grain densities is progressively diminished. At background densities of 1.5 grains/$100\mu^2$ and above, the number of falsely identified tracks was equal to or exceeded the fraction of tracks correctly identified. However, as Berriman

(109) had previously illustrated by the same technique, track visibility at a given fog level is a function of the number of grains/micron of track length.

Quantitation

As discussed earlier, the density or the number of developed grains produced in an emulsion bears a linear relationship to the total number of incident particles. However, this relationship must be interpreted in the light of the rate of latent-image fading and the length of exposure.

There are three ways in which quantitation of radioautographs may be approached: (*a*) densitometry, (*b*) track counting, and (*c*) grain counting. Densitometry is a simple and accurate method of recording average emulsion densities. However, it is limited in application by the size of the aperture which, in the most refined commercially available instruments, is about 0.1 mm.^{2}. Reasonably high optical densities are also required which limits the quantitative sensitivity of the method. Odeblad (76) has described a microdensitometric technique which permits measurements of a circular area 100μ in diameter (.008 mm.^{2}).

The relationship between optical density, D, and the number of developed silver grains per cm.^{2}, n, was derived by Nutting (110) as $D=0.4343\bar{a}n$, where $\bar{a}$ is the mean projective area of the developed grains. The mean projective area of the developed grains of Kodak Limited Autoradiographic stripping plate was determined by Herz (26) by electron microscopic studies and found to be 0.0625μ^2. Andresen *et al.* (58), using this same emulsion and Herz' value for $\bar{a}$, compared grain densities calculated from optical density measurements using Nutting's formula with values obtained by grain counting. They found Nutting's method to give on the average 2.7 times as many grains as were obtained by actual counting.

Boyd & Levi (111) found fair agreement between the C^{14}-content of tissue, as measured in an ionization chamber, and the number of tracks counted in thick (25 and 100μ) NTB2 emulsion. Miller & Hoecker (112) discussed the quantitation of radium, an alpha emitter, and its three alpha-emitting daughters in bone. Kinersly (113) utilized the technique of Hoecker and Roofe (114) for determinations of relative concentrations of Ca^{45} in teeth by track counts. Levi (115) considered the possibilities of quantitating thorium deposits in soft tissues of patients given thorotrast.

One of the greatest difficulties in track counting lies in the proper recognition of the track. This is comparatively simple with α-tracks because of their high grain densities and the fact that they always travel in a straight line. But even in this case those tracks which penetrate nearly perpendicularly to the plane of the emulsion are not easily recognized, especially in a thin emulsion, since they appear as a single grain or a clump of grains. With emulsions of such thickness that a considerable fraction of the α-particle range lies within the emulsion, track recognition is simplified.

The use of thick emulsions, as practiced by Boyd & Levi (111), is particularly useful in quantitation of β-tracks. With energetic β-particles, the

origin of the track may often be difficult or impossible to determine because of the low initial specific energy loss and the fact that fading of the latent image is most pronounced in this area (60). Levi (101) utilized the method of King, Harris & Tkaczyk (11), in which single cells are suspended in liquid emulsion, to improve the ease of track recognition and counting.

A critical study of the problems of quantitation of the radioactive content of small areas by grain counting, so far as the authors are aware, has not yet appeared. Dudley & Pelc (116) have described an apparatus for automatic grain counting designed on the principle of the flying-spot scanner. Andresen *et al.* (58) made quantitative studies of the C^{14}-content of amoebae by both grain counting and Geiger-Mueller methods. These authors found, in Kodak Limited Autoradiographic stripping emulsion, that the grain yield varied from 0.47 to 1.02, the variation being attributed to fading of the latent image. Grain yields in Kodak Limited Autoradiographic stripping emulsion for other β-emitting isotopes have been reported. Using P^{32}, Herz (26) obtained 0.77 grains/β-particle, while Berriman *et al.* (50) found about 1.0. Lamerton & Harriss (52) reported 0.8 for diffusely incident P^{32} electrons and 1.8 for S^{35}. A value of 0.4 for the grain yield from I^{131} β-particles may be assumed on the basis of density measurements made by Berriman *et al.* (50). With the exception of the data of Andresen *et al.*, all these values appear to have been derived from measurements of diffusely incident particles from plane sources. However, it will be noted, if one compares the values for grain yields noted above with the maximum energies of the particles, that grain yield does not increase with decreasing particle energy as expected on the basis of the specific energy loss.

When radioactive inclusions are small compared to the range of the β-particle, a problem arises in determining the area which is to be counted for grains produced by particles originating in the inclusion. Where the sources of the β-particles exist in known, recognizable forms of measurable size, this problem is somewhat simplified, since the mathematical approaches to problems of resolution may be utilized. However, when the source of a β-particle and its size are indeterminate, the quantitation of radioactivity in a small area theoretically becomes an extremely complex problem which is intimately associated with the subject of resolution.

Resolution

Preliminary estimates of attainable resolution often aid in choosing the conditions required for radioautographic procedures. As discussed by Lamerton & Harriss (52), considerations of resolution also have an important bearing on the recognition of a radioautograph and on the limitations of quantitating it by grain counting.

Mathematical approaches to the problem of resolution have been made by assuming that the particle flux diminishes around a small radioactive source according to the inverse square law (that is, by neglecting absorption and backscattering) and that the emulsion response is directly proportional

to flux density. Doniach & Pelc (71) made such calculations on the basis of a point source at various depths in the specimen and on the basis of a rod source of zero diameter perpendicular to the plane of the emulsion. Resolution was defined as the distance from the point of maximum exposure to the point at which the grain density was halved. The results indicated that maximum resolution is achieved when the point source is located at the specimen surface. The authors emphasized the importance of minimizing the gap between specimen and emulsion for best resolution.

Gross *et al.* (91) extended this mathematical treatment, using the same basic assumptions, to plane and cylindrical sources. They showed that increasing emulsion thickness is of secondary importance compared to increasing the distance of the source from the emulsion surface and, further, that resolution is a function of the size and shape of the source. Lamerton & Harriss (52) pointed out the disadvantage of using the inverse square law in such calculations, since the intensity theoretically approaches infinitely high values when the source contacts the emulsion. Instead they used existing theorems, which describe the intensity distribution about sources of various shapes, for calculations of resolution with cylindrical sources. The results show that resolution decreases as the radius of the cylinder increases; and further, that there should be no difference between the resolution obtained when the specimen thickness is x and emulsion thickness is y, or vice versa. These authors defined resolution as follows:

> The resolution of a given autoradiographic technique shall be defined as the distance d, if the images of two uniformly active cylindrical sources of diameter d can just be resolved when the centres are separated by a distance $2d$.

Their calculated values of resolution are listed for general reference in Table IV. They agree with the value of 2.3μ actually measured by Stevens (117), who applied a nuclear type emulsion (Kodak Limited Autoradiographic Plate, 4μ thick) by a stripping technique to an I^{131}-labelled Cobb type test chart. Doniach, Howard & Pelc (118) reported obtaining resolution of 2μ using P^{32} with Kodak Limited Autoradiographic stripping emulsion.

Some aspects of resolution that have not been included in these theoretical approaches are (*a*) effects of grain size, (*b*) exposure time, and (*c*) the effects of the increased rate of energy loss in the terminal portion of the track. Boyd (119) demonstrated the increase in image size as a function of increased grain size (or sensitivity) and, further, illustrated the increase in image size with increasing time of exposure. In discussing Boyd's results, Gross *et al.* (91) emphasized the desirability of low exposures for optimal resolution. These authors also mentioned the adverse effects on resolution of the increasing rate of energy loss in the terminal portion of the track. The increased resolution which may be achieved with very low energy β-particles is illustrated by the results of Chapman-Andresen (120) who obtained resolution of 1μ with tritium in microorganisms, using Kodak Limited Autoradiographic stripping emulsion according to the method of Doniach & Pelc (71).

TABLE IV*

THEORETICAL VALUES OF RESOLUTION

Emulsion thickness	Specimen thickness	Gap	Resolution
2μ	2μ	0	2.1μ
2μ	2μ	0.5μ	3.4μ
5μ	5μ	0	5.1μ
5μ	5μ	0.5μ	6.4μ
5μ	2μ	0	3.3μ
5μ	2μ	0.5μ	5.0μ
20μ	5μ	0	9.3μ
20μ	5μ	4μ	20.6μ

* Lamerton & Harriss (52).

As emphasized by Lamerton & Harriss (52), the recognition and resolution of radioautographs is affected by the contrast between the grain density over the structure of interest and the grain density in the surrounding emulsion. This consideration imposes limitations on the ratio of isotope concentration in structures to concentration in the surrounding medium which must obtain to make recognition possible. For the grain density over a 5μ radius object to be double that of the surrounding area, this ratio was estimated to be 10 for P^{32} and 4 for S^{35} when both specimen and emulsion are 5μ thick. In this instance also, the range of the β-particle in the emulsion and its rate of energy loss is seen to exert an influence.

SUMMARY

The authors have attempted to discuss the fundamental problems associated with the proper application of the radioautographic technique. The method has been utilized in a wide variety of scientific investigations. There is a necessity for strict control over all phases of the handling of the emulsion and preparation of the specimen in order to obtain good results and correct interpretation.

LITERATURE CITED

1. Becquerel, H., *Compt. rend.*, **122,** 1086 (1896)
2. Reinganum, M., *Z. Physik*, **12,** 1076 (1911)
3. Shapiro, M. M., *Revs. Mod. Phys.*, **13,** 58 (1941)
4. Webb, J. H., *Phys. Rev.*, **74,** 511 (1948)
5. Yagoda, H., *Radioactive Measurements with Nuclear Emulsions* (John Wiley and Sons, Inc., New York, N. Y., 356 pp., 1949)
6. Beiser, A., *Revs. Mod. Phys.*, **24,** 273 (1952)

7. Goldschmidt-Clermont, Y., *Ann. Rev. Nuclear Sci.*, **3**, 141 (1953)
8. Dudley, R. A., and Dobyns, B. M., *Science*, **109**, 327 (1949)
9. Comar, C. L., Visek, W. J., Lotz, W. E., and Rust, J. H., *Am. J. Anat.*, **92**, 361 (1953)
10. Arnold, J. S., and Jee, W. S. S., *Stain Technol.*, **29**, 225 (1954)
11. King, D. T., Harris, J. E., and Tkaczyk, S., *Nature*, **167**, 273 (1951)
12. Woodruff, L. A., and Norris, W. P., *Stain Technol.*, **30**, 179 (1955)
13. Mees, C. E. K., *The Theory of the Photographic Process* (The MacMillan Co., New York, N. Y., 1133 pp., 1954)
14. Demers, P., *Can. J. Phys.*, **32**, 538 (1954)
15. Gurney, R. W., and Mott, N. F., *Proc. Roy. Soc.* (*London*), [A] 164, 151 (1938)
16. Mitchell, J. W., *Science et ind. phot.*, **19**, 361 (1948)
17. Mitchell, J. W., *Phil. Mag.*, **40**, 249 (1949)
18. Mitchell, J. W., *Phil. Mag.*, **40**, 667 (1949)
19. Webb, J. H., *J. Opt. Soc. Amer.*, **40**, 3 (1950)
20. Beiser, A., *Phys. Rev.*, **80**, 112 (1950)
21. Hoerlin, H., and Hamm, F. A., *J. Appl. Phys.*, **24**, 1514 (1953)
22. James, T. H., and Higgins, G. C., *Fundamentals of Photographic Theory*, (John Wiley and Sons, Inc., New York, N. Y., 286 pp., 1948)
23. Mayr, G., Bruner, H., and Brucer, M., *Nucleonics*, **11**, (10), 21 (1953)
24. Livingston, M. S., and Bethe, H. A., *Revs. Mod. Phys.*, **9**, 245 (1937)
25. Smith, J. H., *Phys. Rev.*, **71**, 32 (1947)
26. Herz, R. H., *Nucleonics*, 9 (3), 24 (1951)
27. Bogaardt, M., "Calculation of Range/Energy Relations Especially in Photographic Emulsions," *Joint Establishment for Nuclear Energy Research, No.* 6 (Kjeller per Lillestrøm, Norway, 1953)
28. Cork, J. M., *Radioactivity and Nuclear Physics*, 149 (D. Van Nostrand Co., Inc., New York, N.Y., 415 pp., 1950)
29. Ross, M. A. S., and Zajac, B., *Nature*, **162**, 923 (1948)
30. Zajac, B., and Ross, M. A. S., *Nature*, **164**, 311 (1949)
31. Herz, R. H., *Phys. Rev.*, **75**, 478 (1949)
32. Glendenin, L. E., *Nucleonics*, **2** (1), 12 (1948)
33. Steigert, F. E., Toops, E. C., and Sampson, M. B., *Phys. Rev.*, **83**, 474 (1951)
34. Rotblat, J., *Nature*, **167**, 550 (1951)
35. Catala, J., and Gibson, W. M., *Nature*, **167**, 551 (1951)
36. Lattes, C. M. G., Fowler, P. H., and Cuer, P., *Nature*, **159**, 301 (1947)
37. Lattes, C. M. G., Fowler, P. H., and Cuer, P., *Proc. Phys. Soc.* (*London*), **59**, 883 (1947)
38. Yamakawa, K. A., *Phys. Rev.*, **82**, 522 (1951)
39. Van Heerden, P. J., *The Crystal Counter, A New Instrument in Nuclear Physics* (Utrecht thesis), *N. V. Noord-Hollandsche Uitgevers Maatschappij* (Amsterdam, Holland, 1945)
40. Webb, J. H., *J. Opt. Soc. Amer.*, **38**, 312 (1948)
41. Hoerlin, H., *J. Opt. Soc. Amer.*, **39**, 891 (1949)
42. Fowler, P. H., and Perkins, D. H., *Fundamental Mechanisms of Photographic Sensitivity*, 340 (Butterworths Scientific Publications, London, England, 345 pp., 1951)
43. Della Corte, M., Ramat, M., and Ronchi, L., Jr., *Nuovo cimento*, **10**, 509 (1953)
44. Della Corte, M., Ramat, M., and Ronchi, L., Jr., *Nuovo cimento*, **10**, 958 (1953)
45. Della Corte, M., *Nuovo cimento*, **12**, 28 (1954)

46. Dollmann, E. M., *Rev. Sci. Instr.*, **21,** 118 (1950)
47. Lord, J. J., *Phys. Rev.*, **81,** 901 (1951)
48. Dilworth, C. C., *Cosmic Radiation,* 157 (Butterworths Scientific Publications, London, England, 189 pp., 1949)
49. Cobb, J., and Solomon, A. K., *Rev. Sci. Instr.*, **19,** 441 (1948)
50. Berriman, R. W., Herz, R. H., and Stevens, G. W. W., *Brit. J. Radiol.*, **23,** 472 (1950)
51. Dudley, R. A., *Nucleonics*, **12** (5), 24 (1954)
52. Lamerton, L. F., and Harriss, E. B., *Journal of Phot. Sci.*, **2,** 135 (1954)
53. Wainwright, W. W., Anderson, E. C., Hammer, P. C., and Lehman, C. A., *Nucleonics*, **12** (1), 19 (1954)
54. Bell, G. E., *Brit. J. Radiol.*, **9,** 578 (1936)
55. Bell, G. E., *Brit. J. Radiol.*, **9,** 688 (1936)
56. Beiser, A., *Phys. Rev.*, **81,** 153 (1951)
57. Demers, P., Lapalme, J., and Thouvenin, J., *Can. J. Phys.*, **31,** 295 (1953)
58. Andresen, N., Chapman-Andresen, C., Holter, H., and Robinson, C. V., *Compt. rend. trav. lab. Carlsberg, Sér. chim.*, **28,** 499 (1953)
59. McLaughlin, W. L., and Ehrlich, M., *Nucleonics*, **12** (10), 34 (1954)
60. Albouy, G., and Faraggi, H., *Fundamental Mechanisms of Photographic Sensitivity,* 290 (Butterworths Scientific Publications, London, England, 345 pp., 1951)
61. Albouy, G., and Faraggi, H., *J. phys. rad.*, **10,** 105 (1949)
62. Mather, K. B., *Phys. Rev.*, **76,** 486 (1949)
63. Yagoda, H., and Kaplan, N., *Phys. Rev.*, **73,** 634 (1948)
64. Wiener, M., and Yagoda, H., *Rev. Sci. Instr.* ,**21,** 39 (1950)
65. Churchill, J. R., *Trans. Electrochem. Soc.*, **76,** 341 (1939)
66. Strong, W. W., *Phys. Rev.*, **29,** 170 (1909)
67. Ansheles, J. M., *Univ. Boubonov, Ser. 10, No. 3,* **2,** 1 (1936)
68. Boyd, G. A., and Board, F. A., *Science*, **110,** 586 (1949)
69. Board, F. A., *J. Cellular Comp. Physiol.*, **38,** 377 (1951)
70. Everett, N. B., and Simmons, B. S., *Anat. Record*, **117,** 25 (1953)
71. Doniach, I., and Pelc, S. R., *Brit. J. Radiol.*, **23,** 184 (1950)
72. Bourne, G. H., *Biol. Revs. Cambridge Phil. Soc.*, **27,** 108 (1952)
73. Boyd, G. A., and Williams, A. I., *Proc. Soc. Exptl. Biol. Med.*, **69,** 225 (1948)
74. Odeblad, E., *Acta Radiol.*, **39,** 192 (1953)
75. Bartell, L. S., and Brockway, L. O., *J. Appl. Phys.*, **24,** 656 (1953)
76. Odeblad, E., *Acta Radiol., Suppl. 93* (1952)
77. Blundell, M., and Rotblat, J., *Nature*, **167,** 645 (1951)
78. Eidinoff, M. L., Fitzgerald, P. J., Simmel, E. B., and Knoll, J. E., *Proc. Soc. Exptl. Biol. Med.*, **77,** 225 (1951)
79. MacDonald, A. M., Cobb, J., Solomon, A. K., and Steinbreg, D., *Proc. Soc. Exptl. Biol. Med.*, **72,** 117 (1949)
80. Gomberg, H. J., *Nucleonics*, 9 (4), 28 (1951)
81. Holt, M., and Warren, S., *Proc. Soc. Exptl. Biol. Med.*, **73,** 545 (1950)
82. Chapman-Andresen, C., *Compt. Rend. trav. lab. Carlsberg, Sér. chim.*, **28,** 529 (1953)
83. Williams, A. I., *Nucleonics*, **8** (6), 10 (1951)
84. Evans, T. C., *Proc. Soc. Exptl. Biol. Med.*, **64,** 313 (1947)
85. Witten, V. H., and Holmstrom, V., *Lab. Invest.* **2,** 368 (1953)
86. Asboe-Hansen, G., *Cancer Research*, **13,** 587 (1953)

87. Russell, R. S., Sanders, F. K., and Bishop, O. N., *Nature*, **163**, 639 (1949)
88. Taylor, J. H., and Taylor, S. H., *J. Heredity*, **44**, 129 (1953)
89. Leblond, C. P., Stevens, C. E., and Bogoroch, R., *Science*, **108**, 531 (1948)
90. Fitzgerald, P. J., Simmel, E. B., Weinstein, J., and Martin, C., *Lab. Invest.*, **2**, 181 (1953)
91. Gross, J., Bogoroch, R., Nadler, N. J., and Leblond, C. P., *Am. J. Roentgenol. Radium Therapy*, **65**, 420 (1951)
92. Buie, D. H., Hoecker, F., and Roofe, P., *Proc. Soc. Exptl. Biol. Med.*, **75**, 747 (1950)
93. Evans, T. C., and McGinn, W. E., Jr., *Cancer Research*, **13**, 661 (1953)
94. Endicott, K. M., and Yagoda, H., *Proc. Soc. Exptl. Biol. Med.*, **64**, 170 (1947)
95. Bélanger, L. F., and Leblond, C. P., *Endocrinology*, **39**, 8 (1946)
96. Bélanger, L. F., *Anat. Record*, **107**, 149 (1950)
97. Arnold, J. S., *Proc. Soc. Exptl. Biol. Med.*, **85**, 113 (1954)
98. Pelc, S. R., and Howard, A., *Brit. Med. Bull.*, **8**, 132 (1951–1952)
99. Lotz, W. E., and Johnston, P. M., *Nucleonics*, **11**, (3) 54 (1953)
100. Stieff, L. R., and Stern, T. W., *Am. Mineralogist*, **37**, 184 (1952)
101. Levi, H., *Exptl. Cell Research*, **7**, 44 (1954)
102. Towe, G. C., Gomberg, H. J., and Freeman, J. W., *Nat. Advisory Comm. Aeronaut., Tech. Note 3209* (July, 1954)
103. Ray, R. C., and Stevens, G. W. W., *Brit. J. Radiol.*, **26**, 362 (1953)
104. Howard, A., and Pelc, S. R., *Brit. J. Radiol.*, **23**, 634 (1950)
105. Stiller, B., Shapiro, M. M., and O'Dell, F. W., *Rev. Sci. Instr.*, **25**, 340 (1954)
106. Horan, J. R., *Phys. Rev.*, **90**, 717 (1953)
107. Coates, A. C., *Fundamental Mechanisms of Photographic Sensitivity*, 320 (Butterworths Scientific Publications, London, England, 345 pp., 1951)
108. Beiser, A., *Rev. Sci. Instr.*, **23**, 500 (1952)
109. Berriman, R. W., *Fundamental Mechanisms of Photographic Sensitivity*, 272 (Butterworths Scientific Publications, London, England, 345 pp., 1951)
110. Nutting, P. G., *Phil. Mag.*, **26**, 423 (1913)
111. Boyd, G. A., and Levi, H., *Science*, **111**, 58 (1950)
112. Miller, B. L., and Hoecker, F., *Nucleonics*, **8** (5), 44 (1951)
113. Kinersly, T., *Yale J. Biol. Med.*, **27**, 114 (1954)
114. Hoecker, F., and Roofe, P., *Radiology*, **52**, 856 (1949)
115. Levi, H., *Biochim. et Biophys. Acta*, **7**, 198 (1951)
116. Dudley, R. A., and Pelc, S. R., *Nature*, **172**, 992 (1953)
117. Stevens, G. W. W., *Brit. J. Radiol.*, **23**, 723 (1950)
118. Doniach, I., Howard, A., and Pelc, S. R., *Progr. Biophys. and Biophys. Chem.*, **3**, 1 (1953)
119. Boyd, G. A., *J. Biol. Phot. Assoc.*, **16**, 65 (1947)
120. Chapman-Andresen, C., *Exptl. Cell Research*, **4**, 239 (1953)

CELLULAR RADIOBIOLOGY[1,2]

By Robert K. Mortimer and Carl A. Beam

Donner Laboratory, University of California, Berkeley, California

The preceding review article in this series by Sparrow & Forro (334) includes literature up to the end of 1952. The present report is primarily concerned with literature that has appeared in the succeeding two-year period, with emphasis on the presentation of an organized survey rather than on a critical analysis of this literature. The extreme diversity of interests that fall under the above title, as a result of the wide range of effects studied and of organisms and radiations employed, has made organization difficult and in addition has necessitated somewhat arbitrary limits to choice of material. Studies on radiation chemistry and the effects of radiation on macromolecules of biological interest, and—at the other end of the scale—histological manifestations and detailed genetic consequences of radiation damage, have been excluded, even though closely allied in some cases to studies on cellular radiobiology. These subjects are treated in a number of recent reviews (23, 42, 70, 330).

The material has been organized firstly according to the type of radiobiological effect studied, and secondly into subcategories, where possible, according to the type of modifier employed. This system has served indirectly to separate many of the articles in terms of the general class of organism or radiation used.

Recent literature surveys which overlap and in addition supplement some sections of this review are those of Spiegelman & Landman (337) and Zelle (397) on genetics of microorganisms, and Dubois & Petersen (89) on biochemical effects of radiation.

Extensive discussions of practically all aspects of radiation biology are included in a number of books that have appeared recently. The book of Bacq & Alexander (15) provides a coherent account of the present status of research and ideas in radiation chemistry, cellular radiobiology, and vertebrate radiobiology. Dessauer's recent book (80) on "Quantenbiologie," intended as an introductory survey, is also of additional interest because of the fundamental approach to a number of basic radiobiological problems. A revised version of Lea's classic, *Actions of Radiations on Living Cells*, has recently become available (217). Rajewsky (298) presents in a well-organized and easily accessible form a wealth of information, primarily on vertebrate radiobiology. Spear (336) gives a very readable introductory account of

[1] The survey of the literature pertaining to this review was completed in December, 1954.

[2] The following abbreviations are used: DNA for desoxyribonucleic acid; RNA for ribonucleic acid; ATP for adenosine triphosphate; LET for linear energy transfer; RBE for relative biological effectiveness.

many aspects of radiation biology in his recent book *Radiations and Living Cells.*

The first volume of *Radiation Biology* (160), edited by Hollaender, contains a valuable collection of articles written by outstanding scientists representing the major avenues of research in this rapidly expanding field. The proceedings of a number of recent symposia and conferences, of interest to cellular radiobiology, have appeared during the last two years (16, 73, 252). Many of the individual articles from these sources are discussed below. Other recent reviews and critical discussions of general interest to this field are those of Errera (104), Gray (132 to 135), Koller (199), and Stone *et al.* (350). A number of more specific reviews and discussions are considered in the appropriate context.

LETHAL AND MUTAGENIC EFFECTS

The lethal and mutagenic effects of radiation on cells occupy the end position of a chain of chemical and biological disturbances which follow the initial event of energy dissipation. The possible length and complexity of the chain is evidenced below by the diversity of modifiers influencing the end result and by the variety of radiobiological effects that have been proposed to occupy intermediate positions.

Most of the studies to be considered in this section have been performed on microorganisms. Because of the similarity of experimental approach, the many experiments on viruses are considered under the appropriate subheadings along with those on units more clearly cellular. A number of theoretical and general discussions applicable to interpretation of the lethal and mutagenic effects of radiation have appeared recently (34, 78, 140, 165, 235, 329, 367).

General

Many studies have been concerned primarily with determination of the mean lethal dose and target size and shape of irradiated microorganisms and viruses. Goldblith *et al.* (127) have measured the mean lethal γ-ray dose for eleven strains of bacteria. Values obtained ranged from 5,100 r.e.p. for *Pseudomonas* to 53,000 r.e.p. for *Streptococcus.*

Pollard (292) in his recent book on viruses discusses the application of radiation studies to the determination of the size and shape of radiation-sensitive structures within these particles, and a number of recent publications from his group have been directed towards this goal (75, 76, 113, 293, 294, 384). Friedman (113) has assayed x-ray and deuteron-inactivated M-5 phage on three strains of the host, *Bacillus megatherium*, and finds for all three the same degree of phage inactivation. The inactivation cross section for deuterons of 10^{-11} cm.^{2} compares favorably with the electron micrograph cross section of 3.7×10^{-11} cm.^{2}. The cross section for deuteron inactivation of the infective properties of Newcastle's Disease Virus was found to agree quite well with the dimensions of the complete virus obtained from

electron micrographs (384). Davis (76) finds that for inactivation of phage T-1 by electrons, a minimum energy of about 600 electron volts is necessary. She concludes from these findings that highly sensitive genic material is located within the head of the virus and is surrounded by a protecting protein coat about 100 A thick. Similar experiments on bacterial spores have been performed, from which aspects of intracellular morphology are inferred (75). Dimensions of the sensitive region of the serum-blocking antigen of T-1 bacteriophage have been derived from electron, deuteron, and α-particle inactivation studies (293).

Epstein (99) finds a close correlation between radiation-sensitive volume and measured nucleic acid volume for a number of phages. The loss of lysogenicity in phage λ (and acquisition of virulence) was found to be associated with a significant decrease in sensitive volume (100); λ, sensitive or virulent, has about one-third the sensitive volume and nucleic acid volume of its counterpart in size, T-2. Bachofer (9) finds the sensitive volume of dried T-1 bacteriophage to depend both on temperature during irradiation and on the method of drying. About a sevenfold variation in target volume could be obtained by varying the conditions of the experiment. These findings should be of considerable importance in target theory interpretations of direct effects of ionizing radiations.

The inactivation of *Amoeba proteus* by incorporated P^{32} has been studied by Friedrich-Freksa & Kaudewitz (114) as a function of the number of generations after decay of the radioisotope. Maxima in per cent lethals per generation were observed at the fifth and at the thirty-first generations. The first maximum, representing an expression of radiobiological damage, corresponded to that observed after external P^{32}-irradiation. The second maximum however, was interpreted in terms of the inactivation of subgenic units by $P^{32} \rightarrow S^{32}$ transmutations. Stent (348) and Castognoli & Graziosi (63) have measured the rate of inactivation of P^{32}-labeled phage as a function of time after incorporation. Stent computes, on the basis of transmutation inactivation, that only 1 in 13 such decays is effective.

A number of studies have appeared recently in which the induction of lethality has been compared quantitatively with induction of other radiobiological effects. Berrie (32) has found that, while lower incubation temperatures decreased ultraviolet-induced mutation frequency in *Escherichia coli*, an increased lethality was expressed under the same conditions. These results were considered to oppose the causative association of ultraviolet-induced mutations with lethality. Exposures of ultraviolet and diepoxybutane producing comparable decreases in viability were shown by Kölmark (200) to have markedly different effects on reversion rates at two biochemical loci in *Neurospora*. Markert (239) has found pigmented fungus spores to be resistant, by virtue of the filtering action of the pigment, to both lethal and mutagenic actions of ultraviolet light. X-ray-inactivated bacteria were shown to be capable of supporting the growth of phage (110, 204). Kaplan (179) found that the lethal and mutagenic effects of ultraviolet on *Bacterium*

prodigiosum were differentially affected by changes in the gaseous atmosphere during or after irradiation. Whereas anaeribiosis had no influence on lethality, mutation frequency was in some cases depressed. Formation of adaptive enzymes was little influenced by x-ray inactivation of yeast (22) and *E. coli* (393). Ultraviolet and nitrogen mustard, however, decreased both survival and ability to form adaptive enzyme (22, 180). The luminous output of cells of *Achromobacter fischerii* was less affected by x-radiation than was their ability to develop into colonies (154). Loss of motility of *Tetrahymena* was less affected by ultraviolet radiation than was viability (243).

Physical Modifiers

Dose rate, dose fractionation.—Eckart (92) has reported that increasing the intensity decreases the efficiency of ultraviolet for inactivation of T-1 phage. He considers this as evidence against the applicability of the target theory in this case.

A series of related studies have appeared recently in which the relative effectiveness of ultrafractionated and continuous x-ray and electron irradiations is considered (86, 186, 187, 265). For inactivation of *E. coli* (85), ultrafractionated electrons (590 impulses/sec.) were found to be less effective than continuous irradiation; there was no effect of ultrafractionation of x-radiation. Ultrafractionated electrons were found to be less effective, while ultrafractionated x-rays were more effective, for inactivation of *Drosophila* eggs (165).

Inactivation of *Neurospora* conidia by fast neutrons from an atomic test explosion was found to proceed at approximately the same rate as with cyclotron-generated neutrons, indicating no apparent effects of the extremely high dose rates ($\sim 10^{10}$ r.e.p./sec.) obtainable from test explosions (5a).

Linear energy transfer.—The relative effectiveness (RBE) of ionizing radiations of different types, origins, or energies has been the subject of many recent studies. As will be shown, the RBE of different radiations depends not only on their linear energy transfer (LET), but also on factors related to the biological systems studied. Recent reviews devoted to this subject are those of Zirkle (399), Boag (45), and Gray (132, 133, 134).

Lindenmann (222, 223) finds 180-kev x-rays and 31-Mev electrons equally effective for inactivation of *E. coli*. Similar results were obtained by Goldblith *et al.* (128) for inactivation of *Bacillus thermoacidurans* and *E. coli* with x-rays, γ-rays, and 3-Mev cathode rays. Ting, Chinn & Johns (365) find 23.5-Mev x-rays about 75 per cent as effective as 200-kev x-rays for inactivation of four different strains of yeast. The kinetics of inactivation, though different for the different strains of yeast, were similar for the two energies of x-rays. Moos (255) has studied the inactivation of *E. coli B* and *Pseudomonas aeruginosa* with 4-, 39-, and 186-kev and 2-Mev x-rays all delivered at approximately the same dose rate. The lower energy photons were found to be more effective.

Langendorff *et al.* (211) in a comparative study of the lethal effect of x-rays and α-particles on *E. coli* find the more densely ionizing α-particles to be less effective. The RBE,[2] however, depended upon pre- or posttreatment of the cells with heat. Houtermans (167) has shown the relative effectiveness of x-rays and alpha particles for inactivation of *E. coli* to depend on the temperature and phase state of the cellular environment during irradiation. Elkind & Beam (98) found that in yeast the relative effectiveness of these two radiations varied with changes in physiological state and stage of cell division. Interdivisional cells in log phase were more sensitive to x-rays than to α-particles, whereas log phase cells in the process of division, or starved cells, were less sensitive to x-rays. These above studies emphasize the necessity of biological as well as physicochemical interpretations of the relative effectiveness of various radiations.

Tahmisian & Vogel (356) have studied the relative effectiveness of x-rays, γ-rays, and neutrons for destruction of grasshopper eggs. The RBE values of the three radiations were 1.2, 1.0, and 19 respectively. Inactivation of *Neurospora* conidia by fast neutrons, x-rays, and γ-rays has been studied by Atwood & Mukai (5a). A relative effectiveness of 1.5 to 2.0 was found for neutrons compared to x- and γ-radiation. No significant difference was demonstrated in efficiency of production of recessive lethals by the different radiations.

Zirkle & Tobias (401) have determined RBE values of x-rays, deuterons, and α-particles (LET[2] range: 0.73 kev/μ to 190 kev/μ) for inactivation of haploid and diploid yeast and *Stichococcus*. For both haploid and diploid yeast, RBE values changed only slightly for LET values from 0.73 to 30 kev/μ. At the higher linear energy transfer of the polonium α-particles, the RBE increased to a value of about 3 to 5. *Stichococcus* was increasingly susceptible to more densely ionizing radiations over the complete range studied; an RBE value of 11 was obtained for polonium α-particles. Sayeg (319) has extended these studies into regions of still higher linear energy transfer, using in addition to the above radiations a beam of six-times-ionized carbon atoms. He found a similar rise in RBE for inactivation of haploid yeast up to LET values corresponding to polonium α-particles, but at the higher LET values of carbon nuclei the RBE decreased to a value near unity.

Wave length.—Morowitz (256) has found the ultraviolet action spectra for lethal and mutagenic effects in *Bacillus subtilus* spores to correspond approximately to the ultraviolet absorption of the cells; both showed maxima at about 2,700 Å. Franklin (110) has measured the induction of lysis and inactivation in *E. coli* K12 by ultraviolet radiation of different wave lengths. The action spectrum for induction showed a single maximum at 2,650 Å, while the spectrum for cellular inactivation suggested two maxima at 2,650 Å and 2,800 Å. Similar results were observed for inactivation of M-5 bacteriophage (111). These results indicate that induction can be effected by absorption of energy in nucleic acid components, while inactivation results from absorption in either nucleic acid or protein.

The efficiency of inactivation of phages T-1 and T-2 by different wave lengths of ultraviolet has been determined by Zelle & Hollaender (398): A single peak in efficiency at 2,650 Å was found for both organisms when dose was expressed as incident energy. Quantum yields (dose expressed as absorbed quanta), however, were nearly independent of wave length. Less than one absorbed photon in a thousand was effective in causing inactivation. That "quantum yields are likely related inversely to chemical and biological complexity" was evidenced by the lower quantum yields obtained for the more complex phage T-2.

The action spectra for a number of ultraviolet effects in the ciliate *Blepharisma* have been presented by Hirshfield & Giese (158). A composite of nucleic acid and protein absorption best fit the action spectrum obtained for lethality. Giese (119) in his recent review on photobiology has compiled and discussed the action spectra for a number of ultraviolet effects on protozoans.

Environmental Modifiers

Temperature, phase, pressure.—Bachofer *et al.* (9, 13) have studied direct x-ray inactivation of dried T-1 bacteriophage over the temperature range 77°K. to 310°K. The inactivation cross section could be expressed by two terms: the first temperature-independent, the second temperature-dependent and corresponding to an activation energy of 1,100 calories.

The influence of both temperature and phase state on the survival of x-irradiated yeast (389, 390) and T-2 phage (391) has been studied extensively by Wood. An approximately twofold increase in sensitivity, associated with phase change from solid to liquid, was observed for both biological systems. In yeast, the lower sensitivity in solid phase probably results from an immobilization of toxic materials present within the cell, whereas in phage the poisons immobilized are more likely in the surrounding medium. This is evidenced by the lack of additivity of broth protection and freezing protection against x-ray inactivation of phage. In the liquid phase, sensitivities changed only slightly with temperature up to 40°C. In the temperature region 45°C. to 55°C., the x-ray sensitivity of yeast increased rapidly, indicating a synergism between heat and x-ray inactivation. The synergism was also effective when heat treatment (52.5°C.) was applied immediately before or after irradiation.

Houtermans (167) has studied the influence of temperature (−196°C. to 40°C.) and phase state on the sensitivity of *E. coli* to x-rays and α-particles. The α-particle sensitivity of the cells in solid phase was constant, and one-half that expressed in liquid phase. X-ray sensitivity, however, was found to increase about threefold when temperature was increased from −196°C. to 0°C.; sensitivities at 0°C. solid and 0°C. liquid were equal. The change in sensitivity to α-particles associated with the phase change is correlated with a similar change in production of H_2O_2, and is consistent with the possible involvement of this compound as an intermediate in α-particle inactivation

of cells. The different results obtained with x-rays indicate a basically different mechanism of action of this radiation.

The rate of inactivation of bacteriophage by decay of incorporated P^{32} has been shown to be reduced at lower temperatures (63, 348).

Burns (57) has measured the x-ray sensitivity of yeast as a function of hydrostatic pressure during irradiation; no change in radiosensitivity was observed for pressures as high as 10,000 p.s.in. These results were considered as evidence against the association of large molecular volume changes with the production of the primary lesion.

Anoxia.—The oxygen concentration during irradiation is generally considered to influence radiobiological effects at the chemical level, altering the yield and types of active radicals produced. Recent discussions of the oxygen effect have been presented by Gray (135). Stone *et al.* (350), and Lacassagne (206). Lower oxygen concentrations during irradiation nearly always result in reduced radiobiological damage. The literature of the last two years contains several exceptions to this generalization.

Oxygen protection of phage against indirect inactivation by x-rays has been reported by Bachofer & Pottinger (12) and Ebert & Alper (91). The presence of salts in the suspending medium (12) or high pH (4) reduced the protection afforded by oxygen. Experiments employing various combinations of hydrogen, nitrogen, and oxygen showed conclusively that H_2O_2 was not causatively related to phage inactivation (91). The results best fit the hypothesis that inactivation was mediated by reducing rather than oxidizing reactions. Phage that had survived irradiation was found to be more sensitive than unirradiated phage to H_2O_2 and ascorbic acid inactivation. The oxygen concentration during irradiation influenced this effect [Alper (2, 3)].

The genetic effects of x-radiation on *Paramecium* were found by Kimball and Gaither (192) to be decreased under anaerobic conditions. Cell survival and division delay, considered to be nongenetic effects, showed no corresponding decrease. Tahmisian *et al.* (357) find that x-ray induction of size regression in developing grasshopper embryos is reduced tenfold when irradiation is administered in the absence of oxygen. No significant anaerobic protection was observed for neutron inactivation of *Neurospora* (5a).

Graevskii & Ochinskaya (130) report an effective dose reduction of 2.3 and 2.6 respectively for γ- and x-irradiation of *E. coli* in vacuum compared to air. No dose reduction was found for β-irradiation under anaerobic conditions. Birge & Tobias (41) find a twofold dose reduction for x-ray inactivation of haploid yeast under anaerobic conditions. Aerobically and anaerobically grown cells exhibited the same degree of protection and the same kinetics of inactivation. Nybom (276) reports a protection of *Chlamydomonas* against x-ray inactivation by removal of oxygen during irradiation.

Chemical modifiers.—The occurrence of chemical processes following the initial event of energy absorption permits modification by chemical means of the final expression of biological damage. The role of various chemical

modifiers, notably those which reduce the extent of biological damage by competition for active radicals, has been considered in a number of recent reviews and critical discussions (23, 34, 215, 282).

Bachofer *et al.* (10, 11, 12) have reported various degrees of protection against x-ray inactivation of T-1 phage by the presence in the aqueous suspension, during irradiation, of a number of inorganic salts. Many of these (i.e., NO_2^-, CN^-, SO_4^{--}) were considered as reducing agents acting against radiation-produced toxins. High concentrations of ammonium ion were considered to protect by dehydration of the phage particles. A number of metallic salts were found to influence the sensitivity of *Micrococcus pyogenes* to cathode rays (90). Cadmium, cobalt, and nickel chlorides enhanced the effectiveness of the radiation, while lithium, iron, and calcium chlorides afforded protection. Acetonitrile was found to reduce the effects of both ultraviolet radiation and the radiomimetic agent triethylenemelamine on bacteria (326).

Mittler & Laverty (253) have determined the ultraviolet sensitivity of two closely related strains of bacteria, one of which lacked catalase. About twice the dose was required to produce the same degree of inactivation in the catalase-positive as in the catalase-negative strain. The respiratory enzyme poison sodium azide was found to increase both the spontaneous and induced rates of mutation in a number of microorganisms (31, 138), possibly through an inhibition of catalase activity in these cells. Lethality, however, was decreased by the same agent, possibly indicating different mechanisms in mutagenesis and inactivation by ultraviolet. The metabolic inhibitor iodoacetate decreased the extent of ultraviolet inactivation of *Streptomyces* spores (374).

Biagini (35, 36, 37) has made an extensive study of x-ray inactivation and cysteine protection in *E. coli*. X-rays were equally effective upon dried bacteria, dense aqueous suspensions of bacteria (10^{-1} gm./ml.), or broth suspensions of all dilutions. Under these conditions, for which inactivation is presumably direct, cysteine afforded no protection. As the density of aqueous suspensions was decreased to about 10^{-4} gm./ml. the effectiveness of the radiation increased about tenfold, as a result of the increasing importance of indirect effects; the protection afforded by cysteine correspondingly increased to 2. Further reduction of cell density left effectiveness and degree of protection by cysteine unaltered, signifying that the extent of indirect damage for a given number of active radicals had maximized.

A number of protective agents have been found to be effective against x-ray inactivation of *Chlamydomonas* (276). Glutathione was reported to protect completely against the effects observed after exposure of *Paramecium* to irradiated solutions (71, 72).

Postirradiation Modifiers

The modification of radiobiological effects by treatments applied after the beginning of irradiation has received considerable attention in recent

years. It is possible to reactivate otherwise inactivated cells by a number of postirradiation treatments, i.e., exposure to visible light, incubation with certain enzymes or metabolites, and incubation at selected temperatures. Recent surveys pertaining to reactivation of radiation-inactivated cells are those of Latarjet (215, 216), Hollaender & Stapleton (162), Stein & Harm (347), and Bowen (50). A number of articles pertinent to this subject were presented at the Symposium on the Chemistry of Biological After-Effects of Ultraviolet and Ionizing Radiations (252).

Chemical reactivation.—Latarjet and co-workers (215, 216, 251, 360) have investigated the action of the enzyme catalase in restoration of ultraviolet-inactivated bacterial cells. The ability of the cells to be restored decreases with time after irradiation and disappears around the fourth hour. Catalase restoration was possible only in lysogenic strains of bacteria (215, 216, 360). Susceptibilities to catalase restoration and photorestoration in different strains of bacteria appear to occur in a complementary fashion (360). The enzyme peroxidase is also effective in restoration. Alcohol in the medium increases the extent of catalase restoration. It is proposed (215) that these enzymes exert their restorative effect primarily through the initiation of coupled oxidations between certain organic substrates (i.e., alcohol) and organic peroxides formed within the cell, thus diverting these agents from the production of the radio-lesion. Catalase restoration is not observed after roentgen irradiation.

Heinmets *et al.* (145, 146, 147) report reactivation of ultraviolet-inactivated *E. coli* by incubation, after irradiation, with a number of metabolites. Reactivation is most effectively attained at 37°C. and with metabolites belonging to the citric acid cycle. Since this effect could be obtained only for incubation in solution, these experiments do not differentiate clearly between cellular recovery and multiplication. The latter possibility might account for some of the observed increase in viable count.

Temperature reactivation.—A number of recent studies have demonstrated a marked influence of postirradiation temperature on survival and mutation frequency of both x-ray and ultraviolet-irradiated bacterial cells.

Harm & Stein (143, 144, 347) have made an extensive study of the influence of incubation temperature (10°C. to 44.5°C.) on the survival of three strains of *E. coli*. Cells were exposed directly to ultraviolet, exposed to ultraviolet-irradiated medium or peroxide, or placed on unirradiated medium. A similar dependence of survival on incubation temperature was found for cells treated in these three ways. In view of the previously established similarity of inactivation by irradiated medium to that by peroxide, this correspondence in temperature dependence of "direct" and "indirect" inactivation was considered to signify that a large portion of the inactivation by ultraviolet was through the production of cellular poisons. At 44.5°C., at which optimum reactivation is obtained, the survivals of strains B andB/r were identical. A histidineless mutant of *E. coli* showed a much different temperature recovery curve, with an optimum range below 30°C. Photoreac-

tivation and temperature reactivation appeared to act almost independently.

Berrie (32) has studied the influence of postirradiation temperature treatments on survival and mutation of ultraviolet-irradiated *E. coli*. Treatment at 15°C. resulted in greater lethality but fewer mutants among the survivors than treatment at 37°C. A similar reduction in mutation at 16°C. compared to 37°C. has been reported by Witkin (383); the reduced-temperature affected the frequency of induced mutants only in the first postirradiation division.

The influence of postirradiation temperature treatment on survival of irradiated cells is not confined to ultraviolet irradiation. Two groups of investigators have reported a marked effect of temperature treatment on damage caused by ionizing radiations. Langendorff *et al.* (210, 211) were able to reactivate x-irradiated *E. coli* by postirradiation treatment of the cells at 44.5°C. Maximum reactivation (1.6×) was obtained with four hours' treatment at this temperature. The same treatment with α-irradiated cells provided about twice the degree of reactivation (3.3×). On the other hand, pretreatment of the cells for one hour at 37°C. doubled the x-ray sensitivity but left the α-particle sensitivity unaltered. Stapleton *et al.* (343) have studied the influence of postirradiation treatments at a number of temperatures, on survival of three strains of x-irradiated *E. coli*. The temperature giving maximum reactivation varied from one strain to another, but with any strain was suboptimal for growth. For strain B/r, the maximum survival was observed at 18°C., the reactivation corresponding to a dose-reduction factor of 1.5. The rate of recovery increased with temperature and was dependent on the presence of a nutrient environment, suggesting the involvement of physiological processes.

The wide variation in temperature dependence of this recovery effect between different strains of bacteria and for different radiations suggests that much of the previous work in which radiation effects have been assayed at only one temperature requires reconsideration. The above studies show that the relative sensitivities of different strains of bacteria, or effectiveness of different radiations, can be completely altered by postirradiation temperature treatments.

Photoreactivation.—A wide range of effects caused by ultraviolet radiation can be reversed by subsequent exposure to visible light. This reactivating effect appears to be much more general and predictable than either temperature or catalase reactivation, and probably acts at a different level or in a different manner. This is illustrated by the recent study by Harm & Stein (144), in which approximately the same extent of photoreactivation was observed for both temperature-reactivated and nontemperature-reactivated *E. coli*.

Recent discussions on photoreactivation are included in the articles by Bowen (50), Errera (104), Stein & Harm (347), Latarjet (215), and Giese (119).

A number of recent reports have confirmed previous findings that photo-

reactivation takes place only when cytoplasmic material is present. Ultraviolet-inactivated phage cannot be reactivated by subsequent exposure to visible light. Illumination of the host bacterium (51, 156, 196, 219) or plant (27) after infection, however, results in an increased number of active phage. Dried phage, inactivated by ultraviolet light, is not photoreactivable, even after infection (155). Ultraviolet effects in *Urechis caupo* sperm were not reduced by subsequent exposure to visible light. However, effects induced in the eggs were photoreactivable (170).

As in catalase and temperature reactivation, the amount of photoreactivation decreases as the time between irradiation and illumination increases; the rate of this process is temperature-dependent (51, 272, 273, 358). Studies on kinetics of the reactions involved in photoreactivation have been presented by Bowen (51) and Nishiwaki (272, 273). That the basic reactions involved in photoreactivation occur very soon after absorption of the ultraviolet energy is evidenced by the effectiveness of visible light in reducing lethality and mutation when applied at the same time as the ultraviolet (148, 149, 185).

The direct-repair hypothesis, as an explanation of the process of photoreactivation, gains support from recent studies in which reactivated organisms were again exposed to ultraviolet. Lennox *et al.* (219) find reactivated phage-bacterium complexes to be inactivated at the same rate as survivors of a smaller dose of ultraviolet. Repeated alternate treatments of *E. coli* with ultraviolet and visible light revealed a similar relationship; a constant fraction of the organisms treated with ultraviolet was reactivated by visible light in each cycle. Similar experiments with *Streptomyces* (290) appear to indicate a differential effect of photoreactivation on lethality and mutation. Spore populations that had survived five cycles of ultraviolet and visible light exposures contained a considerably higher percentage of mutants. The applicability of the dose-reduction principle to photoreactivation is well illustrated in the recent study by Sarachek (314), in which it was shown that the ratio of light dosage to the dark dosage producing the same degree of inactivation was constant over a wide range of doses for four ploidies of yeast. Newcombe & McGregor have applied this principle to explain photoreactivation of induced mutations in *Streptomyces* (268, 270). Exposure of these organisms to ultraviolet or x-rays results in a high yield of induced mutants; the mutation-versus-dose curve rises to a maximum and then decreases with increasing doses. Reactivation of cells that had received a high dose of ultraviolet resulted in an increased mutation frequency, while the opposite was observed for reactivation of cells that had received doses near the maximum of the mutation response curve. The kinetics of photoreactivation in *Neurospora* (275) is consistent with the assumption that reactivation of the conidia is the consequence of reactivation of a single nucleus per conidium.

The state of hydration of T-1 bacteriophage, as affected by drying, freezing, or ethanol treatment, profoundly influences its ultraviolet sensitivity and photoreactivability (155, 156, 157). Berger *et al.* (31) find that the en-

zyme poison sodium azide reduces not only the effectiveness of ultraviolet light on bacteria, but also the degree of reactivation achieved by subsequent visible light exposure.

Up to 800 quanta of blue reactivating light were found to be necessary to give maximum reactivation of the effects produced in *Colpidium* by one quantum of ultraviolet (120). Extensive attempts to demonstrate photoreactivation of ultraviolet-induced damage in the protozoan *Blepharisma undulans* were unsuccessful (158). No photoreactivation could be obtained for photodynamically inactivated bacteriophage (378) or for x-ray effects in *Streptomyces* (270). A relatively small portion (14 per cent) of the lethal effect induced by ultraviolet in the protozoan flagellate *Astasia longa* was removed by exposure to visible light (325).

Inhibition of respiration, growth, and DNA[2] synthesis in ultraviolet-irradiated *E. coli* all were shown to be reversible by subsequent visible light exposure (185). The tendency of ultraviolet-irradiated *E. coli* to form multinucleate snakes also is photoreactivable (105). Posttreatment with visible light has been shown (283) to markedly reduce the yield of phenocopies induced by ultraviolet light in *Drosophila*. Visible light, while decreasing the effects of ultraviolet on *Chlamydomonas*, increases the sensitivity of this organism to x-rays (276).

Weigle (376, 377) has reported the very interesting finding of ultraviolet reactivation of ultraviolet-inactivated bacteriophage. As with photoreactivation, the reactivating ultraviolet exposure was applied to the bacterium, but could be applied before as well as after infection. X-ray- or nitrogen-mustard-treated bacteria were also capable of restoring ultraviolet-inactivated phage. When applied to the infected bacterium, visible-light reactivation and ultraviolet reactivation were additive. Visible light, when applied to ultraviolet-irradiated bacteria before infection, reversed the restoring ability of these bacteria.

Sarachek & Lucke (316) have reported an ultraviolet-induced resistance to x-ray inactivation in *Saccharomyces*, although their results are not in agreement with those reported by Uretz (371) for combined ultraviolet and x-ray exposures in this organism.

Biological Factors Modifying Radiosensitivity

Division stage.—Houtermans (166) has used a synchronously dividing culture of *E. coli* in a study of the dependence of radiosensitivity on division stage. Sensitivities to both α-particles and ultraviolet light were found to vary considerably; the cells were most insensitive just before division and most sensitive just after division. The recent reports (164, 212, 321) on synchronization of division in microorganisms by means of temperature shifts suggests the possibility of further studies of this type.

A much higher resistance to x-ray-induced lethality of dividing than of nondividing yeast cells has been reported by Beam *et al.* (28). Budding cells, which are considered to be mitosis, exhibited a resistance about ten times

that of nonbudding or interphase cells. A similar though smaller increase in resistance to α-particles has been shown to accompany the onset of budding in yeast (98). An increase in resistance to x-radiation correlated with division of a population of yeast cells has been reported by Sarachek (312). The corresponding change in ultraviolet sensitivity was much less marked (313).

The age and degree of starvation of cultures of *E. coli* (168) and yeast (98, 389) have been shown to influence considerably the shapes or slopes of the survival curves.

Differentiation, pigmentation.—A high correlation between pigmentation and resistance to inactivation and mutation by ultraviolet in *Glomerella* was reported by Markert (239); the pigment apparently protects those cells containing it by absorption of a portion of the incident ultraviolet radiation. Resistance of part of the population of irradiated cells to both lethality and mutation was shown to account for the saturation-type mutation-versus-dose curves obtained. Constantin & Latarjet (68) have isolated and subcultured yeast colonies arising from survivors of successive ultraviolet irradiations, and have obtained by this technique three pigmented mutant strains that were much more resistant to ultraviolet inactivation. The higher radioresistance was attributed to a protection of the nucleus afforded by the cytoplasmic pigments. Mutation from pigmented to nonpigmented in the yeast *Rhodotorula* has been studied by Magni *et al.* (238). Successive reculturing of *E. coli* populations that had survived high doses of x-radiation resulted in populations with increased radioresistance (115). This was considered to arise from the production and selection of radioresistant mutants.

The differentiated spindle form of ascites tumor cells was found to be much more radioresistant than the free round-cell form (214).

Ploidy, nuclear number.—Zirkle & Tobias (401) have reported studies on the relative sensitivity to ionizing radiations of haploid and diploid yeast cells. The diploid cells were found to be more resistant at all doses than the haploid cells. The lower sensitivity of the diploid cells was explained in terms of the expected lower susceptibility to recessive lethal inactivation in this ploidy. Similar studies have been reported by Wood (389) for x-ray inactivation of haploid and diploid yeast cells. On the basis of the recessive lethal model proposed by Zirkle & Tobias, the number of radiosensitive sites essential to cell division was found to be 30. Evidence for x-ray-induced recessive lethal mutations in diploid yeast cells that had received a sublethal dose of x-radiation has been presented (258).

Extensions of x-ray inactivation studies to higher-ploidy yeast cells by Lucke & Sarachek (225) and Mortimer (257) have yielded results that are not in complete agreement with the generally proposed increase of radioresistance with increasing ploidy or with expectations of killing by recessive lethal damage alone. A combination of recessive and dominant lethal killing has been proposed (257) as a possible explanation of the results. The haploid cells would be killed mostly by recessive lethals, while in the higher ploidies killing by dominant lethals would become increasingly important. Other

evidence for the production of dominant lethals in yeast has been obtained [Mortimer (In press)]. The percentage viability of diploid zygotes formed by conjugation of pairs of haploid yeast cells was shown to be reduced by irradiation of one of the parent cells before mating.

Magni (236, 237) has determined the shape of the x-ray survival curves of a number of strains of imperfect yeast. This type of study has been proposed as a tool in furthering the systematics of yeast; the combination of an exponential survival curve and lack of sporulation could indicate that the strain under consideration is haploid. The differences in shapes of x-ray survival curves obtained by Ting *et al.* (365) for four strains of yeast might be explained in terms of ploidy differences. That exponential survival curves are not necessarily indicative of the haploid state of the irradiated cells is demonstrated by the recent study of Nybom (276). Haploid *Chlamydomonas* gametes exhibited sigmoid survival curves for both x-ray and ultraviolet irradiation.

Sarachek & Lucke (314, 315) have studied the influence of ploidy on ultraviolet sensitivity of *Saccharomyces* and conclude that "ploidy plays a subordinate role to other genetical strain differences in determining sensitivity to ultraviolet radiations."

A study of the influence of variations in the average nuclear number of *Neurospora* conidia on ultraviolet sensitivity and photoreactivability has been reported by Norman (275). Extrapolation to zero dose of the linear portion of the survival curves yielded intercepts which agreed very closely with the average nuclear number, a result considered as support for the involvement of nuclear damage in inactivation.

EFFECTS ON CELLULAR BIOCHEMISTRY

This topic has been considered extensively in recent publications of Bacq & Alexander (15), Barron (23), and DuBois & Petersen (89). Some of the recent studies dealing with effects at the biochemical level that result from irradiation of cells are considered below.

A number of recent experiments have demonstrated the apparent stability of existing cellular enzyme systems to high doses of radiation. When the rate of oxygen consumption of bacteria, yeast, or barley seeds was measured soon after exposure to lethal doses of ultraviolet (146, 180, 185) or x-radiation (17, 18, 22, 38, 213, 250), little or no effect of the radiation was detected. When measured under conditions of growth, however, oxygen consumption was markedly reduced compared to that of the control (146, 185, 213, 250), indicating an effect on the ability of the irradiated cells to synthesize respiratory enzymes.

Small doses of x-radiation were reported to have a slight stimulatory effect on respiration of grasshopper eggs (137, 357); higher x-ray doses were found to cause a reduction in respiratory activity (366). A stimulatory effect of ionizing radiations on the respiration of potato tubers has been reported by Sussman (352). The respiration of high-nitrogen-content homogenates

of mouse liver was shown to be uninfluenced by radiation (323). The respiration of low-nitrogen-content homogenates was reduced; the extent of the reduction varied with substrate. Eichel & Roth (97) report a 30 per cent to 50 per cent reduction in respiration of *Tetrahymena* immediately following exposure to high doses of x-rays. The ribonuclease and desoxyribonuclease activities of homogenates from cells receiving the same doses were unaffected. X-ray-induced damage to the respiratory system of yeast, as evidenced by a reduction of mitochondrial staining by indophenol (Nadi reaction), has been reported by Bautz (26).

Exposure of yeast cells to various doses of ultraviolet and nitrogen mustard resulted in correlated decreases in survival and in ability of the cells to form the adaptive enzyme, maltase. In contrast, inactivating doses of x-rays had little effect on enzyme formation (22). Similarly, Yanofsky (393) finds that inactivating doses of x-rays had little effect on the ability of *E. coli* to synthesize lactase. A suppressing effect of ultraviolet on adaptive enzyme formation in *E. coli* B/r has been reported by Heinmets & Kathan (146). Evidence for ultraviolet-induced inhibition of adaptive enzyme formation in *Aerobacter aerogenes* has been presented by Norman (274). A lower survival of irradiated glucose-grown cells was observed when the cells were plated on adaptive substrates instead of on glucose. Cells previously adapted to a particular substrate survived as well on this substrate as on glucose. The difference in sensitivity of *E. coli* strains B and B/r to ultraviolet inactivation was found not to apply to inhibition of adaptive enzyme formation (180). Equal suppressions of galactosidase activity were observed in the two strains following ultraviolet irradiation. Evidence against a close relationship between the activity of the terminal oxidase system and resistance to x-irradiation has been presented by Goucher *et al.* (129)

A decrease in luminous activity of x-irradiated suspensions of *Achromobacter fischerii* has been reported (154, 379). The luminous output was reduced 50 per cent by a dose of 1,800 r (379), indicating an especially sensitive biochemical system. Incorporation of Carbon-14 into most of the biochemical fractions of *Chlorella* was found to be uninfluenced by growth in the presence of tritium (296).

Mitochondrial suspensions isolated from livers of mice that had received a dose of 640 r were unimpaired in their ability to oxidize succinate, while the capacity to couple this oxidation with high-energy phosphorus formation was found to be greatly impaired (241). Billen & Volkin (40) observed no immediate inhibition of succinate oxidation or ATP[2] formation in cell-free extracts of x-irradiated *E. coli;* extracts of cells that had been incubated in glucose buffer for 1 hr. after irradiation showed a marked decrease in phosphorylation. This effect was correlated with an observed disruption and disappearance of the class of cytoplasmic particles associated with ATP synthesis. Under conditions of growth, irradiated *E. coli* were observed to release ATP into the medium (39). That interference with phosphorylation might be related to inhibition of DNA synthesis in irradiated cells has been

considered by Kanazir & Errera (174 to 178). They find a decreased utilization of ATP in ultraviolet-irradiated *E. coli* for a duration comparable to that found for inhibition of DNA synthesis. During this period of inhibition there was an accumulation of acid-soluble organic constituents containing phosphorous, purines, pyrimidines, and pentoses. Kelner (185) has reported an immediate and pronounced inhibition of DNA synthesis in ultraviolet-irradiated *E. coli* B/r; RNA^2 synthesis was found to parallel growth of the cells. Similar results are reported by Klein & Forssberg (197) for x-irradiated ascites tumor cells. Although division was inhibited completely the average cell volume, RNA/cell, and nitrogen/cell were found to increase at a rate not significantly different from the rate of growth of an unirradiated dividing population of cells. DNA synthesis in the irradiated cells, however, was almost completely inhibited. This inhibition was accompanied by a decreased incorporation of glycine into DNA, and by an accumulation of ATP(109).

Further examples of radiation-induced derangement of nucleic acid have been presented by a number of authors. Tillotson & Warren (363) report an immediate decrease in stainable DNA, RNA, and alkaline phosphate in epithelial cells of the intestinal tract of irradiated rats. No change was observed (254) in the ultraviolet absorption of rat carcinoma cells for 48 hr. after x-irradiation, although a decrease in absorption occurred at later times. Partial fragmentation of DNA extracted from ultraviolet-irradiated rat thymocytes has been reported by de Courcy *et al.* (77). Low doses of x-rays were reported (245) to cause a stimulation in nucleic acid synthesis in carcinoma cells. An inhibition of both RNA and DNA synthesis has been observed in x-irradiated *Melanoplus* eggs (281).

CYTOLOGICAL EFFECTS

As was seen in the foregoing sections, the organization of this review has been largely on an operational basis. This is evidenced also in the sections to follow, where such related phenomena as mitotic inhibition and mutation are included among the more directly observable cytological effects of radiation. Pertinent reviews are considered under the appropriate subheadings.

Cytoplasmic Effects

Relatively few studies on observable effects in cytoplasmic structures of irradiated cells have been reported. Irradiation of *Paramecium* with x-rays resulted in decreased motility, increased protoplasmic viscosity, and dysfunction of the contractile vacuoles. Higher doses caused irreversible coagulation, darkening and vacuolization of the protoplasm, swelling and blistering, followed by death of the cell (382). Swollen and vesiculate mitochondria in irradiated *Allomyces* were observed at doses causing no detectable nuclear damage. Higher doses caused pronounced mitochondrial damage as well as obvious nuclear damage and death (306). Glubrecht (125) has studied a number of cytoplasmic effects of ultraviolet in somatic cells of *Allium* and *Tradescantia*. Contraction of the cell vacuole, stainability with erythrosin,

plasmolysis, and cessation of cytoplasmic streaming and of movement of cytoplasmic particles, all were induced by ultraviolet irradiation. Pretreatment of the cells with heat (45°C.) reduced the doses required to cause these effects. The wave-length dependence of some of these effects indicated albumin as a possible primary energy acceptor.

A reversible decrease in protoplasmic viscosity in leaf cells of *Helodea* caused by low doses of β- and γ-radiation, and an irreversible liquefaction caused by higher doses, have been reported by Virgin & Ehrenberg (373). Strugger *et al.* (351) have studied the localized and immediate uptake of fluorochrome dyes in x-ray-damaged protoplasmic regions of *Allium cepa*. Uptake occurred first in damaged areas along the longitudinal walls of the cell, and later spread to other regions as well as to adjacent cells. Blum *et al.* (43) have studied a number of effects of ultraviolet light on *Arbacia* eggs. Rapid cytoplasmic movements, localization of pigments, and cytolysis all were induced by the radiation. No photorecovery could be demonstrated for these effects.

Nuclear Effects

Ultraviolet-induced cloudiness in the nucleus of *Axolotl* cells has been studied by Erdmann (101, 102) and Erdmann & Meyer (103). Sodium thioglycolate, sodium nitrite, and sodium sulfite, effective against ultraviolet-induced coagulation of euglobin solution, were found also to protect against this effect. Cysteine and ascorbic acid were ineffective.

Large intranuclear vacuoles in liver and kidney cells, as well as vacuoles within chromosomes of spleen and ascites tumor cells, have been observed (163) in rats exposed to ionizing radiations. Scherer *et al.* (322) have observed enlargement of the nucleolar apparatus in cells of irradiated mice. Townsend *et al.* (369) find that the formation of the "centrochromatin" region of yeast cells is inhibited by inactivating doses of ultraviolet, whereas comparable doses of x-rays had no such inhibitory effect. These results are discussed in relation to possible disturbances in nucleic acid metabolism.

Trowell (370) has made an extensive study of the radiosensitivity of lymph node cells *in vitro* with pyknosis as a criterion of biological damage. A twelvefold difference in sensitivity between aerobic and anaerobic conditions was observed, a difference much greater than that usually found in biological systems. Swanson & Johnston (355) report about a fourfold dose reduction by anaerobiosis for x-ray-induced pyknosis in *Tradescantia*.

Geckler & Kimball (118) observed a relatively small decrease in the average number of micronuclei in *Paramecium* resulting from x-ray doses that profoundly affected both survival and division rate.

Effects on Nulcear and Cell Division

This section is concerned with those effects of radiation on cell division which become apparent soon after exposure. Recent reviews and critical discussions pertaining to this class of radiobiological effects have been presented

by Carlson (61), Glücksmann (126), and Warren (375). Many articles of interest to this section are included in the proceedings of two recent symposia (16, 73).

The partial-cell irradiation techniques described by Zirkle & Bloom (400) for protons, and by Uretz *et al.* for ultraviolet light (372), are of outstanding interest. Very small portions of amphibian cells were exposed to protons or ultraviolet light, and the cells were followed after irradiation by time-lapse phase microscopy. Following proton irradiations, most of the well-known qualitative effects of ionizing radiations on cell division were observed. The chromosomal effects were, however, localized at the site of irradiation; irradiation of the cytoplasm, spindle, or centriolar region produced no detectable effects. Ultraviolet irradiation of parts of chromosomes interfered with the normal directed movement of the chromosome to the metaphase plate only if the kinetochore was included in the irradiated part.

The nature and extent of the immediate effects of radiation on cell division has been shown to depend strongly upon the division stage in which the cells are irradiated. Carlson (61) describes, for *Chortophaga* neuroblasts, a very critical stage between late and very late prophase: "Irradiation of a cell before it has reached this period usually causes it to stop or even revert mitotically; irradiation after it has passed this period affects its progress through mitosis little if at all." Beatty & Beatty (29) find, in *Tradescantia* microspores irradiated at different stages of their first meiotic division, a period in mid-prophase which appears to be critical. Irradiation of early to mid-prophase chromosomes causes an unspiraling and apparent reversion to earlier stages. Irradiation of mid- and late prophases results in clumping of chromosomes at subsequent metaphase and anaphase. Clumping of metaphase chromosomes in x-irradiated *Tradescantia* has been studied by Swanson & Johnston (355). The interval between irradiation and the first appearance of clumped metaphases decreased and the duration of clumping increased with increasing doses. Rees (303) has studied errors of chromosome separation at anaphase in *Scilla campanula* after x-irradiation. Larger chromosomes and chromosome arms were affected more than expected, suggesting centromere control of chromosome splitting. LaCour & Rutishauser (207, 208) have presented evidence for the identification of these point errors observed at anaphase with aberrations resulting from subchromatid breaks.

The suppression in frequency of visible mitoses, often observed after irradiation, is assumed to represent an interference with the normal progress of cells through division. Carlson *et al.* (62) have studied the influence of x-rays delivered at very low dose rates on the frequency of mitosis in *Chortophaga* neuroblasts. A dose which, if delivered in a few minutes, reduced the mitotic index to zero, caused only a 50 per cent suppression of mitosis if delivered over a period of 6 days (3.4 r/hr.). It was considered that the low dose rates permitted a balance between inhibition and recovery. Koller (198) observed no suppression of mitosis in *Tradescantia* when the irradiation was given at 0.25 and 0.1 r/min.; at the lowest dose rate, an increased frequency

of mitosis after irradiation was observed, an effect also reported for *Chortophaga* (62). Gartner & Peters (116) found higher dose rates of both x-rays and electrons more effective in suppressing mitosis in tissue cultures of chick-heart fibroblasts. Ultrafractionation of the dose decreased the efficiency for inhibiting mitosis in *Vicia* root-tip cells (187).

Changes in oxygen concentration during irradiation were observed (117) to affect the degree of suppression of mitosis in *Chortophaga* neuroblasts, and, in addition, the rate of recovery from this effect. The changes observed under decreased oxygen concentrations could not be easily interpreted in terms of dose reduction alone. The rate of recovery from x-ray-induced mitotic inhibition in corneal epithelium has been shown (112) to be independent of x-ray energy (8 kv. to 240 kv.), intensity (6.5 r/min. to 430 r/min.), or oxygen concentration (5 per cent to 100 per cent).

Mitotic inhibition and resulting accumulation of early prophase stages in x-irradiated tissue cultures of chick-heart fibroblasts have been studied by Peters (284, 286). Half-irradiated cultures showed less inhibition in the irradiated side than was observed in wholly irradiated cultures, while the unirradiated side showed some mitotic inhibition compared to the control. These results suggest the participation of indirect effects beyond the cellular level. Maleic hydrazide, which suppresses mitosis in all actively growing plant tissues, was observed to cause chromosome breakage only in plants with visible heterochromatin (232). These results argue against a direct relation between mitotic inhibition and chromosome breakage.

A number of studies have demonstrated changes in irradiated microorganisms related to division inhibition. Sarachek *et al.* find with increasing doses of x-rays (317) and ultraviolet (314) a decrease in the percentage of yeast cells that have budded after 3 hr. in the presence of nutrients. Complex relations between this parameter and dose for yeast cells of different ploidy are formulated and discussed. Burns (58) has studied division delay in x-irradiated yeast cells by directly observing the time required for individual cells to divide after irradiation. The average division time was found to increase with dose; a sublethal exposure of 10,000 r delayed division by as much as five generation times. Budding cells, which are much more resistant to x-ray-induced lethality (28), were also less susceptible to division delay.

Changes in the growth curves of irradiated microorganisms have been observed by a number of investigators (33, 105, 177, 178, 185, 307); the most frequently observed changes were in duration of lag phase and in rate of growth during log phase. These changes may in part be related to division inhibition, although other effects such as lethality and mutation must be considered. Rubin (307) has shown that chronic irradiation of suspensions of *E. coli* at dose rates as high as 10,000 r/hr. is ineffectual in altering growth rate, final yield of cellular material, or its nucleic acid content. Mutation frequency was a function of dose alone, independent of the amount of growth occurring during irradiation.

The enlargement of cells after irradiation is a well-known radiobiological

effect, generally attributed to a selective inhibition of cytoplasmic division, unaccompanied by an inhibition of growth. This increase in size after irradiation has recently been observed for a number of different cells, e.g., *Chlorella* (295, 297), yeast (340, 341), *E. coli* (105, 341), ascites tumor cells (197), and timothy root cells (55).

The division stages in *Arbacia* eggs most delayed by ultraviolet were found (44) to be those preceding anaphase; only a slight delay could be detected between anaphase and cleavage. Division inhibition in ultraviolet-irradiated *Arbacia* eggs could not be reduced by subsequent exposure to visible light (43). Division delay in *Paramecium* induced by x-ray and nitrogen mustard has been studied by Kimball *et al.* (191). As with ultraviolet, the inhibiting effect was observed to extend through several postirradiation divisions. A number of studies mentioned elsewhere in this review have employed division delay as one of the measures of radiation effects (72, 118, 120, 158, 170, 192). An abnormal budding process in ultraviolet-irradiated yeast is described by Townsend & Sarachek (368).

Chromosomal Effects

Since the preparation of the preceding article in this series (334) there have appeared a number of excellent critical and historical reviews of radiation-induced chromosome structural changes. Chromosomal effects in irradiated animal cells have been surveyed by Kaufmann (183). Giles (122) has presented a critical discussion of radiation-induced chromosome changes in *Tradescantia*. The general problem of chromosome breakage, both spontaneous and induced, has been reviewed by Koller (199). A number of original contributions to this field are contained in the Symposium on Chromosome Breakage (73), and many of them are treated individually in the appropriate connections below.

A review of the controversy regarding healing of broken chromosome ends has been presented by Muller & Herskowitz (262) along with new data relating to this problem. These authors conclude (152, 262), on the basis of X-chromosome breakage experiments, that healing does not occur in *Drosophila* at a frequency detectable by present methods. The breakage of attached-X chromosomes had been proposed as an example of healing of broken ends. If this process involved only breakage followed by healing of the broken ends, the frequency of detachments would be expected to increase linearly with ray dose. A number of recent investigations (152, 203, 279, 280) have, however, shown the frequency of detachments to increase as an exponent of the dose—as does the frequency of translocations. In the majority of cases, the breakage of attached-X chromosomes was accompanied by a translocation with the Y chromosome. Parker (280) has shown that in the absence of a Y chromosome, detachment is occasioned by X-4 translocations, and presents evidence of Y "protection" from this eventuality in the normally constituted genome.

Evidence of nonrandom reunion of broken chromosome ends has been

presented by Haas *et al.* (139) and again discussed by Stone *et al.* (350). Among those translocations affecting four chromosomes, the relative frequency of "two-and-two" translocations to those involving all four chromosomes was much higher than would be expected on the basis of random rejoining.

The distribution of induced breaks along the chromosome strand has been studied by a number of investigators. Revell (305) has compared the distribution of breaks in *Vicia* produced by x-rays with those produced by diepoxide, nitrogen mustard, and tertiary-butyl hydroperoxide. Whereas x-ray-induced breaks showed an apparently random distribution, the chemically-induced breaks appeared to be largely localized in heterochromatic regions. A similar localized action of maleic hydrazide in heterochromatic portions of *Vicia* chromosomes has been reported by McLeish (232, 233). Localization of breakage in *Drosophila* X chromosomes has been observed by Fahmy & Bird (106) following treatments with diepoxide, triazine, or mustard gas. No significant differences in the distributions of breaks could be demonstrated. Barton (25) has shown both ultraviolet- and x-ray-induced breaks of tomato chromosomes to be highly localized in chromatic regions. Localization of breakage in heterochromatic zones of *Cannabis sativa* chromosomes have been demonstrated by Moutschen & Govaerts (259). Breakages were most frequent near the centromere. Oehklers (278) has reported studies on the distribution of breaks induced by a variety of agents in mitotic and meiotic chromosomes. The distribution of spontaneous breaks differs most strikingly from randomness; breaks induced by inorganic salts and nucleic acid derivatives showed similar distributions, suggesting a possible origin of spontaneous mutations.

Shattering of dry-pollen tube chromosomes of *Tradescantia* by ultraviolet has been reported by Lovelace (224).

Dose fractionation, rate.—The fractionation of radiation doses has long been employed in studies of the breakage-reunion process. The reduced yield of 2-hit aberrations accompanying increases of fractionation interval is usually attributed to the decreased probability of coexistence of two breaks as a result of restitution during the fractionation interval. Bora (48, 49) has varied both fractionation interval and intensity in a study of the breakage-reunion process in *Tradescantia*. By extrapolation to instantaneous exposures, the minimum time for a break to remain open was found to be about 3.5 min., a figure which agrees well with previous estimates. The frequency of dicentric bridges induced in *Gesonula punctifrons* by γ-rays was found (300) to be the same for doses delivered at 2.6 r/min. and 0.06 r/min. This lack of intensity effect was considered to be evidence against the necessity in this material of the coexistence of two breaks for the production of these normally 2-hit aberrations. The production of pathological ana- and telophases and micronuclei in root-tip cells of *Vicia faba* was found to be independent of dose rate over the range 5 to 0.5 r/min. (285, 289). Koller (198) has studied the effect of very low-intensity x-rays on *Tradescantia* and has reported a reduced

frequency of chromatid and chromosome breakages and reunions that could not be attributed to restitution alone. Physiological effects, which can coexist with chromosomal effects at sufficiently low dose rates, were considered to influence breakage and reunion frequency.

Lane (209) and Haque (141) have offered new evidence in support of a secondary rise in aberration frequency with extended fractionation intervals, which they have interpreted in terms of recovery from a radiation-induced resistance to breakage. That these findings could not be confirmed by extensive studies by other investigators (79, 318, 346), however, casts doubt on the view that induced resistance to breakage can explain the reduced yield of aberrations. Dose fractionation studies with neutrons (123) were considered as additional evidence against the views of Lane.

Infrared treatment.—Investigation of the effect of combined x-ray and infrared treatment has been continued by Swanson *et al.* (354). The potentiating action of infrared pretreatment upon x-ray-induced chromosome aberrations in *Tradescantia* was found to be associated with wave lengths centered around 0.95 to 0.97 μ. Young *et al.* (396) were unable to demonstrate any increase in recessive lethal production in *Drosophila* by infrared pretreatment. Ives *et al.* (172) have attempted to demonstrate a potentiating effect of infrared on crossing over in *Drosophila*. Although similar to low temperatures in extending the effective period of crossing over, infrared did not affect the cross-over rate.

Temperature.—The influence of low temperatures on the induction of chromosome aberrations by radiation has received some specific consideration. Nybom *et al.* (277) have shown that x-ray damage induced in dry barley seeds—chromosome abnormalities, mutation, or effects on seedling growth—was less when the seeds were irradiated at −190°C. than at 25°C. A similar influence of low temperatures on seedling injury and chromosome aberrations has been reported by Nilan (271) for irradiation of dormant barley seeds at −80°C. and 20°C. Mutation frequency, however, was the same at the two temperatures and was also independent of carbon dioxide or oxygen concentration during irradiation. The results were considered to show that the treatments did not affect primary x-ray damage, but only the reunion of broken ends.

Kurabayashi (202) reports an increase in chromatid breaks and translocations in x-irradiated *Paris tetraphylla* resulting from postirradiation temperature treatment at 0°C. The reduced temperature was considered either to sensitize the chromosome to potential breaks, or to prolong the restitution process. A consideration of low-temperature effects is presented by Haas *et al.* (139) in connection with a detailed discussion of the direct and indirect effects of radiation and the involvement of oxygen in radiation action.

Kind of radiation.—The relative biological effectiveness (RBE) of different ionizing radiations in producing a wide variety of effects has been the subject of recent reviews by Zirkle (399), Boag (45), and Dittrich & Schubert (87).

Kirby-Smith & Daniels (194) have found 60-kev x-rays about twice as effective as Co^{60} γ-rays or 400-kev β-rays in producing chromosome aberrations in *Tradescantia*. These results are discussed in light of the relative ion densities produced by these radiations. Lewis (221) has reported medium-energy x-rays to be more effective than Co^{60} γ-rays in inducing chromosomal rearrangements in *Drosophila*. An approximately equal effectiveness of these two radiations has been reported for production of chromosome aberrations and pollen lethals in *Datura* (338, 395). No difference in effectiveness was found between 200-kev x-rays and fast electrons for production of translocations (159) or breakage of ring chromosomes (52) in *Drosophila*.

The determination of a practical RBE relating radiations whose dose-response curves indicate differences in kinetics must depend either upon comparisons at arbitrary but standardized levels of effect, or upon detailed analysis of the response curves. This applies particularly to comparisons of the efficiencies of neutron and x-ray production of "2-hit" aberrations, for which the neutron dose-action curve is generally linear whereas the x-ray curve is "multihit"; the RBE accordingly decreases with increasing dose. Interest in the relative effectiveness of these two radiations has increased considerably in the last two years, largely in connection with the 1953 nuclear detonation field tests (161). The production of chromosome translocations in *Drosophila* by neutrons and x-rays has recently been reported by a number of investigators (221, 261, 349). Largely because of the different dose-response curves for translocation production by these two radiations, the RBE of neutrons relative to x-rays varied from 7.5 to 1.9 according to the level of effect chosen. Conger (66, 67) and Kirby-Smith & Swanson (195) have compared the effects of x-rays, γ-rays, and fast neutrons upon *Tradescantia* chromosomes. The x-ray dose-response curve for deletions and exchanges was multihit; that of the neutrons was linear. For chromatid and isochromatid breaks, which are produced linearly with both x-rays and neutrons, an RBE of 13 (neutrons: 250 kvp x-rays) was found. Spencer & Blakeslee (338), using the pollen lethal technique in *Datura*, have reported an RBE value for fast neutrons relative to x-rays of 13 to 14. A similar effectiveness for neutrons was found by Yost *et al.* (395) for induction of chromosome aberrations in *Datura*. The types of aberrations and number of aberrations per affected cell were the same for the two radiations.

Spencer *et al.* (339) have examined the effects of thermal neutrons on *Datura stramionium*. These workers find no difference between thermal neutrons and x-rays in the pollen lethality pattern of plants developing from treated seeds or in development of morphological abnormalities of such plants. Yost *et al.* (394) have continued these studies in a preliminary investigation of the relation between chromosome aberrations and gene mutations. In the pollen abnormalities produced by thermal neutrons, those attributable to chromosome aberrations were greatly in excess of those produced by gene mutation. Conger (65) has investigated the effect of slow neutrons on aberration frequency in *Tradescantia* and has provided a basis on

which the effectiveness of this radiation may vary between cells or organisms. Slow neutrons are absorbed largely through capture reactions with boron, nitrogen, and hydrogen. Plants grown in high concentrations of boron yielded more chromosome aberrations than the controls.

The effects of fast neutrons and x-rays on hexaploid wheat and diploid barley have been studied by MacKey (231). Nongenetic killing by x-rays precluded comparison of x-ray mutability in these plants. Neutrons were highly mutagenic to the hexaploid plants, a fact attributable to the relatively high tolerance of the plants for chromosome disturbances.

Caldecott *et al.* (60) have continued the comparison of x-ray and thermal neutron damage in barley, with an analysis of the cytogenetic effects. Among the interesting results demonstrated were (*a*) the same linear realationship between interchanges and mutation frequency for neutrons and x-rays, and (*b*) an unexpected linear or approximately linear dose-effectiveness relationship for both radiations in producing mutations, bridges, and interchanges. An inverse relationship between x-ray sensitivity and water content of barley seeds has been reported (59, 93). The action of neutrons was considered by Ehrenberg *et al.* (93) to be direct and to differ from that of x-rays in being independent of water content or oxygen concentration. An effectiveness of fast protons higher than expected on the basis of their linear energy transfer was observed for damage in barley seeds (94, 96). This discrepancy was attributed to a dissipation of part of the proton energy in lineastic collisions with the production of highly effective low-energy α-particles and protons. Ehrenberg & Gustaffson (95) have reviewed the effects of ionizing radiations on barley. The ratio of isochromatid to chromatid breaks in *Vicia faba* chromosomes was found by Thoday (362) to be higher in material treated with α-particles than in that treated with x-rays.

That the factor determining the relative biological effectiveness of an ionizing particle is not necessarily the type of particle, but the rate at which it loses energy along its path, is well-demonstrated by a recent report of Giles & Tobias (124). Cyclotron-generated deuterons and α-particles, and x-rays, all having approximately equal linear energy transfer, were found to be about equally effective in producing isochromatid aberrations in *Tradescantia.*

Gaseous atmosphere.—The role of oxygen in the production of chromosome abnormalities by ionizing radiations has been the subject of many recent investigations. Some recent reviews pertinent to this area of inquiry are those of Barron (23, 24), Ehrenberg *et al.* (93), Giles (121), Lacassagne (206), and Patt (282).

The interpretation of the "oxygen effect" on the production of chromosome aberrations is still subject to considerable dispute. The more usual interpretation and the one consistent with much other radiobiological information [for discussion see Giles (121, 122)] is in terms of an increased production of oxidizing free radicals in the presence of oxygen, which in turn leads to an increased frequency of chromosome breakage—"differential breakage."

A number of investigations, however, appear to support the idea that the increased aberration frequency produced in the presence of oxygen results from a decreased probability of restitution of the breaks produced under these conditions—"differential reunion." Swanson & Schwartz (353) have discussed these two interpretations and have presented additional evidence which they feel supports the "differential reunion" interpretation. A much lower reduction in frequency of chromatid deletions than of isochromatid deletions and chromatid exchanges was observed when *Tradescantia* was x-irradiated under anoxic conditions. It was reasoned that if oxygen simply influenced the number of primary breaks, the three forms of damage should respond similarly to its absence. Baker & Edington (19), studying the aerobic and anaerobic production of translocations and recessive lethals in *Drosophila*, were unable to distinguish between these two interpretations. In a similar study (20), comparing the relative frequencies of dominant lethals induced in *Drosophila*, the reduction observed in the presence of nitrogen was less than would be expected solely on the basis of a reduced number of primary breaks, a finding considered to support the differential-reunion hypothesis. Read (302) has considered the data of Baker and co-workers and concludes that they can be interpreted entirely in terms of a reduced frequency of primary breaks in the absence of oxygen. Lüning (229) argues that these data as well as his own show the same reduction of recessive lethals as of chromosome breaks in nitrogen, and feels this to be more consistent with differential breakage than with differential restitution. Of interest in this controversy is the study of Kihlman (190), who has shown that 8-ethoxycaffeine (an agent presumably not acting by formation of active radicals) produces more chromosome breaks in *Allium cepa* when applied in the presence of oxygen.

Wolff (385, 386) has reported a decrease in x-ray-induced aberration frequency in *Vicia faba* when the seeds are treated with BAL (2,3-dimercaptopropanol) prior to irradiation. This antioxidant, supposedly similar in action to anoxia, also occasions decreases in a radiation-induced reunion delay, an effect considered to "strengthen the hypothesis that the major effect of anoxia is on the restitution of broken chromosomes, rather than on the intial breakage." Subsequently, however, as a result of a study (387) combining dose fractionation and BAL treatment, it was concluded that chromosome breakage and radiation-induced reunion delay are different and independent effects, and that the difference in aberration yield caused by BAL reflects a difference in initial breakage.

The production of abnormal anaphases in ascites tumor cells by x-rays was shown to be reduced about threefold when the cells were irradiated anaerobically [Conger, see (136)]. A much slighter "dose reduction" was afforded by anoxia against fast neutrons. Other investigations showing a decreased anoxic protection with more densely ionizing radiations are those of Ehrenburg *et al.* (93), Conger [see Giles (121)], and Forrsberg (107, 108).

Nilan (271) reports an increased yield of aberrations in barley when the

seeds were irradiated in atmospheres of CO_2 or O_2. At −80°C., however, these gases reduced the yield of aberrations. Schneiderman & King (324) find the response of *Tradescantias* irradiated with x-rays in atmospheres of CO_2 and O_2 indicates a synergism of the two gases. Both gases were considered to exert their influence on aberration yield through indirect action of the radiation. An extensive study of a number of modifiers on the x-ray sensitivity of *Drosophila virilis* has led Haas *et al.* (139) to conclude that indirect effects may account for more than 50 per cent of the observed genetic damage. Low temperature, dose rate, or atmospheres composed of various combinations of O_2, N_2, CO_2, and CO all influenced the yield of aberrations. These effects were attributed to changes influencing the formation or destruction of active radicals within the cell.

The combined effects of centrifugation and anoxia on x-ray-induced two-hit aberrations in *Tradescantia* and *Vicia* have been studied by Wolff & Von Borstel (388). Centrifugation prior to irradiation reduced aberration frequency; centrifugation after irradiation but before restitution (3 to 4 min.) increased aberration frequency. Irradiation in nitrogen resulted in a reduced yield of aberrations, but the frequency could not be increased by centrifugation. It was concluded that restitution of anaerobically-induced breaks occurs in a shorter time than that of those produced in air.

Chemical modifiers.—The modification of radiation-induced chromosome damage by chemicals has been considered in some recent reports. Wolff (386) has reported sodium hyposulfite and BAL to protect *Vicia faba* chromosomes against x-ray damage; cysteine, glutathione, and ascorbate were ineffective. None of the chemicals afforded protection over that provided by anoxia. Bridge and fragment formation in *Allium cepa* were shown (107, 108) to be reduced about the same amount by cysteine and anoxia, although only a slight extra protection was afforded by cysteine to cells x-irradiated anaerobically. Cysteine protected much less against α-particle damage. Reductions in x-ray-induced chromosome damage in *Tradescantia*, brought about by cysteine, sodium hyposulfite, and sodium cyanide, have been reported by Mikaelsen (249). The protection afforded by sodium hyposulfite and BAL is considered to arise by competition for molecular oxygen, while cysteine is generally considered to act on toxins produced by aerobic decomposition of water. The role of sodium cyanide is more obscure, but its action may involve metabolic changes.

Peters (285, 287, 288) has related the γ-ray production of micronuclei in *Vicia faba* root tip cells to chromosome breakage, and finds their frequency to be increased considerably by postirradiation treatment with megaphen.[3] Reinholz & Aurand (304) found no chemical protection against x-ray damage of plants in which considerable protection was afforded by anoxia.

Action of chemicals on chromosomes.—Recent reviews and discussions relating to this subject are included in articles by Gray (135), Kihlman (188,

[3] Megaphen, as given by Peters, is *N*-(3′-Dimethylamino)-propyl-3-chlorphenothiazin.

189), and Stone *et al.* (350). A number of articles pertaining to the action of chemicals on chromosomes are included in the *Symposium on Chromosome Breakage* (73).

The production of chromosome aberrations and recessive lethals in *Drosophila* by nitrogen mustard and x-rays has been studied by Mehtab (244) and Nasrat *et al.* (267). A lower ratio of aberrations to recessive lethals following nitrogen mustard treatment was reported in both studies. The frequency of translocations was found (267) to increase approximately as the square of the frequency of recessive lethals for nitrogen mustard treatment. The relative paucity of rearrangements following nitrogen mustard treatment was attributed to delayed opening of breaks and a reduced ability of the breaks to recombine. Revell (305) has studied the effects of x-rays, diepoxide, and nitrogen mustard on root cells of *Vicia faba*. The stage of maximum sensitivity to diepoxide and nitrogen mustard, as assayed by chromosomal effects, was found to correspond with the beginning of the resting phase of nuclear division, while that to x-rays was at the end of resting phase. Read (301) observed an earlier expression of growth delay in *Vicia faba* roots for x-ray than for nitrogen mustard treatment, which he correlated with this difference in stage of sensitivity. *Allium cepa* chromosomes were reported (190) to be most sensitive to breakage by 8-ethoxy-caffeine in the second half of interphase.

McLeish (232, 233) has investigated the effects of maleic hydrazide and 8-ethoxy-caffeine on the chromosomes of *Vicia* and has found both these agents to be similar to diepoxide in producing breaks largely in heterochromatin. Because of its structural similarity to the pyrimidines, maleic hydrazide is felt to operate indirectly through reaction or competition with pyrimidine-containing nucleic acid precursors. Breakage of *Tradescantia* chromosomes by ethylene oxide, ketene, and methyl chloride has been reported by Smith & Lotfy (331). It is interesting to note that, though ketene has been found to be ineffective in inducing reverse mutations in *Neurospora*, in keeping with its capacity as a mutachromosomic agent, it is still able to produce "forward" or "loss" mutations in this organism (201).

Deysson & Truhaut (81, 82, 83) have investigated the possibility of chemical protection against damage by radiomimetic agents. Protection was afforded by β-mercaptoethylamine aganist nitrogen-mustard-induced damage although other protective agents tested were ineffective. The same authors have reported (84) a radiomimetic action of actinomyces C and D. Ribonuclease has been reported effective in inducing mitotic abnormalities in onion and lily root cells (184). The occurrence of mitotic abnormalities in *Tradescantia* that had been grown under magnesium or sulfate deficiencies has been reported by Steffensen (344, 345), a finding of additional interest in light of the work on the organization of chromosomes reported by Mazia (242). On the basis of solubilization studies Mazia has proposed that chromosomes are composed of particulate units, containing both protein and DNA, and linked by bridges of divalent cations (Ca, Mg).

Division stage, differentiation.—The relation of stage of division, meta-

bolic state, or degree of differentiation of a cell to its susceptibility to chromosome damage has been considered in a number of recent studies. Many articles pertinent to this section are included in the *Symposium on Chromosome Breakage* (73). Valuable discussions are included in a number of recent articles (135, 199, 260, 350).

Darlington & LaCour (74) have analyzed and classified the different types of x-ray damage observed at meiosis in terms of the time in the division cycle at which they are incurred. The influence of division stage as well as of many other modifying conditions upon radiation effects are discussed by Thoday (361, 362). Evidence is presented (362) that chromosome duplication in *Vicia faba* takes place at the same part of interphase as DNA synthesis (169). In the subsequent part of interphase, most radiation-induced chromatid breaks and exchanges are initiated.

The production of subchromatid breaks in *Lilium* has been associated with irradiation at first meiotic metaphase (69); no such changes occurred following irradiation at pachytene. LaCour & Rutishauser (207, 208) have associated the production of this class of breaks in *Scilla* endosperm with irradiation at prophase rather than metaphase or interphase. The stage for production of subchromatid breaks was considered to correspond to the time of chromosome duplication.

Timonen (364) finds *Allium cepa* cells, arrested in interphase by indole-3-acetic acid treatment, to be highly sensitive to chromosome breakage by x-irradiation. Differentiated cells were refractory to induced chromosome damage. The meiotic stages in maize have been shown to be ones of high radiosensitivity (328, 335). Meiotic cells of *Tradescantia* were shown (142) to be much more susceptible to physiological and structural changes induced by radiation than were postmeiotic cells. Revell (305) reports different stages of sensitivity to chromosome damage in *Vicia*, for diepoxide or x-ray treatment. Diepoxide is most effective in early resting states, x-rays, in late resting stages.

The relative sensitivity of *Drosophila* sperm at different developmental stages has been investigated by several workers. Stone *et al.* (350) find the most sensitive stages for production of translocations and dominant lethals to be in early spermiogenesis, possibly at the end of meiosis. Auerbach (6, 8) has reported different stages of sensitivity for formaldehyde, nitrogen mustard, and x-ray treatments. The maximum sensitivity to x-rays for the production of translocations, large deletions, and recessive lethals was found to occur at late meiosis or early spermiogenesis. Spermatogonia and mature sperm were least sensitive. Increased sensitivity of aging sperm has been reported by Yanders (392) and Lüning (228). Gross rearrangements resulting from irradiation of *Drosophila* females are reported (157, 262) to be more frequent from treated oöcytes than from treated oögonia. More chromosome breakage in *Drosophila* sperm has been observed (228, 230) for irradiation in the impregnated female than in the male, perhaps attributable to a process similar to that which renders aged sperm more liable to breakage (228).

Dominant lethals.—Dominant lethals, because of possible connection

with chromosomal changes and because of the frequency with which they are similarly employed to study the effects of radiation, are considered in the section to follow. In those cases where both effects were studied the reader should refer to the parallel citations in foregoing sections.

Russell *et al.* (310) find approximately the same effectiveness of cyclotron and atomic-test fast neutrons in inducing dominant lethals in the mouse. On the basis of the previously determined RBE of cyclotron neutrons in comparison to x-rays, the RBE of the test neutrons falls between 6.4 and 9.4. Baker & Von Halle (21) and Mickey (248) have compared the effectiveness of atomic-test neutrons with x-rays and cyclotron neutrons, using as an assay system dominant lethal production in *Drosophila*. Since the zygote survival curve for x-rays was not exponential like the neutron curves, the RBE was not constant but varied, as dose increased, from 7 to about 4, in essential agreement with the values obtained for mice (310) and for production of a number of classes of chromosome changes by fast neutrons (see corresponding section under chromosomal effects).

Yanders (392) has studied x-ray-induced dominant lethals in *Drosophila robusta*. His results agree essentially with those reported for *Drosophila melanogaster*, in that the survival curves indicate a multiple-hit-type action. An effect of sperm age upon radiosensitivity similar to that reported by Baker & Von Halle (20) was also reported. The latter authors, as previously noted, employed dominant lethals in a study of the influence of oxygen on radiation effects. The frequency of dominant lethals and translocations in the progeny of x-irradiated *Drosophila virilis* males was shown to be a function of sperm age at the time of irradiation (350). The most sensitive stages for the production of the two types of damage did not coincide completely. Both effects were reduced by anoxia.

Lefevre *et al.* (218) have studied the frequency of notch mutations induced by x-rays in normal, duplicated, and inverted x-chromosomes of *D. melanogaster*. Long deficiencies, including notch, behave as dominant lethals, but it was not certain whether one or two hits is required for their production. A simplified technique for dominant lethal studied in *Drosophila* has been presented by Telfer (359). McQuate (234) found no dominant lethals as the result of ultraviolet irradiation of male *Drosophila*. Kaplan & Lyon (181, 182) observed no protection by β-mercaptoethylamine against x-ray production of dominant and recessive lethals in *Drosophila* and recessive lethals in the mouse, in agreement with the finding (14) that this compound protects mice against x-ray lethality primarily through the liver.

Short exposures of nitrogen mustard were shown by Whiting & von Borstel (381) to produce high yields of dominant lethals in *Habrobracon*. Longer exposures decreased the yield of dominant lethals by increasing sperm inactivation. Nakao (266) has reported effects on silkworms that are attributed to an action of irradiated egg cytoplasm upon components of the sperm nucleus.

Brown & Cave (53, 54, 64) have demonstrated the induction by x-rays of dominant lethals in *Lilium*. The seed sterility (close to 100 per cent at

4000 r) is associated with cytological abnormalities: large irregular nuclei (some of which are polyploid or polytene), micronuclei, and bridges. The sterility is attributed to mitotic failure resulting from these abnormalities.

Chromosome effects and mutation.—The subject of the relation of mutation of chromosome breakage is still very much alive, and a considerable portion of the work involving the induction of mutation by radiations or radiomimetic agents has been overtly or tacitly addressed to this problem. Many of the papers to be discussed under this heading have been covered in preceding sections and therefore are referred to again only briefly. Mutation production in microorganisms has been discussed in an earlier section. The reader's attention is called to a number of recent reviews and discussions of special interest in this topic (260, 309, 342, 350).

Alexander (1) has measured the rate of mutation production at 8 autosomal loci of *Drosophila*. The rates for mature sperm varied from 2.7×10^{-8} per r per locus to 8.75×10^{-8} per r per locus. A considerably lower spermatogonial mutation rate was observed. This variation of sensitivity differs from that previously mentioned for production of chromosome aberrations (6, 8, 350), for which early meiotic stages appear more sensitive than mature sperm. Alexander considers her mutation rate data to support Russell's suggestion that radiation-induced mutation rates are higher in mice than in the fruit fly. Ives *et al.* (173), however, studying mutations in the F_1 generation of *Drosophila*, obtained an average value of 14×10^{-8} per r per locus. Ives (171) concludes that, for the present, the mutation rates in the mouse and the fruit fly appear to be similar. Arguments are presented for limiting future comparisons of mutation rates to autosomal loci tested in the F_1. Marquardt (240) has studied various results of irradiating *Oenothera hookeri* pollen (i.e. mutation, reduction of fertility, and chromosomal effect) and expresses similar reservations concerning methods of estimating radiation effectiveness that depends upon the viability and fertility of the postirradiation F_1 generations.

Bonnier & Lüning (47) find that sensitivity to x-ray induction of recessive lethals is like that to chromosome breakage (46, 230); it is greater in *Drosophila* sperm when irradiated in the impregnated female than when still in the male. Auerbach (6, 8) reports that the peak of susceptibility of *Drosophila* sperm to recessive lethal mutations is the same as for chromosome breakage (late meiosis or early spermiogenesis) in response to x-ray, nitrogen mustard, or formaldehyde treatments.

Fahmy & Bird (106) report that the ratio of recessive lethals associated with rearrangements to those not so associated was highest for x-rays, much lower for triazine, and lowest for diepoxide. A similar higher ratio of translocations to recessive lethals for x-ray treatment than for nitrogen mustard treatment of *Drosophila* has been reported by Mehtab (244) and Nasrat *et al.* (267). McQuate (234) has found the ratio of breaks to recessive lethals induced in *Drosophila* by ultraviolet to be about one-half that observed after x-ray treatment. The ratio of deficiencies to translocations in tomato chro-

mosomes has been reported by Barton (25) to be higher for ultraviolet than for x-ray treatment. Dollinger (88) in a study of three loci in maize found that most of the x-ray- and γ-ray-induced mutations studied were associated with loss of the pertinent chromomeres.

Lewis & Crowe (220) present evidence of revertible x-ray as well as spontaneous mutations in *Oenothera* and *Prunus* which they interpret in terms of previously demonstrated subchromatid breaks (207, 208). Scheibe & Bruns (320) and Bruns (56) have found x-ray induced mutations in clover to be generally expressed in variegated development. Their results are interpreted in terms of Marquardt (240), who has proposed an eightfold subdivision of the chromosome to account for postirradiation development of variegation. Somatic mutations induced in *Ephistia* are interpreted by Pohley (291) in terms of changes in chromosome subunits, followed in subsequent cell generations by segregation of the mutant material. Discussions of delayed mutation and studies on the delayed phenotypic expression of genetic changes in microorganisms are included in a number of recent articles (7, 114, 205, 269, 308, 311).

Young *et al.* (396) found no potentiating effect of infrared posttreatment for recessive lethal production in x-irradiated *Drosophila*. In light of the potentiating action of this treatment on translocation frequency, these authors conclude that recessive lethals and chromosome breaks are unrelated in this organism. Differential effects on mutation and aberration frequency are observed when barley is irradiated at high and low temperatures (271, 277) and in the presence or absence of CO_2 or O_2 (271).

Mickey (248) has compared the relative effectiveness of fast neutrons and x-rays for induction of visible and lethal mutations in *Drosophila*. Whereas considerable variation between different loci was observed, the average RBE for eight specific recessive visible loci was 4. The RBE for sex-linked lethals was 2, for dominant visibles and minutes from 3 to 22 and 5 to 11 respectively. Ives *et al.* (173), in a similar study, find an RBE of 3 to 4 for sex-linked lethals and autosomal visibles.

Belitz (30) has analyzed spontaneous, chemical and fast-neutron-induced sex-linked lethals in *Drosophila* and finds their distribution along the chromosome similar to those reported in earlier studies. An anomalous high effectiveness of fast protons for induction of chlorophyll mutations in barley seeds has been observed (94), an effect attributed to inelastic collisions suffered by the protons. Mutation production in 6n wheat and 2n barley has been studied by MacKey (231), using x-rays and neutrons. Nongenetic killing by x-rays precluded comparison of the two radiations with respect to genetic effects and their dependence upon ploidy. A preponderance of chromosomal over gene types of pollen lethals in *Datura* arising from thermal neutron treatment has been reported (338, 394). The same relative effectiveness of fast neutrons as of x-rays was observed for both types of damage, however (337, 395); this is taken as grounds for re-evaluating the basis of the pollen technique.

Caldecott *et al.* (60) have compared the effectiveness of x-rays and thermal neutrons in inducing a variety of effects in dormant barley seeds. The most striking relation was that between mutation and interchanges, a nearly linear function independent of dosage, kind of radiation, or degree of lethality. The frequencies of chlorophyll mutants and chromosome interchanges were found to be approximately linear functions of x-ray and neutron dose. The dose-action curve for mutation production has been studied by a number of other investigators. Ray & Whiting (299) have obtained a curve for production of visible mutations in *Mormionella* which does not depart significantly from linearity. Mickey (248) and Ives *et al.* (173) report a linear relation for fast-neutron-induced sex-linked lethals in *Drosophila;* the possibility of nonlinearity in the case of visibles is noted (173). Muller *et al.* (263) observe a flattening of the dose-response curve at high x-ray doses. This result, after irradiation of *Drosophila* sperm in early developmental stages, was considered to be attributable to selective killing by chromosome breakage of the more mutable germ cells. A similar lack of proportionality in *Drosophila* was observed (264) between mutation rate and ultraviolet dose. This was considered to arise from unequal illumination of cells in the polar cap and hence selective killing of those mutated. Nonlinear mutation-versus-dose curves are discussed on the basis of heterogeneities, with respect either to doses received by, or to sensitivities of, the irradiated cells.

Michaelis (246) and Michaelis & Kaplan (247) and King (193) have studied the mutagenic action of incorporated β-emitting isotopes in *Epilobium* and *Drosophila* respectively. The mutagenicity of formaldehyde to *Drosophila* sperm has been studied by a number of investigators (155, 156, 332). Altenburg (5) has demonstrated the mutagenicity of tertiary butyl hydroperoxide when applied to eggs in the polar-cap stage. The mutagenic action of miracil and triethylene melamine has been investigated (30, 226). These agents appear to act on late stages of spermatogenesis. DDT [1,1,1-trichloro-2,2,-*bis* (*p*-chlorophenyl)-ethane] was found to be nonmutagenic for *Drosophila* (227).

Sparrow & Singleton (335) and Singleton (327) have studied the effect of chronic gamma irradiation on growing plants and find a nonlinear relationship between mutation frequency and dose rate. A threshold dose rate was necessary in order to exceed the spontaneous mutation rate in maize (327). On the basis of field testing with chronic irradiation it was suggested (333) that plants with large chromosomes are in general more radiosensitive.

LITERATURE CITED

1. Alexander, M. L., *Genetics*, **39**, 409–28 (1954)
2. Alper, T., *J. Gen. Microbiol.*, **11**, 313–24 (1954)
3. Alper, T., *Brit. J. Radiol.*, **27**, 50–54 (1954)
4. Alper, T., and Ebert, M., *Science*, **120**, 608–9 (1954)
5. Altenburg, L. S., *Proc. Natl. Acad. Sci. U. S.*, **40**, 1037–40 (1954)
5a. Atwood, K. C., and Mukai, F., *Am. Naturalist*, **88**, 295–314 (1954)
6. Auerbach, C., *Heredity*, **6**, Suppl., 247–57 (1953)

7. Auerbach, C., *Brit. J. Radiol.*, **27**, 122–24 (1954)
8. Auerbach, C., *Z. ind. Abstam. Verebungsl.*, **86**, 113–25 (1954)
9. Bachofer, C. S., *Science*, **117**, 280–82 (1953)
10. Bachofer, C. S., and Pottinger, M. A., *J. Gen. Physiol.*, **36**, 345–60 (1953)
11. Bachofer, C. S., and Pottinger, M. A., *J. Gen. Physiol.*, **37**, 663–75 (1954)
12. Bachofer, C. S., and Pottinger, M. A., *Science*, **119**, 378–79 (1954)
13. Bachofer, C. S., Ehret, C. F., Mayer, S., and Powers, E. L., *Proc. Natl. Acad. Sci. U. S.*, **39**, 744–50 (1953)
14. Bacq. Z. M., *Science*, **117**, 633–36 (1953)
15. Bacq. Z. M., and Alexander, P., *Fundamentals of Radiobiology*, (Butterworth Scientific Publications, London, England, 389 pp., 1954)
16. Bacq. Z. M., and Alexander, P., *Radiobiology Symposium, Liège, 1954*, (Butterworth Scientific Publications, London, England, 362 pp., 1955)
17. Bair, W. J., *Federation Proc.*, **13**, 5 (1954)
18. Bair, W. J., *U. S. Atomic Energy Commission Document, UR-321* (1954)[4]
19. Baker, W. K., and Edington, C. W., *Genetics*, **37**, 665–77 (1952)
20. Baker, W. K., and Von Halle, E. S., *Proc. Natl. Acad. Sci. U. S.*, **39**, 152–61 (1953)
21. Baker, W. K., and Von Halle, E. S., *Science*, **119**, 46–49 (1954)
22. Baron, L. S., Spiegelman, S., and Quastler, H., *J. Gen. Physiol.*, **36**, 631–41 (1953)
23. Barron, E. S. G., *Radiation Biology*, **1**, 283–314, (A. Hollaender, Ed., McGraw-Hill, New York, N.Y., 1265 pp., 1954)
24. Barron, E. S. G., *Radiation Research*, **1**, 109–24 (1954)
25. Barton, D. W., *Cytologia*, **19**, 157–75 (1954)
26. Bautz, E., *Naturwissenschaften*, **41**, 375–76 (1954)
27. Bawden, F. G., and Kleczkowski, A., *J. Gen. Microbiol.*, **8**, 145–46 (1953)
28. Beam, C. A., Mortimer, R. K., Wolfe, R. G., and Tobias, C. A., *Arch. Biochem. and Biophys.*, **49**, 110–22 (1954)
29. Beatty, A. V., and Beatty, J. W., *Am. J. Botany*, **41**, 242–50 (1954)
30. Belitz, H. J., *Z. ind. Abstam. Verebungsl.*, **86**, 173–84 (1954)
31. Berger, H., Haas, F., Wyss, O., and Stone, W. S., *J. Bact.*, **65**, 538–43 (1954)
32. Berrie, A. M. M., *Proc. Natl. Acad. Sci. U. S.*, **39**, 1125–33 (1953)
33. Beutler, E., Robson, M. J., and Jacobson, L. O., *Proc. Soc. Exptl. Biol. Med.*, **85**, 682–85 (1954)
34. Biagini, C., *Nuntius radiol.* (Firenze), **18**, 97–124 (1952)
35. Biagini, C., *Nature*, **172**, 868–69 (1953)
36. Biagini, C., *Riv. biol.* (*Perugia*), **46**, 147–56 (1954)
37. Biagini, C., and Grossi, V., *Riv. biol.* (*Perugia*), **44**, 493–510 (1952)
38. Billen, D., Stapleton, G. E., and Hollaender, A., *J. Bact.*, **65**, 131–35 (1953)
39. Billen, D., Strehler, B. L., Stapleton, G. E., and Hollaender, A., *Arch. Biochem. and Biophys.*, **43**, 1–10 (1953)
40. Billen, D., and Volkin, E., *J. Bact.*, **67**, 191–97 (1954)
41. Birge, A. C., and Tobias, C. A., *Arch. Biochem. and Biophys.*, **52**, 388–93 (1954)
42. Bloom, W., and Bloom, M. A., *Radiation Biology*, **1**, 1091–1143 (A. Hollaender, Ed., McGraw-Hill, New York, N.Y., 1265 pp., 1954)

[4] Information concerning the availability of this document may be obtained by addressing inquiries to the Office of Technical Service, Department of Commerce, Washington 25, D. C.

43. Blum, H. F., Cook, J. S., and Loos, G. M., *J. Gen. Physiol.*, **37**, 313–24 (1954)
44. Blum, H. F., Kauzmann, E. F., and Chapman, G. B., *J. Gen. Physiol.*, **37**, 325–34 (1954)
45. Boag, J. W., *Nat. Bur. Standards U. S. Rept., 2946*, (1953)
46. Bonnier, G., *Heredity*, **8**, 199–210 (1954)
47. Bonnier, G., and Lüning, K., *Hereditas*, **39**, 193–200 (1953)
48. Bora, K. C., *J. Genetics*, **52**, 140–51 (1954)
49. Bora, K. C., *Brit. J. Radiol.*, **27**, 124–27 (1954)
50. Bowen, G. H., *Cold Spring Harbor Symposia Quant. Biol.*, **18**, 245–53 (1953)
51. Bowen, G. H., *Ann. Inst. Pasteur*, **84**, 218–21 (1953)
52. Brandt, H., and Dittrich, W., *Strahlentherapie*, **91**, 149–56 (1953)
53. Brown, S. W., and Cave, M. S., *Proc. Natl. Acad. Sci. U. S.*, **39**, 97–102 (1953)
54. Brown, S. W., and Cave, M. S., *Am. J. Botany*, **41**, 455–69 (1954)
55. Brumfield, R. T., *Proc. Natl. Acad. Sci. U. S.*, **39**, 366–71 (1954)
56. Bruns, A., *Angew. Botan.*, **28**, 120–56 (1954)
57. Burns, V. W., *Arch. Biochem. and Biophys.*, **53**, 450–56 (1954)
58. Burns, V. W., *U. S. Atomic Energy Commission Document, UCRL-2812* (1954)[4]
59. Caldecott, R. S., *Science*, **120**, 809–10 (1954)
60. Caldecott, R. S., Beard, B. H., and Gardner, C. O., *Genetics*, **39**, 240–59 (1954)
61. Carlson, J. G., *Radiation Biology*, **1**, 763–824 (A. Hollaender, Ed., McGraw-Hill, New York, N.Y., 1265 pp., 1954)
62. Carlson, J. G., Harrington, N. G., and Gaulden, M. E., *Biol. Bull.*, **104**, 313–22 (1953)
63. Castognoli, C., and Graziosi, F., *Nature*, **174**, 599 (1954)
64. Cave, M. S., and Brown, S. W., *Am. J. Botany*, **41**, 469–83 (1954)
65. Conger, A. D., *Genetics*, **38**, 128–33 (1953)
66. Conger, A. D., *Am. Naturalist*, **88**, 215–24 (1954)
67. Conger, A. D., *Science*, **119**, 36–42 (1954)
68. Constantin, T., and Latarjet, R., *Compt. rend. soc. biol.*, **147**, 1906–9 (1953)
69. Crouse, H. V., *Science*, **119**, 485–87 (1954)
70. Dale, W. M., *Radiation Biology*, **1**, 255–81 (A. Hollaender, Ed., McGraw-Hill, New York, N.Y., 1265 pp., 1954)
71. Daniel, G. E., and Park, H. D., *Proc. Soc. Exptl. Biol. Med.*, **83**, 662–65 (1953)
72. Daniel, G. E., and Park, H. D., *J. Cellular Comp. Physiol.*, **42**, 359–67 (1953)
73. Darlington, C. D., Ed., *Symposium on Chromosome Breakage*, (Charles C Thomas, Publisher, Springfield, Ill., 315 pp., 1953)
74. Darlington, C. D., and LaCour, L. F., *Heredity*, **6**, Suppl., 41–45 (1953)
75. Davis, M., *Arch. Biochem. and Biophys.*, **48**, 469–81 (1954)
76. Davis, M., *Arch. Biochem. and Biophys.*, **49**, 417–23 (1954)
77. de Courcy, S. J., Ely, J. O., and Ross, M. H., *Nature*, **172**, 119 (1953)
78. Delbrück, M., *Angew. Chem.*, **66**, 391–95 (1954)
79. DeSerres, F. J., and Giles, N. H., *Genetics*, **38**, 407–15 (1953)
80. Dessauer, F., *Quantenbiologie*, (Springer-Verlag, Berlin, Germany, 178 pp., 1954)
81. Deysson, G., and Truhaut, R., *Bull. soc. chim. biol.*, **35**, 1019–26 (1953)
82. Deysson, G., and Truhaut, R., *Compt. rend.*, **236**, 2329–20 (1953)
83. Deysson, G., and Truhaut, R., *Compt. rend.*, **238**, 1725–27 (1954)
84. Deysson, G., and Truhaut, R., *Compt. rend.*, **239**, 83–85 (1954)
85. Dieckmann, C., *Strahlentherapie*, **92**, 39–42 (1953)
76. Dieckmann, C., Hofmann, D., Kepp, R. K., and Müller, K., *Strahlentherapie*, **92**, 43–47 (1953)

87. Dittrich, W., and Schubert, G., *Strahlentherapie*, **92**, 532–54 (1953)
88. Dollinger, E. J., *Genetics*, **39**, 750–66 (1954)
89. DuBois, K. B., and Petersen, D. F., *Ann. Rev. Nuclear Sci.*, **4**, 351–76 (1954)
90. Dunn, C. G., *J. Bact.*, 66, 421–23 (1953)
91. Ebert, M., and Alper, T., *Nature*, **173**, 987–89 (1954)
92. Eckart, W., *Strahlentherapie*, **94**, 60–63 (1954)
93. Ehrenberg, L., Gustaffson, A., Lundqvist, U., and Nybom, N., *Hereditas*, **39**, 493–504 (1953)
94. Ehrenberg, L., and Anderson, G., *Nature*, **173**, 1086 (1954)
95. Ehrenberg, L., and Gustaffson, A., *Acta. Radiol.*, **41**, 101–4 (1954)
96. Ehrenberg, L., and Nybom, N., *Acta. Agr. Scand.*, **4**, 396 (1954)
97. Eichel, H. J., and Roth, J. S., *Biol. Bull.*, **104**, 351–58 (1953)
98. Elkind, M., and Beam, C. A., *U. S. Atomic Energy Commission Document, UCRL-2845*, (1954)[4]
99. Epstein, H. T., *Nature*, **171**, 394–95 (1953)
100. Epstein, H. T., and Englander, S. W., *Arch. Biochem. and Biophys.*, **52**, 394–99 (1954)
101. Erdmann, K., *Naturwissenschaften*, **40**, 147 (1953)
102. Erdmann, K., *Naturwissenschaften*, **41**, 189 (1954)
103. Erdmann, K., and Meyer, I., *Naturwissenschaften*, **40**, 347 (1953)
104. Errera, M., *Progr. Biophys. and Biophys. Chem.*, **3**, 88–130 (1953)
105. Errera, M., *Brit. J. Radiol.*, **27**, 76–80 (1954)
106. Fahmy, O. G., and Bird, M. J., *Heredity*, **6**, Suppl., 149–59 (1953)
107. Forssberg, A., *Acta Radiol.*, **41**, 56–58 (1954)
108. Forssberg, A., and Nybom, N., *Physiol. Plantarum*, **6**, 78–95 (1953)
109. Forssberg, A., and Klein, G., *Exptl. Cell Research*, **7**, 480–97 (1954)
110. Franklin, R., *Biochim. et Biophys. Acta*, **13**, 137–38 (1954)
111. Franklin, R., Friedman, M., and Setlow, R. B., *Arch. Biochem. and Biophys.*, **44**, 259–64 (1953)
112. Friedenwald, J. S., and Sigelman, S., *Exptl. Cell Research*, **4**, 1–31 (1953)
113. Friedman, M., *J. Bact.*, **68**, 274–78 (1954)
114. Friedrich-Freksa, H., and Kaudewitz, F., *Z. Naturforsch.*, **8b**, 343–55 (1953)
115. Gaden, E., and Henley, E. J., *J. Bact.*, **65**, 727–32 (1953)
116. Gartner, H., and Peters, K., *Strahlentherapie*, **92**, 555–62 (1953)
117. Gaulden, M. E., Nix, M., and Moshman, J., *J. Cellular Comp. Physiol.*, **41**, 451–70 (1953)
118. Geckler, R. P., and Kimball, R. F., *Science*, **117**, 80–81 (1953)
119. Giese, A. C., *Physiol. Zoöl.*, **26**, 1–22 (1953)
120. Giese, A. C., Iverson, R. M., Shepard, D. C., Jacobson, C., and Brandt, C. L., *J. Gen. Physiol.*, **37**, 249–58 (1953)
121. Giles, N. H., *Proc. 2nd Nat. Cancer Conf.*, 984–96 (1954)
122. Giles, N. H., *Radiation Biology*, **1**, 713–61 (A. Hollaender, Ed., McGraw-Hill, New York, N.Y., 1265 pp., 1954)
123. Giles, N. H., DeSerres, F. J., and Beatty, A. V., *Genetics*, **38**, 416–20 (1953)
124. Giles, N. H., and Tobias, C. A., *Science*, **120**, 993–94 (1954)
125. Glubrecht, H., *Z. Naturforsch.*, **8b**, 17–27 (1953)
126. Glücksmann, A., *Brit. J. Radiol.*, **27**, 660–69 (1954)
127. Goldblith, S. A., Proctor, B. E., Davison, S., Lang, D. A., Kan, B., Bates, C. J., and Karel, M., *Radiology*, **60**, 732–35 (1953)
128. Goldblith, S. A., Proctor, B. E., Davison, S., Kan, B., Bates, C. J., Oberle, E. M., Karel, M., and Lang, D. A., *Food Research*, **18**, 659–77 (1953)

129. Goucher, C. R., Woodside, E. E., and Kocholaty, W., *Arch. Biochem. and Biophys.*, **50**, 25–33 (1954)
130. Graevskii, E. Ya., and Ochinskaya, G. K., *Compt. rend. akad. nauk, S.S.S.R.*, **89**, 737–40 (1953)
132. Gray, L. H., *Heredity*, **6**, Suppl., 311–15 (1953)
133. Gray, L. H., *Brit. J. Radiol.*, **26**, 609–18 (1953)
134. Gray, L. H., *Acta Radiol.*, **41**, 63–83 (1954)
135. Gray, L. H., *Radiation Research*, **1**, 189–213 (1954)
136. Gray, L. H., Conger, A. D., Ebert, M., Hornsey, S., and Scott, O. C. A., *Brit. J. Radiol.*, **26**, 638–48 (1953)
137. Grieff, D., Blumenthal, H. T., Chiga, M., and Pinkerton, H., *J. Exptl. Med.*, **97**, 131–34 (1953)
138. Haas, F. L., Wyss, O., Berger, H., and Stone, W. S., *J. Bact.*, **65**, 354 (1953)
139. Haas, F. L., Dudgeon, E., Clayton, F. E., and Stone, W. S., *Genetics*, **39**, 453–71 (1954)
140. Hall, T. A., *Bull. Math. Biophys.*, **15**, 43–47 (1953)
141. Haque, A., *Heredity*, **6**, Suppl., 35–40 (1953)
142. Haque, A., *Heredity*, **6**, Suppl., 57–75 (1953)
143. Harm, W., and Stein, W., *Z. Naturforsch.*, **8b**, 123–33 (1953)
144. Harm, W., and Stein, W., *Z. Naturforsch.*, **8b**, 729–41 (1953)
145. Heinmets, F., *J, Bact.*, **66**, 455–57 (1953)
146. Heinmets, F., and Kathan, R. H., *Arch. Biochem. and Biophys.*, **53**, 205–27 (1954)
147. Heinmets, F., Lehman, J. J., Taylor, W. W., and Kathan, R. H., *J. Bact.*, **67**, 511–22 (1954)
148. Helmke, R., *Zentr. Bakt. Parasitenk*, **161**, 329–32 (1954)
149. Helmke, R., *Strahlentherapie*, **94**, 430–33 (1954)
152. Herskowitz, I. H., *Proc. Natl. Acad. Sci. U. S.*, **40**, 576–85 (1954)
154. Higginbotham, R. D., and Bowers, J. Z., *Proc. Soc. Exptl. Biol. Med.*, **86**, 303–5 (1954)
155. Hill, R. F., and Rossi, H. H., *Science*, **120**, 142–44 (1954)
156. Hill, R. F., and Rossi, H. H., *Radiation Research*, **1**, 282–93 (1954)
157. Hill, R. F., and Rossi, H. H., *Radiation Research*, **1**, 358–68 (1954)
158. Hirshfield, H., and Giese, A. C., *Exptl. Cell Research*, **4**, 283–94 (1953)
159. Höhne, G., and Schubert, G., *Strahlentherapie*, **94**, 72–78 (1953)
160. Hollaender, A., Ed., *Radiation Biology*, **1** (McGraw-Hill, New York, N.Y., 1265 pp., 1954)
161. Hollaender, A., *Am. Naturalist*, **88**, 209–314 (1954)
162. Hollaender, A., and Stapleton, G., *Brit. J. Radiol.*, **27**, 117–21 (1954)
163. Holt, M. W., Sommers, S. C., and Warren, S., *Lab. Invest.*, **2**, 408–18 (1953)
164. Hotchkiss, R. D., *Proc. Natl. Acad. Sci. U. S.*, **40**, 49–55 (1954)
165. Houtermans, T., *Strahlentherapie*, **92**, 423–36 (1953)
166. Houtermans, T., *Z. Naturforsch.*, **8b**, 767–71 (1953)
167. Houtermans, T., *Z. Naturforsch.*, **9b**, 600–2 (1954)
168. Houtermans, T., *Strahlentherapie*, **93**, 130–37 (1954)
169. Howard, A., and Pelc, S. R., *Heredity*, **6**, Suppl., 261–73 (1953)
170. Iverson, R. M., and Giese, A. C., *Science*, **120**, 504 (1954)
171. Ives, P. T., *Am. Naturalist*, **88**, 361–64 (1954)
172. Ives, P. T., Fenton, B. J., Yost, H. T., and Levine, R. P., *Proc. Natl. Acad. Sci. U. S.*, **39**, 1134–41 (1953)

173. Ives, P. T., Levine, R. P., and Yost, H. T., *Proc. Natl. Acad. Sci. U. S.*, **40**, 165–71 (1954)
174. Kanazir, D., *Biochim. et Biophys. Acta*, **13**, 589–90 (1954)
175. Kanazir, D., *Biochim. et Biophys. Acta*, **15**, 592 (1954)
176. Kanazir, D., *Arch. intern. physiol.*, **62**, 565–66 (1954)
177. Kanazir, D., and Errera, M., *Biochim. et Biophys. Acta*, **11**, 451–52 (1953)
178. Kanazir, D., and Errera, M., *Biochim. et Biophys. Acta*, **14**, 62–66 (1954)
179. Kaplan, R. W., *Arch. Mikrobiol.*, **18**, 210–31 (1953)
180. Kaplan, S., Rosenblum, E. D., and Bryson, V., *J. Cellular Comp. Physiol.*, **41**, 153–62 (1953)
181. Kaplan, W. D., and Lyon, M. F., *Science*, **118**, 776–77 (1953)
182. Kaplan, W. D., and Lyon, M. F., *Science*, **118**, 777–78 (1953)
183. Kaufmann, B. P., *Radiation Biology*, **1**, 627–711 (A. Hollaender, Ed., McGraw-Hill, New York, N.Y., 1265 pp., 1954)
184. Kaufmann, B. P., and Das, N. K., *Proc. Natl. Acad. Sci. U. S.*, **40**, 1052–56 (1954)
185. Kelner, A., *J. Bact.*, **65**, 252–62 (1953)
186. Kepp, R. K., *Strahlentherapie*, **92**, 590–98 (1953)
187. Kepp, R. K., *Acta Radiol.*, **41**, 192–200 (1954)
188. Kihlman, B., *Symbolae Botan. Upsalienses*, **11**, 1–96 (1952)
189. Kihlman, B., *Hereditas*, **38**, 9–127 (1952)
190. Kihlman, B., *Nature*, **174**, 561 (1954)
191. Kimball, R. F., Geckler, R. P., and Gaither, N., *J. Cellular Comp. Physiol.*, **40**, 427–59 (1952)
192. Kimball, R. F., and Gaither, N., *Proc. Soc. Exptl. Biol. Med.*, **82**, 471–77 (1953)
193. King, R. C., *J. Exp. Zoöl.*, **122**, 541–75 (1953)
194. Kirby-Smith, J. S., and Daniels, D. S., *Genetics*, **38**, 375–88 (1953)
195. Kirby-Smith, J. S., and Swanson, C. P., *Science*, **119**, 42–44 (1954)
196. Kleczkowski, J., and Kleczkowski, A., *J. Gen. Microbiol.*, **8**, 135–44 (1953)
197. Klein, G., and Forssberg, A., *Exptl. Cell Research*, **6**, 211–20 (1954)
198. Koller, P. C., *Heredity*, **6**, Suppl., 5–22 (1953)
199. Koller, P. C., *Progr. Biophys. and Biophys. Chem.*, **4**, 195–243 (1954)
200. Kölmark, G., *Hereditas*, **39**, 270–76 (1953)
201. Kölmark, G., and Westergaard, M., *Hereditas*, **39**, 209–24 (1953)
202. Kurabayashi, M., *Cytologia*, **18**, 253–65 (1953)
203. Kutschera, G., *Chromosoma*, **6**, 371–80 (1954)
204. Labaw, L. W., Mosley, V. M., and Wyckoff, R. W. G., *J. Bact.*, **65**, 330–36 (1953)
205. Labrum, E. L., *Proc. Natl. Acad. Sci. U. S.*, **39**, 1221–27 (1953)
206. Lacassagne, A., *J. radiol. et électrol.*, **35**, 12–15 (1954)
207. LaCour, L. F., and Rutishauser, A., *Nature*, **172**, 501–2 (1953)
208. LaCour, L. F., and Rutishauser, A., *Chromosoma*, **6**, 696–709 (1954)
209. Lane, G. R., *Heredity*, **6**, Suppl., 23–24 (1953)
210. Langendorff, H., Langendorff, M., and Sommermeyer, K., *Z. Naturforsch.*, **8b**, 117–22 (1953)
211. Langendorff, H., Langendorff, M., and Sommermeyer, K., *Naturwissenschaften*, **41**, 189–90 (1954)
212. Lark, K. G., and Maaløe, O., *Biochim. et Biophys. Acta*, **15**, 345–56 (1954)
213. Laser, H., *Nature*, **174**, 753 (1954)
214. Lasnitzki, I., *Brit. J. Radiol.*, **27**, 228–35 (1954)

215. Latarjet, R., *Acta Radiol.*, **41**, 84–100 (1954)
216. Latarjet, R., Caldas, L. R., Milétic, B., and Morenne, P., *Brit. J. Radiol.*, **27**, 54–56 (1954)
217. Lea, D. E., *Actions of Radiations on Living Cells*, revised ed., (Cambridge University Press, London, England, 416 pp., 1955)
218. Lefevre, G., Ratty, F. J., Jr., and Hanks, G. D., *Genetics*, **38**, 345–59 (1953)
219. Lennox, E. S., Luria, S. E., and Benzer, S., *Biochim. et Biophys. Acta*, **15**, 471–74 (1954)
220. Lewis, D., and Crowe, L. K., *Nature*, **172**, 501 (1953)
221. Lewis, E. B., *Am. Naturalist*, **88**, 225–38 (1954)
222. Lindenmann, J., *Oncologia*, **6**, 1–26 (1953)
223. Lindenmann, J., *Experientia*, **9**, 22–23 (1953)
224. Lovelace, R., *Proc. Natl. Acad. Sci. U. S.*, **40**, 1129–35 (1954)
225. Lucke, W. H., and Sarachek, A., *Nature*, **171**, 1014–15 (1953)
226. Luers, H., *Arch. Geschwulstforsch.*, **6**, 77–83 (1953)
227. Luers, H., *Naturwissenschaften*, **40**, 293 (1953)
228. Lüning, K. G., *Hereditas*, **38**, 321–38 (1952)
229. Lüning, K. G., *Drosophila Information Service*, **27**, 99–100 (1953)
230. Lüning, K. G., *Heredity*, **8**, 211–23 (1954)
231. MacKey, J., *Hereditas*, **40**, 65–180 (1954)
232. McLeish, J., *Heredity*, **6**, Suppl., 125–48 (1953)
233. McLeish, J., *Heredity*, **8**, 385–407 (1954)
234. McQuate, J. T., *Genetics*, **39**, 565–80 (1954)
235. Magni, G. E., *Atti VIII congr. nazl. microbiol.*, 194–99 (1952)
236. Magni, G. E., *Ist. botan. univ. Lab. crittogram Pavia, Atti, Ser. 5*, **10**, 89–97 (1953)
237. Magni, G. E., *Ist. botan. univ. Lab. crittogram. Pavia, Atti, Ser. 5*, **10**, 201–10 (1953)
238. Magni, G. E., Brazolla, A. M., and Bollea, F., *Ist. botan. univ. Lab. crittogram Pavia, Atti, Ser. 5*, **10**, 161–72 (1953)
239. Markert, C. L., *Exptl. Cell. Research*, **5**, 427–35 (1953)
240. Marquardt, H., *Strahlentherapie*, **94**, 608–31 (1954)
241. Maxwell, E., and Ashwell, G., *Arch. Biochem. and Biophys.*, **43**, 389–98 (1953)
242. Mazia, D., *Proc. Natl. Acad. Sci. U. S.*, **40**, 521–27 (1954)
243. Mefferd, R. B., and Loefer, J. B., *Physiol. Zoöl.*, **26**, 341–44 (1954)
244. Mehtab, M., *Nature*, **171**, 262 (1953)
245. Menten, M. L., Feldsted, E. T., and Willms, M., *Exptl. Cell Research*, **7**, 83–94 (1954)
246. Michaelis, P., *Naturwissenschaften*, **41**, 22 (1954)
247. Michaelis, P., and Kaplan, R., *Naturwissenschaften*, **40**, 534 (1953)
248. Mickey, G. H., *Am. Naturalist*, **88**, 241–55 (1954)
249. Mikaelsen, K., *Proc. Natl. Acad. Sci. U. S.*, **40**, 171–78 (1954)
250. Mikaelsen, K., and Halvorsen, H., *Physiol. plantarum*, **6**, 873–79 (1953)
251. Milétic, B., *Compt. rend.*, **238**, 1541–42 (1954)
252. Mitchell, J. S., and Holmes, B., *Brit. J. Radiol.*, **27**, 36–80; 117–44 (1954)
253. Mittler, S., and Laverty, J. A., *Nature*, **171**, 793 (1953)
254. Montgomery, P. O'B., and Warren, S., *Science*, **117**, 589–91 (1953)
255. Moos, W. S., *Nucleonics*, **12** (5), 46–49 (1954)
256. Morowitz, H. J., *Arch. Biochem. and Biophys.*, **47**, 325–37 (1953)

257. Mortimer, R. K., *U. S. Atomic Energy Commission Document, UCRL-1922*, (1952)[4]; *Radiation Research*, **1**, 225 (1954)
258. Mortimer, R. K., and Tobias, C. A., *Science*, **118**, 517–18 (1953)
259. Moutschen, J., and Govaerts, J., *Nature*, **172**, 350 (1953)
260. Muller, H. J., *Radiation Biology*, **1**, 351–473; 475–626 (A. Hollaender, Ed., McGraw-Hill, New York, N.Y., 1265 pp., 1954)
261. Muller, H. J., *Am. Naturalist*, **88**, 437–60 (1954)
262. Muller, H. J., and Herskowitz, I. H., *Am. Naturalist*, **88**, 177–208 (1954)
263. Muller, H. J., Herkowitz, I. H., Abrahamson, S., and Oster, I. I., *Genetics*, **39**, 741–49 (1954)
264. Muller, H. J., Altenburg, L. S., Meyer, H. V., Edmundson, M., and Altenburg, E., *Heredity*, **8**, 153–86 (1954)
265. Müller, K., and Hase, H., *Strahlentherapie*, **92**, 33–38 (1953)
266. Nakao, Y., *Nature*, **172**, 625–26 (1953)
267. Nasrat, G. E., Kaplan, W. D., and Auerbach, C., *Z. ind. Abstam. Verebungsl.*, **86**, 249–62 (1954)
268. Newcombe, H. B., *J. Gen. Microbiol.*, **9**, 30–36 (1953)
269. Newcombe, H. B., *Genetics*, **38**, 134–51 (1953)
270. Newcombe, H. B., and McGregor, J. F., *Genetics*, **39**, 619–27 (1954)
271. Nilan, R. A., *Genetics*, **39**, 943–53 (1954)
272. Nishiwaki, Y., *Yokohama Med. Bull.*, **4**, 346 (1953)
273. Nishiwaki, Y., *Yokohama Med. Bull.*, **5**, 21–31 (1954)
274. Norman, A., *J. Bact.*, **65**, 151–56 (1953)
275. Norman, A., *J. Cellular comp. physiol.*, **44**, 1–10 (1954)
276. Nybom, N., *Hereditas*, **39**, 317–24 (1953)
277. Nybom, N., Lundqvist, U., Gustafsson, A., and Ehrenberg, L., *Hereditas*, **39**, 445–57 (1953)
278. Oehklers, F., *Heredity*, **6**, Suppl., 95–105 (1953)
279. Parker, D. R., *J. Tenn. Acad. Sci.*, **28**, 185 (1953)
280. Parker, D. R., *Proc. Natl. Acad. Sci. U. S.*, **40**, 795–800, (1954)
281. Passonneau, J. V., *Physiol. Zoöl.*, **27**, 119–28 (1954)
282. Patt, H. M., *Physiol. Revs.*, **33**, 35–76 (1953)
283. Perlitsh, M., and Kelner, A., *Science*, **118**, 165–66 (1953)
284. Peters, K., *Z. Zellforsch. u. mikroskop. Anat.*, **39**, 203–11 (1953)
285. Peters, K., *Z. Zellforsch. u. mikroskop. Anat.*, **39**, 414–20 (1954)
286. Peters, K., *Z. Zellforsch. u. mikroskop. Anat.*, **40**, 510–18 (1954)
287. Peters, K., *Naturwissenschaften*, **41**, 89–90 (1954)
288. Peters, K., *Strahlentherapie*, **93**, 263–73 (1954)
289. Peters, K., *Strahlentherapie*, **95**, 283–90 (1954)
290. Pittenger, R. C., and McCoy, E., *J. Bact.*, **65**, 56–64 (1953)
291. Pohley, H. J., *Naturwissenschaften*, **40**, 146–47 (1953)
292. Pollard, E. C., *The Physics of Viruses* (Academic Press, Inc., New York, N.Y., 230 pp., 1953)
293. Pollard, E. C., and Setlow, J., *Arch. Biochem. and Biophys.*, **50**, 376–82 (1954)
294. Pollard, E. C., Adams, W. R., and Robbins, S., *Radiation Research*, **1**, 514–22 (1954)
295. Porter, J. W., and Knauss, H. J., *Plant Physiol.*, **29**, 60–63 (1954)
296. Porter, J. W., and Knauss, H. J., *Radiation Research*, **1**, 253–61 (1954)
297. Porter, J. W., and Watson, M. S., *Am. J. Botany*, **41**, 550–55 (1954)

298. Rajewsky, B., *Strahlendosis und Strahlenwirkung*, (Georg Thieme Verlag, Stuttgart, Germany, 184 pp., 1954)
299. Ray, D. T., and Whiting, D. W., *Biol. bull.*, **106**, 100–6 (1954)
300. Ray-Chaudhuri, S. P., and Pyne, C. P., *Science*, **119**, 685–86 (1954)
301. Read, J., *Brit. J. Radiol.*, **27**, 635–38 (1954)
302. Read, J., *J. Genetics*, **52**, 473–79 (1954)
303. Rees, H., *Heredity*, **6**, Suppl., 235–45 (1953)
304. Reinholz, E., and Aurand, K., *Strahlentherapie*, **94**, 646 (1954)
305. Revell, S. H., *Heredity*, **6**, Suppl., 107–24 (1953)
306. Ritchie, D., *Botan. Gaz.*, **115**, 138–46 (1953)
307. Rubin, B. A., *J. Bact.*, **67**, 361–68 (1954)
308. Rubin, B. A., *Genetics*, **39**, 296–306 (1954)
309. Russell, W. L., *Radiation Biology*, **1**, 825–60 (A. Hollaender, Ed., McGraw-Hill, New York, N.Y., 1265 pp., 1954
310. Russell, W. L., Russell, L. B., and Kimball, A. W., *Am. Naturalist*, **88**, 269–86 (1954)
311. Ryan, F. J., *Proc. Natl. Acad. Sci. U. S.*, **40**, 178–86 (1954)
312. Sarachek, A., *Experientia*, **10**, 377–78 (1954)
313. Sarachek, A., *Exptl. Cell Research*, **6**, 45–55 (1954)
314. Sarachek, A., *Cytologia*, **19**, 77–85 (1954)
315. Sarachek, A., and Lucke, W. H., *Arch. Biochem. and Biophys.*, **44**, 271–79 (1953)
316. Sarachek, A., and Lucke, W. H., *Experientia*, **9**, 374–76 (1953)
317. Sarachek, A., Shult, E. E., and Lindegren, C. C., *Arch. Biochem. and Biophys.*, **51**, 340–49 (1954)
318. Sax, K., and Luippold, H., *Heredity*, **6**, 127–32 (1952)
319. Sayeg, J. A., *U. S. Atomic Energy Commission Document, UCRL-2293* (1954)[4]
320. Scheibe, A., and Bruns, A., *Angew. Botan.*, **27**, 70–74 (1953)
321. Scherbaum, O., and Zeuthen, E., *Exptl. Cell Research*, **6**, 221–27 (1954)
322. Scherer, E., Ringleb, D., and Ventzke, L. E., *Strahlentherapie*, **90**, 41–52 (1953)
323. Schmidlin-Mészáros, J., *Fortschr. Gebiete Röntgenstrahlen*, **81**, 76–84 (1954)
324. Schneiderman, H. A., and King. E. D., *Proc. Natl. Acad. Sci. U. S.*, **39**, 834–38 (1953)
325. Schoenborn, H. W., *Physiol. Zoöl.*, **26**, 312–19 (1953)
326. Schweisfurth, R., and Schwartz, W., *Naturwissenschaften*, **41**, 42–43 (1954)
327. Singleton, W. R., *Genetics*, **39**, 587–603 (1954)
328. Singleton, W. R., and Caspar, A. L., *Genetics* (In press)
329. Six, E., *Z. Naturforsch.*, **9b**, 265–73 (1954)
330. Smith, D. B., *Can. J. Med. Sci.*, **31**, 290–301 (1953)
331. Smith, H. H., and Lotfy, T. A., *Am. J. Botany*, **41**, 589–95 (1954)
332. Sobels, F. H., *Am. Naturalist*, **88**, 109–12 (1954)
333. Sparrow, A. H., and Christensen, E., *Science*, **118**, 697–98 (1953)
334. Sparrow, A. H., and Forro, F., *Ann. Rev. Nuclear Sci.*, **3**, 339–68 (1953)
335. Sparrow, A. H., and Singleton, W. R., *Am. Naturalist*, **87**, 29–48 (1953)
336. Spear, F. G., *Radiations and Living Cells*, (John Wiley and Sons, New York, N.Y., 222 pp., 1953)
337. Spiegelman, S., and Landman, O. E., *Ann. Rev. Microbiol.*, **8**, 181–236 (1954)
338. Spencer, J. L., and Blakeslee, A. F., *Proc. Natl. Acad. Sci., U. S.*, **40**, 441–46 (1954)

339. Spencer, J. L., Singleton, W. R., and Blakeslee, A. F., *Proc. Natl. Acad. Sci. U. S.*, **39**, 288–91 (1953)
340. Spoerl, E., and Carleton, R., *J. Biol. Chem.*, **210**, 521–29 (1954)
341. Spoerl, E., Loveless, L. E., Weisman, T. H., and Balske, R. J., *J. Bact.*, **67**, 394–401 (1954)
342. Stadler, L. J., *Science*, **120**, 811–19 (1954)
343. Stapleton, G. E., Billen, D., and Hollaender, A., *J. Cellular Comp. Physiol.*, **41**, 345–58 (1953)
344. Steffensen, D., *Exptl. Cell Research*, **6**, 554–56 (1954)
345. Steffensen, D., *Proc. Natl. Acad. Sci. U. S.*, **39**, 613–20 (1954)
346. Steffensen, D., and Arnason, T. J., *Genetics*, **39**, 220–28 (1954)
347. Stein, W., and Harm, W., *Z. Naturforsch.*, **8b**, 742–54 (1953)
348. Stent, G. S., *Cold Spring Harbor Symposia. Quant. Biol.*, **18**, 255–59 (1953)
349. Stone, W. S., Alexander, M. L., Clayton, F. E., and Dudgeon, E., *Am. Naturalist*, **88**, 287–93 (1954)
350. Stone, W. S., Haas, F. L., Alexander, M. L., and Clayton, F. E., *Univ. of Texas Publication, #5422*, 244–71 (1954)
351. Strugger, S. P., Krebs, A. T., and Gierlach, Z. S., *Am. J. Roentgenol. Radium Therapy Nuclear Med.*, **70**, 365–75 (1953)
352. Sussman, A. S., *J. Cellular Comp. Physiol.*, **42**, 273–83 (1953)
353. Swanson, C. P., and Schwartz, D., *Proc. Natl. Acad. Sci. U. S.*, **39**, 1241–50 (1954)
354. Swanson, C. P., Rupert, C. S., and Yost, H. T., Jr., *Am. J. Botany*, **40**, 557–64 (1953)
355. Swanson, C. P., and Johnston, A. H., *Am. Naturalist*, **88**, 425–30 (1954)
356. Tahmisian, T. N., and Vogel, H. H., Jr., *Proc. Soc. Exptl. Biol. Med.*, **84**, 538–43 (1953)
357. Tahmisian, T. N., Passonneau, J. N., and Adamson, D. M., *J. Natl. Cancer Inst.*, **14**, 941–52 (1954)
358. Tanada, T., and Hendricks, S. B., *Am. J. Botany*, **40**, 634–37 (1953)
359. Telfer, J. D., *Am. Naturalist*, **88**, 117–18 (1954)
360. Teti, M., *Compt. rend. soc. biol.*, **148**, 210–12 (1954)
361. Thoday, J. M., *Heredity*, **6**, Suppl., 299–309 (1954)
362. Thoday, J. M., *New Phytologist*, **53**, 511–16 (1954)
363. Tillotson, F. W., and Warren, S., *Radiology*, **61**, 249–60 (1953)
364. Timonen, S., *Exptl. Cell Research*, **4**, 142–50 (1953)
365. Ting, T. P., Chinn, H. F., and Johns, H. E., *Rev. can. biol.*, **11**, 389–400 (1952)
366. Tipton, S. R., and St. Amand, G. S., *Physiol. Zoöl.*, **27**, 311–16 (1954)
367. Tobias, C. A., *Acta. Radiologica*, **41**, 105–8 (1954)
368. Townsend, G. F., and Sarachek, A., *J. Bact.*, **65**, 747–49 (1953)
369. Townsend, G. F., Sarachek, A., and Lindegren, C. C., *Cytologia*, **19**, 130–32 (1954)
370. Trowell, O. A., *Brit. J. Radiol.*, **26**, 302–9 (1953)
371. Uretz, R. Z., *Radiation Research*, **1**, 564–65 (1954)
372. Uretz, R. Z., Bloom, W., and Zirkle, R. E., *Science*, **120**, 197–99 (1954)
373. Virgin, H. I., and Ehrenberg, L., *Physiol. plantarum*, **6**, 159–65 (1953)
374. Wainwright, S. D., and Mullaney, J., *Experientia*, **9**, 376–77 (1953)
375. Warren, S., *Chemical Specificity in Biological Interactions*, 17–28, (F. R. Gurd, Ed., Academic Press, Inc., New York, N.Y., 234 pp., 1954)

376. Weigle, J. J., *Proc. Natl. Acad. Sci. U. S.*, **39**, 628–36 (1953)
377. Weigle, J. J., and Dulbecco, R., *Experientia*, **9**, 372 (1953)
378. Welsh, J. N., and Adams, M. H., *J. Bact.*, **68**, 122–27 (1954)
379. Whipple, G. H., *J. Cellular Comp. Physiol.*, **43**, 415–23 (1954)
381. Whiting, A. R., and von Borstel, R. C., *Genetics*, **39**, 317–25 (1954)
382. Wichterman, R., and Figge, F. H. J., *Biol. Bull.*, **106**, 253–63 (1954)
383. Witkin, E. M., *Proc. Natl. Acad. Sci. U. S.*, **39**, 427–33 (1953)
384. Woese, C., and Pollard, E., *Arch. Biochem. and Biophys.*, **50**, 354–67 (1954)
385. Wolff, S., *Nature*, **173**, 501–2 (1954)
386. Wolff, S., *Genetics*, **39**, 356–64 (1954)
387. Wolff, S., and Atwood, K. C., *Proc. Natl. Acad. Sci. U. S.*, **40**, 187–92 (1954)
388. Wolff, S., and von Borstel, R. C., *Proc. Natl. Acad. Sci. U. S.*, **40**, 1138–41 (1954)
389. Wood, T. H., *Proc. Soc. Exptl. Biol. Med.*, **84**, 446–52 (1953)
390. Wood, T. H., *Arch. Biochem. and Biophys.*, **52**, 157–74 (1954)
391. Wood, T. H., *Nature*, **173**, 641–42 (1954)
392. Yanders, A. F., *Genetics*, **39**, 558–64 (1954)
393. Yanofsky, C., *J. Bact.*, **65**, 383–87 (1953)
394. Yost, H. T., Jr., Singleton, W. R., and Blakeslee, A. F., *Proc. Natl. Acad. Sci. U. S.*, **39**, 292–97 (1953)
395. Yost, H. T., Jr., Cummings, J., and Blakeslee, A. F., *Proc. Natl. Acad. Sci. U. S.*, **40**, 447–51 (1954)
396. Young, W. J., Yost, H. T., Jr., Ives, P. T., and Levine, R. P., *Proc. Natl. Acad. Sci. U. S.*, **39**, 488–95 (1953)
397. Zelle, M. R., *Ann. Rev. Microbiol.*, **9**, (1955)
398. Zelle, M. R., and Hollaender, A., *J. Bact.*, **68**, 210–15 (1954)
399. Zirkle, R. E., *Radiation Biology*, **1**, 315–50 (A. Hollaender, Ed., McGraw-Hill, New York, N.Y., 1265 pp., 1954)
400. Zirkle, R. E., and Bloom, W., *Science*, **117**, 487–93 (1953)
401. Zirkle, R. E., and Tobias, C. A., *Arch. Biochem. and Biophys.*, **47**, 282–306 (1953)

REMOVAL OF RADIOELEMENTS FROM THE MAMMALIAN BODY[1]

By Jack Schubert

Division of Biological and Medical Research, Argonne National Laboratory, Lemont, Illinois

INTRODUCTION

The lethal effects of radioactive isotopes were shown early in 1904 by Pierre Curie and two medical colleagues (1). They exposed experimental animals to atmospheres of radon and found that death followed in a matter of hours. In the same experiment Curie demonstrated by means of radioautographs that the radioactive daughters of radon were present to varying extents in all the tissues; it is now known that these contribute to the radiotoxicological effects.

Probably the first death in a human from acute radioactive poisoning was reported by Gudzent in 1912 (2). A 58-year-old woman suffering from arthritis was given frequent injections during a 16-day period of large amounts of Ra^{224} (thorium X). It was hoped that the radium injections would cure her arthritis. Instead she died 26 days after her last injection with the typical symptoms of radiation sickness including bloody stools, hemorrhages, and diarrhea.

Radioactive isotopes when swallowed, inhaled, or injected may cause acute or chronic injury or death solely because of the ionizing radiation emitted by these isotopes within the body. Radioactive poisoning of a chronic type is a slow insidious disease in which a person is usually in good health for many years before detectable symptoms occur. The resulting injuries include various types of anemias, leukemia, crippling lesions of the bone, and bone tumors. Thousands of individuals have suffered injuries or death from chronic radioactive poisoning.

Radioactive substances can produce injury when either outside or inside the body. However, external irradiation is easily avoided by removal of the source or by surrounding the radioisotope with sufficient shielding. When the radioisotope is contained in the body it constitutes a far greater hazard because the internal tissues are irradiated continuously until the isotope is eliminated in the urine and feces, or else loses its radioactivity by natural decay. The most dangerous radioisotopes are those retained in the body for

[1] Inasmuch as there have been no previous reviews of this subject published in this journal or elsewhere, I have taken the liberty of going back to the earliest literature and bringing the subject up to the present. This review also includes interpretative material which has not been published heretofore. The survey of literature pertaining to this review was concluded in July, 1955. I am particularly indebted to Dr. Marcia White Rosenthal who has given freely of her time to correct and edit this article. Responsibility for any errors of omission or commission is the author's.

periods of years and which possess half-lives ranging from a few months to thousands of years.

Until 1939 radioactive poisoning in humans was caused almost entirely by radon (Rn^{222}), and three naturally occurring isotopes of radium: radium (Ra^{222}), mesothorium (Ra^{228}), and thorium X (Ra^{224}). The discovery of nuclear fission and chain-reacting piles resulted in a tremendous increase in both the kinds and amounts of potentially hazardous radioisotopes. Consider the following facts: The production of radium from the time of its discovery in 1898 to the present totals about one and a half kilograms or 1500 curies. Death or injury from pure radium (Ra^{226}) retained in the body has been observed with as little as 0.5 microcurie. Nuclear reactors now produce hundreds of different radioactive isotopes in meagacurie amounts (3). In 1954 the United States Atomic Energy Commission shipped 15,000 curies of radioisotopes from Oak Ridge to be used in research, industry, and medicine.

In Table I are listed those radioactive elements which are the most serious health hazards in atomic energy operations, both from the standpoint of quantities available and amount of use. The health problems associated with these elements exist potentially for miners and millers of uranium and other radioactive ores, personnel of atomic energy plants, residents of areas in

TABLE I

POTENTIALLY HARMFUL RADIOACTIVE ELEMENTS ENCOUNTERED IN ATOMIC ENERGY OPERATIONS*

Element	Chemical symbol	Fission yield in per cent	Half-life	Principal radiation emitted as internal hazard
Plutonium	Pu^{239}	—	24,360 y	α
Radium	Ra^{226}	—	1,622 y	α
Radon	Rn^{222}	—	3.825 d	α
Polonium	Po^{210}	—	138 d	α
Iodine	I^{131}	—	8.1 d	β^-
Cobalt	Co^{60}	—	5.3 y	β^-
Phosphorus	P^{32}	—	14.3 d	β^-
Carbon	C^{14}	—	5600 y	β^-
Promethium	Pm^{147}	2.6	2.6 y	β^-
Cerium	Ce^{144}	6.0	282 d	β^-
Cesium	Cs^{137}	5.9	33 y	β^-
Ruthenium	Ru^{106}	0.4	1.0 y	β^-
Strontium	Sr^{90}	5.8	28 y	β^-

* Data on fission yields and half-lives of fission products provided by L. E. Glendenin and E. P. Steinberg, Personal communication. The half-lives of the other elements are taken from the tables by Hollander, Perlman & Seaborg (4).

which radioactive sewage and wastes are released, people administering or receiving radioactive isotopes and x-rays in medicine, and users of radioactive isotopes in research and industry. Industrial uses where health hazards may exist include the preparation and application of luminous paints, static eliminators, and gas mantles made from thorium and the use of radiation sources for food and pharmaceutical sterilization (5).

Despite the widespread and increasing handling of radioisotopes it is possible to handle even megacurie amounts safely if suitable precautions are taken. However, even under the best conditions, accidents can and do happen. As a result, radioactive isotopes gain entrance into the body by ingestion, inhalation, or by injection into the bloodstream usually through the broken skin.

The necessity for the development of methods of treating radioactive poisoning—particularly the chronic type—is demonstrated by the fact that even in the past decade significant, though not necessarily harmful, levels of radioisotopes have gained entrance into numerous individuals, including the following cases: (*a*) a group of uranium miners were reported in 1954 to have accumulated in the body polonium (Po^{210}) derived from daughter products of radon deposited in the lung (6); (*b*) in 1953 it was reported that in 27 individuals the body levels of plutonium (Pu) ranged from 0.1 to 1.2 μg. (7); (*c*) strontium (Sr^{90}) was inhaled during a laboratory operation (8); (*d*) radium sulfate dust was inhaled by a total of seven persons in three different accidents (8, 9, 10); (*e*) a solution of radium salts was injected intravenously during a suicidal attempt (10).

SCOPE OF PAPER

In most cases, the radioelements with which we are concerned are metals, so that this discussion is limited mainly to poisoning by radioactive metals. Effective treatment for chemical poisoning by metals is available in many cases. Successful treatment, however, for persons who have accumulated radioactive metals in the body is still severely limited except in the earliest stages after exposure. It is our intention to discuss: (*a*) similarities and differences in approach inherent in the treatment of nonradioactive metal and radioactive metal poisons; (*b*) the potential advantages and disadvantages of different treatments; and (*c*) new or untried possibilities for treatment.

GENERAL APPROACHES TO TREATMENT

By treatment we mean the prevention, elimination, or alleviation of the harmful effects caused by a poisonous substance. In the treatment of radioactive poisoning we must deal with many interrelated factors.

Once the route of entry into the body and chemical nature of the poisonous substance is known, then choice of treatment is partially governed by a time element. Immediately after exposure the object of treatment is to minimize absorption of the posion into the bloodstream. After absorption of a nonradioactive poisonous metal one can either hasten its rate of elimination

from the body or inactivate the poison *in situ* so that it can no longer react with surrounding tissue. However, with radioactive poisons the main object is to accelerate excretion or possibly in acute cases to shift the radioelement from radiosensitive to less radiosensitive organs. However, from the chronic standpoint all tissues may be roughly equivalent in susceptibility to radiation effects. Since it is impossible to change the radioactive properties, treatment by inactivation *in situ* is not practical. A treatment designed to remove a radioisotope from the body may either remove it from various organs or may only cause the excretion of the circulating fractions. It is always helpful to determine the total amount of a radioisotope in the blood just before the onset of treatment.

In the sections to follow the problems of treatment are described in more detail. It is well to emphasize that no one treatment can always be generally applied, but the proper treatment must be evaluated in each case; good treatment for one case may be harmful in another, even though the same poison is involved. One must take into consideration factors such as the chemical nature of the metal poison, route of entry into the body, age and health of the patient, time elapsed after exposure, and other factors which will become evident.

The treatment of chronic radioactive poisoning is an extremely difficult problem because the excretion rate of the radioiosotope is very low—0.002 per cent a day or less in many cases. Even if one induces a tenfold increase in the rate of elimination, the actual amounts retained in the body remain essentially unchanged. In order to reduce appreciably the deposits in the body, treatment for chronic cases would have to be maintained for several years. This presents may practical problems such as cooperation of the patient and the effects of prolonged treatment on health.

The chances of reducing the body content of a radioisotope are far greater in the early stages after exposure. During the first few weeks after exposure it is generally found that significant fractions of the deposited radioisotopes are present in the soft tissues and bloodstream from which they are more readily mobilized than from the bone. Also those fractions in the bone, at least in the case of radium and the other alkaline earths, are more readily mobilized at this time. This was explained by Aub *et al.* as follows (11):

> At first, a heavy metal is stored largely in the bone trabeculae, there being from 10 to 16 times as much per gram in the trabeculae as in the cortex of the bone. During the following months there is a redistribution and the concentration becomes equal in both trabeculae and cortex. Because the cortex is far heavier than the trabeculae, this means that most of the radium is stored in cortical bone. . . . The wide distribution in soft-tissues and then the accumulation in the bones implies considerable circulation in the blood and, therefore, a chance for rapid excretion. The first large storage in the trabeculae (where inorganic salts are readily deposited and also readily liberated), would allow a continued though less rapid excretion. When the radium finally accumulates in the cortex, it is to be expected that excretion would be slow and relatively poorly influenced by therapy.

A striking illustration of the transport of calcium and lead from trabeculae and cortex in animals has been reported recently by Aub *et al.* (12). In these experiments alizarin staining was used to follow calcium metabolism, while lead distribution was followed with radiolead.

It is not certain, however, that a significant degree of translocation of radioisotopes from the trabeculae to the cortex occurs in adult humans. Radioautographs of bones in humans taken 20 or more years after exposure show highly concentrated deposits of radium in trabecular bone (13). Further, the deposition of an α-emitting isotope tends to destroy the trabeculae (14).

TREATMENT BY MINIMIZATION OF ABSORPTION OF THE RADIOELEMENT

Oral Ingestion

Treatment after oral ingestion of a radioelement must start as soon as possible. If results from experiments on rats can be extrapolated to man, the only way to minimize absorption of soluble radioisotopes, such as radiostrontium, is to start treatment immediately. Treatment is ineffective if begun only 10 min. after ingestion (15). After oral ingestion, there are three obvious appreaches to treatment: (*a*) use of an emetic; (*b*) minimization of absorption from the gastrointestinal tract by the use of precipitating agents, and (*c*) hastening elimination of the radioactive element by the use of selected cathartics. A knowledge of the chemical properties of radioactive elements is extremely important when choosing a suitable precipitating agent.

In the case of elements which form insoluble hydroxides at physiological pH, treatment, except for a cathartic, may not be needed because the degree of absorption from the gastrointestinal tract is very small. In the case of plutonium and the rare earths, for example, absorption is usually less than 0.01 per cent. Therefore, for Pu, Po, Ce (cerium), and Pm (promethium), the use of precipitating agents can probably be omitted. When very large amounts are swallowed it might be advisable to decrease the solubility of the radioistope by raising the pH of the gastric juice by oral ingestion of nonsystemic antacids such as magnesium oxide, Sippy powders, or aluminum hydroxide. An antacid in combination with a cathartic would appear to be the best approach. In the case of the rare earth elements which are more soluble than plutonium, it is possible that oxalate-containing foods such as rhubarb and spinach or a finely divided carboxylic type cation exchange resin such as Amberlite IRC-50[2] may bind the radioisotopes. In cases of oral ingestion it may be advisable to avoid the use of chelating agents which would increase the solubility of the metal. Nonspecific ion exchange absor-

[2] Produced by Rohm and Haas Co., Washington Square, Philadelphia, Pennsylvania (U.S.A.). The resins are available in low cross-linked forms which undergo considerable swelling in solution. The bulk furnished by the swelled resins may increase the efficiency of removal of the radioisotope from the gastrointestinal tract.

bents such as insoluble zirconium salts might be of value (see section on colloidal carriers).

The alkaline earth group of elements is absorbed to a significant extent from the gastrointestinal tract. Since Ra and Sr form insoluble sulfates, the treatment of choice would appear to be magnesium sulfate in combination with a laxative and possibly an antacid as well. In rats, MacDonald and associates (16) have shown that oral ingestion of magnesium sulfate by rats immediately following the administration by stomach tube of strontium as Sr^{90} decreased the skeletal accumulation of Sr^{90} from 16 per cent to 5 per cent. Also effective were the ammonium salt of an amidopolyphosphate and carboxylic type cation exchange resins. Certain substances including powdered milk actually enhanced the absorption of Sr^{90} from the stomach. The chelating agent, ethylenediaminetetraacetic acid (EDTA) was ineffective.

Copp & Greenberg (15) found that a 5 per cent suspension of tricalcium phosphate in $12\frac{1}{2}$ per cent disodium phophate solution reduced intestinal absorption of Sr only when given immediately after the Sr. None of the following orally administered agents were effective when given 10 min. after the ingestion of radiostrontium by rats: carrier strontium, magnesium sulfate, sodium silicate, sodium bicarbonate, or disodium phosphate.

Experiments with rats have indicated that the maintenance of a high level of calcium intake decreases absorption of Sr and presumably Ra from the stomach (17).

Inhalation

The inhalation of soluble forms of radium and strontium is nearly equivalent to an intravenous injection. Absorption from the lungs is so rapid that treatment is largely similar to that required following injection into the bloodstream. However, the upper nasal passages do retain some of the radioisotope. In one case (8) where a human inhaled $Sr^{90}Cl_2$ from an aqueous solution, the upper nasal passages were sprayed with 0.25 per cent neosynephrine solution with the thought that vasoconstriction might lessen absorption and that shrinkage of the mucous membranes would facilitate a thorough washing. The nasal passages were then washed out with large quantities of isotonic saline solution. About 95 per cent of the Sr^{90} retained in the nose region appeared to have been removed. The use of nasal swabs to remove material clinging to the nasal hairs before irrigation should be valuable. However, most of the inhaled Sr^{90} was absorbed as shown by high urine counts.

Following inhalation of insoluble types of radioactive elements extent of retention in the lungs depends on the particle size of the inhaled substance. The first step in treatment of fractions retained in the lung is the thorough use of a nasal swab (7). In addition it appears advisable to administer a laxative, as was done by Rajewsky & Muth (10), because a large amount of the insoluble material in the lungs is propelled to the mouth, swallowed,

and excreted in the feces. The use of expectorants may also help to hasten elimination.

Drugs which enhance macrophage movements might accelerate the elimination of insoluble particles from the lungs. Easton (18) claims to have accelerated the elimination of intravenously-injected thorium dioxide deposited in the lungs of mice. He used carbon tetrachloride—obviously impractical for humans—as a general accelerator of macrophage movements.

The biological half-life of insoluble substances in the lungs may be months. During this time a slow absorption of the radioelement from the lungs to the bloodstream occurs (19). In such an event it would be helpful if the excretion of the circulating radioisotope could be increased. For Pu and the rare earth elements, at least, this could probably be done by periodic intravenous administration of a combination of zirconium citrate and ethylenediaminetetraacetic acid as is described later. However, the usefulness of these agents in such cases is difficult to assess without experimental evidence.

Puncture of Skin

Following puncture of the skin with an object contaminated with radioisotopes one can only minimize absorption of the fraction retained at the puncture site. Excision and irrigation of the wound site appear most practical. Details of the treatment of contaminated wounds are given by Hathaway & Finkel (20).

TREATMENT AFTER RADIOISOTOPES ARE ABSORBED INTO THE BODY

Decalcification Therapy—Interference with Calcium Metabolism

In 1926 Aub & Minot (see 21) postulated that lead metabolism in the body parallels that of calcium and that the circulation of lead could be controlled by influencing calcium metabolism in the bone. The metabolism of the alkaline earths including radium and strontium is also very similar to that of calcium. Consequently it occurred to Flinn in 1926 (22) that the decalcification techniques of Aub could increase the excretion of radium. He treated three patients with parathormone extract which he claimed increased radium excretion in patients who had accumulated radium in their bodies several years previously.

In 1931 Flinn (23) attempted to cause repair of radium-produced necrotic bone by the administration of viosterol. Since viosterol presumably promotes the laying down of calcium on the bone, Flinn was surprised to find, according to his measurements, that as much as 75 per cent of radium in the body was removed.

The observations of Flinn were not confirmed in studies on four radium dial painters made by Craver & Schlundt (24). They found that viosterol

plus a high calcium diet produced no increase in radium elimination but that the administration of parathyroid extract with a low calcium diet produced about a 50 per cent increase in radium elimination during the period of treatment.

The definitive, classical study of the effects of alterations in calcium metabolism on radium excretion in human subjects was made by Aub and co-workers (11). It was pointed out—and rightly so—that the assay techniques of Flinn were not reliable and that the doses of parathyroid employed by Craver & Schlundt were not large enough to affect calcium metabolism sufficiently.

In a carefully controlled series of experiments on three patients Aub *et al.* (11) found that decalcification therapy increased the urinary excretion of radium four- to eightfold. Treatment consisted of a low calcium diet plus ammonium chloride, thyroid extract, and parathyroid extract. Magnesium gluconate administration also raised the excretion of radium in proportion to its effect on calcium excretion.

One case did not respond to parathyroid extract. The explanation given (11) was that "her osteoclasts were sufficiently damaged so that they were unable to respond to the normal stimulus of parathyroid extract, and were, therefore, unable to liberate bone salts."

When the patients were placed on a high calcium diet with no medication the calcium excretion returned to a very low level but the radium excretion continued high. It was thought that this might have been caused by previous administration of Vitamin D. It is important to note that radium excretion does not always parallel the change in calcium excretion. The excretion of radium does not change as rapidly as that of calcium. One reason given by Aub *et al.* is that when radium is liberated from bone some is stored in the soft tissues. The rate of elimination from soft tissues, as observed in acute cases of radium exposure, is continuously high.

Decalcification therapy has been tried in experimental animals in attempts to promote the excretion of strontium. Small increases in excretion rate were observed but these were at too low a rate to have any appreciable effect on the residue left in the body(17). A low-calcium diet unaccompanied by other medication such as ammonium chloride administration appears to have little value for increasing removal of radioactive alkaline earth metals. In one experiment (25) a group of rats were injected with Ca^{45} and placed on a diet adequate in phosphate but very low in calcium. In these animals the excretion of Ca^{45} was actually reduced. In human subjects, Aub *et al.* (11) also found that the sole use of a low-calcium diet had no effect on radium excretion. These findings are reasonable when it is considered that the body on a low-calcium but adequate phosphate diet attempts to conserve its store of calcium.

No effect at all of decalcification therapies has been observed on the excretion rates of plutonium and the rare earth elements (19). Many experiments have shown that the uptake and excretion of Pu and the rare earths

are unaffected by age of the animal, or by alterations in the degree of mineralization of the bone. Even in bones of rats which are demineralized to the point where the bone contained only one-fourth of the bone salt normally present, no effect on the retention of injected Pu, Yttrium(Y), or Ce is found (17). In the same experiment, when the rats were placed on a phosphate-deficient diet immediaely after injection of the radioisotope, the body retention of Sr was reduced from 76 per cent to only 26 per cent. Similar findings were reported in comprehensive reports by Van Middlesworth (26) and Copp and co-workers (25).

In summary, decalcification therapy is capable of increasing the elimination rate of radium and presumably of strontium in acute and chronic poisoning. In acute exposures to Ra and Sr the increases in elimination caused by decalcification therapy could lower the body content appreciably. However, such therapy appears impractical in the treatment of chronic poisoning because treatment can be given only for limited periods, so that the net depletion of body content of a radioisotope is insignificant. Decalcification therapy has no effect on the retention or excretion of plutonium and rare earth elements. There is no conclusive evidence to show that decalcification therapy might be useful clinically independent of its possible effect on the elimination of radioisotopes.

Complexing or Chelating Agents

Introduction.—When a metal is complexed by different chemical compounds, usually organic in nature, a poorly dissociated molecule is formed. When the complexed metal becomes bound with the ligand in such a manner as to become part of a ring system it is called a chelate. We will use the terms complex and chelate interchangeably, though the term complex is broader; i.e., all chelates are complexes, but not all complexes are chelates.

A chelated metal ion does not undergo its normal chemical reactions except with substances which may possess a stronger affinity for the metal ion that than possessed by the original chelating agent. If the chelate is insoluble and nondiffusible it prevents the injurious effects of the metal ion in the animal body. If the chelate is water-soluble and readily diffusible it is readily excreted. Consequently, there are two rationales for the use of complexing agents in the treatment of metal poisoning: (*a*) the complexing agent selectively combines *in situ* with the toxic metal without removal, or (*b*) it removes the metal ion from combination with cellular constituents with subsequent elimination of the complexed metal from the body. Only the latter is useful in the treatment of radioactive metal poisons.

Historical notes.—In general, only the earliest papers are mentioned in this section. The more recent literature is covered in those sections in which specific results are described.

In the treatment of chemical metal toxicity, many investigators in the past had used complexing agents but for reasons other than their ability to react directly with the metal. The deliberate use of complexing agents be-

TABLE II

FIVE IMPORTANT CHELATING AGENTS USED IN BIOLOGY AND MEDICINE

Chelating Agent	Molecular Weight	Structure	Type of Metal Chelate (M=metal ion)
Tetrasodium salt of ethylenediamine-tetraacetic acid (EDTA)	380.2	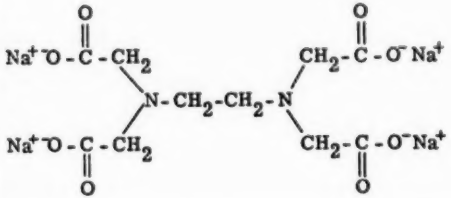	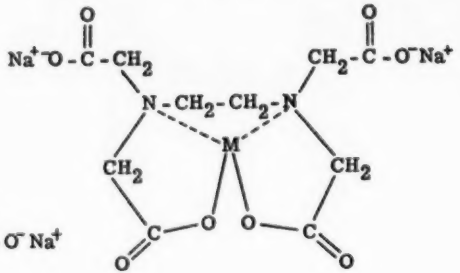
2,3-Dimercapto-1-propanol or 1,2-Dithioglycerol (BAL)	124.2	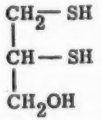	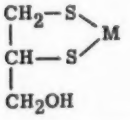

TABLE II (Continued)

Chelating Agent	Molecular Weight	Structure	Type of Metal Chelate (M = metal ion)
Sodium citrate	258.1	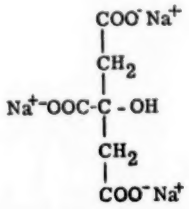	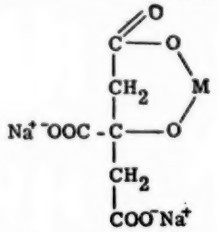
Fe-3 (Commercial chelating agent manufactured by Bersworth Chemical Company, Framingham, Mass.)		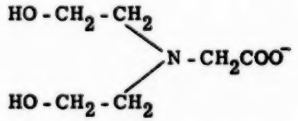	
N-hydroxyethylethylenediamine triacetic acid (Versenol)		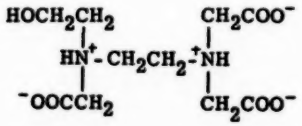	

cause of their metal binding properties for the treatment of heavy metal poisoning was begun just fifteen years ago, in 1940.

During the war years the British developed 2,3-dimercaptopropanol called BAL (British anti-lewisite) to control the harmful effects of arsenical war gases (27, 27a). BAL was subsequently used successfully for the treatment of poisoning by those heavy metals, including arsenic, mercury, and bismuth, which apparently exert their toxic actions through combination with the thiol groups in enzyme proteins. BAL competes successfuly for the —SH groups through the formation of a chelate (see Table II). The BAL-metal combination is readily excreted.

About the same time BAL was employed, Kety (28, 29, 30) attempted to treat lead poisoning by the administration of sodium citrate. He observed that lead forms a fairly strong complex ion with citric acid and measured the stability of the complex ion (29). It occurred to him that the phenomenon of complex formation "might be applicable to the problem of dissolving the insoluble lead compounds of the body tissues, making more lead available for excretion with no increase in lead ion concentration." (29).

In recent years there has become commonly available an extremely powerful group of chelating agents—the polyamino acids. One of the most noted of these agents is ethylendiaminetetraacetic acid (EDTA), shown in Table II. This compound forms especially strong chelates with polyvalent cations. The resulting chelates are water soluble and un-ionized. As early as 1942 biological experiments were carried out with EDTA when its ability to inhibit blood coagulation *in vitro* by complexing calcium was studied (31). In 1949 Bersworth suggested that EDTA be used for removing metals from the body (see 32, p. 509). It has been found that EDTA causes marked increases in excretion of several metals. It has been especially successful for the treatment of lead poisoning (32, pp. 506–10; 33).

Probably the first deliberate attempts to remove radioisotopes from the body by means of complexing agents were made in Chicago beginning about 1945 (34, 35). Painter *et al.* (34, pp. 50–56) used oral and intravenous administration of sodium citrate in an attempt to accelerate plutonium excretion from dogs injected 53 days previously with plutonium. Their reason for the use of sodium citrate was that "plutonium might be dislodged from the tissues by formation of plutonium citrate complex in the blood and subsequent excretion." A 35 per cent increase in the urinary excretion of plutonium was observed during the period of intravenous administration of sodium citrate. Experiments by Schubert (35) showed that administration of sodium citrate within 2 hr. after plutonium injection raised the urinary excretion of Pu several fold. It was pointed out (35) that "the action of sodium citrate in promoting the excretion of plutonium can be attributed to its ability to increase the diffusibility of plutonium and thus facilitate its clearance through the kidney." With regard to the therapy of radioisotope poisoning in general its was stated (36) that "the use of complexing agents . . . may be of . . . value for removing these radioelements with which they form very stable

complex ions." In other studies early administration of sodium citrate was found to enhance excretion of thorium and strontium (37).

Sodium citrate has certain disadvantages for use as a complexing agent. It is rapidly metabolized and in addition it does not generally bind metal ions under physiological conditions as strongly as would appear desirable.

It was only natural that the chelating agent BAL be tried for the treatment of poisoning with radioactive elements. In 1947 Weikel & Lorenz (38) employed BAL in the hope that it would enhance the excretion of radium from mice previously injected with radium salts. In work published in 1953 (39), but performed several years earlier (40), Kawin & Copp investigated the effects of BAL on plutonium excretion in rats. From chemical considerations (based, for example, on reactivity with sulfide ions, $S^{=}$) one would anticipate that BAL would not affect Ra and Pu excretion because these elements do not react appreciably with sulfhydryl groups, and, indeed, no effect was found. However, in the case of polonium (Po), which does react strongly with BAL, marked increases in Po excretion were observed in investigations begun early in 1949 by Hursh (41, 42, 43).

In 1949 Scott, Crowley & Foreman in Hamilton's laboratory at the University of California made a survey of the effect of different chelating agents on the metabolism of radioisotopes of the rare earths (44). The chelating agents tested included citrate, ascorbic acid, nicotinic acid, picolinic acid, isothiopropionic acid, carboxyethyl sulfide, glutathione, cholic acid, dithiocarbanyl, EDTA, BAL, creatine, and in a few cases combinations of two chelating agents. Of all the agents tried, EDTA appeared the most promising in promoting excretion. These studies were continued by Foreman (45) and extended to cerium and plutonium by Foreman & Hamilton (46).

Considerations involved in the use of chelating agents to increase excretion of metals.—The potential effectiveness of a chelating agent in accelerating excretion of a radioisotope *in vivo* can be evaluated in part from chemical considerations: (*a*) affinity of chelating agent for the radioisotope; (*b*) affinity of chelating agent for Ca^{++}, (*c*) hydrolytic reactions of the radioisotope; and (*d*) affinity of radioisotope for cellular constituents. It is desirable that the chelating agent (*a*) form chelates which are water soluble and readily diffusible; (*b*) does not react with normal body constituents, especially calcium (if possible); (*c*) be of low toxicity; (*d*) possess high absorption when taken orally; and that it (*e*) be not metabolized.

In practice, no one chelating agent meets all the requirements. It is not possible to evaluate quantitatively all the various factors listed above. However, some deductions of value can be made from the known formation quotients, i.e., equilibrium constants (Table III) between the chelating agent and metal ions. The ultimate criterion for success of a chelating agent is the extent and rapidity with which it safely removes absorbed radioisotopes from the body.

There are at present principally three chelating agents which have been widely used for treatment of either clinical or experimental metal poisoning.

TABLE III

FORMATION QUOTIENTS INVOLVING EDTA AND CITRIC ACID WITH METAL IONS*

Formation Quotient (log K_f)

$$K_f = \frac{(MKe)}{(M)(Ke)}$$

Metal	EDTA	Ref.	Citrate	Ref.	Metal	EDTA	Ref.
Na^+	1.66	(32)	—	—	Cd (II)	16.4	(32)
Li^+	2.79	(32)	—	—	La (III)	14.7	(47)
Mg^{++}	8.69	(32)	3.2	(32)	Ce (III)	15.4	(47)
Ca^{++}	10.7	(32)	3.16	(49)	Pr (III)	15.75	(47)
Sr^{++}	8.63	(32)	2.85	(49)	Sm (III)	16.55	(47)
Ba^{++}	7.76	(32)	2.54	(50)	Eu (III)	16.7	(47)
Ra^{++}	7.0†	—	2.36	(50)	Gd (III)	16.7	(47)
Pb (II)	18.2	(32)	5.75	(29)	Tb (III)	17.4	(47)
Cu (II)	18.3	(32)	14.2	(32)	Dy (II)	17.75	(47)
Fe (II)	14.15	(32)			Y (III)	17.5	(47)
Fe (III)	25	(32)			Pu (IV)	24†	(48)
$Fe(OH)^{++}$	2.8	(32)			Th (IV)	23†	(48)
Co (II)	16.1	(32)					

* The quoted values of the formation quotient, K_f, are under conditions of ionic strength, 0.1 to 0.16, and temperature of 25°C. M and Ke represent the molar concentrations of the metal and chelate, respectively.

† These values are estimated.

These are EDTA, BAL, and sodium citrate. Of these, EDTA is the most successful in removing rare earths and transuranic elements, while BAL is effective for the removal of polonium, at least under acute experimental conditions. At present, citrates do not appear as promising, mainly because they are rapidly metabolized.

It is particularly important that in the treatment of radioactive poisoning with chelating agents, the amounts administered at a given time be as high as possible. Doses too small can actually result in higher levels deposited in bone than would be the case in the absence of the chelating agent. When Y (51) or lanthanum (La) are chelated with small amounts of EDTA ($\backsim$1 to 5 mg.) enhanced bone deposition is observed. In the case of La^{140}, for example, the injection into mice of La^{140} with about 1 mg. of Na-EDTA resulted in a bone retention of 7.1 per cent of the injected dose of La^{140} compared to 3.0 per cent when $La^{140}Cl_3$ was injected alone (52). This result is explained by the increased diffusibility of the chelated La, shown by the marked decrease in La content in the liver of the La-EDTA-injected rats. In addition, the binding of bone for La is strong so that higher concentrations of EDTA are necessary for effective treatment.

Ethylenediaminetetraacetic acid (EDTA); considerations based on chelation constants.—As is seen in Table III, EDTA forms chelates of exceptional stability. However, since it reacts very strongly with serum calcium it is usually administered as the calcium chelate so as to avoid hypocalcemia. In order for EDTA to combine with a cation M, it is necessary for M to displace Ca^{++} from this chelate. Therefore, in order for EDTA to be highly effective in removing a metal, the metal should possess a binding affinity for EDTA greater than that of calcium for EDTA. Taking the simplest possible example, the reaction can be written:

$$CaV + M = MV + Ca \qquad \text{I}$$

where V represents molar concentration of EDTA, and Ca that of the ionized calcium. The calcium chelate of EDTA, Ca V, is of course $CaV^{=}$. We will, however, omit the charges on ions for simplicity unless necessary for clarity.

The equilibrium quotient, K_q, for reaction I is:

$$K_q = \frac{(MV)(Ca)}{(M)(CaV)} = \frac{K_{MV}}{K_{CaV}} \qquad \text{II}$$

where

$$K_{MV} = \frac{(MV)}{(M)(V)} \qquad \text{III}$$

and

$$K_{CaV} = \frac{(CaV)}{(Ca)(V)}. \qquad \text{IV}$$

Writing equation II in log form we have

$$\log K_q = \log K_{MV} - \log K_{CaV}. \qquad \text{V}$$

Since $\log K_{CaV} = 10.7$, the value of K_{MV} must be large indeed. Rearranging equation II we have

$$\frac{(MV)}{(M)} = \frac{K_{MV}}{K_{CaV}} \times \frac{(CaV)}{(Ca)}. \qquad \text{VI}$$

For practical purposes it is convenient to modify equation VI by eliminating (Ca V). Disregarding the small amount of V bound by M we have, where total $V = V_t$:

$$V = V_t - CaV. \qquad \text{VII}$$

From equation IV we have that

$$V = \frac{CaV}{K_{CaV}Ca}.$$

Substituting into equation VII and rearranging we find:

$$\frac{CaV}{Ca} = \frac{V_t K_{CaV}}{1 + (Ca)K_{CaV}}. \qquad \text{VIII}$$

We can simplify further because $(Ca) \times K_{CaV} \gg 1$ as can be seen from the fact that in blood serum the value of ionized Ca is about $1.3 \times 10^{-3} M$ while $K_{CaV} = 10^{10.7}$. Hence

$$\frac{(CaV)}{(Ca)} = \frac{V_t}{Ca}.$$

Equation VI thus becomes:

$$R_{MV} = \frac{(MV)}{(M)} = \frac{K_{MV}}{K_{CaV}} \times \frac{(V_t)}{(Ca)}. \qquad \text{IX}$$

The important point for therapy is to obtain as high as possible a ratio of chelated M to unchelated M, i.e., $R_{MV} \gg 1$. This is done by maintaining as high and constant a blood level of EDTA as possible, i.e., high V_t. In the case of the rare earths the values of K_{MV} vary from $10^{14.7}$ for La to $10^{17.5}$ for Y (Table III). The value of V_t 1 hr. after intravenous administration of 2.5 gm. of $Na_2CaEDTA$ ($M.W. = 374$) is about 50 mg. per liter of plasma or $.050/374 = 0.00013$ M. The latter part of equation IX becomes

$$\frac{(V_t)}{(Ca)} = \frac{1.3 \times 10^{-4}}{1.3 \times 10^{-3}} = 0.1$$

and, hence, for La we have

$$\frac{LaV}{La} = \frac{10^{14.7}}{10^{10.7}} \times 0.1 = 1000.$$

With such a large ratio for the rare earth which binds the most weakly with EDTA, one would not expect much difference in the effect of EDTA on excretion of the different rare earths. This is not the case.

Equation IX overlooks at least three other factors which become of extreme importance in the net value of R_{MV}. These are the hydrolysis of M, the reactions between M and body constituents such as proteins, and the reactions between the hydroxylated forms of M and the chelating agent. Hydrolysis is of particular importance when dealing with trivalent and tetravalent elements. Consider the following possible reactions:

$$CaV + MOH = MV + Ca + OH^- \qquad \text{X}$$

$$CaV + MOH = (M(OH)V) + Ca \qquad \text{XI}$$

and

$$CaV + LaP = LaV + CaP, \qquad \text{XII}$$

where P represents the binding by those substances present in the body.

Consequently, the net value of the over-all equilibrium quotient resulting from the reaction between a metal, M, and the chelating agent, V, obtained by combining equations I, X, XI, and XII is

$$\log K_q = 3 \log K_{MV} + \log K_{(M(OH)V)} + \log K_{CaP} - (4 \log K_{CaV} + \log K_{MP} + \log K_{MOH}). \qquad \text{XIII}$$

Keeping in mind that $(H^+)(OH^-) = K_W = 10^{-14}$; $(CaP) = K_{CaP}(Ca)(P)$; and the ratio of chelated M to nonchelated M,

$$R_{MV} = \frac{(MV)^3(M(OH)V)}{(M)(MOH)^3(MP)}$$

the expression for R_{MV} becomes

$$R_{MV} = \frac{(K_{MV})^3 K_{(M(OH)V)}}{(K_{CaV})^4 K_{MOH} K_{MP} K_W} \times \left(\frac{V_t}{Ca}\right)^4 \times \frac{(H^+)}{(P)} \cdot \qquad \text{XIV}$$

A rough estimate of R_{MV} can be attempted. Consider the rare earth La, for example. From Table III the value of log $K_{LaV} = 14.7$, log $K_{CaV} = 10.7$, log $K_{La(OH)^{++}} = 5.6$ as given in reference (47), $K_{MP} \cong 10^6$, $V_t/Ca = 0.1$, $H^+ = 10^{-7}$. Log $(La(OH)V)$ is taken to be of the order of 3 based on the value for $(Fe(OH)V)$ given in Table III. These give a value of $R_{LaV} \cong (10^{-4}/P)$, while for yttrium, $R_{YV} \cong (10^3/P)$, a factor of about 10^7.

The efficiency of EDTA for one rare earth relative to another, i.e., R_{M_1V}/R_{M_2V} is nearly proportional to K_{M_1V}/K_{M_2V} because the values of $K_{M_1(OH)} \cong K_{M_2(OH)}$, $K_{M_1P} \cong K_{M_2P}$ and $K_{(M_1(OH)V)} \cong K_{(M_2(OH)V)}$. For example, the difference in stability between the hydroxide of La, the lightest rare earth, $La(OH)^{++}$ and that of the heaviest, $Lu(OH)^{++}$ is only a factor of 10, while the corresponding difference between LaV^- and LuV^- is nearly a factor of 100,000 (actually $10^{4.9}$)—a reflection of chelation involving polydentate ligands[3] (47).

It is found that under identical conditions EDTA is, indeed, more effective against the heavier rare earths than the lighter. With an element like Pu(IV) the situation is more complicated. The very high value of log $K_{PuV} = 24$ is counterbalanced by the hydrolysis of Pu(IV) to form a nearly completely hydroxylated compound at physiological pH, with concomitant polymerization.

The equations presented in this section indicate that under physiological conditions the effectiveness of EDTA can only be improved by increasing the amount of EDTA administered. A better chelating agent, all other factors being equal, would be one which would chelate nearly as strongly as EDTA with trivalent and tetravalent radioisotopes but which would not react with calcium. This would provide at least a factor of $10^{10.7}$ improvement

[3] This is explained by Wheelwright, Spedding & Schwartzenbach (47) as follows: "Larger differences between individual rare earths must be expected in cases of chelating agents in comparison to simple ligands such as OH^- groups. A polydentate complexing agent possesses a number of ligand atoms which are donated to the metal cation during complex formation. Each of these will be bound more firmly by the cation of a heavier member, in comparison to the cation of a lighter member. All of these differences are cumulative in arriving at the stability constants of the two chelate complexes, the logarithms of which are proportional to the free energies to be gained during the addition of the whole polydendate group to the two cations to be compared. In the case of a simple complex such as $M(OH)^{+2}$ one water molecule is replaced by OH^- during complex formation. In the case of MY^- probably all the water molecules of the hydrated cation are expelled and replaced by the atoms of the hexadentate agent Y^{-4}. This explains the comparatively large differences between the individual rare earth cations."

in the over-all chelating efficiency as can be seen from the equations. We are now exploring such a possibility.

Metabolism and toxicity of EDTA.—The metabolism of C^{14}-labeled EDTA has been studied in rats and humans (53, 54). In both species most of the EDTA passes through the body unchanged after parenteral administration. It mixes rapidly with nearly all the body water but does not enter the red blood cells and only very slowly passes the blood-spinal fluid barrier. One hour after intravenous injection to humans 50 per cent is excreted, and within 8 hr. nearly all is eliminated in the urine. The half-time of disappearance from the blood is 1 hr. After oral administration about 90 per cent is eliminated in the feces within two to three days. Absorption after oral administration continues for at least 18 hr. Total absorption reaches a maximum of about 5 per cent, as judged by the amounts appearing in the urine. Maximum absorption from the skin is about 0.001 per cent.

The acute and subacute toxicity of EDTA has been extensively reviewed (55). As the sodium salt, relatively small doses of 20 to 50 mg./kg. produce death in dogs because of hypocalcemia. Approximately 1 gm. per hr. can be administered by infusion to humans. However, when administered combined with an equivalent amount of calcium ion, EDTA is relatively nontoxic. In treatment of radioactive poisoning, EDTA is administered as the calcium salt.[4] Dogs can tolerate as much as 4.0 gm./kg. in a single intravenous injection. In humans, following exposure to plutonium, at least 2.5 gm. of Ca-EDTA have been given in 250 cc. of saline by slow intravenous drip twice daily (56). When given orally at levels of 30 mg./kg. some patients have nausea and abdominal cramps.

When high levels are given regularly by intravenous administration, kidney damage may occur. In four of five cases treated with Na-EDTA kidney damage has been reported upon autopsy (57). In at least two of these it is believed that death was the result of severe kidney damage induced by repeated injections of Na-EDTA (57). Evidence of kidney damage following the administration of repeated large amounts of Ca-EDTA has been reported in rats and humans (58). Foreman states, however, that this damage following repeated injections of Ca-EDTA is reversible and can be prevented by allowing a few days to elapse after a series of injections (58). His tentative recommendations when long term treatment may be required are to inject once or twice daily by slow intravenous drip for five days, followed by two days of rest, and so on.

Effect of EDTA on plutonium and lanthanum excretion in humans.—A technician at Los Alamos cut herself deeply with glass contaminated with a solution of $Pu(NO_3)_4$ in $1M$ HNO_3 (56). This was probably equivalent to an intravenous injection. From the urinary excretion curve it was estimated that she received 25,000 to 30,000 disintegrations per min. (d.p.m.) of

[4] Ca-EDTA as Calcium Disodium Versenate® for injection is available commercially as a very stable, sterile solution from Riker Laboratories, Los Angeles, California.

Pu^{239}. When her urinary excretion of Pu had dropped to 12 d.p.m. per day she was given 2.5 gm. of Ca-EDTA in 250 cc. of saline, slowly by intravenous drip twice daily. A striking rise in Pu excretion from 12 to 1,300 d.p.m. resulted. The effect of EDTA decreased on subsequent days, but it was estimated that in 16 days of treatment about 20 to 25 per cent of the Pu had been removed, in large part from the tissues. This is reasonable assumption because the amounts of Pu excreted exceeded the total amount in the circulating blood at the time treatment was given, as can be deduced from data on metabolism of Pu in humans (59). The patient developed symptoms of kidney damage presumably caused by the EDTA.

A second test of Ca-EDTA was made in a chemist who had been exposed to Pu seven years previously (56). His body burden was estimated to be 1.2 μg. Treatment during a 5-day period with as much as 5 gm. of Ca-EDTA daily produced an average increase of Pu excretion of tenfold over pretreatment levels. This case illustrates the difficulties of treating chronic radioisotope poisoning. In the first place treatment has to be given for months or years in order to reduce appreciably the body burden of Pu. Secondly, during this period the tissues are receiving continued radiation so that even if all the Pu could be removed at the end of, say, five or ten years—a most unlikely event—the patient might not be spared lesions or malignancies.

The effect of EDTA on lanthanum metabolism in humans illustrates some interesting points. A tracer dose of La^{140} as the EDTA complex was injected intravenously into a human (60). The concentration of EDTA was not specified but may be surmised from a previous publication (52) to be a few milligrams. After 48 hr. only 5 per cent of the injected La was excreted. At that time 4 gm. of Ca-EDTA in 500 ml. of a 5 per cent solution of glucose was infused in 3 hr. A sharp rise in La^{140} excretion was observed. By the fifth day post injection urinary excretion dropped to negligible levels. A 7-hour infusion of 8 gm. of Ca-EDTA in 1000 ml. of glucose solution again raised La excretion, but only one-fifth as high as the previous maximum.

In a second study, in an effort to ascertain the maximum possible increase in excretion of La^{140}, Ca-EDTA was administered prior to, and simultaneously with, the La^{140}-EDTA injection. A prior dose of 3 gm. of Ca-EDTA in 300 ml. glucose solution was infused in 2.5 hr. and was followed by a 1.5-hr. infusion containing La-EDTA in 2 gm. of Ca-EDTA. Even in this case the total excretion of La in the first day was only 37 per cent, most of which occurred in the first four hours.

These results with lanthanum are reasonably interpreted by equations I to XIV. Since La is relatively weakly bound by EDTA it is necessary that the concentration of EDTA in the blood be high. Even when La-EDTA is injected simultaneously with several grams of EDTA the ratio of $(LaV)/(La) = R_{La}$ is insufficient to allow more than about one-third of the La to be excreted. If the reactions are amenable to the laws of mass action, a 1000-fold reduction in EDTA concentration, as is the case when La-EDTA

alone was injected, had the effect of reducing R_{La} to the point where, for practical purposes, it is as if uncomplexed La was injected. This, indeed, was observed in an experiment in which La as $LaCl_3$ was injected (60). Approximately 5 per cent of the injected dose was excreted by the kidneys, as was the case following the injection of La-EDTA. This illustrates the importance of the binding strength of a metal with a chelating agent in the effectiveness of the latter; a low value of K_{MV} indicates that a large, possibly toxic, amount of the chelating agent is necessary to remove a significant quantity of the radioelement.

In the case of yttrium, the affinity for EDTA is approximately 400 times that of lanthanum. This is equivalent insofar as R_{MV} is concerned to a 10^7 excess of EDTA. Consequently it would be expected that EDTA would be effective even orally in Y poisoning and be more effective in increasing excretion of yttrium than lanthanum. An illustration of this is shown in experimental animals. Following the injection of uncomplexed Y as YCl_3 into rats, the urinary excretion in 24 hr. was about 5 per cent, which is the same as obtained in the case of La, as would be expected from the nearly identical chemical behavior of rare earth ions at physiological pH. However, when therapeutic doses of EDTA are injected simultaneously with the Y approximately 70 per cent of the Y is excreted in 24 hr. (44) compared to only 37 per cent of La. Thus, a 400-fold increase in the value of K_{MV}—at least for rare earths—results in a twofold decrease in body retention when EDTA is given simultaneously with the rare earth. It would be of particular interest to learn if quantitative predictions for other rare earths can be made from this ratio.

Effects of EDTA on excretion and tissue distribution of radioisotopes in experimental animals.—In general, EDTA can be expected to show varying degrees of effect in removing elements whose K_{MV} exceeds that of calcium. This includes all the rare earths, plutonium, and the transuranic elements. The relative effectiveness of EDTA with the trivalent transuranic elements such as americium (Am) and curium (Cm) can be expected to parallel the rare earths. From electronic and chemical observations it is known, for example, that the rare earth counterpart of Am is europium (Eu), and that of Cm is gadolinium (Gd) (61). A summary of published studies on the effects of EDTA on the metabolism of several different radioisotopes is given in Table IV.

Even under the most favorable conditions, EDTA alone or in combination with BAL, has no effect on the excretion of Sr^{89} from rats (67) or rabbits (68a). Since Ra and Ba react more weakly with EDTA (Table III) than does calcium, it is not expected that the excretion of these alkaline earths would be modified by EDTA.

The most striking effects of EDTA are obtained when it is administered soon after exposure. In the case of Am (III), for instance, EDTA forms a chelate whose stability constant log K_{AmV} is at least 16.7. A single injection of 100 mg. of Ca-EDTA to rats ($\backsim$400 mg./kg.) given intraperitoneally

TABLE IV

PUBLISHED STUDIES ON THE REMOVAL OF RADIOISOTOPES FROM MAMMALS BY THE USE OF ZIRCONIUM SALTS AND THE CHELATING AGENTS—ETHYLENEDIAMINETETRAACETATE, CITRATE, AND BAL

Experimental animal	Therapeutic agents tested	Routes of administration*	Radioisotopes involved	References
Rat	Ca-EDTA	I.V., I.P., oral	Pu^{238}	(62)
Rat	Ca-EDTA Zr Citrate Zr Malate Zr+Ca-EDTA	I.P.	Pu^{239}	(78)
Rat	Ca-EDTA	I.V., I.P., I.M., oral	Pu^{239}, Y^{91}, Am^{241}	(63)
Rat	Ca-EDTA Zr Citrate Zr+Ca-EDTA	I.P.	Pu^{239}	(79)
Rat	Ca-EDTA Ca Citrate	I.P., I.M., oral	Pu^{239}, Y^{91}	(64)
Rat	Ca-EDTA	I.P., I.M., oral	Pu^{239}, Y^{91}, Ce^{144}	(65)
Rat, rabbit	Ca-EDTA, Na-EDTA	I.P.	Y^{91}	(66, 68a)
Rat, rabbit	Ca-EDTA+BAL	I.P., I.M.	$Sr^{89,90}$	(67, 68a)
Rat	Na-EDTA Zr Citrate Na-EDTA+Zr Citrate Na Citrate	I.P., oral	Mixed fission products (255 days old)	(68)
Man	Ca-EDTA	I.V.	La^{140}	(60)
Man	Na-EDTA	I.V.	Ca^{45}	(69)
Man	Ca-EDTA	I.V.	Pu^{239}	(56)
Man	Zr Malate	I.V.	Pu^{239}	(70)
Rat	Zr Citrate, Na Citrate	I.P.	Pu^{239}, Y^{91}	(35, 36, 73, 74)
Rat	Zr Citrate, Na Citrate	I.P.	Th^{230}, $Sr^{89,90}$	(37)
Rat	Zr Citrate	I.P.	Pu^{239}	(75)
Rat	Zr Citrate, Na Citrate	I.P.	Pu^{239}, Y^{90}, Nb^{95}, $Sr^{89,90}$, Ce^{144}	(40)
Rat	Zr Citrate	I.P.	Am^{241}	(77)
Rat	Zr Citrate +Parathormone	I.P.	Pu^{239}, Y^{90}	(40)
Dog	Zr Citrate	I.V.	Pu^{239}	(36, 76)
Dog	Na Citrate	I.V., oral	Pu^{239}	(34)
Rat	BAL	I.M.	Po^{210}	(41, 42)
Rat	BAL	I.M.	Pu^{239}	(39, 40)
Mouse	BAL	Subcut.	Ra^{226}	(38)
Mouse	BAL	I.M.	Sr^{90}, P^{32}, Ra^{224} (ThX)	(71, 72)
Rabbits	BAL	I.M.	Ra^{224} (ThX)	(72)

* I.V. = intravenous. I.P. = intraperitoneally. I.M. = intramuscular.

30 min. after intravenous injection of Am^{241} results in a 25 per cent excretion in the urine within 24 hr., compared to 1 per cent in the untreated rats during the same period. Several days later the animals were fed a diet containing 3 per cent Ca-EDTA. This caused the urinary excretion to increase five- to ten times over the control levels (63). It must be kept in mind that these doses of Ca-EDTA are much higher than would be administered to humans.

In the case of yttrium (log $K_{YV} = 17.5$), a single intravenous injection of 20 mg. ($\backsim$80 mg./kg.) of Ca-EDTA in rats given 2 hr. after intravenous injection of YCl_3 in isotonic saline at pH 6 (63, 64) caused an excretion of 67 per cent of the Y in the urine at the end of 24 hr., compared with 25 to 30 per cent in untreated controls. When EDTA is administered on the twentieth through twenty-third days after Y injection, the urinary excretion of Y rises from a pretreatment level of 0.07 per cent per day to as much as 0.7 per cent—a tenfold increase. Of interest is the fact that Ca-EDTA when given by stomach tube increases Y excretion—a reflection of the large K_{YV} compensating for the low degree of absorption of Ca-EDTA.

The most striking effect on Y excretion by EDTA occurs when EDTA is given before the Y (66). Rats were first given an intraperitoneal injection of 10 mg. of Na-EDTA followed 15 min. later by 50 mg. of Ca-EDTA. One hour after the injection of Ca-EDTA the animals were injected intraperitoneally with carrier-free $Y^{91}Cl_3$. Three days later they were sacrificed. The treated rats excreted a total of 93.3 per cent of the injected Y^{91} compared to 25.3 per cent by the controls. Skeletal retention was only 3.9 per cent compared to 58.0 per cent in the controls.

The time relationships between EDTA and Y injections are important. Results of intraperitoneal injection of Ca-EDTA a 1/2 hr. before Y should not differ significantly from those of 1 hr. because the concentrations of EDTA in the blood and body water are nearly equal at 1/2 and 1 hr. (53). However, if EDTA is administered 3 hr. before Y, a sharp reduction in the urinary excretion of Y and an increase in skeletal deposition would be expected because the blood level of EDTA is from five to ten times less than at the 1-hr. point. The effect of time of EDTA administration on the skeletal concentration of Y is given in reference (66). EDTA is less effective in decreasing the skeletal concentration of Y when given 3 hr. after Y injection than after 1/2 or 1 hr. This is easily explained by the fact that the concentration of Y in the skeleton in untreated animals is about 15 to 20 per cent at 1/2 hr. and increases to about 40 per cent of the injected dose at 3 hr. (80). The increased urinary excretion obtained by EDTA administration at 3 hr. or earlier is evidently only partly derived from the skeleton.

As is to be expected, there is a minimum effective dose of EDTA, even for radioisotopes such as Pu which have a high K_{MV} with EDTA. A dose of 8 mg./kg. of Ca-EDTA is too small to affect significantly the excretion of Pu even when administered simultaneously (62). It is conceivable that doses this small could cause a higher retention of Pu in the skeleton as was discussed earlier in the cases of Y and La. On the other hand, the effectiveness of sufficient Ca-EDTA is independent of Pu concentration, at least in experiments (79) in which the molar ratio of Ca-EDTA to Pu varied from about 3×10^9 to 3×10^4—a factor of 10^5 in range of Pu concentration.

The importance of K_{MV} is shown in an experiment involving rats injected with Ce^{144} (III), log $K_{MV} = 15.4$. When Ca-EDTA ($\backsim$100 mg./kg.) was injected intraperitoneally 18 hr. after intravenous administration of

$CeCl_3$ in a neutral isotonic solution containing citrate, the urinary excretion was increased only about three times the control level (from ∽3 per cent to ∽9 per cent in 24 hr.). When Ca-EDTA was given on the thirteenth through the seventeenth day in doses of 200 mg./kg. twice daily there was scarcely any increase in Ce excretion over the control levels (65). Under similar conditions the excretion of Pu and Y enhanced about tenfold.

When EDTA is administered as a therapy for poisoning by elements with which it reacts only moderately, such as with Ce, then early administration, or even administration prior to the injection of the radioisotope produces relatively small effects. For example, rats were injected with mixed fission products (MFP) 255 days old. The principal fission products were Zr^{95}, Ce^{144}, $Sr^{89,90}$, Y^{91}, and Pr^{143}. Under optimal conditions of treatment, EDTA-treated rats excreted 40 to 50 per cent as compared to 35 per cent by the controls. The skeleton of EDTA-treated rats contained 25 per cent of the injected dose of MFP compared to 30 per cent in the controls. More information on these experiments (68) is given in Table VII (see page 401) in which the effects of EDTA and zirconium salts are compared. Little effect is expected with praseodymium, Pr, because of a relatively low binding capacity for EDTA ($\log K_{PrY} = 15.75$).

An important question is whether prolonged treatment with EDTA can remove radioisotopes once they are fixed in the body, particularly in the skeleton. Partial answers are provided in experiments in which administration of EDTA is begun at least two weeks after the intravenous injection of the radioisotope. In Table V are tabulated the results of such experiments on the effects of Ca-EDTA on Pu excretion and retention in the skeleton and liver. It will be noted that a single massive injection of Ca-EDTA given 30 days after Pu has no effect. However, if Ca-EDTA is given daily for one month or for a total of 30 injections starting a month after Pu injection, a substantial increase in total excretion is observed and skeletal deposition is reduced from 56 per cent of the injected dose of Pu to 41 per cent. Even under optimum conditions the skeletal deposition of Pu can only be reduced a maximum of somewhat less than twofold (Table V). These results do not appear to offer much hope for those cases of chronic poisoning in which treatment is delayed for a year or more.

In similar delayed treatment experiments with Y, Cohn *et al.* (66) began treatment of rats 14 days after Y injection. Rats were injected daily, until sacrificed 29 days after Y injection, with 10 mg. of Na-EDTA followed at varying times during the day by 50 mg. of Ca-EDTA. The treated rats excreted 17 per cent of the Y during the treatment as compared to 4.5 per cent in the controls. The increased amount of Y excreted appeared to be nearly all derived from the skeleton since the treated rats had 48 per cent in the skeleton compared to 62 per cent in the controls.

Vaughan & Tutt (68a) have shown that the effect of EDTA on yttrium excretion in rabbits is greater in young than in old animals. If the EDTA is given immediately after injection of yttrium the skeletal burden is reduced

TABLE V

Effect of Different Dosage Schedules of Ca-EDTA on the Excretion and Distribution of Intravenously Injected Pu in Rats

Total No. of injections of Ca-EDTA	Time of first injection of Ca-EDTA after Pu	Dosage and schedule of treatments with EDTA	Time of sacrifice after radioisotope	Per Cent of Administered Dose of Pu								Ref.
				Urine		Urine+Feces		Skeleton		Liver		
				Controls	Treated	Controls	Treated	Controls	Treated	Controls	Treated	
1	Immediately	*Pre-treatment by* addition of 3.5 per-cent Ca-EDTA to diet 24 hr. prior to Pu. Single injection I.P. of 186 mg. of Ca-EDTA at time of Pu injection	15 days	6	51	27	62	55	31	8.8	3.6	(62)
1	30 min.	*Post-treatment:* 600 mg. Ca-EDTA (2400 mg./kg.) given 30 min. after Pu. Single injection	30 days	—	—	—	—	58	33	15 (soft tissue)	5 (soft tissue)	(79)
1	30 days	*Post-treatment:* 600 mg. Ca-EDTA (2400 mg./kg.) given 30 days after Pu. Single injection	30 days	—	—	—	—	46	50	22 (soft tissue)	18 (soft tissue)	(78)
64	2 hr.	*Post-treatment:* 100 mg. Ca-EDTA (400 mg./kg.) given I.P. 4 times daily for 16 days starting 2 hr. after Pu	16 days	4	32	30	40	55	37	10	10	(63)
11	18 hr.	*Post-treatment:* 25 mg. Ca-EDTA given I.P. at 18 hr. after Pu. 50 mg. Ca-EDTA twice daily on 13th to 17th day	62 days	3.3	13	39	58	50	34	—	—	(64)
25	25 days	*Post-treatment:* 162 mg. Ca-EDTA given I.P. daily from 25th to 50th day post Pu	50 days	6.3	15	26	39	61	52	5.3	4.9	(62)
30	30 days	*Post-treatment:* Ca-EDTA, dosage not stated, but presumably 20 mg. Ca-EDTA, given I.V. daily for 1 month starting 30 days after Pu	60 days	3	20	22	50	56	41	6	2	(56)

appreciably in both age groups, but if it is given two weeks later the effect in the older animals is slight.

These differences may be explained by assuming that chelation occurs with the yttrium present in the blood-stream immediately after injection or released to the blood-stream by the normal process of resorption. The great reduction of Y^{91} in the lower end of the metaphyseal trabeculae of young rabbits treated with versene (EDTA) for 9 days compared with the control suggests that the isotope is removed from areas of high metabolic activity associated with a good blood-supply. In old animals metabolic activity in the bone is slight and little yttrium is released to the blood-stream. The skeletal burden is therefore not appreciably reduced. (68a).

This explanation appears valid and has significance generally in the problem of treating chronic radioactive poisoning.

Several investigators have reported that administration of EDTA as often as four times daily is no more effective than one dose (66, 68a). This finding is not unexpected since the effectiveness of EDTA is dependent primarily on the blood-level of the radioisotope. Following a single dose of EDTA the blood-level of a radioisotope is reduced to a very low level and only gradually increases to a level commensurate with the body burden.

It is claimed (66), that the use of Na-EDTA followed by Ca-EDTA helps to improve the final results. This is explained on the basis that the decalcifying action of the tetrasodium salt of EDTA causes some dissolution of bone resulting in a release of calcium from the bone and a simultaneous release into the blood of bone-fixed yttrium. This explanation does not appear tenable. First, the results may not be unique because no controls were included in which Ca-EDTA alone was administered. Secondly, it has been thoroughly demonstrated that the uptake and release of yttrium by the bone is independent of the degree of calcification or decalcification of bone (17). Finally, a survey of the urinary excretion of Y in experiments in which Ca-EDTA alone was administered with that in which Na-EDTA and Ca-EDTA were given indicates no significant differences [references in Table IV, especially (68a)].

The use of Ca-EDTA in combination with zirconium salts in treatment of radioelement poisoning is discussed later.

Effect of 2,3 dimercaptopropanol (BAL) on excretion and distribution of radioisotopes.—Administration of BAL to experimental animals previously injected with radium (38, 72), strontium (71), phosphorus (71), plutonium (39), or yttrium (44) does not affect the distribution or excretion of these elements. No effect would be expected since, as mentioned earlier, these elements do not react with sulfhydryl compounds to any appreciable extent. Polonium, on the other hand, belongs to a family of elements which react strongly with sulfhydryl groupings.

Hursh (42) administered BAL to rats previously injected intravenously with a solution of polonium chloride at pH 6.5. The BAL was injected intramuscularly beginning 1 hr. after Po^{210} administration in a 10 per cent solu-

tion in peanut oil. Three doses each of 0.04 ml. were given per day for three days. The rats were sacrificed 10 days after receiving Po. The urinary excretion for the 10-day period was increased from 0.64 to 1.39 per cent—a factor of two. The fecal excretion was increased from 25.1 to 52.1 per cent. The Po levels in the bone marrow, blood plasma, spleen, and testes were decreased, while the concentration in the muscle was increased. Increasing the dosage of BAL or initiating treatments at the time of Po injection did not improve the results.

It is of interest to note that in this case the feces were the principal route of enhanced excretion. This is the reverse of the results obtained with EDTA and other chelating agents acting on other elements. While the blood level of Po was lowered, the dialyzable fraction of Po in the blood of treated rats was seven times that of the untreated. This is reasonably explained by supposing that

> BAL exerts its principal effect by forming a BAL-polonium complex, freeing polonium bound to protein . . . by virtue of the strong binding power of its dithiol group. The BAL-polonium complex is readily diffusible and therefore the complex in the blood stream may diffuse into the muscle tissue, may readily filter through the kidney glomerulus, and may be secreted into the gut (42).

Surprisingly, few studies have been made in which increased excretion of a radioisotope has been correlated with increased survival or other criteria of effectiveness. Since BAL decreased the total amount of Po in the body and reduced the level in the more radiation-sensitive organs (from the acute standpoint) it would be expected that the survival time of Po^{210}-poisoned rats would be increased. Hursh (43) found that control rats injected with a lethal dose of Po^{210} (36 μc./kg.) had a median survival time of 22 days compared with 89 days in the BAL-treated rats. Eighty-nine days is considerably longer than the median survival time of 57 days which would have been expected from the amount of Po retained in the body after BAL treatment. It was concluded that the

> detoxifying effect of BAL cannot depend only upon increased excretion but must also consist in a mobilization of polonium from radiation-sensitive tissue such as bone marrow and spleen into radiation-resistant muscle tissue.

Citrates.—As can be seen from Table IV, citrates have been employed frequently in attempts to enhance the excretion of radioisotopes. This is to be expected in view of the fact that they are normal constituents of the tissues and blood of mammals.

Even under optimum conditions the effect of citrates on excretion of Pu and rare earths is relatively insignificant. Studies on the effect of citrate-metal complex formation on the metabolism of several rare earths have been reported (44). In the case of intramuscular injection of the radioisotopes, complexing the rare earth with citrate increased the amount absorbed from the injection site several-fold. While citrate treatment reduced the amount of rare earth deposited in the liver, a large increase in skeletal deposition and kidney deposition was noted.

With thorium and strontium early administration of sodium citrate gave surprisingly large effects (37). Rats were injected intraperitoneally with 200 mg. of sodium citrate (4.0 ml. of a 5 per cent solution) 30 min. after the intraperitoneal injection of Th^{230}. They were sacrificed 8 days later. The control rats excreted a total of 28 per cent of the injected Th^{230} compared to 47 per cent by the treated rats. Nearly all of the increased amount of Th^{230} excreted was derived from the liver which contained 30 per cent of the injected Th^{230} in the controls compared to 14 per cent in the treated rats. Significant reduction in the Th^{230} content of the spleen, pancreas, and kidney was also observed. When the injection of sodium citrate was made 3 days after Th^{230} administration, no effect either on tissue distribution or excretion of the radioisotope was noted. In these experiments only a single injection of sodium citrate was given. In the same experiment when sodium citrate was administered intraperitoneally 30 min. after intraperitoneal injection of $Sr^{89,90}$ the total excretion of $Sr^{89,90}$ was increased from 30 per cent to 46 per cent of the injected dose. In this case most of the increased amount of radioisotope excreted was derived from the skeleton.

The effect of citrate on Th was not unexpected inasmuch as citrates are known to complex Th salts very strongly. This complexing action was further demonstrated by the fact that the diffusibility of Th in blood serum is markedly increased by the addition of sodium citrate (37).

Citrate forms a weaker complex with Sr than with Ca. By making use of an expression, originally given by Kety (29) for lead citrate, to solve for available citrate, one can obtain the ratio of complexed Sr to free Sr in the blood serum:

$$\frac{(SrCit^-)}{(Sr^{++})} = \frac{K_{SrCit^-}}{K_{CaCit^-}} \times \frac{(CaCit^-)}{(Ca^{++})} \qquad \text{XV}$$

where $Cit^{\equiv}$ represents the trivalent citrate anion and K the formation quotient. From the known values of Ca^{++} and citrate in blood serum the ratio $(CaCit^-)/(Ca^{++})$ is found to be 0.063. From the values of K given in Table III:

$$\frac{(SrCit^-)}{(Sr^{++})} = \frac{K_{SrCit^-}}{K_{CaCit^-}} \times 0.063 = \frac{710}{1450} \times 0.063 = 0.031.$$

Hence, most of the Sr in serum is uncomplexed.

When 200 mg. of sodium citrate is injected into a rat whose blood volume is 15 ml., then, assuming no destruction of the injected citrate, the concentration of citrate per ml. $= 200/15 = 13.3$ mg. $= 4.5 \times 10^{-2}$ M. This is a 450-fold increase over the normal blood citrate level which is about 18 to 30 μg. of citrate per ml. or approximately 10^{-4} M (81). This would raise the value of $(CaCit^-)/(Ca^{++})$ to about 24 and the value of $(SrCit^-)/(Sr^{++})$ to about 11. Despite the fact that injected citrates are destroyed rapidly by the body (probably within 2 to 3 hr.) enough Sr is complexed during that time to permit enhanced excretion. It must be realized that most of the increased excretion of a radioisotope caused by a chelating agent occurs in the first few hours after treatment.

Thirty minutes after Sr injection, the amount of Sr in the circulation is approximately 10 to 20 per cent of the amount injected (37). Consequently, the increased urinary excretion of Sr which followed the citrate treatment given at 30 min. was derived from circulating Sr which otherwise would have been deposited in the skeleton. In other words, sodium citrate administration did not remove deposited Sr from the bone. It should be kept in mind that calcium excretion is also increased by citrates. Actually, the citrate levels must be maintained in large molar excess over calcium so that sufficient amounts remain to react with the radioisotope.

If the metabolic destruction of injected citrates could be reduced or if an elevated citrate level could otherwise be maintained in the tissues and blood, it should be possible to improve the ability of citrates to accelerate excretion of radioisotopes. Under these conditions the citrates could be of value in the treatment of many radioactive poisons. In principle this is possible. Since citrates are involved in metabolic cycles it is possible to administer drugs which block the destruction of citrates directly or indirectly. These drugs include nonlethal doses of sodium fluoroacetate which cause large and sustained elevations of citrate levels in the kidney, spleen, and other soft tissues but not in blood (81). Guanidine and guanidine derivatives increase the blood citrate levels two- to threefold (82). Finally, Vitamin D appears to accelerate citric acid production in bone (83). We are investigating the use of these agents for the treatment of poisoning by radioactive and nonradioactive metals.

Miscellaneous chelating agents.—A compound related to EDTA, called Fe-3 and shown in Table II, causes substantial increases in the excretion of Pu and Ce. In an experiment with rats 100 mg. of Fe-3 was injected intraperitoneally each day for five days beginning on the forty-eighth day after injection of a mixture of Pu and Ce (64). The urinary excretion of Pu was increased six- to sevenfold over control levels during the treatment. Some increase was observed during the three days following the cessation of Fe-3 administration. With the same dosage schedule Fe-3 increased the urinary excretion of Ce as much as six times over the level of the control group as compared to a maximum of a threefold increase observed when Ca-EDTA was administered (46). No effect on fecal excretion of Ce was observed.

It is possible that the effectiveness of Fe-3 is related to its ability to form complexes which are more stable in alkaline solution than those of EDTA. Probably more important, it may form weaker chelates with Ca^{++} while reacting to an undiminished degree with transition elements.

Another compound which shows more promise even than EDTA is *N*-hydroxyethylethylenediamine triacetic acid (Versenol)[6] the structure of which is shown in Table II. Versenol administration to humans has been found to cause a marked increase of urinary excretion of iron (84). There-

[6] Versenol is available from the Bersworth Chemical Co., Framingham, Mass.

fore it should react strongly with plutonium, cerium, and similar radioisotopes.

In addition to EDTA, numerous other synthetic derivatives of amino acids may well be useful for the treatment of radioactive poisons. A list of possible compounds can be gleaned from tables in reference (32), pages 532–41.

Other sulfhydryl compounds besides BAL which have been tried for the treatment of experimental plutonium poisoning are methionine and cysteine. No significant effects have been obtained, although it has been observed that cysteine decreased the amount of intramuscularly injected Pu (VI) absorbed from the injection site (26). In later studies, no general alteration in tissue distribution of Pu was found following cysteine administration (40), but the treatment did decrease the absorption of intramuscularly injected Pu (VI). According to Van Middlesworth (26) the latter effect might be explained by a reduction of Pu (VI) to the more poorly absorbed Pu (IV).

Among numerous other chelating agents which have been used in conjunction with rare earths but which do not appear promising for therapy are creatine, cholic acid, glutathione, and trimethylamine tricarboxylic acid (44).

Colloidal Ion Exchange Carriers and Zirconium Salts

Introduction.—Early in 1945 it was thought that the excretion of plutonium from injected animals would be increased by treatment with large amounts of the soluble salts of various metals (35). This suggested treatment was based on the displacing ability of one metal for another, i.e., cation exchange. The metals considered were those possessing a high valence and a metabolism similar to plutonium. Salts of lanthanum, cerium, and zirconium were among those tested. Because of their low toxicity and ability to promote excretion of plutonium, zirconium salts were the most promising.

Subsequent studies, summarized in reference (74), proved that the injection of zirconium salts, especially zirconium citrate, caused marked increases in the excretion of plutonium and the representative rare earth, yttrium. The mechanism of action of zirconuim was postulated to be a carrier action rather than a metal displacement action (40, 73). This carrier concept was demonstrated by experiments involving other metals. The mechanism of action of zirconium salts is explained as follows (74):

> After the entrance of Zr salts into the bloodstream, colloidal aggregates are necessarily formed because of the hydrolyzability of Zr, i.e., above a pH of about 2 an insoluble precipitate of Zr hydroxide is formed. The circulating Pu is adsorbed by these aggregates and the subsequent disposition of the Pu is therefore directly related to the metabolism of the Zr.
>
> If this concept is correct, the salts of other hydrolyzable metals that also form colloids in the blood should be similar in action to the Zr salts. This is borne out by the results with Mn, Fe, Al, and Ti. The salt of a basic, non-hydrolyzable element, magnesium, had no observed influence on Pu metabolism.
>
> The eventual tissue distribution of the circulating colloidal particles, however, is

a function of their particle size distribution . . . Zr colloids of relatively large size are deposited primarily in the liver and spleen. . . . Therefore the tissue or organ distribution of that fraction of Pu removed from the blood can conceivably be varied within considerable limits by means of different carriers.

The injected zirconium exists in the bloodstream as insoluble aggregates which chemically include the phosphates and hydroxides of zirconium. These insoluble zirconium salts function, at pH 7, as a combined anion and cation exchanger of very high capacity ($\backsim$1 millimole per gram) and have an extraordinarily high affinity for ions (K. A. Kraus & H. O. Phillips, private communication). Consequently the more basic ions such as the alkali metals, alkaline earths, and many of the trivalent rare earths are presumably taken up by injected zirconium salts by ion exchange, while the hydrolyzable elements such as Pu and Th are taken up by adsorption or co-precipitation.

Inasmuch as the injected Zr salts function both as anion and cation exchangers, they should be particularly effective against those elements which exist in different charged forms simultaneously such as ruthenium.

In the sections to follow, we will summarize the results of experimental studies using Zr salts to promote excretion of injected radioisotopes. The limitations and potentialities of Zr treatment either alone or in conjunction with EDTA are explored.

Metabolism and toxicity of zirconium salts.—A thorough review of the toxicity and physiological effects of zirconium compounds has recently become available (85). The conclusion is that zirconium salts are remarkably low in toxicity. The acute LD_{50} of zirconium citrate is about 2 gm./kg. Rats receiving a total of 15 injections, given over a period of 5 weeks, of zirconium citrate in single doses of 50 mg. as Zr ($\backsim$175 mg./kg.) showed no ill effects except a transient weight loss (75). Histological examinations of the liver showed no evidence of damage.

Doses of zirconium citrate as high as 400 mg./kg. as Zr were well tolerated by dogs (76). However, the high citrate level in the zirconium solution does depress the ionized calcium content of the blood. This effect may be counteracted by calcium administration (76) to prevent hypocalcemia. When given with calcium gluconate, the administration of zirconium citrate by intravenous drip under conditions approximating those used clinically did not alter the blood pressure or respiratory rate of a dog injected with 1050 mg. Zr (137 mg. Zr/kg.) (Unpublished data).

The lack of overt toxic effects of injected zirconium salts reported above seems at variance with effects observed after injection of zirconium malate (70) and zirconium citrate in man. After several doses of 50 mg. of Zr as zirconium malate, patients became dizzy and developed symptoms of incoordination and other symptoms of vestibular damage similar to those sometimes observed following eighth nerve damage by streptomycin. A significant observation is that those preparations of zirconium salts which cause these adverse effects are unstable on standing, possessing a very short shelf life (86). The explanation of these unexpected toxic effects is probably that

these solutions were sterilized by autoclaving at elevated temperatures. Heat sterilization may cause zirconium chelate to decompose. Decomposition of hydrolyzable metal salts by heat is well known. For example, heat sterilization of ferric cacodylate solutions (National Formulary VIII) results in the formation of colloidal iron oxide (87), increasing the toxicity several-fold. Nonsterilized zirconium salt solutions made in our laboratory and by others are stable without any signs of deterioration for indefinite periods (at least a year). It is apparent, therefore, that solutions of zirconium citrate must be prepared in sterile form without autoclaving. This can be done by mixing sterile water and sterile sodium citrate solutions with zirconyl chloride. The latter solution, when prepared in concentrated form, is presumably sterile.

Following the injection of zirconium citrate solutions prepared according to published directions,[6] more than 90 per cent of the Zr is excreted in the urine, a small amount in the feces, and a small amount is retained in the skeleton and soft tissues (36, 40). Approximately 5 per cent is retained in the muscle and skin, at least for a few days. Kinetic studies on the rates of disappearance of Zr from the blood and rates of incorporation in tissues by Kawin, Copp & Hamilton (40) will be referred to later.

Very little zirconium is absorbed from the gastrointestinal tract when it is given orally as zirconium citrate. Hence, this route of administration is not feasible for the treatment of radioactive poisoning.

Effects of zirconium salts on the excretion and retention of radioisotopes.—Zirconium citrate treatment has some degree of effect on removal of nearly all of the fission products and transuranic elements as shown by the data in Table VI and Table VII.

The effect of zirconium is greater the sooner it is administered after the injection of the radioisotope, just as was the case when chelating agents were used. An important difference, however, is that a single injection of zirconium given before or after administration of the radioisotope will continue to influence the excretion or retention of the radioisotope for periods of days or weeks depending on the initial dose of Zr.

When zirconium citrate is administered in combination with a radioisotope (i.e., simultaneous treatment) the effect on excretion is maximum. In an experiment by Kawin and associates (40) radioyttrium, Y^{90}, and radiozirconium, Zr^{95}, were mixed either with sodium citrate solution or with zir-

[6] A 100 ml. batch of zirconium citrate is prepared as follows (36): To 18 ml. of a filtered solution of pure (iron-free) zirconyl chloride ($ZrOCl_2$) containing from 130 to 140 mg. as Zr. per ml. add, while stirring, 80 ml. of a 12.5 per cent solution by weight of sodium citrate, $Na_3C_6H_5O_7 \cdot 2H_2O$. A precipitate first forms which subsequently dissolves. Two ml. of a 20 per cent NaOH solution are added and the zirconium citrate solution is filtered through quantitative filter paper. The final solution should be clear and colorless. It has a pH of ~6.3 which can be adjusted to 7 if desired, and contains about 25 mg. as Zr per ml. and the equivalent of a 10 per cent sodium citrate solution. Because of its hypertonicity ($Na^+ = \sim 1.1\ M$) it is advisable to dilute it at least threefold for intravenous use.

TABLE VI

EFFECT OF INTRAPERITONEAL ADMINISTRATION OF ZIRCONIUM CITRATE ON THE EXCRETION AND DISTRIBUTION OF DIFFERENT RADIOISOTOPES IN RATS

Radio-isotope	Route of administration	Dose of Zr citrate (mg. as Zr)	Time of injection of Zr after radio-isotope	Time of sacrifice after radio-isotope (days)	Per Cent of Administered Dose						Ref.
					Urine		Skeleton		Liver		
					Controls	Treated	Controls	Treated	Controls	Treated	
Am^{241}	I.V.	40	15 min.	4	5.7	35	31	22	38	18	(77)
Am^{241}	I.V.	40	15 min.	16	8.1	36	35	21	13	12	(77)
Sr^{89}	I.P.	25	1 hour	5	34 (+feces)	40 (+feces)	61	45	—	—	(67)
Sr^{89}	I.P.	25	1 hour (prior to Sr^{89})	5	34 (+feces)	60 (+feces)	61	36	—	—	(67)
Ce^{144}	I.V.	40	Immediately	3	3.6	15	6	6	60	49	(40)
Nb^{95}	I.V.	40	Immediately	3	37	44	14	18	9	12	(40)
Pu^{239}	I.V.	40	Immediately	3	4.7	48	57	16	12	12	(40)
Y^{90}	I.V.	40	Immediately	3	13	71	21	8	28	1.7	(40)

conium citrate. In three days the zirconium-treated rats excreted 97 per per cent of the Y^{90} compared to only 24 per cent by the sodium citrate-treated rats (Table VIII). Following this simultaneous injection of radioisotope and Zr, the tissue distribution and excretion of the two are nearly parallel, indicating that the zirconium is indeed serving as a carrier for the yttrium.

The effect of varying the time of zirconium citrate administration on the metabolism of Pu and Y is shown in Table IX. The sustained action of a single dose of Zr is shown by the fact that it is possible to decrease skeletal deposition of injected Pu or Y even when Zr is administered 8 days before the radioisotopes. The urinary excretion of Pu can be increased even when Zr is injected 23 days earlier (74). Aside from possible effects of zirconium citrate on the degree of reabsorption of radioisotopes during passage through the kidneys, these sustained effects of Zr are probably related to the fact that a small fraction of the Zr circulates in the bloodstream for several days after injection. Kawin, Copp, & Hamilton (40) have demonstrated that a substantial fraction of injected zirconium citrate leaves the serum with a half-life of nearly 5 hr. However, there is little doubt that if the period of observation had been extended, longer-lived fractions would have been found.

Although it has been shown that the skeletal deposition of Pu or Y is markedly reduced when Zr citrate is administered soon after the Pu (Table IX), this is not proof that Pu or Y are actually removed from the skeleton. Control animals given radioisotopes but sacrificed at the time that zir-

TABLE VII*

EFFECT OF TREATMENT WITH ZIRCONIUM CITRATE AND ETHYLENEDIAMINETETRA-ACETATE (EDTA) ON THE EXCRETION AND RETENTION OF MIXED FISSION PRODUCTS BY THE RAT†

Tissue	Per Cent of Administered Dose of Mixed Fission Products						
	Control	Zr Citrate (25 mg Zr per rat)		Na-EDTA (10 mg per rat)		Zr Citrate +Na-EDTA	
		1 hr Pre-	1 hr Post-	1 hr Pre-	1 hr Post-	Zr 1 hr Pre- + EDTA 1 hr Post-	EDTA 1 hr Pre- + Zr 1 hr Post-
Skeleton	30.0±3	9.4±0.8	18±1	25±3	25±3	12±1	17±2
Excreta	35 ±4	50 ±3	43±3	50±9	42±7	51±4	63±2
Liver	25 ±5	14 ±3	16±2	12±2	21±2	10±1	7±0.4
Muscle and skin	5 ±4	16 ±2	12±2	4±0.2	9±5	19±5	10±3

* Based on data in reference (68).

† Each rat received 25 microcuries of mixed fission products, 255 days old, consisting principally of Zr^{95}, Ce^{144}, Y^{91}, $Sr^{89,90}$, and Pr^{143}. The rats were sacrificed 5 days after receiving the mixed fission products. Both the mixed fission products and the treatments were injected intraperitoneally.

conium was injected (1 hr. later), contain the same skeletal levels of Pu or Y as the zirconium-treated animals sacrificed three days later (74). Consequently, it appears that the Zr only prevented any further deposition of Pu or Y in the skeleton after the time of treatment. Additional evidence for this is that Zr causes a very rapid loss of circulating plutonium from the blood. Within 5 min. after Zr injection the blood level of Pu in treated rats is less than half that of the controls, while 1 hr. later the control rats had 53

TABLE VIII

DISTRIBUTION AND EXCRETION IN RATS OF Zr^{95} AND Y^{90} WHEN MIXED WITH SODIUM CITRATE OR ZIRCONIUM CITRATE AND INJECTED INTRAPERITONEALLY*

Tissue	Per Cent of Injected Dose†			
	Zirconium Citrate		Sodium Citrate	
	Yttrium	Zirconium	Yttrium	Zirconium
Femur	0.2±0.05	0.2± 0.05	2.4±0.3	2.4±0.2
Liver	0.4±0.1	0.3± 0.05	5.1±1.0	6.2±0.6
Kidneys	0.2±0.03	0.3± 0.08	3.4±0.3	4.8±0.4
Carcass	2.0±0.5	6.1± 0.8	65.4±4.3	75.8±3.0
Urine	91.2±4.3	86.6±14.8	16.4±2.9	4.3±0.7
Feces	6.0±3.5	6.5± 2.8	7.3±2.3	6.5±0.7
Total Excreta	97.2	93.1	23.7	10.8

* After table in reference (40). The radioisotopes were injected in 1.6 ml. of a 10 per cent sodium citrate solution, or 1.6 ml. of a zirconium citrate solution containing a total of 40 mg. of carrier zirconium. The rats were sacrificed 3 days after injection.

† Values in the table were adjusted to 100 per cent recovery. Actual recoveries were 78.7±7.0. Each value is the mean from 4 or 5 rats. The deviation is expressed as the standard error of the mean.

per cent of the Pu dose in the blood compared to only 6 per cent in the Zr-treated rats (74, 88). Furthermore, within 1 hr. after Zr injection the uptake of Pu by bone reached a plateau, while Pu deposition in the bone of untreated rats continued (88). Similar conclusions as to the mechanism of the effect of Zr on bone deposition of radioisotopes have been reached in the more extensive investigations of Kawin, Copp & Hamilton (40) on the kinetic aspects of radioisotope metabolism following treatment with zirconium citrate.

The effect of the amount of zirconium citrate administered on the excretion and distribution of injected Pu in rats is shown in Figure 1. The amount of Pu excreted into the urine is proportional to the dose of zirconium, while the reduction in skeletal content was nearly independent of the amount of Zr injected or of the number of doses given. As little as 5 mg./kg. as Zr is sufficient to cause a several-fold reduction in the Pu level in the skeleton.

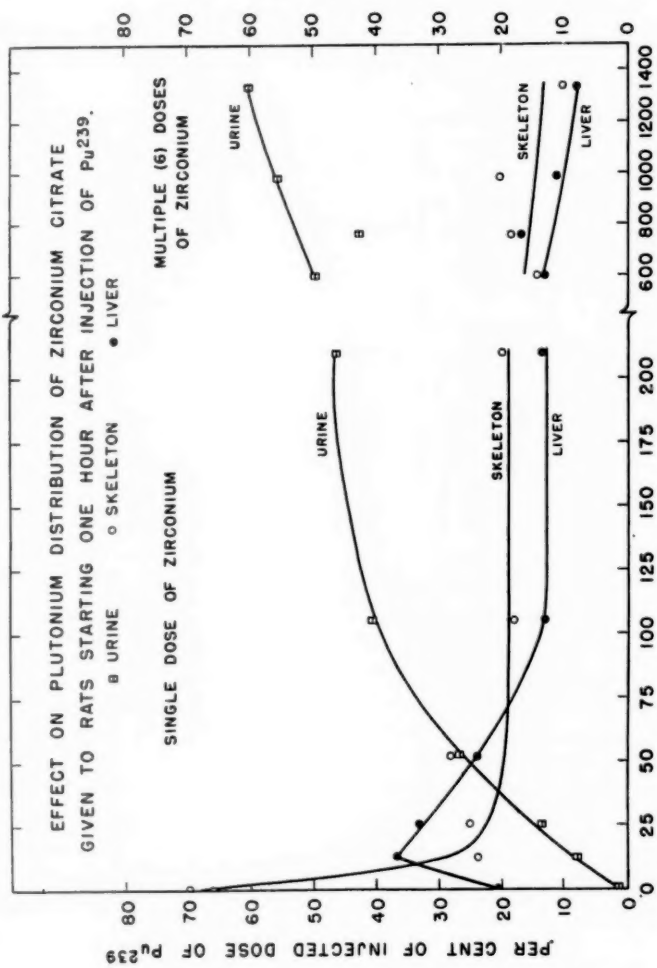
EFFECT ON PLUTONIUM DISTRIBUTION OF ZIRCONIUM CITRATE
GIVEN TO RATS STARTING ONE HOUR AFTER INJECTION OF Pu239.
B URINE o SKELETON • LIVER
SINGLE DOSE OF ZIRCONIUM
MULTIPLE (6) DOSES OF ZIRCONIUM
URINE
SKELETON
LIVER
PER CENT OF INJECTED DOSE OF Pu239
TOTAL AMOUNT OF ZIRCONIUM ADMINISTERED (mg/kg OF BODY WEIGHT)
0 25 50 75 100 125 150 175 200
600 800 1000 1200 1400

FIG. 1. All injections were given intraperitoneally. The rats were sacrificed 72 hr. after plutonium injections. From ref. (73).

TABLE IX

EFFECT OF TIME OF A SINGLE ADMINISTRATION OF ZIRCONIUM CITRATE RELATIVE TO THE INJECTION OF Pu^{239} AND Y^{91} ON RADIOISOTOPE DISTRIBUTION IN RATS*

Time of Injection of Zr Relative to Pu and Y	Dose of Zr Citrate as mg. Zr	Time of Sacrifice after Pu or Y inj. (days)	Per Cent of Administered Dose of Radioisotope												Ref.
			Plutonium^{239}						Yttrium^{91}						
			Urine		Skeleton		Liver		Urine		Skeleton		Liver		
			Controls	Treated	Controls	Treated	Controls	Treated	Controls	Treated	Controls	Treated	Controls	Treated	
Pre-Treated															
1 day	48	3	—	—	67	12	18	22	—	—	61	19	4.4	4.9	(74)
2 days	48	3	—	—	67	23	18	17	—	—	61	25	4.4	2.9	(74)
3 days	48	3	—	—	67	46	18	21	—	—	61	33	4.4	3.5	(74)
Post-Treated															
0.5 hours	51	6	1.4	64	73	12	12	11	27	51	42	16	1.5	1.8	(36)
1.0 hour	40	3	1.3	46	68	20	21	14	—	—	47	38	4.9	3.5	(73)
1.0 hour	30	3	—	—	66	16	21	23	—	—	49	33	8.3	7.1	(74)
24 hours	40	10	—	—	61	40	15	11	—	—	54	41	2.7	2.6	(74)
72 hours	51	6	1.4	7.0	73	61	12	18	27	33	42	43	1.5	2.0	(36)

* All injections were either intraperitoneal or intravenous.

This means that it is possible to minimize skeletal deposition without a concomitant rise in urinary excretion—an important point in the evaluation of the effects of Zr treatment in cases of human radioactive poisoning.

The effect of Zr on Pu excretion is largely independent of the concentration of Pu injected (79) and the valence state of Pu (40, 76).

The effects of Zr may be altered by changing the particle size distribution in the Zr injection solution. It is possible to prepare the zirconium citrate solution so that the ratio of citrate to zirconium is decreased. This has the effect of increasing the particle size of the carrier colloids so that a greater percentage of the Zr is found in the liver and much less is excreted in the urine. When such preparations, or similar ones with other metals, are injected into Pu-injected animals it is found that the amounts of Pu in the skeleton are reduced but that no proportional increase in urinary excretion occurs. Further, the liver possesses higher than normal levels of Pu (74). An excellent experimental demonstration is given by Gofman *et al.* (89, 90) of the relationship between the distribution and excretion of injected colloids relative to their chemical composition (ratio of complexing agent to metal) and particle size.

Preliminary evidence (76) indicates that zirconium citrate treatment may be far more effective in dogs than in rats. Administration of zirconium citrate to dogs injected intravenously 30 min. previously with Pu (IV) actually removed most of the deposited Pu from both the skeleton and soft tissues. It reduced the overall body content tenfold and the skeletal level approximately twentyfold (Table X). In this case Pu was evidently actually removed from the skeleton and other tissues. At the time Zr was injected about 50 per cent of the injected dose of Pu was in the blood [calculation based on extensive metabolic studies on several dogs (34)]. Since 90 per cent of the injected Pu was removed from the dog, approximately 40 per cent must have come directly from the skeleton, liver, and other organs.

Investigations have been made to ascertain whether the use of parathormone might increase the effectiveness of zirconium (40). It was thought that if resorption of bone by parathormone could mobilize Pu and Y, they might be made susceptible to the action of zirconium. However, it was found that parathormone action did not enhance the effect of zirconium on the excretion or internal decontamination of Pu or Y. Neither did the parathormone alone have any effect.

The effectiveness of Zr treatment in chronic radioactive poisoning has not been studied adequately. It is known that the administration of Zr citrate weeks, months, or even years after injection of Pu will cause a significant rise in the urinary output. For example, in a dog treated five months after Pu injection, the urinary excretion of Pu rose following the use of only 4.15 mg./kg. of Zr. A larger injection of Zr (15.8 mg./kg.) about a month later produced a threefold increase in urinary excretion and kept the urinary Pu at a slightly elevated level for the following two to three weeks (36). It is reasonable to conclude that optimal doses of Zr could have produced a

larger increase in the urinary excretion of Pu. An injection of zirconium citrate into this dog two and one-half years after Pu exposure also produced a prompt rise in excretion. However, whether repeated injections of Zr can remove long-standing deposits of Pu or other fission products has not been determined by adequate experimentation. A start has been made by Hackett (75). Thirty-two days after rats were injected intravenously with Pu (IV) one group received three intraperitoneal injections of Zr citrate a week for five weeks. The rats were sacrificed 71 days after Pu injection. Some reduction in skeletal concentration of Pu appears to have been obtained but the data were too scattered to establish significance.

TABLE X*

EFFECT OF ZIRCONIUM CITRATE TREATMENT ON THE EXCRETION AND RETENTION OF INJECTED PLUTONIUM (IV) IN DOGS†

Tissue Analyzed	Per Cent of Administered Dose of Pu (IV)				
	Controls	Zr treated (mg. Zr/kg. per injection)			
		50	100	200	400
Skeleton	81.0	3.8	4.2	7.9	2.6
Liver	19.0	0.5	3.0	1.0	0.5
Spleen	0.009	0.12	0.37	0.11	0.05
Blood	0.1	0.18	0.02	0.005	0.009
Carcass (less organs and skeleton)	0.8	6.5	0.6	1.4	0.3

* Based on data in reference (76).

† The Pu solution injected was plutonium citrate buffered to pH 6. The controls consisted of two dogs while only one dog is represented by each Zr level in the treated groups. Treatment was begun 30 minutes after the injection of Pu and was repeated twice each week for three weeks (6 injections total). Both Pu and Zr were injected intravenously.

There are several considerations in the treatment of radioactive poisoning in humans by zirconium citrate. The most important is that a sufficient dose of zirconium be given as soon as possible after the exposure in order to obtain a maximum excretion and minimum retention of the radioelement. Treatment should be intravenous. If it is desired only to minimize bone deposition, doses as small as 5 to 10 mg./kg. of Zr may be sufficient. With such small doses the urinary excretion may not be appreciably altered. Since the biological half-life of Pu in the soft tissues is far greater than in the bone and since Pu may be more easily removed from the soft tissues, it should be possible to reduce the long term retention of Pu by the soft tissues, particularly if Zr treatment is continued with injections administered approximately once a week. If, in addition to the small doses of Zr, Ca-EDTA is utilized then there is little doubt that the soft tissue levels of the radioiso-

tope would be decreased. The results in animals of combined Ca-EDTA—Zr citrate treatment are covered more fully in the next section.

If the results on dogs given in Table X are confirmed and applicable to humans, then it is conceivable that treatment with Zr citrate given at spaced intervals in doses of at least 50 mg./kg. may shorten the biological half-life of Pu by a factor of approximately 50 or more.

The rate at which the blood level of Pu following Zr treatment returns to or approaches the pretreatment level should be determined. This information would facilitate the design of the most effective treatment schedule and, in addition, allow estimations to be made of the rates at which depletion of the tissue deposits occurred.

Treatment of Radioactive Poisoning by Combined Ca-EDTA and Zirconium Citrate

In acute studies with rats injected with plutonium, zirconium citrate causes greater reductions in bone Pu deposition while EDTA is more effective in reducing soft tissue concentrations. A solution containing both agents would therefore be expected to be more effective than either alone. The experimental results (78, 79) shown in Table XI give striking proof of the

TABLE XI

Comparison of Effects of Zr Citrate and Ca-EDTA on Pu Retention in Rats*

Tissue	Per Cent of Administered Pu Retained			
		Treated Rats		
	Controls	Zr Citrate (50 mg. Zr per rat)	Ca-EDTA (600 mg. per rat)	Zr Citrate +Ca-EDTA† (25 mg. Zr +300 mg. EDTA)
Pu Dose = 0.0014 μg. per rat				
Skeleton	57.7±4.0	12.7± 1.2	33.2±2.6	—
Soft tissue	14.8±3.6	14.8± 3.6	5.1±0.9	—
Total animal	72.6±3.3	27.5± 4.2	38.2±2.6	—
Pu Dose = 140 λg. per rat				
Skeleton	46.3±5.2	13.9± 5.6	27.5±2.7	10
Soft tissue	24.7±4.8	21.2± 5.9	10.8±5.0	12
Total animal	71.0±4.6	35.1±10.9	38.3±3.4	22

* Based on data in references (78) and (79). Rats were given intraperitoneal treatment 30 minutes after the intraperitoneal injection of Pu (IV) citrate. All animals were sacrificed 30 days after Pu injection.

† The values given here were read off a graph in reference (78).

greater effectiveness of the Zr citrate—Ca-EDTA combination in reducing retention of Pu and they furnish a comparison of the individual therapeutic agents under the same experimental conditions. The reduction in skeletal deposition following the combined treatment was no different from that obtained with Zr alone.

In the case of 255-day-old mixed fission products, the combined use of EDTA and zirconium citrate did not improve skeletal decontamination over that obtained with zirconium citrate alone (Table VII). In this case, Zr alone reduced appreciably the skeletal level of radioelements while EDTA alone caused a small decrease in the amount of fission products deposited in the skeleton (68).

Further investigations on the use of combined therapeutic agents for internal decontamination are necessary.

Miscellaneous Approaches, Chemical and Physiological, for the Treatment of Radioactive Poisoning

Attempts to treat radioactive poisoning by several other methods have been made. None of these has had a significant effect, at least for the specific radioisotope tested. They include

(*a*) induced diuresis by injection into dogs of hypertonic saline in the case of Pu (36);

(*b*) disturbance of the organic matrix of bone by induction of scurvy using a scorbutogenic diet in the case of Pu, Sr, and Y (26);

(*c*) use of a protein-free diet in the case of Pu and Sr (26) to disturb bone protein;

(*d*) causation of bone resorption with subsequent use of a diet calculated to induce formation of a layer of new bone, in the hope that the new bone would act as a mass absorber to shield the living cells from radiations from deposited Pu (18);

(*e*) use of endocrine changes such as cretinism which was produced by thyroidectomy of rats at birth. The resulting hypothyroidism inhibited the deposition of radiostrontium in the skeleton. When growth hormone and thyroxin were administered either alone or together to the hypothyroid rats the skeletal concentration of $Sr^{89,90}$ increased to levels which in some cases exceeded those of the normal controls (91).

It is conceivable that stimulation of the cells of the reticuloendothelial system may enable them to cope more adequately with phagocytosis of radioactive particles. Substances such as oestradiol benzoate and choline cause stimulation of these cells (92, 93). Choline has been found to enhance the rate of disappearance from the blood of colloidal $CrP^{32}O_4$ (93).

An interesting possibility in the treatment of radioelement poisoning is the modification of tubular resorption processes in the kidney. In the case of radium, for example, more than 90 per cent of the radium passing through the kidney is resorbed back into the circulation. Even a relatively small decrease in the degree of tubular resorption of radium, caused by use of selec-

tive blocking agents for the renal tubules, could cause a significant increase in the urinary excretion.

Certain pathological conditions such as diabetes or normally-occurring physiological changes of many types, such as those that follow exercise, result in increased blood levels of organic compounds possessing chelating properties. Investigations of the effects of such induced changes in animals, e.g., alloxan-induced diabetes, would be of fundamental interest in the mechanisms of transport and removal of radioactive elements from the body.

LITERATURE CITED

1. Bouchard, C., Curie, P., and Balthazard, V., *Compt. rend. acad. sci.*, **138**, 1384–87 (1904)
2. Gudzent, F., *Berlin. klin. Wochschr.*, **20**, 933–35 (1912)
3. *Control of Radiation Hazards in the Atomic Energy Program*, U. S. Atomic Energy Commission Rept. (U. S. Gov't Print. Office, Washington, D.C., 1950)
4. Hollander, J. M., Perlman, I., and Seaborg, G. T., *Revs. Mod. Phys.*, **25**, 469–651 (1953)
5. Williams, C. R., *J. Ind. Hyg. Toxicol.*, **30**, 294–99 (1948)
6. Sultzer, M., and Hursh, J. B., *Arch. Ind. Hyg. and Occupational Med.*, **9**, 89–100 (1954)
7. Hempelmann, L. H., and Langham, W. H., *U. S. Atomic Energy Commission Document, AECU-2633* (1953)[7]
8. Cowan, F. P., Farabee, L. B., and Love, R. A., *Am. J. Roentgenol. Radium Therapy*, **67**, 805–9 (1952)
9. Marinelli, L. D., Norris, W. P., Gustafson, P. F., and Speckman, T. W., *Radiology*, **61**, 903–14 (1953)
10. Rajewsky, B., and Muth, H., *Strahlentherapie*, **88**, 261–75 (1952)
11. Aub, J. C., Evans, R. D., Gallagher, D. M., and Tibbets, D. M., *Ann. Internal Med.*, **11**, 1443–63 (1938)
12. McLean, R., Calhoun, J. A., and Aub, J. C., *Arch. Ind. Hyg. and Occupational Med.*, **9**, 113–21 (1954)
13. Looney, W. B., and Woodruff, L. A., *Arch. Pathol.*, **56**, 1–12 (1953)
14. Aub, J. C., Evans, R. D., Hempelmann, L. H., and Martland, H. S., *Medicine*, **31**, 221–329 (1952)
15. Copp, D. H., and Greenberg, D. M., *U. S. Atomic Energy Commission Document, MDDC-1001*, pp. 11–26 (1944)[7]
16. MacDonald, N. S., Nusbaum, R. E., Ezmirlian, F., Barbera, R. C., Alexander, G. V., Spain, P., and Rounds, D. E., *J. Pharmacol. Exptl. Therap.*, **104**, 348–53 (1952)
17. Copp, D. H., Axelrod, D. J., and Hamilton, J. G., *Am. J. Roentgenol. Radium Therapy*, **55**, 10–16 (1947)
18. Easton, T. W., *Am. J. Anat.*, **90**, 1–33 (1952)
19. Schubert, J., *Nucleonics*, **8** (No. 2), 13–28 (1951)
20. Hathaway, E. A., and Finkel, A. J., "Medical Care of Wounds Contaminated with Radioactive Materials" (Paper to be presented at Intern. Conf. on Peaceful Uses of Atomic Energy, Geneva, Switzerland, August 8–20, 1955)

[7] Information concerning the availability of this document may be obtained from the Office of Technical Service, Department of Commerce, Washington 25, D. C.

21. Aub, J. C., Fairhall, L. T., Minot, A. S., and Reznikoff, P., "Lead Poisoning," *Medicine*, **4**, 1–250 (1925)
22. Flinn, F. B., and Seidlin, S. M., *Johns Hopkins Hosp. Bull.*, **45**, 269–75 (1929)
23. Flinn, F. B., *J. Am. Med. Assoc.*, **96**, 1763–65 (1931)
24. Craver, L. F., and Schlundt, H., *J. Am. Med. Assoc.*, **105**, 959–60 (1935)
25. Copp, D. H., Hamilton, J. G., Jones, D. C., Thomson, D. M., and Cramer, C., *U. S. Atomic Energy Commission Document, UCRL-1464* (1951)[7]
26. Van Middlesworth, L., *U. S. Atomic Energy Commission Document, MDDC-1022* (1947)[7]
27. Peters, R. A., Stocken, L. A., and Thompson, R. H. S., *Nature*, **156**, 601–19 (1945)
27a. Waters, L. L., and Stock, C., *Science*, **102**, 601–6 (1945)
28. Kety, S. S., and Letonoff, T. V., *Proc. Soc. Exptl. Biol. Med.*, **46**, 476–77 (1941)
29. Kety, S. S., *J. Biol. Chem.*, **142**, 181–92 (1942)
30. Kety, S. S., and Letonoff, T. V., *Am. J. Med. Sci.*, **205**, 406–14 (1943)
31. Dyckerhoff, H., Marx, R., Ludwig, H., *Z. ges. exptl. Med.*, **110**, 412–22 (1942)
32. Martell, A. E., and Calvin, M., *Chemistry of the Metal Chelate Compounds*, (Prentice-Hall, Inc., New York, N. Y., 613 pp., 1952)
33. Rubin, M., Gignae, S., Bessman, S. P., and Belknap, E. L., *Science*, **117**, 659–60 (1953)
34. Painter, E., Russell, E., Prosser, E. L., Swift, M. N., Kisieleski, W., and Sacher, G., *U. S. Atomic Energy Commission Document, AECD-2042* (Ms. dated 1946; declassified 1948)[7]
35. Schubert, J., *Science*, **105**, 389–90 (1947)
36. Schubert, J., *J. Lab. Clin. Med.*, **34**, 313–25 (1949)
37. Schubert, J., and Wallace, H. D., Jr., *J. Biol. Chem.*, **183**, 157–66 (1950)
38. Weikel, J., and Lorenz, E., *Radiology*, **51**, 865–70 (1948)
39. Kawin, B., and Copp, D. H., *Proc. Soc. Exptl. Biol. Med.*, **84**, 576–77 (1953)
40. Kawin, B., Copp, D. H., and Hamilton, J. B., *U. S. Atomic Energy Commission Document, UCRL-812* (1950)[7]
41. Hursh, J. B., *U. S. Atomic Energy Commission Document, UR-83* (1949)[7]
42. Hursh, J. B., *J. Pharmacol. Exptl. Therap.*, **103**, 450–59 (1951)
43. Hursh, J. B., *Proc. Soc. Exptl. Biol. Med.*, **79**, 210–12 (1952)
44. Scott, K. G., Crowley, J., and Foreman, H., *U. S. Atomic Energy Commission Document, UCRL-587* (1949)[7]
45. Foreman, H., *U. S. Atomic Energy Commission Document, UCRL-683* (1950)[7]
46. Foreman, H., and Hamilton, J. B., *U. S. Atomic Energy Commission Document, AECD-3247* (1951)[7]
47. Wheelwright, E. J., Spedding, F. H., and Schwartzenbach, G., *J. Am. Chem. Soc.*, **75**, 4196–4201 (1953)
48. Foreman, H., *U. S. Atomic Energy Commission Document, LA-1851* (1955)[7]
49. Schubert, J., and Lindenbaum, A., *J. Am. Chem. Soc.*, **74**, 3529–32 (1952)
50. Schubert, J., *J. Am. Chem. Soc.*, **76**, 3442–44 (1954)
51. Dudley, H. C., *J. Lab. Clin. Med.*, **45**, 792–99 (1955)
52. Laszlo, D., Ekstein, D. M., Lewin, R., and Stern, K. G., *J. Natl. Cancer Inst.*, **13**, 559–73 (1952)
53. Foreman, H., Vier, M., and Magee, M., *J. Biol. Chem.*, **203**, 1045–53 (1953)
54. Foreman, H., and Trujillo, T. T., *J. Lab. Clin. Med.*, **43**, 566–71 (1954)
55. Rubin, M., Martell, A. E., and Bersworth, F. C., *The Biological Action of the Versenes* (Pamphlet issued by Versenes Incorporated, Framingham, Mass., 84 pp., 1954)

56. Foreman, H., Fuqua, P. A., and Norwood, W. D., *Arch. Ind. Hyg. and Occupational Med.*, **10**, 226–31 (1954)
57. Dudley, H. R., Ritchie, M. B., Schilling, A., and Baker, W. H., *New England J. Med.*, **252**, 331–37 (1955)
58. Foreman, H. (Personal communication, May 26, 1955)
59. Langham, W. H., Bassett, S. H., Harris, P. S., and Carter, R. E., *U. S. Atomic Energy Commission Document, LA-1151* (1950)[7]
60. Hart, H., and Laszlo, D., *Science*, **118**, 3053–54 (1953)
61. Seaborg, G. T., *The Actinide Series in Comprehensive Inorganic Chemistry*, Vol. **1**, 161–223 (D. Van Nostrand Co., Inc., New York, N. Y., 232 pp., 1953)
62. Hamilton, J. G., and Scott, K. G., *Proc. Soc. Exptl. Biol. Med.*, **83**, 301–5 (1953)
63. Foreman, H., *Arch. Ind. Hyg. and Occupational Med.*, **7**, 137–47 (1953)
64. Foreman, H., *J. Am. Pharm. Assoc., Sci. Ed.*, **52**, 629–32 (1953)
65. Foreman, H., and Hamilton, J. G., *U. S. Atomic Energy Commission Document, AECD-3247* (1951)[7]
66. Cohn, S. H., Gong, J. K., and Fishler, M. C., *Nucleonics*, **11**, 56–61 (1953)
67. Cohn, S. H., and Gong, J. K., *Proc. Soc. Exptl. Biol. Med.*, **83**, 550–54 (1953)
68. Gong, J. K., Milne, W. L., and Cohn, S. H., *U. S. Naval Radiol. Defense Lab. Document, USNRDL-426* (1953)
68a. Vaughan, J., and Tutt, M. L., *Lancet*, **265**, 856–59 (1953)
69. Bellin, J., and Laszlo, D., *Science*, **117**, 331–34 (1953)
70. Langham, W. H., *U. S. Atomic Energy Commission Document, WASH-490* (1954)[7]
71. Kisieleski, W. E., Norris, W. P., and Woodruff, L. A., *Proc. Soc. Exptl. Biol. Med.*, **77**, 694–96 (1951)
72. Neumann, K., and Harbers, E., *Naunyn-Schmiedeberg's Arch. exptl. Pathol. Pharmakol.*, **217**, 64–81 (1953)
73. Schubert, J., and White, M. R., *J. Biol. Chem.*, **184**, 191–96 (1950)
74. White, M. R., and Schubert, J., *J. Pharmacol. Exptl. Therap.*, **104**, 317–24 (1952)
75. Hackett, P. L., *Proc. Soc. Exptl. Biol. Med.*, **83**, 710–12 (1953)
76. Joffe, M. H., and Temple, L. A., *Atomic Energy Commission Document, HW-28636*, 92–97 (1952)[7]
77. Langham, W., and Carter, R. E., *Atomic Energy Commission Document, LA-1309* (1951)[7]
78. Katz, J., Weeks, M. H., and Oakley, W. D., *Radiation Research*, **2**, 166–70 (1955)
79. Weeks, M. H., Oakley, W. D., and Thompson, R. C., *Radiation Research*, **2**, 237–39 (1955)
80. Schubert, J., Finkel, M. P., White, M. R., and Hirsch, G. M., *J. Biol. Chem.*, **182**, 635–42 (1950)
81. Lindenbaum, A., White, M. R., and Schubert, J., *J. Biol. Chem.*, **190**, 585–93 (1951)
82. Mårtensson, J., *Acta Med. Scand.*, **125**, 82–94 (1946)
83. Carlsson, A., and Hollunger, G., *Acta Physiol. Scand.*, **31**, 317–33 (1954)
84. Seven, M. J., Gottlieb, H., Israel, H., Reinhold, J. G., and Rubin, M., *Am. J. Med. Sci.*, **228**, 646–51 (1954)
85. *Review of Literature on Toxicity, Physiological Effects and Medical Uses of Zirconium and Its Compounds* (Industrial Hygiene Foundation, Mellon Institute, Pittsburgh, Pa., 15 pp., 1954); this report has appeared in part in *Ind. Eng. Chem.*, **46**, 99A-102A (1954)
86. Kornberg, H., Thompson, R. C., and Wager, R. W., General Electric Company, Hanford, Wash. (Private communication, 1955)

87. Moore, E. E., and Sommers, L. O., *J. Am. Pharm. Assoc., Sci. Ed.*, **39**, No. 5 (1950)
88. Rosenthal, M. W., and Schubert, J., *Atomic Energy Commission Document, ANL-5332* (1954)[7]
89. Gofman, J. W., *J. Lab. Clin. Med.*, **34**, 297–304 (1949)
90. Dobson, E. L., Gofman, J. W., Jones, H. B., Kelly, L., and Walker, L. A., *J. Lab. Clin. Med.*, **34**, 305–12 (1949)
91. Copp, D. H., *Atomic Energy Commission Document, UCRL-332*, 19–21 (1949)[7]
92. Nicol, T., and Zikry, A. A., *Nature*, **170**, 239–40 (1952)
93. Heller, J. H., *Science*, **118**, 353–54 (1953)

VERTEBRATE RADIOBIOLOGY: PHYSIOLOGY[1,2]

By Abraham Edelmann[3]

Biology Department, Brookhaven National Laboratory, Upton, New York

In preparing this article, it became apparent to the author that during the few years which have elapsed since his last review (1), significant advances and changes in ideas had taken place. The descriptive phase of radiobiology has passed, and investigations are more concerned with the mechanisms of the phenomena. The number of scientists engaged in research in this field has increased and concomitantly the number of publications has grown. Additional evidence of not only this growth of interest but also the interdependence of biology, physics, and chemistry in the general field of radiobiology is the rapid growth of the Radiation Research Society and its journal, *Radiation Research*, both dedicated to a degree of integration of the natural sciences to the understanding of radiation effects.

One of the subjects receiving a great deal of interest was that of protection against the action of the rays. Alexander *et al.* (2) have reviewed the methods, both *in vivo* and *in vitro*, in use in evaluating the protective effect of various compounds. The function of the protective substance is possibly competitive removal of free radicals. The HO_2 radical may be important in bringing about the biological aftereffects which result in delayed death. Bonet-Maury & Patti (3) tested various chemicals and biological substances for protective effect. Preirradiation treatment with coal gas, KCN, and malonitrile offered protection, but none of these were effective when given after irradiation. No protection was afforded by the following, given either pre- or postirradiation: catalase, dinitra, sulfocyanide, sodium fluoride, mercury bichloride, hydroquinone, para-aminosalicylic acid (PAS), thiourea, gallic acid, thiomalic acid, formol, antithyroid agents, narcotics, temperature, antidiarrhetic agents, antihemorrhagic agents, Bardach's serum, liver extract, spleen extract, and antihistaminic agents.

Langendorff *et al.* (4) found that combinations of cystine and cortineurine were effective, and reconfirmed the protective action of cysteine and cysteamine. *N*-acetyl-cysteamine, cystinamine, and thiourea were also of benefit while di-thiopropanol (BAL) was not. The effects of *n*-acetyl-cysteamine and thiourea were evidenced even when administered 2 hr. prior to irradiation. These workers also indicated that radiation resistance was not increased by all compounds containing —SH groups.

Additional evidence of the action of cysteamine is furnished by Nelson

[1] The survey of literature pertaining to this review was terminated in June, 1955.

[2] The following abbreviations are used throughout the text: PAS (para-aminosalicylic acid); DNA (deoxyribonucleic acid); RBE (relative biological efficiency); KVP (kilovoltage, peak).

[3] Present address: Nuclear Science and Engineering Corporation, Pittsburgh 36, Pennsylvania.

(5), who found that this substance, given 30 min. before 800 r, exerted beneficial effects as measured by body weight, and time and rate of survival.

Ketones derived from pyrogallol, particularly 4-decanoylpyrogallol and 4-laurolpyrogallol were found to provide effective protection in mice by Lacassagne (6). Experiments on the ability of flavonoids to protect mice from the lethal effects of radiations have been equivocal. Arons *et al.* (7), however, present evidence that pretreatment for 10 days with bioflavenoid affords protection against radiation damage to the nail bed capillaries of humans.

When irradiated rats are joined to unirradiated rats by parabiosis the great majority of irradiated animals receive permanent protection according to Schneider *et al.* (8). Adrenalectomy or splenectomy of both parabionts results in reduced protection, while adrenalectomy or splenectomy of the nonirradiated partner significantly changed the degree of protection. The authors concluded that the spleen is necessary in the nonirradiated partner for permanent protection by parabiosis. Although the results from all parabiosis protection experiments are not in agreement, it appears to the present author that the method is effective. The manner in which parabiotic protection is accomplished may be dual in nature. The unirradiated partner may act as a "detoxifier" of substances produced in the irradiated parabiont and carried to it by the circulation and also it may serve as a supplier or donor of factors necessary to the recovery of the irradiated animal, for example, the spleen or bone marrow "factor."

The blood elements are the most dramatically affected and offer one of the more sensitive and readily studied criteria of radiation damage in mammals. It is therefore not surprising to find continuing advances in this field. Langendorff *et al.* (9) have reconfirmed the effects of spleen shielding and homologous and heterologous transplants in mice. Heterologous liver, transplanted intravenously, also increased the radioresistance of mice, and this is taken as evidence for a humoral factor affecting these responses. Loutit (10), in a short but good review of work attempting to determine whether spleen or bone marrow, or both, exert their effects through a humoral or a cellular mechanism, concludes that the cellular hypothesis has not been excluded. Lorenz & Congdon (11) demonstrated the protective effect of bone marrow transplants. Bone from mouse or rat transplanted intraperitoneally protected mice. Bone marrow formed in the homologous transplants, and it is postulated that this originated from the osseous tissue. Despite the protection afforded the mice by the rat bone, marrow tissue did not form and this is construed as evidence for a humoral factor or factors in this protection mechanism. Confirmatory evidence of the protective effect of bone marrow implants in mice has been produced by May & Arparian (12).

Beef embryo extract is also protective in mice, and Haley *et al.* (13) have fractionated this material and found no effect on total mortality as a result of injections of the fractions, attributable, they feel, to the presence of a beneficial and a detrimental factor in the extracts.

Gershon-Cohen & Hermel (14) studied the changes in whole and differential white counts in rats during the first 24 hr. after 85 to 5000 r. Marked differences occurred in the differential curves between those receiving sublethal and those receiving lethal doses. The authors suggest possible diagnostic and therapeutic applications. An increase in the incidence of bilobed and binucleated lymphocytes in peripheral blood with the peak occurring at one week after 75 r or less is reported by Belleck & Storer (15).

The granulocyte count taken four to seven days after exposure was associated with the survival of mid-lethally irradiated mice in the experiments of Smith *et al.* (16). No association between survival and lymphocyte count was found.

Rust *et al.* (17) reported that burros given 200 r fractionally of $Cobalt^{60}$ γ-rays responded similarly to, but slower than, 400 r. The decrease of platelets was correlated with a bleeding tendency which developed in the ninth irradiation day. One hour after 600 r, a marked hyperferremia is observed in the burro but the maximum response is observed following 1800 r.

Jacobson (18) has reviewed the factors concerned with the survival and recovery of the blood-forming tissue after irradiation.

A decrease in the nucleic acid content of bone marrow after irradiation was found by Schwartz *et al.* (19), while Erickson *et al.* (20) reported that injections of bone marrow suspension caused an overproduction of DNA purines in bone marrow and spleen of previously irradiated rats. The incorporation of C^{14}-tagged adenine into liver DNA purines of mice (21) was decreased by irradiation. A decreased DNA content of mouse mammary carcinoma cells in saline was found after irradiation (22). Harrington & Lavik (23), however, found that while irradiation markedly and constantly inhibited the incorporation of P^{32} into DNA phosphorus, of orotic acid-2-C^{14} into DNA pyremidines, and of sodium formate-C^{14} into DNA guanine, the incorporation of adenine-8-C^{14} into DNA purines was not inhibited.

Irradiation suppressed the inclusion of P^{32} into the protein fraction of rat spleen, and shielding of the spleen resulted in a markedly reduced effect (24). Radiation damage to the spleen was also demonstrated by Scherer & Stolle (25) who reported a decrease in Janus green staining particles of spleen cells after exposure. This is considered to damage elements concerned with the metabolism of enzymes. In this connection, the phosphorylation, oxygen uptake, and P/O ratio of isolated spleen mitochondria are significantly reduced 4 hr. after irradiation (26). However, measurements made by DuBois & Petersen (27) indicate that the adenosine triphosphatase and 5-nucleotidase activity of spleen and thymus of irradiated rats and mice exhibit a transient increased ability to hydrolyze adenosine triphosphate and 5-adenylic acid. Fellas *et al.* (28) reported that the acid-active deoxyribonuclease of rat spleen also increased markedly after whole body irradiation. The change was not apparent in the neutral enzymes of liver or spleen. Complementing these studies, Kowlessar *et al.* (29) found increased acid and neutral deoxyribonuclease activity in the urine of irradiated rats.

Smith *et al.* (30) found the time of increased adenosine triphosphatase activity after irradiation of mice to be shortened by treatment with spleen homogenate. There was little change in total spleen adenosine triphosphatase in mice treated with homogenate, while there was a prolonged decrease in levels of this substance in the nontreated controls.

Irradiation caused decreases in the concentration and turnover of the phosphorus of DNA of regenerating rat liver (31). Sherman & Forssberg (32) found that the specific activity of *ortho* P and acid-labile P from rat livers were markedly increased immediately after irradiation, but were lowered by 1 hr. The specific activity of the adenosine triphosphate fraction was not increased much until 24 hr. The specific activities of these fractions *in vitro* did not differ from the controls. The specific activities of these compounds in muscle were reduced by irradiation.

Schreier *et al.* (33) reported no defect in the ability of starved rats to conjugate benzoic acid-carboxyl-C^{14} as a result of x-irradiation.

A study of enzymes in the lens during the development of radiation-induced cataract has been made by van Heyningen *et al.* (34). During the development of opacity in an irradiated lens, the activities of glyoxalase and acetaldehyde oxidase fall. Aldolase activity falls in the opaque lens. Coenzyme A and nicotinic acid levels also decrease gradually during the development of the opacity. Shock & Puntenney (35) consider the lens itself to be the site of injury in radiation-induced cataract although the ciliary body is temporarily injured.

Cysteine injected to the subconjunctiva protected the epithelium, stroma, and endothelium of the cornea against 40,000 rep of β rays from a strontium^{90} ophthalmological applicator (36).

The central nervous system of both man and monkey have been found to be much more radiosensitive than previously supposed. In a series of studies (37 to 40) Arnold and his associates have found the effects not to be due to blood vessel occlusion. There is a definite selectivity on the part of white matter. Glial cells are adversely affected, and alterations in structure and function can be correlated with the total radiation dose, the intensity of administration, uniformity of dose distribution within the tissue, and the duration of time of observation after exposure. The primate brainstem and hypothalamus are more radiosensitive than cortical areas, responding to moderate dosage of radiations. Since the paraventricular and supraoptic nuclei, as well as the rest of the hypothalamus, are radiosensitive, the authors suggest that perhaps the therapeutic benefits which follow irradiation of the hypophyseal region for pituitary dysfunction are attributable to the effects of x-rays on the hypothalamus. Guinea pigs were given massive doses (1000 to 25,000) of radiation either to the head or entire body by Brace *et al.* (41). They found the higher the dose the earlier the death, with more pronounced symptoms of central nervous system involvement.

The monkey is being used more and more as an experimental animal in radiobiology. Eldred & Trowbridge (42) found the 30-day LD50 to be about

600 r and the LD100 about 800 r. The monkey usually vomits during irradiation. This is followed by a symptomless period and then one of gastrointestinal disturbance, one of hemorrhage and infection, followed by convalescence. Early deaths are associated with the gastrointestinal and hemorrhagic phases, while the late deaths are scattered. The usual changes in the blood picture appear to be the most sensitive index of exposure.

Warren & Kaplan (43) suggest the possibility of using a monkey intelligence test in the analysis of the effects of radiation on psychobiological efficiency. Doses up to 1500 r had no deleterious effects on the performance of monkeys (44). Following a lethal exposure the principal behavioral deficits were an increase in reaction time and failure to respond in the testing situation (45).

Jetter *et al.* (46) found mortality to be increased in dogs exhaustively exercised after 300 r of whole body x-irradiation. Kimeldorf & Baum (47) found similar results in rats exhaustively exercised daily after irradiation. The body, gluteus maximus, kidney, and thymus weights were reduced, while the adrenal weight was increased in animals subjected to daily exhaustive exercise or exposed to x-rays. The spleen and heart were enlarged after exercise, while they were reduced after most x-ray doses. The testis and pituitary weights were reduced by irradiation but not by exhaustive exercise.

More work was done on neutron effects. The relative biological efficiency (RBE) of thermal neutrons from the Los Alamos "Water Boiler" was found to be 1.37×10^{10} $n/\text{cm.}^2/\text{rem}$ compared to 250 KVP x-rays (48). Storer *et al.* (49) reported that animals exposed to lethal doses of neutrons die earlier than those exposed to equal rem doses of x- or γ-rays when rem was determined on a 30-day lethality basis. No unusual effectiveness of neutrons on the intestinal tract was found. Harris *et al.* (50), using spleen and thymus atrophy in mice as a test for the RBE of 14 Mev neutrons, found that an exposure of 1×10^8 $n/\text{cm.}^2$ was equivalent to 1 r of x-rays. On a basis of rep calculated from theoretical single collision curves, the data indicated the RBE of these neutrons to be about 1.6.

The pathology in mice resulting from thermal neutron irradiation was described by Upton *et al.* (51). Qualitatively these are indistinguishable from those of x-radiation. The RBE was similar for most late effects, i.e., the induction of leukemia and other neoplasms and reduction of longevity, as for acute lethality and acute hematologic injury. The RBE of thermal neutrons was several times higher for cataract induction than for acute lethality.

For dominant lethality in the offspring of irradiated male mice, Russell *et al.* (52) found the RBE of detonation neutrons as compared to cyclotron neutrons to be between 0.8 and 1.18; this difference in effectiveness of the two radiations was not statistically significant.

Following 320 to 1000 r of ionizing radiation from an atomic bomb, 100 per cent of exposed swine died (53). Using splenic and thymic weight loss in mice, Worman *et al.* (54) found β rays from tritium to be 1.3 as effective as

radium gammas. A single injection of 1/32 to 1/2 the 30-day LD 50 of U^{233} and U^{238} was found to have no chronic or delayed toxic effects (55).

Increased survival in rats exposed to radiation through grids having holes of various diameter but a constant open- to closed-area ratio resulted in increasingly greater survival as the hole size was decreased according to Kereiakes *et al.* (56). It is thought that the results are attributable to repair initiated in the irradiated areas from adjacent normal tissue.

Hursh *et al.* (57) demonstrated that the average survival time of 60-day survivors of a single dose of 600 r is significantly smaller than that of those receiving 600 r divided into either 10 daily doses of 60 r per day or 30 daily doses of 20 r per day. The same authors (58) found that the LD50 of 60-day survivors of 600 r was reduced after a second exposure. This is believed to result from an irreparable injury produced by the first dose. Baum *et al.* (59) exposed male rats one or more times to 75 r at 7-day intervals. Hematological examinations indicated that the maximal changes were largely independent of the number of exposures and reflected, mostly, the effects of the last irradiation. This was ascribed to the capacity of the hematopoietic system to recover from this dose in the 7-day interval.

Body-weight changes can reflect the degree of radiation damage. Chapman (61), using male mice, confirmed this and found different characteristics of the weight curves at different dose levels, and for the different sexes, males being the more radiosensitive. Body-weight decreases were also followed by Mancić (see 62), who also described an increase in the weight of the liver which he ascribes to increased protein metabolism, and a great increase in fat metabolism. Supplee *et al.* (63) found the liver of irradiated rats to increase in weight as early as 6 hr. after exposure to 600 r. The increase was due mainly to glycogen, but water content was also higher.

Following intravenous administration of colloidal radioactive gold to dogs, with consequent irradiation of the liver, the plasma content of serum albumen was decreased while that of gamma globulin was increased (64). The ascitic fluid was found to contain all plasma proteins, with albumen, γ_2-globulin, fibrinogen, and γ-globulin predominating.

Continued investigations of the lipemia in irradiated rabbits have shown correlations between increases of certain classes of lipoproteins and subsequent time of death (65). Milch *et al.* (66, 66a) reported that irradiation of the rabbit hind limb leads to a hyperlipoproteinemia which is similar to that seen after tourniquet ischemia or other muscle injury.

Following exposure to a strontium-90 source, Witten *et al.* (67) found two waves of erythema in the skin of patients. The first appeared in one to five days, the second in 32 to 59 or 58 to 73 days, depending upon the distance of the source during exposure. Griffith *et al.* (68) contrasted β- and x-ray effects on skin and found the two similar at low doses with the x-ray damage becoming more severe as the dosage is increased. The effects of $cobalt^{60}$ and $radium^{226}$ on rabbit skin were compared by Meschan & Nettleship (69), who found them to be identical except that those of cobalt were

more severe. Ungar & Damgaard (70) observed that β-rays depress local skin reactions to certain inflammatory stimuli, possibly by interfering with a tissue protease system which plays an important role in the inflammatory mechanism. They suggest that perhaps this inhibitory effect can be applied to the early detection of radiation injury.

The spreading of intradermally injected Evans blue is more rapid after whole-body x-irradiation. This radiation-induced permeability of dermal connective tissue occurs during the period of increased vascular permeability and purpura (71).

Moshman & Upton (72) suggest that the depigmentation of the fur of mice is correlated closely enough with the radiation dose to constitute a biological character. This correlation varies with different regions of the coat, the top of the head being most constant.

A review of radiation-induced skin cancer, with 21 case histories, has been prepared by Petersen (73). Bali & Furth (74) report that hemangioendotheliomas can be induced by x-rays. Koletsky *et al.* (75) suggest an indirect or systemic mechanism induced by radiation as possibly operating, in addition to direct tissue injury, in promoting carcinogenesis.

Increased susceptibility to experimental infection is demonstrated by irradiated animals, according to Shechmeister (76), who also reports that sublethal irradiation activates subclinical or latent infection in mice and possibly in rats. The resulting bacteremia is an important factor in radiation death. Scott & Stannard (77) showed that latent *Bartonella muris* infection in the rat can be activated by injecting Polonium^{210} or whole-body x-irradiation. These authors feel that an active bartonella infection in the rat does not exacerbate the lethal effects of an acute radiation dose, although the hematological response can be greatly altered. Bond *et al.* (78) discuss the pathogenesis and pathology of postirradiation infection, its role in the radiation syndrome, and its relation to other sequelae of irradiation. In combating the bacteremia brought on by irradiation, Haley *et al.* (79) feel that medication with antibiotics should start within the first postirradiation week, before massive bacteremia, to be effective.

A significant retardation of wound healing, as measured by tensile strength from the sixth to eleventh day after irradiation, was found in mice by Raventos (80). No effect of irradiation on the sensitivity of rats to painful thermal stimuli was observed by Ballin & Wilding (81), nor did they observe the radiation doses used to affect the analgesic response to morphine sulfate, codeine phosphate, meperidine hydrochloride, and methadone hydrochloride. The codeine, meperidine, and methadon in high dosage did not affect the ultimate lethality in mice.

Gros & Comsa (82) found that a reduction in metabolic rate in guinea pigs by phenothiazine and the methyl ester of piperidine-carboxylic acid increased resistance to irradiation. The effect was at its maximum when the animals were irradiated 10 hr. after injection, and disappeared after 24 hr.

Anesthesia with nitrous oxide may possibly afford some protection but

four other anesthetics did not. A critical change in response to anesthesia may occur immediately after irradiation, however (83).

Radiation reduces the tolerance of guinea pigs to anoxia as shown in experiments by Konecci (84).

Mateyko & Edelmann (85) have shown the rat pituitary to be radiosensitive, responding by alterations in the type of trophin elaborated, i.e., adrenocorticotrophin at the expense of gonadotrophin or thyrotrophin. The isolated adrenal cortex responds to γ radiation by a significant reduction in secretion of certain steroids (86). This perhaps results from the decreased ability of the gland to carry out certain oxidations and hydroxylations after irradiation (87).

Wyman *et al.* (88) found that irradiation of the prospective site of implantation of adrenals was more effective in preventing the transplantation than irradiation of the gland itself. However, once the implant was successful, direct irradiation of the tissue was more effective as regards its ability to grow and its histochemistry. Santisteban *et al.* (89) confirmed the need for adrenal secretions after irradiation.

Lindsay *et al.* (90) have described histological changes in the human thyroid following administration of various forms of internal and external radiations. Levene *et al.* (91) did similar experiments with dogs. Monroe *et al.* (92) reported that the thyroid-irradiated rat accumulated and bound more iodine than the unirradiated controls. A disturbance in the growth rate of rats and monkeys has been described by Hamilton *et al.* (93) following administration of astatine^{211}. It is felt that this is initially attributable to acute radiation injury and then to endocrine changes resulting from lack of thyroid hormone. Differences in effect of iodine^{131} and astatine^{211} are described.

Fleischmann & Brackin (94) found that the testosterone-induced growth of accessory sex organs of castrate male rats is only partially inhibited by x-irradiation.

Following irradiation, Smith & Lewis (95) found a marked increase in the number of atypical mast cells in the cheek pouches of hamsters. There was also a reduction in the total number of mast cells and repopulation was slow.

Clinical observations and data on the survivors of Hiroshima have been published in a series of papers by Ishibashi (96). Looney (97) stresses the importance of locating individuals with histories of previous administration of isotopes. These would provide a major source of clinical material for study of long term effects, if any, of small amounts of isotopes.

Tabershaw & Harris (98) have reviewed health and safety regulations at federal, state, local, and industrial levels. This is of moment because of the increased use of fissionable materials by industry, made possible by the Atomic Energy Act of 1954.

Gould *et al.* (99) suggested γ radiation of pork as a prevention of trichinosis, and Gomberg *et al.* (100, 101) pointed out the economic and practical feasibility of this. Goldblith & Proctor (102) discussed the relative merits of

β particles and γ rays for radiation sterilization of foods and concluded that while γ rays provide a more uniform distribution of energy, the efficiency of utilization is lower than that for β particles. The use of radiation for sterilization and preservation of foods has been discussed in some detail (103, 104). It would appear that the feasibility of this process as regards certain food products is clear and worthy of continued investigation.

LITERATURE CITED

1. Edelmann, A., *Ann. Rev. Physiol.*, **12,** 27–46 (1950)
2. Alexander, P., Fox, M., and Hitch, S. F., *Brit. J. Radiol.*, **27,** 130–31 (1954)
3. Bonet-Maury, P., and Patti, F., *Brit. J. Radiol.*, **27,** 72–76 (1954)
4. Langendorff, H., Koch, R., and Sauer, H., *Strahlentherapie*, **93,** 281–88 (1954)
5. Nelson, A., *Acta Radiol.*, **42,** 485–93 (1954)
6. Lacassagne, A., *Compt. rend.*, **238,** 1279–81 (1954)
7. Arons, I., Freeman, J., Sokoloff, B., and Eddy, W. H., *Brit. J. Radiol.*, **27,** 583–85 (1954)
8. Schneider, M., Wybourn, R. C., Binhammer, R., and Finerly, J. C., *Radiology*, **62,** 234–40 (1954)
9. Langendorff, H., Koch, R., and Sauer, H., *Strahlentherapie*, **93,** 274–80 (1954)
10. Loutit, J. F., *J. Nuclear Energy*, **1,** 87–91 (1954)
11. Lorenz, E., and Congdon, C. C., *J. Natl. Cancer Inst.*, **14,** 955–61 (1954)
12. May, R. M., and Arparian, N., *Compt. rend.*, **239,** 1151–53 (1954)
13. Haley, T. J., McCormick, H. G., and McCulloh, E. F., *U. S. Atomic Energy Commission Document, UCLA-311* (1954)
14. Gershon-Cohen, J., and Hermel, M. B., *Am. J. Roentgenol. Radium Therapy Nuclear Med.*, **71,** 846–52 (1954)
15. Belleck, S., and Storer, J. B., *U. S. Atomic Energy Commission Document, AMRL-162* (1954)
16. Smith, W. W., Gronshery, L., Alderman, I., and Cornfield, J., *Am. J. Physiol.*, **178,** 474–76 (1954)
17. Rust, J. H., Trum, B. F., Heglin, J., McCulloh, E., and Haley, T. J., *Proc. Soc. Exptl. Biol. Med.*, **85,** 258–61 (1954)
18. Jacobson, L. O., *Am. J. Roentgenol. Radium Therapy Nuclear Med.*, **72,** 543–55 (1954)
19. Schwartz, H. P., Riggs, H. E., Glick, C., McGrath, J., Childs, R., Berr, E., Jr., and Stone, F., *J. Phil. Gen. Hosp.*, **4,** 165–68 (1953)
20. Erickson, C. A., Main, R. K., and Cole, L. J., *U. S. Atomic Energy Commission Document, USNRDL-TR-14* (1954)
21. Way, J. L., Mandel, H. G., and Smith, P. K., *Cancer Research*, **14,** 812–16 (1954)
22. Menten, M. L., Feldsted, E. T., and Willms, M., *Exptl. Cell Research*, **7,** 83–94 (1954)
23. Harrington, H., and Lavik, P. S., *U. S. Atomic Energy Commission Document, NYO-4023* (1954)
24. Kuzin, A. M., and Budilova, E. V., *Doklady Akad. Nauk. S.S.S.R.*, **91,** 1183–86 (1953)
25. Scherer, E., and Stolle, F., *Strahlentherapie*, **93,** 317–20 (1954)
26. van Bekkum, D. W., Jongepier, H. J., Nieuwerkerk, H. T. M., and Cohen, J. A., *Brit. J. Radiol.*, **27,** 127–30 (1954)
27. DuBois, K., and Petersen, D. F., *Am. J. Physiol.*, **176,** 282–86 (1954)

28. Fellas, V. M., Meschan, I., Day, P. L., and Douglass, C. D., *Proc. Soc. Exptl. Biol. Med.*, **87,** 231–33 (1954)
29. Kowlessar, O. D., Altman, K. I., and Hempelmann, L. H., *Arch. Biochem. and Biophys.*, **52,** 362–72 (1954)
30. Smith, W. W., Anderson, W., Jr., and Ashwell, G., *Am. J. Physiol.*, **178,** 471–73 (1954)
31. Thomson, J. F., Carttar, M. S., and Tourtellotte, W. W., *Radiation Research*, **1,** 165–175 (1954)
32. Sherman, F. G., and Forssberg, A., *Arch. Biochem. and Biophys.*, **48,** 293–99 (1954)
33. Schreier, K., Altman, K. I., and Hempelmann, L. H., *Proc. Soc. Exptl. Biol. Med.*, **87,** 61–63 (1954)
34. van Heyningen, R., Pirie, A., and Boag, J. W., *Biochem. J. (London)*, **56,** 372–79 (1954)
35. Shock, D., and Puntenney, I., *Quart. Bull. Northwestern Univ. Med. School*, **28,** 359–63 (1954)
36. McDonald, J. E., *Arch. Opthalmol.*, **51,** 301–10 (1954)
37. Arnold, A., Bailey, P., Harvey, R. A., Haas, L. L., and Laughlin, J. S., *Radiology*, **62,** 37–46 (1954)
38. Arnold, A., and Bailey, P., *Am. Med. Assoc. Arch. Pathol.*, **57,** 383–91 (1954)
39. Arnold, A., Bailey, P., and Harvey, R. A., *Neurology*, **4,** 575–85 (1954)
40. Arnold, A., *J. Clin. Endocrinol. and Metabolism*, **14,** 859–68 (1954)
41. Brace, K. C., Andrews, H. L., and Thompson, E. C., *Am. J. Physiol.*, 386–89 (1954)
42. Eldred, E., and Trowbridge, W. V., *Radiology*, **62,** 65–73 (1954)
43. Warren, J. M., and Kaplan, S. J., *U. S. Atomic Energy Commission Document, NP-5371* (1954)
44. Melching, W. H., and Kaplan, S. J., *U. S. Atomic Energy Commission Document, NP-5412* (1954)
45. Kaplan, S. J., Delit, M., Gentry, G., and Melching, W. H., *U. S. Atomic Energy Commission Document, NP-5413* (1954)
46. Jetter, W. W., Lindsley, O. R., and Wohlwill, F. J., *U. S. Atomic Energy Commission Document, NYO-4548* (1954)
47. Kimeldorf, D. J., and Baum, S. J., *U. S. Atomic Energy Commission Document, USNRDL-427* (1954)
48. Brennan, J. T., Harris, P. S., Carter, R. E., and Langham, W. H., *Nucleonics*, **12,** 31–35 (1954)
49. Storer, J. B., Furchner, T. E., Ellinwood, L. E., Sanders, P. C., and Schweitzer, W., *U. S. Atomic Energy Commission Document, LA-1848* (1954)
50. Harris, P. S., Ellinwood, L. E., Anderson, E. C., Davis, R. W., Schweitzer, W., and Sanders, P., *U. S. Atomic Energy Commission Document, LA-1629*(1954)
51. Upton, A. C., Furth, J., and Christenberry, K. W., *Cancer Research*, **14,** 682–90 (1954)
52. Russell, W. L., Russell, L. B., and Kimball, A. W., *Am. Naturalist*, **88,** 269–86 (1954)
53. Tullis, J. L., Dawson, B. G., and Madden, S. C., *Radiology*, **62,** 409–15 (1954)
54. Worman, F. C. V., Turney, D. F., and Lotz, V., *U. S. Atomic Energy Commission Document, LA-1641* (1954)
55. Storer, J. B., Langham, W., Ellinwood, L. E., Furchner, T. E., Schweitzer, W., and Sanders, P., *U. S. Atomic Energy Commission Document, LA-1634* (1954)

56. Kereiakes, J. G., Parr, W. H., Storer, J. B., and Krebs, A. T., *U. S. Atomic Energy Commission Document, AMRL-139* (1954)
57. Hursh, J. B., Van Slyke, F., and Casarett, G., *U. S. Atomic Energy Commission Document, UR-317* (1954)
58. Hursh, J. B., Van Slyke, F., and Casarett, G., *U. S. Atomic Energy Commission Document, UR-318* (1954)
59. Baum, S. J., Kimeldorf, D. J., and Jacobsen, E. M., *U. S. Atomic Energy Commission Document, USNRDL-TR-12* (1954)
60. Greenfield, M. A., Billings, M. S., Norman, A., and Lewis, A. E., *U. S. Atomic Energy Commission Document, UCLA-278* (1954)
61. Chapman, W. H., *U. S. Atomic Energy Commission Document, NM-006012.* 04.67 (1954)
62. Bećarević, A. D., Kaćanski, K. L., and Mancić, D. D., *Bull. Inst. Nuclear Sci., Boris Kidrich (Belgrade)*, **4**, 105–9 (1954)
63. Supplee, H., Weinman, E. O., and Entenman, C., *U. S. Atomic Energy Commission Document, USNRDL-TR-18* (1954)
64. Clouet, D. H., Ball, C. O. T., Meneely, G. R., and Hahn, P. F., *Proc. Soc. Exptl. Biol. Med.*, **87**, 362–65 (1954)
65. Hayes, T. L., and Hewitt, J. E., *U. S. Atomic Energy Commission Document, UCRL-2790* (1954)
66. Milch, L. J., Yarnell, R. A., Stinson, J. V., Collins, J. G., Robinson, L. C., Croye, B. L., and Chang, S. S. M., *Science*, **120**, 713–14 (1954)
66a. Milch, L. J., Redmond, R. F., and Calhoun, W. W., *U. S. Atomic Energy Commission Document, NP-5124* (1954)
67. Witten, V. H., Brauer, E. W., Holmstrom, V., and Loeninger, R., *J. Invest. Dermatol.*, **23**, 271–85 (1954)
68. Griffith, H. D., Philip, J. F., and Swindell, G. E., *Brit. J. Radiol.*, **27**, 107–12 (1954)
69. Meschan, I., and Nettleship, A., *Am. J. Roentgenol. and Radium Therapy Nuclear Med.*, **71**, 306–19 (1954)
70. Ungar, G., and Damgaard, E., *Proc. Soc. Exptl. Biol. Med.*, **87**, 383–86 (1954)
71. Upton, A. C., and Gude, W. D., *Am. Med. Assoc. Arch. Pathol.*, **58**, 258–64 (1954)
72. Moshman, J., and Upton, A. C., *Science*, **119**, 186–87 (1954)
73. Petersen, O., *Acta Radiol.*, **42**, 221–36 (1954)
74. Bali, T., and Furth, J., *Oncologia*, **7**, 231–44 (1954)
75. Koletsky, S., Gustafson, G. E., Goldston, P., and Milanich, V., *U. S. Atomic Energy Commission Document, NYO-4964* (1954)
76. Shechmeister, I. L., *Radiation Research*, **1**, 401–9 (1954)
77. Scott, J. K., and Stannard, J. N., *J. Infectious Diseases*, **95**, 302–8 (1954)
78. Bond, V. P., Silverman, M. S., and Cronkite, E. P., *Radiation Research*, **1**, 389–400 (1954)
79. Haley, T. J., McCulloh, E. F., and McCormick, W. G., *U. S. Atomic Energy Commission Document, UCLA-287* (1954)
80. Raventos, A., *Proc. Soc. Exptl. Biol. Med.*, **87**, 165–67 (1954)
81. Ballin, J. C., and Wilding, J. L., *U. S. Atomic Energy Commission Document, NP-5329* (1954)
82. Gros, C. M., and Comsa, J., *Compt. rend.*, *239*, 832–34 (1954)
83. Burdick, K. H., *U. S. Atomic Energy Commission Document, AF-SAM-21-3501-0005-7* (1954)

84. Konecci, E. B., *U. S. Atomic Energy Commission Document, NP-5516* (1954)
85. Mateyko, G. M., and Edelmann, A., *Radiation Research*, **1**, 470–86 (1954)
86. Ungar, F., Rosenfeld, G., Dorfman, R. I., and Pincus, G., *Endocrinology*, **56**, 30–36 (1953)
87. Rosenfeld, G., Ungar, F., Dorfman, R. I., and Pincus, G., *Endocrinology*, **56**, 24–29 (1955)
88. Wyman, L. C., Whitney, R., Griffin, P. L., and Patt, D. I., *J. Cellular Comp. Physiol.*, **44**, 33–47 (1954)
89. Santisteban, G. A., Bowers, J. Z., and Dougherty, T. F., *Endocrinology*, **55**, 794–807 (1954)
90. Lindsay, S., Dailey, M. E., and Jones, M. D., *J. Clin. Endocrinol. and Metabolism*, **14**, 1179–1218 (1954)
91. Levene, M. B., Andrews, G. A., and Kniseley, R. M., *Am. J. Roeetgenol. Radium Therapy Nuclear Med.*, **73**, 88–97 (1955)
92. Monroe, R. A., Rust, J. H., and Trum, B. F., *Science*, **119**, 65–67 (1954)
93. Hamilton, J. G., Durbin, P. W., and Parrott, M., *J. Clin. Endocrinol. and Metabolism*, **14**, 1161–78 (1954)
94. Fleischmann, W., and Brackin, J. T., Jr., *Endocrinology*, **54**, 227–28 (1954)
95. Smith, D. E., and Lewis, Y. S., *Proc. Soc. Exptl. Biol. Med.*, **85**, 306–7 (1954)
96. Ishibashi, K., *Nagoya J. Med. Sci.*, **14**, 163–205 (1951)
97. Looney, W. B., *Am. J. Roentgenol. Radium Therapy Nuclear Med.*, **72**, 838–48 (1954)
98. Tabershaw, I. R., and Harris, S. J., *Nucleonics*, **12**, 8–13 (1954)
99. Gould, S. E., Gomberg, H. J., and Bethell, F. H., *Am. J. Public Health*, **43**, 1950–57 (1954)
100. Gomberg, H. J., Gould, S. E., Nehemias, J. V., and Brownell, L. E., *Nuclear Engineering Part III Chem. Eng. Progr. Symposium Ser. No. 13*, 89–104 (1954)
101. Gomberg, H. J., Gould, S. E., Nehemias, J. V., and Brownell, L. E., *Nucleonics*, **12**, 38–42 (1954)
102. Goldblith, S. A., and Proctor, B. F., *Nucleonics*, **12**, 32–35 (1954)
103. Denny, C. B., Bohrer, C. W., and Reed, T. M., *U. S. Atomic Energy Commission Document, AECU-2952* (1954)
104. American Meat Inst. Foundation, *U. S. Atomic Energy Commission Document, AECU-2951* (1954)

AUTHOR INDEX

A

Abbott, T. A., 204
Abrahamson, S., 358
Acheson, L. K., Jr., 31
Adair, R. K., 100, 106, 122, 130
Adams, M. H., 338
Adams, W. R., 328
Adamson, D. M., 333, 340
Ahearn, A. J., 208, 246
Ajzenberg, F., 76
Albert, R. D., 78, 88
Albouy, G., 312, 313, 321
Alburger, D. E., 49
Alder, F., 17
Alderman, I., 415
Alexander, G. V., 374
Alexander, M. L., 328, 333, 347, 349, 353, 354, 355, 356
Alexander, P., 226, 227, 228, 234, 327, 328, 340, 344, 413
Alford, W. L., 147
Allen, A. O., 215, 228, 229, 231, 232
Alper, T., 233, 333
Altenburg, E., 358
Altman, K. I., 415, 416
Alvarez, L., 170
Amaldi, E., 27, 35, 101
Amphlett, C. B., 233
Ander, P., 225, 226
Anderson, C. D., 147, 148
Anderson, E. C., 311, 417
Anderson, G., 350, 357
Anderson, L. C., 223, 224
Anderson, M. R., 286
Anderson, R. C., 245
Anderson, R. L., 279
Anderson, W., Jr., 416
Andresen, C. C., see Chapman-Andresen, C.
Andresen, N., 312, 319, 321
Andrews, G. A., 420
Andrews, H. L., 416
Ansheles, J. M., 314
Anta, M. C., 214, 216, 230, 231
Anthanole, V. T., 278
Arfken, G. B., 45
Arnason, T. J., 348
Arnold, A., 416
Arnold, G. P., 77
Arnold, J. S., 300, 317
Arnold, W. H., 148
Arons, I., 414
Arons, W. L., 289, 290
Aronson, R., 78, 81, 87, 88
Arparian, N., 414
Arroe, H., 45
Artsimovitch, L., 101
Asboe-Hansen, G., 316
Ascoli, G., 93
Ashikawa, J. K., 288
Ashkin, J., 118
Ashwell, G., 341, 416
Atwood, K. C., 330, 331, 333, 351
Aub, J. C., 372, 373, 375, 376
Auerbach, C., 353, 354, 356, 357
Aurand, K., 352
Austern, N., 4, 21, 131
Avery, R., 21
Axelrod, D. J., 374, 376, 393
Azimov, S., 147

B

Bacher, R. F., 25
Bachofer, C. S., 329, 332, 333, 334
Bacq, Z. M., 327, 328, 340, 344, 355
Bailey, P., 416
Bailey, T. L., 246
Bair, W. J., 340
Baker, C. J., 126
Baker, W. H., 386, 387, 389, 392
Baker, W. K., 351, 355
Bali, T., 419
Ball, C. O. T., 418
Ballam, J., 146, 148
Ballantine, D. S., 225, 226
Ballin, J. C., 419
Ballou, N. E., 285
Balske, R. J., 346
Balthazard, V., 369
Balwit, J. S., 226, 227, 228
Banarjee, G. I., 278
Banerjee, S., 284, 285
Banks, C. V., 278
Baranger, E., 35
Barbera, R. C., 374
Bardwell. D. C., 226
Bareis, D., 282
Barkas, W. H., 43
Barker, K. H., 153
Barker, R. C., 279
Barnard, G. P., 210, 241
Baron, L. S., 330, 340, 341
Barron, E. S. G., 233, 234, 327, 334, 340, 350
Barschall, H. H., 63, 100, 106, 122, 123, 126
Bartell, L. S., 315
Bartels, J., 207
Bartlett, J. H., 31
Bartlett, M. S., 153
Barton, D. W., 347, 357
Baskett, A. C., 226
Bassett, S. H., 387
Bassili, Y. F., 291
Batalin, A. Kh., 278
Bates, C. J., 328, 330
Bates, D. R., 243
Bates, D. V., 207
Bauer, N., 255
Baum, S. J., 417, 418
Bautz, E., 341
Bawden, F. G., 337
Baxendale, J. H., 233
Beach, J. Y., 255
Beam, C. A., 327-68; 331, 338, 339, 345
Beard, B. H., 350, 358
Beatty, A. V., 344, 348
Beatty, J. W., 344
Bécarević, A. D., 418
Beck, C. K., 184
Becker, R. L., 100, 106, 122
Becquerel, H., 297
Beiser, A., 297, 298, 305, 309, 312, 313, 318, 319
Bekkum, D. W. van, 415
Bélanger, L. F., 317
Belcher, R., 270
Belitz, H. J., 357, 358
Belknap, E. L., 380
Bell, G. E., 311
Bell, R. E., 10
Belleck, S., 415
Bellin, J., 389
Benedict, J. T., 290
Benedict, M., 179
Benillard, P., 278
Bennet, W., 284
Bennett, W. H., 205
Benzer, S., 337
Berger, H., 334, 337
Berger, J. M., 21
Berger, M. J., 84
Bernardini, G., 134, 140
Bernas, A., 229
Bernstein, R. B., 256
Bernstein, S., 81
Bernstein, W., 216, 293
Berr, E., Jr., 415
Berrie, A. M. M., 329, 336
Berriman, R. W., 310, 311, 320, 321
Berry, C. E., 197-212; 203, 204, 206, 209, 251
Bersworth, F. C., 386
Bessman, S. P., 380
Bethe, H. A., 25, 81, 102, 111, 121, 306
Bethell, F. H., 420
Beutler, E., 345

Bevan, A. R., 154, 162, 163
Beydon, J., 286
Beyster, J. R., 77, 126
Biagini, C., 328, 334
Biedenharn, L. C., 2, 9, 111
Billen, D., 336, 340
Binhammer, R., 414
Biram, M. B., 87
Bird, M. J., 347, 356
Birge, A. C., 333
Birger, N., 147
Birks, J. B., 223
Birnbaum, W., 43
Bishop, O. N., 316
Bitter, F., 31
Bjerge, T., 101
Bjornerud, E. K., 147
Blackburn, P. E., 248
Blackett, P. M. S., 152, 174
Blair, J. S., 25
Blakeslee, A. F., 349, 357
Blanchard, C. H., 21
Blaser, J. P., 63
Blatt, J. M., 3, 25, 111, 121
Bleakney, W., 205, 242, 243
Bleuler, E., 131
Blizard, E. P., 73-98; 78, 85, 87, 88, 89, 92
Bloch, C., 121
Bloch, F., 22
Block, M. M., 157
Bloom, M. A., 327
Bloom, W., 327, 344
Blosser, T. V., 84
Blum, H. F., 343, 346
Blumenfeld, H., 151
Blumenthal, H. T., 340
Blundell, M., 316
Boag, J. W., 215, 216, 221, 330, 348, 416
Board, F. A., 314, 315
Bochinski, J., 282, 287
Bock, R., 280
Bockelman, C. K., 100, 106, 122
Bodmer, A. R., 31
Boehm, F., 63
Boelhouwer, C., 226
Bogaardt, M., 306
Bogoroch, R., 316, 317, 322
Bohr, A., 17, 48, 52, 66
Bohr, N., 67, 99, 100, 101
Bohrer, C. W., 421
Bollea, F., 339
Bollinger, L. M., 123
Bond, V. P., 419
Bonet-Maury, P., 413
Bonner, T. W., 75, 126
Bonnier, G., 356
Booth, E. T., 134, 140, 151
Bora, K. C., 347
Borg, R., 289, 290
Born, M., 66
Borst, L. B., 179-96
Borstel, R. C. von, 352, 355
Bortner, T. E., 215, 262
Bothe, W., 145
Bouchard, C., 369
Bourne, G. H., 315
Bouwkamp, C. J., 3
Bowen, E. J., 223
Bowen, G. H., 335, 336, 337
Bowers, J. Z., 330, 341, 420
Boyd, G. A., 314, 315, 316, 320, 322
Brace, K. C., 416
Brackin, J. T., Jr., 420
Brandt, C. L., 338, 346
Brandt, H., 349
Branson, H., 248
Bratenahl, A., 63
Brauer, E. W., 418
Braune, G., 281, 287
Brazolla, A. M., 339
Breazeale, W. M., 185
Breit, G., 27, 45, 105
Brennan, J. T., 417
Brenner, A., 63
Bretton, R. H., 225
Bridge, H., 150
Briscoe, W. A., 207
Brix, P., 45
Broch, E. K., 45
Brockway, L. O., 315
Brode, R. B., 146
Brown, A. H., 207
Brown, R. A., 197, 209
Brown, S. W., 355
Brown, W. W., 152, 157
Brownell, L. E., 420
Brucer, M., 305
Brueckner, K. A., 45, 64, 67, 122
Brumfield, R. T., 346
Bruner, H., 305
Bruns, A., 357
Bryce, W. A., 249
Brysk, H., 215
Bryson, V., 330, 340,341
Budilova, E. V., 415
Bueche, A. M., 226, 227
Buie, D. H., 317
Bunney, L. R., 289, 290
Burcham, W. E., 126
Burdick, K. H., 420
Burhop, E. H. S., 152, 242, 243
Burkig, J. W., 126
Burnelle, L., 249
Burns, V. W., 333, 345
Burton, M., 215, 220, 223, 226, 263
Burwell, J. R., 149
Busey, H. M., 184
Butler, S. T., 131, 133
Butslov, M. M., 175
Buttes, J. P., 280
Buttlar, H. von, 45

C

Cahn, A., 75
Caldas, L. R., 335
Caldecott, R. S., 350, 358
Calhoun, J. A., 373
Calhoun, W. W., 418
Calvin, M., 380, 382, 397
Campbell, E. C., 283
Carleton, R., 346
Carlson, B. C., 46
Carlson, J. G., 344, 345
Carlsson, A., 396
Carr, H. E., 255
Carrick, G. R., 209
Carter, F. E., 387, 389, 400, 417
Carter, R. S., 123, 152
Carttar, M. S., 416
Casarett, G., 418
Casimir, H. B. G., 3
Caspar, A. L., 354
Castognoli, C., 329, 333
Caswell, R. S., 88
Catala, J., 307
Cave, M. S., 355
Certaine, J., 78, 85, 87, 88
Chadwick, J., 25
Chang, S. S. M., 418
Chang, W. Y., 26
Chapiro, A., 216, 221, 222, 225
Chapman, G. B., 346
Chapman, G. T., 78, 89
Chapman, W. H., 418
Chapman-Andresen, C., 312, 316, 319, 321, 322
Charlesby, A., 226, 227, 228
Charpie, R. A., 135
Chase, D. M., 127
Chase, R. L., 293
Chaudhuri, S. P. R., see Ray-Chaudhuri, S. P.
Chemla, M., 280
Cheng, K. L., 278
Chiga, M., 340
Childs, R., 415
Chinn, H. F., 330, 340
Choyke, W. J., 157
Christenberry, K. W., 417
Christensen, E., 358
Christy, R. F., 44, 66
Chupka, W. A., 248
Church, E., 5
Churchill, J. R., 314
Clark, F. H., 76
Clarke, E. M., 243, 244
Clarke, R. L., 134, 135
Clasen, H., 244
Clayton, F. E., 328, 333, 347, 348, 349,352, 353, 354, 355, 356
Clendenin, W. W., 45
Clerc, R. J., 198, 200, 201, 203
Clermont, Y. G., see Goldschmidt-Clermont, Y.
Clifford, C. E., 84
Clokie, H., 288
Clouet, D. H., 418
Coates, A. C., 319
Coats, F. H., 245
Cobb, J., 309, 311, 316

Cochran, E. L., 224
Cohen, B. L., 126, 127, 128, 129, 135
Cohen, J. A., 415
Cohen, J. G., see Gershon-Cohen, J.
Cohen, M. J., 152
Cohn, S. H., 387, 388, 389, 390, 391, 393, 400, 401, 408
Cole, L. J., 415
Coleby, B., 221
Coleman, F. F., 247
Collin, J., 262
Collins, J. G., 418
Collinson, E., 222, 225, 229, 232
Colombo, P., 225
Comar, C. L., 299
Combrisson, J., 218, 225
Comsa, J., 419
Condon, E. U., 253, 256
Congdon, C. C., 414
Conger, A. D., 349, 351
Connally, R. E., 293
Constantin, T., 339
Conway, B. E., 233
Cook, C. F., 126
Cook, G. L., 198
Cook, J. S., 343, 346
Coon, J. H., 63, 126
Cooper, L. N., 26
Copp, D. H., 373, 374, 376, 377, 389, 393, 397, 399, 400, 401, 402, 405, 408
Corben, H. C., 42
Cork, J. M., 307
Cormack, D. V., 216
Cornelius, R. C., 163, 167
Cornfield, J., 415
Corte, M. D., see Della Corte, M.
Coryell, C. D., 290
Cotè, R., 123
Cottin, M., 214, 216, 230, 231, 233
Courcy, S. J. de, 342
Cowan, E. W., 150, 155, 174
Cowan, F. P., 371, 374
Cox, B. C., 217, 244
Craggs, J. D., 246
Cramer, C., 376, 377
Cranberg, L., 126
Craver, L. F., 375
Crawford, F., 170
Crawford, J. W., 94
Crawford, M. F., 45
Cronkite, E. P., 419
Crouse, H. V., 354
Crowe, L. K., 357
Crowley, J., 388, 394, 397
Croye, B. L., 418
Cuer, P., 307
Culler, G., 126, 130
Cummings, J., 349, 357
Curie, P., 369

D

Dabbs, J., 75
D'Agostino, O., 101
Dahlberg, V., 285, 286
Dailey, M. E., 420
Dainton, F. S., 213-40; 214, 215, 221, 222, 225, 229, 232, 233
Dale, W. M., 327
Dalitz, R. H., 21
Damgaard, E., 419
Daniel, G. E., 334, 346
Daniels, D. S., 349
Darden, S. E., 77, 100, 106, 122, 126, 130
Darlington, C. D., 328, 344, 346, 353, 354
Das, N. K., 353
Das Gupta, N. N., 145
Davis, M., 328, 329
Davis, R., 282
Davis, R. J., 278
Davis, R. W., 417
Davison, S., 328, 330
Davisson, C. M., 77
Dawson, B. G., 417
Day, P. L., 415
Day, R. A., Jr., 286
Day, R. B., 126
Dayton, I. E., 127, 132
Dean, J. A., 280
de Courcy, S. J., see Courcy, S. J. de
DeFord, D. D., 277
Deitz, W., 281
Delbrück, M., 328
Delit, M., 417
Della Corte, M., 309, 318
Demers, P., 302, 312
Dennis, G. E., 139
Denny, C. B., 421
DeSerres, F. J., 348
de Shalit, A., see Shalit, A. de
Dessauer, F., 327
Devins, J. C., 220
Devlin, T. R. E., 225
Dewhurst, H. A., 215, 228
Deysson, G., 353
Dibeler, V. H., 243, 246, 255, 262
Dick, J. L., 284
Dieckmann, C., 330
Diehl, H., 280
Dienes, G. J., 225, 226
Dietz, W., 287
Dilworth, C. C., 309
Dingledy, D. P., 248
Dittrich, W., 348, 349
Diven, B. C., 133
Dixon, W. R., 83
Dizdar, Z., 288, 290
Dobrotin, N., 147
Dobson, E. L., 405
Dobyns, B. M., 298
Dodd, J. N., 126
Doering, W. P., 88
Doherty, W., 197
Dolar, D., 289, 290
Dole, M., 226, 227
Dollinger, E. J., 357
Dollmann, E. M., 309
Dondes, S., 220
Doniach, I., 315, 317, 318, 322
Donnally, B. L., 255
Donner, W., 205
Dorfman, L. M., 221
Dorfman, R. I., 420
Dotta, S. K., 278
Dougherty, T. F., 420
Douglas, C. H., 216
Douglas, D. L., 285
Douglass, C. D., 415
Downs, B. W., 61
Draganic, Z., 289, 290
Drell, S. D., 5
Dresner, L., 66
DuBois, K. B., 327, 340, 415
Duchesne, J., 249
Dudenbostel, B. F., 210
Dudgeon, E., 347, 348, 349, 352
Dudley, H. R., 382, 386, 387, 389, 392
Dudley, R. A., 298, 310, 311, 321
Dukey, D. L., 204
Dulbecco, R., 338
Dunn, C. G., 334
Dunning, W. J., 247
Dunton, M. L., 271
Durbin, P. W., 420
Dwyer, F. P., 278
Dyckerhoff, H., 380
Dyrssen, D., 285, 286

E

Easton, T. W., 375, 408
Ebel, A. A., 133
Ebel, J. P., 291
Ebert, M., 216, 221, 233, 333, 351
Eckart, W., 330
Eddy, W. H., 414
Edelmann, A., 413-24; 413, 420
Eden, R. J., 101
Edington, C. W., 351
Edlund, M. C., 179
Edmonds, A. R., 15
Edmundson, M., 358
Ehrenberg, L., 216,343, 348, 350, 351, 357
Ehret, C. F., 332
Ehrlich, M., 312
Ehrmann, J. B., 46
Eichel, H. J., 341
Eidinoff, M. L., 316
Eisberg, L. M., 166
Eisberg, R. M., 25, 135
Eisenbud, L., 100, 102

Ekstein, D. M., 382, 387
Eldred, E., 416
Elkind, M., 331, 339
Ellenburg, J. Y., 285, 286
Ellinwood, L. E., 417, 418
Elliot, J. O., 83
Elliott, A., 197
Elliott, J. B., 163
Elliott, J. P., 49, 66
Ellis, C. D., 25
Eltenton, G. C., 247
Elton, L. R. B., 35
Elving, P. J., 271
Ely, J. O., 342
Emigh, C. R., 151, 152
Emmerich, W. S., 63, 122
Endicott, K. M., 317
Englander, S. W., 329
Engler, N. A., 47
Entenman, C., 418
Epstein, H. T., 329
Erdmann, K., 343
Erickson, C. A., 415
Errera, M., 328, 336, 338, 342, 345, 346
Erskine, G. A., 215
Essex, H., 218, 220
Evan, M. W., 255
Evans, M. G., 247
Evans, R. D., 77, 372, 373, 376
Evans, T. C., 316, 317
Everett, N. B., 314, 315, 316
Ewald, H., 241, 263
Ewing, D. H., 99, 100, 111, 120, 131
Eyring, H., 241-68; 251, 253, 255, 259
Ezmirlian, F., 374

F

Fahmy, O. G., 347, 356
Fairhall, L. T., 375
Fano, U., 77, 81, 83
Farabee, L. B., 371, 374
Faraggi, H., 312, 313, 321
Farmer, F. T., 216, 225, 232
Farmer, J. B., 247
Farrar, R. T., 83
Farwell, G. W., 25, 130
Fechter, H., 25
Fedoruk, S., 215
Feenberg, E., 10, 18, 45, 46
Feld, B. T., 78
Feldsted, E. T., 342, 415
Fellas, V. M., 415
Fenton, B. J., 348
Fermi, E., 101
Fernbach, S., 63, 102, 126, 130
Ferrari, F., 27
Ferrell, R. A., 75
Feshbach, H., 31, 35, 78, 104, 106, 109, 110, 112, 120, 122, 123, 124, 125, 133
Fidecaro, G., 27, 35
Field, F. H., 217, 245, 260, 262
Fields, R. E., 100, 106, 122, 130
Figge, F. H. J., 342
Finerly, J. C., 414
Finkel, A. J., 375
Finkel, M. P., 390
Finston, H. L., 269-96; 272, 287
Fiquet, F., 229
Fireman, E. L., 152
Firestone, R. F., 214
Firsching, F. H., 271, 281
Fischer, G. E., 132
Fischer, W., 287
Fishler, M. C., 389, 390, 391, 393
Fitch, T. E., 87
Fitch, V., 26
Fitzgerald, P. J., 316, 317
Flaschka, H., 272
Fleischmann, W., 420
Flinn, F. B., 375
Flowers, B. H., 7, 14, 49, 66
Flynn, J. H., 256
Foldy, L. L., 7, 21, 81
Foley, H. M., 17, 48
Foner, S. N., 242, 247
Ford, K. W., 25-72; 14, 20, 25, 26, 28, 44, 45, 49, 52, 63, 130, 131
Foreham, H., 382, 386, 387, 388, 389, 390, 392, 393, 394, 396, 397
Forro, F., 327, 346
Forssberg, A., 342, 346, 351, 352, 416
Forster, R. E., 207
Foster, D. G., 280
Fowler, E. C., 154, 157, 165
Fowler, J. F., 225
Fowler, P. H., 307, 309
Fowler, W. B., 158, 165, 166
Fox, L., 210
Fox, M., 94, 234, 413
Fox, R. E., 242, 243, 244, 253, 254
Francel, R. J., 258
Francis, A. E., 133
Francis, J. E., 75
Francis, N. C., 101, 113
Franck, J., 223
Frank, H., 45
Franke, A. A., 289, 290
Franklin, J. L., 217, 245, 260
Franklin, R., 329, 330, 331
Franz, W., 3
Freedman, M. S., 286
Freeman, B. E., 28
Freeman, G. R., 215, 234
Freeman, J., 414
Freeman, J. W., 317
Freemantle, R. G., 126, 130, 132, 133
Freiling, E. C., 289, 290
Freiser, H., 278
Freska, H. F., see Friedrich-Freksa, H.
French, J. B., 3
Fretter, W. B., 145-78; 146, 148, 150, 174, 175
Friedenwald, J. S., 345
Friedman, F. L., 126
Friedman, H. L., 256
Friedman, M., 328, 331
Friedrich-Freksa, H., 329, 340, 357
Friesen, E. W., 150, 174, 175
Friech, O. R., 101
Froman, P. O., 66
Fujinga, T., 277
Fukushima, S., 224
Fulmer, R. E., 275
Fundaminsky, A., 243
Funkhouser, J., 277
Fuqua, P. A., 386, 387, 389, 392
Furchner, T. E., 417, 418
Furth, J., 417, 419

G

Gabbard, R. F., 88
Gaden, E., 334, 339, 340
Gaerttner, E. R., 151, 152
Gaither, N., 333, 346
Gallagher, D. M., 372, 376
Gamble, R. L., 75
Gans, D. M., 101
Gardner, C. O., 350, 358
Garrison, W. M., 230
Gartner, H., 345
Gatha, K. M., 63
Gaulden, M. E., 344, 345
Gebauer, W., 278
Geckler, R. P., 343, 346
Geerk, J., 248
Geilman, W., 278
Gell-Mann, M., 6, 106
Gentner, W., 145
Gentry, G., 417
Gershon-Cohen, J., 415
Gevantman, L. H., 263
Ghiorso, A., 63
Ghormley, J. A., 215, 231, 233
Ghosh, S. K., 145, 150
Gibson, N. A., 278
Gibson, W. M., 126, 130, 133, 307
Gierlach, Z. S., 343
Giese, A. C., 332, 337, 338, 346
Gifford, A. P., 204, 205, 206
Gignac, S., 380
Gilbert, R. S., 285
Giles, N. H., 346, 348, 350, 351
Gillan, G. K., 185
Glass, R. A., 288
Glaser, D. A., 167, 168, 169,

170, 173
Glassgold, A. E., 31
Glasstone, S., 179, 251
Glendenin, L. E., 307
Glick, C., 415
Glines, A., 225
Glubrecht, H., 342
Glücksmann, A., 344
Goeppert-Mayer, M., 48
Goertzel, G., 3, 46, 87, 204
Gofman, J. W., 405
Goishi, W., 285, 286
Goldberger, M. L., 78, 101, 102, 106, 134
Goldblith, S. A., 328, 330, 420
Goldhaber, G. S., see Scharff-Goldhaber, G.
Goldhaber, M., 1-24; 1, 10, 54
Goldman, L. M., 126
Goldschmidt-Clermont, Y., 297
Goldstein, H., 77, 78, 81, 82, 83, 85, 86, 87, 88
Goldston, P., 419
Goldwasser, E. L., 146
Gombas, P., 67
Gomberg, H. J., 316, 317, 420
Gong, J. K., 388, 389, 390, 391, 393, 400, 401, 408
Goodman, C., 17, 56, 133, 139, 179
Goodman, L. S., 126
Gordon, L., 271, 272
Gordon, S., 217, 234
Gorman, J. G., 208
Gottfried, K., 67
Gottlieb, H., 396
Goucher, C. R., 341
Gould, S. E., 420
Govaerts, J., 347
Graevskii, E. Ya., 333
Graham, R. L., 10
Grave, A., 133
Graves, E. R., 63, 126, 139
Gray, L. H., 216, 221, 328, 330, 333, 351, 352, 354
Graziosi, F., 329, 333
Green, A. E. S., 47
Green, M., 284
Greenberg, D. M., 373, 374
Greenlees, G. W., 133
Gregory, B., 148, 150
Greuling, E., 81
Grieff, D., 340
Griffin, P. L., 420
Griffith, H. D., 418
Grigorieff, W. W., 179
Gronshery, L., 415
Gros, C. M., 419
Gross, J., 317, 322
Grossi, V., 334
Grossweiner, L. I., 228, 234
Grove, D. J., 242
Gude, W. D., 419
Gudzent, F., 369
Guest, R. J., 284
Gugelot, P. C., 126, 132, 136, 137, 138, 139
Gunning, H. E., 256
Gupta, N. N. D., see Das Gupta, N. N.
Gurney, R. W., 303
Gustaffson, A., 348, 350, 351, 357
Gustafson, G. E., 419
Gustafson, P. R., 371
Gutbier, H., 217, 246
Guth, E., 35, 39

H

Haas, F. L., 328, 333, 334, 337, 347, 348, 352, 353, 354, 355, 356
Haas, L. L., 416
Hackett, P. L., 389, 398, 406
Hagstrum, H. D., 245, 248
Hahn, B., 26, 61
Hahn, P. F., 418
Hahn, R. B., 277, 279
Haissinsky, M., 214, 216, 230, 231
Halban, H. v., 101
Haley, T. J., 414, 415, 419
Hall, D., 75
Hall, G. G., 244, 245, 251, 261
Hall, L. G., 205
Hall, N. F., 290
Hall, T. A., 328
Halvorsen, H., 340
Halzbecker, Z., 278
Hamill, W. H., 219, 224
Hamilton, J. B., 389, 396 397, 399, 400, 401, 402, 405
Hamilton, J. G., 374, 376, 377, 387, 389, 392, 393, 420
Hamm, F. A., 305
Hammack, K. C., 18
Hammer, C. L., 25
Hammer, P. C., 311
Handley, T. H., 135
Hanks, G. D., 355
Hannan, R. S., 226
Hannay, N. B., 208, 246
Hansen, G. A., see Asboe-Hansen, G.
Hansen, W. W., 3
Hanson, A., 25
Happ, G. P., 258
Haque, A., 348, 354
Harbers, E., 389, 393
Hardwick, T. J., 214
Harkins, W. D., 101
Harm, W., 335, 336
Harmer, D. E., 223
Harrington, H., 415
Harrington, N. G., 344, 345
Harris, D. R., 148
Harris, J. E., 301, 317, 321
Harris, P. S., 387, 417
Harris, S. J., 420
Harriss, E. B., 310, 311, 321, 322, 323
Hart, E. J., 214, 215, 216, 217, 230, 231, 232, 234
Hart, H., 387, 388, 389
Harteck, P., 220
Harvey, J. A., 123
Harvey, R. A., 416
Hase, H., 330
Hasted, J. B., 246
Hathaway, E. A., 375
Hauser, W., 112, 133
Hayes, T. L., 418
Hayward, E., 83, 215
Hayward, H. R., 230
Headington, C. E., 197, 209
Heglin, J., 415
Heinmets, F., 335, 340, 341
Heitler, W., 2
Heller, J. H., 408
Helmke, R., 337
Helwig, H. L., 288
Hemmer, B. A., 221
Hempelmann, L. H., 371, 373, 374, 415, 416
Henderson, I. H. S., 217, 247, 250
Hendricks, S. B., 337
Henglein, A., 225, 263
Henkel, R. L., 126
Henley, E. J., 334, 339, 340
Henley, E. M., 26
Herman, J. A., 271
Hermel, M. B., 415
Herskowitz, I. H., 346, 354, 358
Herz, R. H., 306, 307, 310, 312, 320, 321
Hevesy, G., 101
Hewitt, J. E., 418
Heydenburg, N. P., 17, 56
Heyn, A. H. A., 271
Hickam, W. M., 242, 243, 244
Hickling, A., 215
Hicks, H. G., 285, 286
Higginbotham, R. D., 330, 341
Higgins, G. C., 305
Hildebrand, R. H., 63, 169, 170
Hill, D. L., 25-72; 26, 28, 44, 45, 48, 75
Hill, J. E., 87
Hill, R. F., 337, 358
Hillman, P., 126
Hintenberger, H., 241
Hipple, J. A., 205, 208, 243, 245, 247, 248, 249, 251, 253, 256
Hirsch, G. M., 390
Hirschfelder, J. O., 81
Hirshfield, H., 332, 338, 346
Hirzel, O., 134
Hissel, J., 262
Hitch, S. F., 413
Hoch, M., 248
Hochanadel, C. J., 215, 231, 233

Hockstein, K. G., 280
Hodson, A. L., 148, 152
Hoecker, F., 317, 320
Hoerlin, H., 305, 308
Hofmann, D., 330
Hofstadter, R., 25, 26, 61
Hogan, A. J., 220
Höhne, G., 349
Hollaender, A., 328, 332, 335, 336, 340, 341, 349
Hollander, J. M., 370
Hollunger, G., 396
Holmes, B., 328, 352
Holmstrom, V., 316, 418
Holt, M., 316, 317, 343
Holte, G., 87
Holter, H., 312, 319, 321
Hones, E. W., 152
Honig, R. E., 242, 244
Hood, A., 198, 200, 201, 203
Horan, J. R., 319
Hornig, R. E., 226
Hornsey, S., 351
Horrigan, R. V., 225
Hossain, A., 126, 132
Hotchkiss, R. D., 338
Houtermans, F. G., 45
Houtermans, T., 328, 330, 331, 332, 338, 339
Howard, A., 317, 318, 319, 322, 354
Hoyle, M. G., 9
Hubbel, J. H., 215
Huby, R., 119, 133
Hudson, R. L., 247
Huggett, R. W., 149
Hughes, D. J., 75, 123, 179
Hulbert, H. M., 256
Hull, M. H., 81
Humbach, W., 45
Hummel, R. W., 215, 216, 234
Hungerford, H. E., 85
Hunt, J. P., 219
Hunt, J. W., 215
Hursh, J. B., 371, 389, 393, 394, 418
Hurst, G. S., 215, 262
Hurwitz, H., Jr., 88
Hustrulid, A., 246, 247
Hutchinson, D. A., 234
Huus, T., 17, 56

I

Igo, G. J., 25, 44, 135
Inghram, M. B., 248
Inghram, M. G., 208
Inglis, D. R., 14
Ingold, K. U., 217, 247, 250
Irvine, J., 277
Irvine, J. W., 284
Ishibashi, K., 420
Ishibashi, M., 277
Israel, H., 396
Iverson, R. M., 337, 338, 346
Ives, P. T., 348, 356, 358
Ivin, K. J., 214, 225
Izumo, K., 130, 131

J

Jackson, J. D., 134
Jacobsen, E. M., 418
Jacobsohn, B. A., 42
Jacobson, C., 338, 346
Jacobson, L. O., 345, 415
Jaffey, A. H., 286
Jahn, H. A., 249
James, T. H., 305
Jancovici, B. G., 46
Jankus, V. Z., 30
Jarvis, G. A., 126
Jayson, G. G., 233
Jee, W. S. S., 300, 317
Jensen, J. H. D., 7, 21
Jernakoff, G., 204, 205
Jetter, W. W., 417
Joffe, M. H., 389, 398, 405, 406
Johansson, G., 289
Johns, D. H., 290
Johns, H. E., 215, 216, 330, 340
Johnson, B. H., 198
Johnson, E. R., 231
Johnson, H. L., 248
Johnson, M. H., 64
Johnson, P., 258
Johnston, A. H., 343, 344
Johnston, P. M., 317
Johnston, R., 148
Jones, D. C., 376, 377
Jones, E. J., 208
Jones, G. M. D. B., 150
Jones, H. B., 405
Jones, J. L., see Lennard-Jones, J.
Jones, M. D., 420
Jones, S. L., 280
Jongepier, H. J., 415
Juberman, O., 281, 287
Judson, C. M., 258
Jurney, E. T., 77

K

Kaćanski, K. L., 418
Kafalas, J. A., 284
Kakihana, H., 288
Kamen, M. D., 213, 235
Kan, B., 328, 330
Kanazir, D., 342, 345
Kandel, R. J., 246, 261
Kaplan, N., 314
Kaplan, R., 358
Kaplan, R. W., 329
Kaplan, S., 330, 340, 341
Kaplan, S. J., 417
Kaplan, W. D., 353, 355, 356
Kapur, P. L., 100
Karel, M., 328, 330
Karr, P. R., 81
Kathan, R. H., 335, 340, 341
Katz, J., 389, 392, 407
Kaudewitz, F., 329, 340, 357
Kaufmann, B. P., 346, 353
Kauzmann, E. F., 346
Kawin, B., 389, 397, 399, 400, 401, 402, 405
Keeling, C. D., 226, 227
Keller, J. M., 44
Keller, K. K., 133
Keller, M., 221
Kelly, L., 405
Kelly, P., 229, 234
Kelner, A., 337, 338, 340, 342, 345
Kennedy, J. M., 8, 27
Kennedy, R. J., 84
Kepp, R. K., 330, 345
Kerasek, F. W., 205
Kereiakes, J. G., 418
Kern, W., 225
Kessler, J. O., 151
Kety, S. S., 380, 382
Kiehn, R. M., 133
Kihlman, B., 351, 352, 353
Kim, Y. B., 149
Kimball, A. W., 355, 417
Kimball, G. E., 259
Kimball, R. F., 333, 343, 346
Kimeldorf, D. J., 417, 418
Kind, A., 139
Kinersly, T., 320
King, D. T., 301, 317, 321
King, E. D., 352
King, L. D. P., 184
King, R. C., 358
Kinney, I. W., Jr., 198
Kintner, E. E., 94
Kirby, H. W., 289
Kirby-Smith, J. S., 349
Kirn, F. S., 84
Kisieleski, W., 380, 389, 393, 405
Kisslinger, L. S., 117
Kjeldaas, T., Jr., 242, 243
Kleczkowski, A., 337
Klein, G., 342, 346
Klingenberg, J. L., 278
Knauss, H. J., 341, 346
Kniseley, R. M., 420
Knoll, J. E., 316
Knudsen, A., 26
Koch, R., 413, 414
Kocholaty, W., 341
Koffel, M. B., 247
Kohn, W., 42
Kojima, S., 288
Kokurin, Y., 147
Koletsky, S., 419
Koller, P. C., 328, 344, 346, 347, 354
Kölmark, G., 329, 353
Komlev, A. I., 275
Konecci, E. B., 420
Konopinski, E. J., 111
Kopfermann, H., 45
Kornberg, H., 398
Kossiakoff, A., 242
Kourtschatov, I., 101

Kouts, H. J., 94
Kowlessar, O. D., 415
Krause, G., 281, 287
Krauss, M., 241-68
Krebs, A. T., 343, 418
Kroll, N. M., 7, 42, 44
Kronig, R. de L., 105
Kropf, A., 253
Kume, S., 224
Kuper, J. B. H., 216
Kurabayashi, M., 348
Kurbatov, M. H., 284
Kusch, P., 246
Kutschera, G., 346
Kuzin, A. M., 415
Kynch, G. J., 21

L

Labaw, L. W., 329
Labrum, E. L., 357
Lacassagne, A., 333, 350, 414
LaCour, L. F., 344, 354, 357
Lad, R. A., 248
Lagarrigue, A., 148, 150
Laidler, K. J., 234, 247, 251
Lakin, W., 42
Lamerton, L. F., 311, 311, 321, 322, 323
Lampe, F. W., 219
Landman, O. E., 327, 357
Lane, A. M., 8, 14, 107
Lane, G. R., 348
Lang, D. A., 328, 330
Lang, J. M. B., 121, 122, 140
Langendorff, H., 413, 414
Langendorff, M., 331, 333, 336
Langer, A., 244, 247, 248, 249, 254, 258
Langham, W. H., 371, 374, 387, 389, 398, 400, 417, 418
Langsdorf, A., 154, 155
Lanneau, K. P., 204, 205, 206
Lapalme, J., 312
Lark, K. G., 338
Laser, H., 340
Lasnitzki, I., 339
Laszlo, D., 382, 387, 388, 389
Latarjet, R., 335, 336, 339
Lattes, C. M. G., 307
Laughlin, J. S., 416
Lauritsen, T., 76
Laverty, J. A., 334
Lavik, P. S., 415
Lawrence, E. O., 243
Lawton, E. J., 226, 227, 228
Lazo, R. M., 215
Lea, D. E., 213, 235, 327
Lea, R. M., 166
LeBlanc, J., 123
Leblond, C. P., 316, 317, 322
Leboeuf, M. B., 293
LeCouteur, K. J., 121, 122, 140
Leddicotte, G. W., 285, 286
Leder, L. B., 218
Lederer, M., 291
Lederman, L. M., 151, 163, 167
Leech, J. W., 243
Lefevre, G., 355
Lefort, M., 214, 216, 230, 231, 233
LeGoff, P., 247
Lehman, C. A., 311
Lehman, J. J., 335
Leibnitz, H. M., see Maier-Leibnitz, H.
Leighton, R. B., 147, 148
Leland, W. T., 204
Lemmon, R. M., 221
Lennard-Jones, J., 244, 245, 251, 261
Lennox, E. S., 337
Leprince-Ringuet, L., 148, 150
Letonoff, T. V., 380
Levene, M. B., 420
Levi, H., 317, 320, 321
Levine, R. P., 348, 356, 357, 358
Levison, C. A., 14, 45, 49, 122
Lewin, R., 382, 387
Lewis, D., 357
Lewis, E. B., 349
Lewis, H. W., 152
Lewis, J. J., 224
Lewis, Y. S., 420
Libby, W. F., 285, 286
Lichtenstein, P. G., 146
Liedtke, R. A., 76
Lieth, C., 63
Linacre, J. K., 215
Lind, S. C., 226
Lindegren, C. C., 343, 347
Lindenbaum, A., 382, 395, 396
Lindenbaum, S. J., 130, 140
Lindenmann, J., 330
Lindholm, E., 217, 245
Lindsay, S., 420
Lindsley, O. R., 417
Lingane, J. J., 276, 277, 280
Linlor, W. I., 126
Lint, V. A. J. van, 148
Lippmann, B., 117
Little, K., 227
Livingston, M. S., 306
Livingston, R., 228, 234
Livingston, R. S., 223
Loefer, J. B., 330
Loeninger, R., 418
Looney, W. B., 373, 420
Loos, G. M., 343, 346
Lord, J. J., 309
Lorenz, E., 389, 393, 414
Loria, A., 152
Losee, J. P., 231, 232
Lossing, F. P., 217, 247, 249, 250
Lotfy, T. A., 353
Lotz, V., 417
Lotz, W. E., 299, 317
Loutit, J. F., 414
Lovati, A., 150, 155
Love, R. A., 371, 374
Love, T. A., 85
Lovelace, R., 347
Loveless, L. E., 346
Low, W., 17, 48
Lozier, W. W., 246
Lucke, W. H., 338, 339, 340
Ludwig, H., 380
Luers, H., 358
Luippold, H., 348
Lumpkin, H. E., 197, 198, 260
Lundqvist, U., 348, 350, 351, 357
Lüning, K. G., 351, 354, 356
Luria, S. E., 337
Lyman, E., 25
Lyon, M. F., 355

M

Maaløe, O., 338
McClelland, C. L., 17, 56
McCluggage, W. C., 289
McClure, F. T., 242
McCormick, H. G., 414
McCormick, W. G., 419
McCoy, E., 337
McCue, J. J. G., 133
McCulloh, E. F., 414, 415, 419
MacDonald, A. M., 316
McDonald, J. E., 416
MacDonald, N. S., 374
MacDonald, W. M., 7
McDonell, W. R., 214, 215, 216, 221, 230
McDowell, C. A., 217, 244, 245, 246, 247, 248, 249
McFadden, W. H., 258
McGinn, W. E., Jr., 317
McGowan, F., 56
McGrath, J., 415
McGregor, J. F., 337, 338
McGuire, J. M., 246
McHaney, G. M., 152
McIntyre, J., 25, 26
McIsaac, L. D., 289
Mack, J. E., 50
McKay, H. A. C., 101
MacKey, J., 350, 357
McKinley, W. A., Jr., 35
McLafferty, F. W., 202
McLaren, I. H., 205
McLaughlin, W. L., 312
McLean, R., 373
McLeish, J., 345, 347, 353
McManus, H., 131
McNaughton, G. S., 225, 232
McNevin, W. M., 271
McOmbie, J. F. W., 291
McQuate, J. T., 355, 356
Madden, S. C., 417
Maddock, A. G., 223

Maddock, J. G., 291
Maenchen, G., 163
Magat, M., 225
Magee, J. L., 81, 213, 219, 222, 228, 233, 234, 235, 241, 242, 252, 262
Magee, M., 386
Magni, G. E., 328, 339, 340
Mahmoud, H. M., 45, 122
Maienschein, F. C., 85, 92
Maier-Leibnitz, H., 145
Main, R. K., 415
Majumdar, A. K., 278
Mancić, D. D., 418
Mandel, H. G., 415
Manion, W. P., 223
Mann, M. G., see Gell-Mann, M.
Mann, M. M., 247
Manowitz, B., 225, 226
Margolis, B., 133
Mariani, F., 35
Marinelli, L. D., 371
Mariner, T., 242
Mark, H., 17, 56
Markert, C. L., 329, 339
Marmier, P., 63
Marquardt, H., 356, 357
Marriott, J., 246
Martell, A. E., 380, 382, 386, 397
Mårtensson, J., 396
Martin, C., 317
Martin, H. C., 133
Martin, J. J., 223, 224
Martland, H. S., 373
Marton, L., 218
Marx, R., 380
Massey, H. S. W., 242, 243
Mateyko, G. M., 420
Mather, K. B., 313
Matheson, M. S., 215, 228, 234
Maury, P. B., see Bonet-Maury, P.
Maxwell, E., 341
May, J., 286
May, R. M., 414
Mayer, M. G., 7, 21
Mayer, M. G., see Goeppert-Mayer, M.
Mayer, S., 332
Mayer, S. W., 289, 290
Mayr, G., 305
Mazia, D., 353
Meersche, M. van, 224
Mees, C. E. K., 298, 305, 307, 313, 318
Mefferd, R. B., 330
Mehtab, M., 353, 356
Meiert, J., 248
Melching, W. H., 417
Melpolder, F. W., 197, 209
Mendel, M. G., 278
Meneely, G. R., 418
Menten, M. L., 342, 415
Merkle, T. C., 146
Merritt, G., Jr., 277
Meschan, I., 415, 418
Mesrobian, R. B., 225, 226
Mészáros, J. S., see Schmidlin-Mészáros, J.
Mewherter, A. C., 286
Meyer, H., 148
Meyer, H. V., 358
Meyer, I., 343
Michaelis, P., 358
Mickelwait, A. B., 42
Mickey, G. H., 355, 357, 358
Mikaelsen, K., 340, 352
Milanich, V., 419
Milch, L. J., 418
Milétic, B., 335
Miller, A. A., 228
Miller, B. L., 320
Miller, C. W., 226
Miller, D. H., 154, 157, 165
Miller, D. W., 100, 106, 122
Miller, N., 214, 215, 216, 219, 221, 230, 231
Milne, W. L., 389, 391, 401, 408
Minot, A. S., 375
Miskel, J., 269-96
Missovski, L., 101
Mitchell, J. J., 248
Mitchell, J. S., 328, 352
Mitchell, J. W., 303
Mittelman, P. S., 76
Mittler, S., 334
Miyami, H., 220
Miyazawa, H., 22
Mizzan, E., 279, 286
Mohler, F. L., 243, 246, 255, 262
Momigny, J., 224, 258
Monethrop, P. H., 163
Monroe, R. A., 420
Montgomery, P. O'B., 342
Moon, P. B., 101
Moore, E. E., 399
Moore, F. L., 285, 286
Moos, W. S., 330
Morenne, P., 335
Morgan, W. A., 204, 205
Morowitz, H. J., 331
Morrison, C. G., 115, 116
Morrison, J. D., 242, 244
Mortimer, R. K., 327-68; 338, 339, 345
Moshman, J., 345, 419
Mosley, V. M., 329
Moszkowski, S. A., 8, 64
Moteff, J., 76
Mott, N. F., 242, 303
Mottelson, B. R., 17, 48, 66
Moutschen, J., 347
Moyer, B., 63
Moyer, B. J., 88
Muirhead, H., 115, 116
Mukai, F., 330, 331, 333
Mullaney, J., 334
Muller, F., 148, 150
Muller, H. J., 346, 349, 354, 356, 358
Müller, K., 330
Müller, R. H., 215
Mulliken, R. S., 244
Mullin, C. J., 39
Mund, W., 224
Mura, A., 150
Murakawa, K., 45
Murray, F. H., 87
Murray, R. L., 179, 184
Muschlitz, E. E., Jr., 246
Muth, H., 371, 374
Myers, R. D., 83

N

Nadler, N. J., 317, 322
Nagai, S., 224
Nagle, D. E., 169
Nakao, Y., 355
Nasrat, G. E., 353, 356
Needels, T. S., 155
Nehemias, J. V., 420
Neidigh, R. V., 126, 127, 128, 129
Nelson, A., 413, 414
Nelson, F., 283
Nelson, G. D., 289
Nelson, R. H., 205, 206
Nereson, N., 75, 77, 126
Nervik, W., 289, 290
Nettleship, A., 418
Neuert, H., 217, 242, 244, 246, 248
Neumann, K., 389, 393
Newcombe, H. B., 337, 338, 357
Newman, E., 135
Newth, J. A., 153, 174
Newton, A. S., 215, 221
Nicholson, A. J. C., 242
Nicol, T., 408
Niedner, J. B., 133
Nielsen, C. E., 155, 157
Niemann, K., 281, 287
Nier, A. O., 204, 207
Nieuwerkerk, H. T. M., 415
Niira, K., 219, 249
Nilan, R. A., 348, 351, 357
Nishiwaki, Y., 337
Nix, M., 345
Nobles, R., 126
Nordheim, L. W., 81
Norman, A., 337, 340, 341
Norris, W. P., 297-326; 302, 371, 389, 393
Norwood, W. D., 386, 387, 389, 392
Nottingham, W. B., 243
Noyes, R. M., 219
Nusbaum, R. E., 374
Nutting, P. G., 320
Nybom, N., 333, 334, 338, 340, 348, 350, 351, 352, 357

O

Oakley, W. D., 389, 392, 407
Oberle, E. M., 330
Ochinskaya, G. K., 333
Odeblad, E., 315, 318, 320
O'Dell, F. W., 319
Oehklers, F., 347
Oesper, R. E., 275
O'Hara, C. L., 207
Okazaki, A., 100, 106, 122
Omura, I., 244
O'Neal, M. J., 198, 200, 201, 202, 203
O'Neill, G. K., 139
Oohata, K., 249
Osborn, R. K., 21, 81
Oster, I. I., 358
Oswald, L. O., 163
Otozai, K., 224

P

Padgett, D. W., 88
Pahl, M., 218, 221
Painter, E., 380, 389, 405
Palibin, P., 101
Palmer, J. F., 277
Park, H. D., 334, 346
Parker, D. R., 346
Parmentier, D., 170
Parr, W. H., 418
Parrott, M., 420
Parzen, G., 35
Passonneau, J. N., 333, 340
Passonneau, J. V., 342
Patergnani, E., 139
Patrick, W. N., 223, 225, 263
Patt, D. I., 420
Patt, H. M., 334
Patti, F., 413
Paul, E. B., 134, 135
Paul, W., 25
Pauly, J., 280
Payne, J. H., 289
Peaslee, D. C., 99-144; 63, 104, 110
Peebles, G. H., 83
Peelle, R. W., 85
Peierls, R., 100
Pelc, S. R., 315, 317, 318, 319, 321, 322, 354
Perkins, D. H., 309
Perkins, G. D., 203, 204, 206
Perlitsh, M., 338
Perlman, I., 63, 370
Perry, J. E., 126
Peters, K., 345, 347, 350, 352
Peters, R. A., 380
Petersen, D. F., 327, 340, 415
Petersen, O., 419
Peyrou, C., 148, 150, 153
Philip, J. F., 418
Phillips, G. O., 233
Pickard, J. K., 204
Pidd, R. W., 25
Pilcher, V. E., 123
Pincus, G., 420
Pinkerton, H., 340
Pirie, A., 416
Pittenger, R. C., 337
Plakov, A. G., 175
Plank, J., 278
Platzman, R. L., 213, 235
Pohley, H. J., 357
Pollard, E., 328, 329
Pollard, F. H., 291
Pontecorvo, B., 101
Porter, C., 78
Porter, C. E., 106, 109, 110, 122, 123, 124, 125
Porter, J. W., 341, 346
Potter, R. F., 245
Pottinger, M. A., 333, 334
Powell, W. M., 155, 156, 163
Power, W. H., 289
Powers, E. L., 332
Powers, R. M., 286
Pratt, W. W., 94, 133
Preiser, S., 88
Preiswerk, P., 101
Preston, W. M., 81
Priestley, W., 210
Pritchard, H. O., 246
Proctor, B. E., 328, 330
Proctor, B. F., 420
Prosser, E. L., 380, 389, 405
Prowse, D. J., 126, 132
Pryce, M. H. L., 49
Pryzbylamicy, E. P., 278
Puntenney, I., 416
Pyne, C. P., 347

Q

Quastler, H., 330, 340, 341

R

Racah, G., 15, 27
Radicati, L. A., 6, 8, 14
Ragent, B. I., 126
Rainwater, J., 26, 43, 48
Rajewsky, B., 327, 371, 374
Raka, E. C., 25
Ramat, M., 309, 318
Ramser, J. H., 209
Ramsey, N. F., 126
Rand, A. C., 94
Rasetti, F., 101
Ratty, F. J., Jr., 355
Rau, R. R., 148
Ravenhall, D. G., 31, 35, 61
Raventos, A., 419
Ravilious, C. F., 83
Ray, D. T., 358
Ray, R. C., 318
Ray-Chaudhuri, S. P., 347
Read, J., 351, 353
Redlich, M., 66
Redmond, R. F., 418
Reed, T. M., 421
Rees, H., 344
Rees, J. R., 25, 130, 131
Reese, R. M., 243, 246, 262
Reich, H., 25
Reinganum, M., 297
Reinhold, J. G., 396
Reinholz, E., 352
Relf, K. E., 155, 156
Renner, G., 225
Retallack, J. G., 146
Revell, S. H., 347, 353, 354
Reynolds, G. T., 148
Reynolds, S. A., 280
Reznikoff, P., 375
Richards, E. W. T., 219
Richardson, L. A., 185
Riddell, R. J., Jr., 63
Rigg, T., 216, 229, 232, 234
Riggs, H. E., 415
Rinehart, M., 163, 167
Rinehart, M. C., 75, 167
Ringleb, D., 343
Ringuet, L. L., see Leprince-Ringuet, L.
Ritchie, D., 342
Ritchie, M. B., 386, 387, 389, 392
Robbins, S., 328
Roberts, L. D., 87
Robertson, A. J. B., 242, 247
Robinson, C. F., 203, 204, 205, 206
Robinson, C. V., 312, 319, 321
Robinson, L. C., 418
Robson, M. J., 345
Rochester, G. D., 28, 145
Rock, S. M., 209
Rødstom, G., 216
Rosenfeld, G., 420
Rogers, K., 163, 167
Rohrlich, F., 127, 215
Rolin, M., 230
Ronchi, L., Jr., 309, 318
Roofe, P., 317, 320
Rose, D. G., 226, 227
Rose, M. E., 2, 35
Rosen, A., 126
Rosen, L., 139
Rosenbaum, D., 246
Rosenblum, E. D., 330, 340, 341
Rosenbluth, M., 30
Rosenstock, H. M., 251, 253, 255
Rosenthal, J., 27
Rosenthal, M. W., 402
Ross, J. S., 45
Ross, M., 10, 228
Ross, M. A. S., 307, 308
Ross, M. H., 342
Rosser, W. G. V., 115, 116
Rossi, B., 150
Rossi, H. H., 337, 354, 358
Rotblat, J., 126, 130, 132, 133, 307, 308, 316
Roth, J. S., 341

Rounds, D. E., 374
Rowbottom, J., 215
Roy, J. C., 224
Roys, P. A., 83
Rubin, B. A., 345, 357
Rubin, M., 380, 386, 396
Rulfs, C. L., 278
Rupert, C. S., 348
Russek, A., 22
Russell, E., 380, 389, 405
Russell, L. B., 355, 417
Russell, R. S., 316
Russell, W. L., 355, 356, 417
Rust, J. H., 299, 415, 420
Rutenberg, A. C., 219
Rutherford, E., 25
Rutishauser, A., 344, 354, 357
Ryan, D. E., 278
Ryan, F. J., 357
Ryder, N. V., 152

S

Sacher, G., 380, 389, 405
Sachs, R. G., 4, 10, 21
Saeland, E., 216
St. Amand, G. S., 340
Sakata, S., 5
Saldick, J., 215
Salmon, L., 293
Samos, G., 272, 287
Sampson, M. B., 307, 308
Samuel, A. H., 222, 228, 234
Sanders, F. K., 316
Sanders, P., 417, 418
Santisteban, G. A., 420
Sarachek, A., 337, 338, 339, 340, 343, 345, 346
Sargent, C. P., 163, 167
Satchler, G. R., 8
Satpathy, S., 276
Sauer, H., 413, 414
Sax, K., 348
Saxon, D. S., 63, 127
Sayeg, J. A., 331
Scadden, E. M., 285
Schafer, W. D., 77
Schardt, A. W., 293
Scharff-Goldhaber, G., 14
Schawlow, A. L., 44, 45
Scheibe, A., 357
Scherbaum, O., 338
Scherer, E., 343, 415
Schiff, L. I., 30, 35, 39
Schilling, A., 386, 387, 389, 392
Schissler, D. O., 255, 260
Schlundt, H., 375
Schmidlin-Mészáros, J., 341
Schneider, M., 414
Schneiderman, H. A., 352
Schoenborn, H. W., 338
Scholes, G., 233
Schrank, G., 132
Schreier, K., 416
Schubert, G., 348, 349
Schubert, J., 369-412; 375, 376, 380, 381, 382, 389, 390, 395, 396, 397, 402, 404, 405, 408
Schulz, R., 225
Schumann, R. P., 285
Schumb, W. C., 290
Schupak, F., 271
Schwartz, C., 15
Schwartz, D., 351
Schwartz, H. P., 415
Schwartz, W., 334
Schwartzenbach, G., 382, 385
Schwarz, H. A., 231, 232, 233
Schweisfurth, R., 334
Schweitzer, W., 417, 418
Schwemin, A., 170
Schwinger, J., 30, 43, 117
Scott, J. K., 419
Scott, J. M. C., 123
Scott, O. C. A., 351
Scott, K. G., 387, 388, 389, 392, 394, 397
Scott, M., 25
Seaborg, G. T., 63, 370, 387, 388
Sears, B. J., 9
Sebban, J., 225
Seevers, D. O., 152
Segrè, E., 101
Seidlin, S. M., 375
Serber, R., 102
Setlow, J., 328, 329
Setlow, R. B., 331
Seven, M. J., 396
Severinghaus, J. W., 207
Shalit, A. de, 22
Shapiro, M. M., 297, 319
Sharp, W. T., 8, 131
Sheard, D. R., 214
Shechmeister, I. L., 419
Shepard, D. C., 338, 346
Shephard, W. D., 166
Shepherd, H. J., 226
Sheppard, C. W., 226
Sherma, H. D., 284, 285
Sherman, F. G., 416
Sherman, L., 126, 130
Shimamoto, Y., 3
Shock, D., 416
Shor, S. W. W., 84, 85
Shrauzer, G. N., 278
Shuler, K. E., 247
Shull, F. B., 133
Shult, E. E., 347
Shure, K., 83
Shutt, R. P., 154, 157, 158, 162, 165, 166
Siebemeir, G., 287
Siegert, A. J. F., 21
Siekemeir, G., 281
Sigelman, S., 345
Silver, E. G., 140
Silverman, M. S., 419
Simmel, E. B., 316, 317
Simmons, B. S., 314, 315, 316
Simmons, D. H., 126
Simon, A., 9, 93
Singleton, W. R., 349, 354, 357, 358
Sink, R. L., 209
Sircar, S. S. G., 276
Six, E., 328
Skinner, C. E., 278
Skonieczny, R. F., 279
Slater, N. B., 252
Slattery, R. E., 81
Slaughter, G. G., 157
Slavatinskii, S., 147
Sluis, V. J. H., see Vander Sluis, J. H.
Small, P. A., 225
Smaller, B., 228, 234
Smith, C., 248
Smith, D. B., 327
Smith, D. E., 420
Smith, E. R., 288
Smith, F. M., 43
Smith, H. H., 353
Smith, J. H., 35, 306
Smith, J. R., 126
Smith, J. S. K., see Kirby-Smith, J. S.
Smith, L. G., 242, 246, 248
Smith, P. K., 415
Smith, W. W., 415, 416
Smolkin, G. E., 175
Smutz, M., 282, 287
Sneddon, I., 121
Snowden, M., 145, 154, 162, 163
Snowdon, S. C., 126
Sobels, F. H., 358
Sokoloff, B., 414
Solomon, A. K., 289, 290, 309, 311, 316
Sommermeyer, K., 333, 336
Sommers, L. O., 399
Sommers, S. C., 343
Spain, P., 374
Sparrow, A. H., 327, 346, 354, 358
Spear, F. G., 327
Speckman, T. W., 371
Spedding, F., 282, 287
Spedding, F. H., 382, 385
Spencer, J. L., 349, 357
Spencer, L. V., 81, 83, 84
Spiegelman, S., 327, 330, 350, 351, 357
Spiess, F. N., 283
Spinks, J. W. T., 215, 216, 234
Spoerl, E., 346
Spontak, J., 197, 209
Spruch, L., 21
Stadler, L. J., 356
Stahl, R. H., 126
Stannard, J. N., 419
Stapleton, G., 335, 336, 340, 341
Stech, B., 8, 22
Steffensen, D., 348, 353
Steigert, F. E., 307, 308

Stein, G., 233
Stein, W., 335, 336
Steinbach, J. F., 284, 285
Steinberg, D., 316
Stelson, P., 56, 139
Stent, G. S., 329, 333
Stephens, W. E., 205
Stephenson, R., 179
Stern, K. G., 382, 387
Stern, T. W., 317
Sternglass, E. J., 215
Stevens, C. E., 316
Stevens, C. M., 204
Stevens, G. W. W., 310, 311, 318, 321, 322
Stevens, H. M., 291
Stevenson, D. P., 243, 245, 247, 248, 249, 251, 256, 257, 258, 259, 260
Stevenson, M. L., 170
Stevenson, P. C., 285, 286, 289, 290
Stewart, D. W., 258
Stieff, L. R., 317
Stiller, B., 319
Stine, C. R., 272
Stinson, F., 84
Stinson, J. V., 418
Stock, C., 380
Stocken, L. A., 380
Stolle, F., 415
Stone, W. S., 328, 333, 334, 337, 347, 348, 349, 352, 353, 354, 355, 356
Stone, F., 415
Storer, J. B., 415, 417, 418
Storrs, C. L., 78, 89
Strauch, K., 133
Street, J. C., 146, 152
Strehler, B. L., 341
Strong, W. W., 314
Strugger, S. P., 343
Succi, C., 154, 155
Sultzer, M., 371
Sundaram, A. K., 284, 285
Sunyar, A. W., 1, 10, 19, 54
Supplee, H., 418
Sussman, A. S., 340
Suttle, J. F., 216
Sutton, H. C., 232, 233
Suura, H., 30
Suzuki, M., 220
Svedberg, T., 216
Swallow, A. J., 233
Swanson, C. P., 343, 344, 348, 349, 351
Swiatecki, W. J., 66
Swickard, E. O., 77
Swift, M. N., 380, 389, 405
Swindell, G. E., 418
Sworski, T. J., 231, 232
Szegö, G., 54
Szilard, L., 101
Szwarc, M., 247

T

Tabershaw, I. R., 420
Tagliaferri, G., 150, 154
Tahmisian, T. N., 331, 333, 340
Tait, J. H., 87
Takeda, G., 118
Talmi, I., 46
Tanada, T., 337
Taplin, G. V., 216
Taschek, R. F., 133
Tate, J. T., 246, 247
Taube, H., 219
Taylor, A. E., 109, 126
Taylor, E. H., 228, 234
Taylor, J. H., 316
Taylor, J. J., 83
Taylor, S. H., 316
Taylor, T. B., 102, 126
Taylor, T. I., 204
Taylor, W. W., 335
Tehakinan, A., 278
Teichmann, T., 102
Telegdi, V. L., 6
Telfer, J. D., 355
Teller, E., 64, 249
Temmer, G. M., 17, 56
Temple, L. A., 389, 398, 405, 406
Terra, L., 150
Teti, M., 335
Tewari, S. N., 291
Thie, J. A., 39
Thirring, W. E., 106
Thoday, J. M., 350, 354
Thomas, B. W., 197
Thomas, R., 5
Thomas, R. G., 102, 103, 104, 105, 107, 110
Thompson, E. C., 416
Thompson, R., 245
Thompson, R. C., 389, 392, 398, 407
Thompson, R. H. S., 380
Thompson, R. W., 149
Thompson, S. O., 255
Thomson, D. M., 376, 377
Thomson, J. F., 416
Thorburn, R., 246
Thorndike, A. M., 158, 165, 166
Thouvenin, J., 312
Tibbets, D. M., 372, 376
Tickner, A. W., 249
Tillman, J. R., 101
Tillotson, F. W., 342
Tillu, M. M., 278
Timonen, S., 354
Ting, T. P., 330, 340
Tipton, S. R., 340
Titus, W. F., 133
Tkaczyk, S., 301, 317, 321
Tobias, C. A., 328, 331, 333, 338, 339, 345, 350
Todd, A., 226, 227
Tolbert, B. M., 221
Toops, E. C., 307, 308
Tourtellotte, W. W., 416
Touschek, D., 121
Towe, G. C., 317
Townes, C. H., 17, 44, 48, 64
Townsend, G. F., 343, 346
Trainor, L. E. H., 7, 140
Tralli, N., 3
Treiman, S. B., 148
Tribalate, S., 286
Trilling, G. H., 148
Trowbridge, W. V., 416
Trowell, O. A., 343
True, W., 66
Truhaut, R., 353
Trunillo, T. T., 386
Trum, B. F., 415, 420
Tsimbalista, L. I., 275
Tucker, H., 278
Tullis, J. L., 417
Turk, E., 279
Turkevich, J., 255
Turney, D. F., 417
Tutt, M. L., 388, 389, 391, 393

U

Uebersfeld, J., 218, 225
Ungar, F., 420
Ungar, G., 418
Untermeyer, S., 186
Upton, A. C., 417, 419
Uretz, R. Z., 338, 344

V

van Bekkum, D. W., see Bekkum, D. W. van
Van Cleve, A. B., 215, 234
Vander Sluis, J. H., 9
Van Heerden, P. J., 308
van Heyningen, R., 416
van Lint, V. A. J., see Lint, V. A. J. van
van Meersche, M., see Meersche, M. van
Van Middlesworth, L., 377, 397, 408
Van Norman, R. W., 207
Van Slyke, F., 418
Van Vleck, J. H., 249
Vaughan, J., 388, 389, 391, 393
Ventzke, L. E., 343
Vermeil, C., 233
Vier, M., 386
Villars, F., 21
Villi, C., 27
Virgin, H. I., 343
Visek, W. J., 299
Vlanne, P. N., 278
Vogel, A. I., 277
Vogel, H. H., Jr., 331
Voigt, A., 289
Volkin, E., 341
Volkin, H. C., 88

Volkov, A. B., 10
Volmar, Y., 291
von Borstel, see Borstel, R. C. von
von Buttlar, H., see Buttlar, H. von
Von Halle, E. S., 351, 355
von Weizacker, C. F., see Weizacker, C. F. von
Vought, R. M., 242

W

Wäffler, H., 134
Wager, R. W., 398
Wagner, C. D., 257
Wagner, F., Jr., 286
Wahl, P., 225
Wahrhaftig, A. L., 241-68; 251, 253, 255
Wainwright, S. D., 334
Wainwright, W. W., 311
Waldron, J. D., 217, 242, 248
Walker, J. K., 197-212; 205, 206, 207
Walker, L. A., 405
Walker, W. D., 166
Wall, N. S., 25, 130, 131
Wallace, H. D., Jr., 381, 389, 395, 396
Wallace, P. R., 3
Wallenstein, M. B., 251, 253, 255
Walsh, P. D., 217
Walt, M., 77, 100, 106, 122, 123, 126
Walter, J., 259
Walter, J. L., 278
Walter, J. I., 278
Walton, R. B., 100, 106, 122
Wang, C. F., 133
Waniek, R. W., 140
Wanlass, S. D., 147
Wannier, G. H., 243
Warner, C., 215
Warren, J. M., 417
Warren, J. W., 242, 244, 245, 246, 248
Warren, S., 316, 317, 342, 343, 344
Washburn, H. W., 203, 204, 206, 251
Watanabe, K., 219
Waterman, H. I., 226
Waters, L. L., 380
Watson, F. N., 84
Watson, K. M., 113, 118
Watson, M. S., 346
Watson, R. E., 31
Watt, B. E., 75, 87
Way, J. L., 415
Way, K., 76
Webb, J. H., 297, 305, 306, 308
Weddle, O. H., 155
Weeks, B. M., 230
Weeks, M. H., 389, 392, 407
Wegner, H. E., 25, 130
Weicksel, J. A., 258
Weigle, J. J., 338
Weikel, J., 389, 393
Weil, H., 291
Weills, J. T., 186
Weinman, E. O., 418
Weinstein, J., 317
Weisman, T. H., 346
Weiss, J., 216, 219, 221, 229, 232, 233, 234
Weiss, J(erome), 216, 231
Weisskopf, V. F., 3, 8, 25, 67, 78, 99, 100, 104, 106, 107, 109, 110, 111, 120, 121, 122, 123, 124, 125, 126, 131, 140
Weizacker, C. F. von, 46
Wells, R. A., 291
Welsh, J. N., 338
Welton, T. A., 78, 87, 88
Weneser, J., 1-24; 5, 14
Wertheim, M. S., 44
Westcott, C. H., 101
Westergaard, M., 353
Wheeler, J. A., 26, 42, 48, 64, 67
Wheelwright, E. J., 382, 385
Wherry, T. C., 205
Whipple, G. H., 341
White, G. R., 77, 83
White, H. E., 243
White, M. R., 389, 390, 395, 396, 397, 401, 402, 403, 404
Whitehead, W. D., 126
Whiting, A. R., 355
Whiting, D. W., 358
Whitmore, B. G., 139
Whitney, R., 420
Whittemore, W. L., 158, 165, 166
Wichmann, E., 42
Wichterman, R., 342
Wick, G. C., 87
Widdoes, L. C., 185
Wiener, M., 314
Wigner, E., 66, 105
Wigner, E. P., 76, 86, 100, 102, 107, 243, 244
Wilding, J. L., 419
Wilets, L., 42, 45
Wiley, W. C., 205
Wilkins, J. E., Jr., 77, 81, 82, 83, 85
Wilkinson, D. H., 7
Wilkinson, J., 214, 216, 230, 231
Willard, J. E., 214
Williams, A. I., 315, 316, 317
Williams, C. R., 371
Williams, R., 63
Williams, R. R., Jr., 219, 224, 263
Willms, M., 342, 415
Wilson, C. T. R., 145
Wilson, G., 204, 205
Wilson, J. G., 145, 150, 174
Wilson, R. N., 31, 35
Wilson, R. R., 46
Winsche, W. E., 282
Winther, A., 17
Wiswall, R. H., Jr., 282
Witkin, E. M., 336
Witten, V. H., 316, 418
Woese, C., 328, 329
Wohlwill, F. J., 417
Wolfe, G., 81
Wolfe, R. G., 338, 345
Wolfendale, A. W., 28
Wolfenstein, L., 112, 118
Wolff, S., 351, 352
Wood, E., 109, 126
Wood, J. G., 170
Wood, K., 242
Wood, T. H., 332, 339
Woodruff, L. A., 297-326; 302, 373, 389, 393
Woods, R. D., 63, 127
Woodside, E. E., 341
Worman, F. C. V., 417
Wright, B. T., 126
Wright, R. W., 163
Wybourn, R. C., 414
Wyckoff, H. O., 84
Wyckoff, R. W. G., 329
Wyman, L. C., 420
Wyss, O., 334, 337

Y

Yagoda, H., 297, 298, 313, 314, 315, 316, 317
Yamakawa, K. A., 308
Yamamoto, T., 224
Yanders, A. F., 354, 355
Yang, C. N., 66
Yanofsky, C., 330, 341
Yarnell, R. A., 418
Yasaitis, E. L., 228, 234
Yeater, M. L., 151, 152
Yennie, D. R., 31, 35, 61
York, C. M., 147
Yost, H. T., Jr., 348, 349, 356, 357, 358
Young, G., 86
Young, W. J., 348, 357
Young, W. S., 197, 209
Yukawa, H., 5

Z

Zabel, C. W., 77
Zajac, B., 307, 308
Zavoiskii, E. K., 175
Zeldes, H., 228, 234
Zelikoff, M., 219
Zelle, M. R., 327, 332
Zemany, P. D., 226, 227
Zerby, C. D., 84, 85
Zeuthen, E., 338
Zhdanov, G., 147

Zikry, A. A., 408
Zirkle, R. E., 215, 330, 331, 339, 344, 348
Zook, W. C., 271
Zupancic, C., 17, 56
Zweifel, P. F., 88

SUBJECT INDEX

A

Accelerators
  detectors associated with, 145-75
  shielding of, 73-94
Acidity, control of, 271
Actinometry, 216-17
Adiabatic correlation, 247
Alkanes, in mass spectrometry, 198-203
Alloys, analysis of, 207-8
Alpha decay
  and nuclear charge distribution, 66
Alpha particles
  biological effects of, 327-58
  elastic scattering of, 130-31
  emission of, 66
  energy loss of, 306
  grain yields from, 310-11
  radiation decomposition by, 230
  range in emulsions of, 305-9
  scattering by nuclei of, 25, 63
  sources of, 214
  yield in neutron reactions of, 135
Alpha spectra, 292
Americium poisoning, 389
Ammonia
  radiation decomposition of, 220
Analysis
  by mass spectrometers, 197-211
Anesthesia
  and radiation protection, 419-20
Argon-41, in research reactors, 185, 190
Aromatic chemicals, mass spectral analysis of, 202
Artifacts in emulsions, 312-15
Atom bomb explosions
  radiation effects of, 330, 355, 417
Attenuation, nuclear radiation, 73-94
Automatic data reduction
  in mass spectrometry, 208-11

B

Background
  in photographic emulsions, 319
Background radiation
  research reactors and, 190
Bacteremia
  in radiation injury, 419
Bacteria
  radiation effects on, 327-58
BAL (British Anti-Lewisite)
  and radioactive poisoning, 380-81, 393-94
Beryllium
  in research reactors, 180
Beta particles
  cloud chamber detection of, 157
  in CO_2 decomposition, 220
  in decomposition of aqueous systems, 231
  energy loss of, 306
  energy loss in emulsions, 306
  and eye cataracts, 416
  grain yields from, 310-11, 321
  radiation injury by, 417-18
  range in emulsion of, 305-9
Beta spectra, 292
Bevatron, cloud chamber use with, 155, 157, 163-64
Blood
  radiation effects and, 414
Bone marrow, and radiation protection, 414
Born approximation
  in electron-nucleus scattering, 30, 39
Boron-10
  shielding and, 76
Bremsstrahlung, 39
Bubble chambers, 145-46, 167-75
  liquid hydrogen type, 169-73
  track lifetime in, 174
Buildup factors, 80, 83

C

Calcium-45
  in radioautography, 299-300
Calcium metabolism
  and radioactive poisoning, 375-77
Calibration matrix, 200
Capture gamma rays, 76
Carbon dioxide
  radiation decomposition of, 220
Carcinogenesis
  systemic mechanism of, 419
Cataracts, radiation induced, 416
Cell division
  radiation effects on, 342-58
  and radiosensitivity, 338-40
Cellular radiobiology, 327-58
  biochemical effects in, 340-42
  cytological effects in, 342-58
  lethal effects in, 328-40
  mutagenic effects in, 328-40
  oxygen concentration effects in, 333
  post-irradiation modifiers in, 334
  radiosensitivity modifiers in, 332-34, 338-40
  temperature effects in, 332-33
Channel quantum numbers, 102-3
Charge, nuclear
  angular shape of, 26, 47-68
  and bound electrons, 44-46
  and bound -mesons, 41-43
  distribution of, 25-68
    basic parameters in, 28-29
    electron scattering and, 61-63
    isotope shifts and, 56-60
    -mesonic x-rays and, 26-28, 60-61
    nonelectric measures of, 63-66
    theories of, 66-68
  electric quadrupole transitions and, 50-54
  electron scattering and, 30-40
  gamma decay and, 54-56
  mirror nuclei and, 46-47
  quadrupole moments and, 48-50
  radial shape of, 26-47, 63, 66-67
  radius of, 25-47
Chelates
  and radioactive poisoning, 377-94, 396-97
  in radiochemical separation, 269-71
Chemistry, radiation, 213-35
  of alkyl monohalide systems, 224
  of aqueous solutions, 229-35
  of biologically significant solutes, 233

central problem of, 213
chemical dosimetry and, 216-17
ferrous sulfate oxidation and, 215-16
of ice, 228
of inorganic gases, 220-21
low energy electron impact and, 241-63
and organic compound reactions, 221-28
physical dosimetry and, 215
polymerization and, 224-25
primary processes in, 217-20
rotating sector technique and, 215
sources for studies in, 214
of two component systems, 223
of water, 218-19, 228-35
Chlorophyll mutations, 357-58
Chromatography
and radiochemical separation, 291
Chromosomes
breakage of, 346-47, 356
chemical action on, 352-53
infrared radiation effects on, 348
radiation effects on, 343-58
chemical modifiers and, 352
oxygen and, 350-51
temperature and, 348
Citrates
and radioactive poisoning, 394-408
Cloud chambers, 145-67
background fog in, 151
calibration of, 148, 158
at Columbia University, 163
condensation efficiency of, 149-51
deadtime reduction in, 151
diffusion type, 145-67
atmospheric pressure operation of, 155-57
basic mechanism of, 154
in cosmic ray studies, 156
high pressure, 157-67
double chamber technique, 146-49
efficiency of, 153
errors of, 149, 152-53
expansion type, 145-53
at Harwell, 162-63
high pressure hydrogen type, 154
ionization measurements in, 149-50
large, 150-51
low pressure, 157
momentum measurements in, 150
multiplate, diffusion type, 156-57
thermal effects in, 152-53
triple, 147
Coal gas
and radiation protection, 413
Collective model of nucleus, 17-21
Complexing agents
and radioactive poisoning, 377-94, 396-97, 407-8
Complexones, 269-71
Compound nucleus, 99-101, 107-12
Compton process, 77, 80
Computers
in mass spectrometry, 208-11
Computing machines, 87
Conductivity
induced by x-rays, 225
Core, nuclear, 17-21
Cosmic rays
detection of, 146-67
Cosmotron, cloud chamber for, 159-62, 166
Costs of nuclear reactors, 181, 184
Coulomb energy
of mirror nuclei, 46-47
CP-5, 186-87
Cross section , removal, 78, 88-92
Cross sections
for ionization by electrons, 242-45
neutron, 77-78
Cupferron
in radiochemical separation, 275-76
Cycloalkanes, in mass spectrometry, 198-203
Cysteamine
and radiation protection, 413
Cysteine
and radiation protection, 334, 343
and radioactive poisoning, 397
Cytological effects
of radiation, 342-58

D

Deadtime
in cloud chambers, 151-52
Decalcification therapy, 375-77
Densitometry, 320
Detectors, nuclear particle, 145-67
see also Bubble chambers, Cloud chambers
Deuterated hydrocarbons, 253-58
Deuterons
inelastic scattering of, 132-33
Diffusion chambers
see Cloud chambers
Digital computers, 208-11
Diketones, beta
in radiochemical separation, 281
Dissociation
bond energies in, 259
see Chemistry, radiation
Distillation
and radiochemical separation, 282, 287
DNA
and radiation injury, 415
Dose, radiation, 80
Dosimetry, 215-17
DPPH solutions, 221-22
Drugs
and radiation injury, 419

E

EDTA
effect on Pu, La excretion, 386-88, 392
effect on Y excretion, 388-90
metabolism of, 386
and radioactive poisoning, 380-94
in radiochemical separation, 269-72
toxicity of, 386
and Zr citrate treatment, 407-8
Elastic scattering
of alpha particles, 130-31
of neutrons, 130
of protons, 126-30
Electrochemistry
in radiochemical separation, 276-77
Electromagnetic radiation
interaction with nuclei of, 1-22
and collective model, 17-21
and many-particle shell model, 13-17
and one-particle shell model, 7-13
multipole expansion of, 2-6
and nuclear charge, current densities, 21-22
Electrons
binding of, 44-46
ionization by, 242-45
low energy, 241-63
scattering by nuclei of, 25-28, 30-40, 61-63
for high energy electrons, 32-35
for low energy electrons,

31
for medium energy electrons, 32-35
Emulsions, nuclear
in cloud chamber work, 174
scanning of, 162
Emulsions, photographic
artifacts and, 312-15
atmosphere oxygen and, 313
background in, 319
chemical effects on, 312-15
coating of, 316
compositions of, 304
densitometry and, 320
distortion of, 319
exposure of, 317-18
grain counting in, 320
humidity effects on, 304, 312, 315, 317
hydrogen peroxide and, 313-14
hydrogen sulfide and, 314
latent image effects in, 312-19
moisture content of, 304
particle range in, 307-9
processing of, 318
resolution in, 321-23
response mechanism of, 304-6
sensitivity of, 307-9
specific energy loss in, 305
temperature influence on, 309
track counting in, 320
types available, 302-3
Enzymes
radiosensitivity of, 340-42
Explosion-proofing, 203-4
Eyes
radiosensitivity of, 416

F

Ferrous sulfate
oxidation of, 215-16, 233
Fission, 74-76
Fission products
hazards of, 187, 191
poisoning by, 401
Fluorescence
photographic emulsions and, 315
Food
radiation sterilization of, 420-21

G

Gamma rays
attenuation of, 77-86
capture, 76
effect on aqueous systems of, 231
from fission, 75-76
induced chlorination by, 223
in nuclear transitions, 54-55, 64
oxidation by, 216
sources of, 214
see also Chemistry, radiation
Glutathione
and radiation protection, 334
Graphite
in research reactors, 179
Grey wedge
in pulse analysis, 283, 293

H

Hazards
of radioactive poisons, 369-409
Health physics
see Shielding
Heats of formation
of ions, radicals, 260
Heavy water
in research reactors, 180, 186
Helium-3
magnetic moment of, 21
High pressure diffusion chamber, 157-67
Hiroshima bombing
data on survivors of, 420
Hydrocarbons
analysis of, 197-202
bond dissociation energies of, 259-62
mass spectra of, 242, 246, 253-62
Hydrogen
in cloud chambers, 154, 169
neutron absorption in, 91
neutron scattering in, 86-87
Hydrogen peroxide
effect on latent image of, 313
Hydrogen sulfide
effect on latent image of, 314
Humidity
nuclear emulsions and, 304, 312, 315, 317

I

Ice
radiation chemistry of, 228
Industrial applications
of mass spectrometry, 197-211
Instrumentation
explosion-proofing of, 203-4
in research reactors, 191-92
see Mass spectrometry
Iodine-131
in radioautography, 321-23
Ion exchange
column, precipitation on, 272-74
and radiochemical separation, 287-90
Ion exchange resins
in radioactive poisoning, 373-74, 397-408
Ionization
in cloud chamber tracks, 149-50
in mass spectrometry, 241-63
probability of, 242-45
Ion pair
energy to form, 262
energy to produce, 216
Ion resonance, 204
Ions
fragment, 245-46
heats of formation of, 260
in mass spectral analysis, 200, 204-6
metastable, 253-54
negative, 246
Ion sources, 202, 207
Isotope dilution analysis, 208
Isotope shift, 44-45, 56-60

K

Kernel method, 92

L

Lamb shift, 44, 46
Lanthanum-140 poisoning, 387-89
Latent image
chemical effects on, 312-15
development of, 318-19
mechanism of formation of, 304-5, 309-12
Lead, nuclear radius of, 42-43
Lethal dose
for microorganisms, 328-40, 354-56
Level densities, 121, 136
Licenses
for U.S. research reactors, 183
Lifetimes
of nuclear particles, 153
of nuclear transitions, 11-14, 16, 54-56, 64
Linear energy transfer, 330
Lipemia
and radiation injury, 418
Liquids
superheating of, 167
Lithium-6
shielding and, 76
Lithium-7 recoils, 214
Lubricating oils
mass spectral analysis of, 198-200

M

Magic nuclei, 76
Magnetic moments
in nucleon radiation interaction, 21
Magnets
for bubble chambers, 173
for cloud chambers, 148, 153, 155, 159, 163
Mammals
radioelements removal from, 369-409
Many-particle shell nucleus, 13-17
Mass spectrometry, 197-211, 241-63
alloy analysis by, 207
applications of, 206-8
automatic data reduction in, 208-11
calibration matrix for, 198-201
computers for, 208-11
of deuterated molecules, 253-58
of free radicals, 247
heavy gas oil analysis by, 198
high molecular weights and, 197-202
high temperature source in, 202
instrumentation in, 204-7
isotope dilution technique in, 207
intermolecular reactions in, 262-63
lubricating oil analysis by, 198-200
metal analysis by, 207
organic chemical analysis by, 202
process monitoring and, 202-7
quasi-equilibrium theory and, 250-62
rearrangement peaks in, 257-58
wax analysis by, 200-2
Mesons
charged
in nuclear forces, 21
detection of, 146, 163-65
n, p reactions and, 166
-Mesons
bound, 41-43
determination of mass of, 146
interaction with nuclei of, 26-28, 40-43, 60-61
scattering by nuclei of, 43-45
-Mesons
production of V-particles by, 165-66
Mesothorium poisoning
see Radium poisoning
Metallo-organic compounds
mass spectral analysis of, 202
Metals, analysis of, 207-8
Methane
mass spectrum of, 248-50
Mirror nuclei, 46-47
Moderators
in research reactors, 179-80
Molecular reactions, 262-63
Molecular weights
mass spectral analysis of, 197-202
Molecules, polyatomic
mass spectra of, 250
Moments method, 81
Momentum
cloud chamber measurement of, 147, 150, 152
Monoaromatics, in mass spectrometry, 198-203
Monte Carlo calculation
in nuclear reaction theory, 133-34
Monte Carlo method, 84
Monkey
in radiosensitive studies, 416-17
Multipole expansion, 2-6
Mutagenic effects, 328-40
Mutation rate, 356-58
Mutations, and chromosome breakage, 356-58

N

Naphthalenes, in mass spectrometry, 198-203
Nervous system
radiosensitivity of, 416
Neutrons
absorption cross section of, 123
angular distribution in scattering of, 130
attenuation of, 74-78, 86-94
in chemical dosimetry, 216
distribution in nuclei of, 26-48
from fission, 75
inelastic scattering of, 77, 133
meson production with, 166
radiation decomposition by, 230
radiation injury by, 417-18
radiobiological effects of, 330, 349-50, 357
reactions with protons, 166
scattering by nuclei of, 63
total cross section of, 122-23
see also Reactors, research
Nitrogen-14
shielding and, 76
Nitrogen mustard, 330, 341, 353
Nitrous oxide
radiation decomposition of, 218
and radiation injury, 419-20
Nuclear charge
see Charge, nuclear
Nuclear emulsions
see Emulsions, photographic
Nuclear models
collective, 17-21
many-particle shell, 13-17
one-particle shell, 7-13
optical model, 99, 113-19, 131-40
in radiation-nuclear interaction, 6-21
statistical model, 99, 119-22, 131-40
Nuclear reactions
see Reactions, nuclear ; Reactors, research
Nuclear temperatures, 121, 136, 139-40
Nuclei
interaction of radiation with, 1-22
Nucleic acids
and radiation injury, 415
Nucleon-nucleon interaction
see Reactions, nuclear
Nucleus
angular shape of, 47-63
charge distribution in, 25-68
compressibility of, 45-46, 56-60
Coulomb excitation of, 56
-meson binding with, 41-43
radius of, 25, 28, 30-46
see also Charge, nuclear

O

Omegatron, 204
One-particle shell nucleus, 7-13
Optical model of nucleus, 99, 113-19, 123, 127-30
comparison with statistical model, 131-40
Organic compounds
mass spectral analysis of, 202
Oxidation
in radiation chemistry, 233-34
Oxygen
effect on latent image of, 313
and radiobiological effects 333, 350-51

P

Pair production, 77, 80
Paper chromatography, 291
Parabiosis
  and radiation protection, 414
Penetration, nuclear radiation, 73-94
Petroleum
  mass spectral analysis of, 198-202
  refining of, 198, 201-3, 206-7
Phosphates, butyl
  in radiochemical separation, 281
Phosphorus-32
  in radioautography, 301, 321-23
Photochemistry, 217-20
Photoelectric effect, 77, 80
Photographic emulsions
  see Emulsions, photographic
Photography
  in cloud chamber work, 160, 166, 174
Photoluminescence
  photographic emulsions and, 315
Photoneutrons
  in D_2O reactors, 192
Photons
  see Gamma rays, x-Rays
Photoreactivation, 336-38
Pigmentation
  and radiosensitivity, 339
Piles
  see Reactors
Plastics
  irradiation of, 218, 225-28
Platinum
  elastic scattering of protons on, 127
Ploidy
  and radiosensitivity, 339-40
Plutonium-239
  in radioautography, 302
Plutonium poisoning, 369-409
Poisons, radioactive, 369-409
  ingestion of, 373-74
  inhalation of, 374-75
  in skin punctures, 375
  tabulation of, 370
  treatment for, 371-409
    by Ca-EDTA, Zr citrate, 407-8
    by complexing agents, 377-97
    by decalcification, 375-77
    by ion exchange, 397-407
    by minimizing absorption, 373-75
    by zirconium salts, 397-407
Poisons, reactor, 189
Polonium
  as α source, 214
Polonium poisoning, 389
Polymerization
  by radiation, 224-25
Postirradiation treatment, 335-38
Potassium cyanide
  and radiation protection, 413
Precipitation
  homogeneous, 271
  on ion exchnage columns, 273-74
  radiochemical separation with, 269-81
Process control
  with mass spectrometry, 202-7
Protons
  in cloud chamber calibration, 148, 158
  distribution in nuclei of, 26-68
  elastic scattering of, 126-30
  inelastic scattering of, 132, 135-39
  in radiobiological studies, 344
  scattering by nuclei of, 63
Psychobiological effects of radiation, 417
Pulse height analysis, 283, 293

R

Rad, 80
Radiation chemistry
  see Chemistry, radiation
Radiation, electromagnetic
  see Electromagnetic radiation
Radiation injury
  body wieght changes and, 418
  and depigmentation, 419
  and infection susceptibility, 419
  lethal dosage for rats, 418
  from nonuniform exposure, 418
  and tissue permeability, 419
Radiation protection
  with coal gas pretreatment, 413
  with cysteamine, 413-14
  and eye cataracts, 416
  with KCN, 413
  with malonitrile
  in microorganisms, 332-34, 343
  and parabiosis, 414
  preirradiation treatment and, 413
Radiations
  shielding from, 73-94
Radicals
  formation of, 217-20
  mass spectrometry and, 247
  radiation protection and, 413
Radioactive poisoning
  see Poisons, radioactive
Radioautography, 297-323
  apposition of emulsions and, 316-17
  artifacts in, 312-15
  emulsions for, 298-305
  examination and interpretation of, 319
  exposure of emulsions in, 317-18
  latent image effects in, 312-15
  physical principles of, 303-12
  processing of emulsions and, 318-19
  quantitation in, 320-21
  resolution in, 321-23
  specimen preparation in, 315-16
  see also Emulsions, photographic
Radiobiology, cellular
  see Cellular radiobiology
Radiobiology, vertebrate
  see Vertebrate radiobiology
Radiochemical separation, 269-93
  by chromatography, 291
  by distillation, 282, 287
  by electrochemical techniques, 276-77
  instrumentation for, 292-93
  by ion exchange, 287-90
  by precipitation, 269-81
  by solvent extraction, 281-82
  summary tabulation of, 292
  by volatilization, 282, 287
Radioisotopes
  carrier-free production of, 282
Radiolysis, 213-35
Radiosensitivity
  in cellular radiobiology, 332-34, 338-42
  modification of, 332-34, 338-40, 343
Radium poisoning, 369, 374-77, 389
Raleigh reactor, 184
Range
  of alphas, betas in emulsions, 305-9
Rare earths
  separation of, 282
RBE, 327, 331, 348-50
Reactions, nuclear
  angular distribution of

products of, 111-12, 132-33
compound nucleus and, 107-11
eigenstate decomposition and, 102-7
of intermediate energy heavy particles, 99-140
optical model and, 113-19
proton scattering and, 126-30
statistical model and, 119-22
total neutron cross sections and, 122-23
Reactor
radiation chemistry and, 216, 226, 230
Reactors, research, 179-96
control of, 191
costs of, 181
design,construction of, 187-94
heat removal in, 191
industrial interests in, 181-82
initial operation of, 194-96
legal problems and, 182-84
refueling of, 188
safety of, 187-89
shielding of, 189-90
startup problems in, 192
tabulations of, 179-81
types of, 184-87
university interest in, 181-82
utility of, 181-84
Reactors, shielding of, 73-94
Refinery, mass spectrometry and, 201-3, 206-7
Removal cross section, 78, 88-92
Research reactors
see Reactors, research
Resolution
in mass spectrometry, 204-6
in radioautography, 321-23
Resonance widths, 123
Rubidium-86
gamma ray of, 76

S

Safety
in research reactors, 187-92
Scattering
of gammas, 77-83
of neutrons, 77
Scattering, elastic
see Elastic scattering
Scintillator detectors
and β, γ spectra, 293
in luminescent chamber, 175
Separations processes
see Radiochemical separation
Shell model
and angular shape of nucleus, 66
and nuclear charge distribution, 48-50
Shielding, 73-94
of BNL reactor, 94
of cloud chambers, 162
fission process and, 74-76
gamma attenuation in, 78-86
inhomogeneous, 93-94
interaction process in, 77-78
of Materials Testing Reactor, 94
Monte Carlo method and, 84
neutron attenuation in, 86-94
ORNL reactors and, 89-90
radiation sources in, 74-77
removal cross sections and, 78, 88
in research reactors, 189-90
Silver bromide
see Emulsions, photographic
Sodium citrate
and radioactive poisoning, 380, 402
Solarization, 305
Solid state
and photographic grain development, 304
Solids
isotope analysis of, 207-8
Solvent extraction
and radiochemical separation, 281-82
Spleen
and radiation injury, 415
Statistical model of nucleus, 99, 119-22
comparison with optical model, 131-40
ideal validity of, 139
level densities in, 121-22
Sterilization, food, 420-21
Stopping power
in photographic emulsions, 307
Strontium-90 poisoning, 374-77, 389
Sulfahydryl compounds
and radioactive poisoning, 380-94, 397
Sulfur, in petroleum refining, 198
Superheating of liquids, 167-69
Swimming pool reactors, 181-82
Synchrotron, proton
cloud chambers with, 157-67

T

Temperature
and microorganism radiosensitivity, 332
Testosterone
and radiation injury, 420
Thioacetamide
in radiochemical separation, 273
Thymus
radiation injury and, 415
Thyroid
radiation injury of, 420
Toxicity
of radioisotopes, 369-409
Transitions, nuclear
electromagnetic radiation and, 1-22
Transport theory, 81-83
Trichinosis
radiation prevention of, 420-21
Tritium
magnetic moment of, 21
Tritium recoils, 214

U

Ultraviolet radiation
biological effects of, 327-58
mutation with, 329, 331-32
oxidation by, 216-17
in photoreactivation, 336-38
Uranium
enriched reactor fuel, 180
in research reactors, 179-80
Urea, hydrolysis of, 271

V

Versenol
and radioactive poisoning, 396
Vertebrate radiobiology
physiology, 413-21
Viruses
radiation effects on, 327-58
Volatilization
radiochemical separation and, 282, 287
V particles
detection of, 165

W

Water
effect on latent image of, 313
gamma attenuation in, 84
neutron attenuation in, 87, 91
radiation chemistry of, 218-19, 228-35
radiation effects on, 184, 186, 218-19, 228-35
Water boiler reactors

181-82, 184
Waxes
mass spectral analysis of, 200-1, 203
Window effects, 139
Wounds
and radioactive poisons, 375

X

Xenon-135
in research reactors, 189
X-ray film, 298-323
X-rays
biological effects of, 327-58
comparison with β-ray injury, 418
fine structure in, 44
isotope shift in, 44
in mu-meson capture, 26, 28, 41-43, 60-61
oxidation by, 216

Y

Yeast
radiation effects on, 331, 338-40
Yttrium-91 poisoning, 388-408

Z

Zirconium citrate
metabolism toxicity of, 398-99
and radioactive poisoning, 397-408
and radioisotope excretion, 399-407

CHAPTER TITLE INDEX
Volumes 1–5

Titles of volume chapters are arranged in groups according to general descriptive topics. Within each group, titles are arranged in chronological order. It should be understood that the topic categories are arbitrary and have been chosen only to assist in identifying related chapters. For more detailed indexing see the Subject Index at the end of each volume.

ACCELERATORS

"High Energy Accelerators: Standard Cyclotron",	M. S. Livingston,	1: 157-62
"High Energy Accelerators: Synchrocyclotron",	M. S. Livingston,	1: 163-68
"High Energy Accelerators: Linear Accelerators",	J. C. Slater,	1: 199-206
"Recent Progress in Accelerators",	E.L.Chu, L.I. Schiff,	2: 79-92
"Recent Developments in Proton Synchrotrons",	J.P. Blewett,	4: 1-12

CHEMISTRY, NUCLEAR AND RADIO-

"Chemistry of the Actinide Elements",	J.J.Katz, W.M.Manning,	1: 245-62
"Analytical Nuclear Chemistry",	C.J. Rodden,	1: 343-62
"Isotopes",	J. Bigeleisen,	2: 221-38
"Separation Techniques Used in Radiochemistry",	P.C.Stevenson, H.G. Hicks,	3: 221-34
"Fission Radiochemistry (Low Energy Fission)",	L.E.Glendenin, E.P.Steinberg,	4: 69-80
"Radiochemical Separation Techniques",	H.L.Finston, J. Miskel,	5: 269-96

COSMIC RAYS

"Nuclear Interactions of Cosmic Rays",	R.V. Adams,	1: 107-36
"Origin and Propagation of Cosmic Rays",	L. Biermann,	2: 335-64
"Mesons and Heavy Unstable Particles in Cosmic Rays",	L. Leprince-Ringuet,	3: 39-66

DETECTORS

"Detection of Nuclear Particles",	W.H. Jordan,	1: 207-44
"Photographic Emulsions",	Y. Goldschmidt-Clermont,	3: 141-70
"Nuclear Particle Detection: Fast Electronics",	R.E. Bell,	4: 93-110
"Characteristics of Scintillators",	R.K. Swank,	4: 110-40
"Cerenkov Counters",	J. Marshall,	4: 141-56
"Cloud Chambers and Bubble Chambers",	W.B. Fretter,	5: 145-78
"Radioautography Techniques",	W.P. Norris, L.A. Woodruff,	5: 297-326

FISSION

"High Energy Fission",	R.W. Spence, G.P. Ford,	2: 399-410
"Fission Radiochemistry (Low Energy Fission)",	L.E. Glendenin, H.G. Hicks,	3: 221-34
"Design of Nuclear Reactors for Research",	L. B. Borst	5: 179-96

INTERACTION OF NUCLEAR RADIATIONS AND MATTER

"Radiation Effects in Solids",	G. J. Dienes,	2: 187-220
"Extranuclear Interactions of Electrons and Gamma Rays",	D.R. Corson, A.O. Hanson,	3: 67-92
"Radiation Chemistry",	J.L. Magee,	3: 171-92
"Chemical Effects of Nuclear Transformations",	J.E. Willard,	3: 193-220
"Penetration of Heavy Charged Particles in Matter",	E.A. Uehling,	4: 315-50
"Radiation Chemistry",	F.S. Dainton,	5: 213-40

LOW TEMPERATURE PHENOMENA

"Low Temperature Phenomena",	C.T. Lane,	1: 413-40

MESONS

"Meson Physics",	R.E. Marshak,	1: 1-42
"Subnuclear Particles",	J.S. Blair, G.F. Chew,	2: 163-86
"Reactions of π-Mesons with Nucleons",	E.M. Henley, M.A. Ruderman, and J. Steinberger	3: 1-38
"The Interaction Between π-Mesons and Nucleons",	M. Gell-Mann, K.M. Watson,	4: 219-70
"Heavy Mesons",	C. Dilworth, G.P.S.Occhialini, and L. Scarsi	4: 271-314

(See also COSMIC RAYS)

METALLURGY

"Progress in Metallurgy",	B.A. Rogers, F.H. Spedding,	1: 441-64

NEUTRONS
"Neutron Optics", D.J. Hughes, 3: 93-118
"The Standardization of Neutron Measurements", A. Wattenberg, 3: 119-40

NUCLEAR GEOLOGY, COSMOLOGY
"Geochemistry", M. Fleischer, J.C. Rabbit, 1: 465-78
"Origin and Abundance Distribution of the Elements", R.A. Alpher, R.C. Herman, 2: 1-40
"Energy Production in Stars", E.E. Salpeter, 2: 41-62
"Production and Distribution of Natural Radiocarbon", E.C. Anderson, 2: 63-78
"Radioactivity in Geology and Cosmology", T.P. Kohman, N. Saito, 4: 401-62

NUCLEAR MOMENTS, STRUCTURE
"Recent Developments in the Theory of Nuclear Structure", E. Feenberg, 1: 43-66
"Energy Levels of Light Nuclei", T. Lauritsen, 1: 67-96
"Nuclear Moments", N. Ramsey, 1: 97-106
"Nuclear Moments", B.T. Feld, 2: 239-60
"Radiofrequency and Microwave Spectroscopy of Nuclei", G.E. Pake, 4: 33-50
"Distribution of Charge in Nuclei", D. Hill, K.W. Ford, 5: 25-72

NUCLEAR REACTIONS
"Nuclear Reactions Induced by High Energy Particles", D.H. Templeton, 2: 93-104
"Recent Studies of Photonuclear Reactions", K. Strauch, 2: 105-28
"Advances in Nucleon-Nucleon Scattering Experiments and their Theoretical Consequences", G. Breit, R.L. Gluckstern, 2: 365-98
"Theories of Photonuclear Reactions", J. S. Levinger, 4: 13-32
"Nuclear Reactions of Intermediate Energy Heavy Particles", D.C. Peaslee, 5: 99-144

POSITRONIUM
"Positronium", S. DeBenedetti, H.C. Corben, 4: 191-218

RADIATION HAZARDS
"Radiation Dosimetry and Protection", L.D. Marinelli, 3: 249-70
"Practical Aspects of Radiation Injury", L.H. Hempelmann, and J.G. Hoffman, 3: 369-92
"Removal of Radioelements from the Mammalian Body", J. Schubert, 5: 369-412

RADIOACTIVITY
"Angular Correlation of Nuclear Radiation", H. Frauenfelder, 2: 129-62
"Experimental Clarification of the Theory of Beta-Decay", E.J. Konopinski, L.M. Langer, 2: 261-304
"Beta-Decay Energetics", C.D. Coryell, 2: 305-34
"Alpha Radioactivity", I. Perlman, F. Asaro, 4: 157-90
"Gamma Radiation from Nuclei", M. Goldhaber, J. Weneser, 5: 1-24

RADIOBIOLOGY
"Cellular Radiobiology", A.H. Sparrow, F. Forro, Jr., 3: 339-68
"Cellular Radiobiology", R.K. Mortimer, C.A. Beam, 5: 327-68
"Biochemical Effects of Radiation", K.P. DuBois, D.F. Petersen, 4: 351-76
"Some Aspects of the Biological Action of High Energy Radiations", H.M. Patt, 1: 495-524
"Genetic Effects of Radiation", R.F. Kimball, 1: 479-94
"Vertebrate Radiobiology: Embryology", R. Rugh, 3: 271-302
"Vertebrate Radiobiology: Histopathology and Carcinogenesis", J. Furth, A.C. Upton, 3: 303-38
"Vertebrate Radiobiology: Lethal Actions and Associated Effects", J.F. Thomson, 4: 377-400
"Vertebrate Radiobiology: Physiology", A. Edelmann, 5: 413-24

Volumes 1–5

RADIOISOTOPES		
"Isotopic Tracers in Chemical Systems",	R.R. Edwards,	1: 301-42
"Radioisotopes in Biochemical and Medical Research",	C.A. Villee,	1: 525-68
"Radioisotopes in Soils Research and Plant Nutrition",	S.B. Hendricks, L.A. Dean,	1: 597-610
"Isotopes",	J. Bigeleisen,	2: 221-38
"Standardization of Radioactive Sources",	G. Manov,	4: 51-68
SHIELDING		
"Nuclear Radiation Shielding", (See also RADIATION HAZARDS)	E. P. Blizard,	5: 73-98
SPECTROSCOPY		
"Atomic and Molecular Spectroscopy",	G.H. Dieke,	1: 363-412
STABLE ISOTOPES, MASS SPECTROSCOPY		
"Mass and Relative Abundance of Isotopes".	A.O. Nier,	1: 137-56
"Electromagnetic Separation of Stable Isotopes",	C.P. Keim,	1: 263-92
"Chemical Separation of Stable Isotopes",	G.H. Clewett,	1: 293-300
"Stable Isotopes in Biochemical Research".	D.Rittenberg, T.D. Price,	1: 569-96
"Isotope Effects in Chemical Reactions",	P.E. Yankwich,	3: 235-48
"Stable Isotope Dilution as an Analytical Tool",	M.G. Inghram,	4: 81-92
"Mass Spectrometric Analysis of Electron Impact Processes",	H. Eyring, A.R. Wahrhaftig, and M. Krauss	5: 241-68
"Industrial Applications: Mass Spectrometry",	C.E. Berry, J.K. Walker,	5: 197-212

INDEX OF CONTRIBUTING AUTHORS
Volumes 1–5

A listing of volume and page numbers for each contributing author in the first five volumes.

A

Adams, R.V., 1: 107
Alpher, R.A., 2: 1
Anderson, E.C., 2: 63
Asaro, F., 4: 157

B

Beam, C.A., 5: 327
Bell, R.E., 4: 93
Berry, C.E., 5: 197
Biermann, L., 2: 335
Bigeleisen, J., 2: 221
Blair, J.S., 2; 163
Blewett, J.P., 4: 1
Blizard, E.P., 5: 73
Borst, L.B., 5: 179
Breit, G., 2: 365

C

Chew, G.F., 2: 163
Chu, E.L., 2: 79
Clewett, G.H., 1: 293
Corben, H.C., 4: 191
Corson, D.R., 3: 67
Coryell, C.D., 2: 305

D

Dainton, F.S., 5: 213
Dean, L.A., 1: 597
DeBenedetti, S., 4: 191
Dieke, G.H., 1: 363
Dienes, G.J., 2: 187
Dilworth, C., 4: 271
DuBois, K.P., 4: 351

E

Edelmann, A., 5: 413
Edwards, R.R., 1: 301
Eyring, H., 5: 241

F

Feenberg, E., 1: 43
Feld, B.T., 2: 239
Finston, H.L., 5: 269
Fleischer, M., 1: 465
Ford, G.P., 2: 399
Ford, K.W., 5: 25
Forro, F., Jr., 3: 339
Frauenfelder, H., 2: 129
Fretter, W.B., 5: 145
Furth, J., 3: 303

G

Gell-Mann, M., 4: 219
Glendenin, L.E., 4: 69
Gluckstern, R.L., 2: 365
Goldhaber, M., 5: 1
Goldschmidt-Clermont, Y., 3: 141

H

Halpern, I., 1: 175
Hanson, A.O., 3: 67
Hempelmann, L.H., 3: 369
Hendricks, S.B., 1: 597
Henley, E.M., 3: 1
Herman, R.C., 2: 1
Hicks, H.G., 3: 221
Hill, D., 5: 25
Hoffman, J.G., 3: 369
Hughes, D.J., 3: 93

I

Inghram, M.G., 4: 81

J

Jordan, W.H., 1: 207

K

Katz, J. J., 1: 245
Keim, C.P., 1: 263
Kimball, R.F., 1: 479
Kohman, T.P., 4: 401
Konopinski, E.J., 2: 261
Kraushaar, W.L., 1: 175
Krauss, M., 5: 241

L

Lane, C.T., 1: 413
Langer, L.M., 2: 261
Lauritsen, T., 1: 67
Leprince-Ringuet, L., 3: 39
Levinger, J.S., 4: 13
Livingston, M.S., 1: 157, 163, 169

M

Magee, J.L., 3: 171
Manning, W.M., 1: 245
Manov, G., 4: 51
Marinelli, L.D., 3: 249
Marshak, R.E., 1: 1
Marshall, J., 4: 141
Miskel, J., 5: 269
Mortimer, R.K., 5: 327

N

Nier, A.O., 1: 137
Norris, W.P., 5: 297

O

Occhialini, G.P.S., 4: 271

P

Pake, G.E., 4: 33
Patt, H.M., 1: 495
Peaslee, D.C., 5: 99
Perlman, I., 4: 157
Petersen, D.F., 4: 351
Price, T.D., 1: 569

R

Rabbit, J.C., 1: 465
Ramsey, N., 1: 97
Rittenberg, D., 1: 569
Rodden, C.J., 1: 343
Rogers, B.A., 1: 441
Ruderman, M.A., 3: 1
Rugh, R., 3: 271

S

Saito, N., 4: 401
Salpeter, E.E., 2: 41
Scarsi, L., 4: 271
Schiff, L.I., 2: 79
Schubert, J., 5: 369
Slater, J.C., 1: 199
Sparrow, A.H., 3: 339
Spedding, F.H., 1: 441
Spence, R.W., 2: 339
Steinberg, E.P., 4: 69
Steinberger, J., 3: 1
Stevenson, P.C., 3: 221
Strauch, K., 2: 105
Swank, R.K., 4: 111

T

Templeton, D.H., 2: 93
Thomas, J.E., Jr., 1: 175
Thomson, J.F., 4: 377

U

Uehling, E.A., 4: 315
Upton, A.C., 3: 303

V

Villee, C.A., 1: 525

W

Wahrhaftig, A.R., 5: 241
Walker, J.K., 5: 197
Watson, K.M., 4: 219
Wattenberg, A., 3: 119
Weneser, J., 5: 1
Willard, J.E., 3: 193
Woodruff, L.A., 5: 297

Y

Yankwich, P.E., 3: 235